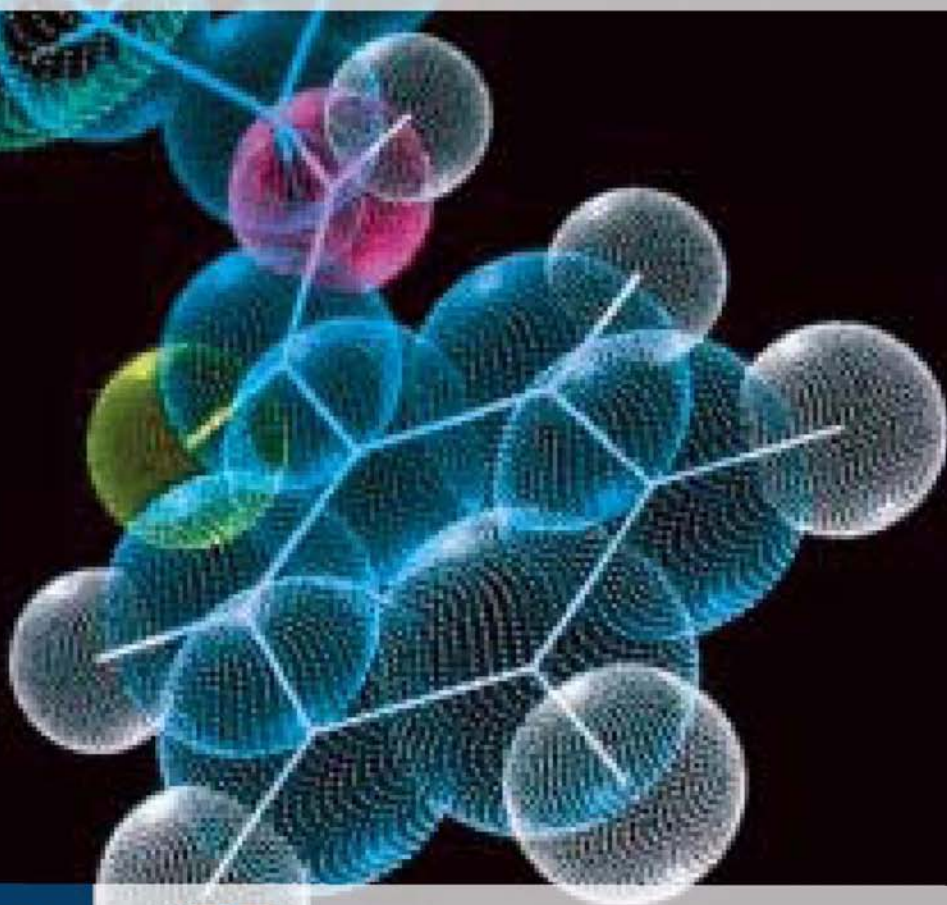


# Molecular Biopharmaceutics

Edited by Bente Steffansen, Birger Brodin  
and Carsten Uhd Nielsen



**(P<sub>h</sub>P)**  
Pharmaceutical Press

**UUA** pharmacy  
series

## **Molecular Biopharmaceutics**

## **ULLA Pharmacy Series**

### **Series Editor-in-Chief**

Prof Anthony C Moffat

The School of Pharmacy, University of London, UK

### **Members of the Editorial Advisory Board**

Prof Patrick Augustijns, Katholieke Universiteit Leuven, Laboratory for Pharmacotechnology and Biopharmacy, Belgium

Prof Franco Bernini, University of Parma, Dipartimento di Scienze Farmacologiche, Biologiche e Chimiche Applicate, Italy

Prof Meindert Danhof, LACDR, Director of Research, The Netherlands

Prof Lennart Dencker, Uppsala University, Faculty of Pharmacy, Department of Pharmaceutical Biosciences, Sweden

Prof Elias Fattal, University Paris South, Faculty of Pharmacy, France

Prof Sven Frokjaer, University of Copenhagen, The Faculty of Pharmaceutical Sciences, Denmark

Prof Flemming Jorgensen, University of Copenhagen, The Faculty of Pharmaceutical Sciences, Department of Medicinal Chemistry, Denmark

Prof Denis Labarre, University Paris South, Faculty of Pharmacy, France

Prof Fred Nyberg, University Paris South, Faculty of Pharmacy, France

Prof Patrizia Santi, University of Parma, Dipartimento Farmaceutico, Italy

Prof Nico Vermeulen, LACDR-Section of Molecular Toxicology, Department of Chemistry & Pharmacochemistry, The Netherlands

Other titles in the ULLA pharmacy series include:

*Pharmaceutical Toxicology*

*Paediatric Drug Handling*

*International Pharmacy Practice Research*

*Biomedical and Pharmaceutical Polymers*

*Proteomics and Metabolomics in Pharmaceutical Science*

*Managing and Developing Learning in Healthcare*

NB: some of the titles listed are forthcoming/not yet published

# Molecular Biopharmaceutics

Aspects of drug characterisation,  
drug delivery and dosage form evaluation

Edited by

**Bente Steffansen**

Associate Professor  
Department of Pharmaceutics and Analytical Chemistry  
Faculty of Pharmaceutical Sciences  
University of Copenhagen, Denmark

**Birger Brodin**

Associate Professor  
Department of Pharmaceutics and Analytical Chemistry  
Faculty of Pharmaceutical Sciences  
University of Copenhagen, Denmark

**Carsten Uhd Nielsen**

Associate Professor  
Department of Pharmaceutics and Analytical Chemistry  
Faculty of Pharmaceutical Sciences  
University of Copenhagen, Denmark



London • Chicago **(PP)<sub>h</sub>**  
**Pharmaceutical Press**

**Published by the Pharmaceutical Press**

An imprint of RPS Publishing

1 Lambeth High Street, London SE1 7JN, UK

100 South Atkinson Road, Suite 200, Grayslake, IL 60030-7820, USA

© Pharmaceutical Press 2010

**(PP)** is a trade mark of RPS Publishing

RPS Publishing is the publishing organisation of the Royal Pharmaceutical Society of Great Britain

First published 2010

Typeset by Thomson Digital (India) Limited, Noida, India

Printed in Great Britain by TJ International, Padstow, Cornwall

ISBN 978 0 85369 722 0

All rights reserved. No part of this publication may be reproduced, stored in a retrieval system, or transmitted in any form or by any means, without the prior written permission of the copyright holder.

The publisher makes no representation, express or implied, with regard to the accuracy of the information contained in this book and cannot accept any legal responsibility or liability for any errors or omissions that may be made.

The right of Bente Steffansen, Birger Brodin and Carsten Uhd Nielsen to be identified as author of this work has been asserted by them in accordance with the Copyright, Designs and Patents Act, 1988.

A catalogue record for this book is available from the British Library.



# Contents

*ULLA pharmacy series* x

*Preface* xi

*About the editors* xii

*Contributors* xiv

*Abbreviations* xv

<b>Part 1</b>	<b>Introduction</b>	<b>1</b>
	<i>Bente Steffansen, Carsten Uhd Nielsen and Birger Brodin</i>	
1.1	Molecular biopharmaceutics	1
1.2	Important definitions and terms	1
1.3	Experimental methods within molecular biopharmaceutics	2
1.4	Classification of drug substances	2
1.5	The book chapters	3
	References	4
<b>Part 2</b>	<b>Physicochemical characterisation of drug candidates</b>	<b>5</b>
<b>2.1</b>	<b>Acid/base properties, solubility and distribution of drug candidates</b>	<b>7</b>
	<i>Bente Steffansen, Carsten Uhd Nielsen and Birger Brodin</i>	
2.1.1	Acid/base properties of drug candidates	7
2.1.2	Solubility in aqueous solution	18
2.1.3	Partition properties of drug candidates	23
2.1.4	Solvation and solid-state limited solubility	28
2.1.5	Solid-state characterisation	29
2.1.6	Conclusions	31
	References	31
<b>2.2</b>	<b>Mechanisms of decomposition of drug candidates</b>	<b>35</b>
	<i>Bente Steffansen, Carsten Uhd Nielsen and Birger Brodin</i>	
2.2.1	Hydrolysis	35

2.2.2	Oxidation	43	
2.2.3	Non-oxidative photolytic degradation	46	
2.2.4	Degradation by racemisation	47	
2.2.5	Polymerisation	47	
2.2.6	Conclusions	48	
	References	48	
<b>2.3</b>	<b>Kinetics of decomposition in aqueous solution</b>		<b>51</b>
	<i>Bente Steffansen, Carsten Uhd Nielsen and Birger Brodin</i>		
2.3.1	First-order and pseudo zero-order kinetics of irreversible reactions	52	
2.3.2	Second-order and pseudo first-order kinetics of irreversible reactions	54	
2.3.3	Pseudo first-order kinetics of reversible reactions	57	
2.3.4	Pseudo first-order reactions of irreversible consecutive reactions	59	
2.3.5	Influence of pH on decomposition rate	60	
2.3.6	Influence of temperature on decomposition rate	62	
2.3.7	Influence of ionic strength on decomposition rate	64	
2.3.8	Influence of buffers on decomposition rate	66	
2.3.9	Influence of enzymes on decomposition rate	67	
2.3.10	Conclusions	68	
	References	69	
<b>2.4</b>	<b>Chemical approaches to improving bioavailability properties of oral drug candidates</b>		<b>71</b>
	<i>Kristina Luthman and Bente Steffansen</i>		
2.4.1	Lipinski's rule of five	71	
2.4.2	Salt formation	72	
2.4.3	Bioisosteric replacement	76	
2.4.4	Prodrug formation	84	
2.4.5	Conclusions	97	
	References	98	
<b>2.5</b>	<b>Preformulation in the industry step by step</b>		<b>101</b>
	<i>Heidi Lopez de Diego</i>		
2.5.1	Early discovery	102	
2.5.2	Lead optimisation	104	
2.5.3	Late discovery	105	
2.5.4	Early development	106	
2.5.5	Full development	111	

<b>Part 3</b>	<b>Membrane transport of drug candidates</b>	<b>113</b>
<b>3.1</b>	<b>Structure and function of absorption barriers</b>	<b>115</b>
	<i>Birger Brodin, Bente Steffansen and Carsten Uhd Nielsen</i>	
3.1.1	Epithelial morphology	115
3.1.2	The epithelial cell and tight junctions	117
3.1.3	The gastrointestinal tissue barriers	118
3.1.4	The respiratory tract	123
3.1.5	The skin	125
3.1.6	Barrier tissues in the brain	126
3.1.7	The eye	129
3.1.8	Conclusions	131
	References	131
<b>3.2</b>	<b>Passive diffusion of drug substances: the concepts of flux and permeability</b>	<b>135</b>
	<i>Birger Brodin, Bente Steffansen and Carsten Uhd Nielsen</i>	
3.2.1	How do molecules move in solution? The concepts of flux, migration and diffusion	135
3.2.2	Fluxes across barriers and the permeability coefficient	137
3.2.3	Unstirred water layers	141
3.2.4	Fluxes across a barrier under non-steady-state conditions	142
3.2.5	Fluxes of a charged solute in the presence of an electrical potential gradient	144
3.2.6	Use of flux ratios to analyse transport mechanisms	145
3.2.7	Conclusions	146
3.2.8	Examples	147
	References	151
<b>3.3</b>	<b>Carrier-mediated transport kinetics</b>	<b>153</b>
	<i>Carsten Uhd Nielsen, Bente Steffansen and Birger Brodin</i>	
3.3.1	Carrier function and mechanisms	154
3.3.2	Description of carrier-mediated transport kinetics	160
3.3.3	Methods for studying transport via carriers	171
3.3.4	Conclusions	173
	References	173
<b>3.4</b>	<b>Classification of human transporters</b>	<b>175</b>
	<i>Pascale Anderlé</i>	
3.4.1	Classification according to transport mechanisms	177
3.4.2	Transporter classification system	180



3.4.3	Gene ontology	183
3.4.4	Human Genome Organization (HUGO) symbols	185
3.4.5	Pfam	186
3.4.6	Practical approach: <i>SLC15A1</i> and <i>ABCB1</i>	186
3.4.7	Conclusions	191
	References	191
<b>3.5</b>	<b>Absorptive transporters</b>	193
	<i>Carsten Uhd Nielsen, Bente Steffansen and Birger Brodin</i>	
3.5.1	Searching for absorptive transporters	194
3.5.2	Conclusions	210
	References	211
<b>3.6</b>	<b>Efflux transporters</b>	213
	<i>Carsten Uhd Nielsen, Birger Brodin and Bente Steffansen</i>	
3.6.1	ATP-binding cassette (ABC) transport proteins in the intestine	214
3.6.2	Efflux transporters in the liver	218
3.6.3	Efflux transporters in the kidney	219
3.6.4	Efflux transporters in the brain	221
3.6.5	Conclusions	222
	References	222
<b>3.7</b>	<b>Preclinical evaluation of drug transport</b>	225
	<i>Anna-Lena Ungell</i>	
3.7.1	Mechanisms of drug transport across membranes	226
3.7.2	Tools to assess drug transport during phases of drug discovery	228
3.7.3	Cell cultures	232
3.7.4	Optimising experimental conditions	238
3.7.5	Screening for transporter interaction	239
3.7.6	Influence of metabolism during transport	242
3.7.7	Use of preclinical models for prediction of drug transport in humans	243
3.7.8	The Biopharmaceutics Classification System	245
	References	247

<b>Part 4</b>	<b>Describing and predicting bioavailability</b>	<b>255</b>
<b>4.1</b>	<b><i>In vitro</i> dissolution</b>	<b>257</b>
	<i>Betty Lomstein Pedersen and Anette Müllertz</i>	
4.1.1	Dissolution mechanism theories	258
4.1.2	Factors influencing dissolution <i>in vitro</i>	260
4.1.3	Factors influencing dissolution <i>in vivo</i>	261
4.1.4	Dissolution equipment described in the pharmacopoeias	265
4.1.5	Selection of dissolution media for <i>in vitro</i> dissolution studies	269
4.1.6	Conclusions	272
	References	273
<b>4.2</b>	<b>The Biopharmaceutics Classification System in drug discovery and development</b>	<b>277</b>
	<i>Chi-Yuan Wu</i>	
4.2.1	Prediction of oral drug absorption	279
4.2.2	Application of the Biopharmaceutics Classification System	285
4.2.3	The Biopharmaceutics Drug Disposition Classification System	291
	References	295
<b>4.3</b>	<b>Biosimulation studies</b>	<b>297</b>
	<i>Isabel Gonzalez-Alvarez and Marival Bermejo</i>	
4.3.1	What is modelling and simulation?	297
4.3.2	How to construct and verify a model	300
4.3.3	How can a biosimulation model be applied for preclinical investigations and dosage form development?	301
4.3.4	Conclusions	329
Appendix 4.3.1	Objective functions	330
Appendix 4.3.2	How does non-linear regression work?	332
Appendix 4.3.3	Software tools, companies and institutions developing biosimulation packages	339
	References	340

# ULLA pharmacy series

## Series Editor-in-Chief

**Professor Anthony C Moffat**, The School of Pharmacy, University of London, UK

The ULLA pharmacy series is a new and innovative series of introductory textbooks for postgraduate students and science monographs for practising scientists.

The series is produced by the ULLA Consortium (European University Consortium for Advanced Pharmaceutical Education and Research). The Consortium is a European academic collaboration in research and teaching of the pharmaceutical sciences that is constantly growing and expanding. The Consortium was founded in 1990 and consists of pharmacy departments from leading universities throughout Europe:

- Faculty of Pharmacy, University of Uppsala, Sweden
- The School of Pharmacy, University of London, UK
- Leiden/Amsterdam Centre for Drug Research, University of Leiden, The Netherlands
- Leiden/Amsterdam Centre for Drug Research, Vrije Universiteit Amsterdam, The Netherlands
- The Faculty of Pharmaceutical Sciences, University of Copenhagen, Denmark
- Faculty of Pharmacy, University Paris-Sud, France.

The editorial board for the ULLA series consists of several academics from these leading European institutions who are all experts in their individual field of pharmaceutical science.

The titles in this series are primarily aimed at PhD students and will also have global appeal to postgraduate students undertaking masters or diploma courses, undergraduates for specific courses, and practising pharmaceutical scientists.

Further information on the Consortium can be found at [www.u-l-l-a.org](http://www.u-l-l-a.org).

## Preface

*Molecular Biopharmaceutics* concerns physicochemical characterization, membrane transport and bioavailability of mainly small (pro)drug substances/candidates. The book describes experimental and predictive methods, ie from chemical stability, dissolution, passive diffusional and carrier-mediated membrane permeability to biosimulation of oral absorption and bioavailability. These methods are all applied in modern molecular biopharmaceutical science, in industrial preformulation and preclinical pharmaceutical development, as well as suggested in various regulatory guidelines.

The book would not have been written without the experimental laboratory work, done by our 'Drug Transporters in ADME' research group at Faculty of Pharmaceutical Sciences, University of Copenhagen. We therefore wish to thank laboratory technicians Birgitte Eltong, Bettina Dinitzen, and Maria Læssøe Pedersen, who are running the various equipment and cells. We also wish to thank the PhD's that have been running many experiments during their stay in our laboratories, and thereby indirectly contributed to the book: André Huss Eriksson, Rikke Andersen, Luise Kvistgaard Gram, Karina Thorn, Gerda Marie Rist, Sidsel Frølund, Helle Bach Søndergaard, Mie Larsen and Diana Højmark Omkvist.

Finally, we would also like to thank groups that have supported our experimental work and networking – The Danish Research Council, The European Network of Excellence-BioSim, The Danish Drug Research Academy, The Carlsberg foundation, The Hørslev Found, The Honorable Traveling Found of Marie Lønggaard, The Alfred Benzon Found and The Danish Apoteker Society Found.

Bente Steffansen  
Birger Brodin  
Carsten Uhd Nielsen  
August 2009

## About the editors

**Carsten Uhd Nielsen** (CUN) is Associate Professor of Transporters in ADME at the Faculty of Pharmaceutical Sciences (PHARMA), University of Copenhagen. His research has focused on epithelial drug transport via transporters and the impact of transporters in defining oral bioavailability. Carsten Uhd Nielsen graduated with MSc(Pharm) in 1997 from the Royal Danish School of Pharmacy. After a brief period in industry, in 2001 he obtained his PhD in drug delivery via transporters under the Center of Drug Delivery and Transport. He has served as Programme Director for the MSc in Pharmaceutical Sciences programme at PHARMA and has been on the committee developing the final BSc project in Pharmaceutics. Carsten Uhd Nielsen has furthermore worked with postgraduate teaching as both a PhD advisor and as a member of the PhD Study Board at PHARMA. From 2007 to 2009 he was on part-time leave from PHARMA working on barrier models for Bioneer:FARMA, an affiliation of the biotech company Bioneer.

**Birger Brodin**, MSc PhD in Biology, graduated from the August Krogh Institute, University of Copenhagen in 1994. After a Carlsberg-granted postdoctoral scholarship, he was employed as Post Doc by the Center for Drug Design and Transport at the Department of Pharmaceutics and Analytical Chemistry, The Faculty of Pharmaceutical Sciences (PHARMA), University of Copenhagen, where he is Associate Professor at present.

Birger Brodin has been working with the biophysics of drug transporters in the ‘Drug Transporters in ADME’ section at PHARMA since 1998. His main area of research has been peptide transporters, where he has authored a number of scientific papers, reviews and popular science articles. Birger Brodin is an elected member of the Academic Advisory Board, PHARMA, Head of the Cell Culture Facility, PHARMA, Group Leader of the ‘Drug Transporters in ADME’ section and Course Director of PhD and graduate courses. He is a member of the American Association of Pharmaceutical Scientists, The Danish Society for

Biochemistry and Molecular Biology, The Scandinavian Physiological Society and The Federation of European Physiological Society.

**Bente Steffansen** is Associate Professor in Transporters in ADME at The Faculty of Pharmaceutical Sciences (PHARMA), University of Copenhagen. She graduated with MSc(Pharm) in 1989 from The Royal Danish School of Pharmacy and obtained her PhD under the Danish Research Academy in Ocular Drug Delivery in 1994. During her PhD study she also worked for 1½ years as Research Scientist at The University of Kentucky, USA, and later as Visiting Scientist at University of Uppsala. Her research is focused on studying drug delivery processes, such as transporter-mediated ADME processes, prodrug delivery and biosimulation. Bente Steffansen has more than 50 research publications and is a member of the European Biosim network of excellence. She serves as the Program Director for the Master in Pharmaceutical Regulatory Affairs at PHARMA and supervises many Bachelor, Master and PhD students. She is a member of the Chemical Committee under the National Pharmacopoeia Board.

## Contributors

**Pascale Anderlé, PhD** Assistant Professor, ISREC, Swiss Institute for Experimental Cancer Research, 1066 Epalinges, Lausanne, Switzerland

**Marival Berjemo, PhD** Associate Professor, Department of Engineering, Pharmacy Section, Miguel Hernandez University, Alicante, Spain

**Birger Brodin, PhD** Associate Professor, Faculty of Pharmaceutical Sciences, University of Copenhagen, Denmark

**Isabel Gonzalez-Alvarez, BS, MS, PhD** Assistant Professor, Department of Engineering, Pharmacy Section, Miguel Hernandez University, Alicante, Spain

**Betty Lomstein Pedersen, PhD** Research Scientist, Novo Nordisk A/S, Denmark

**Heidi Lopez de Diego, MS, PhD** Preformulation, H Lundbeck A/S, Denmark

**Kristina Luthman, PhD** Professor, Department of Chemistry, Medicinal Chemistry, Göteborg University, Sweden

**Anette Müllertz, PhD** Associate Professor, Department of Pharmaceutics and Analytical Chemistry, Danish University of Pharmaceutical Sciences, Denmark

**Carsten Uhd Nielsen, PhD** Associate Professor, Faculty of Pharmaceutical Sciences, University of Copenhagen, Denmark

**Bente Steffansen, PhD** Associate Professor, Faculty of Pharmaceutical Sciences, University of Copenhagen, Denmark

**Anna-Lena Ungell, PhD** Associate Professor Pharmaceutics, Team leader and Principal Scientist, DMPK & Bioanalytical Chemistry, AstraZeneca R&D Mölndal, Sweden

**Chi-Yuan Wu, BS, MS, PhD** Senior Scientist, Pharmacokinetics and Drug Metabolism, Research and Development, Amgen, Thousand Oaks, California, USA

# Abbreviations

<b>AAPS</b>	American Association of Pharmaceutical Scientists
<b>ABC</b>	ATP-binding cassette
<b>ACAT</b>	advanced CAT (model)
<b>ACE</b>	angiotensin-converting enzyme
<b>ADAM</b>	advanced dissolution, absorption and metabolism (model)
<b>ADME</b>	absorption, distribution, metabolism and elimination
<b>ADP</b>	adenosine disphosphate
<b>AIC</b>	Akaike information criterion
<b>AOA</b>	acycloxyalkoxy
<b>API</b>	active pharmaceutical ingredient
<b>AQ</b>	absorption quotient
<b>ASA</b>	acetyl salicylic acid
<b>ATP</b>	adenosine triphosphate
<b>AUC</b>	area under the curve
<b>AZT</b>	azidothymidine
<b>BCRP</b>	breast cancer-resistance protein
<b>BCS</b>	Biopharmaceutics Classification System
<b>BDDCS</b>	Biopharmaceutics Drug Disposition Classification System
<b>BHPH</b>	bis-(p-hydroxyphenyl)-pyridyl-2-methane
<b>BSA</b>	bovin serum albumin
<b>BSEP</b>	bile salt export pump
<b>CA</b>	coumarinic acid
<b>CAT</b>	compartmental transit and absorption
<b>Caco-2</b>	human colon carcinoma cells
<b>CBER</b>	Center for Biologics Evaluation and Research
<b>CCK</b>	cholecystokinin
<b>CD</b>	candidate drug
<b>CDER</b>	Center for Drug Evaluation and Research
<b>CHN</b>	carbon hydrogen nitrogen
<b>CHO</b>	Chinese hamster ovary
<b>CL</b>	clearance



<b>CNS</b>	central nervous system
<b>CNT</b>	concentrative nucleoside transporter
<b>CV</b>	coefficient of variation
<b>CYP</b>	cytochrome P
<b>DMPK</b>	drug metabolism and pharmacokinetic
<b>DMSO</b>	dimethylsulfoxide
<b>DSC</b>	differential scanning calorimetry
<b>DVS</b>	dynamic vapour sorption
<b>EC</b>	enzyme classification
<b>EMA</b>	European Medicines Agency
<b>ENT</b>	equilibrative nucleoside transporter
<b>ER</b>	efflux ratio
<b>FA</b>	fraction absorbed
<b>FaSSGF</b>	fasted-state simulated gastric fluid
<b>FaSSIF</b>	fasted-state simulated intestinal fluid
<b>FBP</b>	folate-binding protein
<b>FDA</b>	Food and Drug Administration
<b>FeSSGF</b>	fed-state simulated gastric fluid
<b>FeSSIF</b>	fed-state simulated intestinal fluid
<b>FIP</b>	International Pharmaceutical Federation
<b>5-FU</b>	5-fluorouracil
<b>GABA</b>	$\gamma$ -aminobutyric acid
<b>GI</b>	gastrointestinal
<b>GITS</b>	gastrointestinal therapeutic system
<b>GLUT</b>	glucose transporter
<b>GO</b>	Gene Ontology
<b>GSE</b>	general solubility equation
<b>GST</b>	glutathione-S-transferase
<b>HAT</b>	heteromeric amino acid transporter
<b>HGNC</b>	Human Genome Nomenclature Committee
<b>HMIT</b>	H <sup>+</sup> - <i>myo</i> -inositol
<b>HMM</b>	hidden Markov model
<b>HPLC</b>	high-performance liquid chromatography
<b>HSA</b>	human serum albumin
<b>HTS</b>	high-throughput screening
<b>HUGO</b>	Human Genome Organization

<b>IAMS</b>	immobilised phospholipids onto a silica surface
<b>IC<sub>50</sub></b>	concentration at 50% inhibition
<b>IF</b>	intrinsic factor
<b>IR</b>	immediate release
<b>IUBMB</b>	International Union of Biochemistry and Molecular Biology
<b>iv</b>	intravenous
<b>IVIVC</b>	<i>in vitro</i> – <i>in vivo</i> correlation
<b>LC</b>	liquid chromatography
<b>LG</b>	lead generation
<b>LO</b>	lead optimisation
<b>MCT</b>	monocarboxylate transporter
<b>MDCK</b>	Madin–Derby canine kidney (cells)
<b>MDR</b>	multidrug-resistant/multidrug resistance
<b>MHD</b>	10-hydroxy-carbazepine
<b>MMC</b>	migrating motor complex
<b>MPA</b>	mycophenolatic acid
<b>MRP</b>	multidrug-resistance-associated protein
<b>MS</b>	mass spectroscopy
<b>MW</b>	molecular weight
<b>NHE</b>	Na <sup>+</sup> /H <sup>+</sup> exchanger
<b>OAT</b>	organic anion transporter
<b>OATP</b>	organic anion-transporting polypeptide
<b>OB</b>	oral bioavailability
<b>OCT</b>	organic cation transporter
<b>OF</b>	objective function
<b>OMCA</b>	oxymethyl-modified coumarinic acid
<b>PAMPA</b>	parallel intraluminal permeability approach
<b>PCA</b>	principal component analysis
<b>PEG</b>	polyethylene glycol
<b>P-gp</b>	P-glycoprotein
<b>Ph Eur</b>	<i>European Pharmacopoeia</i>
<b>Pi</b>	inorganic phosphate
<b>PLS</b>	partial least squares
<b>po</b>	oral
<b>POT</b>	proton-dependent oligopeptide transporter
<b>PSA</b>	polar surface area

<b>QSAR</b>	quantitative structure–activity relationship
<b>QSPR</b>	quantitative structure–property relationship
<b>RBC</b>	red blood cell
<b>RFT</b>	reduced folate transporter
<b>RP-HPLC</b>	reverse-phase HPLC
<b>SAR</b>	structure–activity relationship
<b>SLC</b>	solute carrier
<b>SLS</b>	sodium lauryl sulphate
<b>SMCT</b>	sodium-coupled monocarboxylate transporter
<b>SMVT</b>	sodium-coupled multivitamin transporter
<b>SNP</b>	single nucleotide polymorphism
<b>SPAN</b>	sorbitan ester
<b>SQ</b>	secretion quotient
<b>SULT</b>	sulphotransferase
<b>TC</b>	transporter classification
<b>TCDB</b>	transporter classification database
<b>TEER</b>	transepithelial electrical resistance
<b>TGA</b>	thermogravimetric analysis
<b>ThT</b>	thiamine transporter
<b>TI</b>	target identification
<b>TMS</b>	transmembrane segment
<b>TS</b>	transition state
<b>UGT</b>	uridine diphosphate glucuronosyl transferase
<b>UIR</b>	unit impulse response
<b>UR</b>	uptake ratio
<b>USP</b>	<i>US Pharmacopoeia</i>
<b>UV</b>	ultraviolet
<b>wt</b>	wild-type
<b>XPRD</b>	X-ray powder diffraction

# Part 1

## Introduction

*Bente Steffansen, Carsten Uhd Nielsen and Birger Brodin*

### 1.1 Molecular biopharmaceutics

The goal of the present book is to describe aspects of molecular biopharmaceutics related to drug characterisation, drug delivery and dosage form evaluation of small active pharmaceutical ingredients.

Although molecular biopharmaceutics is a complex and developing academic scientific area, it is relevant to both industrial preformulation, formulation and preclinical scientists as well as chemical assessors within regulatory affairs. This book is primarily aimed at biopharmaceutical scholars and scientists within academia. However, we believe that employees in industrial pharmaceutical development as well as chemical assessors in pharmaceutical regulatory affairs may find the book valuable.

### 1.2 Important definitions and terms

*Bioavailability* is defined in this book as the rate and extent to which an active substance or moiety is absorbed from the pharmaceutical dosage form, and becomes available at its site of action (Food and Drug Administration (FDA), 2000; European Medicines Agency (EMA), 2001).

*Leads* are defined as a series of structurally related chemical compounds that have shown interesting pharmacological activity and from which drug candidates may be selected. *Drug candidates* are defined as pharmacologically active compounds undergoing evaluation of their potential as future drug substances. *Drug substances* are defined as active ingredients within a dosage form. A drug candidate/substrate is together named as an *active pharmaceutical ingredient (API)*. A drug substance is,

however, first accepted as such when it is registered within a dosage form in a single country such as Japan, or in regions such as Europe or USA, according to respective national Japanese, central European or US regulations. Thus a drug substance is the API within a drug product which is registered as a specific dosage form. The final dosage form is defined as the *drug product*. The European and US regulations are administered by the EMEA and by the FDA respectively.

### **1.3 Experimental methods within molecular biopharmaceutics**

Molecular biopharmaceutics encompasses the field of characterising, describing, evaluating, optimising and predicting bioavailability, and methods applied in this field are described in the book.

Experimental methods applied within molecular biopharmaceutics were initially taken primarily from physical chemistry and physiology but related to aspects of interest for studying steps of importance for bioavailability, namely drug absorption, distribution, metabolism and elimination (ADME). Thus, physicochemical and physiological phenomena, for example acid/base properties, solubility, partition, stability and permeability within physiologically relevant environments, and of relevance for ADME, are studied. Biochemical and molecular biology methods have also been employed over recent years to study ADME phenomena such as absorptive, metabolic, distributive and eliminative pathways as well as expression of endogenous enzymes and transporters of relevance to ADME. Thus, modern molecular biopharmaceutical science is interdisciplinary and methods applied in the field are also applied and relevant to industrial preclinical and (pre)formulation drug development. Regulatory authorities are focused on requiring not only experimental documentation based on physicochemical methods, such as dissolution and permeability studies, but also documentation based on biochemical and molecular biology methods. An example is studies of drug interactions with enzymes and membrane transporters (FDA, 2006; EMEA, 2008).

### **1.4 Classification of drug substances**

Drug substances may be classified according to pharmacological or chemical properties or to routes of administration. Examples are the classifications ‘antidepressive’, ‘steroid’ or ‘ocular’ drug substances. However,

drug substances may also be characterised by their biopharmaceutical properties, for example based on physicochemical parameters of importance for ADME such as those described by Lipinski's rule of five (Chapter 2.4) or by the Biopharmaceutics Classification System (BCS). Recently, classification of drug substances, in the Biopharmaceutical Drug Disposition Classification System (BDDCS), has also been based on biochemical pathways such as metabolism and elimination pathways, as well as on substrate properties in relation to absorptive and/or exsorsptive membrane transporters (Chapter 4.2).

These classification systems thus organise drug substances into categories with related properties, in contrast to the *European Pharmacopoeia* (Ph Eur, 2009) and the *US Pharmacopoeia* (USP, 2009) which simply organise drug substances by alphabetical order.

## 1.5 The book chapters

This book is divided into three main Parts – Parts 2, 3 and 4. In Part 2, methods of importance for physicochemical characterisation of drug substances and candidates are described. Chapter 2.1 focuses on how acid/base, solubility, lipophilicity and solid state properties of (pro)drug candidates and substances may be characterised. Chapters 2.2 and 2.3 respectively examine mechanisms and kinetics of drug decomposition. In Chapter 2.4, examples of chemical approaches to improving bioavailability are described and Chapter 2.5 presents examples of how physicochemical methods may be applied in industrial preformulation.

Part 3 concerns how membrane transport is studied. The first Chapter, 3.1, describes the structure and function of absorptive barriers. This is followed by Chapter 3.2, which examines the kinetics of passive diffusion-driven flux and permeability; next, Chapter 3.3 discusses the kinetics of carrier-mediated flux and permeability. Classification of human transporters is described in Chapter 3.4 and absorptive and efflux transporters are respectively described in Chapters 3.5 and 3.6. The last chapter, 3.7, gives examples of how transport studies are used in preclinical evaluation.

Part 4 presents ways in which bioavailability may be described and predicted from various molecular biopharmaceutical studies. Chapter 4.1 concerns how *in vitro* dissolution is studied and how it may be applied to predict bioavailability. Chapter 4.2 describes how BCS and BDDCS may be applied in the industrial pharmaceutical development process to predict bioavailability, and examines molecular biopharmaceutical methods of importance in this process. Part 4 ends with Chapter 4.3, which

describes and reviews how biosimulation of drug absorption may be applied in predicting bioavailability.

Enjoy!

## References

- EMA Committee for Proprietary Medicinal Products (2001). *Note for Guidance on the Investigation of Bioavailability and Bioequivalence*. <http://www.emea.europa.eu/pdfs/human/qwp/140198en.pdf> (accessed 28 April 2009).
- EMA Committee for Medicinal Products Human Use (CHMP) (2008). *Concept Paper/Recommendation on the Need for Revision of (CHMP) Note for Guidance on the Investigation of Drug Interactions*. <http://www.emea.europa.eu/pdfs/human/ewp/29793108en.pdf> (accessed April 29 2009).
- European Pharmacopoeia*, 6th edn (2009). <http://online6.edqm.eu/ep604/> (accessed 28 April 2009).
- FDA, Center for Drug Evaluation and Research (2000). *Guidance for Industry, Waiver of in vivo Bioavailability and Bioequivalence Studies for Immediate-release Solid Oral Dosage Forms Based on a Biopharmaceutics Classification System*. <http://www.fda.gov/downloads/Drugs/GuidanceComplianceRegulatoryInformation/Guidances/UCM070246.pdf> (accessed 2 June 2009).
- FDA, Center for Drug Evaluation and Research and Center for Biologic Evaluation and Research (2006). *Guidance for Industry, Drug Interaction Studies, Study Design, Data Analysis, and Implications for Dosing and Labeling*. <http://www.fda.gov/cder/guidance/6695dft.pdf> (accessed 29 April 2009).
- US Pharmacopoeia (2009). <http://www.usp.org/> (accessed 28 April 2009).

## Part 2

### Physicochemical characterisation of drug candidates

2.1	Acid/base properties, solubility and distribution of drug candidates	7
2.2	Mechanisms of decomposition of drug candidates	35
2.3	Kinetics of decomposition in aqueous solution	51
2.4	Chemical approaches to improving bioavailability properties of oral drug candidates	71
2.5	Preformulation in the industry step by step	101

The aim of Part 2 is to provide an overview of physicochemical characterisation of (pro)drug candidates/substances. Physicochemical characterisation of compounds is part of molecular biopharmaceutics and is typically encompassed in preformulation and preclinical development in the pharmaceutical industry. Thus physicochemical properties of (pro) drug candidates and substances are important issues in optimal drug delivery, i.e. the design of optimal formulations containing optimal bioavailable drug substances.

In Chapter 2.1, acid/base properties, solubility, lipophilicity and solid-state properties are described, focusing on theory and methods applied to characterise (pro)drug candidates and substances.

In Chapter 2.2 mechanisms of decomposition of (pro)drug candidates and substances are described. The chapter focuses on describing the most relevant mechanisms affecting drug stability, such as hydrolysis, oxidation and photolytic degradation, and how these mechanisms may be influenced by external factors such as water, oxygen and light.



In Chapter 2.3, the kinetics of decomposition of (pro)drug candidates and substances in aqueous solution, including biofluids, are described. The chapter focuses on describing reaction kinetics of zero, first and second order and how these may be applied in characterising (pro)drug candidates and substances. Furthermore, the chapter examines how kinetic parameters such as rate constant, half lives, and shelf lives are applied to document stability (European Medicines Agency (EMA), 2006). Finally, the chapter describes how these kinetic parameters may be influenced by various factors such as pH, temperature, ions, buffers and enzymes.

In Chapter 2.4, examples of chemical approaches to improving the bioavailability properties of oral drug candidates are described. The chapter describes Lipinski's rule of five, and how it may be applied in selecting chemical strategies to optimise the bioavailability of (pro)drug candidates and substances (Lipinski *et al.*, 2001). Approaches such as salt formation, chemical stabilisation of peptides, and prodrug strategies are described. The chapter includes examples of salts used to optimise bioavailability and pharmaceutical formulation. An overview of intestinal peptidases relevant to stabilising peptide and protein drug candidates is presented, as well as examples of prodrug candidates registered in the EU.

In Chapter 2.5, industrial preformulation is described step by step. The chapter gives an industrial perspective on how drug candidates are evaluated in terms of physicochemical characterisation. The chapter focuses on examining to what extent characterisation takes place in the various stages of drug development.

## References

- EMA (2006). *Note for Guidance on Stability Testing: stability testing of new drug substance and products* (CPMP/ICH/2736/99). <http://www.ema.europa.eu/pdfs/human/ich/273699en.pdf> (accessed 29 April 2009).
- Lipinski CA, Lombardo F, Dominy BW, Feeney PJ (2001). Experimental and computational approaches to estimate solubility and permeability in drug discovery and development settings. *Adv Drug Deliv Rev* 46: 3–26.

# 2.1

## Acid/base properties, solubility and distribution of drug candidates

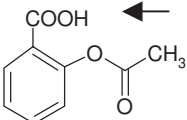
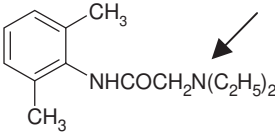
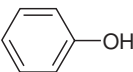
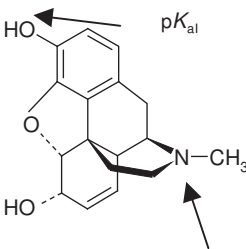
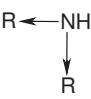
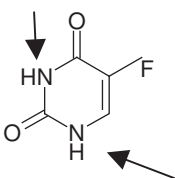
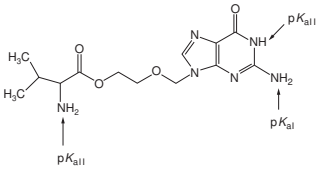
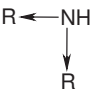
*Bente Steffansen, Carsten Uhd Nielsen and Birger Brodin*

Physicochemical properties of drug candidates, such as acid/base properties, which are characterised by the ionisation/acidity constant ( $K_a$ ), aqueous solubility ( $S$ ) and partition ( $P$ ) and distribution ( $D$ ) between two immiscible phases (often  $n$ -octanol and water), as well as solid-state characteristics, are fundamental properties used in the sciences of biopharmaceutical and pharmaceutical chemistry. Furthermore, physicochemical characterisation of drug candidates is essential for industrial preformulation and for the preclinical development selection process of drug candidates. For solute acidic and basic drug candidates,  $S$  and  $D$  are generally dependent on the concentration of protons  $[H^+]$ .  $K_a$ ,  $S$ ,  $P$ ,  $D$  and  $[H^+]$  are often very large or very small numbers. Thus, for convenience, they may be expressed in logarithmic terms by  $-\log K_a = pK_a$ ,  $\log S$ ,  $\log P$ ,  $\log D$ , and  $-\log[H^+] = pH$  respectively. The aim of this chapter is to introduce the theory and some methods that are used to characterise drug candidates with regard to their molecular acid/base properties, molecular solubility, molecular partition and distribution between two immiscible phases, as well as their solid-state characterisation.

### 2.1.1 Acid/base properties of drug candidates

Lewis describes an acid as an electron pair acceptor and a base as an electron pair donor (Lewis, 1923). Conjugated Lewis acid and base pairs may therefore not necessarily involve proton transfer. However, Brøndsted–Lowry defines an acid as any substance that can ionise in aqueous solution to create a solvated hydrogen ion, i.e. an oxonium ion ( $H_3O^+$ ).  $H_3O^+$  is often abbreviated  $H^+$ . Thus, a Brøndsted–Lowry acid is a proton donor and a Brøndsted–Lowry base a proton acceptor. The ionisation process always involves the two, which are known as conjugated acid–base pairs (Brøndsted, 1923). The  $pK_a$  functional groups of selected (pro)drug substances are shown in Table 2.1.1.

**Table 2.1.1**  $pK_a$  functional groups of selected (pro)drug substances

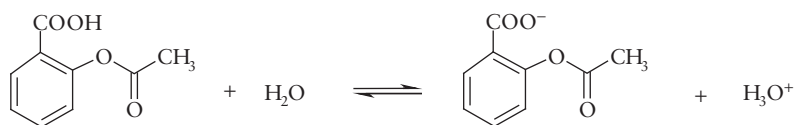
$pK_a$ functional groups	Structures of selected drug substance	$pK_a$
RCOOH		
Carboxylic acid	ASA	$pK_{aI} = 3.5$
$R_2-NH$		
Secondary amine	Lidocaine	$pK_{aI} = 7.84$
		
Phenol		$pK_{aI} = 8.17$
$R_3N$		
Tertiary amine	Morphine	$pK_{aII} = 9.26$
		
NH-acidic		$pK_{aI} = 8.0$
	5-Fluorouracil	$pK_{aII} \approx 13$
$R-NH_2$		
Primary amine (aciclovir)		$pK_{aI} = 2.0$
$R-NH_2$		
Primary amine (valine)	Valaciclovir	$pK_{aII} = 7.2$
NH-acidic (amide)		
		
		$pK_{aIII} = 9.1$

Notes: Arrows in the NH-acidic structure indicate the direction of electron-withdrawing effect, whereas arrows in the drug substance structures point at  $pK_a$  functional groups.

In this chapter, the focus is on drug candidates that are Brønsted–Lowry acids or bases, in which pH-dependent proton transfer takes place. This proton transfer can be determined by the ionisation/acidity constant,  $K_a$ , for the ionisation process.

### 2.1.1.1 Drug candidates with acid properties

For a monoprotic acid, i.e. an acid containing only one replaceable hydrogen atom per molecule such as the drug substance acetyl salicylic acid (ASA), the ionisation process takes place as illustrated in Scheme 2.1.1. Here the proton-donating acidic neutral species of ASA is represented together with water on the left side of the arrows, and the proton-accepting basic ionised species of ASA is represented together with the oxonium ion on the right side of the arrow.



Neutral species of ASA + water

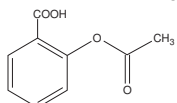
Charged species of ASA + oxonium ion

(Scheme 2.1.1)

The equation for calculating the ionisation/acidity constant  $K_a$  of the monoprotic ASA in dilute solution is given in Equation 2.1.1:

$$K_a = \frac{[\text{RCOO}^-][\text{H}^+]}{[\text{RCOOH}]} \quad (2.1.1)$$

in which  $\text{H}_3\text{O}^+$  is shortened to  $\text{H}^+$  for monoprotic acids and



to  $\text{RCOOH}$ , and in which  $[\text{RCOO}^-]$ ,  $[\text{RCOOH}]$  and

$[\text{H}^+]$  represent concentrations of ionised species, neutral species and protons involved in the process, respectively. If drug substances are not in dilute solution, concentrations should be substituted by activities, which are difficult to measure. Thus, for practical reasons  $K_a$  is generally determined in dilute aqueous solution. This is the reason why concentrations rather than activities will be used in the present chapter, assuming that experiments take place in dilute aqueous solution. Therefore,  $[\text{RCOOH}]$  can be described by Equation 2.1.2:

$$[\text{RCOOH}] = \frac{[\text{RCOO}^-][\text{H}^+]}{K_a} \quad (2.1.2)$$

The total concentration of drug candidate  $[R]_T$  can be described as the sum of species, as is apparent from Equation 2.1.3:

$$[R]_T = [\text{RCOOH}] + [\text{RCOO}^-] \quad (2.1.3)$$

According to Equation 2.1.3 it is possible to calculate the neutral species fraction  $f_{\text{RCOOH}}$  by Equation 2.1.4:

$$f_{\text{RCOOH}} = \frac{[\text{RCOOH}]}{[\text{RCOOH}] + [\text{RCOO}^-]} \quad (2.1.4)$$

So, by combining Equations 2.1.2 and 2.1.3, Equation 2.1.5 arises. Thus, the neutral species fraction  $f_{\text{RCOOH}}$  of any monoprotic drug candidate that is an acid may be calculated from  $[\text{H}^+]$  and  $K_a$ , i.e. pH and  $\text{p}K_a$  respectively, using Equation 2.1.5:

$$f_{\text{RCOOH}} = \frac{[\text{H}^+]}{[\text{H}^+] + K_a} \quad (2.1.5)$$

According to Equation 2.1.1, the  $-\log K_a$  ( $\text{p}K_a$ ) for monoprotic acids is defined as the pH value at which 50% of the compound is protonated  $[\text{RCOOH}]$  and 50% is deprotonated  $[\text{RCOO}^-]$ . Thus for monoprotic acids,  $K_a$  may be determined once the species distribution at a given pH is known. This is described for ASA and monoprotic acids in general by Equations 2.1.6 and 2.1.7 respectively.

$$\text{p}K_a = \text{pH} + \log \frac{\left[ \text{Chemical structure of ASA (protonated)} \right]}{\left[ \text{Chemical structure of ASA (deprotonated)} \right]} \quad (2.1.6)$$

$$\text{p}K_a = \text{pH} + \log \frac{[\text{RCOOH}]}{[\text{RCOO}^-]} \quad (2.1.7)$$

Equation 2.1.7 is easily transformed into the well-known Henderson-Hasselbalch equation (Hasselbalch, 1916) as shown in Equation 2.1.8:

$$\text{pH} = \text{p}K_a + \log \frac{[\text{RCOO}^-]}{[\text{RCOOH}]} \quad (2.1.8)$$

Once the  $pK_a$  values are known, the Henderson–Hasselbalch equation may be used to calculate the ratio between ionised and neutral species at a given pH of any drug candidate or excipient that is a monoprotic acid.

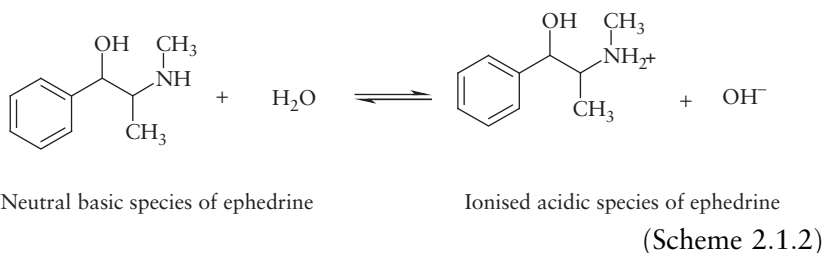
Similarly, the ionised species fraction  $f_{RCOO^-}$  for drug candidates that are monoprotic acids may be calculated by Equation 2.1.9.

$$f_{RCOO^-} = \frac{K_a}{[H^+] + K_a} \quad (2.1.9)$$

Thus, an acidic drug candidate, i.e. a monoprotic acid such as ASA, with a  $pK_a$  value of approximately 3.5 will primarily be represented by its neutral species in gastric juice at pH 1–3, whereas it will be primarily represented by its ionised species in intestinal fluids at pH 5.5–8 and in blood at pH 7.4. The pH of relevant physiologic media and the absorption area at which the biological media are represented are shown in Table 2.1.2.

### 2.1.1.2 Drug candidates with base properties

For a monoprotic base such as ephedrine (see the illustration in Scheme 2.1.2), i.e. a base accepting one  $H^+$  per molecule, the ionisation/base constant  $K_b$  for the ionisation process in aqueous solution can be described by Equation 2.1.10:

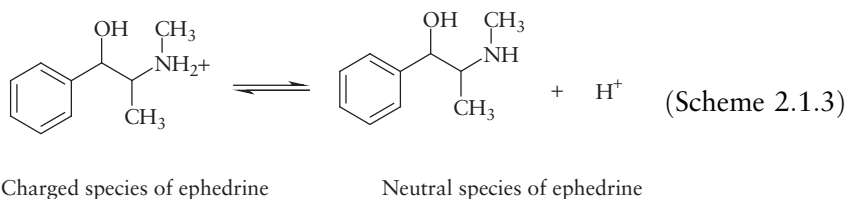


$$K_b = \frac{[RH^+][OH^-]}{[R]} \quad (2.1.10)$$

However, in preformulation and preclinical development,  $K_a$  rather than  $K_b$  values are determined. Thereby,  $K_a$  values are generally used to describe ionisation properties of both acidic and basic drug candidates. As  $pK_a + pK_b = pK_w$ , where  $pK_w$  is the ionisation product for water, i.e. 14.00 at 25 °C, it is easy to transform  $pK_b$  into  $pK_a$  values and vice

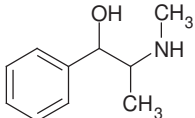
versa. If the  $pK_b$  of ephedrine is determined to be 4.35 at 25 °C, it transforms into a  $pK_a$  for ephedrine of 9.65.

Thus, the ionisation process of ephedrine may alternatively take place as illustrated in Scheme 2.1.3, in which it is implied that ionisation takes place in dilute aqueous solution:



The  $K_a$  for the monoprotic base ephedrine and for monoprotic bases in general may be calculated by Equation 2.1.11,

$$K_a = \frac{[R_3N][H^+]}{[R_3NH^+]} \quad (2.1.11)$$

in which  is shortened to  $R_3N$ . Fractions of neutral and ionised species of drug candidates that are monoprotic bases can be calculated by Equations 2.1.12 and 2.1.13 respectively.

$$f_{R_3N} = \frac{K_a}{[H^+] + K_a} \quad (2.1.12)$$

$$f_{R_3NH^+} = \frac{[H^+]}{[H^+] + K_a} \quad (2.1.13)$$

Thus, a monoprotic base such as ephedrine with a  $pK_a$  value of approximately 9.6 may be primarily represented by its ionised species in both gastric juice and intestinal fluid, as well as blood (see Table 2.1.2).

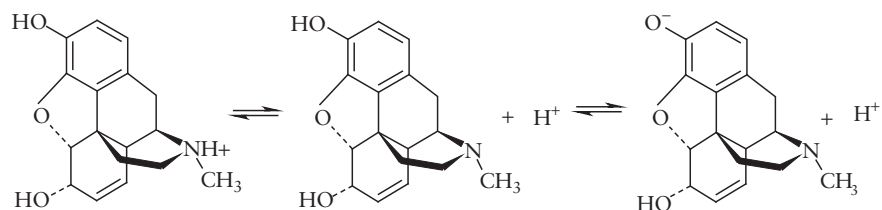
### 2.1.1.3 Amphiphilic drug candidates

For a drug substance that has two acid/base functionalities, and therefore two  $pK_a$  values, such as morphine ( $pK_{aI}=8.17$ ;  $pK_{aII}=9.26$ ), the

**Table 2.1.2** pH in various biological media together with surface area at which the biological media is represented (Wilson, 1967; Newton and Kluza, 1978; Madara, 1991; Dressman *et al.*, 1993; Gray and Dressman, 1996; Kutchai, 1996; Charman *et al.*, 1997; Dressman *et al.*, 1998; Avdeef, 2001)

<i>Biological fluid</i>	<i>pH</i>	<i>Absorption area (m<sup>2</sup>)</i>
Salivary fluid	6.4	–
Gastric juice	1–2.1 (fasted) 5.0 (0–0.1 h after eating)	0.11
Pancreatic juice	7.9–8.4	–
Duodenal fluid	2.4–6.8	60
Jejunal fluid	5.8–6.2 (fasted) 4.5–5.5 (0–1 h after eating)	60
Ileal fluid	6.5–8.0	60
Colonic fluid	5.0–8.0	0.25
Blood	7.40 (arterial) 7.39 (venous)	–
Cerebrospinal fluid	7.35	–
Urine	5.7 (male) 5.8 (female)	–
Lachrymal fluid (tears)	7.4	–
Aqueous humour fluid	7.21	–

ionisation process takes place as illustrated in Scheme 2.1.4, in which it is implied that the ionisation takes place in dilute aqueous solution:



Morphine

Acidic positive charged species

Ampholytic neutral species

Basic negative ionised species

(Scheme 2.1.4)

Morphine is an ampholyte with a basic  $pK_{aI}$  of 8.17 and an acidic phenolic  $pK_{aII}$  of 9.26.



Once the pH, the  $pK_a$  values,  $[H^+]$  and the  $K_a$  values are known, the various species fractions of the acidic, ampholytic and basic species may be calculated by Equations 2.1.14, 2.1.15 and 2.1.16 respectively.

$$f_{\text{acid}} = \frac{[H^+]^2}{[H^+]^2 + K_{\text{al}}[H^+] + K_{\text{al}}K_{\text{all}}} \quad (2.1.14)$$

$$f_{\text{ampholyte}} = \frac{[H^+]K_{\text{al}}}{[H^+]^2 + K_{\text{al}}[H^+] + K_{\text{al}}K_{\text{all}}} \quad (2.1.15)$$

$$f_{\text{base}} = \frac{K_{\text{al}}K_{\text{all}}}{[H^+]^2 + K_{\text{al}}[H^+] + K_{\text{al}}K_{\text{all}}} \quad (2.1.16)$$

#### 2.1.1.4 $pK_a$ values determined by pH metric titration

For experimental determination of  $pK_a$  values of drug candidates, it is necessary to expose the molecule to an environment with a changing pH. This may be investigated by monitoring a specific species-dependent property of the drug candidates, such as species-dependent conductivity, solubility, potential, or absorbance (Albert and Serjeant, 1984). Potentiometric or pH metric titration is the method most often used to determine  $pK_a$  values. Therefore, this method will be described next.

In pH metric titrations, known values of a precisely standardised strong acid (typically HCl) or base (typically KOH) are added to a solution of a proteogenic drug candidate, during which pH is continuously measured with a hydrogen-sensitive electrode. Titrations using acid or base titrants, as described above, are called acidimetric and alkalimetric titrations respectively. The drug candidate being assayed should be dissolved in water or in water:methanol mixtures, i.e. by the Yasuda-Shedlowski technique, which is described in more detail later.

It is possible to measure precise and accurate  $pK_a$  values in aqueous dilute solution by pH metric titration under controlled conditions, i.e. in a well-stirred system where the temperature and apparent ionic strength are kept constant and where correction for the content of  $CO_2$ , which is dissolved in the base titrant, is performed. The  $pK_a$  values are dependent on ionic strength within the solution. Because ionic strength may change during titration, due to variations in species distribution of the drug candidate, the ionic strength within the solution should be kept at a relatively high concentration compared to the ionic strength arising

from the drug candidate, which varies during titration depending on its ionisation state. An ionic strength of approximately 0.16M KCl, which corresponds to an isotonic solution, is therefore often used in preformulation and preclinical evaluation of drug candidates.

Graphical presentation of the pH metric titration is performed well by a Bjerrum difference plot (Bjerrum, 1941). In these plots, titrant volumes are recalculated to the average number of bound protons per drug candidate molecule ( $\bar{n}_H$ ), which is then plotted versus the pH. Such a plot can be obtained by subtracting a titration curve containing no drug candidate (blank titration) from a titration curve with a known drug candidate concentration.

A Bjerrum difference plot for the monoprotic base ephedrine is shown in Figure 2.1.1. The Bjerrum plot of ephedrine shows that each ephedrine molecule loses one proton in the pH range of 8.5 to 11. It is seen that for pH values below approximately 8.5, the average number of bound protons per molecule of ephedrine  $\bar{n}_H$  is 1, whereas zero protons are bound to ephedrine for pH values above approximately 10.8.

Furthermore, it is apparent from Figure 2.1.1. that the  $pK_a$  of ephedrine is approximately 9.5.

A Bjerrum difference plot may be transformed into plots of pH versus % species distribution, when species distribution is correlated to proton release. Theoretically, % species distribution of a basic drug substance such as ephedrine is easily calculated from the species fraction, as indicated in Equations 2.1.12 and 2.1.13, by multiplying the fractions by 100.

Amine and phenol functionalities of buprenorphine are characterised by  $pK_a$  values that are determined to be 8.3 and 9.6 respectively. The ionisation process of buprenorphine is shown in Scheme 2.1.5.

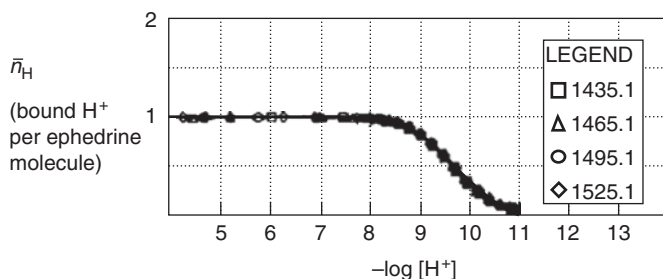
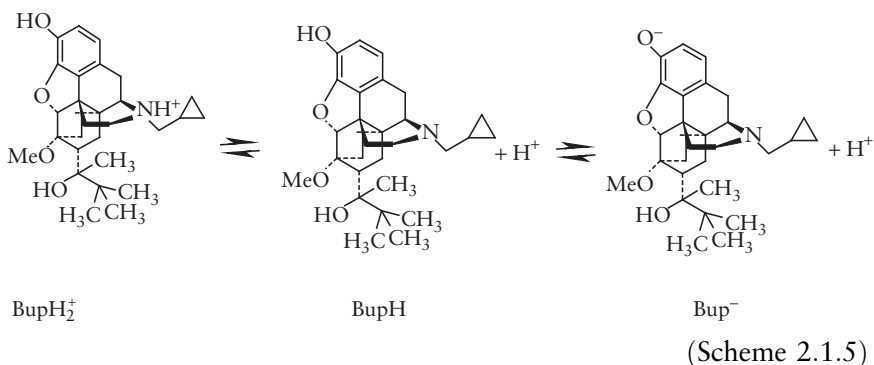


**Figure 2.1.1** Bjerrum difference plot of ephedrine. Average number of bound protons per molecule of ephedrine ( $\bar{n}_H$ ) versus pH.



A species distribution curve of buprenorphine as a function of pH is shown in Figure 2.1.2. Theoretically, % species distribution of the ampholyte buprenorphine can easily be calculated from the species fraction indicated in Equations 2.1.14, 2.1.15 and 2.1.16, by multiplying the fractions by 100. Thus, at a pH lower than 10 the positively charged species of buprenorphine ( $\text{BupH}_2^+$ ) is represented. At a pH interval between 6 and 11, the neutral ampholytic species of buprenorphine ( $\text{BupH}$ ) is represented, whereas the negatively charged species of buprenorphine ( $\text{Bup}^-$ ), is represented at pH values higher than 8.

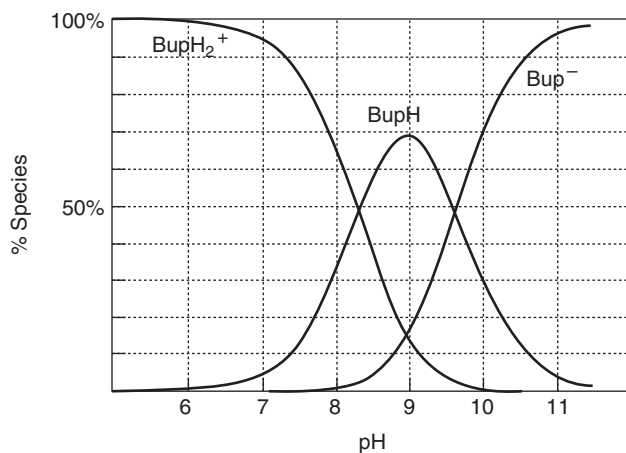


**Figure 2.1.2** Species distribution of buprenorphine as a function of pH, protonated positive species ( $\text{BupH}_2^+$ ), neutral species ( $\text{BupH}$ ) and negative species ( $\text{Bup}^-$ ) of buprenorphine. Reproduced from *Sirius Technical Application Notes Volume 1* (1994). Riverside: Sirius Analytical Instruments Ltd.

From Figure 2.1.2 it is apparent that at an intestinal fluid pH of 6–9, all three species of buprenorphine will be present. This is convenient for its solubility in intestinal fluid and permeability across the intestinal membrane. This is explained by the pH-partition hypothesis in which it is described that a neutral species has better diffusional permeability across the intestinal membrane than an ionised species, but an ionised species has better solubility in aqueous intestinal fluid than a neutral species. Diffusional permeability is further described in Chapter 3.1 and the pH-partition hypothesis in Section 2.1.3 and by Shore *et al.* (1957) and Neuhoff *et al.* (2005).

For drug candidates with low aqueous solubility, which may play a part during titration, the Yasuda–Shedlowski technique can be used to estimate the  $pK_a$ . With this technique, the linear relationship between, for example, methanol content in the titration media (0–60% methanol content) and apparent  $pK_a$  values, i.e.  $p_oK_a$  values, are determined to estimate true aqueous  $pK_a$  values (Shedlovski, 1962; Takács-Novák *et al.*, 1997). The  $p_oK_a$  values for ASA and ephedrine are shown in Table 2.1.3. As is apparent from this table, the  $p_oK_a$  for ASA increases and the  $p_oK_a$  for ephedrine decreases with increasing methanol content in the titration media. The increase in  $p_oK_a$  for ASA with increased methanol concentration may be explained by methanol lowering the dielectric constant of the titration media. This disfavors the increased ionisation of acids during alkalimetric titration, resulting in an increased  $p_oK_a$  for ASA. The ionisation of ASA is illustrated in Scheme 2.1.1. In contrast, the decreased dielectric constant of the titration medium with increased methanol content favours increased neutralisation of the base ephedrine

**Table 2.1.3** Apparent  $pK_a$  ( $p_oK_a$ ) for ASA and for ephedrine at various methanol concentrations

% Methanol	$p_oK_a$ ASA	$p_oK_a$ ephedrine
0	4.55 <sup>a</sup>	9.46 <sup>a</sup>
10	4.68	9.39
20	4.84	9.32
30	5.02	9.11
40	5.21	9.01
50	5.43	8.92
60	5.67	8.81

Note: <sup>a</sup>Estimated aqueous  $pK_a$  from linear regression of  $p_oK_a$  as function of methanol content.

and thus a decreased  $p_oK_a$  during alkalimetric titration. The neutralisation of ephedrine is illustrated in Scheme 2.1.2.

### 2.1.2 Solubility in aqueous solution

The solubility of drug candidates in aqueous solution is mainly used to investigate its importance for formulating aqueous solutions, e.g. parenteral formulations, and for evaluating the influence of solubility on bio-availability. Consequently, solubility may be investigated in aqueous buffer solutions as well as in various relevant biological media. It is relevant to study drug candidate solubility in biological media as it is observed that generally only dissolved fractions of drug candidates are available for absorption into the blood.

The influence of acid/base and solid-state properties of drug candidates on solubility in aqueous solution is described in this chapter, whereas dissolution methods to describe the solubility rate of drug candidates are described in Chapter 4.1.

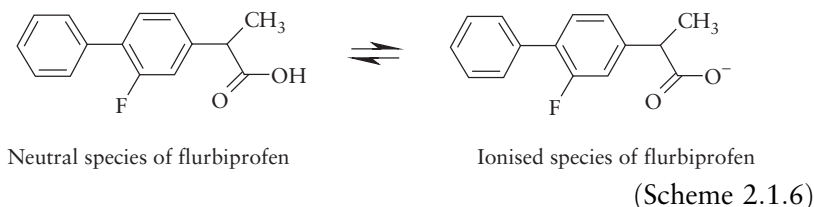
The *European Pharmacopoeia* (Ph Eur, 2009) describes the solubility of drug substances as shown in Table 2.1.4.

Even though ionised species generally dissolve better than their corresponding neutral species, the solubility terms described in Ph Eur do not take species-dependent solubility into consideration. Thus, the solubility is simply determined in aqueous solution without considering what the pH of the aqueous solution may change to during the experiment, i.e. after addition of a drug candidate. The Ph Eur solubility terms are good first estimations of the aqueous solubility of drug candidates and may be used in the initial selection process. This process is used to determine whether the solubility of the drug candidate may be limited for

**Table 2.1.4** Descriptive terms of drug substrate solubility according to Ph Eur

<i>Ph Eur descriptive term</i>	<i>Solubility (mg ml<sup>-1</sup>)</i>
Very soluble	>1000
Freely soluble	100–1000
Soluble	33–100
Sparingly soluble	10–33
Slightly soluble	1–10
Very slightly soluble	0.1–1
Practically insoluble	<0.1

choice of dosage form and permeability across biological membranes. However, the aqueous solubility of compounds that have acid/base properties may be pH dependent because ionised species are generally more soluble in aqueous solution than neutral species. For monoprotic weak acids such as flurbiprofen ( $\text{RCOOH}$ ), see Scheme 2.1.6, the total apparent solubility of an acid,  $S_T$ , at any pH can be described by Equation 2.1.17.



In Equation 2.1.17,  $S_{\text{RCOOH}}$  and  $S_{\text{RCOO}^-}$  refer to the solubility of the neutral and the ionised species respectively.

$$S_T = S_{\text{RCOOH}} + S_{\text{RCOO}^-} \quad (2.1.17)$$

However, if  $S_{\text{RCOOH}}$  and  $S_{\text{RCOO}^-}$  are considered as the respective concentrations in solution, i.e.  $[\text{RCOOH}]$  and  $[\text{RCOO}^-]$ , Equation 2.1.17 corresponds to Equation 2.1.3. Based on the assumption that  $S_{\text{RCOO}^-}$  is much larger than  $S_{\text{RCOOH}}$ , and by applying Equations 2.1.3 and 2.1.4, it is apparent that  $S_T$  at any pH can be described by Equation 2.1.18.

$$S_T = \frac{[S_{\text{RCOOH}}]}{f_{\text{RCOOH}}} \quad (2.1.18)$$

In Equation 2.1.18,  $f_{\text{RCOOH}}$  is the fraction of neutral species, which may be calculated from Equation 2.1.5 once the pH of the aqueous solution and the  $\text{pK}_a$  of the monoprotic drug candidates are known. Equation 2.1.18 may be described in logarithmic terms by Equation 2.1.19.

$$\log S_T = \log S_{\text{RCOOH}} - \log f_{\text{RCOOH}} \quad (2.1.19)$$

Thus, for drug candidates that are monoprotic acids, one may determine the solubility of the neutral species, which is also called intrinsic solubility ( $S_{\text{RCOOH}}$ ). The intrinsic solubility of a monoprotic acid is experimentally determined in aqueous solution at 2 pH units below its  $\text{pK}_a$ , and then  $S_T$  at any pH may be estimated by Equation 2.1.19.

### 2.1.2.1 Solubility–pH profiles

Solubility–pH profiles of drug candidates with acid/base properties may be fully determined experimentally by titration during which the drug substance precipitates (Avdeef, 1996, 2001).

Bjerrum plots of such titrations may be recalculated into solubility–pH profiles where  $\log S_T$  values are shown as a function of pH. In Figure 2.1.3 the solubility–pH profile of the monoprotic acid flurbiprofen is illustrated.

From the solubility–pH profile of flurbiprofen, it is apparent that the intrinsic solubility of flurbiprofen may be determined below pH 2 and that the solubility increases with ionised species concentration as described by Equation 2.1.19.

For a monoprotic weak base such as lidocaine, the total apparent solubility  $S_T$  can be described by Equation 2.1.20 in which  $S_{R_3NH^+}$ , and  $S_{R_3N}$  refer to the solubility of the neutral and the ionised species respectively.

$$S_T = S_{R_3NH^+} + S_{R_3N} \quad (2.1.20)$$

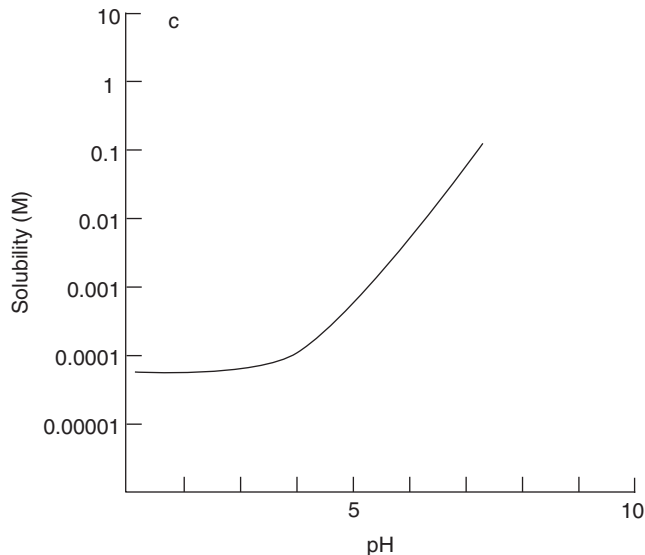
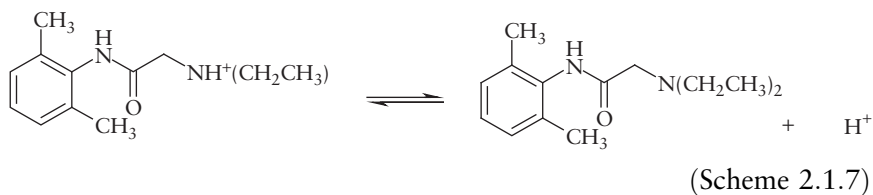


**Figure 2.1.3** Solubility–pH profile of flurbiprofen; the  $pK_a$  was determined to 4.03 ( $\pm 0.04$ ) at 25 °C and ionic strength of KCl at 0.15 M. Reproduced from Avdeef A (1998). pH-metric solubility 1. Solubility–pH profiles from Bjerrum plots. Gibbs buffer and  $pK_a$  in the solid state. *Pharm Pharmacol Commun* 4: 165–178.

The ionisation scheme for lidocaine is illustrated in Scheme 2.1.7.



However, based on the assumption that the solubility of the ionised species shows much larger aqueous solubility than its neutral species, the apparent solubility of monoprotic drug candidates that are bases may be determined at any pH by Equation 2.1.21.

$$\log S_T = \log S_{R_3N} - \log f_{R_3N} \quad (2.1.21)$$

In Equation 2.1.21,  $f_{R_3N}$  is the fraction of the neutral species.  $f_{R_3N}$  may be easily calculated by Equation 2.1.12 once the pH in the aqueous solution and the  $pK_a$  of the drug candidate are known. Thus, for drug candidates that are monoprotic bases one may determine the aqueous solubility of its neutral species, i.e. its intrinsic solubility ( $S_{R_3N}$ ). In practice, this intrinsic solubility is determined in an aqueous solution at 2 pH units above the  $pK_a$  value of the drug candidate. In Table 2.1.5  $S_T$  values of lidocaine as well as  $f_{R_3N}$  at various pH levels are shown. This is estimated by Equation 2.1.21 by using a lidocaine  $pK_a$  of 7.84 at 25 °C and a lidocaine intrinsic solubility of 0.004 g ml<sup>-1</sup>.

In drug discovery it is common to determine aqueous solubility at a single pH value to calculate solubilities at other pH values by

**Table 2.1.5** Lidocaine solubility ( $S_T$ )

pH	$f_{R_3N}$	$S_T$ (g ml <sup>-1</sup> )
5	$1.44 \times 10^{-3}$	2.778
6	$1.42 \times 10^{-2}$	0.282
7	$1.26 \times 10^{-1}$	0.032
8	$5.91 \times 10^{-1}$	0.007
9	$9.35 \times 10^{-1}$	0.004
10	$9.93 \times 10^{-1}$	0.004
11	1.000	0.004

Notes:  $S_T$  at various pH values is estimated from Equation 2.1.21 by using  $S_{R_3N}$  at 0.004 g ml<sup>-1</sup> and  $pK_a$  of 7.84.



Equation 2.1.21 as described above. However, Artursson and co-workers have shown that such calculated solubility values for at least amine drug substances can differ largely from experimental values. The accuracy of the calculated pH-dependent aqueous solubility of 25 cationic drug substances is summarised by Bergström *et al.* (2004).

The total solubility of an amphoteric drug substance such as buprenorphine may be described by Equation 2.1.22:

$$S_T = S_{\text{ampholyte}} + S_{R_3NH^+} + S_{RCOO^-} \quad (2.1.22)$$

in which  $S_{\text{ampholyte}}$ ,  $S_{R_3NH^+}$  and  $S_{RCOO^-}$  are solubilities of neutral, positive and negative species, respectively. Assuming that positive and negative species show infinite solubilities in aqueous solution, the solubility of amphoteric drug candidates may be described by Equation 2.1.23.

$$\log S_T = \log S_{\text{ampholyte}} - \log f_{\text{ampholyte}} \quad (2.1.23)$$

$\log f_{\text{ampholyte}}$  may be calculated by Equation 2.1.15 once the pH of the aqueous solution and the  $pK_a$  values for the amphoteric drug candidate are known.

An experiment-based solubility–pH profile of the diprotic ampholytic drug substance buprenorphine is shown in Figure 2.1.4.

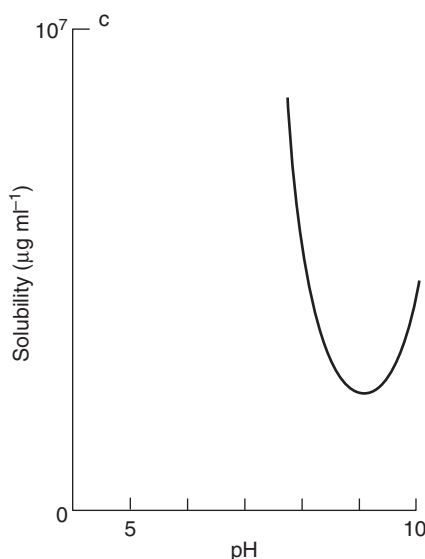


**Figure 2.1.4** Solubility–pH profile of buprenorphine. Reproduced from Avdeef A (1998). pH-metric solubility 1. Solubility–pH profiles from Bjerrum plots. Gibbs buffer and  $pK_a$  in the solid state. *Pharm Pharmacol Commun* 4: 165–178.

From Figures 2.1.2 and 2.1.4 as well as Scheme 2.1.5 it is apparent that the aqueous solubility of buprenorphine is dependent on pH and that the solubility of neutral BupH species is much lower than the solubilities of ionised BupH<sub>2</sub><sup>+</sup> and Bup<sup>−</sup> species. The profile may be theoretically described by Equation 2.1.23.

Apart from the pH-dependent solubility of drug candidates described above, it is equally important to assess the dissolution, i.e. the solubility rate. This is particularly done for evaluating their oral bioavailability. This is because oral drug candidates should be dissolved during intestinal transit, i.e. within 3–6 h, in order to be absorbed into the blood circulation. The solubility rate is assessed through dissolution studies, which are described in detail in Chapter 4.1.

The influence of drug candidate solubility on bioavailability is considered in the Biopharmaceutics Classification System (BCS), introduced by the US Food and Drug Administration (FDA), in which drug substances are classified as low- or high-solubility drug substances, i.e. one dose is respectively dissolved or not in 250 ml water in the pH range 1–8 (FDA, 2000). The BCS is described in detail in Chapter 4.3.

### 2.1.3 Partition properties of drug candidates

The partitioning of a solute drug candidate between two immiscible liquids, often *n*-octanol and aqueous buffer, is often referred to as its partition coefficient (*P*) (Leo *et al.*, 1971). The *P* of a drug candidate is mainly applied to investigate its formulation properties in two-phase formulation, e.g. emulsions, as well as for evaluating its passive diffusional permeability properties across lipophilic biological membranes which is of importance for its bioavailability, see Lipinski's rule of five in Chapter 2.4. For drug candidates with ionisation properties, *P* is normally defined as the partitioning of neutral species between *n*-octanol and aqueous buffer. Thus, *P* is a constant and refers to molecules or species partitioning between two immiscible phases. If volumes of water and organic phases of *V*<sub>w</sub> and *V*<sub>o</sub> respectively are different, this will have an influence on *P*.

The partition coefficient of monoprotic acids and bases is generally related to their neutral species as described by Equations 2.1.24 and 2.1.25.

$$P = \frac{[\text{RCOOH}]_{\text{o}}}{[\text{RCOOH}]_{\text{w}}} \frac{V_{\text{w}}}{V_{\text{o}}} \quad (2.1.24)$$

$$P = \frac{[\text{R}_3\text{N}]_{\text{o}}}{[\text{R}_3\text{N}]_{\text{w}}} \frac{V_{\text{w}}}{V_{\text{o}}} \quad (2.1.25)$$

The distribution coefficient,  $D$ , of drug candidates is related to  $P$  but refers to total species distribution between two immiscible phases, which varies with pH when compounds that can ionise are assessed.  $D = P$  in the pH region where a substance is fully un-ionised. However, the distribution of compounds that can ionise is pH dependent because neutral species are more lipophilic than charged ones. Thus, when the drug substance is fully represented by its neutral species, it is maximally partitioning into the lipid/organic phase. Based on the assumption that the neutral species distribute to a much larger degree into the lipid/organic phase than the ionised species, the  $D$  of monoprotic acids and bases can be expressed by Equations 2.1.26 and 2.1.27 respectively.

$$D_{\text{acid}} = P \times f_{\text{RCOOH}} \quad (2.1.26)$$

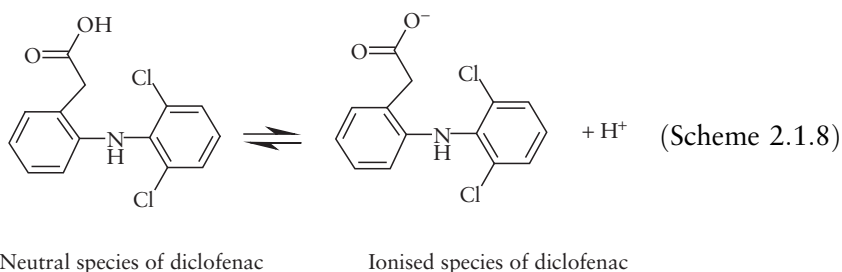
$$D_{\text{base}} = P \times f_{\text{R}_3\text{N}} \quad (2.1.27)$$

Thus, by determining  $P$  for the monoprotic drug candidates,  $D$  may be estimated by Equations 2.1.26 and 2.1.27 for acids and bases respectively, which by logarithmic terms transforms into Equations 2.1.28 and 2.1.29.

$$\log D_{\text{acid}} = \log P + \log f_{\text{RCOOH}} \quad (2.1.28)$$

$$\log D_{\text{base}} = \log P + \log f_{\text{R}_3\text{N}} \quad (2.1.29)$$

In Scheme 2.1.8 the ionisation process for the acidic drug compound diclofenac is illustrated.



The  $\log D$ -pH profile of diclofenac is shown in Figure 2.1.5, which may be described by Equation 2.1.28 in the pH region 1–9. Above pH 9, the profile is described by  $\log D$  for its ionic species, which is approximately 0.7. The carboxylic acid functionality of diclofenac has a  $\text{p}K_{\text{a}}$  of 4.0 (Sirius Technical Application Note 2, 1995).

As illustrated in Figure 2.1.5, the  $\log D$  of diclofenac decreases with pH in the pH range 4.0–9.0. Thus, diclofenac may penetrate better into a

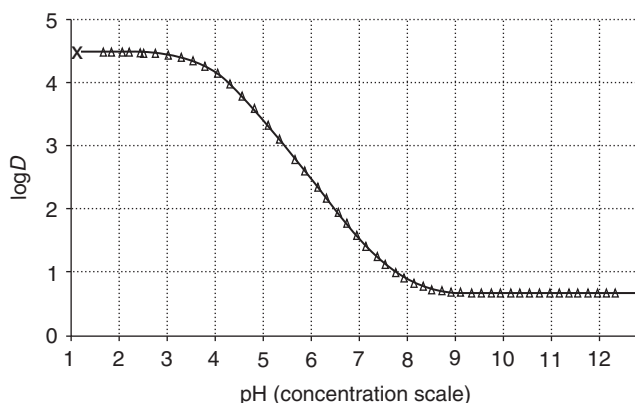
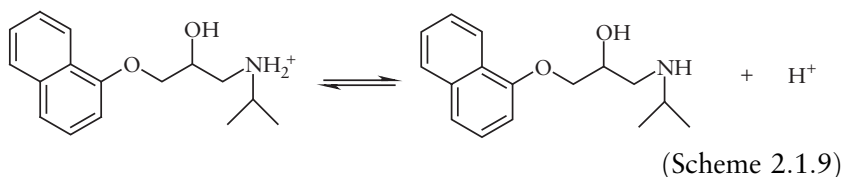


**Figure 2.1.5**  $\log D$ -pH profile of the acidic drug substance diclofenac between *n*-octanol and water as function of pH. It is seen that the un-ionised species of diclofenac distributes better to *n*-octanol than the ionised species. Reproduced from *Sirius Technical Application Notes Volume 2* (1995). Riverside: Sirius Analytical Instruments Ltd.

lipophilic environment, such as phospholipids in cell membranes, when delivered from acidic media such as the gastric juice at pH 1–3, than when delivered from intestinal fluid at pH 5.5–8. In general, it is hypothesised that when a pH gradient is present across a lipophilic cell membrane, the neutral species of an acidic drug substance, delivered from acidic gastric or intestinal fluids to the lipophilic cell membrane barrier, arises as its ionised form at an intracellular or blood pH of 7.4. In this way the concentration gradient of the neutral species, across the lipophilic membrane, is maintained, which drives passive diffusion of the neutral species. This hypothesis is called the pH-partition hypothesis.

The ionisation process of the basic drug substance propranolol is shown in Scheme 2.1.9.



The  $pK_a$  of propranolol is determined to be 9.72 and its  $\log P$ , i.e. the partitioning of its fully neutral and fully ionised species between *n*-octanol and water is determined to be 3.41 and 0.48 respectively (Clarke and Cahoon, 1987). An illustration of  $f_{R_3N}$  and  $\log D$  at various pH levels is shown in Table 2.1.6.

pH- $\log D$  profiles may be determined through experiments by first titrating drug candidates in water, followed by titration in non-mixed

**Table 2.1.6** Fraction of neutral propranolol  $f_{R_3N}$  as well as  $\log D$  of propranolol at various pH values

pH	$f_{R_3N}$	$\log D$
4	0	*0.48
5	0	*0.48
6	0	*0.48
7	0.002	0.69
8	0.019	1.68
9	0.160	2.61
10	0.656	3.22
11	0.950	3.38

Notes:  $f_{R_3N}$  is calculated from Equation 2.1.12 and  $\log D$  from Equation 2.1.29, except for \* $\log D$  which is 0.48, i.e.  $\log D$  of the fully ionised species.

solvents of *n*-octanol and water. This may be performed by equipment such as the GlpKa meter developed by Sirius Instruments as illustrated next for the drug substance morphine.

The ionisation process of morphine is shown in Scheme 2.1.4, and a Bjerrum difference plot as a result of morphine sulphate titration in aqueous solution is shown by the solid curve in Figure 2.1.6.

The solid curve shows that all protons are bound to morphine at a pH lower than 6 and that morphine loses two protons per molecule in the pH interval 6–11. Thus, morphine has two overlapping  $pK_a$  values in this pH range. However, the Bjerrum difference plot produced from

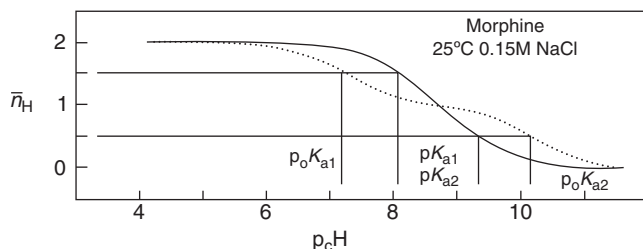


**Figure 2.1.6** Bjerrum plot; that is average amount of bound protons  $n_H$  as function of  $-\log[H^+]$  ( $p_cH$ ) as a result of alkalimetric titration of morphine sulphate in aqueous solutions (solid line) and in non-miscible mixed solvents of water and *n*-octanol (dotted line) at 25 °C and at ionic strength at 0.15 M KCl. Apparent  $p_oK_{a1}$  and  $p_oK_{a2}$  determined in non-miscible mixed solvents and  $pK_{a1}$  and  $pK_{a2}$  determined in aqueous solution. Reproduced from Avdeef A (1996). Assessment of distribution–pH profiles, In: Pliska V, Testa B, van der Waterbeemd, eds. *Lipophilicity in Drug Action and Toxicology*. Weinheim: VCH Publishers Weinheim, 111–139.

titration of morphine sulphate in aqueous solution does not show whether the protons arise from basic or acidic functionalities in morphine. This may be solved by also titrating morphine sulphate in non-mixed solvents such as *n*-octanol and water mixtures, i.e. a pH–log*D* profile determination. As illustrated in Figure 2.1.6, the amine functionality in morphine has a lower  $pK_a$  than the phenolic functionality because the first  $pK_a$  determined in non-miscible mixed solvent (dotted curve) is lower than when determined in water (solid curve). This indicates that neutral deprotonated amine species of morphine are distributed to the octanol phase and therefore not recognised by the electrode, which results in a lower apparent  $p_oK_a$  than when measured in aqueous solution. In contrast, the second  $pK_a$  of morphine may arise from the phenol functionality. For phenol the protonated neutral species is distributed to octanol to a much larger degree than its negative ionised species. Thus it follows that the  $p_oK_a$  values determined from non-mixed solvents (dotted curve) are larger than when determined in aqueous solution (solid curve).

The Bjerrum plot may be translated into a pH–log*D* profile by Equation 2.1.30.

$$\log D_{\text{ampholyte}} = \log P + f_{\text{ampholyte}} \quad (2.1.30)$$

This is shown for morphine in Figure 2.1.7, where it is seen that log*D* of morphine is highest in the pH interval 7–11, and consequently morphine is optimally delivered to the intestinal lipophilic membrane barrier from an intestinal fluid pH of 7–10.

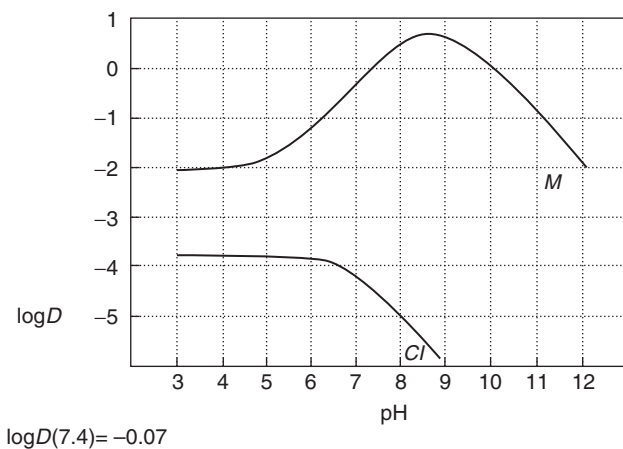


**Figure 2.1.7** pH–log*D* profile of morphine hydrochloride performed in *n*-octanol and water. Morphine (M) and chloride (Cl). Reproduced from *Sirius Technical Application Notes Volume 2* (1995). Riverside: Sirius Analytical Instruments Ltd.

### 2.1.4 Solvation and solid-state limited solubility

$\log P$  has also been used as a solvation parameter. Of particular interest is the general solubility equation (GSE) (Equation 2.1.31) developed by Yalkowski and co-workers (Jain and Yalkowski, 2001)

$$\log S = 0.05 - 0.01(T_m - 25) - \log P \quad (2.1.31)$$

in which  $S$  is intrinsic solubility, i.e. the solubility of the neutral species of the drug substance in molar units, and  $T_m$  is its melting point used as a solid-state parameter. From Equation 2.1.31 it can be seen that intrinsic solubility is related to both the solvation parameter  $\log P$  and the solid-state parameter  $T_m$ .

Bergström and co-workers have applied Equation 2.1.31 to classification of poor-solubility drug substances into solvation-limited and solid-state-limited poor-solubility drug substances (Wassvik *et al.*, 2006; Bergström *et al.*, 2007, Wassvik *et al.*, 2008). For 15 drug substances investigated, nicknamed as ‘grease balls’, with solubility ranging from 2.9 nM to 1.1  $\mu$ M and  $\log P$  between 3.5 and 6.8, they found a good correlation between  $\log P$  and  $\log S$ , whereas no correlation was observed between  $T_m$  and  $S$  (Bergström *et al.*, 2007). Consequently, they suggested the solubility of these ‘grease balls’ is solvation limited. In another study they investigated 20 poor-solubility drug substances nicknamed ‘brick dusts’ with  $S$  ranging from  $-1.75$  to  $-4.83$  and  $\log P$  close to 2. Good correlation was observed between  $\log S$  and  $T_m$  and/or melting enthalpy  $\Delta H$ , but no correlation between  $\log P$  and  $\log S$ . Consequently the solubility of these ‘brick dust’ molecules, characterised by features such as rigidity and high aromaticity, were suggested to be solid-state limited (Wassvik *et al.*, 2008).

These observations are highly relevant for selecting and formulating poor-solubility drug candidates. Whereas solvation-limited poor-solubility ‘grease ball’ candidates represent highly lipophilic species that are unable to form bonds with water molecules, the solid-state-limited poor-solubility ‘brick dust’ candidates represent stable crystals in which the strong intermolecular bonds within the crystal restrict the solubility of the candidate with water. For ‘grease ball’ candidates, the solubility may be improved largely by incorporating excipients such as disintegrants, solubility enhancers or lipids in the formulation, whereas this is generally not the case for ‘brick dust’ candidates. For ‘brick dust’ candidates, the strong intermolecular bonds should be weakened, for example by changing the shape of the crystal unit cells (polymorphic forms) or crystal habits as described in Section 2.1.5 or by salt or prodrug formation (see Chapter 2.4).

### 2.1.5 Solid-state characterisation

During selection of drug candidates, crystal forms are characterised by means of investigating their influence on dissolution. This is, as described in Section 2.1.4, especially important for solid-state-limited low-solubility drug candidates where dissolution may be limiting for bioavailability.

Drug candidate crystals may be held together by non-covalent interactions, which influences the melting point of the crystals. A specific crystal consists of repeating unit cells, i.e. it contains the same size and the same number of molecules or ions arranged in the same way, thus creating crystal lattices. Unit cells may be arranged in cubic, hexagonal, trigonal, tetragonal, orthorhombic, monoclinic or triclinic crystal lattices. Cubic, tetragonal, orthorhombic and hexagonal structures are illustrated in Figure 2.1.8.

The form of the unit cells may be characterised in three dimensions. The width, depth and height of the unit cell are represented by  $b$ ,  $a$  and  $c$ , respectively (see Figure 2.1.8), and the angles between  $b$  and  $c$ ,  $a$  and  $c$ , and  $b$  and  $a$  may then be characterised as  $\alpha$ ,  $\beta$  and  $\gamma$  respectively.

Cubic crystals are formed as cubes when  $a = b = c$  and  $\alpha = \beta = \gamma = 90^\circ$  as illustrated in Figure 2.1.8. The tetragonal crystal is a rectangular prism in which  $a = b \neq c$  but  $\alpha = \beta = \gamma = 90^\circ$  as illustrated in Figure 2.1.8. In orthorhombic unit cells  $a \neq b \neq c$  and  $\alpha = \beta = \gamma = 90^\circ$ , i.e. there are three right-angled axes with different lengths as illustrated in Figure 2.1.8. In the regular hexagonal crystal all sides and angles are equal, i.e. all angles are  $120^\circ$  as seen in Figure 2.1.8.

In the triclinic crystal,  $a \neq b \neq c$  and  $\alpha, \beta, \gamma \neq 90^\circ$ . In the monoclinic crystal  $a \neq b \neq c$  and  $\alpha = 90^\circ$ , whereas  $\beta$  and  $\gamma \neq 90^\circ$ . In the trigonal (rhombohedral) crystal,  $a = b = c$  and  $\alpha = \beta = \gamma \neq 90^\circ$ .

Some unit cells may be further described as simple, base-, face- or body-centred unit cells. In simple unit cells, molecules/ions are only represented in the corners. In base-centred unit cells, as well as being

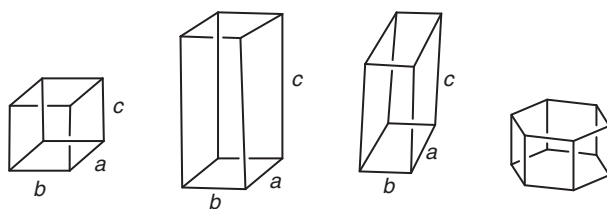


**Figure 2.1.8** Lattice structures. From left to right: cubic, tetragonal, orthorhombic and hexagonal.



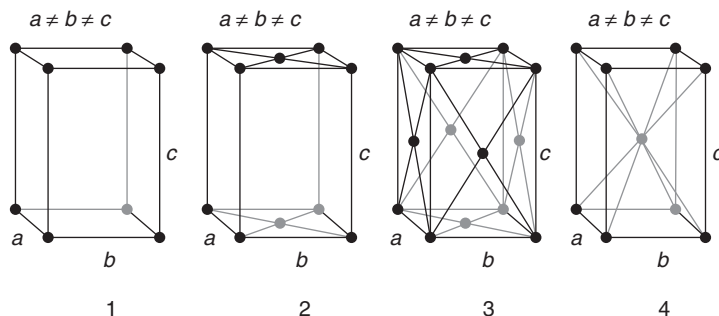


**Figure 2.1.9** Simple orthorhombic crystal structures (1), base centred (2); face centred (3); and body centred (4). The width, depth and height are represented by  $b$ ,  $a$  and  $c$  respectively, and the angles between  $b$  and  $c$ ,  $a$  and  $c$ , and  $b$  and  $a$  are represented respectively by  $\alpha$ ,  $\beta$ , and  $\gamma$ . From Wikipedia.org [http://en.wikipedia.org/wiki/Orthorhombic\\_crystal\\_system](http://en.wikipedia.org/wiki/Orthorhombic_crystal_system)).

represented in the corners, molecules/ions are also represented in the two base planes of the unit cells. In face-centred unit cells, as well as being represented in the corners, molecules/ions are also centred at each (sur)face. In body-centred unit cells, as well as being represented in each corner, molecules/ions are also centred in the middle (body) of the cells. Simple, base-, face- and body-centred orthorhombic unit cells are depicted in Figure 2.1.9 (2–4).

The shape of the unit cells is generally described by Miller indices, which will not be further described; however, specific drug candidates may crystallise into different polymorphic forms where the molecules/ions arrange themselves in more than one way, either by packing differently in the crystal lattice or by orienting themselves differently in the lattice. These unit cells variations can be characterised by analysing X-ray diffraction patterns of the drug candidate. Properties such as dissolution and melting point are also often different between polymorphic forms, and therefore unit cell variation may also be characterised by analysing their phase transition temperature by differential scanning calorimetry (DSC), to obtain melting point entropies,  $\Delta S$ , and enthalpies,  $\Delta H$ . Polymorphic forms may also show different crystal habits, that is, similar unit cells, but different apparent crystal shapes. Apparent crystal shapes may be acicular, prismatic, pyramidal, tabular or lamellar. The different crystal habits may have different dissolution rates. Thus for solid-state-limited low-solubility drug candidates, crystal habits may have an influence on dissolution and thus bioavailability, as well having a possible influence on formulation properties.

Thus, it is important to characterise the various polymorphic forms of a specific drug candidate, including possible crystal habits, with regard to rational pharmaceutical development.

### 2.1.6 Conclusions

Characterisation of acid/base properties, solubility, lipophilicity and solid-state properties of drug candidates is essential for biopharmaceutical and formulation sciences as well as for industrial formulation and preclinical selection processes. For drug candidates with acid/base properties it is convenient to determine the  $pK_a$  to further determine species-dependent solubility and lipophilicity. This is important because species-dependent solubility and lipophilicity may have a major influence on both the formulation and biopharmaceutical properties of drug candidates. Furthermore, they may influence the chemical stability of the drug candidate. Solid-state properties of drug candidates are especially relevant for characterisation of poor-solubility drug candidates because solid-state properties may significantly influence formulation strategies as well the physical and chemical stability of these candidates. The chemical stability of drug candidates is discussed in Chapter 2.1.2.

### References

- Albert A, Serjeant EP (1984). *Determination of Ionization Constants*, 3rd edn. London: Chapman and Hall, London.
- Avdeef A (1996). Assessment of distribution–pH profiles. In: Pliska V, Testa B, van der Waterbeemd, eds. *Lipophilicity in Drug Action and Toxicology*. Weinheim: VCH Publishers, 111–139.
- Avdeef A (1998). pH-metric solubility. 1. Solubility–pH profiles from Bjerrum plots. Gibbs buffer and  $pK_a$  in the solid state. *Pharm Pharmacol Commun* 4: 165–178.
- Avdeef A (2001). Physicochemical profiling (solubility permeability and charge state). *Curr Top Med Chem* 1: 277–351.
- Bergström CAS, Luthman K, Artursson P (2004). Accuracy of calculated pH-dependent aqueous solubility. *Eur J Pharm Sci* 22: 387–398.
- Bergström CAS, Wassvik CM, Johansson K, Hubatsch I (2007). Poorly soluble marketed drugs display solvation limited solubility. *J Med Chem* 50: 5858–5862.
- Bjerrum J (1941). *Metal-amine Formation in Aqueous Solution*. Copenhagen: Haase.
- Brøndsted JN (1923). Einige bemerkungen über den begriff der säuren und basen. *Rec. Trav Chim Pays-Bas* 42: 718.
- Charman WN, Porter CJ, Mithani SD, Dressman JB (1997). Physicochemical and physiological mechanisms for the effects of food on drug absorption: the role of lipids and pH. *J Pharm Sci* 86: 269–282.

- Clarke FH, Cahoon NM (1987). Ionization constants by curve fitting: determination of partition and distribution coefficients of acids and bases and their ions. *J Pharm Sci* 76: 611–621.
- Dressman J, Bass P, Ritschel WA, *et al.* (1993). Gastrointestinal parameters that influence oral mechanisms. *J Pharm Sci* 82: 857–872.
- Dressman JB, Amidon GL, Reppas C, Shah V (1998). Dissolution testing as a prognostic tool for oral drug absorption: immediate release dosage forms. *Pharm Res* 15: 11–22.
- European Pharmacopoeia*, 6th edn (2009). <http://online6.edqm.eu/ep604/> (accessed 28 April 2009).
- FDA, Center for Drug Evaluation and Research (2000). *Guidance for Industry, Waiver of in vivo Bioavailability and Bioequivalence Studies for Immediate-release Solid Oral Dosage Forms based on a Biopharmaceutics Classification System*. <http://www.fda.gov/downloads/Drugs/GuidanceComplianceRegulatoryInformation/Guidances/UCM070246.pdf> (accessed 2 June 2009).
- Gray VA, Dressman JB (1996). Change of pH requirements for simulated intestinal fluid TS. *Pharm Forum* 22: 1943–1945.
- Hasselbalch KA (1916). Die berechnung der wasserstoffzahl des blutes auf der freien und gebunden kohlen-saure desselben und die sauerstoffbindung des blutes als function der wasserstoffzahl. *Biochem Z* 78: 112–120.
- Jain N, Yalkowski SH (2001). Estimation of aqueous solubility I: application to organic nonelectrolytes. *J Pharm Sci* 90: 234–252.
- Kutchai, HC (1996). Digestive system. In: Levy MN, Koeppe BM, Stanton, BA, eds. *Berne & Levy Principles of Physiology*, 4th edn, Part six, St Louis: Elsevier Mosby Yearbook, 429–586.
- Leo A, Hansch C, Elkins D (1971). Partition coefficients and their uses. *Chem Rev* 71: 525–616.
- Lewis GN (1923). *Valence and Structure of Atoms and Molecules*. New York: The Chemical Catalogue Co, 141.
- Madara JL (1991). Functional morphology of epithelium of the small intestine. In: Field M, Frizzell RA, eds. *Handbook of Physiology Section 6: The Gastrointestinal System Volume IV, Intestinal Absorption and Secretion*. Bethesda: American Physiological Society, 83–120.
- Neuhoff S, Artursson P, Zamora I, Ungell AL (2005). pH-dependent passive and active transport of acidic drug transport across Caco-2 cells. *Eur J Pharm Sci* 25: 211–220.
- Newton DW, Kluza RB (1978). pK values of medicinal compounds in pharmacy practice. *Drug Intell Clin Pharm* 12: 546–554.
- Shedlovski T (1962). The behavior of carboxylic acids in mixed solvents. In: Pesce B, ed. *Electrolytes*. New York: Pergamon Press, 146–151.
- Shore PA, Brodie BB, Hogben CA (1957). The gastric secretion of drugs: a pH partition hypothesis. *J Pharmacol Exp Ther* 119: 361–369.
- Sirius Technical Application Notes Volume 1* (1994). Riverside: Sirius Analytical Instruments Ltd.
- Sirius Technical Application Notes Volume 2* (1995). Riverside: Sirius Analytical Instruments Ltd.

- Takács-Novák K, Box KJ, Avdeef A (1997). Potentiometric  $pK_a$  determination of water-insoluble compounds: validation study in methanol/water mixtures. *Int J Pharm* 151: 235–248.
- Wassvik CM, Holmén AG, Bergstrøm CAS, Zamora I, Artursson P (2006). Contribution of solid-state properties to the aqueous solubility of drugs. *Eur J Pharm Sci* 29: 294–305.
- Wassvik CM, Holmén AG, Draheim R, Artursson P, Bergstrøm CAS (2008). Molecular characteristics for solid state limited solubility. *J Med Chem* 51: 3035–3051.
- Wilson JP (1967). Surface area of the small intestine in man. *Gut* 8: 618–621.



# 2.2

## Mechanisms of decomposition of drug candidates

*Bente Steffansen, Carsten Uhd Nielsen and Birger Brodin*

Characterisation of the stability of drug candidates in aqueous solution is fundamental in the sciences of biopharmaceutical and pharmaceutical chemistry, as well as in industrial preformulation and preclinical development. In industry, stability investigations of drug candidates in aqueous solution generally take place during lead optimisation and late discovery (see Chapter 2.5), whereas stability investigations of drug products generally takes place during pharmaceutical development.

Despite the large structural variety of drug and prodrug candidates, most degradation reactions can be classified as hydrolysis, oxidation, isomerisation, racemisation or polymerisation reactions. These may be initiated by environmental factors such as light, humidity and oxygen. Also, whether the drug candidate is in solid state or aqueous solution may influence its stability. In aqueous solution, factors such as pH, temperature, ionic strength, or the presence of catalysts, e.g. metal ion impurities or buffers, may influence the stability of drug and prodrug candidates. A systematic stability test therefore includes studies of both the mechanism and rate (kinetics) by which drug and prodrug candidates are degraded. The aim of the present chapter is to describe reaction mechanisms of importance for stability of drug candidates and of relevance for drug formulation and bioavailability. The kinetics of stability are described in Chapter 2.3.

### 2.2.1 Hydrolysis

The most important class of hydrolysis reactions influencing the stability of prodrug and drug candidates is the hydrolysis of carboxyl functional groups. Carboxyl drug and prodrug candidates are carboxylic acid derivatives that are different from carbonyl candidates, which also include aldehydes and ketones and are generally stable towards hydrolysis. The development of prodrugs is often based on the rational introduction of a vulnerable carboxyl functional group to parent drug candidates such



**Figure 2.2.1** General molecular structures of a carboxyl compound (a), and an acyl functional group (b). R is an organic unit and X is OR, NR, SR, or Cl, the free bond (–) may be bound to X or R and the bold carbon (**C**) is named as the acyl carbon.

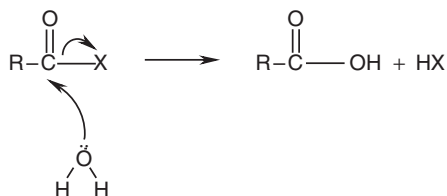
as alcohols, carboxylic acids or amines. Many prodrugs are therefore designed to contain carboxyl functional groups. Thus, it is of great importance to understand the degradation mechanisms of carboxyl candidates. Hydrolysis or water-catalysed reactions of carboxyl candidates take place by acyl transfer reactions. The general molecular structures of carboxyl compounds and acyl groups are shown in Figure 2.2.1a and b, respectively.

Many prodrug and drug candidates are carboxyl compounds such as esters, amides, imides, succinimides, lactams, thiol esters, lactones, acid anhydrides or acid chlorides. Table 2.2.1 shows some selected drug substances that are carboxyl compounds.

Hydrolysis reactions are initiated by an electron pair or nucleophilic attack. Electron pairs may be donated by  $\text{H}_2\text{O}$ . This electron pair or nucleophilic attack on the acyl carbon, with a partial positive charge, is illustrated in Figure 2.2.2.

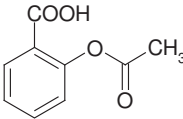
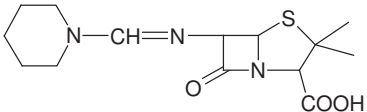
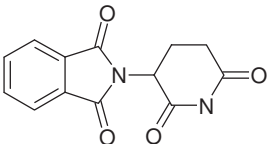
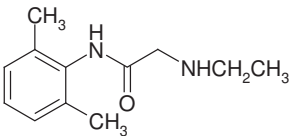
The leaving group  $\text{HX}$ -, that is  $\text{HOR}'$ ,  $\text{HNR}'$ ,  $\text{HSR}'$  arises from hydrolysis of esters, amides, and thiol esters respectively. This acyl transfer reaction, i.e. hydrolysis, is probably the most common reaction of carboxyl compounds and is one of the most frequent degradation routes for drug substances.

Figure 2.2.3 shows such an example, the degradation pathways for acetyl salicylic acid (ASA). The reaction results in the formation of salicylic acid and acetic acid. The kinetics of the degradation of ASA are explained in more detail by Garrett (1957).

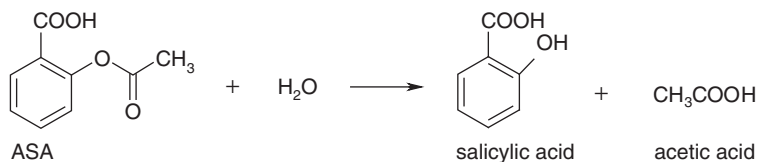


**Figure 2.2.2** Hydrolysis, i.e. nucleophilic attack by  $\text{H}_2\text{O}$  on an acyl carbon in a carboxyl compound, resulting in the corresponding carboxylic acid and leaving the group  $\text{HX}$ . X is e.g. OR, NR or SR, and R is an organic unit.

**Table 2.2.1** General structures of selected carboxyl compounds and examples of drug substances that are carboxyl compounds

<i>Hydrolysable carboxyl compounds</i>	<i>Drug substance examples</i>
$\text{R}-\overset{\text{O}}{\parallel}{\text{C}}-\text{OR}'$ <p>Ester</p>	 <p>Acetyl salicylic acid (ASA)</p>
$\text{R}-\left[\text{CH}_2\right]_n-\text{N}-\overset{\text{O}}{\parallel}{\text{C}}-$ <p>Lactam</p>	 <p>Mecillinam</p>
$\text{RC}-\overset{\text{O}}{\parallel}{\text{N}}-\overset{\text{O}}{\parallel}{\text{CR}}$ <p>Imide</p>	 <p>Thalidomide</p>
$\text{R}-\overset{\text{O}}{\parallel}{\text{C}}-\text{NHR}'$ <p>Amide</p>	 <p>Lidocaine</p>

The hydrolysis of amides is another important class of hydrolysis reactions relevant for pharmaceutical stability investigations. Since the electronegativity of nitrogen (3.0) is less than that of oxygen (3.5), the acyl carbon in an amide is, in general, of lower partial positive charge than in an ester. Consequently, amides are often more stable towards hydrolysis than esters. However, if nitrogen is in a terminal position as it

**Figure 2.2.3** Hydrolysis of acetyl salicylic acid (ASA) resulting in the formation salicylic acid and acetic acid.



is in the amino acids asparagine (Asn) and glutamine (Gln), the acyl carbon is generally more easily attacked by nucleophiles than in secondary amines. Thus, deamidation of primary amines, such as Asn and Gln, takes place and asparaginic acid (Asp) and glutaminic acid (Glu), respectively are formed. These reactions are generally not very fast in neutral solution, but may be extensively catalysed by acids and bases as well as by intramolecular nucleophilic attack as described below. Thus, deamidation is an important reaction for most drug candidates that are peptides and proteins, even though it is unpredictable for influencing therapeutic activity. Therefore, no influence on therapeutic effects is seen in the case of deamidation reactions in insulin, but in the case of adrenocorticotrophin, deamidation reactions decrease its therapeutic effect (Gráf *et al.*, 1973).

In addition, hydrolysis may be responsible for the release of parent drug substance from an ester prodrug. Prodrugs are described in Chapter 2.4. In Figure 2.2.4 the hydrolysis of the ester prodrug valaciclovir is shown. The hydrolysis is initiated by electron pair attack donated by  $\text{H}_2\text{O}$ , resulting in the release of parent aciclovir together with the amino acid valine (Val). The kinetics of degradation of valaciclovir are described in Chapter 2.3 and in more detail by Thomsen *et al.* (2003a,b).

Hydrolysis may also be catalysed either by stronger nucleophiles than water or by acids due to protonisation of acyl oxygen. Examples of compounds that can catalyse hydrolysis reactions are specific and general acids and bases. Consequently, hydrolysis reactions are pH dependent. The kinetics of pH-dependent hydrolysis are described in Chapter 2.3. Other examples of catalysts are electrophiles and nucleophiles as well as enzymes with esterase or peptidase activity. Examples are shown in Table 2.2.2.

The first step in a hydrolytic acyl transfer reaction of esters in alkaline solution can involve a nucleophile attack by the specific base catalyst on the acyl carbon, i.e.  $\text{OH}^-$  creates a tetrahedral intermediate as shown in Figure 2.2.5a. This reaction is reversible. However, depending on which of the C-OH or the C-OR' bonds are strongest, either the

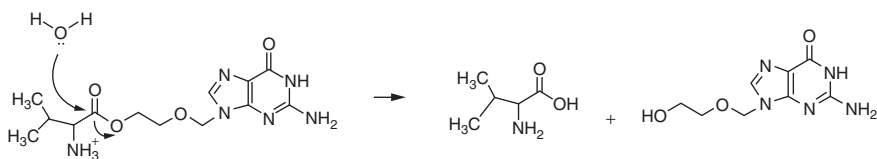


**Figure 2.2.4** Hydrolysis of the ester prodrug valaciclovir to the parent aciclovir and the amino acid valine.

**Table 2.2.2** Examples of compounds catalysing hydrolysis reactions. Regarding gastrointestinal peptidases see Table 2.4.3 as well as Steffansen *et al.*, 2005

<i>Hydrolysis catalysts</i>	<i>Structures of various catalysts</i>
Specific acid	$\text{H}_3\text{O}^+$
Specific base	$\text{OH}^-$
Water	$\text{H}_2\text{O}$
General acid (proton donor), i.e. Brønsted acid (see Section 2.1.1)	Examples: several buffers: $\text{H}_3\text{PO}_4$ , $\text{H}_2\text{CO}_3$ , $\text{CH}_3\text{CH}_2\text{COOH}$
General base (proton acceptor), i.e. Brønsted base (see Section 2.1.1)	Examples: several buffer systems: $\text{CO}_3^{2-}$ $\text{HCO}_3^-$
Electrophile (electron pair acceptor), i.e. Lewis acid (see Section 2.1.1)	Examples: metal ions such as $\text{Na}^+$ , $\text{K}^+$ as well as acyl carbon (cf. Figure 2.2.1)
Nucleophile (electron pair donor), i.e. Lewis base (see Section 2.1.1)	Examples: amines and alcohols $\text{R}-\ddot{\text{O}}\text{H}$ $\text{R}-\ddot{\text{N}}\text{H}_3$
Enzymes with esterase or peptidase activity	Examples: carboxyesterases, aminopeptidases, carboxypeptidases

corresponding alcohol is formed or the ester is reformed. In the hydrolysis process illustrated in Figure 2.2.5b, the alcohol is formed and the specific base catalyst  $\text{OH}^-$  is reformed.

It has been suggested that ring-opening hydrolysis of the mecillinam in the pH range 7–9 may be catalysed by the intramolecular non-protonated nucleophilic amidino group. The reaction is also catalysed by specific base catalysis (Bundgaard 1977; Bundgaard and Larsen, 1977). The intramolecular nucleophilic attack by the amidino group is illustrated in Figure 2.2.6.

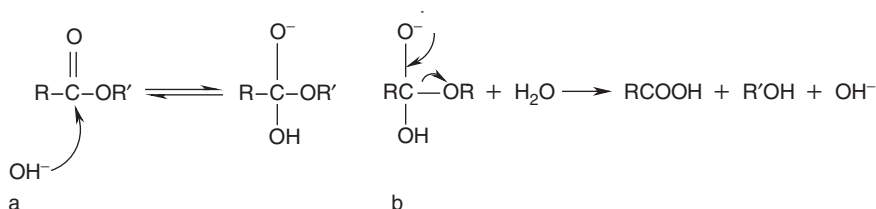


**Figure 2.2.5** Hydrolysis of an ester in alkaline solution involving nucleophilic attack by the specific base catalyst  $\text{OH}^-$  on the acyl carbon with partial positive charge, which results in the reversible formation of the tetrahedral intermediate (a) followed by the breakage of the C-OR' bond to produce the corresponding carboxylic acid  $\text{RCOO}^-$  and alcohol  $\text{R}'\text{OH}$  (b).

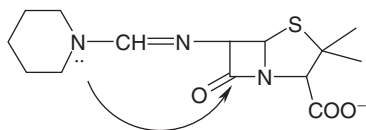


**Figure 2.2.6** Intramolecular nucleophilic attack by the amidino group in mecillinam.

Intramolecular nucleophilic attack often takes place in a similar way in peptides enclosing Asn and Gln. This is illustrated in Figure 2.2.7, where an electron pair from the secondary peptide bond attacks the  $\beta$ -acyl carbon, i.e. in the side chain of Asn, to form a pentacyclic imide intermediate that opens up to form either the corresponding Asp-containing peptide or the corresponding iso-Asp-peptide. This reaction explains one of the most important chemical instability reactions of peptides and proteins.

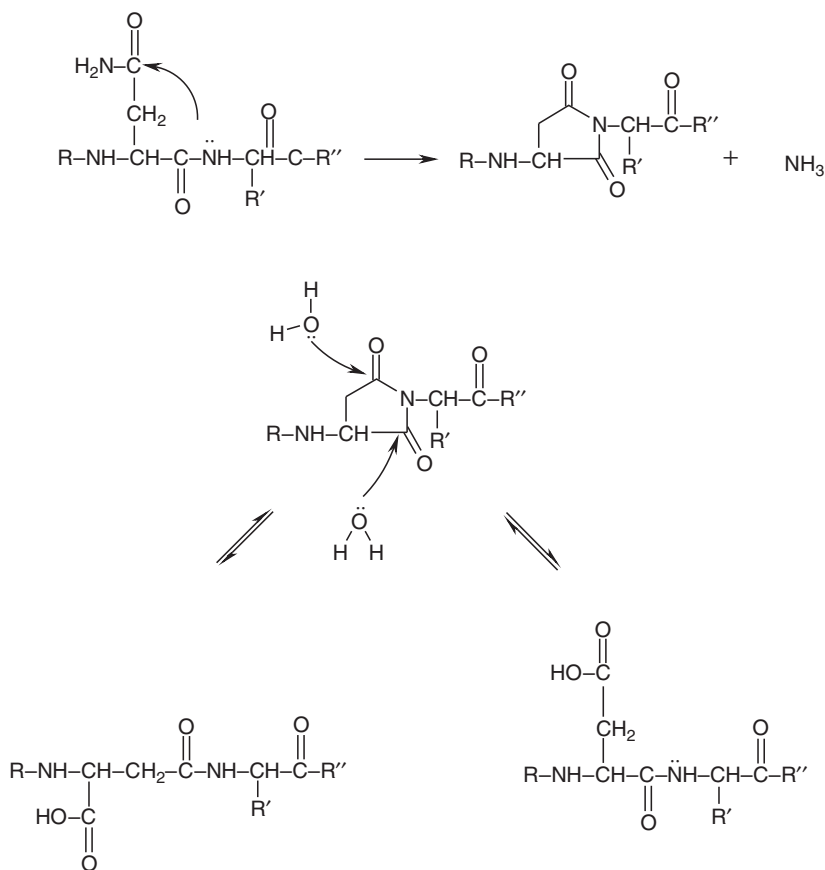


**Figure 2.2.7** Deamidation in peptides and proteins enclosing the amino acid asparagine (Asn).

However, carboxyls are catalysed not only by bases or nucleophiles but often also by acids. Protonation of acyl oxygen by acids further polarises the carboxyl group, which attracts nucleophiles within its neighbourhood to attack acyl carbon and thus catalyses the reaction. Steffansen and co-workers (Steffansen *et al.*, 2005) have suggested this reaction takes place in the acid-catalysed ester hydrolysis of the proposed main degradation pathway of the model prodrug Glu(aciclovir)-Sar that, via two parallel reactions, forms parent aciclovir and a suggested cyclic impurity (see Figure 2.2.8).

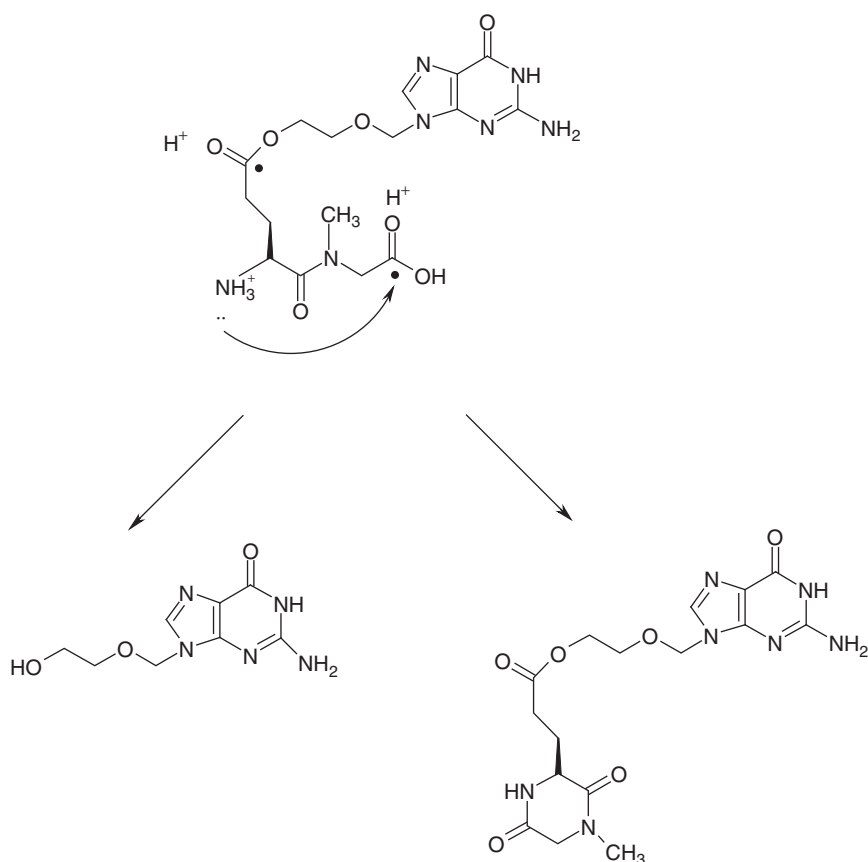


**Figure 2.2.8** Specific acid-catalysed hydrolysis of Glu(aciclovir)-Sar to release parent aciclovir and a suggested cyclic impurity. Acyl carbons are marked by •. Redrawn from Thomsen AE, Friedrichsen GM, Sørensen AH, *et al.* (2003a). Prodrugs of purine and pyrimidine analogues for the intestinal di/tri-peptide transporter PEPT1: affinity for PEPT1 in Caco-2 cells, drug release in aqueous media and in vitro metabolism. *J Control Rel* 86: 279–292.

Mechanisms of degradation reactions investigated in aqueous solutions may differ with pH. Thus, even though the parallel specific acid-catalysed hydrolysis reaction of Glu(aciclovir)-Sar takes place at  $\text{pH} < 4$ , the specific acid-catalysed aciclovir formation increases with increasing pH, whereas the specific acid-catalysed formation of the cyclic impurity increase with decreasing pH (Thomsen *et al.*, 2003a,b).

Another example of hydrolysis mechanisms being pH dependent is the specific acid-catalysed hydrolysis of erythromycin 2'-acetate, i.e. at  $\text{pH} \leq 4.0$ , where erythromycin 2'-acetate prodrug is quantitatively and irreversible degraded to its corresponding impurity anhydroerythromycin via dehydration of the initially formed 6.9 hemiketal erythromycin (Atkins *et al.*, 1986; Kurath *et al.*, 1971; Steffansen and Bundgaard, 1989). The reaction scheme for this acid-catalysed conversion of erythromycin 2'-acetate is shown in Figure 2.2.9.

However, erythromycin 2'-acetate is reacting as a true prodrug in the pH range of 7–10, i.e. it is quantitatively hydrolysed by specific base-catalysed reaction to its corresponding drug substance erythromycin. The reaction scheme for this reaction is illustrated in Figure 2.2.10.

In order to identify possible impurities arising from decomposition reactions, it is of utmost importance to investigate the mechanisms behind the hydrolysis reactions of (pro)drug candidates.

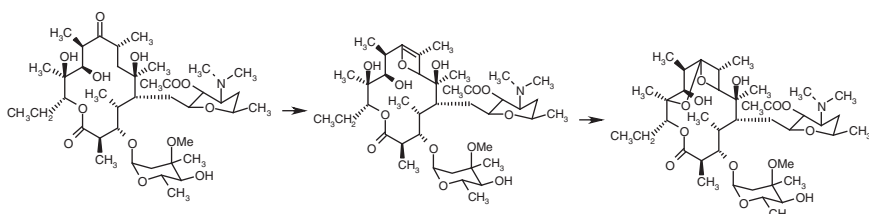


**Figure 2.2.9** Acid-catalysed degradation of 2'-acetate erythromycin to impurity 2'-acetate anhydroerythromycin via 2'-acetate erythromycin 6.9-hemiketal.

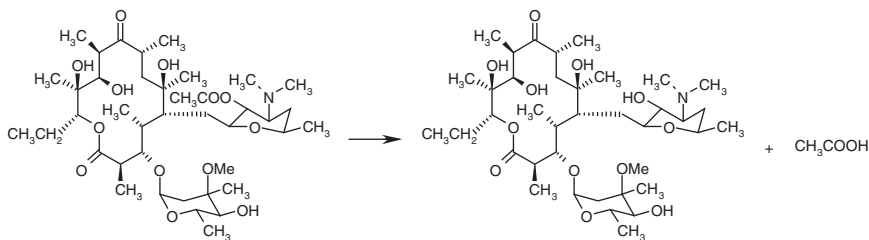


**Figure 2.2.10** Hydrolysis of the prodrug 2'-acetate erythromycin at pH 7.4 to the corresponding drug substance erythromycin.

For drug and prodrug substances that decompose due to hydrolysis, it is clearly important to formulate the drug product as a solid dosage form that limits the access of water to the drug substances. However, in humid conditions the drug substance is exposed to a limited amount of water even in a solid dosage form. Therefore, the solid dosage form should be formulated with excipients that do not catalyse hydrolysis, so that the drug substance shows maximal stability. It is therefore of great importance to investigate and understand the hydrolysis reactions of drug candidates even though they are developed by means of a solid dosage form.

### 2.2.2 Oxidation

Whereas hydrolysis involves a two-electron transfer reaction, oxidation proceeds through one-electron transfer, i.e. free radical transfer reactions. Many drug substances and candidates exist in a reduced form, e.g. alcohols, alkylbenzenes, aldehydes, alkenes, amines, so that the presence of oxygen in the atmosphere may create oxidised degradation products.

Oxidation is complementary to reduction, i.e. oxidation and reduction involve electron release and uptake processes, respectively. These electron transfer processes take place only to some extent with regard to redox processes involving covalent bonds such as in alcohols. Although covalently bound carbon is encompassed by the same numbers of electrons before and after its oxidation process, the oxidation state may change because electrons are regarded as belonging to the most electronegative atom involved in the bond.

Some oxidation reactions are initiated by energy such as light. However, not all photolytic reactions are oxidative in nature (see Section 2.2.3).

An example of non-photolytic oxidation is phenol oxidising to ketone, which can be catalysed in alkaline solution and is thus pH dependent. The base initiates the reaction by making a free radical at the phenol oxygen. The free radical then initiates a chain reaction by which a new free radical is formed. In Figure 2.2.11 (right), the free radical is placed in a para-position to the ketone; however, that is just to provide an illustration since this free radical initiates further, inter- or intramolecular, degradation. Thus base-catalysed oxidation of phenols, which in the case of the amino acid tyrosine (Tyr) is very complex, is, nevertheless, often seen. Since tyrosine is a building block of many protein and peptide drug candidates, this oxidation reaction has great importance for stability investigations of many of these drug candidates. The same type of reaction takes place in morphine and epinephrine (adrenaline) oxidations.

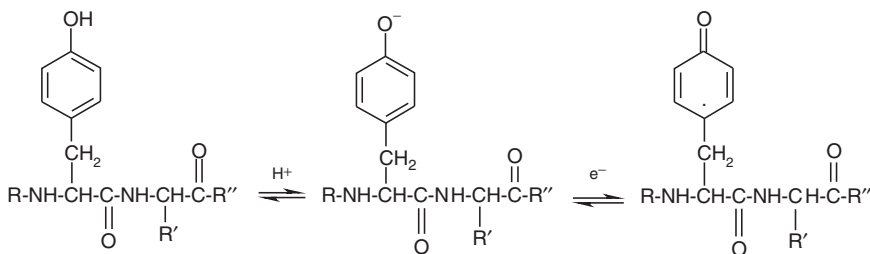


**Figure 2.2.11** Redox equilibrium of the amino acid tyrosine.

The oxidation states of carbon may change from  $-4$  in  $\text{CH}_4$  to  $+4$  in  $\text{CCl}_4$ . In oxidation state zero, carbon has four accessible electrons in its outer electron shell.

The oxidation of a primary alcohol, where the alcohol carbon ( $\text{C}^*$  in Figure 2.2.12 left) is bound by single bonds to one alcohol (an oxidation state of  $-1$ ), two hydrogens (each in an oxidation state of  $+1$ ), and one carbon atom, the five electrons in its outer electron shell are considered to belong to  $\text{C}^*$ . Consequently, the  $\text{C}^*$  atom is in its oxidation state  $-1$ . This is illustrated in Figure 2.2.12 left, where electrons considered to belong to the  $\text{C}^*$  are marked by a bold  $\mathbf{x}$  and those marked with a regular  $\mathbf{x}$  are considered to belong to neighbouring atoms. However, when  $\text{C}^*$  releases two electrons during oxidation of the compound from phenol to aldehyde,  $\text{C}^*$  changes its oxidation state from  $-1$  to  $+1$ . The carbonyl carbon in aldehyde is illustrated as bold  $\mathbf{C}$  with the three bold  $\mathbf{x}$ 's in Figure 2.2.12 right. In other words, compared to free carbon in oxidation state zero, which has four electrons in its outer electron shell, alcohol-bound carbon has five and carbonyl carbon involved in aldehyde functionality has three. Consequently its oxidation state changes from  $-1$  to  $+1$ .

Apart from in  $\text{O}_2$ , where oxygen is in an oxidation state of zero, oxygen is normally in its oxidation state of  $-2$ , and it is more electronegative (3.5) than carbon (2.5). Hydrogen, on the other hand, is (apart from  $\text{H}_2$ ) normally in an oxidation state of  $+1$  and is less electronegative (2.2) than carbon (2.5). Electrons involved in covalent bonds are considered to

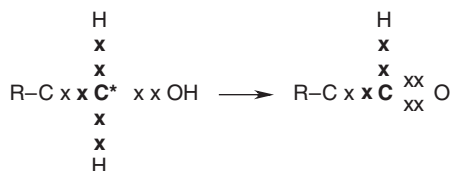


**Figure 2.2.12** Oxidation of primary alcohol to aldehyde. For explanation, see text.

belong to the most electronegative atom involved in the bond. Bold C\* in Figure 2.12 illustrates alcohol-bound carbon in its oxidation state of  $-1$  (left) and bold C carbonyl carbon in aldehyde functionality is in its oxidation state of  $+1$  (right). Bold x illustrates electrons considered to belong to C\* or C, whereas regular x's are considered to belong to neighbouring atoms. Thus, compared to free carbon, which has four electrons, C\* involved in the primary alcohol functionality has five (x), and carbonyl carbon C involved in aldehyde has three (x). Thus, bold C\* goes from having an excess of one electron, in order to reach an oxidation state of  $-1$ , to having a deficiency of one electron, in order to reach an oxidation state of  $+1$ , when alcohol is oxidised to aldehyde.

Other oxidation reactions are light-induced oxidation processes such as takes place in riboflavin. The two carbons within the second and third ring systems each take up one electron, and riboflavin is thus reduced by two. The neighbouring nitrogen atoms are not involved in the redox process, since nitrogen has six electrons in the outer electron shell throughout the reaction. The oxidation process of riboflavin is illustrated in Figure 2.2.13.

Oxidative reactions may also be catalysed by electron donors such as the metal ions  $\text{Fe}^{3+}$ ,  $\text{Cu}^{2+}$  or  $\text{Co}^{3+}$ . Since  $\text{Fe}^{3+}$  and  $\text{Cu}^{2+}$  particularly are often present in distilled water, drug candidates that may oxidise should be formulated from ion-free water.

Methods of avoiding oxidation reaction are dependent on the oxidation mechanism. For example if oxygen itself is involved in the process, the method will need to exclude oxygen, for example by exchanging the air in containers for an inert gas or by packaging in hermetically sealed containers. In cases where oxidation is base catalysed, the pH may be

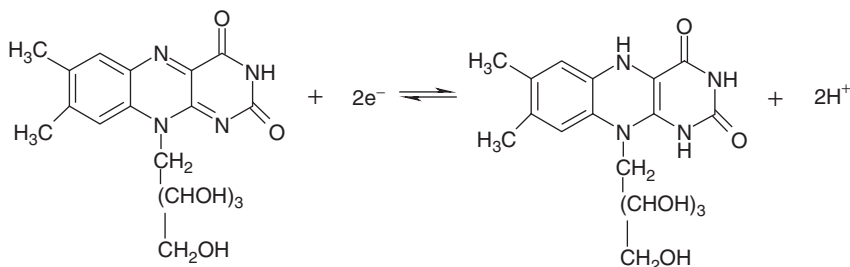


**Figure 2.2.13** Redox equilibrium between riboflavin (left) and dihydroriboflavin (right). In the oxidation process, two carbon atoms in the second and third ring systems are reduced. Redrawn from Connors KA, Amidon GL, Stella VJ (1986). *Chemical Stability of Pharmaceuticals. A Handbook for Pharmacists*, 2nd edn. New Jersey: Wiley-Interscience Publication John Wiley and Sons 3–847.



reduced to 3–4. If the oxidation is photolytic, the oxidative process may be minimised by avoiding light. Impurities of metal ions such as  $\text{Cu}^{2+}$  or  $\text{Fe}^{3+}$  may catalyse oxidation reactions, but by adding chelating agents such as EDTA, redox processes can be limited. Alternatives are addition of antioxidants (reducing agents) such as sodium thiosulphate and ascorbic acid.

### 2.2.3 Non-oxidative photolytic degradation

Photolytic reactions may be oxidative in nature as described above. However, they may also be excitative in which a drug candidate develops into an excited state species as a consequence of absorption of light or radiation energy. The absorbed energy can then be lost by radiation, fluorescence, phosphorescence, heat loss or collision with other molecules, i.e. quenching. During this energy loss, chemical decomposition may occur. One example is photolysis-induced *cis-trans* isomerisation where carbon–carbon  $\pi$ -electrons may be excited by light, which allows rotation and thus *cis-trans* isomerisation. One example of such light-induced reaction is the *cis*-conformation of licochalcone A, which isomerises in the presence of light to form impurities of the corresponding *trans*-form. This is illustrated in Figure 2.2.14.

One way to limit photolytic isomerisation is to avoid the wavelengths initiating the excitation reaction. The whole production procedure should be performed in artificial light where compromising wavelengths are avoided. The drug product should be packaged in containers that exclude all light or that filter those wavelengths that catalyse the reaction.

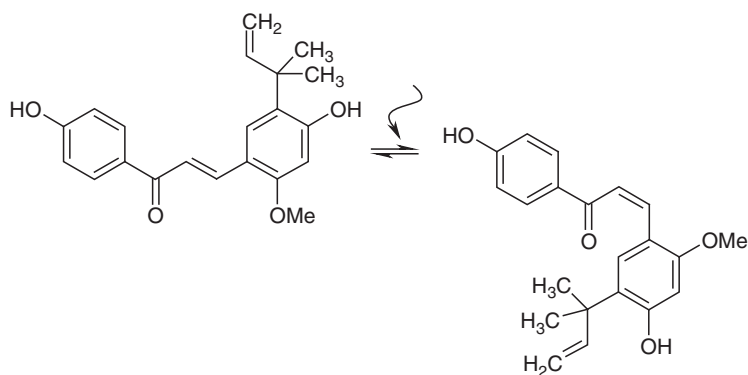


**Figure 2.2.14** *cis-trans* isomerisation of licochalcone A.

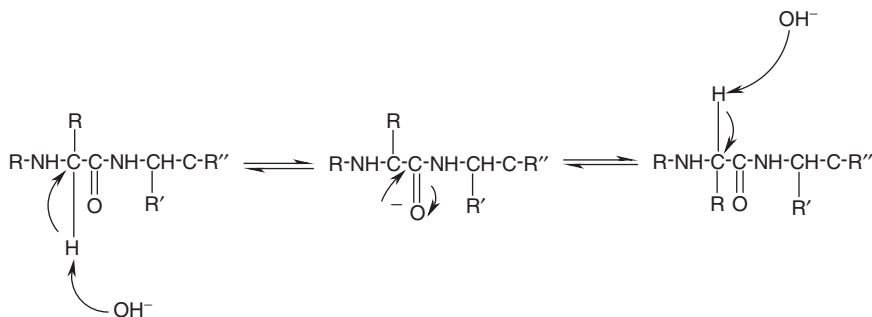


**Figure 2.2.15** Racemisation from L- to D-amino acids.

### 2.2.4 Degradation by racemisation

Possible racemisation may take place in drug candidates that include a chiral centre, i.e. carbon bound to four different groups. There are many examples, and one is amino acids except for glycine, where base-catalysed racemisation of L-amino acids forms impurities of corresponding D-amino acids. This is due to acidic properties of the alpha-hydrogen of amino acids. The acidity of the alpha-hydrogen is increased in amino acids with electronegative side chains, which weakens the carbocation properties of the acyl carbon, see Figure 2.2.1. The racemisation reaction is shown in Figure 2.2.15 and may take place in all drug candidates that are peptides or proteins.

### 2.2.5 Polymerisation

Polymerisation reactions between identical drug substance molecules may form large and complex degradation products. This is especially seen for several  $\beta$ -lactam antibiotics. The polymerisation of  $\beta$ -lactams has been shown to occur via various reactions; however, one example is aminolysis between the free carboxylic acid formed in the ring-opened impurity of ampicillin, ampicilloic acid, and the side-chain amine of another ampicillin molecule as shown in Figure 2.2.16 (Bundgaard and Larsen, 1977).

Polymerisation impurities may be immunogenic, and polymerisations of penicillins, in the form of an aqueous solution, play a major role in penicillin allergy and should therefore be avoided. That is one of the reasons why many penicillins are formulated as solid drugs or as granulations to be dissolved shortly before administration.

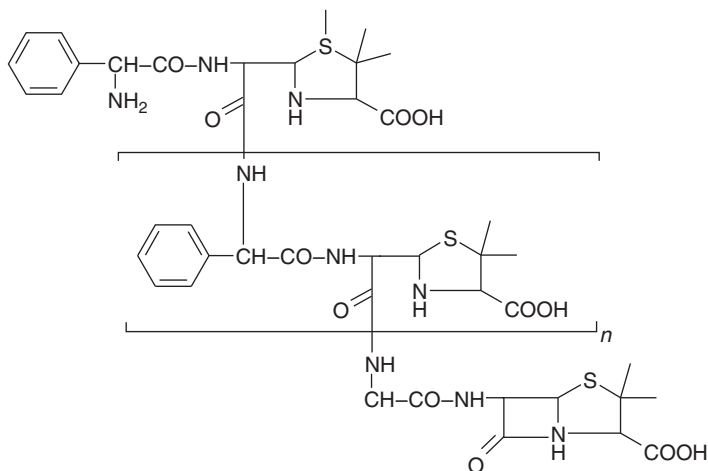


**Figure 2.2.16** Polymerisation of ampicillin.

## 2.2.6 Conclusions

Degradation of prodrug and drug candidates and substances may often be initiated by environmental factors within the atmosphere such as humidity, which may induce hydrolysis; oxygen, which may induce oxidation; or light, which among others may induce *cis-trans* isomerisation. However, it is often possible to identify vulnerable functional groups that are sensitive to one or more of these inducing factors, such as carboxyl, carbonyl, alcohol, chiral centres or double bonds within the molecules. This is important for explaining the degradation mechanisms and describing the kinetics of these reactions, which should be used in the documentation of the stability of a drug substance, i.e. the active pharmaceutical ingredient (API), and the final drug product.

## References

- Atkins PJ, Herbert TO, Jones NB (1986). Kinetic studies on the decomposition of erythromycin A in aqueous acidic and neutral buffers. *Int J Pharm* 30: 199–207.
- Bundgaard H (1977). Aminolysis of the 6 $\beta$ -amidinopenicillanic acid mecillinam. Imidazole formation and intramolecular participation of the amidino side chain. *Acta Pharm Suec* 14: 267–278.
- Bundgaard H, Larsen C (1977). Polymerization of penicillins IV. Separation isolation and characterization of ampicillin polymers formed in aqueous solution. *J Chromatogr* 132: 51–59.

- Connors KA, Amidon GL, Stella VJ (1986). *Chemical Stability of Pharmaceuticals. A Handbook for Pharmacists*, 2nd edn. New Jersey: Wiley-Interscience Publication John Wiley and Sons 3–847.
- Garrett ER (1957). The kinetics of solvolysis of acyl esters of salicylic acid. *J Am Chem Soc* 79: 3401–3408.
- Gráf L, Hajós G, Patthy A, Cseh G (1973). The influence of deamidation on the biological activity of porcine adrenocorticotropin hormone ACTH. *Horm Metab Res* 5: 142–143.
- Kurath P, Jones PH, Egan RS, Perun TJ (1971). Acid degradation of erythromycin A and erythromycin B. *Experientia* 27: 362.
- Larsen CS, Bundgaard H (1977). Kinetics and mechanism of degradation of mecillinam in aqueous solution. *Arch Pharm Chemi Sci* 5: 66–86.
- Steffansen B, Bundgaard H (1989). Erythromycin prodrugs: kinetics of hydrolysis of erythromycin and various erythromycin 2'-esters in aqueous solution and human plasma. *Int J Pharm* 56: 159–168.
- Steffansen B, Nielsen CU, Frokjaer S (2005). Delivery aspects of small peptides and substrates for peptide transporters. *Eur J Pharm Biopharm* 60: 241–245.
- Thomsen AE, Friedrichsen GM, Sørensen AH, *et al.* (2003a). Prodrugs of purine and pyrimidine analogues for the intestinal di/tri-peptide transporter PEPT1: affinity for PEPT1 in Caco-2 cells, drug release in aqueous media and in vitro metabolism. *J Control Rel* 86: 279–292.
- Thomsen AE, Friedrichsen GM, Sørensen AH, *et al.* (2003b). Erratum to Prodrugs of purine and pyrimidine analogues for the intestinal di/tripeptide transporter PEPT1: affinity for hPEPT1 in Caco 2 cells drug release in aqueous media and in vitro metabolism. *J Control Release* 88: 343.



## 2.3

### Kinetics of decomposition in aqueous solution

*Bente Steffansen, Carsten Uhd Nielsen and Birger Brodin*

The stability of (pro)drug candidates in an aqueous solution can be described not only mechanistically (see Chapter 2.2) but also kinetically, in terms of both the rate and order of degradation. Such kinetic stability investigations are relevant in molecular biopharmaceutics, as well as in preclinical development, in order to investigate the rate of possible *in vitro* metabolism of drug candidates and/or their release from prodrugs. Investigations may take place in relevant buffer solutions at a specific pH or in artificial biological media with or without specific enzymes, or in genuine biological media, such as intestinal, gastric, lachrymal, salivary and/or other blood fluids. The pH values of a number of potentially relevant biofluids are shown in Table 2.1.2. Furthermore, *in vitro* metabolism or release from prodrugs may be investigated in various tissue homogenates, for example intestinal, hepatic, or nephritic homogenates, or in homogenates of various relevant cell cultures such as enterocytic, hepatocytic, erythrocytic or proximal tubular cell homogenates. Kinetic investigations in biopharmaceutical and preclinical development are often described by degradation orders, rate constants and half lives ( $t_{1/2}$ ), and sometimes, if specific enzymes are identified as rate limiting, by Michaelis–Menten kinetics, and thus by  $K_m$  and  $V_{max}$  values (see Chapter 3.3).

However, kinetic stability investigations are also an integral part of the documentation of impurities arising from possible decomposition reactions that may take place during storage of the pharmaceutical product as well as an integrated part of establishing their shelf life. Shelf-life investigations are normally initiated during preformulation and pharmaceutical formulation development, through the study of such kinetics as reaction order and rate constants of (pro)drug substances in various aqueous solutions at specific pH, temperature and ionic strengths. The criterion generally accepted by authorities in the field is that a maximum of 5% of the formulated (pro)drug substance may be decomposed during storage. For this reason, shelf-life investigations often deal with the time

taken for 5% of the drug substance, i.e. the API (active pharmaceutical ingredient), to decompose, determined as  $t_{5\%}$ .

Besides determining the half life ( $t_{1/2}$ ) and shelf life ( $t_{5\%}$ ) of drug candidates, it is also important to understand the kinetics and thus the order of the decomposition reactions. Furthermore, one needs to identify and describe the influence of various factors, for example enzymes, pH, solubility, excipient and temperature, on the kinetics and thus on the rate of degradation reactions.

The purpose of this chapter is to present the importance of zero-, first- and second-order kinetics in the description of stability kinetics of (pro)drug candidates and of relevance for formulation and bioavailability. Furthermore, the influence of pH, temperature, buffers and ionic strength on the decomposition kinetics of (pro)drug candidates and thus on the establishment of shelf life will be described. Finally, a description of the influence of biofluid (pH and enzymes) on *in vitro* metabolism and *in vitro* release kinetics of prodrugs will be given.

### 2.3.1 First-order and pseudo zero-order kinetics of irreversible reactions

The spontaneous decomposition reaction of a drug candidate A, in which the reaction is purely dependent on the decomposition of A to form metabolites or impurities by an irreversible reaction, is illustrated in Scheme 2.3.1. The same kind of reaction may take place in the release of drug candidate ( $A^*$ ) from prodrug PA.



The rate of such a decomposition reaction  $v$  may be described by Equation 2.3.1 in which  $[A]$  is the concentration of (P)A,  $k$  is the rate constant of its decomposition reaction and  $[A]_t$  is the concentration of (P)A at a given time  $t$ .

$$v = -\frac{d[A]}{dt} = k[A]_t \quad (2.3.1)$$

The definition of the overall order of a reaction is defined as the sum of its concentration term exponents in a rate equation (Connors *et al.*, 1986). The sum of concentration term exponents in Equation 2.3.1 is one ( $[A]^1$ ), the reaction being purely dependent on (P)A, and consequently the degradation is of the first order. The rate constant  $k$  is thus the first-order rate constant given at  $\text{time}^{-1}$ . The rate constant  $k$  is independent of the

initial concentration  $[A]_0$ , whereas the numbers of (P)A degraded per time unit (e.g. mol (P)A degraded  $\text{min}^{-1}$ ) change with time. It is easier to understand this relation when Equation 2.3.1 is integrated into Equation 2.3.2 and rearranged to form Equation 2.3.3, since the first-order degradation may be described by a logarithmic function.

$$[A]_t = [A]_0 e^{-kt} \quad (2.3.2)$$

$$\log[A]_t = \log[A]_0 - \frac{k}{2.303} t \quad (2.3.3)$$

From Equation 2.3.3 it can be seen that the degradation of (P)A can be illustrated graphically by a linear first-order plot of  $\log[A]_t$  versus  $t$  with a slope  $-k/2.303$ . An example of such a graph is shown in Figure 2.3.1. Equation 2.3.3 may be rearranged to Equations 2.3.4 and 2.3.5 in order to calculate the half life ( $t_{1/2}$ ) of (P)A, which is the time ( $t$ ) it takes (P)A to reach one half of  $[A]_0$ , and the shelf life ( $t_{5\%}$ ), which is the time it takes to reach 95% of  $[A]_0$  respectively;  $k_{\text{obs}}$  is the observed rate constant.

$$t_{1/2} = \frac{\ln 2}{k_{\text{obs}}} \quad (2.3.4)$$

$$t_{5\%} = \frac{\ln 100/95}{k_{\text{obs}}} \quad (2.3.5)$$

In cases where only dissolved (P)A spontaneously decomposes to form an impurity, metabolite or  $A^*$  according to Scheme 2.3.1, and where (P)A is formulated in a suspension, the accessible amount for degradation, i.e.  $[A]_0$ , corresponds to the solubility ( $S$ ) of (P)A. As soon as one molecule of (P)A is decomposed, there is room for another molecule to dissolve from the suspension, and consequently  $[A]_0$  is constant and the rate of degradation is then described by Equation 2.3.6. In Equation 2.3.6, the concentration term exponent may be considered as constant, i.e. zero, and the observed pseudo zero-order rate constant  $k_{\text{obs}} = k[A]_0$  subsequently describes the reaction kinetics.

$$v = -\frac{d[A]}{dt} = k[A]_0 = k_{\text{obs}} \quad (2.3.6)$$

Equation 2.3.6 can be integrated to form Equation 2.3.7:

$$[A]_t = [A]_0 - k_{\text{obs}} t \quad (2.3.7)$$

From Equation 2.3.7 it can be seen that the degradation of (P)A may be illustrated graphically by a linear plot of  $[A]_t$  versus  $t$  with a slope of  $-k_{\text{obs}}$



given as a concentration term per unit time. Thus pseudo zero-order  $k_{\text{obs}}$  is dependent on  $[A]_0$ . However, the number of moles decomposed per time unit does not change with time as long as the suspension is maintained. The half life ( $t_{1/2}$ ) and shelf life ( $t_{5\%}$ ) of (P)A may be calculated from Equations 2.3.8 and 2.3.9 respectively.

$$t_{1/2} = \frac{[A]_0}{2k} \quad (2.3.8)$$

$$t_{5\%} = \frac{[A]_0}{20k} \quad (2.3.9)$$

Very few decomposition reactions of (pro)drug candidates are genuine first-order or pseudo zero-order reactions. However, many may be described by second-order and pseudo first-order kinetics as described in Section 2.3.2.

### 2.3.2 Second-order and pseudo first-order kinetics of irreversible reactions

Second-order reactions occur, for example, if a dissolved (pro)drug substance (P)A reacts at a ratio of 1:1 with another similar dissolved (pro) drug molecule (P)A to form a product by an irreversible reaction according to Scheme 2.3.2. The rate of such decomposition may be described by Equation 2.3.10:



$$v = -\frac{d[A]}{dt} = k[A]^1[A]^1 = k[A]^2 \quad (2.3.10)$$

Two concentration term exponents ( $[A]^2$ ) are involved, and thus the reaction may be described by second-order kinetics. Equation 2.3.10 may be transformed into Equation 2.3.11 and rearranged to form Equation 2.3.12 in which  $k$  is the second-order rate constant given as concentration<sup>-1</sup> time<sup>-1</sup>.

$$\int_{[A]_0}^{[A]_1} -\frac{d[A]}{[A]^2} = \int_0^t kt \quad (2.3.11)$$

$$\frac{1}{[A]_t} - \frac{1}{[A]_0} = kt \quad (2.3.12)$$

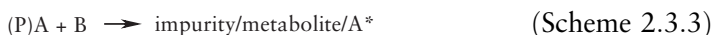
From Equation 2.3.12, it can be seen that the decomposition may be illustrated graphically by a linear plot of  $1/[A]_t - 1/[A]_0$  versus  $t$  with a slope of  $-k$  given as concentration<sup>-1</sup> time<sup>-1</sup>. Equation 2.3.12 may be rearranged to give Equations 2.3.13 and 2.3.14 from which  $t_{1/2}$  and  $t_{5\%}$  may be calculated respectively.

$$t_{1/2} = \frac{1}{k[A]_0} \quad (2.3.13)$$

$$t_{5\%} = \frac{0.052}{[A]_0 k} \quad (2.3.14)$$

An example of such a second-order reaction is the dimerisation of ampicillin, in which two identical ampicillin molecules form ampicillin dimers that further polymerise, as illustrated in Figure 2.2.16 (Bundgaard, 1976).

Second-order reactions may also take place between (P)A and a second substance B, e.g. an excipient, to form impurity or metabolite or A\* by an irreversible reaction according to Scheme 2.3.3.



The rate of degradation  $\nu$  may then be described by Equation 2.3.15, in which  $k$  is the second-order rate constant of the reaction.

$$\nu = -\frac{d[A]}{dt} = -\frac{d[B]}{dt} = -k[A]^1[B]^1 \quad (2.3.15)$$

If  $[A]_t = [A]_0 = [P]_t$  and  $[B]_t = [B]_0 = [P]_t$ , where  $[A]_0$  and  $[B]_0$  are initial concentrations of (P)A and B respectively, and  $[P]_t$  is the product formed at time  $t$ , then Equation 2.3.15 may be rearranged to give Equation 2.3.16:

$$\ln \frac{[A]_0 - [P]_t}{[B]_0 - [P]_t} = ([A]_0 - [B]_0)kt + \ln \frac{[A]_0}{[B]_0} \quad (2.3.16)$$

The decomposition may be illustrated graphically by a linear plot of  $\ln \frac{([A]_0 - [P]_t)}{([B]_0 - [P]_t)}$  versus  $t$  with slope  $([A]_0 - [B]_0)kt$ .

Many second-order reactions may be kinetically simplified to pseudo first-order reactions. An example of this is the irreversible second-order hydrolysis of the ester prodrug valaciclovir to form parent aciclovir and valine, which is shown in Figure 2.2.4 (Thomsen *et al.*, 2003a,b). In

general terms, if a (pro)drug candidate (P)A reacts irreversibly with e.g. water (B) at a ratio of 1:1 to produce drug substance A\* (Scheme 2.3.3), the rate of degradation  $\nu$  can be described by the Equation 2.3.16 in which  $k$  is the second-order rate constant, and the sum of concentration term exponents ( $[A]^1 + [B]^1$ ) is two.

However, in the case of  $[B] \gg [A]$ , the kinetics of the reaction may be described by Equation 2.3.17, which may be rearranged to form Equations 2.3.18 and 2.3.19. The apparent sum of concentration term exponents is then reduced from two in Equation 2.3.17 to one in Equations 2.3.18 and 2.3.19, namely from  $([A]^1 + [B]^1)$  to  $([A]^1)$ , and consequently the apparent kinetics are termed pseudo first-order, in which the observed pseudo first-order rate constant ( $k_{\text{obs}} = k[A]$ ) is given as unit  $\text{time}^{-1}$ .

$$-\frac{d[A]}{dt} = k_{\text{obs}}[A] \text{ and } k_{\text{obs}} = k[B] \quad (2.3.17)$$

$$[A]_t = [A]_0 e^{-k_{\text{obs}} t} \quad (2.3.18)$$

$$\log[A]_t = \log[A]_0 - \frac{k_{\text{obs}}}{2.303} t \quad (2.3.19)$$

From Equation 2.3.19 it can be seen that the degradation of (P)A can be illustrated graphically by a linear first-order plot of  $\log[A]_t$  versus  $t$ .

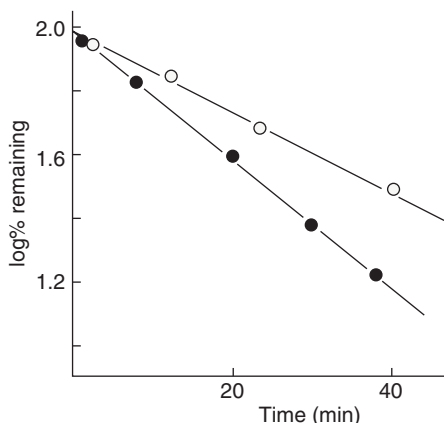


**Figure 2.3.1** The log of % remaining erythromycin 2'-acetate prodrug versus time, representing a pseudo first-order plot of erythromycin 2'-acetate degradation in an aqueous buffer solution at pH 4.00 (●) and pH 7.4 (○) at  $37 \pm 2^\circ\text{C}$ . Reproduced from Steffansen B, Bundgaard H (1989). Erythromycin prodrugs: kinetics of hydrolysis of erythromycin and various erythromycin 2'-esters in aqueous solution and human plasma. *Int J Pharm* 56: 159–168.

**Table 2.3.1** Time points at which % remaining erythromycin 2'-acetate prodrug was analysed in an aqueous buffer solution pH 7.4 at  $37 \pm 2^\circ\text{C}$ 

Time (min)	% Remaining erythromycin 2'-acetate prodrug	Log % remaining erythromycin 2'-acetate prodrug
0	100	2.00
3	95.5	1.98
15	75.8	1.88
26	50.1	1.70
41	31.6	1.50

Another example of irreversible pseudo first-order hydrolysis besides that of valaciclovir is the hydrolysis of erythromycin 2'-acetate prodrug (PA). An example of a first-order plot is shown in Figure 2.3.1 in which a plot of overall % degradation of PA in aqueous buffer solution of pH 4.00 (filled circle) and pH 7.40 (open circle) at  $37 \pm 2^\circ\text{C}$  is shown (Steffansen and Bundgaard, 1989). The slope of such graphs is represented by  $-k_{\text{obs}}/2.303$ .

The data illustrated in Figure 2.3.1 are given in Table 2.3.1. Using these data,  $k_{\text{obs}}$  may be calculated by linear regression (time versus  $\log k_{\text{obs}}$ ) as  $0.0053 \text{ min}^{-1}$ . When one has calculated  $k_{\text{obs}}$  of the decomposition reaction, its corresponding half life ( $t_{1/2}$ ) and shelf life ( $t_{5\%}$ ) may be calculated using Equations 2.3.4 and 2.3.5, to be approximately 129 min and 10 min respectively.

### 2.3.3 Pseudo first-order kinetics of reversible reactions

First-order reactions may also be reversible (Scheme 2.3.4), in which two first-order rate constants are involved, one that describes the rate of the forward reaction ( $k_{+1}$ ) and a second that describes the rate of the reverse reaction ( $k_{-1}$ ). At equilibrium the amount going forward must equal the amount going in reverse.



The rate,  $v = d[\text{A}]/dt$ , of such reversible decomposition for which the forward and reverse reactions are of the first order, e.g. the *cis-trans*

isomerisation of licochalcone A (see Figure 2.2.14) may be described by Equation 2.3.20.

$$-\frac{d[A]_0}{dt} = k_{+1}[A] - k_{-1}[B] \quad (2.3.20)$$

The integrated form of Equation 2.3.20 is Equation 2.3.21, which may be rearranged into Equation 2.3.22, where  $[A]_0$  represents the initial concentration of the drug candidate,  $[A]_t$  the concentration at time  $t$  and  $[A]_{eq}$  the equilibrium concentration.

$$\log \frac{[A]_0 - [A]_{eq}}{[A]_t - [A]_{eq}} = \frac{(k_{+1} + k_{-1})}{2.303} t \quad (2.3.21)$$

$$\log([A]_0 - [A]_{eq}) = -\frac{k_{+1} + k_{-1}}{2.303} t + \log([A]_t - [A]_{eq}) \quad (2.3.22)$$

A linear plot of  $\log([A]_0 - [A]_{eq})$  versus  $t$  has a slope of  $-(k_{+1} + k_{-1})/2.303$  and intercept  $\log([A]_t - [A]_{eq})$ . By rearranging Equation 2.3.22 into Equations 2.3.23 and 2.3.24, the shelf life and half life respectively of drug candidates decomposed by reversible first-order reactions may be calculated:

$$t_{5\%} = \frac{\ln 100/95}{k_{+1} + k_{-1}} \quad (2.3.23)$$

$$t_{1/2} = \frac{\ln 2}{k_{+1} + k_{-1}} \quad (2.3.24)$$

### 2.3.3.1 Parallel irreversible pseudo first-order kinetics

Decomposition of drug candidates may also proceed via two or more parallel pseudo first-order reactions in which two pseudo first-order rate constants are involved. In Scheme 2.3.5,  $k_1$  is the rate constant for the drug candidate, (P)A, decomposing to B, and  $k_2$  is the rate constant for (P)A decomposing to C. This is the case for the acid-catalysed hydrolysis of the model prodrug Glu(aciclovir)-Sar which decomposes into aciclovir ( $A^*$ ) as well as a suggested cyclised impurity (Thomsen *et al.*, 2003a,b). The proposed degradation pathway for Glu(aciclovir)-Sar is shown in Figure 2.2.8.



The rate of such parallel reactions may be described by Equation 2.3.25.

$$-\frac{d[A]}{dt} = k_1 + k_2[A]_t \quad (2.3.25)$$

When measuring the disappearance of (P)A, the observed rate constant is the sum of the rate constants for the parallel decompositions, i.e.  $k_{\text{obs}} = k_1 + k_2$  and Equation 2.3.25 equals Equation 2.3.19. Thus  $t_{1/2}$  and  $t_{5\%}$  for the disappearance of A may be calculated by Equations 2.3.4 and 2.3.5 respectively.

However, it may be desirable to determine the separate values of  $k_1$  and  $k_2$ , since such rate constants may give important information about, for example, the rate of impurity formation. Separate values for  $k_1$  or  $k_2$  may be determined by measuring the products B and C. The equation describing the production of B is given by Equation 2.3.26:

$$\frac{d[B]}{dt} = k_1[A]_t \quad (2.3.26)$$

By integrating Equation 2.3.26, in which  $[A]_t = k_1/k_{\text{obs}}[A]_0 e^{-k_{\text{obs}}t}$  one gets Equation 2.3.27:

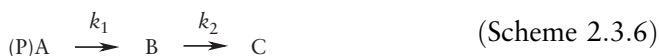
$$\log([B]_{\infty} - [B]_t) = \log(k_1/k_{\text{obs}}[A]_0) - k_{\text{obs}}t/2.303 \quad (2.3.27)$$

Equation 2.3.27 describes a plot of  $\log([B]_{\infty} - [B]_t)$  versus  $t$ , which is linear with a slope of  $-k_{\text{obs}}t/2.303$  and an intercept  $\log(k_1/k_{\text{obs}}[A]_0)$ , from which  $k_1$  may be calculated according to Equation 2.3.28.

$$k_1 = [B]_{\infty} k_{\text{obs}} / [A]_0 \quad (2.3.28)$$

### 2.3.4 Pseudo first-order reactions of irreversible consecutive reactions

Irreversible consecutive reactions may proceed if drug candidate (P)A degrades to impurity B, which then further degrades to impurity C by respective first-order rate constants  $k_1$  and  $k_2$ , as illustrated in Scheme 2.3.6.



The rate of decomposition may be described by Equations 2.3.29 to 2.3.31.

$$\frac{d[A]}{dt} = -k_1[A] \quad (2.3.29)$$

$$\frac{d[B]}{dt} = -k_2[B] + k_1[A] \quad (2.3.30)$$

$$\frac{d[C]}{dt} = k_2[B] \quad (2.3.31)$$

Equations 2.3.29 to 2.3.31 integrate to give Equations 2.3.32 to 2.3.34 respectively.

$$[A]_t = [A]_0 e^{-k_1 t} \quad (2.3.32)$$

$$[B]_t = [A]_0 \frac{k_1}{k_2 - k_1} (e^{-k_1 t} - e^{-k_2 t}) \quad (2.3.33)$$

$$[C]_t = [A]_0 - [A]_t - [B]_t \quad (2.3.34)$$

The half life and shelf life describing the pseudo first-order disappearance of (P)A may be calculated from Equations 2.3.4 and 2.3.14 respectively. An example of an irreversible consecutive reaction is that of the decomposition of 2'-acetate-erythromycin prodrug (PA) in acidic solution to 2'-acetate anhydroerythromycin via 2-acetate erythromycin 6,9-hemiketal, as illustrated in Figure 2.2.9.

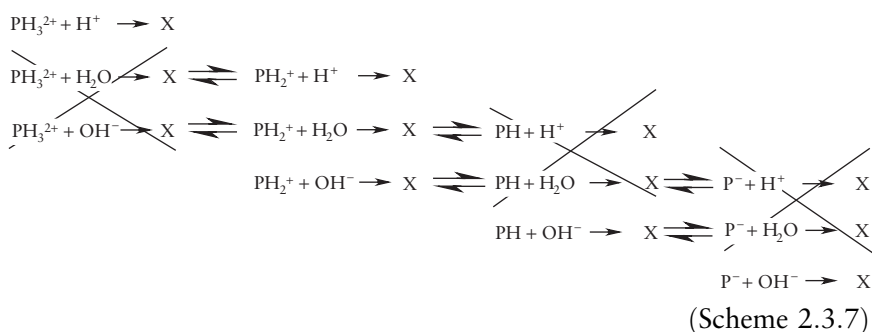
### 2.3.5 Influence of pH on decomposition rate

The stability of (pro)drug candidates in aqueous solution is often dependent on pH, and as a consequence the process is catalysed by concentrations of specific acids ( $H^+$ ) and/or bases ( $OH^-$ ). Information regarding the influence of pH on the stability of drug candidates may be obtained by systematic determination of observed pseudo first-order rate constants  $k_{obs}$  versus pH, while maintaining other factors such as temperature and ionic strength at constant values. If the pH is preserved by buffer solutions during an investigation of specific acid- and base-catalysed degradation of drug candidates, it is then necessary to investigate separately the influence of possible buffer concentrations on  $k_{obs}$  (see Section 2.3.2.5).

Obtained pseudo first-order  $k_{obs}$  values from pH rate experiments may be illustrated as a pH–rate profile, i.e. by depicting  $\log k_{obs}$  versus pH. A pH rate profile may be very helpful in the investigation of decomposition mechanisms, but it may also be very helpful in determining shelf life and evaluating possible pH-dependent metabolism. A pH profile may have any number of characteristic features, depending on the specific

acid/base-catalysed processes involved, as well as the possible species distribution arising from acidic and/or basic functionalities of the (pro) drug candidate.

An example of pH-dependent decomposition is the hydrolysis of the ester prodrug valaciclovir (P) as it forms the drug substance aciclovir and the amino acid pro-moiety valine. Valaciclovir has three  $pK_a$  values, namely 2.0, 7.2 and 9.1, associated with two primary amine functionalities and one NH-acidic functionality, cf. Table 2.1.1. Consequently, 12 potential reactions may be involved in the hydrolysis of valaciclovir, as illustrated in Scheme 2.3.7, where  $PH_3^{2+}$  is the triprotonised,  $PH_2^+$  the diprotonised,  $PH$  the monoprotonised, and  $P^-$  the fully deprotonised prodrug species.



The pH-rate profile of valaciclovir is denoted by bold squares in Figure 2.3.2. By comparing the pH-rate profile with possible reactions it is suggested that (1) below  $pK_{aI}$  the profile is described by a specific acid-catalysed reaction of the triprotonised species, (2) at  $pK_{aI} < pH < pK_{aII}$  it is described by specific acid, water-catalysed (spontaneous) and specific base-catalysed hydrolysis of the diprotonised species, (3) at  $pK_{aII} < pH < pK_{aIII}$  it is described by specific base-catalysed hydrolysis of the monoprotonised species, and (4) at  $pH > pK_{aIII}$  it is described by specific base-catalysed hydrolysis of the fully deprotonised species.

Those reactions believed not to occur are marked by crosses in Scheme 2.3.7. Thus the proposed rate equation is given in Equation 2.3.35 (Thomsen *et al.*, 2003a,b).

$$\begin{aligned}
 k_{obs} = & k'_{H^+} \cdot [H^+] \cdot f_{PH_3^{2+}} + k_{H^+} \cdot [H^+] \cdot f_{PH_2^+} + k_o f_{PH_2^+} + k_{OH^-} \cdot [OH^-] \cdot f_{PH_2^+} \\
 & + k'_{OH^-} [OH^-] \cdot f_{PH} + k''_{OH^-} [OH^-] \cdot f_{P^-}
 \end{aligned}
 \quad (2.3.35)$$

In Equation 2.3.35  $f_{PH_3^{2+}}$  is the species fraction of triprotonised,  $f_{PH_2^+}$  the species fraction of diprotonised,  $f_{PH}$  the species fraction of



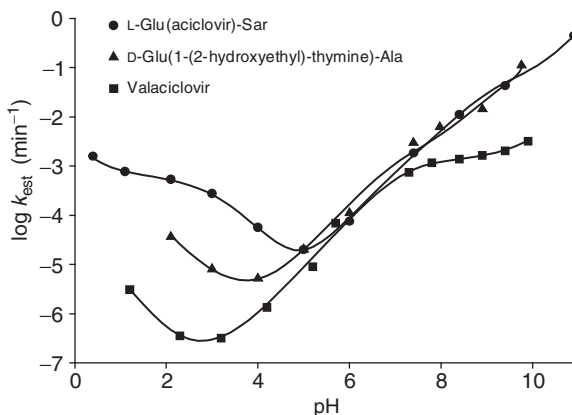


**Figure 2.3.2** The pH-rate profile of  $\log k_{\text{obs}}$  ( $\text{min}^{-1}$ ) versus pH for valaciclovir (bold squares), L-Glu(acyclovir)-Sar (bold circles) and D-Glu[1-(2-hydroxyethyl)thymine]Ala (bold triangles) at 37 °C. The solid valaciclovir curve was obtained by fitting experimental data to Equation 2.3.34, using experimentally determined pKa values. Reproduced from Thomsen AE, Friedrichsen GM, Sørensen AH, *et al.* (2003a). Prodrugs of purine and pyrimidine analogues for the intestinal di/tri-peptide transporter PEPT1: affinity for PEPT1 in Caco-2 cells, drug release in aqueous media and in vitro metabolism. *J Control Rel* 86: 279–292.

monoprotionised and  $fP^-$  the species fraction of fully deprotonised pro-drug P. Species fractions may be calculated as described in Section 2.1.1.

The profiles of pH rates are a very useful tool in pharmaceutical development. Using such profiles the pharmaceutical developer may gain an overview of the influence of pH on the decomposition kinetics of (pro) drug candidates. This is important not only in terms of determining and documenting the shelf life of (pro)drugs, but also in preclinical development, where it can help to evaluate possible acid/base-catalysed metabolism and elimination issues. One example is the possible influence of various environmental pH values *in vivo*, i.e. possible acid/base-catalysed metabolism of orally administered (pro)drug candidates during their gastrointestinal passage (see the pH of various biological fluids – Table 2.1.2). However, one should bear in mind that metabolism and elimination may often be enzyme-catalysed processes; these points are further described in Section 2.3.9.

### 2.3.6 Influence of temperature on decomposition rate

The decomposition rate in an aqueous solution of many (pro)drug candidates is dependent on temperature. For many small molecular drug substances such as ASA, the influence of temperature on degradation rate

may be described by the Arrhenius equation (Equation 2.3.36) that in logarithmic terms becomes Equations 2.3.37 and 2.3.38.

$$k_{\text{obs}} = Ae^{-E_a/RT} \quad (2.3.36)$$

$$\ln k_{\text{obs}} = \ln A - \frac{E_a}{RT} \quad (2.3.37)$$

$$\log k_{\text{obs}} = \log A - \frac{E_a}{2.303RT} \quad (2.3.38)$$

In Arrhenius Equations 2.3.36–2.3.38,  $k_{\text{obs}}$  is the observed rate constant;  $E_a$  is the activation energy, which usually ranges from 50 to 150 kJ mol<sup>-1</sup> and is the energy barrier to be overcome if a reaction is to take place when reactants collide;  $R$  is the gas constant, i.e. 8.303 J K<sup>-1</sup> mol<sup>-1</sup>;  $A$  is the frequency factor indicating collision numbers per unit time per mole, which is assumed to be independent of temperature for any given reaction.  $T$  is the temperature given in K; 2.303 is a constant that relates the log scale to the ln scale. Thus, from Equation 2.3.38, it can be seen that a plot of  $\log k$  versus  $1/T$  should be linear with a slope of  $-E_a/2.303R$  and an intercept of  $\log A$ . The Arrhenius plot for water-catalysed hydrolysis, termed ‘spontaneous’ hydrolysis is shown for acetyl salicylic acid (ASA) in Figure 2.3.3 and is cited from Garrett, 1957.

For many small molecular drug substances and candidates, an advanced form of the Arrhenius equation, Equation 2.3.39, is applied in order to estimate shelf life at room temperature from temperature-accelerated studies performed at temperatures that are typically between 40 °C and 80 °C. In the EMEA note for guidance on stability testing, long-term, intermediate and accelerated stability testing temperatures of 25 °C, 30 °C and 40 °C respectively are suggested (EMEA, 2006).

$$\log \frac{k_2}{k_1} = -\frac{E_a}{2.303R} \left[ \frac{1}{T_1} - \frac{1}{T_2} \right] \quad (2.3.39)$$

Thus, by isolating  $k_1$  from Equation 2.3.39, one can calculate its value by inserting  $k_2$  values determined from accelerated conditions, using Equation 2.3.40.

$$\log k_2 = -\frac{E_a}{2.303R} \left[ \frac{1}{T_1} - \frac{1}{T_2} \right] + \log k_1 \quad (2.3.40)$$

The Arrhenius equation holds true as long as no change in reaction mechanism is observed with temperature. However, a change in reaction mechanism may typically be observed by a reaction order change and/or

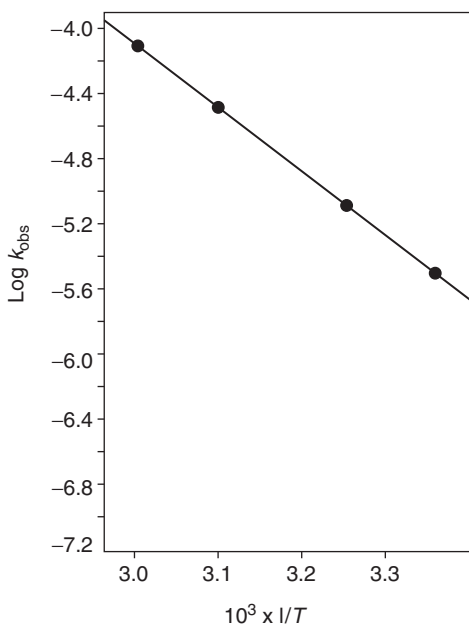


**Figure 2.3.3** Arrhenius plot for so-called 'spontaneous' hydrolysis of acetyl salicylic acid (ASA).  $k_{\text{obs}}$  is given in  $\text{s}^{-1}$ . Reproduced from Garrett ER (1957). The kinetics of solvolysis of acyl esters of salicylic acid. *J Am Chem Soc* 79: 3401–3408.

impurity changes with temperature. Examples of this are some macromolecular drug candidates such as proteins, in which the decomposition rate at room temperature may be, for example, a deamidation reaction as shown in Figure 2.2.7. However at temperatures such as  $60^\circ\text{C}$ , for example, denaturation reactions such as a change in tertiary structure may take place. In such cases the decomposition rate may not be accurately described by the Arrhenius equation.

### 2.3.7 Influence of ionic strength on decomposition rate

Biological media contain electrolyte at a concentration of approximately 0.16M, and therefore there is considerable relevance in preclinical development in investigating the influence of ionic strength on hydrolysis. The same holds true for the pharmaceutical development of parenteral drugs as well as that of eye drops where such electrolytes such as NaCl are added in order to achieve an isotonic solution. The influence of electrolyte concentration on  $k_{\text{obs}}$  in dilute solutions, i.e. ionic strengths less than

$0.01 \text{ mol kg}^{-1}$ , may be described by the Brøndsted-Bjerrum Equation 2.3.41:

$$\log k = \log k_0 + 1.036 A z_A z_B I^{1/2} \quad (2.3.41)$$

For ionic strengths between  $0.01$  and  $0.1 \text{ mol kg}^{-1}$ , a modified form of the Brøndsted-Bjerrum equation, Equation 2.3.42 may be applied:

$$\log k = \log k_0 + 1.036 A z_A z_B \left[ \frac{I^{1/2}}{1 - I^{1/2}} \right] \quad (2.3.42)$$

In the Brøndsted-Bjerrum equation,  $z_A$  and  $z_B$  are the charges of the reacting molecules,  $I$  is the ionic strength of the solution and  $A$  is a constant dependent on the dielectric constant of the solution, i.e.  $0.509$  in water at  $298 \text{ K}$ . The influence of ionic strength ( $I$ ) on the hydrolysis rate is often determined at varying  $\text{KCl}$  concentrations but constant  $\text{pH}$ , temperature and buffer concentration.

An example is the observed decrease in the rate of ester hydrolysis and thus a  $k_{\text{obs}}$  decrease from  $2.17 \times 10^{-3}$  to  $0.11 \times 10^{-3} \text{ min}^{-1}$ , with  $I$   $0.05$ – $0.5 \text{ M}$  by  $\text{KCl}$ , of the zwitterionic species of the model prodrug  $\text{Glu}(\text{OBzl})\text{-Sar}$  when investigated in  $0.02 \text{ M}$  phosphate buffer,  $\text{pH } 7.4$  at  $37^\circ\text{C}$  (Lepist *et al.*, 2000).

It can be seen from Equation 2.3.42 that the influence of  $I$  on  $k_{\text{obs}}$  is charge dependent. Thus when  $I$  increases,  $k_{\text{obs}}$  for  $\text{OH}^-$ -catalysed hydrolysis in molecules carrying a negative charge or positive charge may increase or decrease respectively. In the present case,  $k_{\text{obs}}$  decreases with  $I$  and consequently it is suggested that the amine positive charge in the zwitterionic species of  $\text{Glu}(\text{OBzl})\text{-Sar}$  plays a larger role than that of the carboxylic negative charge. This point is illustrated by Figure 2.3.4 where negative  $\text{Cl}^-$  electrolytes are attracted by the protonised amine. This negative cloud of chloride ions inhibits the nucleophil attack by the

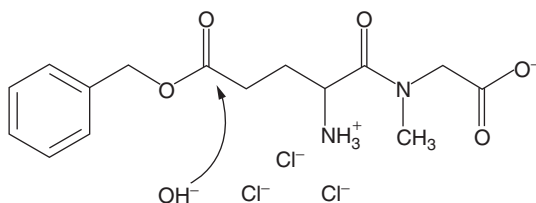


**Figure 2.3.4** Nucleophil attack by specific base catalyst  $\text{OH}^-$  on the acyl carbon of  $\text{Glu}(\text{OBzl})\text{-Sar}$  can be inhibited by  $\text{Cl}^-$ . Data from Lepist E-I, Kusk T, Larsen DH, *et al.* (2000). Stability and *in vitro* metabolism of dipeptide model prodrugs with affinity for the oligopeptide transporter. *Eur J Pharm Sci* 11: 43–50.

negative specific base catalyst  $\text{OH}^-$  on the acyl carbon of Glu(OBzl)-Sar and consequently decreases its hydrolysis rate (Lepist *et al.*, 2000).

### 2.3.8 Influence of buffers on decomposition rate

General acid/base catalysis may, for example, occur from buffers used to maintain constant pH within an aqueous solution. Buffers may be present in biological media, two examples being phosphate and ammonia, the major urinary buffers. The main buffer in blood is carbonate, while other buffer systems in biological media rely on phosphate and lactate. The influence of these general acids and bases on the hydrolysis rate is therefore of relevance for preclinical development where metabolism and elimination studies may be performed *in vitro*. Buffers are also used in pharmaceutical formulations, and their influence on the shelf life of a drug is an important and relevant point to study. Buffer catalysis may be described by buffer catalysis constants ( $k_{\text{cat}}$ ), which may be calculated from slopes of  $k$  versus buffer concentration. Such studies are made at constant temperature, ionic strength and pH. The influence of buffers on  $k$  may be described mathematically using Equation 2.3.43.

Buffer catalysis may also be observed in pH–rate profile experiments. If that is the case, extrapolated y intercepts from buffer catalysis studies, i.e.  $k$  at zero buffer concentration ( $k_{\text{zero}}$ ), should be depicted as  $k_{\text{obs}}$  values in the pH profile.

$$k = k_{\text{zero}} + k_{\text{cat}}[\text{buffer concentration}] \quad (2.3.43)$$

Table 2.3.2 shows  $k_{\text{cat}}$  for various buffers that have an influence on the hydrolysis rate of the model prodrug Glu(OBzl)-Sar.

Based on the data presented in Table 2.3.2, it seems that  $\text{OH}^-$ -catalysed ester hydrolysis of Glu(OBzl)-Sar, i.e. at  $\text{pH} > 5$ , is especially sensitive to buffer catalysis. Of those buffers investigated, carbonate has the largest  $k_{\text{cat}}$ . However, from the present study it is not possible to elucidate which species of single buffers are catalysing the hydrolysis of Glu(OBzl)-Sar, since the buffers are applied at pH values in the region of  $\text{pK}_{\text{a}}$  values, and consequently at least two buffer species are present. Nevertheless, one might postulate that the  $k_{\text{cat}}$  for  $\text{PO}_4^{3-}$  species is larger than the  $k_{\text{cat}}$  for  $\text{HPO}_4^{2-}$  species since the  $k_{\text{cat}}$  for a total phosphate buffer increases with pH as does  $\text{PO}_4^{3-}$ , while  $\text{HPO}_4^{2-}$  decreases. Moreover, one might propose that the  $k_{\text{cat}}$  for  $\text{HCO}_3^-$  is larger than that for the  $k_{\text{cat}}$  of  $\text{CO}_3^{2-}$ , since the  $k_{\text{cat}}$  for total carbonate decreases with pH while  $\text{CO}_3^{2-}$  increases and  $\text{HCO}_3^-$  decreases.

**Table 2.3.2** Buffer catalyst constants for a number of buffers inducing catalysis of Glu(OBzl)-Sar hydrolysis in an aqueous solution at constant pH investigated at  $I=0.5$  and at  $37^\circ\text{C}$ ; data from Lepist E-I, Kusk T, Larsen DH, *et al.* (2000). Stability and *in vitro* metabolism of dipeptide model prodrugs with affinity for the oligopeptide transporter. *Eur J Pharm Sci* 11: 43–50

Buffer	pH	$k_{\text{cat}} (\text{M}^{-1} \text{min}^{-1})$
Phosphate	2.0	$7.01 \times 10^{-4}$
Phosphate	3.0	$5.47 \times 10^{-4}$
Acetate	4.0	$8.67 \times 10^{-5}$
Acetate	5.0	$6.89 \times 10^{-5}$
Phosphate	6.0	$1.30 \times 10^{-3}$
Phosphate	7.4	$2.61 \times 10^{-2}$
Phosphate	8.0	$8.25 \times 10^{-2}$
Carbonate	9.0	0.49
Carbonate	9.5	0.42

Even though buffers are present in most biological media, and for that matter tissues, the overwhelming reason for drug metabolism remains enzyme-catalysed degradation, which will be briefly described in the following Section 2.3.9.

### 2.3.9 Influence of enzymes on decomposition rate

The release of drug substances from prodrugs as well as the metabolism of drug substances may be catalysed by acids or bases, or indeed be spontaneous, i.e. water catalysed. However, abundant *in vivo* catalysts are also digestive and metabolising enzymes. The kinetics of enzyme-catalysed reactions are characterised by the saturable Michaelis–Menten kinetics which can be described mathematically by Equation 3.3.3. Since enzyme-catalysed degradation of (pro)drug substances is described by saturable kinetics, it may be applied to evaluate possible drug–drug, food–drug and excipient–drug interaction arising from these compounds being substrates for specific enzymes. Examples of identified intestinal pancreatic, brush border or cytosolic peptidases involved in the metabolism of peptide drug candidates, as well as the release of drug substances from some amide and ester prodrugs are given in Table 2.4.3, and the importance of metabolism investigation during discovery and development is discussed in Chapter 4.2.

In preclinical development and molecular biopharmaceutics, the rate of *in vitro* metabolism of drug candidates may be investigated by

determining the half life of first- or zero-order candidate metabolism in various dilute tissue homogenates such as hepatic, nephritic and intestinal preparations, or in biological fluids such as gastric, intestinal, urine, blood plasma, lacrymal or cerebrospinal fluid. However, by using tissue homogenates and biological fluids one is faced with the issue of ethics and the disadvantages connected with this field. For this reason, *in vitro* metabolism may be evaluated in suspensions of various cell culture homogenates. In some cases, membrane transporters such as P-glycoprotein (P-gp) are believed to deliver drug substance substrates to sites of metabolising enzymes such as CYP450s, which may be elegantly studied in whole tissues. There may, however, also be experimental disadvantages in using whole tissues, tissue homogenates, biological fluids or suspensions of cell culture homogenates, for instance if more than one enzyme is involved in the metabolic processes under investigation. Although *in vitro*–*in vivo* correlation may be performed on metabolic half lives, there are weaknesses associated with such studies, for instance a lack of Michaelis–Menten parameter characterisation, i.e.  $V_{\max}$  and  $K_m$ , and thus compromised understanding of those enzymes involved. Moreover, if biological materials arising from experimental animals, especially different species, are used, one needs to address the issue of variation between experimental animal and human enzymes which may compromise any *in vitro*–*in vivo* correlations.

An additional experimental problem is that enzymes are easily deactivated during tissue preparation and it is therefore important to characterise enzyme activity of known substrates by Michaelis–Menten parameters. Enzyme-catalysed *in vitro* metabolism may also be characterised in artificial gastric, pancreatic or intestinal fluids as suggested in the *US Pharmacopoeia*. Thus, specific drug candidate–enzyme interaction kinetics should be investigated in solutions of known specific enzymes and characterised by the Michaelis–Menten parameters, i.e.  $K_m$  and  $V_{\max}$ , whereas the overall rate of *in vitro* metabolism may be studied in various specific tissue or cell homogenates as well as in specific biological or artificial fluids. The American FDA has released *Guidance for Industry, Drug Metabolism/Drug Interaction Studies in the Drug Development Process* (FDA, 1997).

### 2.3.10 Conclusions

The kinetics of stability and *in vitro* metabolism of drug candidates, as well as the *in vitro* release of drug candidates from prodrugs, is often characterised in the molecular biopharmaceutical and formulation

sciences, as well as during industrial pharmaceutical and preclinical development. During pharmaceutical development and in the formulation sciences the kinetics of (pro)drug candidate stability may be characterised, mainly in order to determine parameters of impurity and shelf life. During preclinical development and in the biopharmaceutical sciences, *in vitro* metabolism of drug candidates and *in vitro* release of drug candidates from prodrugs may be characterised in order to evaluate and elucidate the influence of possible catalysts, such as acids, bases and enzymes, on ADME and on pharmacokinetic parameters.

## References

- Bundgaard H (1976). Polymerization of penicillins: kinetics and mechanism of di- and polymerization of ampicillin in aqueous solution. *Acta Pharm Suec* 13: 9–26.
- Connors KA, Amidon GL, Stella VJ (1986). *Chemical Stability of Pharmaceuticals. A Hand Book for Pharmacists*, 2nd edn. New Jersey: Wiley-Interscience Publication John Wiley & Sons 3–847.
- EMA (2006). *Note for Guidance on Stability Testing: stability testing of new drug substance and products* (CPMP/ICH/2736/99). <http://www.emea.europa.eu/pdfs/human/ich/273699en.pdf> (accessed 29 April 2009).
- FDA (1997). *Guidance for Industry, Drug Metabolism/Drug Interaction Studies in the Drug Development Process: studies in vitro*. <http://www.fda.gov/downloads/Drugs/GuidanceComplianceRegulatoryInformation/Guidances/ucm072104.pdf> (accessed 3 June 2009).
- Garrett ER (1957). The kinetics of solvolysis of acyl esters of salicylic acid. *J Am Chem Soc* 79: 3401.
- Lepist E-I, Kusk T, Larsen DH, *et al.* (2000). Stability and *in vitro* metabolism of dipeptide model prodrugs with affinity for the oligopeptide transporter. *Eur J Pharm Sci* 11: 43–50.
- Steffansen B, Bundgaard H (1989). Erythromycin prodrugs: kinetics of hydrolysis of erythromycin and various erythromycin 2'-esters in aqueous solution and human plasma. *Int J Pharm* 56: 159–168.
- Thomsen AE, Friedrichsen GM, Sørensen AH, *et al.* (2003a). Prodrugs of purine and pyrimidine analogues for the intestinal di/tripeptide transporter PEPT1: affinity for hPEPT1 in Caco 2 cells drug release in aqueous media and *in vitro* metabolism. *J Control Release* 86: 279–292.
- Thomsen AE, Friedrichsen GM, Sørensen AH, *et al.* (2003b). Erratum to Prodrugs of purine and pyrimidine analogues for the intestinal di/tripeptide transporter PEPT1: affinity for hPEPT1 in Caco 2 cells drug release in aqueous media and *in vitro* metabolism. *J Control Release* 88: 343.





# 2.4

## Chemical approaches to improving bioavailability properties of oral drug candidates

*Kristina Luthman and Bente Steffansen*

Potential oral drug candidates are generally identified in high-throughput screening campaigns focused on their *in vitro* pharmacological activity. However, the importance of bioavailability properties is also appreciated and therefore usually included in the selection process, for example based on parameters described by ‘Lipinski’s rule of five’ (Lipinski *et al.*, 2001). Nevertheless, there is still a great need for optimising bioavailability properties of drug candidates not only to include the Lipinski parameters but also to take into account biological factors such as substrate properties directed towards membrane transporters and metabolising enzymes as suggested by the FDA (US Department of Health and Human Services, FDA, Center for Drug Evaluation and Research (CDER) and Center for Biologics Evaluation and Research (CBER), 2006); this is also discussed in Parts 3 and 4. In this optimisation process, chemical approaches such as salt formation, bioisosteric replacement, and prodrug formation may be applied. The aim of this chapter is to describe and exemplify such chemical approaches used to improve the bioavailability properties of drug candidates.

### 2.4.1 Lipinski’s rule of five

Lipinski’s rule of five is based on an analysis of key physicochemical properties of drug substances in the World Drug Index (<http://www.daylight.com/dayhtml/doc/theory/index.html>).

The rule is based on four physicochemical parameters that are globally associated with solubility and permeability, and it states that drug substances are most likely to have good bioavailability when the following four parameters are fulfilled: the number of hydrogen bond (H-bond) donors < 5, the number of H-bond acceptors < 10, the molecular weight (MW) is < 500, and the logarithm of the calculated octanol/water

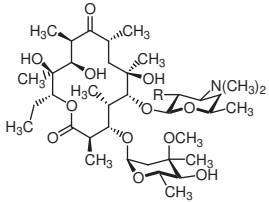
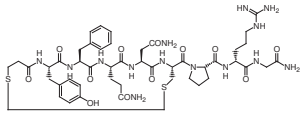
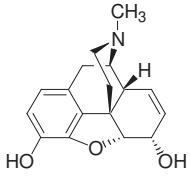
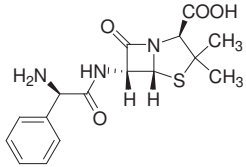
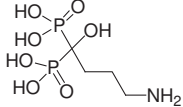
partition coefficient,  $\log P < 5$ , (Lipinski *et al.*, 2001). Since the cut-off values for each of the four parameters were five or a multiple of five, the rule was simply named the ‘rule of five’. Hydrogen bond acceptors and donors in the rule of five refer to hydrogen bonds formed between a hydrogen atom covalently bound to an electronegative atom such as N or O, and another electronegative atom, normally N or O. The hydrogen atom that is covalently bound to e.g. N or O is called the *hydrogen bond donor* and the electronegative atom (N or O) receiving the hydrogen bond is called the *hydrogen bond acceptor*.  $\log P$  in the rule of five refers to the logarithm of the partition coefficient  $P$  of the un-ionised species as described in Section 2.1.3. Hydrogen-bond donors and acceptors as well as  $\log P$  for some selected drug substances are shown in Table 2.4.1.

Lipinski’s rule of five is thus a simple and inexpensive tool to apply in the industrial ‘early drug discovery phase’, where it is the rule of thumb for medicinal chemists. All drug substances shown in Table 2.4.1, except for ivermectin, are registered as oral drug formulations. As seen from the table, several of these drug substances do not fulfil all Lipinski’s rules; however, the rule states that if two or more parameters are not within the limits the compound is expected to show poor absorption properties. To improve the predictability using the rule of five, Veber *et al.* have suggested additional parameters to be included such as polar surface area (PSA) ( $< 140 \text{ \AA}^2$ ), the sum of H-bond donors and acceptors ( $< 12$ ) and the number of rotatable bonds ( $< 10$ ) (Veber *et al.*, 2002). However, other important physicochemical parameters such as the degree of ionisation in relevant biological media ( $\text{pK}_a$  values) are not considered in the rule of five. The biopharmaceutical and preclinical scientists will also identify a number of apparent limitations to the rule, which include biological properties such as substrate properties towards metabolising enzymes and membrane transporters. These properties are not taken into consideration in the rule of five even though, as described in Parts 3 and 4, they may have a major influence on the bioavailability. Furthermore, the rule, which is based on physicochemical parameters that are globally associated with solubility, does not discriminate between solubility and dissolution. Thus it should not be used uncritically in the selection of oral drug candidates.

### 2.4.2 Salt formation

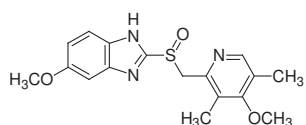
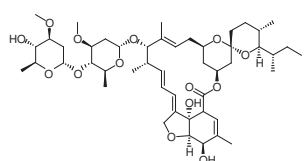
For some drug candidates, it is not the solubility but the dissolution, i.e. the solubility rate (see Chapter 4.1), that is limiting for bioavailability. Dissolution properties may sometimes be improved by salt formation simply by the stronger tendency of salts to dissociate in water. If the acid

**Table 2.4.1** Oral bioavailability (OB) (%) of selected drug substances according to the Danish Medicine Catalogue ([www.medicin.dk](http://www.medicin.dk))

<i>Drug/prodrug molecule</i>	<i>OB (%)</i>	<i>MW</i>	<i>H-bond acceptors</i>	<i>H-bond donors</i>	<i>logP</i> <i>*logD<sub>7.4</sub></i>
 R = OH: erythromycin R = OCOCH <sub>2</sub> CH <sub>2</sub> COOH: succinate ester prodrug	Varies	714.92 (814.96 prodrug)	14 (16 prodrug)	5 (4 prodrug)	*1.98
 Desmopressin	0.1	1041.2	26	17	−3.72
 Morphine	20–60	285.7	4	1	0.90
 Ampicillin	40	317.34	7	3	−2.00
 Alendronate	0.7	313.43	8	7	−2.77

(continued)

**Table 2.4.1** (Continued)

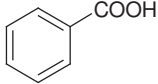
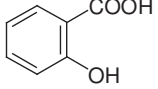
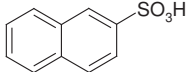
Drug/prodrug molecule	OB (%)	MW	H-bond acceptors	H-bond donors	logP *logD <sub>7.4</sub>
 Omeprazole	20–40	313.42	6	1	*2.38
 Ivermectin	Not available	875.1	14	3	6.70

Notes: MW, molecular weight; H-bond acceptors, hydrogen bond acceptors; H-bond donors, hydrogen bond donors; logP, logarithm of the distribution of the neutral drug substance between octanol and water; logD<sub>7.4</sub> logarithm of the observed distribution of the drug substance between octanol and water at pH7.4.

or base used to form the salt is strong, the salt can be expected to completely dissociate in aqueous solution and thus increase the dissolution. Drug candidates that are acids, such as carboxylic acids, may often be crystallised as, for example, sodium ( $pK_a$  16.0 for sodium) or potassium ( $pK_a$  14.8) salts. Sodium hydroxide and potassium hydroxide are strong bases, and their respective cations  $Na^+$  and  $K^+$  are thus Lewis acids (see Section 2.1.1 and Table 2.2.2). They will normally form salts with drug candidates that completely dissociate in aqueous solution. The tendency to dissociate depends in part on the strength of the Lewis acid, i.e. dissociation decreases with decreasing  $pK_a$ . Thus for salts of the same drug candidate, the tendency to dissociate is larger for its lithium salt ( $pK_a$  13.8) than for its calcium salt ( $pK_a$  12.9) > magnesium salt ( $pK_a$  11.4) > diethanolamine salt ( $pK_a$  9.7) > zinc salt ( $pK_a$  9.0) > choline salt ( $pK_a$  8.9) > aluminium salt ( $pK_a$  5.0).

Furthermore, salt formation may affect the micro-pH within and close to the formulation, controlled by the strong salt-forming acid or base which, independently of pH in the gastrointestinal juice or dissolution medium, may increase the apparent dissolution. Table 2.4.2 shows the chemical structures of the acids most frequently used in salt formation of basic drug candidates.

**Table 2.4.2** Acids used in salt formation of drug substances that are bases

<i>Acid structure used for salt formation</i>	<i>Name of acid and <math>pK_a</math></i>	<i>Salt formed</i>
$\begin{array}{c} \text{COOH} \\   \\ \text{CHOH} \\   \\ \text{CHOH} \\   \\ \text{COOH} \end{array}$	Tartaric acid, $pK_a$ 3.00	Tartrate
$\begin{array}{c} \text{COOH} \\   \\ \text{CH}_2 \\   \\ \text{CH}_2 \\   \\ \text{COOH} \end{array}$	Succinic acid, $pK_{aI}$ 4.2, $pK_{aII}$ 5.6	Succinate
$\begin{array}{c} \text{COOH} \\   \\ \text{CH} \\    \\ \text{CH} \\   \\ \text{COOH} \end{array}$	Maleic acid, $pK_{aI}$ 1.92, $pK_{aII}$ 6.23	Maleate
HCl	Hydrochloric acid, $pK_a$ -6.10	Hydrochloride
H <sub>3</sub> PO <sub>4</sub>	Phosphoric acid, $pK_{aI}$ 2.15, $pK_{aII}$ 7.20, $pK_{aIII}$ 12.38	Phosphate
H <sub>2</sub> SO <sub>4</sub>	Sulphuric acid, $pK_{aI}$ -3.00, $pK_{aII}$ 1.96	Sulphate
$\begin{array}{c} \text{H} \diagdown \text{COOH} \\   \\ \text{OH} \end{array}$	Lactic acid, $pK_a$ 3.10	Lactate
$\begin{array}{c} \text{COOH} \\   \\ \text{CH}_2 \\   \\ \text{HO}-\text{C}-\text{COOH} \\   \\ \text{CH}_2 \\   \\ \text{COOH} \end{array}$	Citric acid, $pK_{aI}$ 3.13, $pK_{aII}$ 4.76, $pK_{aIII}$ 6.40	Citrate
	Benzoic acid, $pK_a$ 4.20	Benzoate
	Salicylic acid, $pK_a$ 3.00	Salicylate
CH <sub>3</sub> SO <sub>3</sub> H	Methanesulphonic acid (mesylic acid), $pK_a$ -1.20	Mesylate
	Naphthalenesulphonic acid (napsylic acid), $pK_a$ 0.17	Napsylate
CH <sub>3</sub> COOH	Acetic acid, $pK_a$ 4.76	Acetate

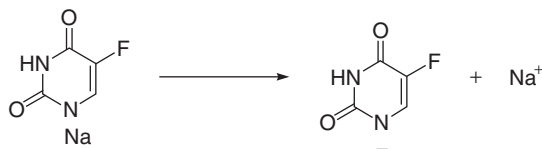


**Figure 2.4.1** Dissociation of the sodium salt of 5-fluorouracil in aqueous solution.

When salts of drug candidates become too soluble and hygroscopic, this can lead to instability of both the solid formulation and the drug candidate, as some of the substance will dissolve in its own absorbed moisture. This may not only disintegrate the tablet or capsule formulation during storage but also initiate hydrolytic degradation of the drug substance within the formulation (see Section 2.2.1). In this case a weaker salt-forming acid or base should be applied.

Salts of drug substances may also be used in liquid formulations when it is necessary to keep the substance in solution but desirable to avoid buffer excipients that are not suitable in injection liquids if the pH will deviate too much from the physiological pH of 7.4. An example is the iv (intravenous) aqueous injection solution of the anticancer drug 5-fluorouracil (5-FU). The dissociation scheme of the sodium salt of the NH acidic 5-FU in aqueous solution is shown in Figure 2.4.1.

The aqueous solubility of 5-FU ( $pK_a$  8.0) is approximately 11 mg ml<sup>-1</sup> (neutral species), whereas the sodium salt of 5-FU forms aqueous solutions in concentrations above 50 mg ml<sup>-1</sup> at pH 9. At this pH the salt dissociates into the negatively charged species of 5-FU and thereby increases its solubility. The 50 mg ml<sup>-1</sup> concentration is more convenient to use than the 11 mg/ml solutions, due to the smaller injection volumes needed. Although pH 9 deviates considerably from pH 7.4 in the blood (see Table 2.1.2), it is necessary to keep 5-FU in solution when administered iv; therefore the sodium salt of 5-FU is applied in formulations used for iv injection. Drug solubility can also be enhanced using prodrug strategies (see Section 2.4.4) or for solvation-limited ‘grease ball’ candidates (see Section 2.1.4) by using solubilisers as ingredients in the pharmaceutical formulation.

### 2.4.3 Bioisosteric replacement

Stabilisation of metabolically sensitive functional groups such as esters or amides can be obtained by introducing bioisosteric replacements (Patani and LaVoie, 1996; Chen and Wang, 2003). Bioisosteric moieties should be designed to show similar size, shape, electron distribution, lipophilicity/

hydrophilicity,  $pK_a$ , and hydrogen-bonding capacity as the group being replaced. However, they do not necessarily overlap atom upon atom, but show similar biological properties.

This section will focus on the stabilisation of peptides against hydrolytic cleavage by protease enzymes. The sensitive parts of the peptides are the amide bonds (peptide bonds) that are connecting amino acids. Peptides are endogenous compounds involved in many important physiological processes, and as peptides have been associated with certain disease states, peptide receptors and processing enzymes have become interesting pharmacological targets for drug-discovery efforts. Peptides are often found to be less useful as drugs in themselves due to their low oral bioavailability. This has mainly been associated with their inefficient penetration of the intestinal membrane, and their rapid degradation by endogenous peptidases both in the gastrointestinal tract and in blood. Intestinal peptidases are summarised in Table 2.4.3.

Although extensive efforts have been put into the areas of formulation and delivery of peptides, it is generally considered that oral delivery of peptides still represents a significant challenge. One example of an orally administered peptide drug is ciclosporin (Sandimmun<sup>®</sup>), a cyclic undecapeptide used as an immunosuppressant. It is administered as oral solutions or soft capsules. In these formulations ciclosporin is formulated with oils such as ricinus and maize oil together with ethanol, propyleneglycol and DL- $\alpha$ -tocopherol. Alternatively, ciclosporin is formulated as an infusion concentrate in which it is dissolved in oils. Ciclosporin is a substrate to the efflux transporter P-glycoprotein (P-gp) (see Chapter 3.6) and may also be a substrate for other transporters as well as for the metabolising cytochrome P-450 enzymes. Consequently, drug–drug interactions between ciclosporin and a wide range of drug substances that interact with P-gp and/or P-450 are observed, which may partly explain its highly variable bioavailability. Ciclosporin contains D-amino acids which, together with the cyclic structure, stabilise the compound against protease degradation.

Another interesting example of an orally administered peptide drug is desmopressin (see Table 2.4.1), a synthetic replacement for antidiuretic hormone prescribed for diabetes insipidus. Although it only shows 0.1% oral bioavailability, it can be administered as tablets, and the extreme potency of desmopressin makes even very low plasma concentrations highly efficacious. Desmopressin is stabilised against metabolism by several important structural features including an N-terminal deamination and a C-terminal amidation, as well as the presence of a D-amino acid and an intramolecular disulphide bond.



**Table 2.4.3** Enzyme types, enzyme commission number, common name and preferred cleavage site, for human intestinal pancreatic, brush border or cytosolic peptidases. Data cited from Bai *et al.* 1992; Woodley 1994; Andersen 2006; Steffansen *et al.*, 2005; <http://www.ebi.ac.uk/thornton-srv/databases/enzymes/>; <http://www.ebi.ac.uk/intenz/index.jsp>; <http://www.expasy.org/>; <http://www.genome.ad.jp/>; <http://www.brenda-enzymes.info/>

<i>Type of peptidases</i>	<i>Enzyme Commission Number and common name</i>	<i>Preferential cleavage site</i>
Pancreas endopeptidase	EC 3.4.21.4, trypsin	Arg-Xaa, Lys-Xaa
Pancreas endopeptidase	EC 3.4.21.1, chymotrypsin	Tyr-Xaa, Trp-Xaa, Phe-Xaa, Leu-Xaa, Met-Xaa
Pancreas endopeptidase	EC 4.21.36, elastase	Ala-Xaa
Pancreas endopeptidase	EC 3.4.21.70, protease E	Ala-Xaa
Pancreas exopeptidase	EC 3.4.17.2, carboxypeptidase A	Release of Val Leu Ile Phe Tyr Trp C-terminal amino acid
Pancreas exopeptidase	EC 3.4.17.2, carboxypeptidase B	Release of Lys Arg C-terminal amino acid
Brush border exopeptidase	EC 3.4.11.7, aminopeptidase A or glutamyl aminopeptidase	Release of Glu Asp N-terminal amino acid
Brush border exopeptidase	EC 3.4.11.2, aminopeptidase N or alanyl aminopeptidase	Release of N-terminal amino acid
Brush border exopeptidase	EC 3.4.11.9, aminopeptidase P, Pro-X aminopeptidase	Release of Pro N-terminal amino acid
Brush border exopeptidase	EC 3.4.11.16, aminopeptidase W, Trp-X aminopeptidase	Release of Trp Tyr Phe N-terminal amino acid
Brush border endopeptidase	EC 3.4.21.9, enteropeptidase	Activates trypsinogen by selective cleavage of Leu <sup>6</sup> -Ile <sup>7</sup> bond
Brush border endopeptidase	EC 3.24.11, neprilisin, endopeptidase 24.11	Between hydrophobic amino acid
Brush border endopeptidase	EC 3.4.24.18, endopeptidase 2, meprin A	Not described
Brush border oligopeptidase	EC 3.4.15.1, angiotensin-converting enzyme, peptidyl-dipeptidase A	Release of C-terminal dipeptide
Brush border oligopeptidase	EC 3.4.14.5, dipeptidyl peptidase IV	Release of N-terminal dipeptide
Cytosolic peptidase	EC 3.4.13.3, carnosinase, X-His peptidase	Xaa-His
Cytosolic peptidase	EC 3.4.13.18, cytosolic non-specific peptidase	Preferentially hydrophobic dipeptides

Another way to improve the plasma half life and decrease the protein binding and renal clearance of peptide drugs has been the formation of macromolecular polyethylene glycol (PEG) conjugates of peptides (Roberts *et al.*, 2002; Veronese and Pasut, 2005).

One strategy to improve the oral bioavailability of peptide-based drug candidates is to introduce structural modifications that lead to decreased metabolism, or increased absorption, i.e. increased intestinal permeability. Backbone-modified peptides, often called pseudopeptides, in which sensitive amide bonds have been replaced with bioisosteric moieties, should be designed to be metabolically stable but also have to retain their pharmacological activity

#### 2.4.3.1 Peptidomimetic strategies

Peptide backbone mimetics belong to the so-called type I peptidomimetics which historically were the first peptidomimetics (Ripka and Rich, 1998). This group includes amide bond isosteres and mimetics of secondary structures. Replacement of peptide bonds with an isosteric moiety often leads to pseudopeptides possessing increased stability towards metabolic enzyme-catalysed hydrolysis (M), but also other ADME properties in addition to metabolism may be affected by pseudopeptidic strategies

Important considerations in the selection of an amide bond replacement have been its ability to exhibit geometrical, conformational, electrostatic and hydrogen-bonding properties that are similar to the amide bond itself. An amide bond replacement can be introduced into a peptide by synthesis of a dipeptide analogue of the general structure Xxx-Ψ[A-B]-Yyy. Next, some examples of important bioisosteric amide-bond replacements and their use in bioactive peptides will be discussed.

#### 2.4.3.2 Amide-based bioisosteres

The synthetically most accessible means to stabilise a peptide against enzyme-catalysed degradation is probably the exchange of L-amino acids for D-amino acids or to introduce N-methylations, i.e. methyl groups on the amide nitrogen atom (see Figure 2.4.2) (Hodgson and Sanderson, 2004). However, such modifications may induce severe conformational constraints and thereby decrease the recognition and binding properties of the pseudopeptide in relation to its pharmacological target.

The retro-inverso peptides xxx-Ψ[NHCO]-yyy (see Figure 2.4.2) (Goodman and Chorev, 1979; Chorev and Goodman, 1993) not only

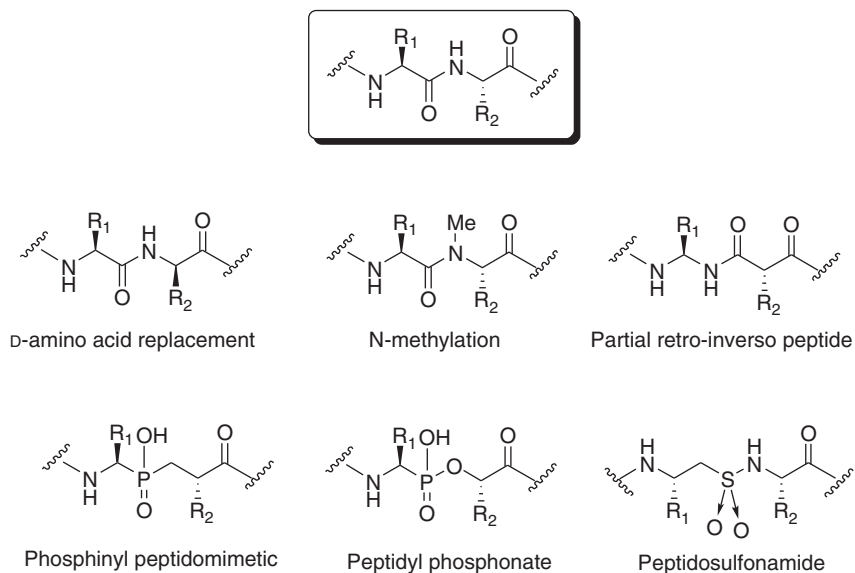


**Figure 2.4.2** Structure of some important amide bond isosteres.

reverse the direction of the peptide bonds but also have the L-amino acids exchanged for D-amino acids. Incorporation of a retro-inverse isostere results in a pseudopeptide with a similar topology to the native peptide; however, it is no longer sensitive to peptidase degradation.

A recent example of the use of a small retro-inverse peptide, to improve its ADME properties, is the Tat antagonist R.I.CK-Tat9 (N-acetyl-ckrrrqrrrkrNH<sub>2</sub>), which has been used either alone or in combinations with, for example, saquinavir, in *in vitro* studies for anti-HIV activities. The compounds were used as multifunctional PEG-based bioconjugates, and their increased anti-HIV activity was suggested to emanate from an enhanced intracellular uptake and a synergistic inhibitory effect of saquinavir and the Tat peptide (Wan *et al.*, 2006). The strongly basic Tat peptide sequence is known to have cell-penetrating properties and has been used as a vehicle for transport of cargo molecules across plasma membranes.

Replacements of amide bonds by bioisosteric groups mimicking the transition state (TS) of the hydrolysis of the amide has been widely used in the development of protease inhibitors. Examples of possible TS mimetics are the phosphine xxx-Ψ[PO(OH)]-yyy, phosphonate xxx-(Ψ[PO<sub>2</sub>(OH)])-yyy and sulfonamide xxx-Ψ[SO<sub>2</sub>NH]-yyy, shown in Figure 2.4.2, and the dihydroxyethylene and hydroxyethylene isosteres shown in Figure 2.4.3. Pseudopeptides containing phosphinyl-based TS mimetics have found

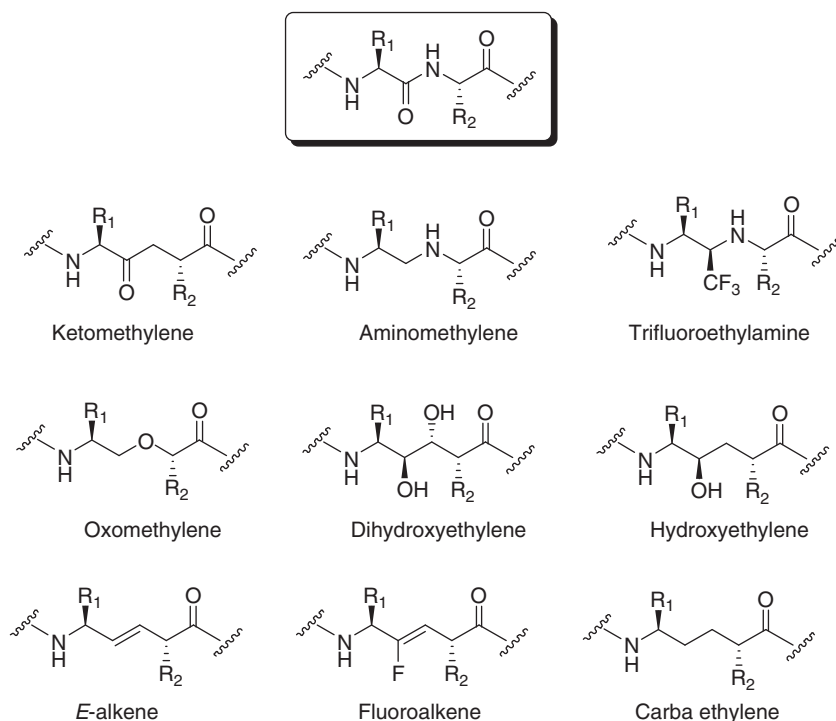


**Figure 2.4.3** Amide bond bioisosteres.

applications as stable zinc, serine and aspartate protease inhibitors. The corresponding phosphonates have also shown potent inhibitory activity toward aspartate proteases. Hydroxyethylene moieties are incorporated in all marketed HIV-protease inhibitors, e.g. indinavir, to mimic the TS for the hydrolysis reaction.

Peptidosulfonamide analogues of Leu-enkephalin and TAP have been shown to display improved stability towards pepsin and trypsin degradation (De Bont *et al.*, 1999). Another important property of this type of bioisostere is the increased acidity of the sulfonamide N-H compared to the amide. This will lead to stronger hydrogen-bonding interactions as have been shown for some oligopeptidosulfonamide ‘tweezer’ molecules used as synthetic receptors (Loewik *et al.*, 1996).

Some other popular peptide bond surrogates, which have found application in the development of metabolically stable pseudopeptides, are shown in Figure 2.4.3.

The inherent properties of the amide bond have been studied using mimetics in which either the NH or the carbonyl moieties have been removed. The ketomethylene isostere  $\text{xxx-(}\Psi[\text{COCH}_2\text{)]-yyy}$ , which is

not recognised by peptidases and is consequently metabolically stable, has been shown to possess interesting substrate properties towards the absorptive peptide transporter PEPT1. Absorptive transporters and their importance for drug delivery are further described in Chapter 3.5. The hydrogen-bonding interaction of ketomethylene isosteres with PEPT1 is due to the presence of the carbonyl group in the isosteric moiety. For example, Phe $\Psi$ [COCH<sub>2</sub>]Gly, Phe $\Psi$ [COCH<sub>2</sub>]Asp, Val $\Psi$ [COCH<sub>2</sub>]Gly and Val $\Psi$ [COCH<sub>2</sub>]Asp mimetics have been shown to be excellent substrates for PEPT1 and consequently suggested as pro-moieties for low-permeability drug candidates (Våbenø *et al.*, 2004a,b). Such a prodrug delivery approach is further described below in Section 2.4.4. A hydrogen-bonding interaction with PEPT1 via the carbonyl group in the original peptide is believed to be crucial, and in the ketomethylene isosteres that interaction is still intact. In these mimetics, the increased conformational flexibility of the ketomethylene moiety is compatible with PEPT1 interaction.

The aminomethylene mimetic xxx-( $\Psi$ [CH<sub>2</sub>NH])-yyy is a reduced amide in which the increased basicity of the secondary amine will confer dramatic changes in electrostatic properties compared to the parent amide. In some studies an increased cell permeability of pseudopeptides has been shown, in addition to increased stability toward hydrolytic enzymes; however, in other studies the cell permeability has been considerably decreased. Thus, to improve the amide bond-mimicking properties of the aminomethylene isostere, the basicity of the secondary amine has to be decreased. Introducing a trifluoromethyl group in the  $\alpha$ -position to the amine (xxx- $\Psi$ [CH(CF<sub>3</sub>)NH]-yyy) has been shown to more accurately mimic the hydrogen-bonding properties of the amide (Sani *et al.*, 2007). This replacement has been successfully used in highly pharmacologically potent and selective cathepsin K inhibitors. According to X-ray crystallographic studies of complexes between the pseudopeptides and the pharmacological target (cathepsin K), an important hydrogen bond in the complex is intact (Black *et al.*, 2005).

The *E*-alkene (xxx- $\Psi$ [CH=CH]-yyy) is a well-known bioisosteric unit; it has an almost identical geometry to the amide bond (see Figure 2.4.4). It was first used by Hann *et al.* as an amide bond replacement in Leu-enkephalin, where it was shown that the *E*-alkene was tolerated as a Tyr-Gly but not a Gly-Gly replacement (Hann *et al.*, 1980, 1982).

One important consideration related to the use of *E*-alkene isosteres is that any backbone hydrogen-bonding interaction will be disrupted. This feature has recently been used advantageously when incorporated into the A $\beta$  Alzheimer amyloid peptide. Replacing only one out of 39

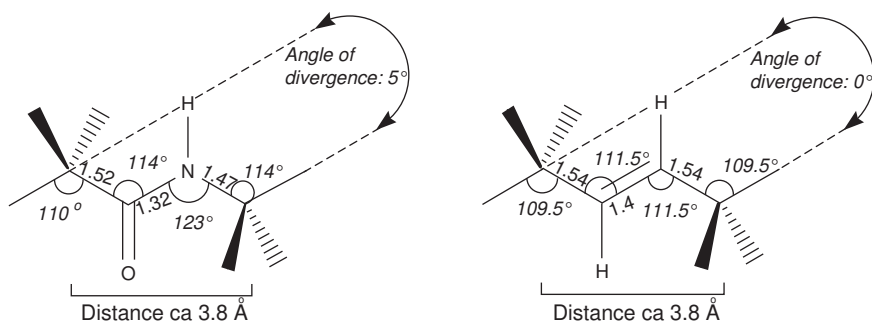


**Figure 2.4.4** Bond lengths and bond angles of amides and *E*-alkenes are almost the same. Adapted from Hann MM, Sammes PG, Kennewell PD, Taylor JB (1980). On double bond isosteres of the peptide bond; an enkephalin analog. *J Chem Soc Chem Commun* 234–235.

amide bonds by an *E*-alkene mimetic prevented the transformation of A $\beta$  into amyloid fibrils (Fu *et al.*, 2005).

Using the *E*-alkene isostere as starting point, other dipeptidomimetics can be designed and synthesised which show improved electrostatic and/or hydrogen-bonding properties. These new mimetics can also be designed to introduce different lipophilic or stereochemical effects in comparison with the parent structure. Such changes might be advantageous for transport, receptor binding, or membrane interaction. One such example is the more electrostatically favourable fluoroalkene mimetic (xxx- $\Psi$ [CF=CH]-yyy), which has been used to study conformational preferences of peptides and also for studies of ligand/receptor interactions. The first example of the use of fluoro-olefin peptide isosteres was the introduction of Phe( $\Psi$ [CF=CH])Gly in substance P (Allmendinger *et al.*, 1990). This compound showed almost the same activity as substance P itself, but exhibited increased chemical stability and receptor-binding affinity compared to the *E*-alkene analogue. In a recent study, *Z*- and *E*-fluoroalkene dipeptide mimetics were used to investigate the conformational *cis*- and *trans*-amide bond preferences for oligopeptide transport via PEPT1. It was shown that the *E*-fluoroalkene and *E*-alkene isosteres possessed higher affinities for PEPT1 compared to the *Z*-isomers (Niida *et al.*, 2006).

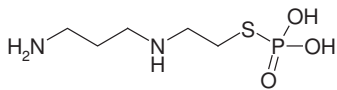
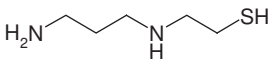
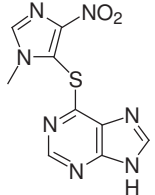
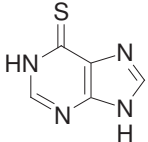
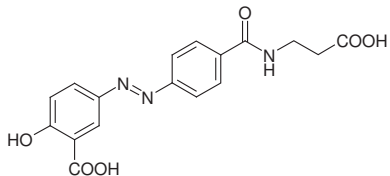
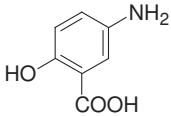
The aim of bioisosteric replacement of peptide bonds is to stabilise peptidic drug candidates against metabolism and to increase permeability without compromising its pharmacological activity. This is, as described, a quite complex strategy that needs to be developed for each specific case. Another strategy for improving the bioavailability of drug candidates is the prodrug approach, which will be briefly described in the following section.

### 2.4.4 Prodrug formation

Low solubility and low permeability properties of drug candidates can sometimes be circumvented by prodrug formation. In Table 2.4.4 examples of European-registered prodrugs and their corresponding parent drug substances are shown.

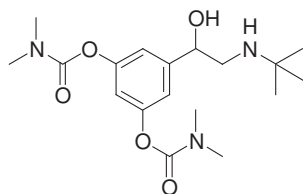
One prodrug strategy that is often applied to improve the solubility of drug candidates is to introduce a pro-moiety containing phosphate, sulphate or succinate groups, which can ionise in relevant biological media. An example is the succinate prodrug of chloramphenicol for iv administration (see Table 2.4.4). A carboxylic acid group in the succinate pro-moiety, with a  $pK_a$  value far below physiological pH, will be ionised at pH 7.4 and thereby increase the aqueous solubility of chloramphenicol-succinate ester compared to the parent chloramphenicol. Chloramphenicol itself is an alcohol with a  $pK_a$  value far above pH 7.4, and consequently it is present as neutral species, with lower aqueous solubility, than the corresponding ionised succinate-ester prodrug.

**Table 2.4.4** Examples of European registered prodrugs and parent drug substances, taken from Steffansen B, Thomsen AE, Frokjaer S (2003) Prodrugs. In: van de Waterbeemd H, Lennernäs H, Artursson P, eds. *Methods and Principles in Medicinal Chemistry, Estimation of Permeability, and Oral Absorption*. Weinheim: Wiley VCH, 532–546

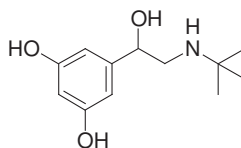
Prodrug	Drug
<p>Amifostine iv administration</p> 	<p>Dephosphorylated aminofostine</p> 
<p>Azathioprine</p> 	<p>6-Mercaptopurine</p> 
<p>Balsalazide</p> 	<p>Mesalazine</p> 

**Table 2.4.4** (Continued)

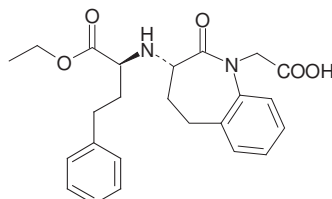
Bambuterol



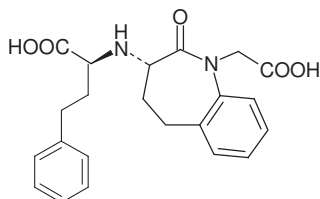
Terbutaline



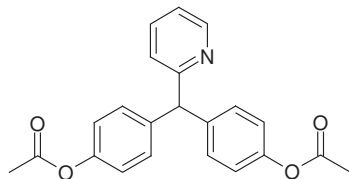
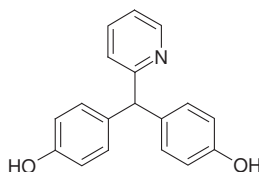
Benazepril



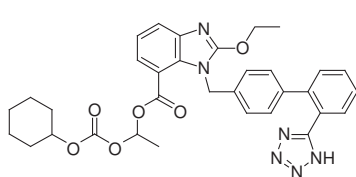
Benazeprilat



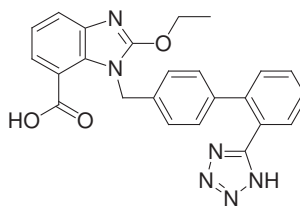
Bisacodyl

bis-(p-Hydroxyphenyl)-pyridyl-  
2-methane  
(BHPH)

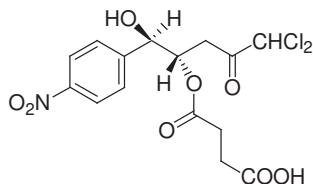
Candesartan cilexetil



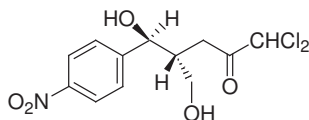
Candesartan



Chloramphenicol succinate



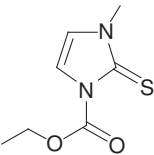
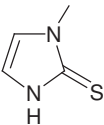
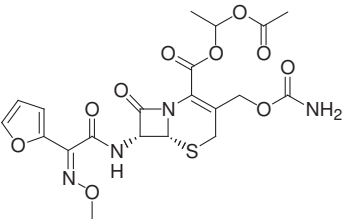
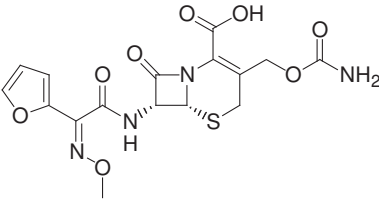
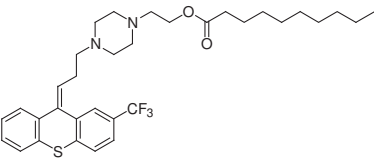
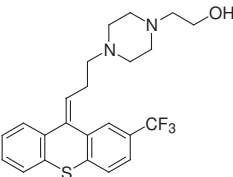
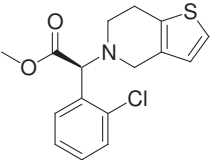
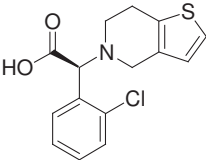
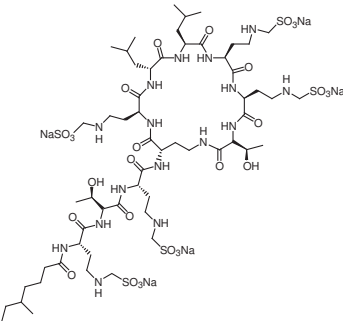
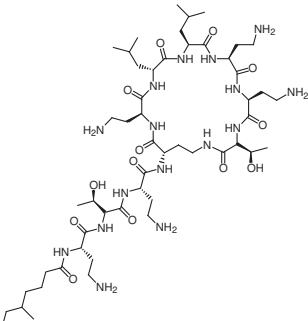
Chloramphenicol



(continued)

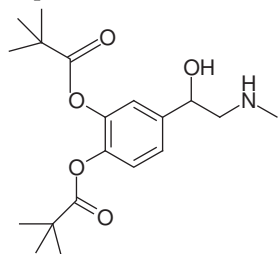


**Table 2.4.4** (Continued)

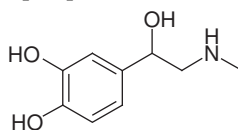
<i>Prodrug</i>	<i>Drug</i>
<p>Carbimazole</p> 	<p>Methimazole</p> 
<p>Cefuroxime axetil</p> 	<p>Cefuroxime</p> 
<p>(Z)-flupentixol decanoate</p> 	<p>(Z)-flupentixol</p> 
<p>Clopidogrel</p> 	<p>The corresponding acid</p> 
<p>Colistimethate</p> 	<p>Colistin (polymyxin E)</p> 

**Table 2.4.4** (Continued)

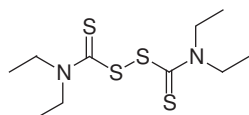
Dipivefrine



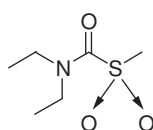
Epinephrine (adrenaline)



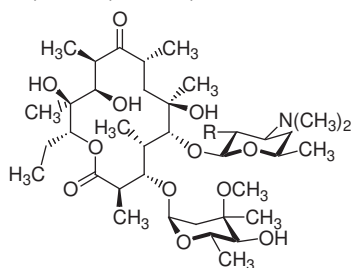
Disulfiram



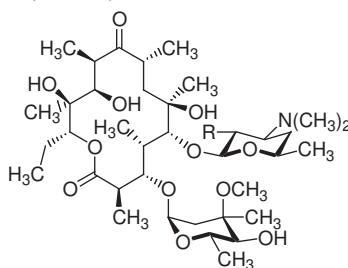
S-Methyl-N,N-diethylthiocarbamate sulfone



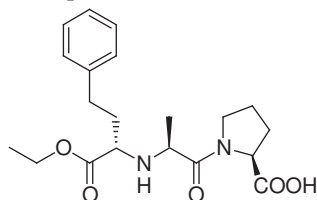
Erythromycin ethylsuccinate



Erythromycin

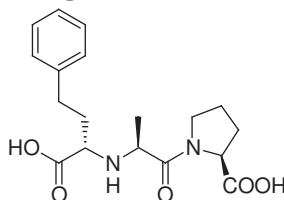
R=OCOCH<sub>2</sub>CH<sub>2</sub>COOEt

Enalapril

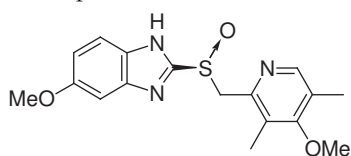


R=OH

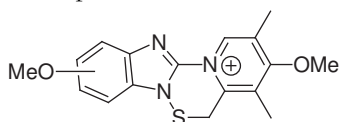
Enalaprilat



Esomeprazole



Esomeprazole sulfenamide



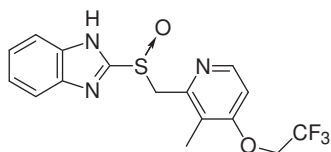
S-enantiomer of omeprazole

(continued)

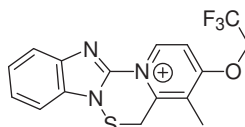


**Table 2.4.4** (Continued)

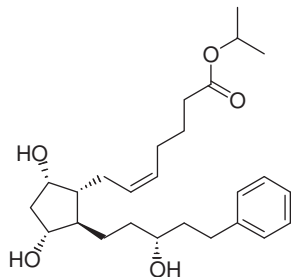
Lansoprazole



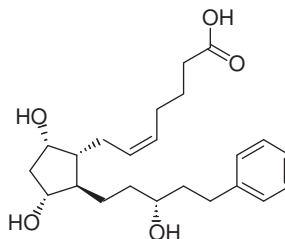
The corresponding sulfenamide



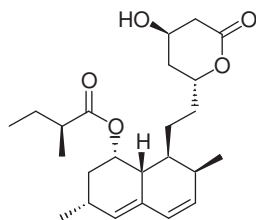
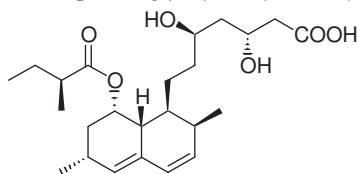
Latanoprost



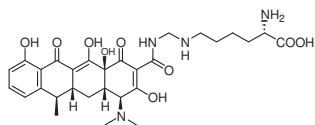
The corresponding acid



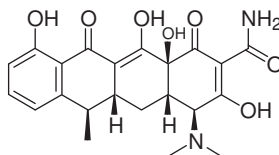
Lovastatin (lactone)

Corresponding  $\beta$ -hydroxycarboxylic acid

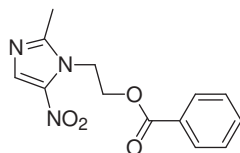
Lymecycline



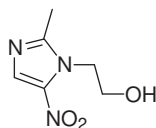
Tetracycline



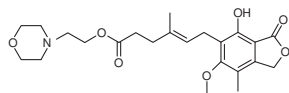
Metronidazole benzoate



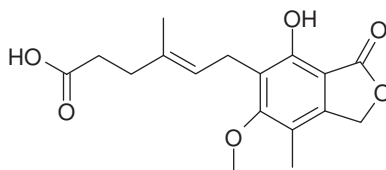
Metronidazole



Mycophenolate mofetil

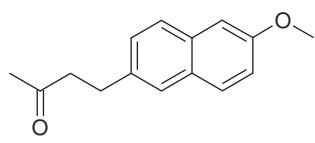
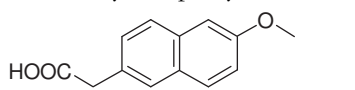
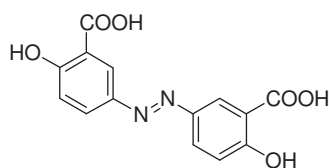
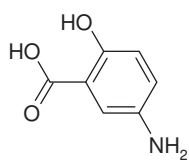
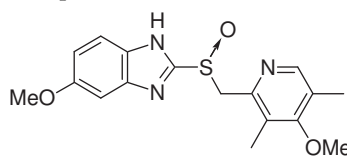
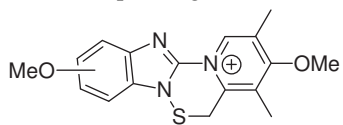
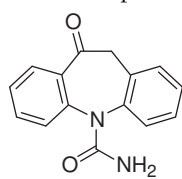
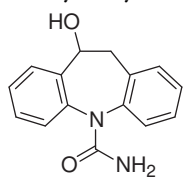
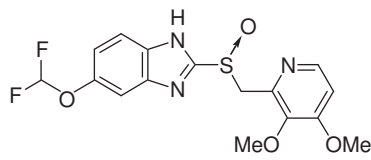
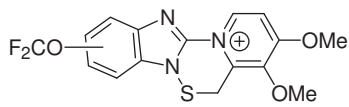
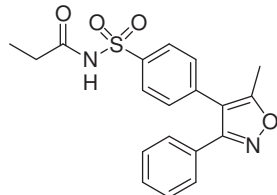
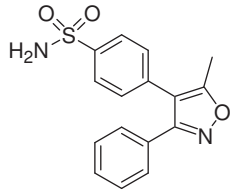


Mycophenolatic acid (MPA)



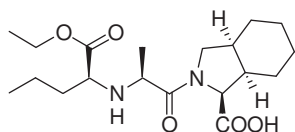
(continued)

**Table 2.4.4** (Continued)

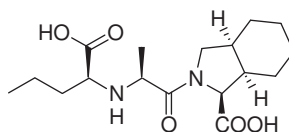
<i>Prodrug</i>	<i>Drug</i>
Nabumetone 	6-Methoxy-2-naphthylacetic acid 
Olsalazine 	Mesalazine 
Omeprazole 	The corresponding sulfenamide 
racemic Oxcarbazepine 	10-Hydroxy-carbazepine (MHD) 
Pantoprazole 	The corresponding sulfenamide 
Parecoxib 	Valdecoxib 

**Table 2.4.4** (Continued)

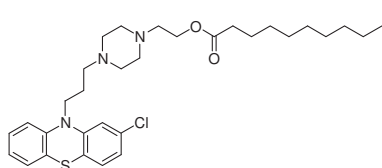
Perindopril



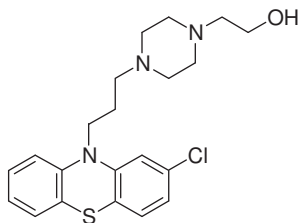
Perindoprilat



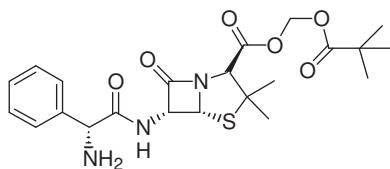
Perphenazine decanoate



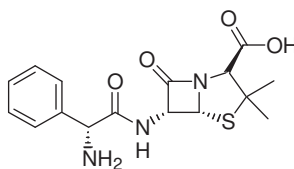
Perphenazine



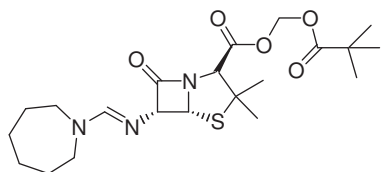
Pivampicillin



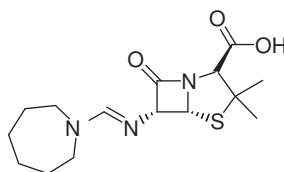
Ampicillin



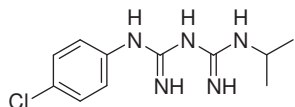
Pivmecillinam



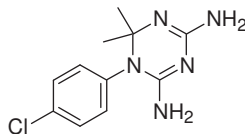
Mecillinam



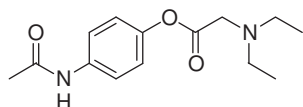
Proguanil



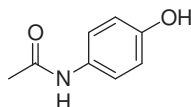
Cycloguanil



Propacetamol

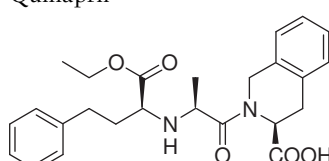
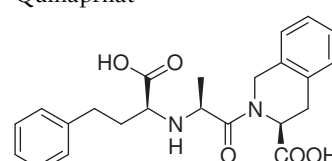
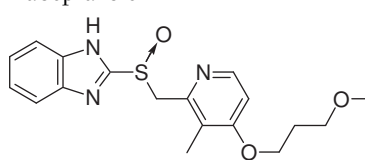
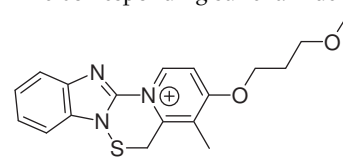
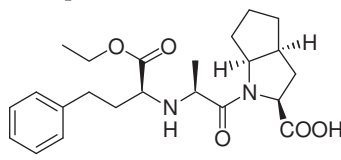
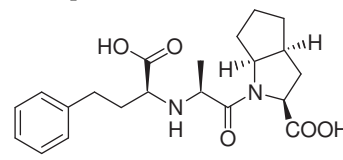
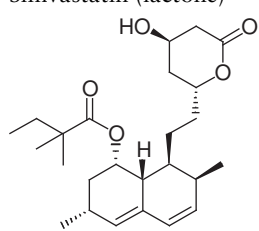
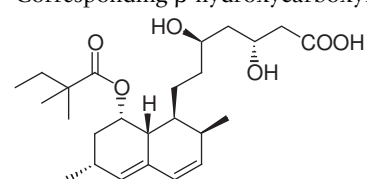
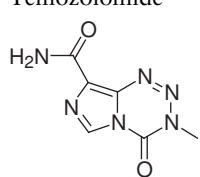
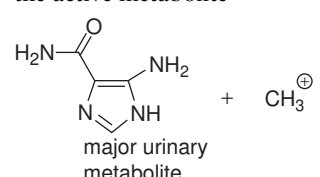
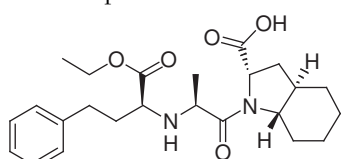
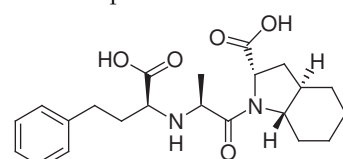


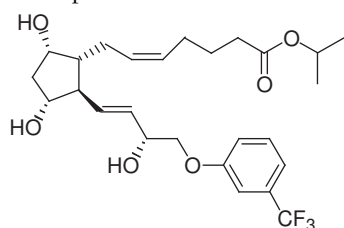
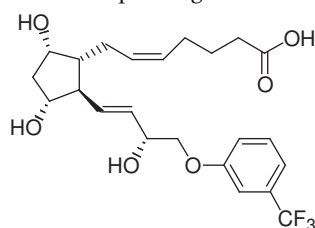
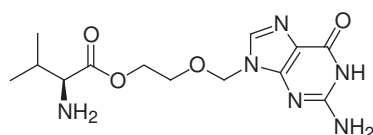
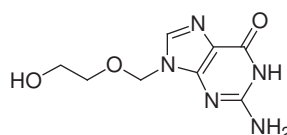
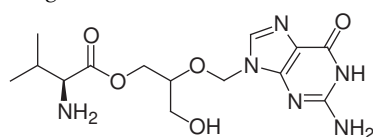
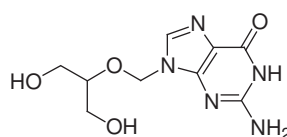
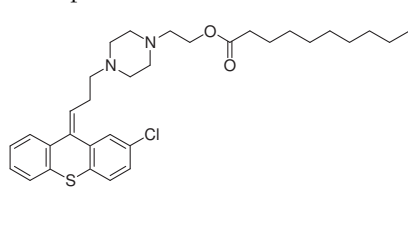
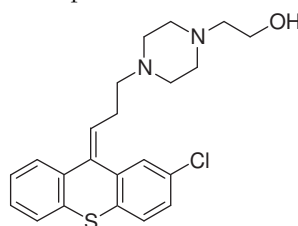
Paracetamol



(continued)

**Table 2.4.4** (Continued)

<i>Prodrug</i>	<i>Drug</i>
<p>Quinapril</p> 	<p>Quinaprilat</p> 
<p>Rabeprazole</p> 	<p>The corresponding sulfenamide</p> 
<p>Ramipril</p> 	<p>Ramiprilat</p> 
<p>Simvastatin (lactone)</p> 	<p>Corresponding <math>\beta</math>-hydroxycarboxylic acid</p> 
<p>Temozolomide</p> 	<p>The methyl cation is the active metabolite</p>  <p>major urinary metabolite</p>
<p>Trandolapril</p> 	<p>Trandolaprilat</p> 

**Table 2.4.4** (Continued)**Travoprost****The corresponding acid****Valaciclovir****Aciclovir****Valganciclovir****Ganciclovir****Zuclopentixol decanoate****Zuclopentixol**

Strategies to improve the permeability by prodrug formulation may be to develop prodrugs that have increased passive diffusional permeability properties across the enterocytic membrane compared to the parent compound, or to develop prodrugs as substrates for absorptive intestinal membrane transporters such as the peptide transporter PEPT1. However, regardless of the strategy, a prerequisite is that the drug candidates contain functional group(s) such as carboxylic acid, alcohol, thiol or amine functionalities which can be applied in the formation of bioreversible linkages between the pro-moiety and the drug candidate. The most frequently applied prodrug linkage is the ester linkage; however, many other



linkages may also be used. Some of the most conventional examples are shown in Table 2.4.5, together with chemical structures of derivable functional groups.

Thus, drug candidates that are alcohols, amines, thiols, or carboxylic acids may be formulated as the corresponding ester, amide, thioester and ester prodrugs, respectively. Conventional ester linkages are in general rapidly cleaved in the gastrointestinal fluids and thus characterised by very short half lives *in vivo*, due to esterase-catalysed hydrolysis. In cases where the prodrug linkage is hydrolysed in gastrointestinal fluids, the prodrug formulation does not necessarily increase the oral bioavailability of the parent drug candidate. However, in cases where the ester linkage is sterically hindered by either the drug substance or a bulky promoiety, its hydrolysis may be only slowly catalysed either by esterases or by acids and/or bases. This sterically hindered ester linkage will normally lead to a decreased release rate of the parent drug candidate from the prodrug compared to drug release from prodrugs, which are not designed to have sterically hindered ester linkages. Consequently, in cases where the prodrug permeability rate is faster than its gastrointestinal metabolism rate, the prodrug candidate may show an increased bioavailability compared to the parent drug candidate.

Such a prodrug strategy was applied in the formation of a bioreversible ester linkage between the  $\beta$ -carboxylic acid in the Glu-Sar promoiety and the alcohol functionalities in hydroxyethyl-thymine candidate and aciclovir (Thomsen *et al.*, 2003a,b). In this prodrug candidate approach, the promoiety but not the linker is stabilised by N-methylation (see Figure 2.4.2). The resulting Glu(aciclovir)-Sar and Glu(hydroxyethylthymine)-Sar prodrug candidates, which show affinity to the intestinal absorptive peptide carrier hPEPT1, release aciclovir/hydroxyethylthymine in a non-enzyme-catalysed but specific base-catalysed manner, whereas the promoiety Glu-Sar itself is fully stabilised. Thus, aciclovir is released by a half life of 6.1 days in upper intestinal fluid (pH 6.0) and 344 minutes in blood (pH 7.4), respectively, and consequently the Glu(aciclovir)-Sar prodrug candidates should hypothetically survive during the intestinal transit time of approximately 3 hours while releasing aciclovir in a controlled manner in blood (Thomsen *et al.*, 2003a,b). The Glu(aciclovir)-Sar prodrug candidate and its release of aciclovir is shown in Figure 2.2.8, the pH-rate profile describing the pH-dependent release rate of aciclovir in Figure 2.3.2 and the pH of various biological fluids in Table 2.1.2. Glu(aciclovir)-Sar and Glu(hydroxyethylthymine)-Sar have both been shown to have strong affinities for PEPT1; however none of them were translocated by the transporter, and consequently their bioavailabilities in rats was

**Table 2.4.5** Examples of functional groups that may be applied for prodrug formation

Functional group	Prodrug form	Linkage
$\begin{array}{c} \text{O} \\ \parallel \\ \text{R}-\text{C}-\text{OH} \end{array}$	$\begin{array}{c} \text{O} \\ \parallel \\ \text{R}-\text{C}-\text{O}-\text{R}' \end{array}$	Ester
$\begin{array}{c} \text{O} \\ \parallel \\ \text{R}-\text{C}-\text{OH} \end{array}$	$\begin{array}{c} \text{O} \\ \parallel \\ \text{R}-\text{C}-\text{O}-\text{CH}-\text{O}-\text{C}-\text{R}' \\ \quad \quad \quad \mid \quad \quad \parallel \\ \quad \quad \quad \text{R}'' \quad \quad \text{O} \end{array}$	$\alpha$ -Acyloxyalkyl esters
$\begin{array}{c} \text{O} \\ \parallel \\ \text{R}-\text{C}-\text{OH} \end{array}$	$\begin{array}{c} \text{O} \\ \parallel \\ \text{R}-\text{O}-\text{C}-\text{O}-\text{R}' \end{array}$	Carbonate esters
$\begin{array}{c} \text{O} \\ \parallel \\ \text{R}-\text{C}-\text{OH} \end{array}$	$\begin{array}{c} \text{O} \\ \parallel \\ \text{R}-\text{C}-\text{NH}-\text{R}' \end{array}$	Amides
R-OH	$\begin{array}{c} \text{O} \\ \parallel \\ \text{R}-\text{O}-\text{C}-\text{R}' \end{array}$	Esters
R-OH	$\begin{array}{c} \text{O} \\ \parallel \\ \text{R}-\text{O}-\text{CH}-\text{O}-\text{C}-\text{R}' \\ \quad \quad \quad \mid \\ \quad \quad \quad \text{R}'' \end{array}$	$\alpha$ -Acyloxyalkyl ethers
R-OH	$\begin{array}{c} \text{O} \\ \parallel \\ \text{R}-\text{O}-\text{C}-\text{N}-\text{R}' \\ \quad \quad \quad \mid \\ \quad \quad \quad \text{H} \end{array}$	Carbamate
R-OH	$\begin{array}{c} \text{O} \\ \parallel \\ \text{R}-\text{O}-\text{P} \begin{array}{l} \nearrow \text{OR}' \\ \searrow \text{OH} \end{array} \end{array}$	Phosphate esters
R-NH <sub>2</sub>	$\begin{array}{c} \text{O} \\ \parallel \\ \text{R}-\text{N}-\text{C}-\text{O}-\text{R}' \\ \quad \quad \mid \\ \quad \quad \text{H} \end{array}$	Carbamate
R-SH	$\begin{array}{c} \text{O} \\ \parallel \\ \text{R}-\text{S}-\text{C}-\text{R}' \end{array}$	Thioesters
R-SH	$\begin{array}{c} \text{O} \\ \parallel \\ \text{R}-\text{S}-\text{CH}-\text{O}-\text{C}-\text{R}' \end{array}$	$\alpha$ -Acyloxyalkyl thioethers
R-SH	R-S-S-R'	Disulphides

shown to be almost zero (Eriksson *et al.*, 2005; Thomsen *et al.*, 2004). The use of an N-methyl amide bioisoster as peptide bond replacement to stabilise against cleavage by peptidases and yet keep affinity for absorptive PEPT1 carrier seems not to be a generally applicable approach to increasing PEPT1-mediated bioavailability, whereas the ketomethylene promoiety approach seems more promising (Våbenø *et al.*, 2004a,b; Andersen *et al.*, 2006).

Santos and co-workers designed and synthesised several 5'-O-dipeptide ester prodrug candidates of azidothymidine (AZT) in which the peptide bond is not stabilised. Some of these prodrug candidates show affinity for PEPT1 and are suggested to release the parent AZT by plasma amino- and diaminopeptidase-catalysed hydrolysis. Whether these prodrugs are stable within gastrointestinal environments has not yet been investigated (Santos *et al.*, 2008).

Other ester linkages are stable towards esterase activity in gastrointestinal fluids, but the hydrolysis is catalysed by enterocytic esterases. In such cases the ester prodrug is cleaved within the enterocyte and consequently the parent drug candidate is released in the intracellular compartment of the enterocytes. This is suggested to be the case for the valine ester prodrugs of aciclovir and ganciclovir (valaciclovir and valganciclovir, Table 2.4.4), which are both shown to be substrates for hPEPT1 (Han *et al.*, 1998a,b; Thomsen *et al.*, 2003a,b). It is suggested that the ester linkage between the carboxylic acid in the valine promoiety and the alcohol functionality in aciclovir is cleaved by the intracellular esterase valase which is present in both enterocytes and hepatocytes (Kim *et al.*, 2003). Consequently no parent valaciclovir prodrug but only aciclovir reaches the blood circulation *in vivo* (Beauchamp *et al.*, 1992; Burnette and Miranda, 1994). The bioavailability of aciclovir is approximately 20%, which increases to approximately 60% when administered as valaciclovir. The chemical structure of valaciclovir is shown in Figure 2.2.4 and Table 2.4.4.

Other more chemically advanced prodrug linkages are the acyloxy-alkoxy- (AOA), coumarinic-acid- (CA) and oxymethyl modified coumarinic acid (OMCA)-based linkers made by Borchardt and co-workers in the cyclic prodrugs of the [Leu5]-enkephalin analogue DADLE (Bak *et al.*, 1999; Wang *et al.*, 1999; Ouyang *et al.*, 2002). The chemical structures of these prodrug candidates are shown in Figure 2.4.5. The parent drug candidate is suggested to be released by enzyme-catalysed hydrolysis (Wang *et al.*, 1999). The strategy behind the design of these prodrug candidates was to increase the lipophilicity and thus oral bioavailability of DADLE. However, other factors than lipophilicity

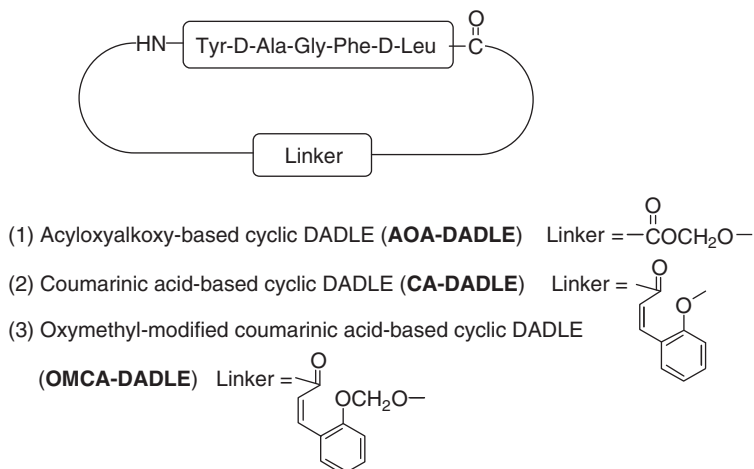


**Figure 2.4.5** Chemical structures of DADLE and its cyclic prodrugs (AOA-DADLE, CA-DADLE, and OMCA-DADLE). Reproduced from Ouyang H, Chen W, Andersen TE, Steffansen B, Borchardt RT (2009a). Factors that restrict the intestinal cell permeation of cyclic prodrugs of an opioid peptide (DADLE): (I) role of efflux transporters in the intestinal mucosa. *J Pharm Sci* 98: 337–348.

restricted the intestinal cell permeation of these cyclic prodrugs. The restricting factors have recently been partially elucidated, the prodrugs being substrates for exsorptive intestinal transporters such as P-gp, breast cancer-resistant protein (BCRP) and multidrug-resistance-associated protein (MRP2) (Ouyang *et al.*, 2009a).

All together the prodrug approach may improve drug bioavailability when designing prodrug candidates with improved permeability or solubility properties. Strategies for improving permeability across biological membranes such as the membrane of the small intestine may be to design prodrug candidates that are more lipophilic than the parent drug candidate or to design prodrug candidates as substrates for absorptive membrane transporters such as hPEPT1. Intestinal absorptive transporters have recently been reviewed (Steffansen *et al.*, 2004).

## 2.4.5 Conclusions

This chapter has presented some examples of how chemical approaches, i.e. salt formation, bioisosteric replacement, and prodrug formation, may be applied as strategies to improve the bioavailability of drug candidates. Optimising bioavailability is classically based on Lipinski's rule of five; however, many other factors have also been proven to limit the

bioavailability of drug candidates. These factors may involve metabolic enzymes and/or membrane carriers that may increase or limit the bioavailability and cause interactions between drug candidates (US Department of Health and Human Services, FDA, CDER and CBER, 2006). Modern drug development should be based on such challenges, and consequently subsequent chapters describe how membrane transporters that influence drug bioavailability may be investigated.

## References

- Allmendinger T, Felder E, Hungerbuehler E (1990). Fluoroolefin dipeptide isosteres. II. Enantioselective synthesis of both antipodes of the Phe-Gly dipeptide mimic. *Tetrahedron Lett* 31: 7301–7304.
- Andersen R, Nielsen CU, Begtrup M, *et al.* (2006). *In vitro* evaluation of N-methyl amide tripeptidomimetics as substrates for the human intestinal di/tri-peptide transporter hPEPT1. *Eur J Pharm Sci* 28: 325–335.
- Bai JP-F, Hu M, Subramanian P, Mosberg J, Amidon GL (1992). Utilization of peptide carrier system to improve intestinal absorption targeting prolidase as a prodrug-converting enzyme. *J Pharm Sci* 81: 113–116.
- Bak A, Siahaan TJ, Gudmundsson OS, *et al.* (1999). Synthesis and evaluation of the physicochemical properties of esterase-sensitive cyclic prodrugs of opioid peptides using an (acyloxy)alkoxy linker. *J Pept Res* 53: 393–402.
- Beauchamp LM, Orr GF, de Miranda P, Burnette T, Krenitsky TA (1992). Amino acid ester prodrugs of acyclovir. *Antiviral Chem Chemother* 3: 157–164.
- Black WC, Bayly CI, Davis DE, *et al.* (2005). Trifluoroethylamines as amide isosteres in inhibitors of cathepsin K. *Bioorg Med Chem Lett* 15: 4741–4744.
- Burnette TC, de Miranda P (1994). Metabolic disposition of the acyclovir prodrug valacyclovir in rat. *Drug Metab Dispos* 22: 60–64.
- Chen X, Wang W (2003). The use of bioisosteric groups in lead optimisation. *Annu Rep Med Chem* 38: 333–346.
- Chorev M, Goodman M (1993). A dozen years of retro-inverso peptidomimetics. *Acc Chem Res* 26: 266–273.
- De Bont DBA, Sliedregt-Bol KM, Hofmeyer LJF, Liskamp RMJ (1999). Increased stability of peptidesulfonamide peptidomimetics towards protease catalyzed degradation. *Bioorg Med Chem* 7: 1043–1047.
- Eriksson AH, Elm PL, Begtrup M, *et al.* (2005). hPEPT1 affinity and translocation of selected Gln-Sar and Glu-Sar dipeptide derivatives. *Mol Pharm* 2: 242–249.
- Fu Y, Bieschke J, Kelly JW (2005). E-Olefin dipeptide isostere incorporation into a polypeptide backbone enables hydrogen bond perturbation: probing the requirements for Alzheimer's amyloidogenesis. *J Am Chem Soc* 127: 15366–15367.
- Goodman M, Chorev M (1979). On the concept of linear modified retro-peptide structures. *Acc Chem Res* 12: 1–7.
- Han H-K, De Vruhe RLA, Rhie JK, *et al.* (1998a). 5'-amino acid esters of antiviral nucleosides acyclovir and AZT are absorbed by the intestinal PEPT1 peptide transporter. *Pharm Res* 15: 1154–1159.

- Han H-K, Oh D-M, Amidon GL (1998b). Cellular uptake mechanism of amino acid ester prodrugs in Caco 2/hPEPT1 cells overexpressing a human peptide transporter. *Pharm Res* 15: 1382–1386.
- Hann MM, Sammes PG, Kennewell PD, Taylor JB (1980). On double bond isosteres of the peptide bond: an enkephalin analog. *J Chem Soc Chem Commun* 234–235.
- Hann MM, Sammes PG, Kennewell PD, Taylor JB (1982). On the double bond isostere of the peptide bond: preparation of an enkephalin analog. *J Chem Soc Perkin Trans 1*: 307–314.
- Hodgson DRW, Sanderson JM (2004). The synthesis of peptides and proteins containing non-natural amino acids. *Chem Soc Rev* 33: 422–430.
- Kim I, Chu X-Y, Kim S, Provoda CJ, Lee K-D, Amidon GL (2003). Identification of a human valacyclovirase: biphenyl hydrolyase-like protein as valacyclovir hydrolase. *J Biol Chem* 278: 25348–25356.
- Lipinski CA, Lombardo F, Dominy BW, Feeney PJ (2001). Experimental and computational approaches to estimate solubility and permeability in drug discovery and development settings. *Adv Drug Del Rev* 46: 3–26.
- Loewik DWPM, Mulders SJE, Cheng Y, Shao Yi, Liskamp RMJ (1996). Synthetic receptors based on peptidosulfonamide peptidomimetics. *Tetrahedron Lett* 37: 8252–8256.
- Niida A, Tomita K, Mizumoto M, *et al.* (2006). Unequivocal synthesis of (Z)-alkene and (E)-fluoroalkene dipeptide isosteres to probe structural requirements of the peptide transporter PEPT1. *Org Lett* 8: 613–616.
- Ouyang H, Vander Velde DG, Borchardt RT, Siahaan TJ (2002). Synthesis and conformational analysis of coumarinic acid based cyclic prodrug of an opioid peptide with modified sensitivity to esterase-catalyzed bioconversion. *J Pept Res* 59: 183–195.
- Ouyang H, Chen W, Andersen TE, Steffansen B, Borchardt RT (2009a). Factors that restrict the intestinal cell permeation of cyclic prodrugs of an opioid peptide (DADLE): (I) role of efflux transporters in the intestinal mucosa. *J Pharm Sci* 98: 337–348.
- Ouyang H, Chen W, Andersen TE, Steffansen B, Borchardt RT (2009b). Factors that restrict the intestinal cell permeation of cyclic prodrugs of an opioid peptide (DADLE): part (II) role of metabolic enzymes in the intestinal mucosa. *J Pharm Sci* 98: 349–361.
- Patani GA, LaVoie EJ (1996). Bioisosterism: a rational approach in drug design. *Chem Rev* 96: 3147–3176.
- Ripka AS, Rich DH (1998). Peptidomimetic design. *Curr Opin Chem Biol* 2: 441–452.
- Roberts MJ, Bentley MD, Harris JM (2002). Chemistry for peptide and protein PEGylation. *Adv Drug Del Rev* 54: 459–476.
- Sani M, Volonterio A, Zanda M (2007). The trifluoroethylamine function as peptide bond replacement. *Chem Med Chem* 2: 1693–1700.
- Santos C, Morais J, Gouveia L, *et al.* (2008). Dipeptide derivatives of AZT: synthesis, chemical stability, activation in human plasma, hPEPT1 affinity and antiviral activity. *Chem Med Chem* 3: 970–978.
- Steffansen B, Thomsen AE, Frokjaer S (2003). Prodrugs. In: van de Waterbeemd H, Lennernäs H, Artursson P, eds. *Methods and Principles in Medicinal*

- Chemistry, Estimation of Permeability, and Oral Absorption*. Weinheim: Wiley VCH, 532–546.
- Steffansen B, Nielsen CU, Brodin B, *et al.* (2004). Intestinal solute carriers: a overview of trends and strategies for improving oral drug absorption. *Eur J Pharm Sci* 21: 3–16.
- Steffansen B, Nielsen CU, Frokjaer S (2005). Delivery aspects of small peptides and substrates for peptide transporters. *Eur J Pharm Biopharm* 60: 241–245.
- Thomsen AE, Friedrichsen GM, Sørensen AH, *et al.* (2003a). Prodrugs of purine and pyrimidine analogues for the intestinal di/tripeptide transporter: affinity for PEPT1 in Caco-2 cells, drug release in aqueous media and *in vitro* metabolism. *J Control Rel* 86: 279–292.
- Thomsen AE, Friedrichsen GM, Sørensen AH, *et al.* (2003b). Erratum to Prodrugs of purine and pyrimidine analogues for the intestinal di/tripeptide transporter PEPT1: affinity for hPEPT1 in Caco 2 cells drug release in aqueous media and *in vitro* metabolism. *J Control Release* 88: 343.
- Thomsen AE, Christensen MS, Bagger MA, Steffansen B (2004). Acyclovir prodrugs for intestinal di/tripeptide transporter PEPT1: comparison of *in vivo* bioavailability in rats and transport in Caco-2 cells. *Eur J Pharm Sci* 23: 319–325.
- US Department of Health and Human Services, FDA, CDER and CBER (2006). Guidance for Industry, Drug Interaction Studies – Study Design, Data Analysis, and Implications for Dosing and Labeling, Draft Guidance. <http://www.fda.gov/CDER/guidance/6695dft.pdf> (accessed 1 May 2009).
- Våbø J, Nielsen CU, Ingebrigtsen T, *et al.* (2004a). Dipeptidomimetic ketomethylene isosteres as pro-moieties for drug transport via the human intestinal di/tripeptide transporter hPEPT1: design, synthesis, stability and biological investigations. *J Med Chem* 47: 4755–4765.
- Våbø J, Lejon T, Nielsen CU, *et al.* (2004b). Phe-Gly dipeptidomimetics designed for the di/tripeptide transporters PEPT1 and PEPT2: synthesis and biological investigations. *J Med Chem* 47: 1060–1069.
- Veber DF, Johnson SR, Cheng HY, *et al.* (2002). Molecular properties that influence the oral bioavailability of drug candidates. *J Med Chem* 45: 2615–2623.
- Veronese FM, Pasut G (2005). PEGylation, successful approach to drug delivery. *Drug Disc Today* 10: 1451–1458.
- Wan L, Zhang X, Gunaseelan S, *et al.* (2006). Novel multi-component nanopharmaceuticals derived from poly(ethylene)glycol, retro-inverso-Tat nonapeptide and saquinavir demonstrate combined anti-HIV effects. *AIDS Res Ther* 3: 12. <http://www.aidsrestherapy.com/content/3/1/12> (accessed 1 May 2009).
- Wang B, Nimkar K, Wang W, *et al.* (1999). Synthesis and evaluation of the physicochemical properties of esterase-sensitive cyclic prodrug of opioid peptides using phenyl propionic acid and coumarinic acid linkers. *J Pept Res* 53: 370–382.
- Woodley JF (1994). Enzymatic barriers for GI Peptide and protein delivery. *Crit Rev Ther Drug Carrier Syst* 11: 61–95.

# 2.5

## Preformulation in the industry step by step

*Heidi Lopez de Diego*

In the pharmaceutical industry, preformulation studies are initiated in the early stage of drug discovery and extend all the way through the development of the drug until registration. The results from the preformulation studies form an integral part of the registration package. In this chapter, the preformulation studies performed at the different stages of development of a new drug will be described.

The development is divided into the following stages: early discovery, where the lead series are identified; lead optimisation; late discovery, approaching the selection of the development candidate; early development, that is prior to the clinical studies; and full development, which means during the clinical studies. Of course it would be an advantage to know everything about the physicochemical properties of the compound at an early stage, so that these properties could be taken into account in all aspects of development. It is, however, time consuming to undertake salt selection and polymorphism screening, and it is waste of resources to do this on the vast amount of compounds that never even enter clinical trials. On the other hand, a salt shift, or appearance of a new stable polymorphic modification with significant different properties at a late stage of development may involve a lot of extra work and cause delay in registration of the new drug. Therefore it has to be decided at which stage of development each investigation should be performed, in a way that minimises the risk of delay, and at the same time uses as few resources as possible working on compounds that never turn into a marketed product.

Every company has its own preformulation programme and differences in the strategy are observed. These variations reflect differences in company politics, the size of the company, resources, specialist knowledge and available in-house techniques. As an example, high-throughput salt screening and polymorph screening are performed at an early stage of development in large companies with their own high-throughput facilities, while smaller companies without this equipment normally do salt



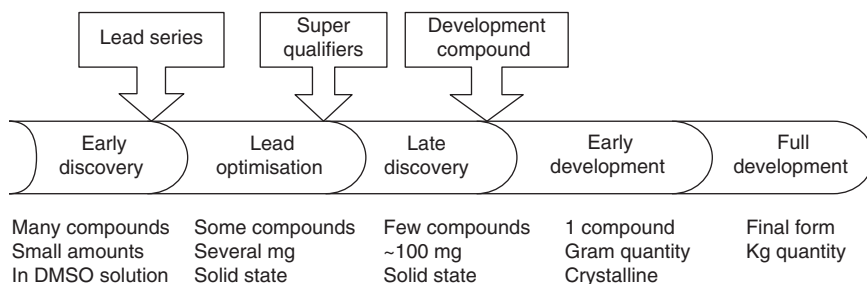


**Figure 2.5.1** Schematic representation of the development stages.

selection and polymorphism investigation at a later stage. Furthermore, every compound and project has its own peculiarity, so even though a preformulation programme and policy exist, deviations from the programme will occur to solve specific challenges for a given compound.

The number of compounds, the amount and purity of each compound, and the demands in relation to precision of the analytical results change throughout the development. In the following, the preformulation studies performed at each stage of development are described. A schematic representation of the development stages is given in Figure 2.5.1.

### 2.5.1 Early discovery

In the early discovery phase the purpose of preformulation studies is to guide the chemist to compounds with properties that are acceptable for a drug. It is not enough that the compound is biologically active; it should also be able to reach the target in the human body. If, for example, compounds in a series are insoluble, very lipophilic, or very unstable, it will be impossible, or at least very difficult and time consuming to transform one of these compounds into a bioavailable drug. It would be preferable if another series is selected or the compounds are modified in a way that gives better physicochemical properties.

At the early discovery stage, the keyword is ranking. A large number of compounds are being investigated and they have to be ranked from a physicochemical point of view. We are not seeking precise values; the compounds at this stage often only exist in very small amounts and with low purity, so the aim is to divide the compounds into groups as: good, acceptable, bad or unacceptable, using a small amount of compound and a short time on each compound. The techniques at this stage are often denoted ‘high-throughput screening’. Even placing the compounds into

the groups itemised above may be difficult. At the early stage of development, there is usually no information available about the biological potency. It is clear that a very potent compound will be administered in low dose and therefore the requirement for solubility is much less than for a compound that ultimately has to be given in a dose of 500 mg. Furthermore, the expected route of administration may affect the grouping. The demands on solubility, lipophilicity and stability differ for a compound in a cream as compared to a compound for oral administration.

The typical parameters of interest at this point are: acid/base properties, stability, solubility and lipophilicity. The available substance for the investigations is often only few microlitres of a dimethylsulfoxide (DMSO) solution.

#### **2.5.1.1 Acid/base properties**

The acid/base properties give information about how other properties changes with pH (e.g. lipophilicity and solubility) and about whether the solubility may be changed by selecting a salt for development.  $pK_a$  values are not measured at this stage, but from the structure of the molecule it can be judged whether the compound has any acid- or base character within the pH range of interest ( $pH \sim 1-10$ ). Some companies use computer programs for calculation of approximate  $pK_a$  values.

#### **2.5.1.2 Stability**

The stability is seldom measured at this stage, but the molecular structure gives information about whether obvious stability problems may be expected.

#### **2.5.1.3 Solubility**

Low solubility is one of the major challenges in the modern pharmaceutical industry. Nephelometry may be used for solubility ranking. Microtitre plates are loaded with different concentrations of the compounds in buffer solution and placed in the nephelometer, where laser light is used to measure the turbidity of the solutions. If a solution has a concentration that is higher than the solubility of that particular compound, precipitation will occur, leading to a turbid solution. One of the major drawbacks of this method is the danger of formation of supersaturated solutions due to lack of precipitation of crystalline material. Another drawback, if the solutions are prepared from DMSO solutions, is that effect of the

presence of DMSO may differ from compound to compound and thereby upset the ranking.

Some companies use computer programs for calculation of approximate solubility.

#### 2.5.1.4 Lipophilicity

The lipophilicity of a homologous series of compounds may be ranked by high-performance liquid chromatography (HPLC). In this method, the retention times of a series of compounds with known  $\log D$  values are measured on reverse-phase HPLC (RP-HPLC) through a lipid column using a buffer solution, and a standard plot of retention time versus  $\log D$  is constructed. Then, from the plot, the  $\log D$  values of the unknown compounds may be estimated from their retention times.

The major drawback of this method is that the compounds should be of similar structure (homologous series) to get the correct order of magnitude.

### 2.5.2 Lead optimisation

The purpose of preformulation studies in the lead optimisation phase is to help the medicinal chemist in optimising the series as regards physicochemical properties. If, for example, low solubility is the problem, it may be improved by introducing a polar group into the molecule. At this stage the compounds are solids and the amount available for preformulation studies is typically  $\sim 10$  mg.

The properties of principal interest are  $pK_a$ ,  $\log P/\log D$ , aqueous solubility and stability. Not all parameters are measured on all compounds. Depending of the general properties of the series, focus is placed on different parameters. Furthermore the solubility in different vehicles (e.g. cyclodextrins) is important information for animal experiments.

#### 2.5.2.1 $pK_a$

The  $pK_a$  values are determined by titration. Often the solubility of the compound is too low to allow titration in pure water. In these cases the titration is performed in water–methanol mixtures with variation in methanol content, and the  $pK_a$  value in pure water is determined by extrapolation to zero methanol content.

### 2.5.2.2 $\log D$

The  $\log D$  profile may be determined by titration if the compound has a  $pK_a$  value in the relevant range and it is known. Titration is performed with known amounts of octanol present. The shift in the apparent  $pK_a$  value is related to the water–octanol equilibrium and makes it possible to calculate the entire  $\log D$  versus pH profile.

Another possibility is to use the shake-flask method.

### 2.5.2.3 Solubility

The solubility is determined at a fixed pH value. Phosphate buffer pH 7.4 is often chosen as a solvent. The solubility is typically determined using the shake-flask method (e.g. by adding excess of solid to the buffer, leaving it shaking at constant temperature (often 22 °C or 25 °C) for 1–2 days and then measuring the concentration in the supernatant using HPLC).

If sufficient compound is available (~20 mg), the solubility is determined in relevant vehicles (e.g. cyclodextrin solutions) to support the choice of formulation for animal experiments.

### 2.5.2.4 Stability

The stability is measured in solution, often under very stressed conditions (e.g. exposed to light in a light cabinet, placed at high temperature in solution of different pH). The concentration is measured by HPLC before and after exposure to the stressed condition.

## 2.5.3 Late discovery

At a later stage in the discovery process, a few promising compounds are selected. These are sometimes called super qualifiers. At this stage the compounds exist as fairly pure solid compounds and in larger amounts. This means that normally 100–200 mg can be used for preformulation studies. The preformulation task is to characterise them and judge whether they have suitable properties for development, highlight problems, and give input to possible solution.

At this point,  $pK_a$  values and the  $\log D$  profile are normally already known. The crystallinity is verified by X-ray powder diffraction (XRPD). If the compound is not crystalline, efforts are made to crystallise it. The aqueous solubility is re-determined at e.g. pH 7.4, and after the solubility measurement, the precipitate is analysed for crystallinity and identity

(XRPD). It is important for solubility determination that the solid is crystalline, as amorphous material has higher solubility. If it subsequently crystallises the solubility will drop significantly (easily by up to 10 times). From the solubility at pH 7.4 and the  $pK_a$  value, the solubility profile (solubility versus pH) can be calculated. This profile is used for judging whether, for example, solubility problems may be overcome by selecting another salt. If so, a mini salt screening is considered.

Properties such as  $pK_a$ , lipophilicity, stability in solution at fixed pH and solubility at fixed pH (in the pH range where the solubility of pure base (acid) determines the overall solubility) are inherent compound properties that are independent of the salt form selected. Therefore they cannot be improved by selecting another salt.

Other properties such as crystallinity, melting point, thermal stability and hygroscopicity are salt dependent. Also, the solubility at low pH for bases and at high pH for acids depends on the salt.

The obtained form of the compound is characterised with respect to crystallinity (XRPD), melting point (DSC), thermal stability (thermogravimetric analysis (TGA)), hygroscopicity (dynamic vapour sorption (DVS)) and solubility in water without pH adjustment. Furthermore, the solid-state stability may be determined under highly stressed conditions (light and high temperature and humidity).

From the results of these investigations, it is judged whether the present form may be used for the early development, or another salt is needed.

#### 2.5.4 Early development

In this stage, the compound has to be turned into a new drug; nevertheless, its properties may be problematic. Hopefully the preformulation work during discovery has resulted in selection of a compound with adequate properties, and in this case it is 'just' a matter of optimising the compound in relation to selecting the best salt, finding the more stable polymorphic modification and characterising its properties. However, if it happens that a particular compound with a unique pharmacological profile is insoluble, unstable and very lipophilic, and if all attempts to modify the molecule towards better physicochemical properties lead to lack in biological activity, the problems with bioavailability have to be overcome in the development.

The purpose of the preformulation studies is to find the best form of the compound for development into a drug, and to characterise it with respect to all physicochemical properties. The first step is to evaluate

whether the compound may be developed into a stable bioavailable drug or whether it should be considered for developing a prodrug. Then the best salt for development has to be identified (if the compound has acid or base properties). When the salt is selected it has to be characterised. Part of the characterisation is performed during the salt screening, as physicochemical properties form the basis for the selection (e.g. aqueous solubility, intrinsic dissolution rate, stability, thermal behaviour, hygroscopicity) but solubility versus temperature, solubility in organic solvents, possible solvate formation and polymorphism screening also remain to be carried out.

The characterisation is described here as a case study (compound XX).

#### 2.5.4.1 Background

XX is a new development candidate. The following parameters have been determined in the discovery phase: it is a base with one  $pK_a$  value = 8.5. It has a solubility of  $180 \mu\text{g ml}^{-1}$  at pH 7.4.  $\text{Log}P = 2.6$  and  $\text{log}D_{7.4} = 2.2$ . The  $\text{log}D$  profile has been determined by titration. It is unstable in acidic solution. It will be developed for oral administration. So far it has been precipitated as an oxalate salt.

It is not expected to give problems where physicochemical properties are concerned, although acidic salts should be avoided as they could give rise to an acidic microenvironment in the formulation, leading to possible degradation.

So far the free base of the compound has not been isolated as a crystalline solid. The solubility at pH 7.4 may therefore be overestimated. Efforts are made to crystallise the base.

#### 2.5.4.2 Preformulation work

The free base is crystallised and used for re-determination of the aqueous solubility at pH 7.4. The result gives  $30 \mu\text{g ml}^{-1}$ . The new solubility versus pH curve is shown in Figure 2.5.2, together with the previous one. It appears that the compound is much less soluble than expected from the initial investigation.

At the same time it is observed in the biology department that they cannot make the cyclodextrin solutions at  $15 \text{ mg ml}^{-1}$  for animal dosing as they could previously. The reason is that the free base precipitates. New solubility determinations in cyclodextrins are performed and the dosing programme has to be changed.

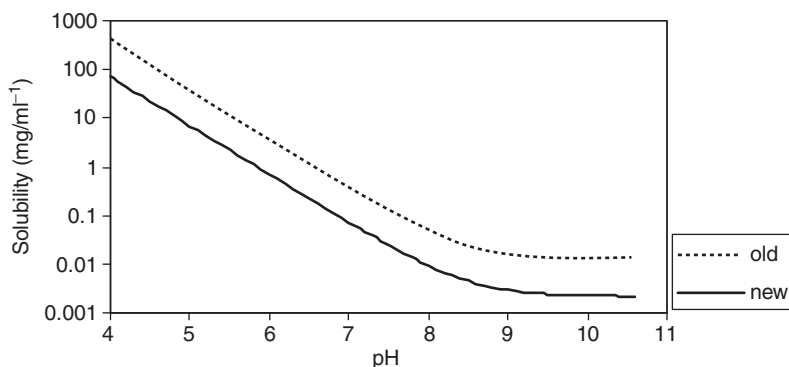


**Figure 2.5.2** Solubility versus pH calculated from the old value at pH 7.4 ( $180 \mu\text{g ml}^{-1}$ ) and from the new value ( $30 \mu\text{g ml}^{-1}$ ).

The free base is characterised. It is found to be non-hygroscopic and crystalline, with low solubility and a low intrinsic dissolution rate in hydrochloric acid. It is therefore clear that a salt screening should be performed. The more important parameters for this salt screening are the solubility and the dissolution rate, although the salt must not give rise to acidic solution.

#### 2.5.4.3 Salt screening

The properties of the oxalate salt are already known. A series of other acids are selected, and a small amount of salt of each acid is made. The first criterion for an acceptable salt is that it is crystalline and has a well-defined stoichiometry. For most compounds these properties are closely connected, a crystalline compound is well defined; but in some cases the solubility of a 1:1 salt and a 2:1 salt is so close that the mixtures precipitate, which gives the overall precipitation odd stoichiometry.

The prepared salts are analysed by XRPD. The stoichiometry of the crystalline ones is then checked by microanalysis (carbon hydrogen nitrogen (CHN)). The solubility of those that are well defined and crystalline is then determined. pH is measured in the saturated solution, and the precipitate from the solubility determination is analysed by XRPD to check that the solubility measure is really the solubility of the crystalline salt.

The three more-soluble salts are selected for further characterisation, and larger amounts of these salts are made (200–500 mg of each). XRPD is performed to ensure that the same polymorphic modification as last time is obtained. It happens very often that the first small amount made is a metastable modification.

The larger amount is characterised by:

- intrinsic dissolution rate
- thermal properties (TGA and DSC)
- solid-state stability (light, heat and humidity, e.g. 80°C, 80% relative humidity); the stability is tested under very stressed conditions in order to be able to rank the compounds in a short time
- hygroscopicity (DVS).

From these results the most promising salt is selected.

Now the basic properties of this salt are known. A large batch is made for general early development activities, and part of the batch is used for further characterisation. The first task is to check that the same crystal modification is obtained (XRPD). Upscaling from small batches only prepared for salt-screening purposes to larger scale may lead to other crystal forms (polymorphism).

Then the solubility in different organic solvents is measured. This has two purposes. One is to actually determine the solubility of the salt in organic solvent and the other is to get information on possible solvate formation and polymorphism.

The solubility in organic solvents is determined by addition of excess of compound to the solvent and then shaking the suspensions for several days (shake-flask method).

The solubility is determined as the concentration of compound in the supernatant.

The precipitate is isolated and analysed by XRPD. In methanol and ethanol, the X-ray powder diffractogram of the precipitate is similar to the pattern of the salt batch used.

In toluene, the diffractogram of the precipitate differs from the original diffractogram. This implies that either a new polymorphic modification is obtained or a solvate is formed. The precipitate is then analysed using TGA. The TGA thermogram is shown in Figure 2.5.3.

The curve shows a weight loss of about 10% corresponding to a solvate (hemi-toluenate). This means that a solvate has been formed from toluene. The sample is heated to 120°C, and subsequently analysed by XRPD. From the TGA curve it is evident that at this temperature the solvent is liberated. The XRPD differs from both the solvate diffractogram and the original batch diffractogram. This means that a new polymorph has been formed. The modification obtained was less stable than the original form (proved afterwards by cross-seeding).



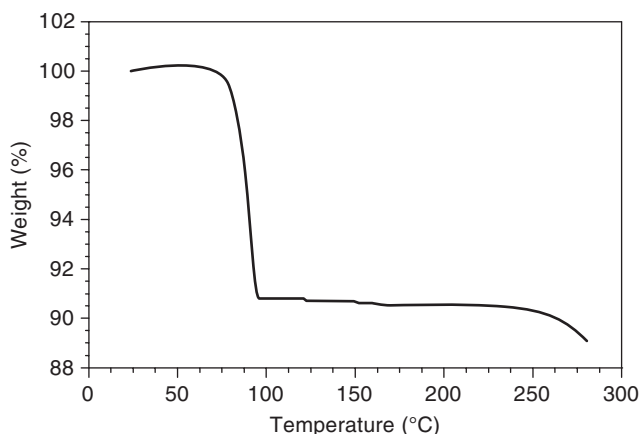


**Figure 2.5.3** TGA thermogram of the precipitate from toluene.

Other aromatic solvents also led to formation of solvates. All these solvates formed metastable polymorphic modifications after desolvation. Therefore, it is concluded that aromatic solvents should be avoided in the final step of the process.

The saturated solutions from the solubility determinations are left for slow evaporation of the solvents. The solids obtained from these experiments are analysed by XRPD to see if new polymorphs are obtained. No new form was obtained. Some of the precipitates seem to be larger crystals (slow evaporation is the optimal condition for crystal growth). These are investigated under the microscope, and the crystals obtained from methanol seem to be large single crystals. Therefore this precipitate is used for crystal structure determination by single crystal X-ray analysis.

#### 2.5.4.4 Polymorphism investigation

Polymorphism investigation is one of the most demanding tasks in the preformulation package. Some information has already been obtained from the experiments for determination of solubility in organic solvents. Furthermore, all the batches produced are followed up in the chemical development process.

Polymorphism screening is performed by making crystallisations from a large number of solvents and solvent mixtures under different conditions (high and low temperature, fast and slow cooling, stirring, no stirring etc), always avoiding the presence of crystal seeds.

All precipitations are analysed by XRPD. If new diffractograms are obtained, TGA is used to check whether it is a solvate or a new polymorphic modification.

If new polymorphs are obtained, the next step is to determine the relative thermodynamic stability of the forms. It has to be clarified whether it is monotropy (the same form is the more stable at all temperatures) or enantiotropy (a transition temperature exists where one form is the more stable form at temperatures below this temperature and the other form is stable above this temperature). The relative thermodynamic stability at room temperature is determined by cross-seeding experiments, where saturated solutions of each polymorph are seeded with another one and the mixtures are left for days to weeks. Subsequently the precipitate is analysed. The metastable form is then transformed into the stable form. The DSC-thermograms (melting point and enthalpy) are used for more information of the relative stability issues (the higher-melting form is the more stable in the case of monotropy; the lower-melting form has the higher enthalpy of fusion in the case of enantiotropy). The solubility of each form is measured at different temperatures to find the eventual transition temperature (in the case of enantiotropy).

If a more stable form appears, that one is normally chosen for development.

In that case the entire characterisation has to be repeated for that form.

#### **2.5.4.5 Compatibility**

Examination of compatibility with excipients is performed when formulation development is initiated.

#### **2.5.5 Full development**

Now all should be done. It may, however, happen that new polymorphic forms appear during scaling-up of the process. Therefore the new batches should be followed, not only by the analytical team, but also by the preformulation group.

Further characterisation may also be needed for particular formulations.



## Part 3

### Membrane transport of drug candidates

3.1	Structure and function of absorption barriers	115
3.2	Passive diffusion of drug substances: the concepts of flux and permeability	135
3.3	Carrier-mediated transport kinetics	153
3.4	Classification of human transporters	175
3.5	Absorptive transporters	193
3.6	Efflux transporters	213
3.7	Preclinical evaluation of drug transport	225

The aim of Part 3 is to provide an overview of drug transport across biological barriers. Tissues such as the intestine or the lung perform functions that are vital to the maintenance of the human body. One of the functions of such epithelial barriers is to separate the body from the exterior. In the intestine the epithelial cells separate ingested food from the systemic circulation, and the lung tissues separate inhaled air from the blood circulation. A normal function of biological membranes is thus to serve as a barrier. In drug delivery the biological membranes are normally viewed as barriers to drug transport, regardless of the fact that they may not always be barriers to all drug substances or candidates.

In Chapter 3.1 ‘Structure and function of absorption barriers’, the focus is on the nature of the various epithelial and endothelial barriers. The following Chapters 3.2–3.6 provide a thorough description of the mechanisms moving molecules across membranes, and the concept of drug permeability. These chapters provide tools for understanding and describing transport via passive or active transport mechanisms. Since

membrane transporters are important for bioavailability of drug substances, classifications of transporters via classical functional concepts as well as genetic concepts are provided. The last chapter of this section is about the preclinical evaluation of drug transport. This chapter gives an industrial perspective on how drug candidates are evaluated in terms of transport properties as well as metabolism. The impact of transporters on bioavailability and potential risk of transporters as mediators of drug–drug interactions have also gained the attention of the regulatory authorities. A draft *Guidance for Industry* from the US Department of Health and Human Services, Food and Drug Administration (FDA), Center for Drug Evaluation and Research (CDER) and Center for Biologics Evaluation and Research (CBER) states:

... not every drug–drug interaction is metabolism-based, but may arise from changes in pharmacokinetics caused by absorption, distribution and excretion interactions. Drug–drug interactions related to transporters are being documented with increasing frequency and are important to consider in drug development (US Department of Health and Human Services, FDA, CDER and CBER, 2006).

## Reference

- US Department of Health and Human Services, FDA, CDER and CBER (2006). *Guidance for Industry, Drug Interaction Studies – Study Design, Data Analysis, and Implications for Dosing and Labeling*, Draft Guidance. <http://www.fda.gov/CDER/guidance/6695dft.pdf> (accessed 12 May 2009).

# 3.1

## Structure and function of absorption barriers

*Birger Brodin, Bente Steffansen and Carsten Uhd Nielsen*

New drugs are normally formulated so they can be administered via non-invasive pathways. This is due to a number of diverse factors such as patient compliance, safety, production costs and product stability. The conventional oral tablet remains one of the most popular choices when selecting new formulations of a drug substance. However, a number of issues must be addressed when the drug substance is intended to permeate a barrier and act at a site distant to its dissolution site. The aim of this chapter is to provide an overview of morphology and permeability properties of the most important drug barriers in the body. This will hopefully provide the reader with a basic understanding of some of the factors that must be taken into account when designing new drug formulations for transepithelial delivery.

### 3.1.1 Epithelial morphology

Layers of specialised cells, epithelia, cover nearly all surfaces of the body, both external and internal. Epithelia constitute the barriers between the body and the external environment and have two main functions: (1) they protect the internal environment of the body from the external environment, and (2) they allow exchange of relevant nutrients, water, gases and waste products with the environment. Human epithelia are specialised so that the predominant exchange of gases takes place in the lungs, the predominant absorption of nutrients takes place in the small intestine, the skin is mainly protective, and so forth. However, when one tries to analyse the function of various epithelia, it must always be taken into account that the tissues serve these two functions: protection of the internal environment of the body and exchange of relevant compounds with the exterior.

Epithelia can be classified morphologically by (1) their number of cell layers, (2) the shape of the cells, and (3) the presence of apical surface specialisations such as cilia or keratin (Wheater *et al.*, 2006). This is shown in Table 3.1.1.

**Table 3.1.1** Epithelial classifications; epithelia can be classified by numbers of cell layers, shape or specialisation of cells. Often an epithelium will be described with a combination of these terms

<i>Number of cell layers</i>	<i>Shape of cells</i>	<i>Specialisations</i>
1: Simple epithelium	Flat, irregular: squamous epithelium	Apical cilia: ciliated epithelium
>1: Stratified epithelium	Cuboidal: cuboidal epithelium Tall columnar: columnar epithelium	Keratin in apical layers: keratinising epithelium

As a general rule, simple epithelia normally perform functions such as absorption or secretion, whereas stratified epithelia to a larger extent serve protective roles. The morphologies of various types of epithelia are shown in Figure 3.1.1. Simple squamous epithelia are often found lining airways, in body cavities and blood vessels, permitting passive transport of liquids and gases between body compartments. Cuboidal epithelia are usually found in ducts and tubules of the kidney and glands. Columnar epithelia are found in highly absorptive epithelia such as the small intestine. The presence of keratin or cilia has traditionally been used to subdivide epithelia further. Keratin is found in the outermost layer of stratified, squamous epithelium, the skin for instance, and provides resistance to mechanical stress and protects the underlying tissue from loss of liquid. Cilia serve the function of generating a flow of liquid/mucus and are found in the airways as well as in other types of tissue. A specialised stratified epithelial type, the transitional epithelium, is found in organs that can stretch, such as the bladder or urethra. In transitional epithelia, the cell layers can slide over each other allowing distension and contraction.

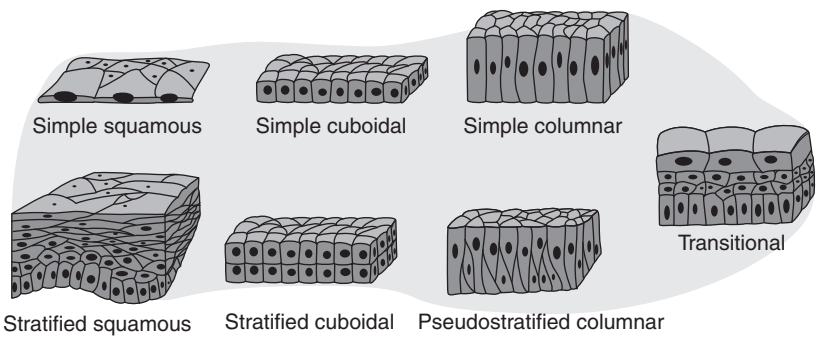


**Figure 3.1.1** Morphologies of basic epithelial types.

Functionally, epithelia can also be classified as ‘tight’ or ‘leaky’ on the basis of their resistance to paracellular water and solute flow. The colon and collecting ducts of the kidney are typically tight epithelia where uptake of salts and water is transcellular. The small intestine and the proximal tubule of the kidney are examples of leaky epithelia where a substantial paracellular transport can occur. Both tight and leaky epithelia possess tight junctions, but differ in their permeability. This is also reflected in the electrical resistance of the epithelia, with leaky epithelia having transepithelial resistance values below  $200 \Omega \text{cm}^2$  and tight epithelia having resistances above this value (Marrero *et al.*, 1998).

### 3.1.2 The epithelial cell and tight junctions

Epithelial cells generate boundaries between the body and its external environment. In order to maintain a constant intracellular environment, the cells must be able to allow controlled passage of water, nutrients and waste products. Two important features of epithelial cells make this possible: (1) tight junctions, and (2) polarity of protein expression. Absorptive epithelial cells are illustrated in Figure 3.1.2.

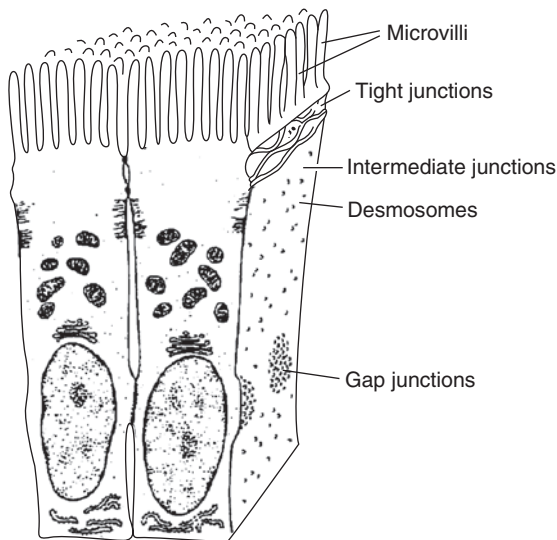


**Figure 3.1.2** Absorptive epithelial cells. Tight junctions define the border between the apical and lateral membranes, and enable polarised expression of proteins. Adapted from Weinstein RS, McNutt NS (1972). Cell junctions. *N Engl J Med* 286: 521–524.



Tight junctions connect epithelial cells at their apical end. Epithelial cells can also be interlinked via a set of protein contacts such as gap junctions, desmosomes, integrins etc. Three types of membrane domains can be distinguished: (1) apical plasma membrane facing the exterior, (2) lateral plasma membrane facing neighbouring cells, and (3) basal plasma membrane. The latter two are normally treated together and termed the basolateral membrane. The epithelial cells rest on 'the basement membrane', a filamentous protein/polysaccharide network secreted by the epithelial cells and by the underlying connective tissue. Beneath the basement membrane lie connective tissue and blood vessels. The barrier function of epithelia is determined by the passive permeability of the tight junctions and of the epithelial cells, as well as the selective barrier properties of the cells, which are determined by a range of transport proteins. The tight junctions constitute a barrier for paracellular diffusion of molecules, but also a barrier for lateral diffusion of membrane proteins within the membrane. Epithelial cells can therefore maintain a polarised membrane protein expression pattern, enabling vectorial transport of water and nutrients. Important specialisations in absorptive epithelia are the microvilli, small projections of the plasma membrane, which can significantly increase the nominal surface area for absorption.

### 3.1.3 The gastrointestinal tissue barriers

The gastrointestinal (GI) tract is a long tube traversing the body. Its primary function is breakdown of food to absorbable entities, uptake of nutrients and water, and excretion of indigestible food components. The GI tract is divided into segments with different functions and is illustrated in Figure 3.1.3.

The oral cavity is designed for chewing and wetting food components. The epithelia in the mouth are mainly protective; however, a number of glands secrete liquid along with some digestive enzymes. The main function of the oesophagus is to move food to the stomach by peristaltic muscle action. The role of the stomach is to digest and solubilise food particles and kill microbes. This is accomplished by release of pepsin and hydrochloric acid. The stomach also regulates release of dissolved food into the small intestine through the pyloric sphincter. Digestion continues in the small intestine, aided by enzymes released from the exocrine glands of the pancreas as well as by enterocytic enzymes, (intestinal peptidases are summarised in Table 2.4.3, Chapter 2.4). The

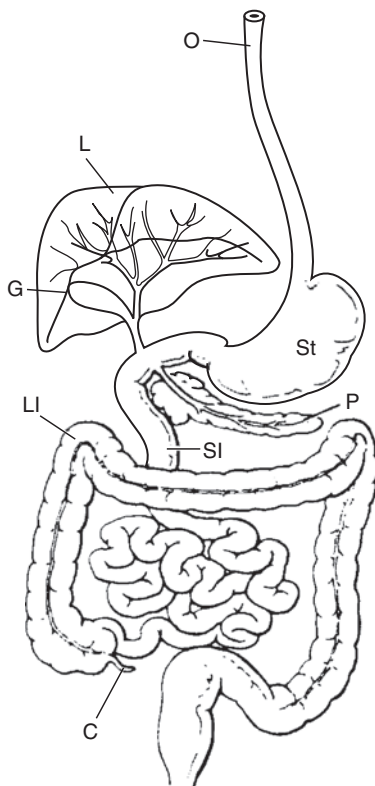


**Figure 3.1.3** The GI tract (mouth and pharynx not included). C, colon; G, gall bladder; L, liver; LI, large intestine; O, oesophagus; P, pancreas; SI, small intestine; St, stomach. Adapted from Eckert R, Randall D, Augustine G (1988). *Animal Physiology. Mechanisms and adaptation*, 3rd edn. New York: WH Freeman and Company.

small intestine is responsible for uptake of most of the food constituents such as proteins, carbohydrates and fat. The colon is the site for reabsorption of water from the intestinal contents, and the primary role of the rectum is to cause defecation, via muscle action. A detailed description of the anatomy of the GI tract is beyond the scope of the present text; however, in the following we shall focus on GI barrier structures that are relevant in drug absorption and delivery.

### 3.1.3.1 The oral cavity, pharynx and oesophagus

The primary function of the epithelial barriers of the oral cavity is to provide an environment for wetting and chewing food particles, while maintaining a barrier for micro-organisms and protection against

mechanical stress due to chewing and mastication. The oral cavity is thus covered with stratified, squamous epithelia, which can withstand moderate mechanical abrasion and is an effective barrier for large hydrophilic molecules and micro-organisms. Glands open up into the oral cavity and moisten tissue as well as food contents. This protects the epithelium of the oral cavity from desiccation and lubricates the food bolus before passage to the stomach. In terms of drug delivery, the oral cavity raises some challenges. The transit time of a food bolus is normally very short, so formulations for the oral cavity are usually designed to act on the buccal or sublingual epithelia, where they can avoid being swallowed. However, the continuous flow of saliva will tend to carry drug substance further down the GI tract. The mouth also is well equipped with sensory nerves, and drug formulations should thus act as quickly as possible in order to avoid compliance problems. The advantages of drug delivery from the oral cavity to the blood are the avoidance of hepatic first-pass metabolism of the drug, and avoidance of the acidic environment in the stomach, which may cause breakdown of certain drug substances.

The pharynx and the oesophagus mainly serve as a passage way from the mouth to the stomach, and due to the fast passage time and low permeability of the epithelia, they will not be treated further.

### 3.1.3.2 The stomach

The function of the stomach is to initiate digestion of food components, to grind food components into chyme and to release the chyme for further digestion and absorption. The epithelium of the stomach is a simple columnar epithelium, its main role being the secretion of a protective mucus layer. Specialised gland cells also produce hydrochloride and precursors of digestive enzymes. Very little absorption occurs in the stomach; there are, however, some notable exceptions. Alcohol can be absorbed to some extent through the stomach wall, as well as some weak acids, including the common drug substance acetyl salicylic acid (aspirin), which are more lipid soluble as their neutral species rather than anionic species.

The main role of the stomach is to control the rate of chyme influx into the small intestine. The gastric emptying rate is increased by gastric distension and decreased by duodenal distension. Duodenal fat or acid content also decreases gastric motility, and a number of other sensory inputs might also influence the emptying rate, e.g. pain, depression and fear. Variances in gastric emptying rates may have a large impact on the bioavailability of drug substances. Functional characteristics of the

**Table 3.1.2** Functional characteristics of gastrointestinal segments influencing drug dissolution and absorption; reproduced from Daugherty AL, Mrsny RJ (1999). Trans cellular uptake mechanisms of the intestinal epithelial barrier. Part one. *Pharm Sci Technol Today* 4: 144–151

<i>GI segment</i>	<i>Surface area (m<sup>2</sup>)</i>	<i>Segment length (m)</i>	<i>Residence time (h)</i>	<i>pH of segment</i>
Stomach	3.5	0.25	1.5	1–2
Duodenum	1.9	0.35	0.5–0.75	4–5.5
Jejunum	184.0	2.8	1.5–2.0	5.5
Ileum	276.0	4.2	5–7	7.0–7.5
Colon and rectum	1.3	1.5	1–60	7.0–7.5

stomach segment influencing drug and nutrient dissolution and absorption are shown in Table 3.1.2.

### 3.1.3.3 The small intestine

The chyme is passed from the stomach into the small intestine, via the pyloric sphincter. Functional characteristics of the various intestinal segments influencing drug and nutrient dissolution and absorption are shown in Table 3.1.2. The small intestine is a coiled tube, approximately 7–8 m long, consisting of three segments: the duodenum, the jejunum and the ileum. The duodenum is a short structure (35 cm) where the bile-pancreatic duct empties its contents of bile, digestive enzymes and bicarbonate. It is followed by the jejunum (~2.8 m) and the ileum (~4.2 m). There is no clear-cut distinction between the small intestinal segments. The small intestine is specialised in absorbing nutrients. It is highly folded with large folds (plicae) extending into the intestinal lumen. The surface is covered by small finger-like projections (villi) (see Figure 3.1.4), and the epithelial cells covering the villi are covered with microvilli.

The degree of folding decreases along the length of the small intestine. The total surface area of the small intestine has been estimated at ~300–500 m<sup>2</sup>. A meal will normally be digested and absorbed before it reaches the terminal end of the jejunum. The intestine therefore has a considerable overcapacity.

The villi are covered with a simple columnar epithelium consisting mainly of absorptive enterocytes. The intestinal epithelium is generally considered to be a leaky epithelium with resistances of the order of 100  $\Omega$  cm<sup>2</sup> (Greger, 1996). The small intestinal epithelium mediates

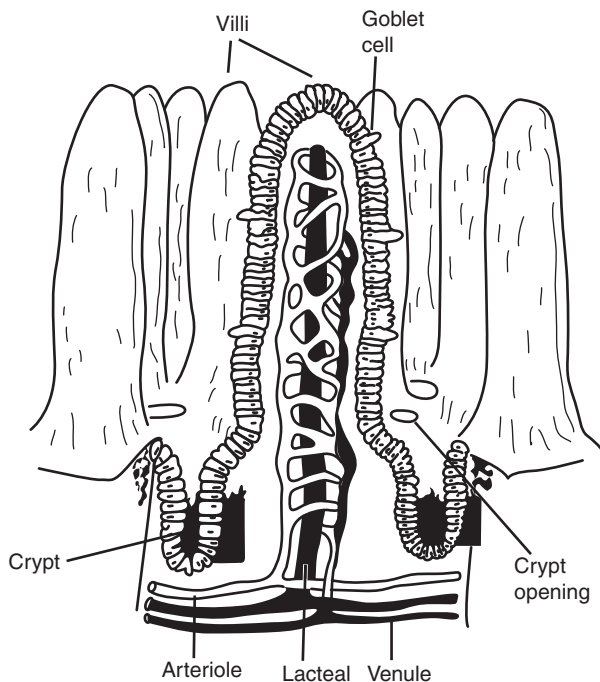


**Figure 3.1.4** Villi of the small intestine. Enterocytes are generated in the crypts, where division occurs. They migrate towards the tip of the villi, becoming progressively more mature. Adapted from Eckert R, Randall D, Augustine G (1988). *Animal Physiology. Mechanisms and adaptation*, 3rd edn. New York: WH Freeman and Company.

absorption of dietary protein and carbohydrates via a range of membrane transport proteins. The uptake mechanism of lipids is still controversial. Although the classical point of view is that lipids diffuse passively into the intestinal cells, a number of reports have indicated that lipid transport proteins may mediate the uptake (Kampf and Kleinfeld, 2007). Smaller compounds may also pass paracellularly via the ‘leaky’ tight junctional complexes. Molecules as large as mannitol may cross paracellularly, and mannitol is often used as a marker for paracellular transepithelial flux in intestinal drug transport studies.

The huge surface area, the relatively long transit time, and the wide range of nutrient transporters present, make oral administration an obvious first-choice strategy for new formulations. However, some factors regarding the intestinal barrier must be taken into consideration with respect to oral administration. The drug candidate in question must either be stable in the acidic environment of the stomach, or protected by an

acid-resistant coating that disintegrates when the formulation reaches the small intestine. The drug candidate should also be able to withstand attack from the digestive enzymes present in the lumen of the small intestine. The physicochemical properties of the drug candidate should accommodate uptake by passive diffusion, or be a substrate for one of the intestinal transporters. Furthermore, the drug candidate should not readily undergo first-pass metabolism in the liver, since compounds taken up from the small intestine enter the portal vein, from where they are transported directly to the liver before reaching the systemic circulation.

#### **3.1.3.4 The colon and the rectum**

The colon is a tube, ~120 cm long, consisting of three relatively straight segments: the ascending, transverse and descending colon. The function of the colon is to store and concentrate undigested matter and propagate the luminal content towards the rectum. This is reflected in the morphology of the colon, where plicae or villi are absent, and the intestinal tissue is thicker. Absorption in the colon is mainly limited to absorption of sodium, chloride and water, but vitamins produced by colonic bacteria are also absorbed. Intestinal contents can reside in the colon for 18–24 h, and are moved towards the rectum by muscular action. Colon transit time varies considerably depending on age, nutritional status and lifestyle factors. The contents are passed to the rectum. The main function of the rectum is to mediate defecation. The rectum is a thick, highly vascularised structure with no role in absorption of nutrients. However, due to the high vascularisation and its accessible epithelial surface, drug substances can be taken up from the rectal lumen if they are able to permeate passively across the epithelium, i.e. have suitable lipophilicity.

#### **3.1.4 The respiratory tract**

The main role of the respiratory tract is to mediate exchange of gases (oxygen, carbon dioxide) between the blood and the atmosphere. Minor specialised functions are also present, such as olfactory organs in the nasal cavity and the vocal cords in the larynx. The respiratory tract can roughly be divided into the conductive part and the respiratory part. Air is taken up via the nose into the nasal cavity, where it is heated and larger particles are trapped. Air moves via the trachea, the bronchi and the bronchioles to the respiratory part, consisting of the respiratory bronchioles, the alveolar ducts, alveolar sacs and finally the alveoli.

### 3.1.4.1 The nose

The nose and the nasal cavity are designed to take up air, clean it of particles and humidify it. Air is inhaled via the nostrils and passes into the nasal cavity and via the nasopharynx to the trachea. The nasal epithelium is divided into two major cell types, mucus-producing goblet cells and cilia-covered cells that move the thin mucus layer towards the nasopharynx. The epithelium is a pseudostratified columnar ciliated epithelium with goblet cells immersed. The submucosa is extremely vascularised, providing a means of heating the inhaled air towards body temperature. Submucosa furthermore contains glands that secrete mucus and liquid, which aids in humidifying inhaled air. The nasal cavities have an area of  $\sim 150 \text{ cm}^2$ . The nasal epithelium has properties that make it an obvious target for transepithelial drug delivery, e.g. a mucus layer which might trap particles, a fairly thin epithelial barrier without keratinisation, extensive submucosal vascularisation and no hepatic first-pass metabolism. However, nasal drug delivery also offers a number of challenges. Formulations must be deposited in the nasal cavities and stay there long enough to permit absorption; formulations must not interfere with ciliary function or irreversibly alter the epithelial integrity. The olfactory epithelium is situated in the upper part of the nasal cavity and covers  $\sim 10 \text{ cm}^2$ . It has been suggested that drug substances taken up in the olfactory epithelium might pass directly from the nasal cavity to the brain, thus circumventing the blood–brain barrier (Behl *et al.*, 1998; Illum, 2004). However, the existence of this proposed phenomenon is still controversial (Merkus and van den Berg, 2007).

### 3.1.4.2 The lung

The lungs are composed of a number of different tissue structures, forming two large sacs situated in the thorax. The upper parts of the lungs are tubes of decreasing diameter (trachea and bronchi), which primarily serve to conduct air to the lower parts. Gas exchange occurs in a number of small sacs at the end of the bronchioles, called alveoli. Gas exchange occurs in the alveoli, where the large surface area ensures rapid exchange. The maximal area available for gas exchange in the adult lung ranges from 50 to 100  $\text{m}^2$ . Lung epithelial morphology depends on function. The trachea and bronchi, which function as conductive tubes, are covered with a columnar ciliated epithelium. The alveoli are lined with two types of epithelial cells; type I and II pneumocytes. Type I pneumocytes are large squamous cells, constituting by far the largest part of the alveolus surface

area. Type II pneumocytes are smaller rounded cells, secreting surfactant. Exchange of gases occur across type I pneumocytes, while type II pneumocytes possess a number of transport proteins involved in fluid and salt transport. The alveoli are surrounded by a network of capillaries in close contact with the alveolar wall. The type I pneumocytes and the endothelial cells of the capillaries share a basement membrane, and the thickness of the 'air–blood barrier', pneumocyte – basement membrane – endothelial cell, is  $\sim 0.6 \mu\text{m}$  (Brain, 2007).

Systemic drug administration via the lungs is an attractive alternative to the more conventional oral administration pathway, due to the large absorbing surface area and direct access to the systemic circulation, thus avoiding hepatic first-pass metabolism. Especially for proteins, the pulmonary pathway seems to be a good alternative to oral delivery, since proteins are normally broken down rapidly in the GI tract (see Chapter 2.4). However, lung delivery involves the use of inhalation devices with the risk of large dose variations due to low compliance.

### 3.1.5 The skin

The skin is a continuous protective epithelium covering the external surface of the body. The skin of an adult is approximately  $2 \text{ m}^2$  and is the largest organ in the body. Skin thickness varies greatly in an individual, from  $<1 \text{ mm}$  on the eyelids to  $\sim 5 \text{ mm}$  on the upper back. Major roles of the skin are to prevent water loss from the organism, and to provide a physical and immunological barrier against pathogens. The skin also provides protection against mechanical, chemical and thermal stimuli, and participates in thermoregulation. Properties of the skin vary both at the level of the individual and between individuals. Age, race and diseases are all causes for skin variations. The outer boundary of the skin is the epidermis, a squamous stratified keratinised epithelium. The epidermis rests on the dermis, a thick vascularised layer containing glands, nerves and hair follicles. Epidermis and dermis structures of the skin are shown in Figure 3.1.5.

Below the dermis is the hypodermis, the subcutaneous layer of adipose tissue and larger blood vessels. The epidermis is the actual barrier towards the outside environment, and it is across this cell layer that drug substance permeation must occur. The barrier of the epidermis resides in the outer layer, the stratum corneum, where dead keratinised cells constitute a barrier for water and hydrophilic compounds (Elias, 1991). The stratum corneum can be considered a protein-lipid matrix, which



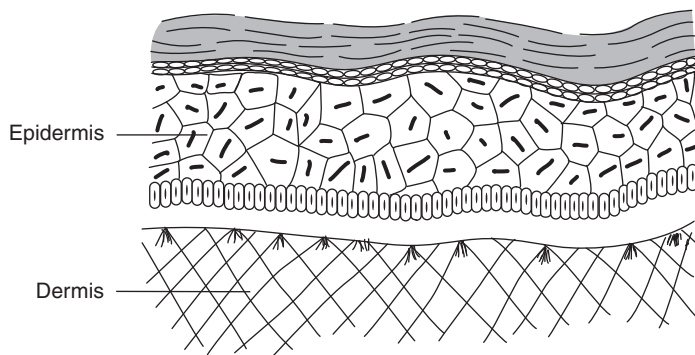


**Figure 3.1.5** Epidermis and dermis of the skin. The proliferative layer of the epidermis generates cells, which gradually move upwards to end up as flattened, water-impermeable keratinised cells at the outermost boundary (stratum corneum).

restricts the passive diffusion of both lipophilic and hydrophilic compounds (Curdy *et al.*, 2000). This barrier has a very high transepithelial resistance, estimated to be of the order of  $550 \text{ k}\Omega \text{ cm}^2$  (Kalia and Guy, 1995), indicating that the stratum corneum has a very low paracellular passage of ions (and larger hydrophilic compounds). However, this resistance drops markedly upon hydration. This is often exploited when designing formulations for skin administration. Once a compound has crossed the stratum corneum it may diffuse in the intercellular spaces to the dermis. From the dermis, drug substances can escape to the systemic circulation via blood vessels. Drugs might also act locally on nerve endings, inflammation and skin diseases.

The major challenge of drug administration via the skin is to overcome the barrier residing in the stratum corneum. The fact that permeability is increased upon hydration is exploited in formulations such as creams and patches. Another approach commonly used is increasing the stratum corneum permeability of candidates by formulating them as prodrugs with higher lipophilicity than the parent compound (Fang and Leu, 2006) or to include permeability enhancers in the formulations. Prodrugs are further described in Chapter 2.4.

### 3.1.6 Barrier tissues in the brain

The capillaries of the brain make up a very effective barrier for transport of drug substances and solutes between the blood and the cerebrospinal fluid. In the brain, the endothelial cells of the capillaries form an extremely tight continuous monolayer, as opposed to normal continuous

capillaries with a substantial higher permeability, or fenestrated capillaries with pores allowing for exchange of fluid and solvents.

The brain endothelial cells are linked together via extensive tight junctions (see Figure 3.1.6). The presence of tight junctions makes the tissue practically impermeable for larger hydrophilic molecules (Brightman and Reese, 1969), with the exception of some nutrient molecules, which are transported through the cells via nutrient transporters (Boado *et al.*, 1999; McAllister *et al.*, 2001; Paulson, 2002). Lipophilic molecules, which in other tissues normally would pass by simply diffusing through the lipid bilayers of the cells, are extruded by the activity of efflux pumps: transport proteins situated in the apical membrane of the brain endothelial cells. Thus the blood–brain barrier provides a ‘passive’ physical barrier, i.e. the tight monolayer of cells, and an ‘active’ barrier, i.e. the efflux pumps. Efflux pumps are present in other barrier tissues as well, but in the blood–brain barrier they play a predominant role in determining drug pharmacokinetics.

The transepithelial electrical resistance (TEER) across the blood–brain barrier is  $>1500\ \Omega\text{cm}^2$  (Crone and Olesen, 1982; Butt *et al.*, 1990), with experimental estimates reaching levels as high as  $6000\text{--}8000\ \Omega\text{cm}^2$  (Smith and Rapoport, 1986; Butt *et al.*, 1990). This is due to the very low ionic conductivity of the junctional structures in the blood–brain barrier in combination with the low ion permeability of the endothelial cells.

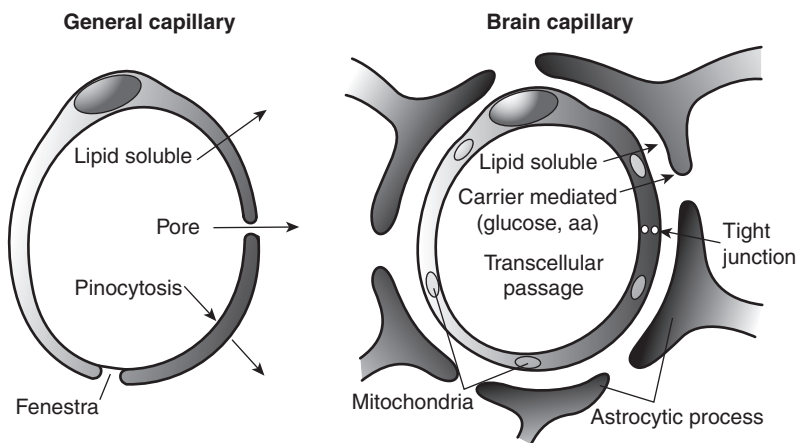


**Figure 3.1.6** The blood–brain barrier endothelial cells as compared to fenestrated capillaries. aa, amino acids.

The blood–brain barrier is considered the most important challenge factor in the development of central nervous system (CNS) drugs (Pardridge, 2007). In order to cross the blood–brain barrier, a drug substance can either cross paracellularly, transcellularly via diffusion through lipid bilayers, or transcellularly via membrane transport proteins. Drug substances with physicochemical properties that enable them to diffuse through lipid bilayers might, however, be apically extruded by the battery of efflux pumps extruding lipophilic substrates (Leslie *et al.*, 2005). Drug substances permeating via uptake transport proteins might show limited uptake due to saturation of the uptake transporters.

The most accurate method of determining the blood–brain barrier permeability of a drug substance is the *in situ* perfusion method (Reichel, 2006). However, this method is costly and not suited for screening studies. Over the last two decades, a number of research groups have therefore tried to generate *in vitro* blood–brain barrier models, but with variable success. Attempts have included endothelial cells isolated from bovine brain (Rim *et al.*, 1986, Shah *et al.*, 1989), astrocyte-conditioned media (Arthur *et al.*, 1987), co-cultures of endothelial and glial cells (Stanness *et al.*, 1999), and generation of blood–brain barrier cells from stem cells (Weidenfeller *et al.*, 2007). However, most attempts have failed to reproduce the tightness of the tissue, with TEER values of the models ranging from 30 to 100  $\Omega\text{cm}^2$ . The generation of an *in vitro* model of the blood–brain barrier is thus a major challenge for both industry and academia.

The extreme tightness of the blood–brain barrier and the activity of efflux proteins make administration of drug substances to the brain a great challenge. It has been estimated that up to 98% of the hit compounds coming out of traditional high-throughput screening programmes would fail to cross the blood–brain barrier due to low permeability (Pardridge, 2002). Screening programmes, based on Lipinski's rule of five and focusing on selecting substrates with blood–brain barrier permeability, have been implemented, thus selecting substrates with 'CNS-likeness' (see Figure 3.1.7).

Thus CNS drugs have a smaller optimal range of molecular weight, lipophilicity, and hydrogen-bond donors as well as hydrogen-bond acceptors compared to general therapeutics.

However, these screening criteria still remain rough guidelines and should be combined with knowledge of the substrate profiles of the brain efflux transporters.

<b>Drug-likeness</b> (Lipinski's 'rule of five') <ul style="list-style-type: none"> <li>• MW &lt;500</li> <li>• clogP &lt;5</li> <li>• HBD &lt;5</li> <li>• HBA &lt;10</li> </ul>	<b>Lead-likeness</b> <ul style="list-style-type: none"> <li>• MW &lt;350–400</li> <li>• clogP &lt;4</li> <li>• Solubility or scope for polar functions</li> </ul>	<b>CNS-likeness</b> <ul style="list-style-type: none"> <li>• MW &lt;450</li> <li>• clogP &lt;3</li> <li>• HBD &lt;4</li> <li>• HBA &lt;8</li> </ul>
--	---	---

**Figure 3.1.7** High-throughput screening criteria. The original 'rule of 5' and its modification for lead and CNS compounds, respectively. MW, molecular weight; clogP, calculated logP; HBD, number of hydrogen-bonding donors; HBA, number of hydrogen-bonding acceptors. For Lipinski's rule of five see Chapter 2.4.1.

Another factor, which makes prediction of blood–brain barrier permeability a difficult task, is the fact that blood–brain barrier properties might vary during disease conditions. Overcoming the obstacle of brain drug administration thus remains one of the major challenges in the field of drug delivery.

### 3.1.7 The eye

The eye is a complex structure, composed of many different cell types and tissue components. The design of formulations for topical delivery to the eye is challenging. The globe of the eye (the eyeball) is shown in Figure 3.1.8. The inner part of the eye (the anterior and the posterior chambers) is protected anteriorly from the environment by the corneal and the scleral epithelium. The cornea is a transparent 0.5–0.7 mm five-layer-thick membrane, consisting of an outward-facing epithelial layer, a thick fibrillated stroma, and finally an endothelium lining the anterior chamber. The cornea is covered by a film of lacrimal fluid at the exterior surface. Corneal epithelium is of the squamous-stratified type, with extensive networks of tight junctions resulting in low paracellular passage and high electrical resistance.

The remaining part of the eye exposed to the exterior, including the inside of the eyelids, is covered by conjunctival epithelium. The conjunctiva is a stratified columnar epithelium which is leakier than the cornea. However, transcorneal permeation is the main route of drug substance entrance from the lacrimal fluid to the anterior chamber (Urtti, 2006).

The posterior part of the eye is shielded from xenobiotics in the blood by the blood–retinal barrier, which shares some similarities with the blood–brain barrier described above (Antonetti and Wolpert, 2003). The blood–retinal barrier is composed of the retinal pigment epithelium and the endothelial cells of the retinal vasculature.

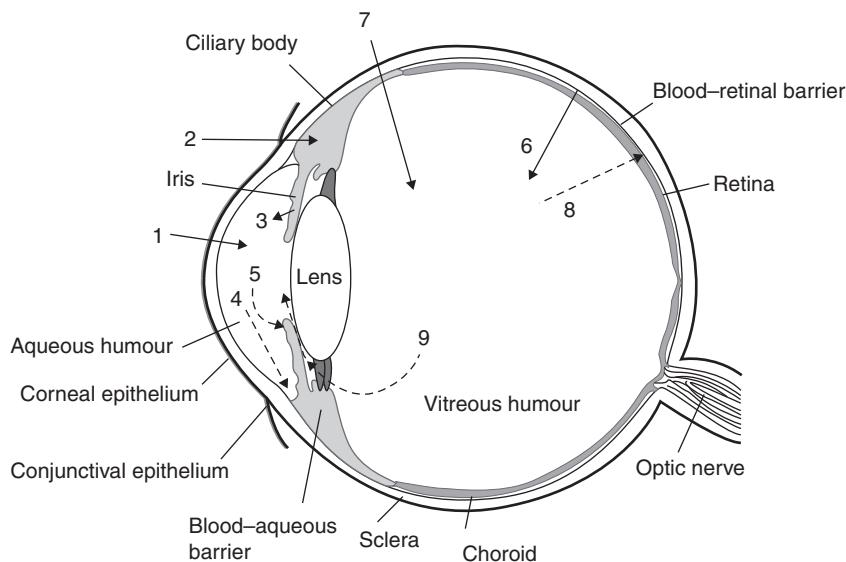


**Figure 3.1.8** Schematic representation of the eye and an overview of drug entrance and elimination pathways (depicted by arrows). (1) Transcorneal permeation; (2) permeation via the conjunctiva and sclera; (3) transport over the blood–aqueous barrier; (4) elimination from the aqueous humour into the trabecular meshwork and Schlemm’s canal, a drainage system; (5) elimination from the aqueous humour, across the blood–aqueous barrier into the blood; (6) transport from the blood into the posterior part of the eye, across the blood–retina barrier; (7) intravitreal drug administration; (8) drug elimination from the vitreous humour, across the blood–retina barrier; (9) drug elimination from the vitreous humour to the anterior chamber.

The anterior part of the eye can be treated with topical fluid formulations, for example eye drops. However, drainage from the ocular surface is fast, and the bioavailability of topically administered eye drops is low. Bioavailability to the posterior segments after topical administration of eye drops is generally close to zero due to fast clearance, low corneal permeability and long diffusion pathway. Systemic drug delivery to the posterior segment is hindered by the blood–ocular barriers, consisting of the blood–aqueous barrier and the blood–retina barrier. The posterior segment of the eye can generally only be reached via massive intravenous dosing or intravitreal administration. However, not all drug substances can be administered at high systemic concentrations due to systemic side effects, and intravitreal administration has its limitations due to its invasive nature. Therefore many posterior segment diseases, for example diabetic retinopathies and neural changes induced by glaucoma,

lack effective treatments (Urtti, 2006). Consequently ocular drug delivery to the posterior part of the eye remains a challenge.

### 3.1.8 Conclusions

The epithelial tissues of the body represent barriers for topical and systemic treatment by drug substances. Internal epithelia, i.e. endothelia, act in addition as barriers between the systemic circulation and the target such as the brain and the posterior segments of the eye. Detailed knowledge of the barrier in question will aid the formulation scientist in making proper choices of dosage forms and in selecting relevant preclinical studies such as permeability studies across relevant cell culture models or excised tissue models of the barrier in question. Such preclinical studies can be used to select and discard drug and formulation candidates at an early stage in the pharmaceutical drug development process.

### References

- Antonetti DA, Wolpert EB (2003). The blood–brain barrier: biology and research protocols. In: Nag S, ed. *Methods in Molecular Medicine*, volume 89. Totowa, NJ: Humana Press Inc., 365–374.
- Arthur FE, Shivers RR, Bowman PD (1987). Astrocyte-mediated induction of tight junctions in brain capillary endothelium: an efficient in vitro model. *Brain Res* 433: 155–159.
- Behl CR, de Meireles JC, Pimplaskar HK, *et al.* (1998). Effects of physicochemical properties and other factors on systemic nasal drug delivery. *Adv Drug Deliv Rev* 29: 117–133.
- Boado RJ, Li JY, Nagaya M, Zhang C, Pardridge WM (1999). Selective expression of the large neutral amino acid transporter at the blood–brain barrier. *Proc Natl Acad Sci U S A* 96: 12079–12084.
- Brain JD (2007). Inhalation, deposition and fate of insulin and other therapeutic proteins. *Diabetes Technol Ther* 9(suppl 1): s4–s15.
- Brightman MW, Reese TS (1969). Junctions between intimately apposed cell membranes in the vertebrate brain. *J Cell Biol* 40: 648–677.
- Butt AM, Jones HC, Abbot NJ (1990). Electrical resistance across the blood–brain barrier in anesthetized rats: a developmental study. *J Physiol* 429: 47–62.
- Crone C, Olesen SP (1982). Electrical resistance of brain microvascular endothelium. *Brain Res* 241: 49–55.
- Curdy C, Kalia YN, Falson-Rieg F, Guy RH (2000). Recovery of human skin impedance in vivo after iontophoresis: effect of metal ions. *AAPS Pharm Sci* 2(3): E23.
- Daugherty AL, Mrsny RJ (1999). Transcellular uptake mechanisms of the intestinal epithelial barrier. Part one. *Pharm Sci Technol Today* 4: 144–151.

- Eckert R, Randall D, Augustine G (1988). *Animal Physiology. Mechanisms and adaptation*, 3rd edn. New York: WH Freeman and Company.
- Elias PM (1991). Epidermal barrier function: intercellular lamellar lipid structures, origin, composition and metabolism. *J Control Release* 5: 199–208.
- Fang J-Y, Leu Y-L (2006). Prodrug strategy for enhancing drug delivery via skin. *Curr Drug Discov Technol* 3: 211–224.
- Greger R (1996). Epithelial transport. In: Greger R, Windhorst U, eds. *Comprehensive Human Physiology* volume 2. Berlin, Heidelberg: Springer-Verlag, 1217–1233.
- Illum L (2004). Is nose-to-brain transport in man a reality? *J Pharm Pharmacol* 56: 3–17.
- Kalia YN, Guy RH (1995). The electrical characteristics of human skin *in vivo*. *Pharm Res* 12: 1605–1613.
- Kampf JP, Kleinfeld AM (2007). Is membrane transport of FFA mediated by lipid, protein or both? *Physiology* 22: 7–29.
- Leslie EM, Deeley RG, Cole SP (2005). Multidrug resistance proteins: role of P-glycoprotein, MRP1, MRP2, and BCRP (ABCG2) in tissue defense. *Toxicol Appl Pharmacol* 204: 216–237.
- Marrero A, Ostrovskiy DA, Matkowskyj KA, *et al.* (1998). Electrophysiological characterisation of human distal colon using a novel technique. *Dig Dis Sci* 43: 2439–2445.
- McAllister MS, Krizanac-Bengez L, Macchia F, *et al.* (2001). Mechanisms of glucose transport at the blood–brain barrier: an *in vitro* study. *Brain Res* 409: 20–30.
- Merkus FW, van den Berg MP (2007). Can nasal drug delivery bypass the blood–brain barrier? Questioning the direct transport theory. *Drugs R D* 8: 133–144.
- Pardridge WM (2002). Drug and gene targeting to the brain with molecular Trojan horses. *Nat Rev Drug Discov* 1: 131–139.
- Pardridge WM (2007). Blood–brain barrier delivery. *Drug Discov Today* 12: 54–61.
- Paulson OB (2002). Blood–brain barrier, brain metabolism and cerebral blood flow. *Eur Neuropsychopharmacol* 12: 495–501.
- Reichel A (2002). The role of blood–brain barrier studies in the pharmaceutical industry. *Current Drug Metab* 7: 183–203.
- Rim S, Audus KL, Borchardt RT (1986). Relationship of octanol/buffer and octanol/water partition coefficients to transcellular diffusion across brain microvessel endothelial cell monolayers. *Int J Pharm* 32: 79–84.
- Shah MV, Audus KL, Borchardt RT (1989). The application of bovine brain microvessel endothelial cell monolayers grown onto polycarbonate membranes *in vitro* to estimate the potential permeability of solutes through the blood–brain barrier. *Pharm Res* 6: 624–627.
- Smith QR, Rapoport SI (1986). Cerebrovascular permeability coefficients to sodium, potassium and chloride. *J Neurochem* 46: 1732–1742.
- Stanness KA, Neumaier JF, Sexton TJ, *et al.* (1999). A new model of the blood–brain barrier: co-culture of neuronal, endothelial and glial cells under dynamic conditions. *NeuroReport* 10: 3725–3731.
- Urtti A (2006). Challenges and obstacles of ocular pharmacokinetics and drug delivery. *Adv Drug Deliv Rev* 58: 1131–1135.

- Weidenfeller C, Svendsen CN, Shusta EV (2007). Differentiating embryonic neural progenitor cells induce blood-brain barrier properties. *J Neurochem* 101: 555–565.
- Weinstein RS, McNutt NS (1972). Cell junctions. *N Engl J Med* 286: 521–524.
- Wheater PR, Burkitt HG, Daniels VG (2006). *Functional Histology. A text and colour atlas*, 5th edn. Edinburgh, London and New York: Churchill Livingstone.





# 3.2

## Passive diffusion of drug substances: the concepts of flux and permeability

*Birger Brodin, Bente Steffansen and Carsten Uhd Nielsen*

Experimental studies of the movement of molecules in solutions and molecular transport across artificial or biological barriers are used by the pharmaceutical scholar in a variety of contexts, ranging from simple diffusion and dissolution studies, to complex *in vivo* pharmacokinetic investigations. Movement of molecules in solutions and molecular transport across barriers may be described mathematically, and knowledge about these descriptions will aid in the design of experiments and interpretation of data. A number of textbooks explain the mathematical background necessary for transport studies (for example Schultz, 1980; Steen-Knudsen, 2002). In the present chapter, however, focus will be on presenting only the most commonly used equations and explaining the parameters involved, and the circumstances under which these equations can be applied. The aim of this section is thus to provide a basic framework of concepts describing transport of drug substances across biological barriers, hopefully enabling the reader to choose appropriate experimental models and data analysis for a given problem related to flux and permeability studies.

### **3.2.1 How do molecules move in solution? The concepts of flux, migration and diffusion**

Mass transport of molecules in a solution or molecular transport across a barrier is normally measured by fluxes. The flux of a solute is simply defined as the mass or number of molecules moving through a given cross-sectional area during a given period of time (Equation 3.2.1):

$$J = \frac{m}{A t} \quad (3.2.1)$$

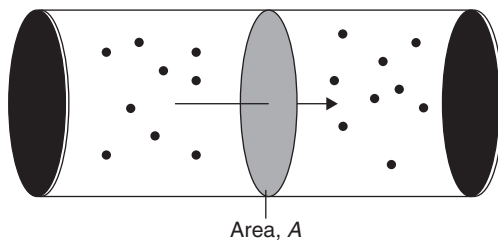


**Figure 3.2.1** Flux, i.e. movement of molecules (•) through cross-sectional area ( $A$ ) in a given time period ( $t$ ).

where  $J$  is the flux of a mass of compound  $m$ , moving through a cross-sectional area  $A$  during time  $t$  as illustrated in Figure 3.2.1. The unit for a flux value could thus be  $\text{mol cm}^{-2} \text{min}^{-1}$ , or alternatively  $\mu\text{g cm}^{-2} \text{h}^{-1}$ .

Movement of molecules in solution or molecular transport across barriers can be caused by migration or diffusion. Migration is movement of molecules caused by an external force that is acting on each of the solute molecules. Such external forces can be gravity, electrical fields (in case of charged solutes) or hydrodynamic flow. Diffusion is the random thermal movement of molecules in a solution, and thus diffusion may only cause a net transport of molecules in the presence of a concentration gradient.

The velocity of diffusion is related to the diffusion coefficient of a solute, a constant related to the properties of a given molecule in a given solvent. The diffusion coefficient ( $D$ ) is dependent on the size of the solute molecule and the viscosity of the solvent as described by the Stokes–Einstein equation (Equation 3.2.2):

$$D = \frac{RT}{6\pi\eta N_0 r_A} \quad (3.2.2)$$

where  $R$  is the gas constant,  $T$  absolute temperature,  $r_A$  the radius of spherical solute,  $N_0$  Avogadro's number, and  $\eta$  the viscosity of the solution. Thus the diffusion coefficient decreases with increasing molecule size and increasing viscosity of the solvent.

Diffusional flux can be described by the relationship commonly known as Fick's law (or Fick's first law), normally accredited to the German physiologist Adolf Fick (Equation 3.2.3):

$$J(x, t) = -D \frac{\delta C(x, t)}{\delta(x)} \quad (3.2.3)$$

Fick's Law is a partial differential equation, describing a flux,  $J$ , down a concentration gradient,  $\delta C$ , in a plane over time,  $t$ , for a solute,  $x$ , with a diffusion coefficient  $D$ . This version of Fick's law is rarely used for interpreting simple transport studies. However, when assuming a time-independent linear concentration profile (Equation 3.2.4), Fick's law becomes more straightforward to use, as we shall see later.

In transport studies conducted in biopharmaceutical science or in preclinical development, most experimental designs aim at eliminating migrational flux components to solely study diffusional fluxes. Migrational fluxes will not be described further in this chapter, apart from being mentioned in relation to electrical fields in Sections 3.2.5 and 3.2.6.

### 3.2.2 Fluxes across barriers and the permeability coefficient

The most common biopharmaceutical use of flux studies is transport investigations of drug candidates or prodrug candidates, across a barrier tissue, such as small intestinal cell culture models or tissue models. A typical setup for the conduction of this type of experiment will include a donor compartment with a defined initial concentration of compound, a defined volume, a barrier structure with a defined cross-sectional area and thickness, and a receiver compartment with a defined initial concentration and a defined volume (see Figure 3.2.2).

Stirring should be complete in both donor and receptor compartments, in order to ensure that there is no concentration gradient within the two compartments, and thus the only gradient present is across the barrier structure separating the two compartments. Fluxes are then measured simply, by taking samples from the receiver compartment at given time points after addition of the test compound to the donor solution. In the simple situation, where the flux across the barrier only moves an insignificant amount of solute test compound from the donor chamber, the concentration gradient across the barrier is essentially constant, and the flux will thus be of zero order, i.e. be constant, since flux occurs as a function of the concentration gradient. In such cases, a simple version of Fick's law can be used to relate fluxes and concentration gradients (Equation 3.2.4):

$$J = P (C_{\text{donor}} - C_{\text{receiver}}) \quad (3.2.4)$$

where  $P$  is the permeability coefficient,  $C_{\text{donor}}$  and  $C_{\text{receiver}}$  are the concentrations of the drug substance in the donor and receiver compartments, respectively, and  $J$  is the flux from the donor to receiver compartment of the drug substance in question. Occasionally the notations  $P_{\text{apparent}}$  ( $P_{\text{app}}$ )

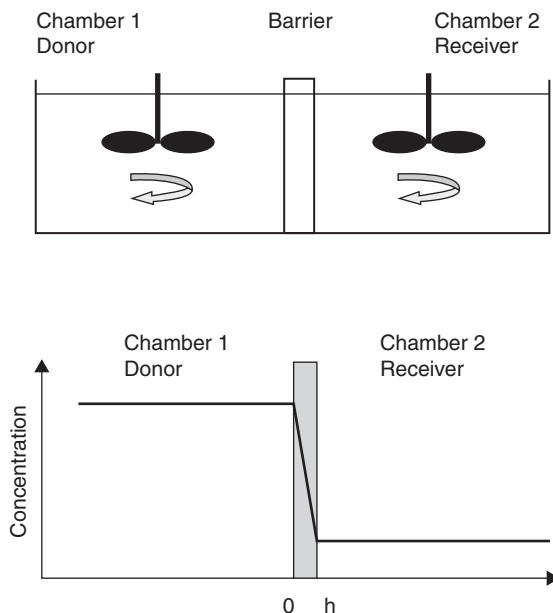


**Figure 3.2.2** Top: a two-compartment system for transepithelial flux measurements. A barrier (a tissue or an artificial membrane) is bathed in stirred solutions. Bottom: concentration gradient in the two-compartment system. Normally perfect stirring is assumed, i.e. it is assumed that there are no concentration gradients within each of the two compartments and that the whole concentration drop occurs across the barrier.

or  $P_{\text{effective}}$  ( $P_{\text{eff}}$ ) are used when dealing with experimentally obtained permeability coefficients, in order to underscore their vulnerability to bias due to experimental conditions. Assuming that the concentration gradient,  $C_{\text{donor}} - C_{\text{receiver}}$ , across the barrier is linear and constant, i.e. time independent, Fick's law can be simplified to the equation shown in Equation 3.2.4 and further simplified if it is assumed that the drug substance concentration in the donor compartment is constant and that the concentration in the receiver chamber is virtually zero as compared to the donor concentration. The concentration gradient thus becomes equal to the concentration of the drug substance in the donor chamber at time zero, as shown in Equation 3.2.5:

$$J = P C_{\text{donor}} \Leftrightarrow P = \frac{J}{C_{\text{donor}}} \quad (3.2.5)$$

It follows from Equations 3.2.4 and 3.2.5 that the flux is proportional to the concentration gradient and that the permeability is simply the constant that relates flux and concentration gradient. It follows that the

permeability of a drug substance in a given barrier can be estimated from a simple flux experiment at a given concentration gradient, and that the determined permeability value can readily be compared with other permeability values obtained at other concentration gradients. The obtained permeability value can thus be compared with permeability values obtained from a similar experimental setup and, on basis of previous experience, the drug substance in question could be categorised in terms of permeability.

However, a number of experimental considerations must be made, before the estimated permeability value is valid.

- 1 The concentration gradient should be constant or nearly constant throughout the experiment. Normally, experiments are performed under sink conditions, i.e. the concentration in the receiver compartment is initially zero and is assumed to increase insignificantly during the time course of the experiment. The acceptable increase in  $C_{\text{receiver}}$  depends on the required precision, but we suggest that the concentration gradient should not change more than 10% during the experiment. The change in concentration gradient is easily measured, either by measuring the concentration in the donor and receiver chamber before and after the experiment, or by using the measured flux value to estimate how much compound has moved during the experiment. If, in fact, the concentration gradient changes considerably, data can be processed assuming non-steady-state conditions, see Section 3.2.4.
- 2 The concentration gradient should be the only gradient present across the tissue. This implies that concentrations of all other compounds than the drug should be kept similar in the donor and the receiver compartment, that no hydrodynamic gradient should exist and that no electrical gradient should be present when permeabilities of charged drug compounds are measured.
- 3 It should be ensured that the transport of drug is purely passive. This is normally performed by investigating drug transport at a range of concentration gradients. If transport is purely passive, a linear relationship between flux and concentration gradient will be observed. For active transport see Chapter 3.4.
- 4 Unstirred water layers surrounding the barrier in question should be minimised. In experimental practice, this is normally accomplished by choosing the highest possible stirring rate, i.e. a rate that minimises concentration gradients in the donor and receiver compartment but does not damage the barrier (properties).

Permeability data may be used for a number of purposes. The permeability constant obtained in a cell model or an *in vitro* tissue model can be used to predict the bioavailability of a given drug substance, or permeabilities of a series of related drug candidates can be compared for selection of a drug candidate with a high permeability. Permeability comparisons must, however, be done with caution. Table 3.2.1 shows the permeabilities of a number of compounds in the Caco-2 cell model and intestinal tissue, respectively. It is evident that the relative ranking of compounds is meaningful, but the absolute values vary between models.

The permeability is a constant that consists of a number of model-specific variables, i.e. the diffusion coefficient of the drug in the barrier ( $D$ ), the thickness of the barrier ( $h$ ) and the partition coefficient of the drug into the barrier ( $\alpha$ ) (Equation 3.2.6, see also Chapter 2.1 for a discussion on partition coefficients).

$$P = \frac{\alpha D}{h} \quad (3.2.6)$$

When comparing permeability data obtained in different experimental setups such as for example intestinal epithelial cell culture models and *in situ* perfusion models, the lipid composition may vary between the two systems, causing different values of  $D$  and  $\alpha$ . The thickness of the barrier,  $h$ , i.e. the height of the cell layer can also vary. Variations in

**Table 3.2.1** Permeabilities of drug and reference compounds in Caco-2 cells and human intestine

Compound	Permeability in Caco-2 cells, apical–basolateral ( $\text{cm s}^{-1}$ )	Intestinal permeability in rat (r) or human (h) ( $\text{cm s}^{-1}$ )	Bioavailability (%)
Mannitol	$0.069 \times 10^{-5}$	$0.3 \times 10^{-5}$ (r)	Low
Atenolol	$0.13 \times 10^{-5}$	$1.5 \times 10^{-5}$ (h)	45
Ranitidine	$0.01 \times 10^{-5}$	$1.5 \times 10^{-5}$ (r)	~50
Terbutaline	$\sim 0.1 \times 10^{-5}$	$3.0 \times 10^{-5}$ (h)	65
Ondansetron	$1.8 \times 10^{-5}$	n/a	100
Metoprolol	$3 \times 10^{-5}$	$15 \times 10^{-5}$ (h)	100
Antipyrine	$5 \times 10^{-5}$	$50 \times 10^{-5}$ (h)	100

Notes: Values are taken from Gan *et al.* (1993); Collett *et al.* (1999); Rege *et al.* (2001); Lennernas (1998); Brusewitz *et al.* (2007); Laitinen *et al.* (2003).

n/a, not available.

the thickness of the unstirred water layers surrounding the tissues can furthermore cause differences in permeability values obtained in the two models. In order to underline that permeability estimates can be prone to errors, it is quite common to use the notation  $P_{\text{effective}}$  ( $P_{\text{eff}}$ ) or  $P_{\text{apparent}}$  ( $P_{\text{app}}$ ) when referring to permeability estimates from flux experiments.

### 3.2.3 Unstirred water layers

In simple two-compartment systems, barrier permeabilities, estimated from flux measurements, are determined assuming that the concentrations in compartments 1 and 2 are constant throughout the individual compartments. The only concentration gradient present will thus be the gradient across the barrier. However, this simplification does not always hold true. In some cases the permeability measurements are dependent on the stirring conditions. This phenomenon is due to the presence of unstirred water layers close to the tissue, and it is caused by local concentration gradients in the solutions surrounding the tissue. Unstirred water layers can be viewed as two additional barriers in the transport pathway, a barrier in compartment 1 and a barrier in compartment 2 (see Figure 3.2.3).

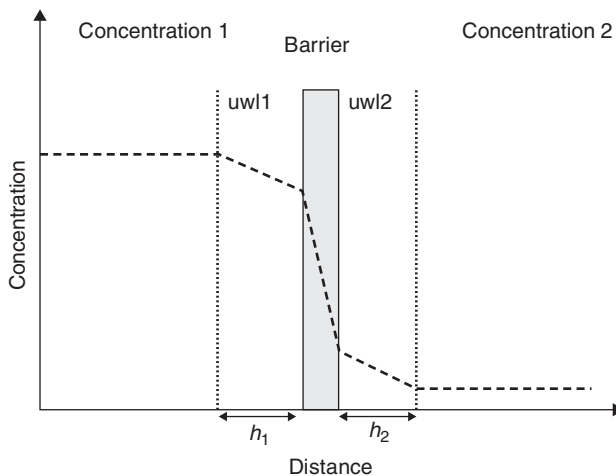


**Figure 3.2.3** Unstirred water layers (uwl) can be present close to the tissue barrier due to imperfect stirring of the experimental solutions. The unstirred water layers can be regarded as two extra barriers, with thickness  $h_1$  and  $h_2$ , in series with the tissue barrier.



Steady-state flux across an unstirred water layer can be described by the simplified Fick's expression, and an equation can easily be set up describing the measured permeability as a function of the real barrier permeability and the permeabilities in the two unstirred water layers (Equation 3.2.7):

$$\frac{1}{P_{\text{eff}}} = \frac{1}{P_{\text{uw1}}} + \frac{1}{P_{\text{barrier}}} + \frac{1}{P_{\text{uw2}}} \Leftrightarrow \frac{1}{P_{\text{eff}}} = \frac{h_1}{D_{\text{uw1}}} + \frac{1}{P_{\text{barrier}}} + \frac{h_2}{D_{\text{uw2}}} \quad (3.2.7)$$

where  $P_{\text{eff}}$  is the actual estimated permeability across the tissue and the unstirred water layers,  $P_{\text{uw1}}/P_{\text{uw2}}$ ,  $h_1/h_2$  and  $D_{\text{uw1}}/D_{\text{uw2}}$  are the permeabilities, thickness and diffusion coefficients of uw1 and 2, respectively, and  $P_{\text{barrier}}$  is the true permeability of the tissue barrier.

However, the permeabilities,  $P_{\text{uw1}}$  and  $P_{\text{uw2}}$  are not readily determined, and therefore the real permeability is not easily derived. A simpler approach for dealing with unstirred water layers is to determine the permeability ( $P_{\text{eff}}$ ) at a range of different stirring rates, and since the estimated permeability will approach the true permeability asymptotically, the true permeability can be estimated from a mathematical fit of the obtained data. An alternative approach is to choose an experimental setup and just compare  $P_{\text{eff}}$  values under identical conditions, while knowing that they might be underestimated due to the presence of the unstirred water layers.

This possible influence of unstirred water layers must be kept in mind when absolute permeabilities are compared between different experimental setups with different stirring rates and different barrier structures.

### 3.2.4 Fluxes across a barrier under non-steady-state conditions

In experiments with highly permeable compounds, the transport of a drug candidate from the donor compartment to the receiver compartment cause a first-order decrease of the concentration of drug candidate in the donor chamber and an accompanying increase in its concentration in the receiver chamber (see Figure 3.2.4). In this situation, the concentration gradient cannot be considered constant, and the permeability cannot be calculated directly from Equations 3.2.4 or 3.2.5.

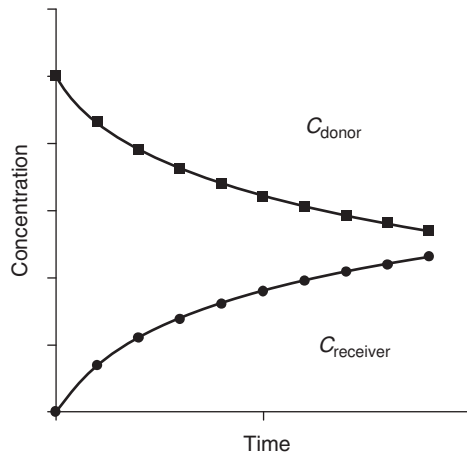


**Figure 3.2.4** Non-stationary diffusion of a solute from a donor compartment to a receiver compartment, in a two-compartment system with equal volumes of solution on both sides of the barrier, and initially only solute present in the donor compartment. Both  $C_{\text{donor}}$  and  $C_{\text{receiver}}$  will approach the same value asymptotically.

This is observed when flux of a lipophilic drug candidate is measured across a barrier tissue for a sufficiently long time period. The problem can be solved in two ways, either by keeping the volumes of the donor and receiver compartments very large, i.e. by constantly flushing the donor and receiver compartments with fresh experimental solutions (a flow-through system), or alternatively by treating the obtained data using a set of equations that take the changing concentration gradient into account. When a significant flux occurs across a barrier with a constant permeability, the concentration of drug candidate in the donor chamber will decrease with one-phase exponential decay, and the concentration in the receiver chamber will increase with one-phase exponential association. When the concentration of drug is plotted in a log diagram against time, the slope of the curve will be related to the permeability.

The calculation of the permeability from non-stationary fluxes demands knowledge of  $C_{\text{donor}}$  at time zero ( $C_{\text{donor}, t=0}$ ), the volumes of the donor and receiver compartments ( $V_{\text{donor}}$  and  $V_{\text{receiver}}$ ), the tissue area ( $A$ ) and the concentration of at least one (but ideally 3–5) receiver samples at different time intervals ( $C_t$ ). From these input values, other values can be derived, for use in the calculation, such as the total mass of compound in the system ( $m_{\text{total}}$ ), which is equal to the mass initially added to the donor compartment ( $m_{i, t=0}$ ) and can be calculated as  $C_{\text{donor}, t=0} \times V_{\text{donor}}$ . Then

the following equations can be applied:

$$C_{\infty} = \text{the final concentration in both compartments} \\ = \frac{m_{i,t=0}}{V_{\text{donor}} + V_{\text{receiver}}} \quad (3.2.8)$$

$$\frac{C_{\infty} - C_{\text{receiver},t}}{C_{\infty}} = e^{-kt} \quad (3.2.9)$$

$$k = AP \frac{C_{\text{donor}} + C_{\text{receiver}}}{C_{\text{donor}} + C_{\text{receiver}}} \quad (3.2.10)$$

The constant  $k$  can be isolated mathematically or found by plotting time and concentration data in a logarithmic plot, and  $P$  can be isolated easily from Equation 3.2.10.

When applying this treatment to experimental data, it must be verified that mass balance exists, as lipophilic drugs often adsorb to pipettes and glass and plastic surfaces.

### 3.2.5 Fluxes of a charged solute in the presence of an electrical potential gradient

The estimation of a permeability value as described in Equations 3.2.4 and 3.2.5 implies that the only factor responsible for mass transport across the barrier in question is the concentration gradient of the solute. If an electrical potential gradient is present across the tissue and the solute is charged, the driving force for mass transport is a combination of the electrical and chemical gradients, and the estimated permeability will be influenced by the electrical potential gradient (see Figure 3.2.5).

The presence of electrical fields generated by an electrically active tissue can be dealt with in two ways, either by setting up the barrier tissue in an Ussing chamber setup, allowing voltage clamp of the barrier and thereby reducing the electrical potential to zero by applying current from an external current source, or by measuring the electrical potential gradient during the experiment and estimating the permeability by using Equation 3.2.11 (also known as the Nernst–Planck equation):

$$J = zPv \frac{C_2 - C_1 e^{zv}}{1 - e^{zv}} \quad (3.2.11)$$

where  $J$  is the flux of charged compound from compartment 1 to compartment 2,  $z$  is the charge of the substrate,  $P$  is the permeability of the compound,  $C_1$  and  $C_2$  are the concentrations of the compound in

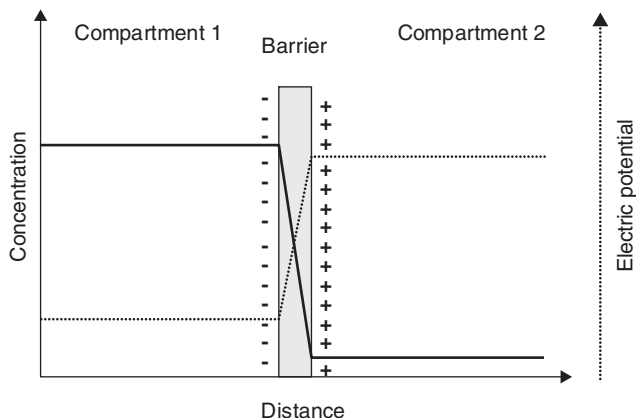


**Figure 3.2.5** Flux of a charged solute across a barrier with an electric potential difference between compartment 1 and compartment 2. If an electrical potential exists across a barrier, it will impose a force on charged drug molecules. The direction of the force will depend on whether the compound is positively or negatively charged. When drug transport is studied across electrically active epithelia or across cell membranes, or when currents carried by an electrophoretic process should be predicted, electrical fields must thus be taken into consideration.

compartments 1 and 2, respectively, and  $v$  is the normalised electrical potential difference across the barrier (Equation 3.2.12):

$$v = \frac{VF}{RT} \quad (3.2.12)$$

In this equation,  $v$  is the potential difference across the barrier (with compartment 1 as reference),  $F$  is Faraday's number,  $R$  is the gas constant and  $T$  is the absolute temperature. Using Equations 3.2.11 and 3.2.12, one can either calculate the permeability of a charged compound in the presence of an electric field, by measuring values of flux,  $J$ , and potential,  $V$ , and then calculating  $P$  from Equation 3.2.11, or calculate how much compound will be moved by a given electrical field across a tissue with a given permeability, by inserting the potential  $V$  and the permeability in the equation.

### 3.2.6 Use of flux ratios to analyse transport mechanisms

The transport mechanism of a compound across a given tissue barrier can be analysed in terms of flux ratios, in order to investigate whether the transepithelial transport is active, i.e. energised by ATP-consuming

pumps, or passive (see Section 3.3.1). The flux ratio equation deals with unidirectional fluxes of radiolabelled compounds (Ussing, 1949; Dawson, 1977). A unidirectional flux can be defined as a flux from one compartment to another, across a barrier, measured by radiolabel, without considering counterflux of the same compound. If a charged compound does not interact with other compounds and its transepithelial transport is solely driven by the electrochemical potential difference across the barrier, then the ratio between the unidirectional fluxes can be described as follows:

$$\frac{J^{1-2}}{J^{2-1}} = \left[ \left( \frac{C_1}{C_2} \right) e^{\left( \frac{-zFV}{RT} \right)} \right] \quad (3.2.13)$$

where  $J^{1-2}$  and  $J^{2-1}$  are the fluxes from compartment 1 to 2 and vice versa,  $V$  is the potential difference between compartment 1 and 2 ( $V_2 - V_1$ ),  $C_1$  and  $C_2$  are the concentrations in the respective compartments,  $z$  is the charge of the compound,  $F$  is Faraday's number,  $R$  is the gas constant and  $T$  is the absolute temperature. What Equation 3.2.13 actually states is that the ratio between the unidirectional fluxes should equal the concentration ratio times a factor describing the electric gradient across the barrier. It follows from the equation that for a non-charged solute, this factor becomes 1, and the flux ratio will thus equal the concentration ratio. A flux-ratio analysis is thus a very simple method of investigating whether a transepithelial transport process is passive or energised.

### 3.2.7 Conclusions

Mass transport across a barrier, e.g. intestinal epithelium or other pharmaceutically relevant barriers, can be caused by diffusion or migration. Transport by simple diffusion can be measured as flux, and characterised by a permeability for the transported solute. The permeability can be calculated using the measured flux and the concentration gradient. Permeabilities can be compared between a series of related compounds in order to select drug candidates in a screening process, or used to predict *in vivo* bioavailability of a given drug substance. Care must be taken in experimental design and when interpreting permeabilities, in order to distinguish permeabilities of compounds with carrier-mediated flux components from permeabilities of compounds that are solely driven by diffusion.

### 3.2.8 Examples

#### Example 3.2.1: calculation of the permeability of a drug compound in the Caco-2 cell intestinal model

The apical to basolateral (equivalent to lumen–blood) flux,  $J^{a-b}$ , of a new drug candidate **x**, has been measured across 21-day-old Caco-2 cell mono-layers grown on permeable filter support. **x** has been added to the apical solution at a concentration of 50 mM. Samples have been taken from the basolateral solution at intervals of 15 min. The concentration of the compound has been measured using radiolabelled **x**. At time zero and at the end of the experiment, donor samples have been taken (see Table 3.2.2).

##### *Experimental parameters:*

Volumes of the experimental solutions: apical volume = 0.5 ml, basolateral volume = 1.0 ml. Sample volume, receiver solution (basolateral) = 100  $\mu$ l; sample volume, donor solution (apical) = 20  $\mu$ l. Cross-sectional area of tissue = 1 cm<sup>2</sup>.

##### *Calculations:*

In order to obtain the flux across the tissue, the amount of substance which has moved per time unit must be calculated. This is done, first by calculating the amount (mass) of substance present in the receiver solution at time =  $t$ , by multiplying the sample concentration by the volume of

**Table 3.2.2** A theoretical data set, showing concentration values sampled at different time points, and the derived flux values

Sample number	Time, $t$ (min)	[Drug <b>x</b> ] in donor sample (mM)	[Drug <b>x</b> ] in receiver sample, (mM)	Mass of Drug <b>x</b> in receiver solution (nmol)	Mass <sub>total</sub> (nmol)	Flux (nmol (cm <sup>2</sup> min) <sup>-1</sup> )
1	0	50	0	0	0	0
2	15	–	0.02	20	20	1.33
3	30	–	0.07	70	72	3.47
4	45	–	0.15	150	159	5.80
5	60	–	0.25	250	274	7.67
6	75	–	0.35	350	399	8.33
7	90	–	0.44	440	524	8.33
8	105	–	0.51	510	638	7.60
9	120	48	0.58	580	759	8.07

experimental solution, i.e.:

$$C_n \times V_r = \text{mass} \quad (3.2.14)$$

However, since substance has been removed from the receiver solution, every time a sample has been taken, a correction must be introduced. The total mass that has crossed the barrier at a given time is thus:

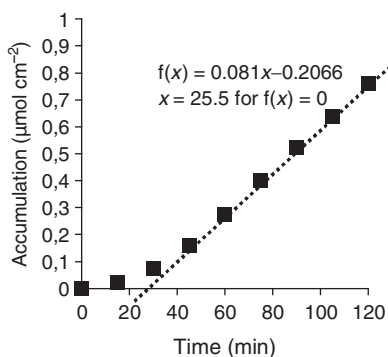
$$\text{Mass}_{\text{total}} = V_s \left( \sum_{n=1}^n C_{n-1} \right) + C_n \times V_r \quad (3.2.15)$$

where  $C_1, C_2, \dots, C_n$  are the sample concentrations in samples 1, 2,  $\dots, n$ ,  $V_r$  is the volume of the receiver solution and  $V_s$  is the volume of the sample.

The data can be plotted, either in a plot of accumulated  $x$  versus time (Figure 3.2.6, graph 1) or as a plot of flux of  $x$  versus time (Figure 3.2.6, graph 2). Both these types of plots have advantages and drawbacks. Graph 1 simply displays the mass of substance per area which has crossed the cell monolayer at a given time. The flux can then be found as the slope of the linear part of the relation. In this example, the flux is  $0.0081 \mu\text{mol} (\text{cm}^2 \text{min})^{-1}$  or  $8.1 \text{ nmol} (\text{cm}^2 \text{min})^{-1}$ . The intercept with the  $x$  axis is called the *lag time* and in the example shown this is 25.5 min. The lag time is obtained by setting  $f(x) = 0$ .

Graph 2 in Figure 3.2.6 displays the same data set, but with the flux instead of accumulation on the  $y$  axis. Thus the bar at the  $x$  value 15 min is the mean flux during time 0–15 min, the bar at 30 min is the mean flux at 15–30 min etc. The flux, or transport rate, reaches steady state after

Graph 1



Graph 2

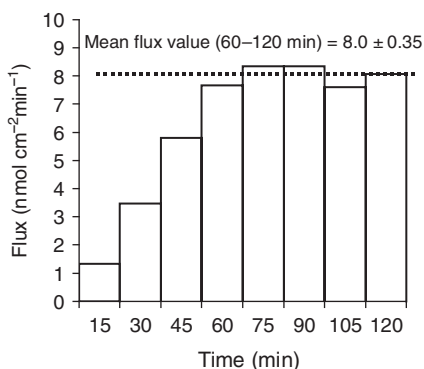


**Figure 3.2.6**

~60 min, as judged by visual inspection of the data. The steady-state flux can thus be determined as the mean of the flux values obtained in the steady-state period (60–120 min). The value  $8.0 \text{ nmol cm}^2 \text{ min}^{-1}$  is obtained from the present data set, a value corresponding fairly well with the determination from graph 1. When plotted in a graph like graph 2, parameters such as the time of steady-state and possible depletion of donor compound will be more visible to the investigator, whereas graph 1 demands fewer calculations and yields the lag-time.

The permeability can now be calculated using Equation 3.2.5 (thus ignoring the slight concentration drop in the donor chamber during the experiment):

$$\begin{aligned}
 P &= \frac{J \frac{\text{nmol}}{\text{cm}^2 \text{ min}}}{C_{\text{donor}} \frac{\text{mmol}}{\text{l}}} = \frac{8 \text{ nmol l}}{50 \text{ mmol cm}^2 \text{ min}} = 0.16 \frac{10^{-9} \text{ l}}{10^{-3} \text{ cm}^2 \text{ min}} \\
 &= 0.16 \frac{10^{-9} 10^3 \text{ cm}^3}{10^{-3} \text{ cm}^2 \text{ min}} = 0.16 10^{-3} \frac{\text{cm}}{\text{min}} = 9.6 10^{-3} \frac{\text{cm}}{\text{h}} = 2.6 10^{-6} \frac{\text{cm}}{\text{s}}
 \end{aligned}
 \tag{3.2.16}$$

### Example 3.2.2: calculation of the permeability of a drug in the Caco-2 cell intestinal model under non-steady-state conditions

The apical to basolateral (equivalent to lumen-blood) flux,  $J^{a-b}$ , of a new drug compound y, has been measured across 21-day-old Caco-2 cell monolayers grown on permeable filter support. As in the previous example, y has been added to the apical solution at a concentration of 50 mM. Samples have been taken from the basolateral solution at varying intervals, see below. The concentration of the compound has been measured using radiolabelled compound y. At time zero and at the end of the experiment, donor samples have been taken (see Table 3.2.3).

#### *Experimental parameters:*

Volumes of the experimental solutions: apical volume = 0.5 ml, basolateral volume (at  $t=0$ ) = 1.0 ml. Sample volume, receiver solution (basolateral) = 10  $\mu\text{l}$ ; sample volume, donor solution (apical) = 10  $\mu\text{l}$ . Cross-sectional area of tissue =  $1 \text{ cm}^2$ .

#### *Calculations:*

In order to obtain the flux across the tissue, the amount of substance that has moved per time unit is calculated as in the previous example. The flux values indicate that a large percentage of the added dose has moved across



**Table 3.2.3** A theoretical data set, showing concentration values sampled at different time points under non-stationary flux conditions

Sample number	Time, <i>t</i> (min)	[Drug y] in donor sample (mM)	[Drug y] in receiver sample (mM)
1	0	50	0
2	10	–	8
3	30	–	14
4	90	16.6	16.6

the barrier during the measurement period, therefore a non-steady-state flux analysis is performed.

The concentration of compound y at time infinity in both compartments is calculated, using Equation 3.2.8:

$$C_{\infty} = \frac{m_{1,t=0}}{V_{\text{donor}} + V_{\text{receiver}}} = \frac{50 \text{ mM } 0.5 \text{ ml}}{0.5 \text{ ml} + 1 \text{ ml}} = 16.7 \text{ mM} \quad (3.2.17)$$

The concentrations measured can be fitted to Equation 3.2.9:

$$\frac{C_{\infty} - C_{\text{receiver},t}}{C_{\infty}} = e^{-kt} = \frac{16.7 \text{ mM} - C_{\text{receiver},t}}{16.7 \text{ mM}} = e^{-kt} \quad (3.2.18)$$

The *k* value can be estimated graphically or by isolation, and can be used to calculate the permeability according to Equation 3.2.10:

$$\begin{aligned} k &= 62.7 \text{ } 10^{-3} \text{ min}^{-1} = AP \frac{V_{\text{donor}} + V_{\text{receiver}}}{V_{\text{donor}} V_{\text{receiver}}} \\ &= 1 \text{ cm}^2 P \frac{0.5 \text{ ml} + 1 \text{ ml}}{0.5 \text{ ml } 1 \text{ ml}} \Leftrightarrow P = 62.7 \text{ } 10^{-3} \text{ min}^{-1} \frac{\text{cm}^3}{3 \text{ cm}^2} \end{aligned} \quad (3.2.19)$$

obtaining a *P* value of  $0.0209 \text{ cm min}^{-1}$  or  $3.5 \times 10^{-4} \text{ cm s}^{-1}$ .

### Example 3.2.3: flux ratio analysis

The unidirectional fluxes of a novel drug substance, testicine, have been measured in Caco-2 cell monolayers. The monolayers have been incubated with 1 mM of isotope-labelled testicine in both the apical and basolateral compartment, and steady-state fluxes have been determined. The apical and basolateral test solutions are identical. Testicine has a negative charge. The monolayers are mounted in an Ussing chamber, allowing for

measurement of the potential difference ( $V$ ) from the apical to the basolateral side.

The following parameters are obtained during the experiment:

$$J_{\text{apical-basolateral}} = 15 \text{ nmol} \times \text{cm}^{-2} \times \text{min}^{-1}$$

$$J_{\text{basolateral-apical}} = 10 \text{ nmol} \times \text{cm}^{-2} \times \text{min}^{-1}$$

$$V = V_{\text{basolateral}} - V_{\text{apical}} = 10 \text{ mV} = 0.010 \text{ J C}^{-1}$$

$$\text{Temperature} = 20^\circ \text{C}$$

$F$ ,  $R$  and  $T$  have the values:

$$F = 96\,487 \text{ C mol}^{-1}$$

$$R = 8.3144 \text{ J (K mol)}^{-1}$$

$$T_{20^\circ \text{C}} = 293 \text{ K}$$

The experimentally determined flux ratio thus becomes:

$$\frac{J^{1-2}}{J^{2-1}} = \frac{15}{10} = 1.5 \quad (3.2.20)$$

and the calculated flux ratio becomes

$$\left(\frac{C^1}{C^2}\right) e^{\left(\frac{-zFV}{RT}\right)} = \left(\frac{1}{1}\right) e^{\left(\frac{-(-1) 96487 \text{ C mol}^{-1} 0.01 \text{ J C}^{-1}}{8.31144 \text{ J K}^{-1} \text{ mol}^{-1} 293 \text{ K}}\right)} = 1.49 \quad (3.2.21)$$

The flux ratio analysis thus indicates that no active transporters are involved in the transepithelial transport process, which appears to be driven solely by the transepithelial electrochemical gradient.

## References

- Brusewitz C, Schendler A, Funke A, Wagner T, Lipp R (2007). Novel poloxamer-based nanoemulsions to enhance the intestinal absorption of active compounds. *Int J Pharm* 329: 173–181.
- Collett A, Higgs NB, Sims E, Rowland M, Warhurst G (1999). Modulation of the permeability of H<sub>2</sub> receptor antagonists cimetidine and ranitidine by P-glycoprotein in rat intestine and the human colonic cell line Caco-2. *J Pharmacol Exp Ther* 288: 171–178.
- Cox DS, Raje S, Gao H, Salama NN, Eddington ND (2002). Enhanced permeability of molecular weight markers and poorly bioavailable compounds across Caco-2 cell monolayers using the absorption enhancer, zonula occludens toxin. *Pharm Res* 19: 1680–1688.

- Dawson DC (1977). Tracer flux ratios: a phenomenological approach. *J Membr Biol* 31: 351–358.
- Gan LS, Hsyu PH, Pritchard JF, Thakker D (1993). Mechanism of intestinal absorption of ranitidine and ondansetron: transport across Caco-2 cell monolayers. *Pharm Res* 10: 1722–1725.
- Laitinen L, Kangas H, Kaukonen AM, *et al.* (2003). N-in-one permeability studies of heterogeneous sets of compounds across Caco-2 cell monolayers. *Pharm Res* 20: 187–197.
- Lennernas H. (1998). Human intestinal permeability. *J Pharm Sci* 87: 403–410.
- Rege BD, Yu LX, Hussain AS, Polli JE (2001). Effect of common excipients on Caco-2 transport of low-permeability drugs. *J Pharm Sci* 90: 1776–1786.
- Schultz SG (1980). *Basic Principles of Membrane Transport*. Cambridge: Cambridge University Press.
- Steen-Knudsen O (2002). *Biological Membranes. Theory of transport, potentials and electric impulses*. Cambridge: Cambridge University Press.
- Ussing HH (1949). The distinction by means of tracers between active transport and diffusion. *Acta Physiol Scand* 19: 43–56.

# 3.3

## Carrier-mediated transport kinetics

*Carsten Uhd Nielsen, Bente Steffansen and Birger Brodin*

Over the last few decades it has become clear that a number of drug substances are transported across epithelial or endothelial biological barriers in a saturable way. For many of these compounds it has been shown that the explanation for this saturability is that they are substrates for transporters. Transport of these compounds is thus mediated by transport proteins present in the biological membrane. Such proteins exert physiological functions in which they transport endogenous molecules or exogenous nutrients, toxins or vitamins from one compartment to another. They are specialised transporters in terms of bringing or excluding one class of compounds from the exterior to the interior of the human body, or from one interior compartment to another. Thus, besides being saturable they are also selective and specific in their recognition of substrates. Nevertheless, some drug substances are transported by one or more transporters and must in this way mimic the biological presence of their 'natural substrates'. Transporter-mediated transfer of a compound from one compartment to another may influence its pharmacokinetics. In some cases, if the concentration of drug substance is lower than the maximal transport capacity of the transport system then its transport is controlled by transporter. In other situations, drug transfer may be limited if the concentration needed is much higher than the capacity of the transport system. It is therefore necessary for the scientist working in molecular biopharmaceutical settings to be able to describe the kinetics of drug transfer via a transport protein, to investigate whether a drug candidate is a substrate for a transporter or not, and, furthermore, to evaluate the impact of these observations on the usefulness of a given new drug candidate. In the following sections carrier types and functions will be described and the basic equations for describing transport of molecules via a carrier protein will be given, with a special focus on carriers located in the intestine.

### 3.3.1 Carrier function and mechanisms

The chemical and physical properties of cell membranes make them practically impermeable for ions and hydrophilic compounds. The cell relies on specialised transport protein for exchanging ions and hydrophilic nutrients with its surroundings. The transport proteins are typically integral proteins, which span the lipid bilayer of the cell membrane multiple times. The cell maintains an asymmetric distribution of ions due to two fundamental types of membrane transport protein – carriers and channels. The concentrations of ions outside and inside the cell are listed in Table 3.3.1.

Carriers are functionally characterised by their substrates, their driving force and their substrate specificity. The transport of substrate via a carrier is passive in nature since the transport rate is dependent on the concentration gradient of the transported substrates. However, if the carrier is viewed in the dynamic cellular system, it may, for symports or antiports, be secondary or tertiary dependent on an active transporter in order to maintain the gradients for the co-transported substrate. In general, carriers must be able to perform at least four functions in order to move a substrate across the cell membrane, i.e. transport the substrate; these are illustrated and explained in Figure 3.3.1.

Depending on the nature of these processes, the carrier is classified. In the following the concepts of carriers – uniports, symports, antiports and active transporters – will be illustrated, using examples that are relevant for the biopharmaceutical student or scientist. Channels do not

**Table 3.3.1** Approximate concentrations of important ions inside and outside a generalised mammalian cell

Ion	Concentration (mM)		Equilibrium potential (mV)
	Inside the cell	Outside the cell	
Na <sup>+</sup>	5 to 15	150	91 to 62
K <sup>+</sup>	150	5.5	–88
Cl <sup>–</sup>	9	125	–70
Ca <sup>2+</sup>	10 <sup>–4</sup>	1 to 2	129 to 132
Mg <sup>2+</sup>	0.5	1 to 2	9 to 19
<sup>a</sup> H <sup>+</sup>	4 × 10 <sup>–5</sup>	1.6 × 10 <sup>–4</sup> to 4 × 10 <sup>–5</sup>	–37 to 0

Notes: Equilibrium potential (mV) is calculated at 37 °C using the Nernst equation.

<sup>a</sup>The proton concentration inside the cell is calculated based on an intracellular pH of 7.4, and for outside the cell on a pH range of 6.8 to 7.4.

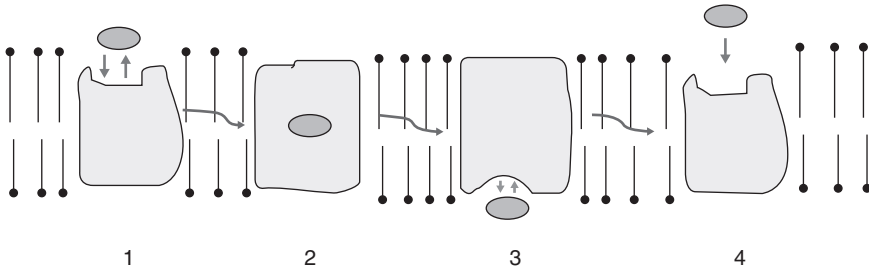


**Figure 3.3.1** Illustration of the conformational changes associated with translocation of substrate:

- 1 recognition of the substrate is the process where the substrate binds to the carrier
- 2 translocation of the substrate is the process where the carrier undergoes a conformational rearrangement with the result of moving the substrate from outside the cell to the inside of the cell
- 3 release of the substrate where the substrate is dissociated from the carrier and present in the cytosol of the cell
- 4 recovery of the conformation of the carrier to the orientation in which it is ready to bind another substrate.

need to bind the substrate in order to transport the solute across the membrane. Channels form hydrophilic pores that the solute, typically inorganic ions, can pass through from one compartment to another.

### 3.3.1.1 Uniports

Uniports are carriers that only move one substrate in one direction in the transport process (Figure 3.3.2). This implies that there is no additional

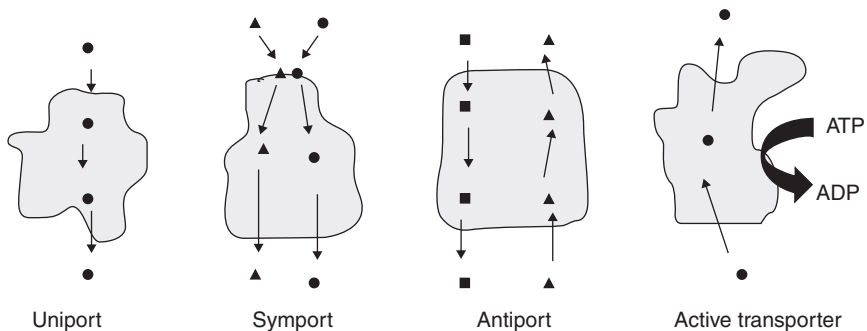


**Figure 3.3.2** Illustration of the various forms of carriers.

ion or substrate involved in the translocation of a substrate across the cell membrane. The transport of a neutral substrate is thus dependent only on the concentration gradient of the single substrate, and the concentration of substrate outside and inside the cell will define the rate of substrate transfer via the carrier. In other words the transport process will occur downhill, i.e. down the concentration gradient, and no intracellular accumulation occurs. However, the carrier will still perform a vital function since it facilitates the transfer of a substrate that is otherwise not normally transportable from the outside/inside of the cell to the inside/outside. For charged compounds, the electrical potential across the cell membrane may influence the transport of a compound. A combination of a chemical and electrical gradient is termed an electrochemical gradient. Typical uniports are found in the solute carrier family 2, SLC2, of glucose transporters. SLC2 family members facilitate the diffusion of glucose across membranes of different tissues, and they are referred to as glucose transporters or GLUTXs, where X is a number indicating the isoform of the transporter. Other uniport carriers are found in the facilitative nucleoside transporter family, SLC29, which transports nucleosides, and the  $\text{Na}^+$ -independent, system L-like amino acid transporter family, SLC43, which transports neutral amino acids. Different isoforms of these transporters are found in different tissues and have different localisations at the cellular level of polarised cells, i.e. at the apical or basolateral membranes.

### 3.3.1.2 Symports

Carriers that have two or more substrates moving in one direction during the transport process are called symports (see Figure 3.3.2). This means that in addition to the substrate, which could be an amino acid, a dipeptide or a nucleoside molecule, there is also an ion or substrate involved in the translocation process across the cell membrane. The transport of a substrate is thus dependent on both the concentration gradient of the substrate itself and the concentration of co-substrate. The typical symport substrate would be a solute such as an amino acid, a di/tripeptide or a nucleoside, and typical co-substrates are ions such as  $\text{Na}^+$  or  $\text{H}^+$ . The rate of transport via the carrier will depend on both the concentration gradient of the substrate and the concentration gradient of the co-substrate(s). The total driving force for the transport process is thus the sum of the electrochemical gradients working on the cellular system. This enables the cell to accumulate the substrate intracellularly by utilising the gradients of the co-substrates. This is also known as uphill

transport or a concentrative capacity of the transport system. This is seen for members of the proton oligopeptide cotransporter family, SLC15, where di/tripeptides are transported along with protons (Brodin *et al.*, 2002). In the small intestine the  $H^+$ /peptide transporter, PEPT1, transports di/tripeptides from the intestinal lumen into an enterocyte along with a proton. The influx of protons causes a decrease in intracellular pH, which activates the  $Na^+/H^+$  exchanger, and proton efflux occurs by exchanging protons for sodium ions. This maintains the intracellular pH around approximately 7.4, and, due to the slightly acidic microclimate of the intestine (pH  $\sim$ 6.8), the pH gradient is maintained. Since the total driving force is responsible for the transport of di/tripeptides via PEPT1, the cell is able to accumulate an amount of peptide substrate inside the cell – even though the concentration gradient of the peptide is in the opposite direction. As mentioned earlier, symports may have two substrates moving in the same direction. In addition to a dependence on the amino acid gradient,  $ATB^{0,+}$  (SLC6A14) from the solute-linked carrier family 6, which transports neutral and cationic amino acids is also dependent on both sodium and chloride as driving forces. Thus three substrates are moving in the same direction. This involvement of two co-substrates makes the concentrative capacity of the carrier higher than for an amino acid carrier coupled to sodium alone (Ganapathy *et al.*, 2005).

### 3.3.1.3 Antiports

Carriers that have two substrates moving in opposite directions during the transport process are called antiports (see Figure 3.3.2). For antiports, one substrate involved in the translocation process will exchange another substrate across the cell membrane. The transport of a substrate is thus dependent on both the concentration gradient of the substrate itself and the concentration of co-substrate. The typical example of an antiport would be the  $Na^+/H^+$  exchanger (NHE), for which a  $Na^+$  ion is exchanged for a  $H^+$  across the cell membrane. The rate of transport via the carrier will depend on the concentration gradient of the substrates going in opposite directions. Antiports are also involved in the exchange of amino acids across the basolateral membranes of cells.

### 3.3.1.4 Active transporters

In the previous sections the different types of carriers were described. Carriers are passive in nature and the transport rate of substrate depends



on the electrochemical gradients involved, which determine the driving force for the transport process. However, other integral proteins exist where the translocation of substrates is coupled to the direct consumption of cellular ATP. Transport proteins utilising ATP for transporting their substrates are called active transporters, or primarily active transporters or pumps. The hydrolysis of ATP:  $\text{ATP}^{4-} + \text{H}_2\text{O} \rightarrow \text{ADP}^{3-} + \text{H}^+$ , yields energy ( $\Delta G' = -30 \text{ kJ mol}^{-1}$ ), which is utilised in the transport process for transporting the substrate in the opposite direction to the chemical gradient. As seen in Table 3.3.1, the intracellular concentration of  $\text{Na}^+$  is low compared to the extracellular concentration; nevertheless, one of the cell's most fundamental functions is the active transport of  $\text{Na}^+$  out of the cell and influx of  $\text{K}^+$  via  $\text{Na}^+/\text{K}^+$ -ATPase. Another class of active transporters that is important for the biopharmaceutical student or researcher is the active multidrug transporters. These transporters are described in Chapters 3.4 and 3.6. Briefly, they use the energy from the hydrolysis of ATP to transport a wide range of endogenous and therapeutically active molecules out of various cells and are called efflux transporters.

### 3.3.1.5 Carriers and active transporters in the dynamic cellular system

Carriers and transporters may be described functionally when viewed alone. However, in the dynamic cell the carriers or transporters work in concert with other carriers and ion channels. Even though the transport of a substrate via a carrier is passive in nature, the maintenance of gradients responsible for their transport in a dynamic cell system may be dependent on active transporter(s). Therefore the carriers in a cell system may be described according to their dependence on active transporters. This is illustrated in Figure 3.3.3.

In situation 1 the true active transporter is illustrated. The transport of substrate is coupled to the hydrolysis of ATP, and is dependent on the ATP level and the concentration of substrate. In situation 2 the transport of substrate via a symport is illustrated. In the case of glucose, the influx of glucose is coupled to the transport of  $\text{Na}^+$  and occurs via the sodium-dependent glucose transporter SGLT1. The  $\text{Na}^+$  ion moving into the cell is transported across the basolateral membrane via the active  $\text{Na}^+/\text{K}^+$ -ATPase. The transport of glucose via SGLT1 is thus secondarily dependent on an active transporter, and at the cellular level it is a secondarily active transporter. Glucose is either consumed inside the cell or

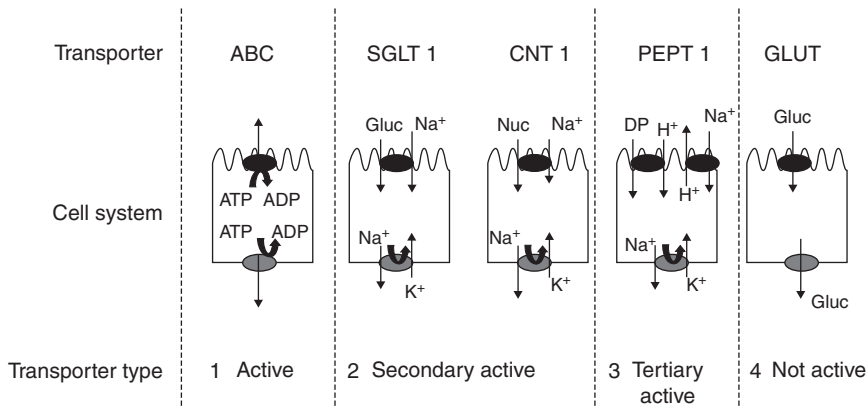


**Figure 3.3.3** Illustration of the various forms of carriers working in a dynamic cell. Gluc, glucose; Nuc, nucleotide; DP, dipeptides; ABC, ATP-binding cassette family transporter; SGLT1, the sodium-dependent glucose transporter; CNT1, the concentrative nucleotide transporter; PEPT1, the di/tripeptide transporter. These transporters are discussed further in Chapter 3.4.

transported across the basolateral membrane via the uniport GLUT5. In situation 3 the intestinal peptide transporter, PEPT1, is a carrier responsible for the cellular accumulation of di/tripeptides. The influx of substrate is dependent on protons, and if no other mechanisms were working in the cell the intracellular environment would eventually exist in equilibrium with the extracellular fluid, and the concentration of substrate and protons will be the same on each side of the cell membrane. In the dynamic cell system, the protons are exchanged across the apical membrane for sodium, thereby creating a sink for protons and resulting in an uphill transport of substrate. The  $\text{Na}^+$  ion moving into the cell is transported across the basolateral membrane via the active  $\text{Na}^+/\text{K}^+$ -ATPase. The influx of peptide and protons is thus indirectly dependent on the functional activity of the active  $\text{Na}^+/\text{K}^+$ -ATPase, and in the dynamic cell PEPT1 is termed a tertiary active transporter. The influx of peptide substrate is tertiarily dependent on an active transporter. At the transporter level alone, PEPT1 is a symport (see Section 3.3.1.2 Symports), and at the cellular level it is a tertiary active transporter. The peptide substrate does not stay in the cell; it is either metabolised to amino acids or transported out of the cell across the basolateral membrane. In situation 4 the influx and efflux of substrate in a dynamic viable cell is mediated by two identical or distinct carriers, and the total cellular transport is not directly or indirectly dependent on any active transporters.

### 3.3.2 Description of carrier-mediated transport kinetics

The identification of carrier type and how the carrier operates at a cellular level is normally necessary for an appropriate mathematical description of the transport of substrate. In this section transporter kinetics are discussed, whereas non-saturable kinetics are described in Chapter 3.2.

#### 3.3.2.1 The carrier seen as an enzyme

The mathematics used to describe transport via carriers is derived from the kinetics known for enzymes since the early 1900s. For enzymes the reaction between one substrate, S, and enzyme, E, forming a product, P, is initially given by:



In contrast, the simplified transport of one substrate via a transport protein, T, is initially given by:



The enzyme mediates the bioconversion of a substrate to a product, whereas the transport protein moves the substrate from one compartment to another without changing the structure of the substrate. Originally described for enzymes, the initial velocity is given by the Michaelis–Menten equation:

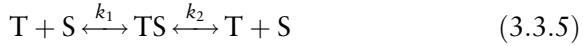
$$V_o = \frac{V_{\max}[S]}{K_m + [S]} \quad (3.3.3)$$

$V_o$  is the initial velocity (molarity/time),  $V_{\max}$  is the maximal velocity at a constant enzyme concentration (molarity/time),  $S$  is the substrate concentration (molarity), and  $K_m$  is the equilibrium constant when  $V_o$  is equal to one-half of  $V_{\max}$ . Equation 3.3.3 is also used for transport proteins present in tissues or cell cultures and the velocity is sometimes normalized with respect to the transport area, thereby yielding the flux,  $J$  (moles/area/time), across the system:

$$J_o = \frac{J_{\max}[S]}{K_m + [S]} \quad (3.3.4)$$

In the following, the derivation of the Michaelis–Menten equation is given under steady-state conditions. According to Equation 3.3.2, the

following reactions are involved in transport of a substrate: under steady-state conditions in which the concentration of transport protein is maintained constant and the transporter–substrate complex is constant:



If the amount of substrate is lower than the amount required to completely occupy all the transport proteins present, a population of free transporters (transporters not binding a substrate) must exist:

$$[\text{transporter}]_{\text{free}} = [\text{transporter}]_{\text{total}} - [\text{transporter}]_{\text{bound}} \quad (3.3.6)$$

If we look at a situation where the rate constant for the release of substrate,  $k_2$ , is higher than  $k_{-2}$  (rate constant in the opposite direction to  $k_2$ ), the following can be stated:

$$(k_{-1} + k_2)[TS] = k_1([T] - [TS])[S] \quad (3.3.7)$$

Collecting the rate constants yields an equilibrium, which is here termed the Michaelis–Menten constant:

$$(k_{-1} + k_2)/k_1 = K_m = ([T]_{\text{total}} - [TS])[S]/[TS] \quad (3.3.8)$$

Solving this equation for  $[TS]$  gives the following steps:

$$([T]_{\text{total}} - [TS])[S] = [TS]K_m \quad (3.3.9)$$

$$[TS]K_m = ([T]_{\text{total}}[S]) - ([TS][S]) \quad (3.3.10)$$

$$[TS]([K_m + [S]]) = [T]_{\text{total}}[S] \quad (3.3.11)$$

And finally:

$$[TS] = ([T]_{\text{total}}[S])/[K_m + [S]] \quad (3.3.12)$$

Since the velocity of the transport process depends on the rate of the release of substrate from the transporter:

$$V = k_2[TS] \quad (3.3.13)$$

The expression of the rate equation is obtained by substituting the value of  $[TS]$  from Equation 3.3.13 into Equation 3.3.12:

$$V = (k_2[T]_{\text{total}}[S])/[K_m + [S]] \quad (3.3.14)$$

And, since  $k_2[T]_{\text{total}}$  equals the maximal velocity at a given transporter concentration,  $V_{\text{max}} = k_2[T]_{\text{total}}$ , Equation 3.3.14 can be rearranged

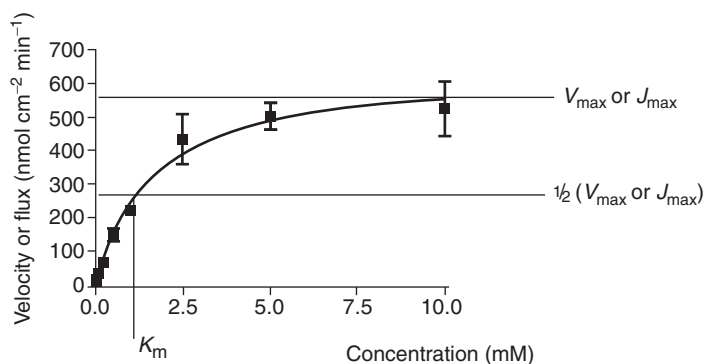


**Figure 3.3.4** Illustration of a Michaelis–Menten curve. The velocity or flux for a saturable transport process is described as a function of the total concentration of substrate at one given transporter concentration.

to give the familiar Michaelis–Menten expression given earlier in Equation 3.3.3:

$$V_o = \frac{V_{\max}[S]}{K_m + [S]} \quad (3.3.15)$$

The velocity's dependence on concentration is illustrated in Figure 3.3.4.

### 3.3.2.2 The carrier seen as an adsorption surface

The carrier transport derived based on enzyme kinetics is one way of viewing transporter kinetics; another is to view the carrier as a surface available for adsorption of substrates at discrete points (Neame and Richards (1972)). The carrier is seen as composed of a number of mobile adsorption sites in which the substrate is adsorbed at one surface and later released from another surface. By using the Langmuir adsorption equation, the derivation of an expression describing the transport rate via a carrier yields basically the Michaelis–Menten-type equation given in Equation 3.3.3.

### 3.3.2.3 The maximal velocity and the amount of enzyme present

In Figure 3.3.4, the typical Michaelis–Menten curve is illustrated. It can be seen that as the concentration is increased the velocity of the transport process is also increased. However, two important observations can also

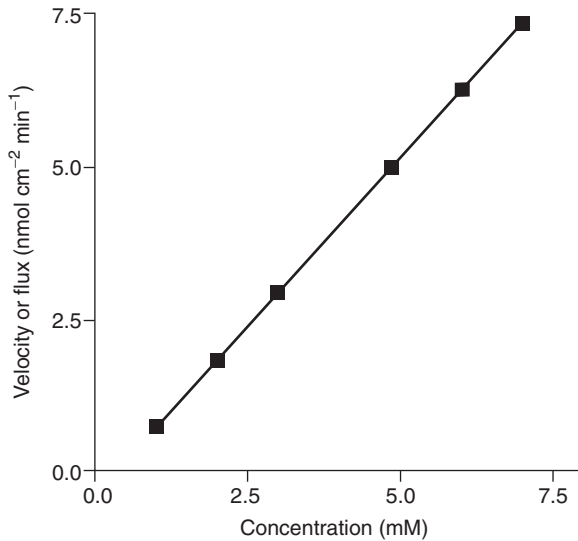


**Figure 3.3.5** Illustration of the dependence of velocity on the transporter concentration: the effect of the transporter concentration,  $[T]_{\text{total}}$  (mM), on the velocity,  $V$ , (M/time) of a transporter-mediated transport at a fixed constant concentration of substrate,  $[S]$ .

be made: (1) as the concentration of substrate is increased to well above the concentration equal to  $K_m$ , the velocity,  $V$ , gradually approaches a constant velocity at which it is constant and equal to the maximal velocity,  $V_{\text{max}}$ , at the given amount of transporters present; (2) as the concentration is increased the change in velocity, i.e. the slope of the curve in Figure 3.3.4, decreases gradually to zero. It is important to remember that  $V_{\text{max}}$  is dependent on the total number of transporters present, as illustrated in Equation 3.3.14. This is particularly important when evaluating experimental results obtained from different experimental system (see Sections 3.3.3 and 3.3.4). If the amount of transporter varies between the experiments, the velocity will vary accordingly, and problems will arise when the analysis of the experiments is conducted. As seen in Figure 3.3.5, there is a linear relationship between the velocity of the transport process and the amount of transporter present in the experimental or cellular system.

### 3.3.2.4 The Michaelis–Menten constant

The Michaelis–Menten constant is an equilibrium constant, which is experimentally determined from the initial concentration of substrate at half-maximum velocity, or at half-saturation of  $T$  with  $S$ . As seen

in Equation 3.3.8, the constant is based on how well a substrate binds to its transport protein. However, the constant may be dependent on substrate binding to at least two conformations of the transport protein, which in simplified terms mean its conformations at intra- and extracellular positions. The  $K_m$  value may be viewed as an indicator for how good a substrate is for a given transporter. However, since both  $k_1$  and  $k_2$  (Equation 3.3.8) may be rate-determining parameters in the expression for  $K_m$ , a change in  $K_m$  may for a transporter be a result of binding of substrate in the two different binding situations. From Equation 3.3.8 it is also seen that the  $K_m$  value is independent of the absolute amount of transporter present in the investigated system. The amount of transporter must, of course, be constant in the experiments giving the velocities at given concentrations.

### 3.3.2.5 What happens if other ligands or substrates are present?

The kinetics of transporter-mediated transport of a single substrate via one transporter are described above. However, transporters normally have several substrates, which are structurally similar, and therefore the transport of a given substrate will be influenced by the presence of other substrates. Moreover, lead series of novel compounds from a drug discovery programme or newly developed compounds from rational synthetic design are often investigated or even targeted for their ability to interact with transporters. In the following section the kinetics and experimental tools for investigating interactions of leads and drug candidates with transporters are described.

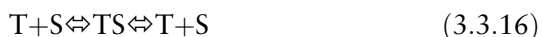
#### 3.3.2.5.1 *Substrate, ligand, or transportate?*

First, let us look at the types of interaction between a compound and a transporter that we are likely to encounter. In traditional enzyme terminology, the term ‘substrate’ is used for a molecule that which binds to the enzyme and undergo a series of reactions, which results in the formation of a product. The term ‘ligand’ is used in the literature on receptors, where a molecule binds to a receptor, which subsequently initiates a cascade of biological responses. On the other hand, an inhibitor is a molecule that binds to an enzyme (or receptor) and interferes with the enzyme’s activity by preventing either the formation of the ES complex or the generation of a product. How does this translate into looking at transporters? In terms of transporters, a substrate is a molecule which is moved

from one compartment to another by the transporter (see Section 3.3.2.1). Hence, the term ‘substrate’ in the field of transporters has a slightly different meaning from the term ‘substrate’ for an enzyme. Nevertheless, the term ‘substrate’ is most often used for a molecule that is moved from one compartment to another by a transporter, i.e. translocated. The term ‘transportate’ (Brandsch *et al.*, 2004) has been suggested for a molecule translocated by a carrier protein, and this may more appropriately describe the process; however, the future will show if this term is being widely accepted in the field. Normally, a compound that binds to a transporter without being translocated is referred to as a ‘ligand’. However, the term ‘ligand’ brings associations with a molecule that binds to a receptor and elicits a biological response, and therefore the term ‘inhibitor’ may be a more precise one to use.

### 3.3.2.5.2 Competitive inhibitors

In preclinical studies as well as molecular biopharmaceutical research, experiments are often performed in order to investigate whether a novel compound is binding to a given transport protein. This is frequently tested against a known substrate. The first analysis of binding assumes that the substrate and the novel compound (here termed I for inhibitor) interact with the same binding site of the transporter:



This kinetic scheme, in which I binds to the transport protein, is known as competitive inhibition. Conceptually, in a competition assay, we then look at a new compound as an inhibitor. However, by measuring the transport of S via T, we can easily extract information with regard to whether I decreases the transport of S in a concentration-dependent manner or not. The different types of reversible inhibition can then be distinguished experimentally, by investigating inhibitor effects on the kinetic parameters for the transport process. These inhibitor effects are summarised in Table 3.3.2. However, from competition assays one may not be able to distinguish between an inhibitor and a transportate, but only whether a new compound binds or not to the transporter. Initially we do not know if the binding is reversible or irreversible, but that can be tested by washing I out of the experimental system. The ability of the



**Table 3.3.2** Effects of reversible inhibitors on kinetic constants

<i>Type of inhibitor</i>	<i>Effect</i>	<i>Rate law</i>	<i>Calculation of <math>K_i</math> from <math>IC_{50}</math></i>
Competitive: I only binds to T	Raises $K_m$ $V_{max}$ is unchanged	$V = \frac{V_{max}[S]}{K_m(1 + \frac{[I]}{K_i}) + [S]} \quad (3.3.19)$	$K_i = \frac{IC_{50}}{(1 + \frac{[S]}{K_m})} \quad (3.3.22)$
Uncompetitive: I only binds to TS	Lowers $K_m$ and $V_{max}$ $V_{max}/K_m$ is unchanged	$V = \frac{V_{max}[S]}{K_m + (1 + \frac{[I]}{K_i})[S]} \quad (3.3.20)$	$K_i = \frac{IC_{50}}{(1 + \frac{K_m}{[S]})} \quad (3.3.23)$
Non-competitive: I binds to T and TS equally	Lowers $V_{max}$ and $K_m$ remains unchanged	$V = \frac{V_{max}[S]}{K_m(1 + \frac{[I]}{K_i}) + (1 + \frac{[I]}{K_i'})[S]} \quad (3.3.21)$	$IC_{50} = \frac{K_m + [S]}{(\frac{K_m}{K_{i1}} + \frac{[S]}{K_{i2}})} \quad (3.3.24)$
I binds to T and TS unequally	Lowers $V_{max}$ and raises or lowers $K_m$		

compound to interact with T may, from the kinetic scheme in Equations 3.3.16 and 3.3.17 be described by Equation 3.18:

$$K_i = \frac{[T][I]}{[TI]} \quad (3.3.18)$$

and the effect on the transport rate of S is given in Equation 3.3.19 (Table 3.3.2).  $K_i$  is a constant for the dissociation of I from the TI complex, and is called the inhibition constant.  $K_i$  is often termed 'affinity', and is an often used parameter in the evaluation of series of 'substrates' for transporters. However, from Equation 3.3.18 it is apparent that the  $K_i$  value is not easily determined because the concentration of both transporter and transporter-inhibitor complex should be known. However, the determination of the  $K_i$  value is facilitated by the use of radiolabelled standard compounds. The standard compounds are well characterised as substrates for specific transporters. Some of these standard compounds are available as radiolabelled isotopes, and this offers a natural starting point for investigation of the interaction between a transporter and novel compounds. An example of this is transport via PEPT1 (mentioned in Section 3.3.1.2 Symports), where the stabilised dipeptide Gly-Sar (either  $^3\text{H}$ - or  $^{14}\text{C}$ -labelled) has been characterised over a couple of decades, and is now widely used as a standard substrate for investigating transport via PEPT1. Novel compounds are typically characterised by their ability to inhibit the transport of Gly-Sar via PEPT1 in a concentration-dependent manner. Examples of this are seen in Figure 3.3.6.

The concentration of the new compound, which is able to inhibit 50% of the Gly-Sar uptake via PEPT1 is the concentration at 50% inhibition, i.e. the  $\text{IC}_{50}$  value. The lower this value, the higher the ability of the compound to inhibit the uptake of Gly-Sar, and the tighter the binding. The  $\text{IC}_{50}$  value can be used to calculate the  $K_i$  value of the competitive inhibitor (new compound) by determining the  $\text{IC}_{50}$  value along with the  $K_m$  value for the standard substrate (Equation 3.3.22). The concentration of standard substrate, [S], should be known; however since the radiolabelled standard compounds normally have a high specific activity, the assay concentration of S is normally much lower than its  $K_m$  value, and therefore the difference between its  $\text{IC}_{50}$  value and its  $K_i$  value is almost insignificant.  $\text{IC}_{50}$  values and  $K_i$  values are referred to as affinity values. Affinity values provide important information about transporter recognition and apparent binding strength of molecules. The affinity values are used to rank a lead series of new compounds with respect to their binding, and as such provide a basis for selecting molecules for further analysis. Affinity values are also used for molecular modelling purposes and for

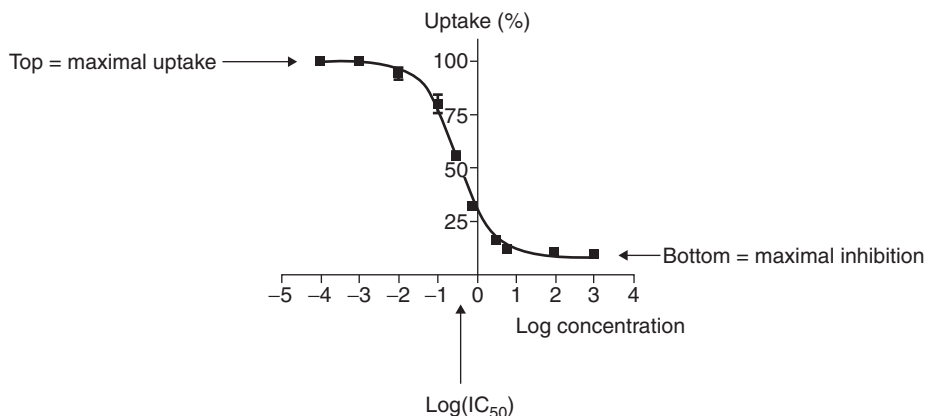


**Figure 3.3.6** Illustration of the dependence of inhibitor concentration on uptake.

exploring binding sites of transporters. It is therefore very important to be able to compare results obtained by others. Therefore care should be taken when comparing  $IC_{50}$  values with the  $K_i$  values, when comparing results obtained with different standard substrates, and when using different protocols of for example pH in solution, the presence or absence of  $Na^+$ . Also affinity values using different tissues or species must be compared with care.

In the dynamic cellular system, effects related to the carrier protein rather than to the solute may be of importance. Functional upregulation of transport activity and/or capacity may be seen in response to cellular events. Biological processes increasing the available number of carriers will increase the  $V_{max}$ , and modulation of the carrier via second messengers may alter the  $K_m$  value of the carrier. In the field of molecular biology of carriers' point mutation or genetic variants, the study of altered transport capacity ( $V_{max}$ ) or transport activity ( $K_m$ ) is highly relevant.

### 3.3.2.5.3 Uncompetitive inhibitors

Uncompetitive inhibitors only bind to the transporter–substrate complex:



The effect on kinetic parameters of such a substrate is shown in Table 3.3.2. It is important to remember that transporters are different from enzymes, and that the transporter–substrate complex exists in two,

probably different, conformations facing either the extracellular or intracellular side. The uncompetitive binding of an inhibitor or transportate may occur at both sides.

#### 3.3.2.5.4 *Non-competitive inhibitors*

For non-competitive inhibition, binding of inhibitor to carrier binding sites of both the empty transporter and the transporter–substrate complex may occur:



In other words, the inhibitor may act by either decreasing the turnover rate of the carrier and/or decreasing the amount of carriers available for substrate binding. The effect on substrate transport rate of a non-competitive inhibitor is derived from enzyme kinetics, but since carriers and enzymes are distinct, the equation in Table 3.3.2 (Equation 3.3.21) is a point of reference more than an absolute guidance (Neame and Richards, 1972).

#### 3.3.2.6 **Mixed kinetics including multiple carriers and passive diffusion**

The transport of a compound may occur via a single transporter as is seen for hydrophilic nutrients across a biological barrier. However, for compounds generated by the pharmaceutical industry or the academic researcher, the structural properties of the molecules may be such that the compound is a substrate for different types of carriers. Furthermore, alongside carrier-mediated transport, the compound may be able to permeate a membrane in a non-saturable manner.

##### 3.3.2.6.1 *Transport via one carrier along with passive diffusion*

In a number of cases the study of carrier-mediated transport processes is complicated by parallel non-saturable transport processes. In an experimental system the compound may be able to passively cross the membrane in which the carrier is expressed. If, for example, we look at the

study of a carrier in an epithelial barrier, which could be the barrier of an enterocyte, the compound may diffuse into the cell. The total transport rate of compound from the extracellular medium into the cell is thus not sufficiently described by Equation 3.3.30:

$$V_o = \frac{V_{\max}[S]}{K_m + [S]} \quad (3.3.30)$$

but must be combined with the expression of Fick's first law (see Section 3.2.1):

$$V = K_D \Delta[S] \quad (3.3.31)$$

In Equation 3.3.31, the uptake rate,  $V$ , has the unit of mol/time, and the concentration gradient,  $\Delta[S]$ , has the unit of mol/volume, which means that  $K_D$  has the unit of volume/time. Combining Equations 3.3.3 and 3.3.31 yields the equation for uptake of a compound by a carrier-mediated and a non-saturable transport process:

$$V_o = \frac{V_{\max}[S]}{K_m + [S]} + K_D \Delta[S] \quad (3.3.32)$$

As already mentioned, the transport rate across a biological barrier is often normalised with respect to the transport area, thereby giving the flux of a compound. In a situation where a transport process is a combination of one carrier-mediated and a non-saturable transport, the following expression describes the flux:

$$J_o = \frac{J_{\max}[S]}{K_m + [S]} + P_{\text{app}} \Delta[S] \quad (3.3.33)$$

where  $P_{\text{app}}$  is the apparent permeability coefficient. The origin of this constant is described in Chapter 3.2. Which of the transport processes involved in the transfer of compound from one compartment to the other is the main transport pathway in a given situation, is a result of the kinetic constants involved in relation to the concentration of compound.

### 3.3.2.6.2 Transport via two or multiple carriers

Transporters are generally relatively specific with respect to the substrates they accept; however some compounds may be substrates for more than one type of transporter. A substrate may also be transported by transporters belonging to the same transporter family, where different isoforms are expressed in the same cell or tissue. In these situations the description

of the rate of transport is a combination of the rate expression for the processes involved. For example if two transporters are transporting a substrate in one direction, the velocity of the process is defined by:

$$V_{\text{Total}} = \frac{V_{\text{max}}^1[S]}{K_m^1 + [S]} + \frac{V_{\text{max}}^2[S]}{K_m^2 + [S]} + \dots + \frac{V_{\text{max}}^n[S]}{K_m^n + [S]} \quad (3.3.34)$$

where 1 denotes the parameters for one transporter and 2 denotes the parameters for the other transporter, and  $n$  is the  $n$ 'th transporter involved in the overall transport. If the transporters work in different directions, the velocity of the process is found by subtracting one rate equation from the other:

$$V_{\text{Total}} = \frac{V_{\text{max}}^1[S]}{K_m^1 + [S]} - \frac{V_{\text{max}}^2[S]}{K_m^2 + [S]} \quad (3.3.35)$$

If transporter 1 has the highest transport capacity at the given concentration, the transport direction is defined as positive. Equations 3.3.34 and 3.3.35 may be combined with an expression for non-saturable transport similarly to Equations 3.3.32 and 3.3.33 (Table 3.3.2) when appropriate for the description of the experimentally obtained data.

### 3.3.3 Methods for studying transport via carriers

Transport via carriers may be investigated in several different systems using several different techniques. In the following two sections a brief description of different systems for studying carriers and different techniques will be provided. The sections are meant as an overview, and the reader is advised to consult more specific literature for detailed information about the systems and techniques if further interested.

#### 3.3.3.1 Systems for measuring transport via carriers

The choice of model system for investigating transport via carriers is highly dependent on the purpose of the study in question. There are various advantages and disadvantages associated with almost any system. It is therefore important to have a well-defined question before selecting a model. In general, a simple system allows for easier interpretation of the results. In general terms there are two purposes of investigating a carrier in biopharmaceutical work. One is to understand what the impact of a given transporter is in relation to a biological response. This could be the

impact on bioavailability of a drug, the response mediated by inhibiting the uptake of a neurotransmitter, or the effect of a carrier in renal reabsorption or excretion. For these purposes human pharmacokinetic or dynamic studies could be very relevant, although they are both laborious and expensive. Animals or perfused animal tissues may also be used, or excised tissues from animal. Tissue preparation could be used in the Ussing chamber or more simply as everted rings or sacs. Cell culture models, most notably the Caco-2 cell model, are also widely used for predicting the impact of transporters on intestinal transport of drug candidates. For investigating whether a compound is a substrate for a transporter or for probing the binding site or mode of action of a transporter, simpler systems could be used. These systems could be transient or stable transfection of a cell line with the cDNA for the transporter in question into mammalian cells (Hela, Cos7, HEK293, CHO or LLC-PK1). Heterologous expression of carriers is also widely carried out in yeast cells (*Pichia pastoris*) or *Xenopus laevis* oocytes.

### 3.3.3.2 Techniques for measuring transport via carriers

The study of carrier-mediated transport kinetics has benefited greatly from the development of advanced analytical methods along with many skilled biochemical and molecular biological techniques. In general, the techniques for studying transport via carrier fall into two categories: where the movement of substrate is measured directly or indirectly. Direct measurement of substrate is where the substrate is radiolabelled and the transport can be followed directly by counting the radioactivity present in different compartments. If radiolabelled molecules are not available, the researcher must depend on analytical methods (high-performance liquid chromatography (HPLC) or liquid chromatography/mass spectroscopy (LC-MS)-based methods or fluorescence assays) with a sufficiently low detection limit to be able to detect very small quantities of compound present inside the cells expressing the carrier of interest. The indirect methods are based on the function of the carrier in the system where it operates. For example for PEPT1, which is a  $H^+$ -co-transporter, the movement of substrate is coupled to the movement of protons. This movement of protons will affect both the intracellular pH and the membrane potential of the cell expressing PEPT1 (assuming that the substrate is neutral at the pH used in the experiment). By measuring the change in either intracellular pH or membrane potential it is possible to indirectly determine if a compound is a substrate for PEPT1. The intracellular pH

or membrane potential can be measured using fluorescent probes or with greater accuracy by using microelectrodes.

### 3.3.4 Conclusions

Carriers are fundamental in the movement of solutes across cell membranes. Furthermore, they have been shown to move drug substances across cell membranes. It is therefore important to have a basic knowledge about how carriers are classified and how they work. The function of transporters and the description of their kinetics have been discussed in this chapter.

### References

- Brandsch M, Knutter I, Leibach FH (2004). The intestinal H<sup>+</sup>/peptide symporter PEPT1: structure–affinity relationships. *Eur J Pharm Sci* 21: 53–60.
- Brodin B, Nielsen C U, Steffansen B, Frokjaer S (2002). Transport of peptidomimetic drugs by the intestinal di/tri-peptide transporter, PepT1. *Pharmacol Toxicol* 90: 285–296.
- Ganapathy ME, Ganapathy V (2005). Amino acid transporter ATB0, + as a delivery system for drugs and prodrugs. *Curr Drug Targets Immune Endocr Metabol Disord* 5: 357–364.
- Neame KD, Richards TG (1972). *Elementary Kinetics of Membrane Carrier Transport*. London: Blackwell Scientific Publications.





# 3.4

## Classification of human transporters

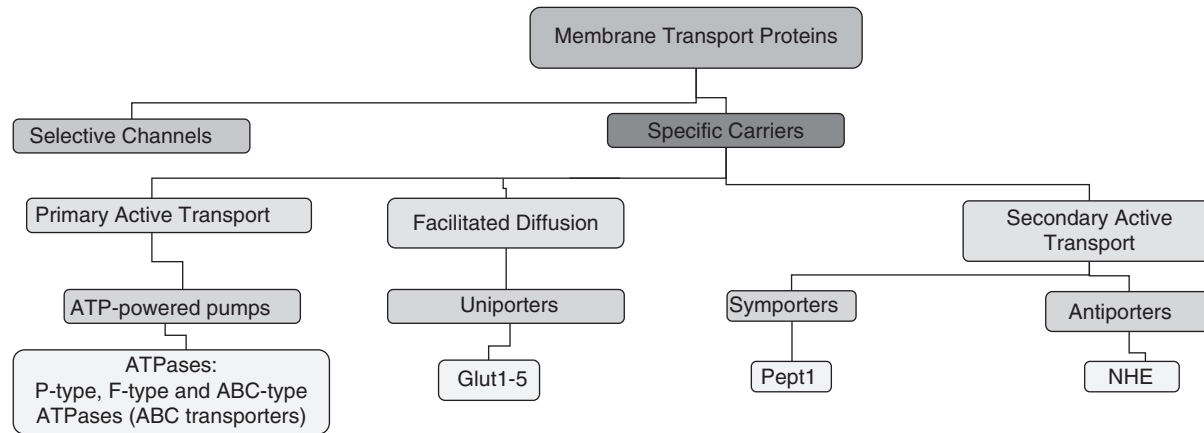
*Pascale Anderlé*

The plasma membrane represents a barrier between the cell and its environment. It is, however, essential that such separation is not complete. A large number of molecules must constantly move between the inside and outside of the cell, most frequently one at a time, but also in large groups. Hence, the plasma membrane functions as a selectively permeable membrane with well-defined selectivity with respect to which molecules cross and which direction they are allowed to travel.

Molecules can be transported either passively or actively across the membrane. Passive transport is driven by the kinetic energy of the molecules being transported (simple diffusion) or by membrane transporters that facilitate that diffusion (facilitated diffusion). They are always transported down their concentration gradient. In fact very few molecules enter or leave cells, or cross organelle membranes, without the help of proteins. Active transport, on the other hand, depends upon the production of cellular energy in the form of adenosine triphosphate (ATP) hydrolysis (Lodish *et al.*, 2000).

There are two classes of membrane transport proteins – carriers and channels (see Figure 3.4.1). Both form continuous protein pathways across the plasma membrane. Whereas transport by carriers can either be active or passive, solute flow through channel proteins is always passive (Alberts *et al.*, 2002).

Transport systems are essential to every living cell. They allow all essential nutrients to enter the cell and its compartments, regulate the cytoplasmic concentrations of metabolites by excretion mechanisms, control the concentration of ions inside the cell, which is very different from that outside the cell, export macromolecules such as complex carbohydrates, proteins, lipids, and DNA, catalyse export and uptake of signalling molecules that mediate intercellular communication, prevent toxic effects of drugs and toxins by mediating active efflux, and participate in biological warfare by exporting biologically active agents that



#### Primary active transport

Energy derived from hydrolysis of ATP to ADP liberating energy from high energy phosphate bond

#### Facilitated diffusion

Like any diffusion, transport from an area of higher concentration to lower concentration. Passive transport is powered by the potential energy of a concentration gradient and does not require the expenditure of metabolic energy

#### Secondary active transport

Use of energy from another source – another secondary diffusion gradient set up across the membrane using another ion. Because this secondary diffusion gradient initially established using an ion pump, as in primary active transport, the energy is ultimately derived from the same source – ATP hydrolysis.

**Figure 3.4.1** Overview of mechanisms of transport according to Lodish *et al.* (2000).

insert into or permeate the membranes of target cells (Saier, 2000). Transport is an essential aspect of all life-endowing processes: metabolism, communication, biosynthesis, reproduction and both co-operative and antagonistic inter-organism behaviours.

Transporters also play an important role in diseases and drug therapies. Numerous Mendelian disorders caused by mutations in transporter and channel genes underscore their physiological relevance. Membrane transporters play a key role in drug entry and extrusion from cells endowed with efflux pumps such as the ABC (ATP-binding cassette) transporters. Moreover, electrochemical gradients across membranes are relevant to drug partitioning into and out of cells and cell organelles, such as mitochondria. Transporters are frequently responsible for drug–drug and nutrient–drug interactions (Anderlé *et al.*, 2004). In cancer therapy, these proteins can cause chemoresistance as the drugs are secreted out of the cells by efflux pumps. On the other hand, targeting transporters for drug delivery has also been shown to increase chemosensitivity (Huang *et al.*, 2004).

Membrane transporters, ion exchangers and ion channels are encoded by numerous gene families, comprising 4.1 % of genes in the human genome (Venter *et al.*, 2001). The immense importance of these proteins and the increasing amount of data available on them mean that a systematic classification of transport systems is essential. Such a classification contributes to a comprehensive understanding of the basic functions of these proteins in any living cell (Saier *et al.*, 2006).

There are various ways to classify genes and proteins that function as transporters. In the following sections we will present the different major classification systems that currently exist and demonstrate the underlying ideas and structures of these systems. We will also discuss the problem of classifying such complex protein families and outline the different strategies for classification using two example transporters.

### **3.4.1 Classification according to transport mechanisms**

A basic strategy to classify membrane transporters is undoubtedly one based on the mechanisms of transport (Lodish *et al.*, 2000; Alberts *et al.*, 2002). This system forms the basis for most of the current more detailed classification systems. In summary, there are three major classes of membrane transport proteins: carriers, channels and ATP-powered pumps. All are integral transmembrane proteins and exhibit a high degree of specificity for the substance transported. It has to be noted that the

nomenclature can vary. For instance, the term 'transporter' can also refer to the term 'carrier'. The rate of transport by the three types differs considerably due to the differences in their mechanism of action (see Figure 3.4.1). A solute can be transported by any of three distinct, but related processes: (1) facilitated diffusion; (2) primary active transport; and (3) secondary active transport (see Figure 3.4.1).

In general, two principal modes of facilitated diffusion can be distinguished in biological systems: channel type and carrier type. There are, however, significant differences between channels and carriers that function on the basis of facilitated diffusion. Therefore, these two transporter systems are considered to be distinct and, as a consequence, are classified differently. In the following sections we will discuss the various mechanisms of transport and the corresponding transporter systems.

#### **3.4.1.1 Facilitated diffusion: channels**

Channel proteins transport water or specific types of ions down their concentration or electric potential gradients, which is an energetically favourable reaction. In contrast to carrier proteins, channel proteins simply form open pores in the membrane, allowing small molecules of the appropriate size and charge to pass freely through the lipid bilayer. They form a protein-lined passageway across the membrane, through which multiple water molecules or ions move simultaneously, a relatively rapid rate – up to  $10^8$  molecules  $s^{-1}$ . The solute passes in a diffusion-limiting process from one side to the other via a channel or a pore that is lined by appropriately hydrophilic (for hydrophilic substrates), hydrophobic (for hydrophobic substrates), or amphipathic (for amphipathic compounds) amino acid residues of the constituent proteins. The plasma membrane of all animal cells contains potassium-specific channel proteins that are generally open and are critical to generating the normal, resting electric potential across the plasma membrane. Many other types of channel proteins are usually closed, and only open in response to specific signals.

One group of channel proteins is the porins, which allow the free passage of ions and small polar molecules through the outer membranes of bacteria. Channel proteins also permit the passage of molecules between cells connected at gap junctions. The plasma membranes of many cells also contain water channel proteins (aquaporins), through which water molecules are able to cross the membrane much more rapidly than they can diffuse through the phospholipid bilayer. The best-characterised channel proteins, however, are the ion channels, which mediate the

passage of ions across plasma membranes. Although ion channels are present in the membranes of all cells, they have been especially well studied in nerves and muscles, where their regulated opening and closing is responsible for the transmission of electric signals (Lodish *et al.*, 2000). Channels are also widely used as drug targets, but, according to Treherne (2006), are still largely under-exploited as drug targets.

#### **3.4.1.2 Facilitated diffusion: uniporters**

In contrast to uniporters, channel proteins form open pores through the membrane, allowing the free diffusion of any molecule of the appropriate size and charge. Uniporters, on the other hand, transport one molecule at a time down a concentration gradient. Unlike channels, they undergo conformational changes that allow the molecule to pass through the membrane and be released on the other side. This type of transporter, for example, moves small, hydrophilic substrates such as glucose or amino acids across the plasma membrane into mammalian cells. Similar to enzymes, uniporters accelerate a reaction that is already thermodynamically favoured, and the movement of a substance across a membrane down its concentration gradient will have the same negative  $\Delta G$  value whether or not a protein transporter is involved (Lodish *et al.*, 2000). This type of movement is referred to as facilitated transport or facilitated diffusion. In contrast to passive diffusion, which follows Fick's law, facilitated diffusion is specific for a given compound and its transport rate is saturable. Moreover, its transport rate is significantly higher compared to passive diffusion, as the transported molecule is never in direct contact with the hydrophobic core of the membrane. In contrast to active transport systems, the direction of transport in facilitated diffusion is reversible, depending on the concentration gradient.

#### **3.4.1.3 Secondary active transport: symporters and antiporters**

Unlike uniporters, secondary active transporters are able to import or export ions and small molecules, such as glucose and amino acids, against a concentration gradient. They couple the movement of one type of ion or molecule against its concentration gradient to the movement of a different ion or molecule down its concentration gradient. In other words, they mediate coupled reactions in which an energetically unfavourable reaction is coupled to an energetically favourable reaction. As they have the

ability to transport two different solutes simultaneously, these carriers are also called co-transporters. When the transported molecule and co-transported ion move in the same direction, the process is called symport; when they move in opposite directions, the process is called antiport. As this transport mechanism involves catalysing an ‘uphill’ movement of certain molecules, these carriers are referred to as ‘active transporters’, but unlike the pumps, they do not hydrolyse ATP (or any other molecule) during transport. A very well-known example for a symporter is the dipeptide transporter PEPT1. The uptake of di- and tripeptides is associated with proton translocation in the same direction. Therefore, the transport rate is pH dependent (Daniel and Kottra, 2004). In contrast, the sodium/proton exchangers (NHE), which contribute to sodium and cytoplasmic pH homeostasis, are classical antiporters (Orlowski and Grinstein, 2004).

#### **3.4.1.4 Primary active transport: pumps**

Primary active transporters move ions or small molecules ‘uphill’ against a concentration gradient or electric potential across a membrane, which requires energy. In primary active transport, solute movement is coupled directly to an exergonic reaction (i.e. hydrolysis of ATP to ADP and inorganic phosphate (Pi), which releases energy). The overall reaction – ATP hydrolysis and the ‘uphill’ movement of ions or small molecules – is energetically favourable. Such pumps maintain the low calcium ( $\text{Ca}^{2+}$ ) and sodium ( $\text{Na}^{+}$ ) ion concentrations inside almost all animal cells relative to those in the medium, and generate the low pH inside animal-cell lysosomes, plant-cell vacuoles, and the lumen of the stomach. There are four principal classes. While the P, F, and V classes transport ions only, the ABC superfamily class transports small molecules as well as ions. The members of the ABC superfamily play a very important role in chemoresistance (Dean *et al.*, 2001a,b; Huang *et al.*, 2004).

#### **3.4.2 Transporter classification system**

In 1998, Milton Saier and his collaborators laid the basis for a comprehensive transporter classification system which was adopted in 2002 by the International Union of Biochemistry and Molecular Biology (IUBMB). The development of this classification system has been strongly influenced by the recent and fast progress in genomic sequencing and in computational biology. This transporter classification (TC) system provides a comprehensive overview of transport from structural, functional and evolutionary standpoints. The classification system is comparable to

the enzyme classification (EC) system approved by the Enzyme Commission. In contrast to the EC, the TC is not solely based on function, but 'additionally on phylogeny. Two different enzymes catalysing the exact same reaction sometimes exhibit completely different amino acid sequences and three-dimensional structures, function by entirely different mechanisms, and apparently evolved independently of each other. As the TC system takes into account the phylogenetic origins of transport systems it provides a reliable guide to protein structure, mechanism and function, although there may be some exceptions (Saier, 1999, 2000; Saier and Paulsen, 2001; Busch and Saier, 2002).

In the TC, the transporters are grouped on the basis of five criteria. Consequently, five different digits are assigned to each transporter system. The first digit corresponds to the transporter class, the second to the subclass, the third specifies the transporter family (or superfamily), the fourth the subfamily (family in a superfamily), and the fifth defines the substrate or range of substrates transported, as well as the polarity of transport (see Figure 3.4.2).

Any two transporters in the same subfamily that transport the same substrates using the same mechanisms are given the same TC number, regardless of whether they are orthologs or paralogs. Orthologs are genes that are evolutionary related, share a function, and have divergent speciation. Paralogs, on the other hand, have a common ancestor but have diverged by gene amplification and no longer have a common function. Basically, orthologs have the same function but occur in different species, while paralogs exist in the same genome but have different functions. The mode of regulation is not taken into account in the TC system. The primary level of classification (e.g. distinction of classes) is based on transport and energy-coupling source. Currently, there are seven classes recognised in the TC (see Figure 3.4.3).

The next level of classification is the families. While the classes and subclasses distinguish functionally different types of transporters, the families and subfamilies provide a phylogenetic basis for classification. In order for two proteins to belong to the same family, they must exhibit a region of a minimum of 60 residues in comparable portions of the two proteins that has a comparison score in excess of nine standard deviations (Saier, 2000). A minimum of 60 residues is arbitrarily selected because

1. Digit Class	2. Digit Subclass	3. Digit Family	4. Digit Subfamily	5. Digit Substrate
-------------------	----------------------	--------------------	-----------------------	-----------------------

**Figure 3.4.2** Description of the TC number associated with each transporter.



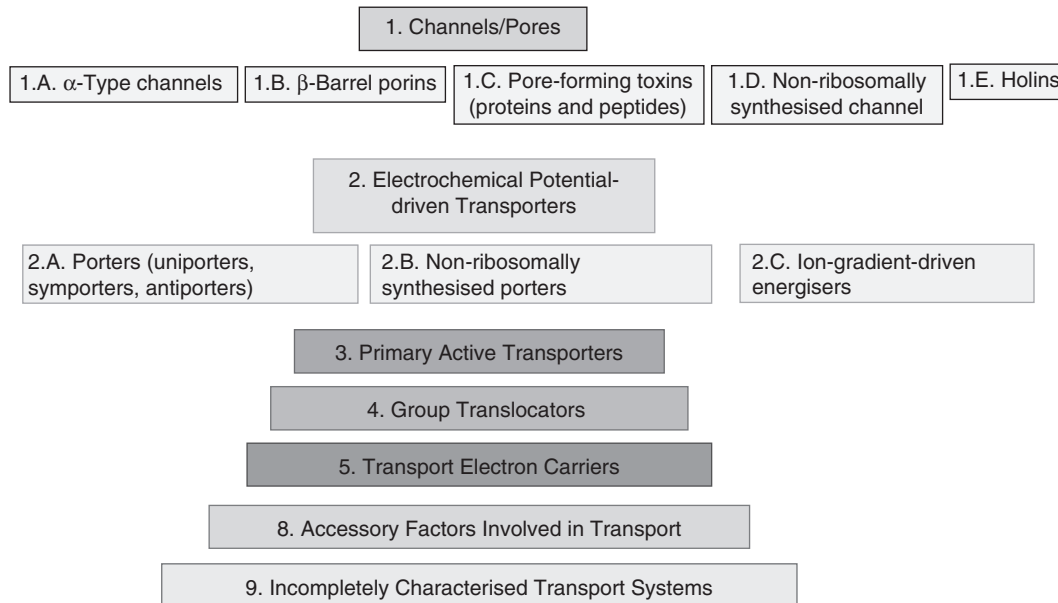


**Figure 3.4.3** Classes and subclasses of the TC system. Classes 6 and 7 have not yet been assigned. These classes are reserved for novel types of transporters that do not fall into the other classes.

many protein domains in water-soluble protein are of about this size. More than 400 families are currently included in the TC system (Saier *et al.*, 2006).

#### 3.4.2.1 Transporter Classification Database (TCDB)

In parallel to the TC system, Milton Saier and collaborators established a relational, web-integrated database. The transporter classification database (TCDB; [www.tcdb.org/tcdb/](http://www.tcdb.org/tcdb/)) contains sequence, classification, structural, functional and evolutionary information about transport systems for many different living organisms. All data are a summary of published information of over 10000 references. Currently, there are about 3000 distinct proteins organised in more than 400 families based on the TC system (Ren *et al.*, 2004; Saier *et al.*, 2006).

The classification system can be accessed through an intuitive web interface. The user can start at the top of the hierarchy and descend through the taxonomy. At the deepest level, individual protein information such as Swiss-Prot accession number, the primary sequence, source organism and the protein name, length, molecular weight and probable topology can be retrieved. Several links, such as links to the SwissPfam database (see below), the ExPASy server, the Swiss Institute of Bioinformatics BLAST Network service, and transmembrane segment (TMS) prediction are provided. A link to the FASTA formatted protein sequence, as well as a link to the hydropathy and amphipathicity plots for the protein, are also available. The TCDB can also be searched by entering the TC family name or TC number. Additionally, it is possible to search by keyword, disease name, and protein name. Also included is a section detailing human transporters that have been approved by the Human Genome Nomenclature Committee (HGNC), which will be discussed later (see Section 3.4.4). Importantly, each of these proteins has been cross-referenced with the TC system (Ren *et al.*, 2004; Saier *et al.*, 2006).

In conclusion, the TCDB is an essential tool in exploring the structures and functions of transporters and gaining a good understanding of how transporters are classified according to the TC system.

#### 3.4.3 Gene ontology

The recent sequencing efforts and the resulting information about the genomes of different organisms have made it clear that a large fraction of the genes specifying the core biological functions are shared by all eukaryotes. The knowledge of the biological role of such shared proteins in one

organism can certainly illuminate its role in other organisms. As a consequence, in 2000 the Gene Ontology Consortium constructed a tool, the Gene Ontology (GO), to facilitate the biologically meaningful annotation of genes and their products in a wide variety of organisms (Ashburner *et al.*, 2000; [www.geneontology.org](http://www.geneontology.org)). The main aim is the possibility of an automated method of transferring biological annotation from experimentally well-studied model organisms to less well-known organisms, based on gene and protein sequence similarity. Ontologies are structured vocabularies in the form of directed acyclic graphs that represent a network in which each term may be a 'child' of one, or more than one, 'parent'.

The current GO system consists of three completely independent categories: (1) molecular function; (2) biological process; and (3) cellular component.

'Molecular function' GO terms describe activities at the molecular level. They represent activities rather than the entities (molecules or complexes) that perform the actions, and do not specify where or when, or in what context, the action takes place. Molecular functions generally correspond to actions that can be performed by individual gene products, but some activities are performed by assembled complexes of gene products. In contrast, a 'biological process' represents a series of events accomplished by one or more ordered assemblies of molecular functions. It has to be noted that a 'biological process' is not equivalent to a pathway. The GO system does not specifically focus on representing any of the dynamics or dependencies that would be required to describe a pathway. A 'cellular component' is a component of a cell with the possibility that it is part of some larger object, which may be an anatomical structure or a gene product group. Each annotation of a given gene is attributed to a source, which may be a literature reference, another database or a computational analysis. Such a GO evidence code provides a useful estimation of the annotation quality.

#### **3.4.3.1 Human membrane transporters and GO**

To date there are in total 27 894 human gene products annotated to the ontologies, of which a little fewer than 40% have not been electronically inferred (i.e. not purely based on sequence similarity, [www.geneontology.org](http://www.geneontology.org)). Using GOA as a reference, we identified 2365 human gene products in Swiss-Prot that have been annotated as proteins with 'transporter activity' or with any daughter term – isoforms and subunits were counted independently.

The GO database is cross-referenced by the TC system ([www.geneontology.org](http://www.geneontology.org)). In other words, each gene is associated with a TC code if possible. It has to be noted though that the hierarchical structure in the TC system does not correspond to the classification system in the GO database. One major difference is that in GO a transporter can be annotated with different GO terms, while in the TC a given protein gets only one TC code. Using two model transporters we will later discuss the differences between the two classification systems.

#### **3.4.4 Human Genome Organization (HUGO) symbols**

The Human Genome Organization (HUGO) was created in 1988. Some of the objectives of this association are to assist with the co-ordination of research on the human genome and to help with the exchange of data between scientists (Bodmer, 1991). One organisation, the Human Genome Nomenclature Committee (HGNC), is responsible for approving a unique gene name and gene symbol for each individual gene and storing this information in their HGNC database. Guidelines for the human gene nomenclature can be found on their web page ([www.genenames.org/guidelines.html](http://www.genenames.org/guidelines.html)).

To date, the HGNC contains more than 40 transporter families of the so-called *SLC* (solute carrier) series. This family includes a major part of transporter-related genes. In the HUGO system, the remaining transporter genes are ATP-driven transporters, channels, ionotropic receptors, aquaporins, transporter and channel subunits, and auxiliary/regulatory transport proteins ([www.genenames.org/guidelines.html](http://www.genenames.org/guidelines.html)) (Hediger *et al.*, 2004). The *SLC* families have been presented in detail in the prepared *SLC* mini-review series of *Pflügers Archiv* (Hediger, 2004). Hediger and his co-workers have prepared a database containing all *SLC* members ([www.bioparadigms.org/slc/menu.asp](http://www.bioparadigms.org/slc/menu.asp)). Similar to the *SLC* families, useful links to web pages which describe the various transporter families and provide some additional information on their members can be found on the HGNC web page. Overall, the HGNC requires that the nomenclature schemes apply a ‘stem’ (or ‘root’) symbol for members of a gene family or grouping, with a hierarchical numbering system to distinguish the individual members. However, the strategy on how genes are grouped into families is not very well documented.

Even though the HUGO symbols are cross-referenced in the TCDB, the way transporters are classified into the various families in the HGNC does not necessarily correspond to the classification in the TC.

### 3.4.5 Pfam

The Pfam-A database contains a collection of curated multiple sequence alignments for each family, as well as profile hidden Markov models (profile HMMs) for finding these domains in new sequences (Sonnhammer *et al.*, 1998; Bateman *et al.*, 2000). A multiple sequence alignment is an alignment of three or more sequences, with gaps inserted in the sequences such that residues with common structural positions and/or ancestral residues are aligned in the same column. Defining profile HMMs is a probabilistic approach to representing a motif in a sequence. Each family in Pfam is represented by two multiple sequence alignments and two profile HMMs. The Pfam families are grouped in so-called clans. A clan contains two or more Pfam families that have evolved from a single evolutionary origin. Proof of their evolutionary relationship is usually determined by similar tertiary structures, or, when structures are not available, by common sequence motifs. Clans have been introduced in Pfam as some protein families are highly divergent, thus making it very difficult to represent the family with a single HMM. These families are closely related, so sequences may significantly hit more than one member of the clan ([www.sanger.ac.uk/Software/Pfam/browse/clans.shtml](http://www.sanger.ac.uk/Software/Pfam/browse/clans.shtml)).

For all protein sequences that do not belong to any Pfam family, a new family is generated in the so-called Pfam-B database. As of release 19.0, Pfam contained 8183 Pfam families, which match 75% of protein sequences in Swiss-Prot and TrEMBL (and 53% of all residues) (<http://pfam.sanger.ac.uk>; Bateman *et al.*, 2000). Cross-references to the TC and GO databases (QuickGO) are integrated into the Pfam database.

### 3.4.6 Practical approach: *SLC15A1* and *ABCB1*

In the following we will use *SLC15A1* and *ABCB1*, two important drug targets, as examples of how these genes and their corresponding gene products can be classified by the different systems.

#### 3.4.6.1 Classification based on transport mechanisms

PEPT1, the gene product of *SLC15A1*, has been shown to transport dipeptides and tripeptides and structurally related compounds. The uptake of these compounds into cells is directly coupled to a proton influx. As a consequence, increased proton efflux via the NHE exchanger can be observed (Daniel and Kottra, 2004). Taken together, as shown in Figure 3.4.1, PEPT is a typical secondary active transporter or

symporter. The term ‘tertiary active transporter’ has also been associated with *SLC15A1* (see Section 3.3.1.5 and Brandsch *et al.*, 2004). It has to be noted though that this concept has not yet been taken into account by the major classification systems.

On the other hand, it has been shown that the gene product of *ABCB1*, P-glycoprotein, acts as an ATP-dependent pump (Silverman, 1999). It is a typical ABC-type ATPase.

#### 3.4.6.2 TC system

Searching the TC with the keyword ‘SLC15A1’, the TC number 2.A.17.4.1 can be retrieved. It is classified as a ‘Peptide: H<sup>+</sup> symporter (transports cationic, neutral and anionic dipeptides; also transports  $\beta$ -lactam antibiotics, the antitumor agent, bestatin, and various protease inhibitors)’. Figure 3.4.4 outlines the detailed classification. The first digit indicates that SLC15A1 belongs to the class of carriers whose transport is driven by an electrochemical potential. The subclass (second digit) specifies that SLC15A1 is a porter, more specifically a symporter (see Figure 3.4.4). It is a member of the proton-dependent oligopeptide transporter (POT) family (third digit) and transports dipeptides, tripeptides and structurally related compounds (fifth digit).

As for *ABCB1*, the TC number ‘3.A.1.201.1’ represents ‘Broad specificity multidrug resistance (MDR) efflux pump (exports amphiphilic compounds of unrelated chemical structure); peptide efflux pump; phospholipid (e.g. phosphatidyl serine), cholesterol and sterol flippase (also called *ABCB1* and p-gp)’ (see Figure 3.4.4). *ABCB1* forms part of the family ‘ATP-binding cassette superfamily’ (third digit). The mechanism of transport is driven by P–P-bond hydrolysis (second digit) and, thus, *ABCB1* can be considered a typical primary active transporter (first digit.) In addition, both transporters can be found in the TCBD under the section ‘Transporters from humans’, listed with the official gene symbol according to HUGO.

#### 3.4.6.3 GO

Figure 3.4.5 summarises the nodes in the GO tree where *SLC15A1* and *ABCB1* are annotated according to GOA ([www.geneontology.org](http://www.geneontology.org)). In contrast to the TC system, in GO the two genes can be classified in different ways. On one hand, the transporters can be associated with different unique GO terms, on the other hand, the specific GO terms can be found in the different locations and hierarchical levels in the classification tree.

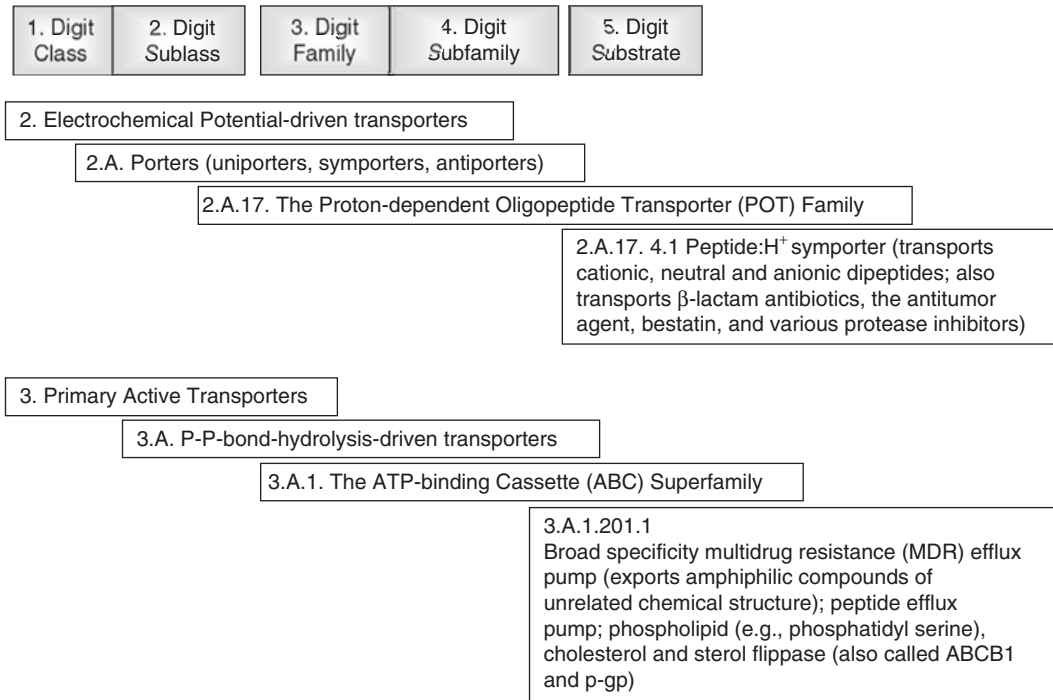


**Figure 3.4.4** Classification of the gene products SLC15A1 and ABCB1 in the TC system.

**SLC15A1****Function**

**oligopeptide transporter activity** (IEA)

GO:0015198 : oligopeptide transporter activity (3)

**peptide:hydrogen symporter activity** (TAS)

GO:0005215 : transporter activity

GO:0005386 : carrier activity

GO:0015290 : electrochemical potential-driven transporter activity

GO:0015291 : porter activity

GO:0005427 : proton-dependent oligopeptide transporter activity

GO:0015333 : **peptide:hydrogen symporter activity**

GO:0015293 : symporter activity

GO:0015294 : solute:cation symporter activity

GO:0015295 : solute:hydrogen symporter activity

GO:0015333 : **peptide:hydrogen symporter activity**

GO:0015075 : ion transporter activity

GO:0008324 : cation transporter activity

GO:0015294 : solute:cation symporter activity

GO:0015295 : solute:hydrogen symporter activity

GO:0015333 : **peptide:hydrogen symporter activity**

GO:0015197 : peptide transporter activity

GO:0015198 : oligopeptide transporter activity

GO:0005427 : proton-dependent oligopeptide transporter activity

GO:0015333 : **peptide:hydrogen symporter activity**

GO:0015293 : **symporter activity** (4) (IEA)

GO:0005215 : **transporter activity** (1) (IEA)

**Process**

GO:0007586 : **digestion** (3) (TAS)

GO:0006857 : **oligopeptide transport** (5, 5, 6) (IEA)

GO:0015031 : **protein transport** (4,4,5,5,5) (IEA)

**Component**

GO:0008372 : **cellular component unknown** (1) (ND)

GO:0016021 : **integral to membrane** (4) (IEA)

GO:0005887 : **integral to plasma membrane** (5, 5, 5) (TAS)

GO:0016020 : **membrane** (2) (IEA)

GO:0005624 : **membrane fraction** (3) (TAS)

**ABCB1****Function**

**ATP binding** (TAS)

GO:0005488 : binding

GO:0000166 : nucleotide binding

GO:0017076 : purine nucleotide binding

GO:0030554 : adenylyl nucleotide binding

GO:0005524 : ATP binding

**ATPase activity** (IEA)

GO:0003824 : catalytic activity (1)

GO:0016887 : ATPase activity (7)

**ATPase activity, coupled to transmembrane movement of substances** (TAS)

GO:0042626 : ATPase activity, coupled to transmembrane movement of substances (13)

GO:0000166 : **nucleotide binding** (2) (IEA)

GO:0005215 : **transporter activity** (1) (TAS)

**Process**

GO:0042493 : **response to drug** (4) TAS

GO:0006810 : **transport** (3, 2, 2) TAS

**Component**

GO:0009986 : **cell surface** (2) IEP

GO:0016021 : **integral to membrane** (4) TAS

GO:0016020 : **membrane** (2) IEA

GO:0005624 : **membrane fraction** (3) TAS

**Figure 3.4.5** Classification of SLC15A1 and ABCB1 according to GO. The complete hierarchical tree is only shown for some selected GO terms. For the others, the hierarchical level is indicated in parentheses, defining ‘molecular function’, ‘biological process’ and ‘cellular component’ as 0. The evidence codes are indicated for each GO term: IEA = inferred from electronic annotation, TAS = traceable author statement, IEP = inferred from expression notation, ND = no biological data available.



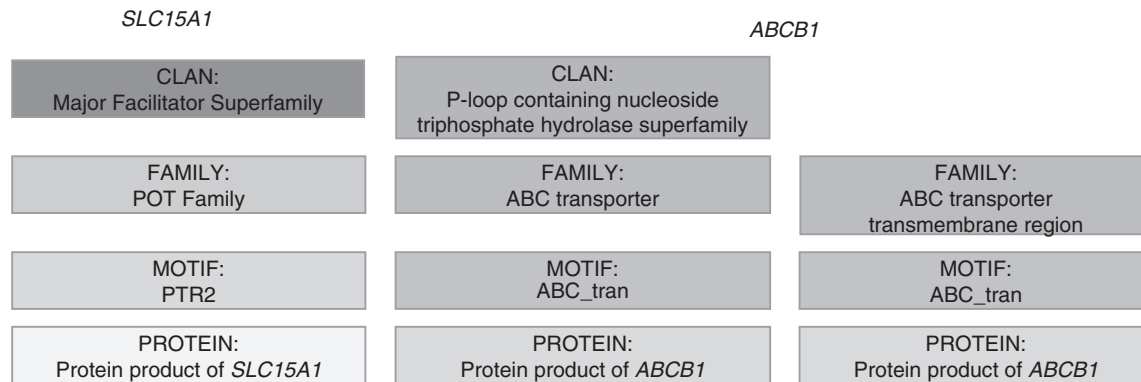


**Figure 3.4.6** Classification of the gene products of *SLC15A1* and *ABCB1* in the Pfam-A database.

### 3.4.6.4 Pfam

Searching the Pfam database, which focuses on relevant protein motifs via the Sanger website ([www.sanger.ac.uk/Software/Pfam/search.shtml](http://www.sanger.ac.uk/Software/Pfam/search.shtml)), reveals that the protein product of *SLC15A1* has a so-called PTR2 domain which defines the *POT* family. In contrast to the TC system where the *POT* family and the major facilitator superfamily are two independent families, in the Pfam system the *POT* family is considered to make part of the clan ‘the major facilitator superfamily’.

As for the protein product of *ABCB1*, two motifs can be found in the Pfam database: ABC\_tran and ABC\_membrane. The family ‘ABC transporter transmembrane region’ (ABC\_membrane) represents a unit of six transmembrane helices. Many members of the other family, the ‘transporter family’ (ABC\_tran), have two such regions (see Figure 3.4.6).

### 3.4.7 Conclusions

We have discussed the importance of transporters in living cells and their role in drug delivery. The increasing amount of data available on these proteins provokes the need for a systematic classification of transport systems. We have shown that classification strategies can actually contribute to a comprehensive understanding of the basic functions of these proteins in any living cell.

There are various ways to organise the vast amount of data available on transporters. Each of the systems presented has a different overall goal and uses different parameters to classify genes, or their products, respectively. Therefore, each system has limitations. Its advantages and disadvantages depend on the users’ scientific questions. All the systems presented are integrated in publicly available databases. There is certainly a trend to converge these databases and to provide cross-references. However, a one-to-one comparison is very difficult as the various classifications systems have similar goals, but differ significantly in their structures.

### Acknowledgment

I would like to thank Dr Viviane Praz for providing the latest statistics of the GO annotations.

### References

- Alberts B, Johnson A, Lewis J, *et al.* (2002). *Molecular Biology of the Cell*. New York: Garland Publishing.
- Anderle P, Huang Y, Sadee W (2004). Intestinal membrane transport of drugs and nutrients: genomics of membrane transporters using expression microarrays. *Eur J Pharm Sci* 21: 17–24.

- Ashburner M, Ball CA, Blake JA, *et al.* (2000). Gene ontology: tool for the unification of biology. The Gene Ontology Consortium. *Nat Genet* 25: 25–29.
- Bateman A, Birney E, Durbin R, *et al.* (2000). The Pfam protein families database. *Nucleic Acids Res* 28: 263–266.
- Bodmer WF (1991). HUGO: the Human Genome Organization. *FASEB J* 5: 73–74.
- Brandsch M, Knutter I, Leibach FH (2004). The intestinal H<sup>+</sup>/peptide symporter PEPT1: structure-affinity relationships. *Eur J Pharm Sci* 21: 53–60.
- Busch W, Saier MH Jr (2002). The transporter classification (TC) system, 2002. *Crit Rev Biochem Mol Biol* 37: 287–337.
- Daniel H, Kottra G (2004). The proton oligopeptide cotransporter family SLC15 in physiology and pharmacology. *Pflügers Arch* 447: 610–618.
- Dean M, Hamon Y, Chimini G (2001). The human ATP-binding cassette (ABC) transporter superfamily. *J Lipid Res* 42: 1007–1017.
- Dean M, Rzhetsky A, Allikmets R (2001). The human ATP-binding cassette (ABC) transporter superfamily. *Genome Res* 11: 1156–1166.
- Hediger MA, Romero MF, Peng JB, *et al.* (2004). The ABCs of solute carriers: physiology, pathological and therapeutic implications of human membrane transport proteins. Introduction. *Pflügers Arch* 447: 465–468.
- Huang Y, Anderle P, Bussey KJ, *et al.* (2004). Membrane transporters and channels: role of the transportome in cancer chemosensitivity and chemoresistance. *Cancer Res* 64: 4294–4301.
- Lodish H, Berk A, Zipursky SL, *et al.* (2000). *Molecular Cell Biology*. New York: WH Freeman & Co.
- Orlowski J, Grinstein S (2004). Diversity of the mammalian sodium/proton exchanger SLC9 gene family. *Pflügers Arch* 447: 549–565.
- Ren Q, Kang KH, Paulsen IT (2004). TransportDB: a relational database of cellular membrane transport systems. *Nucleic Acids Res* 32: D284–D288.
- Saier MH Jr (1999). A functional-phylogenetic system for the classification of transport proteins. *J Cell Biochem* 84–94.
- Saier MH Jr (2000). A functional-phylogenetic classification system for transmembrane solute transporters. *Microbiol Mol Biol Rev* 64: 354–411.
- Saier MH Jr, Paulsen IT (2001). Phylogeny of multidrug transporters. *Semin Cell Dev Biol* 12: 205–213.
- Saier MH Jr, Tran CV, Barabote RD (2006). TCDB: the Transporter Classification Database for membrane transport protein analyses and information. *Nucleic Acids Res* 34: D181–186.
- Silverman JA (1999). Multidrug-resistance transporters. In: Sadee AA, ed. *Membrane Transporters as Drug Targets*. New York: Kluwer Academic/Plenum Publishers, 353–386.
- Sonnhammer EL, Eddy SR, Birney E, Bateman A, Durbin R (1998). Pfam: multiple sequence alignments and HMM-profiles of protein domains. *Nucleic Acids Res* 26: 320–322.
- Treherne JM (2006). Exploiting high-throughput ion channel screening technologies in integrated drug discovery. *Curr Pharm Des* 12: 397–406.
- Venter JC, Adams MD, Myers EW, *et al.* (2001). The sequence of the human genome. *Science* 291: 1304–1351.

# 3.5

## Absorptive transporters

*Carsten Uhd Nielsen, Bente Steffansen and Birger Brodin*

In Chapter 3.3 the various carrier types and their basic kinetics were described, and in Chapter 3.4 classification systems for human transporters were discussed. In this chapter, carriers, which are involved in transporting nutrients from the exterior to the interior of the body, will be described with respect to their relevance for the biopharmaceutical scholar. In this context the absorptive carrier is viewed as a carrier that transports nutrients from an exterior area, e.g. the intestine, the lung, or the cornea, into the epithelial cells and subsequently to the systemic circulation, i.e. the interior of the body. Carriers are integral players in the absorption, distribution, metabolism, and excretion (ADME) of many drug molecules. The challenge for the biopharmaceutical researcher is thus to sufficiently optimise ADME properties of drug candidates in order to reach drug compound(s) that have appropriate pharmacokinetic profiles for the dosage regimen and disease they are developed for. Alternatively, carriers themselves may also be pharmacological targets in which modulation of their activity is a part of the treatment of a disorder. This is especially seen for carriers in the CNS. The activity of L-glutamate transporters that belong to the *SLC1* gene family present in different CNS cell types is a pharmacological target for developing inhibitors for the treatment of CNS disorders or injury. Likewise transporters for  $\gamma$ -aminobutyric acid (GABA) (*SLC32A1*) are pharmacological targets in drug discovery programmes. The focus in the present chapter, however, will be primarily on nutrient carriers, which are relevant with regard to delivering drug candidates across epithelial barriers, and as such are important for the bioavailability of these compounds. In some cases it has retrospectively been shown that a transporter has influence on oral absorption of a drug compound and subsequently on its oral bioavailability. This has been seen for valaciclovir and  $\beta$ -lactam antibiotics, whose bioavailability partly depends on the transport

activity of the intestinal di/tripeptide transporter PEPT1. However, absorptive transporters are also relevant in drug-discovery and drug-development settings, since they offer a possibility for designing integral structural features in drug candidates by means of improving ADME properties, e.g. by designing analogues or prodrugs as substrates for absorptive transporters. Moreover, knowledge about molecular structural features of importance for interactivity with transporters may add to rational pharmaceutical formulation development since some pharmaceutical excipients may have molecular features that may interact with transporters as well. Alternatively, some pharmaceutical excipients may alter transporter function, by inhibiting or activating its regulation on both a short- and long-term basis, or by having influence on its co-substrate, e.g.  $\text{Na}^+$  or  $\text{H}^+$ . Thus, if that is the case, it seems possible, by using recipients that increase (or decrease if desirable) the driving force of the transporter, to increase transport capacity and subsequently the absorption fraction of the drug candidate substrate. Such preclinical studies may as well add to knowledge with regard to possible drug–drug interactions and/or drug–food interactions.

### 3.5.1 Searching for absorptive transporters

In this chapter, some absorptive transporters of relevance for pharmaceutical exploitation will be presented. The chapter will also focus on transporter properties that are advantageous for the biopharmaceutical scientist to consider, as well as strategies to utilise transporters for increasing intestinal permeation. The field of transporters is a rapidly evolving research area, and the present chapter is based on the current available knowledge. However, it is advisable to consult the HUGO Nomenclature Committee database for ongoing updates. At present the database includes more than 40 transporter families of the so-called *SLC* (solute carrier) gene series. The *SLC* families represent a major portion of the transporter-related genes but additional *SLC* transporters are constantly being identified. The *SLC* tables were originally prepared by the authors of the *SLC* mini-review series of *Pflügers Archiv* (Heidiger *et al.*, 2004). Apart from latest updates of the *SLC* families and their members, the database also links to relevant gene databases and reviews in the literature. This database is thus a gateway to a wealth of information, whereas the following only describes a selection of known absorptive transporters. Chapter 3.4 discusses the databases available for information, search and classification of transporters.

### 3.5.1.1 Absorptive transporters present in the intestine and kidney

Table 3.5.1 presents selected absorptive transporters that are mainly expressed in the intestinal and renal epithelial cells. The human intestine has transport systems for the diverse group of hydrophilic ‘nutrients, e.g. vitamins, minerals, amino acids, peptides and hexoses, which are transported across the lipophilic cell membranes of the epithelial enterocytes via carriers. Likewise, transporters expressed in the kidney are responsible for reabsorption of nutrients present in the ultrafiltrate. In Table 3.5.1 the carriers have been organised according to their transport mode. The gene name of the carrier is given along with its protein name. The general types of natural substrates are listed and the major tissue distribution and cellular localisation is provided. As an example the proton-dependent symports consist of transporters for amino acids, di- and tripeptides and minerals. Within the group of proton-dependent peptide transporters two different genes, *SLC15A1* and *SLC15A2*, have gene products that are peptide transporters. These proteins are called PEPT1 and PEPT2, respectively. The natural substrates of PEPT1 and PEPT2 are dipeptides ( $A_1A_2$ ) and tripeptides ( $A_1A_2A_3$ ). The cellular localisation of PEPT1 and PEPT2 is in the apical membrane, which is the side of the enterocytes facing the exterior (luminal) side of the intestinal and kidney tissues.

#### 3.5.1.1.1 Amino acid transporters

In the intestinal fluid, amino acids are the results of protein hydrolysis. Amino acids form a group of molecules with large physicochemical differences; they may be small neutral molecules like glycine, or large hydrophobic ones like tryptophan. Amino acids may be neutral, cationic or anionic, which may depend on pH, but the battery of transporters responsible for cellular absorption and vectorial transport in the intestine and kidney is relatively specialised. The organisation of amino acid transporters is rather confusing, since historically the transport systems have been characterised in tissue preparation and named according to their function and thus named by transport system names. However, with the advances in molecular biology the cDNAs encoding membrane transporter proteins have been cloned and named by gene and protein names. Thus, transporters are referred to by transport system names arising from functional studies in tissues, as well as by transporter names arising from cDNA and protein studies. These names are mixed in the literature; however, in this chapter we aim to use gene (*SLC*) and protein names.

**Table 3.5.1** Selected absorptive transporters for nutrients, vitamins, and minerals in epithelial cells

	<i>Gene name</i>	<i>Protein</i>	<i>Substrates</i>	<i>Tissue</i>	<i>Cellular location</i>
Proton-dependent symports					
Peptides	<i>SLC15A1</i>	PEPT1	A <sub>1</sub> A <sub>2</sub> , A <sub>1</sub> A <sub>2</sub> A <sub>3</sub>	Intestine, kidney	Apical
	<i>SLC15A2</i>	PEPT2	A <sub>1</sub> A <sub>2</sub> , A <sub>1</sub> A <sub>2</sub> A <sub>3</sub>	Kidney, lung	Apical
Amino acids	<i>SLC36A1</i>	PAT1	Gly, Ala, Pro	Intestine, kidney, lung	Apical
	<i>SLC36A</i>	PAT2	Gly, Ala, Pro	Kidney, lung	Apical
Minerals	<i>SLC11A2</i>	DMT1	Fe <sup>2+</sup> , Cd <sup>2+</sup> , Co <sup>2+</sup> , Cu <sup>2+</sup> , Mn <sup>2+</sup>	Intestine, kidney, lung	Apical
Sodium-dependent symports					
Amino acids	<i>SLC6A19</i>	B <sup>0</sup> AT1	Neutral amino acids	Intestine, kidney	Apical
Bile acids	<i>SLC10A2</i>	ASBT	Bile acids	Ileum, kidney, biliary tract	Apical
Vitamins	<i>SLC23A1</i>	SVCT1	Ascorbic acid	Kidney, intestines	Apical
Nucleosides	<i>SLC28A1</i>	CNT1	Pyrimidine nucleosides	Small intestine, kidney	Apical
	<i>SLC28A2</i>	CNT2	Purine nucleosides	Kidney, intestine	Apical
	<i>SLC28A3</i>	CNT3	Purine and pyrimidine nucleosides	Intestine, lung	Apical
Hexoses	<i>SLC5A1</i>	SGLT1	Glucose	Small intestine, kidney	Apical
Sodium-chloride-dependent symports					
Amino acids	<i>SLC6A14</i>	ATB(0+)	Neutral, cationic amino acid	Colon, lung	Apical

Uniports					
Nucleosides	<i>SLC29A1</i>	ENT1	Purine pyrimidine nucleosides	Ubiquitous	Plasma membrane (basolateral in polarised renal epithelial cells) and perinuclear membranes
	<i>SLC29A2</i>	ENT2	Purine pyrimidine nucleosides nucleobases	Ubiquitous, plasma membrane	Basolateral in polarised renal epithelial cells. Particularly abundant in skeletal muscle
Hexoses	<i>SLC2A5</i> <i>SLC2A2</i>	GLUT5 GLUT2	Fructose Glucose, galactose, fructose, mannose, glucosamine	Small intestine, kidney Intestine, kidney	Apical Basolateral



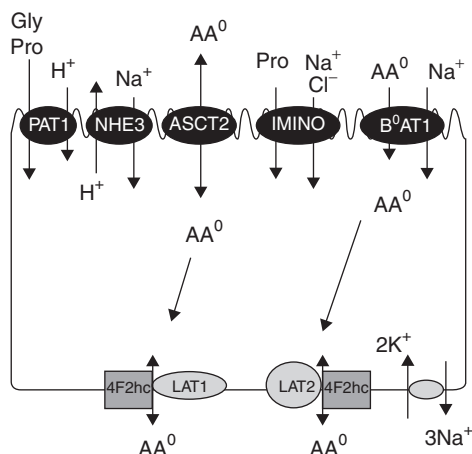


**Figure 3.5.1** Transport of neutral amino acids ( $\text{AA}^0$ ) in the small intestine and the kidney. PAT1 is the proton-dependent amino acid transporter, ASCT2 is the neutral amino acid exchanger; IMINO is the sodium- and chloride-dependent proline transporter;  $\text{B}^0\text{AT1}$  is the neutral amino acid transporter; NHE3 is the apical sodium proton exchanger 3; LAT is a glycoprotein-associated amino acid transporter (gpaAT) of L-type 1; LAT1 (SLC7A5) or 2; LAT2 (SLC7A8); 4F2hc (SLC3A2) is a heavy chain amino acid transporter protein.

In Figure 3.5.1 the transport of neutral amino acid in the intestine and the proximal tubule is illustrated. At least four different amino acid transporters transport neutral amino acids ( $\text{AA}^0$ ) across the apical membrane of intestinal and renal epithelial cells, with overlapping substrate specificity. The PAT1 (SLC36A1) transporter primarily transports proline and glycine. Proline is also transported by the IMINO/SIT (SLC6A20) transporter; however, the transporters differ in the driving forces, proton versus sodium, and in the  $K_m$  values, 0.13 mM versus 2.8 mM, for PAT1 and IMINO, respectively (Broer *et al.*, 2005). The  $\text{B}^0\text{AT1}$  (SLC6A19) transporter transports ‘large’ aliphatic amino acids such as leucine, valine, isoleucine and methionine, with the highest-affinity  $K_m$  values of approximately 1 mM, whereas phenylalanine, glutamine and alanine have affinities that are three-fold higher (Broer *et al.*, 2005). The ASCT2 (SLC1A5) transporter is an exchanger, which exchanges alanine, serine, cysteine, asparagine, threonine and glutamine for each other. ASCT2 is an obligatory antiporter and it is therefore not mediating a net absorption of amino acid. In the colon,  $\text{ATB}^{0,+}$  (SLC6A14) is another amino acid transporter for neutral amino acids.

Charged amino acids are transported by heteromeric amino acid transporters (HATs), which are composed of a light and a heavy subunit

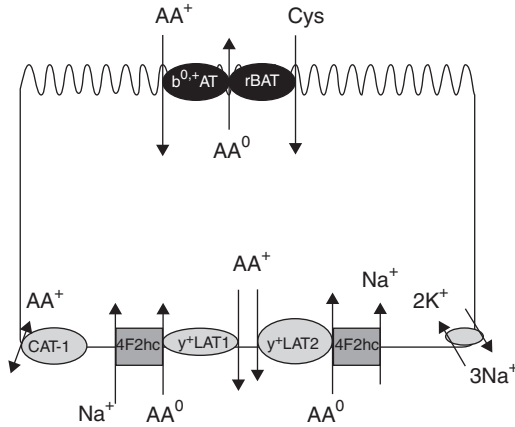


**Figure 3.5.2** Transport of charged amino acids ( $\text{AA}^+$ ) in the small intestine and the kidney.  $\text{b}^{0,+}\text{AT}$  is a sodium-independent amino acid transporter for neutral and cationic amino acids (exchanger); rBAT is a protein, which associates with  $\text{b}^{0,+}\text{AT}$  to form a transport system, which exchanges cysteine and positively charged (dibasic) amino acids with  $\text{AA}^0$  (Palacin and Kanai, 2004; Verrey *et al.*, 2004; see Figure 3.5.2).

linked by a disulphide bridge. The heavy subunits are SLC3 members, namely, rBAT (SLC3A1) and 4F2hc (SLC3A2). These proteins are type II membrane glycoproteins, which means that they have one single trans-membrane domain and the C-terminus is located outside the cell. rBAT heterodimerises with the light chain protein  $\text{b}^{0,+}\text{AT}$  (SLC7A9), to constitute the transport system, which exchanges cysteine and positively charged (dibasic) amino acids with  $\text{AA}^0$  (Palacin and Kanai, 2004; Verrey *et al.*, 2004; see Figure 3.5.2).

As seen in Figures 3.5.1 and 3.5.2, the amino acids moving into the epithelial cells are transported or exchanged across the basolateral membrane by several different transport systems composed of a light- and a heavy-chain protein. These systems are present to maintain cellular homeostasis and aid in vectorial absorption or re-absorption.

#### 3.5.1.1.2 Di/tripeptide transporters

Small peptides consisting of 2–3 amino acid residues are an important nutritional source of amino acids. These di- and tripeptides are transported across biological membranes via the transport capacity of two peptide transporters (see Table 3.5.1 and Figure 3.5.3), which belong to the SLC15 family. As discussed in Chapter 3.4, peptide transporters are proton-dependent symports. In the small intestine, PEPT1 is responsible

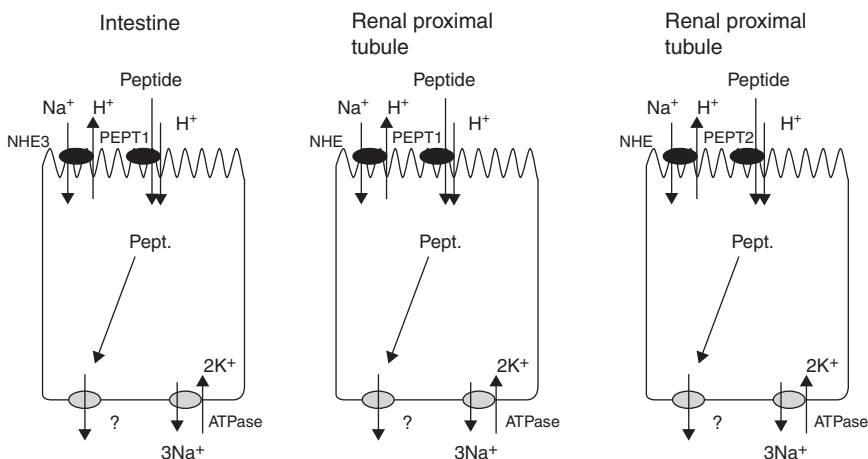


**Figure 3.5.3** Transport of small peptides (2–3 amino acid residues) in the small intestine and the kidney. In this context a peptide consists of either 2 or 3 amino acid residues. The '?' indicates that the basolateral transporter for peptide substrates transported into the epithelial cell via PEPT1 or PEPT2 has not been identified. NHE3 is the apical sodium proton exchanger 3.

for a large fraction of the amino acid uptake in the form of dipeptides or tripeptides. The di- or tripeptides are present in the intestinal lumen and are a result of dietary breakdown of protein coming from the ingested food. In the kidneys, di- or tripeptides arising from metabolism of hormones, neuropeptides or cytokines are reabsorbed by PEPT1 and PEPT2. In the kidney, both peptide transporters are expressed in a sequential manner in order to ensure an efficient reabsorption of amino acid nitrogen. In both the small intestine and the kidney, the apical uptake is mediated via well-characterised PEPT. Most of the substrates transported into the cell via PEPTs are rapidly metabolised inside the cell to the constituent amino acids, but some peptidomimetics are not metabolised. Therefore, for transepithelial transport to occur, these peptidomimetics must exit the cell via basolateral efflux. The efflux of peptidomimetics is mediated via a transport protein, which has been partly characterised with respect to pH dependency and substrate specificity. However, the molecular nature of the transporter is at present unknown, since a basolateral peptide transporter so far has not been cloned. It is unknown if the carrier-mediated transport process, which has been functionally characterised, is due to one or more transporter(s). It is important to consider the apical as well as the basolateral transport step in the overall evaluation of transepithelial transport pathways of both standard nutrients and novel drug

candidates, and therefore knowledge about the transporter responsible for the basolateral efflux step for PEPT substrates is eagerly anticipated.

### 3.5.1.1.3 Hexose transporters

Transport of glucose and related hexoses across biological membranes is mediated by members of two different SLC families, the sodium-dependent SLC5 family and the sodium-independent SLC2 family. The SLC5 family consists of 11 members where their functions, based on expression studies, have been ascribed to 9 out of the 11. SGLT1 is the primary apical sodium-dependent transporter for glucose; however the SLC5 family also has a vitamin transporter, SLC5A6, where the gene product, SMVT, transports biotin and pantothenate. The SLC2 family comprises 13 members, the glucose transporters (GLUTs) 1–12 and a  $H^+$ -*myo*-inositol (HMIT). GLUTs function as simple uniport carriers with the transport direction defined by the electrochemical gradient. Glucose has a key role in providing metabolic energy and being a building block for biosynthesis of biomolecules, and glucose transporters are expressed in every cell of the body. The different isoforms are expressed in different tissues, which is illustrated in Figure 3.5.4.

In Figure 3.5.4 the focus is on the GLUT expression in the intestine and the kidney. In the intestine, transepithelial hexose transport is mediated via an apical influx of glucose and galactose via SGLT1, and fructose via GLUT5. For transepithelial transport of hexoses to occur,

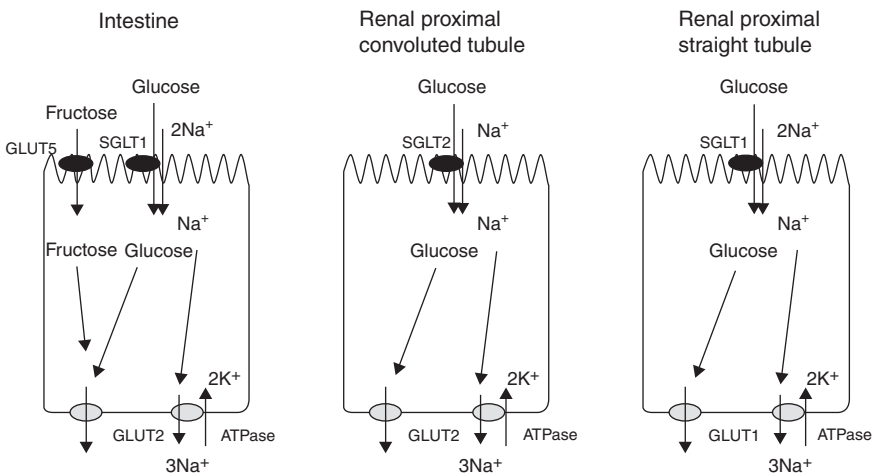


**Figure 3.5.4** Transport of hexoses in epithelial cells of the intestine and the kidney via members of the SLC2 and SLC5 families.

the transport into the cell must be followed by exit from the cell via basolateral efflux. This efflux of hexoses is mediated via GLUT2. Since SGLT1 is sodium dependent, sodium is exchanged for potassium across the basolateral membrane.

#### 3.5.1.1.4 Nucleoside transporters

Purine and pyrimidine nucleosides and their metabolic products are important precursors for the biosynthesis of DNA and RNA. Moreover, nucleosides participate in numerous other biological processes. Nucleosides are, like a number of other nutrients, relatively hydrophilic molecules, and their ability to be absorbed and distributed in the body is highly dependent on transporters. Members of the SLC families 28 and 29 are responsible for the transport of nucleosides. In epithelial cells, transport via members of the SLC28 family is dependent on the sodium gradient across the cell membrane, and these transporters are expressed in the apical membrane (see Figure 3.5.5 and Table 3.5.1). The transporters of the SLC29 family are independent of sodium in the transport process, and are thus facilitative or equilibrative transporters. In epithelial

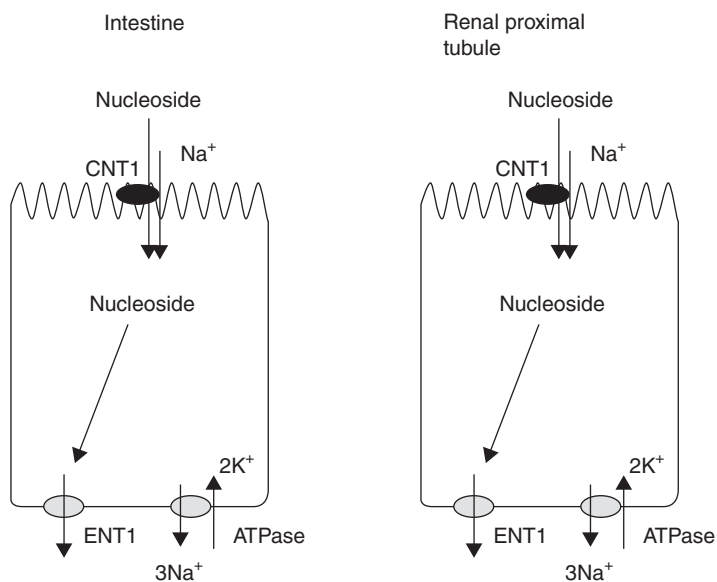


**Figure 3.5.5** Transport of nucleosides in epithelial cells of the intestine and kidney. CNT1,  $\text{Na}^+$ -dependent concentrative nucleoside transporter type 1; ENT1:  $\text{Na}^+$ -independent equilibrative nucleoside transporter type 1.

cells they are expressed in the basolateral membrane. The concentrative nucleoside transporters CNT1–3 transport uridine and certain uridine analogues. In general, hCNT1 is selective for pyrimidines, except a modest transport of adenosine by hCNT1, and hCNT2 is selective for purines. hCNT3 is non-selective for both purine and pyrimidine nucleosides. The equilibrative nucleoside transporters hENT1 and hENT2 transport both purine and pyrimidine nucleosides, although the substrate affinities are lower than for the CNTs. For transepithelial transport of nucleosides, the CNTs and ENTs function in series to bring a nucleoside from the surface of the epithelial barrier into the systemic circulation.

### 3.5.1.1.5 Vitamin transporters

Vitamins are a group of structurally diverse compounds, which need to be obtained from the diet. They are involved in a wealth of biological processes, where, among other things, they act as cofactors for metabolic processes. Since they are essential to the body, it is important to consider their oral absorption. Vitamins are generally divided into two groups based on their solubility: vitamins A, D, E and K are lipid soluble and the group of B vitamins and vitamin C are water soluble. Overall, the vitamins A, D, E, and K have  $\log P$  values  $>5$ , and are therefore highly lipophilic, and so are absorbed from the intestinal fluid by passive non-saturable diffusion. The more hydrophilic vitamins of the group of B vitamins and vitamin C rely on carriers in order to be both absorbed from the intestinal fluid and re-absorbed in the kidney. L-Ascorbic acid, the reduced form of vitamin C, is an effective antioxidant and scavenger of free radicals, and moreover an important cofactor in several enzymatic reactions. Two sodium-dependent carriers for L-ascorbic acid, SVCT1 and SVCT2, have been cloned, and these are the products of the *SLC23A1* and *SLC23A2* genes, respectively. SVCT1 is widely expressed in epithelial barriers such as the intestine, kidney, and lung, whereas SVCT2 is expressed in the tissues of the brain, eye and placenta (see Table 3.5.1 and Figure 3.5.6). Several other transporters have been demonstrated to be involved in the intestinal absorption and renal re-absorption of the water-soluble B vitamins: these include the thiamine transporters 1 (ThT1) and ThT2, the reduced-folate transporter-1 (RFT-1), and the sodium-coupled multivitamin transporter (SMVT) for biotin, pantothenate and lipoate. In Figure 3.5.6, the intestinal transport of a selected B vitamin has been illustrated. Nicotinic acid (niacin, B<sub>3</sub>) has been suggested to be absorbed in the intestine by the monocarboxylate transporter (SLC16), MCT1; however it is possible that the sodium-coupled

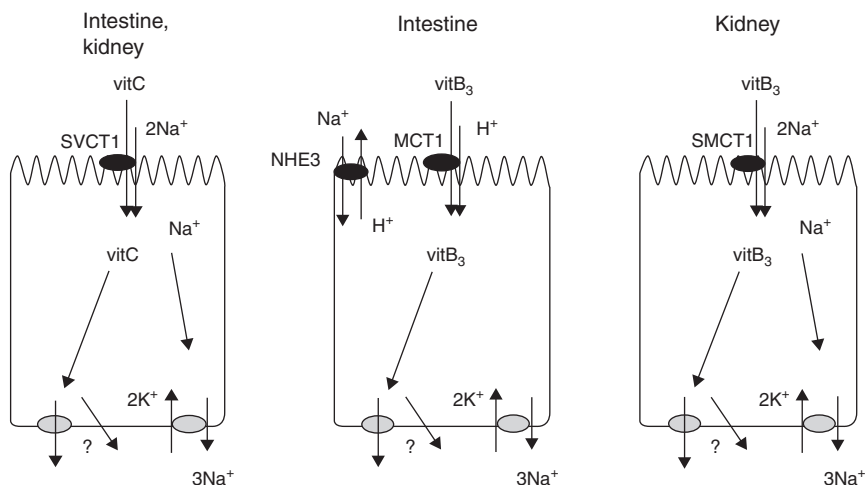


**Figure 3.5.6** Transport of vitamins in epithelial cells of the intestine and kidney. vitC, vitamin C; SVCT 1, sodium-coupled vitamin C transporter 1; MCT 1, monocarboxylate transporter 1; SMCT 1, sodium-coupled monocarboxylate transporter 1; vitB<sub>3</sub>, vitamin B<sub>3</sub>.

monocarboxylate transporter (SLC5A8), SMCT1, also participates in the absorption of vitamin B<sub>3</sub> in segments such as the ileum and colon. In the kidney it has been proposed that the reabsorption of B<sub>3</sub> is mediated by SMCT1 (Gopal *et al.*, 2005).

Besides the carriers described above, other mechanisms also participate in vitamin absorption and re-absorption. In the kidney proximal tubules, endocytosis of folate bound to folate-binding protein (FBP) occurs via endocytosis. In the intestine, receptor-mediated endocytosis is observed for vitamin B<sub>12</sub> in complex with the transport protein intrinsic factor (IF), following binding to the receptor protein cubilin.

### 3.5.1.2 Important absorptive transporters in drug delivery and biopharmaceutics

In Section 3.5.1.1, some of the absorptive transporters present in the intestine and kidney were described. These transporters perform an important function in relation to normal growth and function of human and animals. Why are they relevant for the student of pharmaceuticals? Medicine is made to act in a biological system. The biological system may be the human body or an animal. It has been estimated that 40% of the drug molecules on the market interact with transporters. Several of these 40% are intended to act on a transporter in the CNS. However, as the knowledge on transporters increases, the classical view of enzymes and

receptors as the main drug targets will be altered to include transporters in the drug discovery phase, and must then be integrated in the development of pharmaceuticals in the drug development phase. The plasma–time profile of a drug or drug candidate may depend to various degrees on the transport capacity and tissue expression of transporter. Factors such as substrate specificity, transporter capacity, expression profiles, and genetic variation will determine to what extent the transporters will be relevant for a given individual. The development of a pharmaceutical formulation must be able to appropriately accommodate the knowledge about capacity and expression of absorptive transporters in order to maximise the fraction of administered dose absorbed. Knowledge about transporters and their function and expression may also be useful in describing abnormal pharmacokinetic profiles of a drug molecule in the discovery or development phases. Some examples of drugs interacting with transporters are given in Table 3.5.2. Thus, inclusion of the increasing knowledge about transporter interactions with drug candidates already in the drug discovery phase and throughout the pharmaceutical development phase makes transporters an integral factor to be considered in drug development and may increase the success rate of rational drug development.

### 3.5.1.3 Impact of transporters on intestinal absorption/ intestinal drug delivery

Besides the intrinsic kinetic and regulatory characteristics of a given transporter, a number of other parameters should be taken into consideration when utilising transporters for drug delivery or when dealing with unusual or unexpected pharmacokinetics. One of these elements is the *expression of the transporter(s) in tissue segments*. Knowledge regarding intestinal expression of a relevant transporter for a drug candidate may influence the design of its pharmaceutical formulation. For example, since hPEPT1 is expressed in the small intestine, one may choose an instant-release formulation of a possible drug candidate substrate for hPEPT1. In contrast, since the amino acid transporter ATB<sup>0,+</sup> is expressed in the colon, then subsequently a colon-specific drug-release formulation will be relevant for a drug candidate substrate to ATB<sup>0,+</sup> in order to maximise absorption from the relevant tissue segment. The likelihood of drug–drug and drug–food interactions should be considered in relation to the expression of transporter. The effect of segmental pH variations may also influence not only the driving force regarding transport for proton-dependent transporters, but also the ionisation state of the substrates. A transporter may recognise a substrate differently



**Table 3.5.2** Selected absorptive transporters relevant in drug delivery and biopharmaceutics; some typical drug molecules transported via the transporters have been listed

<i>Natural substrate</i>	<i>Gene name</i>	<i>Protein</i>	<i>Drug molecules</i>	<i>References</i>
Proton-dependent symports				
Peptides	<i>SLC15A1</i>	PEPT1	$\beta$ -lactam antibiotics, valaciclovir, angiotensin-converting enzyme (ACE)-inhibitors, bestatin, various amino acid or dipeptidomimetic prodrugs	Dantzig, 1998; Brodin <i>et al.</i> , 2002; Nielsen <i>et al.</i> , 2002
Amino acids	<i>SLC15A2</i>	PEPT2		
	<i>SLC36A1</i>	PAT1	GABA, GABA analogues, vigabatrin, D-cycloserine, D-serine	Thwaites and Anderson, 2007
	<i>SLC36A</i>	PAT2		
Sodium-dependent symports				
Nucleosides	<i>SLC28A1</i>	CNT1	Zidovudine (3'-azido-3'-deoxythymidine, AZT), lamivudine (2',3'-dideoxy-3'-thiacytidine, 3TC), and zalcitabine (2',3'-dideoxycytidine, ddC), cytarabine [1-( $\beta$ -D-arabinofuranosyl)cytosine, AraC], gemcitabine (20,20-difluorodeoxycytidine, dFdC)	Gray <i>et al.</i> , 2004
	<i>SLC28A2</i>	CNT2	Didanosine (2',3'-dideoxyinosine, ddI), ribavirin	Gray <i>et al.</i> , 2004
	<i>SLC28A3</i>	CNT3	Cladribine, gemcitabine, FdU, 5-fluorouridine, fludarabine and zebularine	Gray <i>et al.</i> , 2004
Sodium-chloride-dependent symports				
Amino acids	<i>SLC6A14</i>	ATB <sup>0,+</sup>	NOS inhibitors, D-serine, amino acid prodrugs of aciclovir	Ganapathy and Ganapathy, 2005

depending on its ionisation state as well as its stereochemistry. This indicates the importance of considering *substrate specificity* of the ADME-relevant transporter(s).

It is a highly relevant, but also difficult, task to evaluate the *kinetic parameters*,  $K_m$  and  $V_{max}$  with regard to administered dose. *In vitro* studies may give information about the binding of a drug candidate to a transporter, or even yield data on the translocation. However, what are the likely consequences of drug candidate substrate binding/translocation on its intestinal absorption and ultimately its oral bioavailability? Let us say we are developing a prodrug for the peptide transporter, hPEPT1. From the literature we know that the natural substrates for hPEPT1 have affinities in the range of 0.1–3 mM (Nielsen *et al.*, 2002). Furthermore, we know for one distinctive class of substrates, the  $\beta$ -lactam antibiotic, that the likely cut-off value for where the affinity of a compound is too low to translate into a relevant bioavailability is approximately 15 mM (Bretschneider *et al.*, 1999). This indicates that the prodrug we are developing should have affinities in the lower millimolar range, i.e. 0.1–5 mM, unless it has a structural resemblance to  $\beta$ -lactam antibiotics. The concentration of the prodrug in the intestine would then determine the transport rate. The concentration in the intestine is rarely measured, but may for convenience be estimated as described in the Biopharmaceutics Classification System (BCS) (see Chapter 4.3) as the concentration yielded by the dose divided by 250 ml water. Because the transport of prodrug, measured as its flux, is approximately linear in the concentration range from 0 to the  $K_m$  value, then an increase in its dose would give a proportional increase in its flux across the intestine. Increasing the dose, to give concentrations higher than the  $K_m$  value, will not give a proportional increase in the flux. The flux will be saturated by increasing the concentration of prodrug if its absorption is specifically transporter mediated. The involvement of transporters in the absorption step may therefore be one cause of non-linear pharmacokinetics. Apart from relating the  $K_m$  values to dose, it may also be relevant to relate  $V_{max}$  or  $J_{max}$  to dose, since  $V_{max}/J_{max}$  determines the maximal transport capacity of the transport system. However,  $V_{max}$  values are mainly obtained from *in vitro* systems, and it is difficult to estimate the *in vivo*  $V_{max}$  of a transport system.

In some cases, *variations in the transporter genes* may have effects on the pharmacokinetic profiles of a drug compounds. Differences can be ascribed to processing and stability of the transcribed mRNA, to processing, stability, and sorting of the resulting proteins, or to changes in the kinetic parameters ( $K_m$  and  $V_{max}$ ) of the proteins. Single nucleotide polymorphisms (SNPs) present in the coding region of a gene may thus

lead to altered drug responses or even to other phenotypic differences, such as diseases. For a large number of transporters, the most updated information on genetic variations may be found in the following two databases: [www.ncbi.nlm.nih.gov/Entrez/](http://www.ncbi.nlm.nih.gov/Entrez/) and [www.pharmgkb.org/](http://www.pharmgkb.org/).

#### **3.5.1.4 Influx transporters present in the liver and kidney**

Besides the absorptive transporters present in the intestine and re-absorptive transporters in the kidney, the basolateral influx transporters in the kidney and liver are very important for overall pharmacokinetics. Some of the re-absorptive transporters in the kidney have been described in the previous sections. In this section, other influx carriers will be discussed with regard to their expression in the kidney and liver. Absorptive transporters in tissues other than the intestine and the kidney are not yet well investigated; however, in order for tissues to be relevant for transporter-mediated drug delivery to the systemic circulation, via a given epithelial barrier, then the transporter must be present in large tissue organs such as the lung. Furthermore, its expression in the tissue must be sufficiently high in order to deliver the relevant dose for treating the disease in question. In the lung a number of transporters such as peptide and amino acid transporters have been identified. Future studies may shed light on delivery of drug compounds via transporters expressed in the lung.

##### *3.5.1.4.1 Organic anion-transporting polypeptides*

Organic anion-transporting polypeptides (OATPs) are membrane transport proteins that mediate sodium-independent transport of substrates from the blood into hepatocytes. The substrates are a wide range of amphipathic organic molecules such as some bile salts, organic dyes, steroid conjugates, thyroid hormones, anionic oligopeptides and some drug compounds, e.g. some xenobiotics (Hagenbuch and Meier, 2004). The nomenclature of OATPs has been rather confusing, and for further information on the history and nomenclature of these the reader is referred to the review by Hagenbuch and Meier (2004). We will use the new SLCO-nomenclature and the new protein names as given in the review.

In the liver, protein-bound drug compounds are extracted from the circulation. The free drug is taken up by the hepatocytes for further hepatic handling such as metabolism and export (see Chapter 3.6). In the uptake process from the blood into hepatocytes, OATPs play an important role as outlined in Figure 3.5.7. The transport mechanism of OATPs seems to be an anion exchange, in which the cellular uptake of

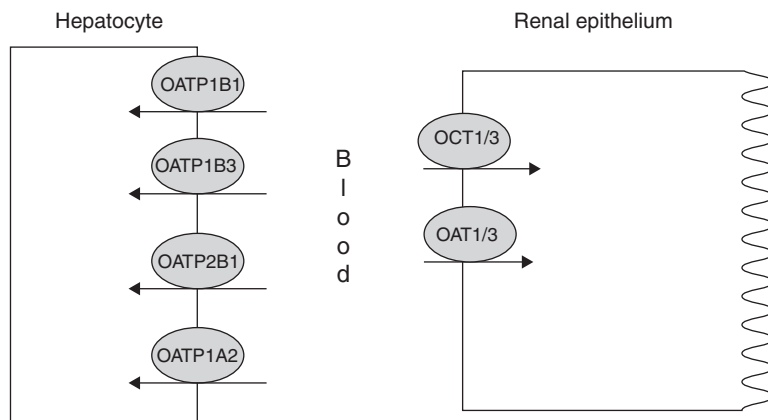


**Figure 3.5.7** Organic anion-transporting polypeptides (OATPs), organic cation transporters (OCTs), and organic anionic transporters (OATs) in the liver and the kidney.

organic compounds is coupled to an efflux of cellular bicarbonate, glutathione and/or glutathione-*S*-conjugates (Hagenbuch and Meier, 2004). The transport direction is thus dependent on these gradients, which are driving forces for the transport process (see Chapter 3.6).

OATP1B1 (SLCO1B1) transports bile salts and organic anions. Specifically, OAPT1B1 transports conjugated and unconjugated bilirubin, steroid conjugates, thyroid hormones  $T_4$  and  $T_3$ , and drugs such as pravastatin, rifampicin and methotrexate. The carrier is exclusively expressed in the liver. OATP1B3 (SLCO1B3) has similar substrates to OATP1B1, and thus transports bile salts and organic anions. Moreover, OATP1B3 transports digoxin and cholecystokinin (CCK-8) and the opioid peptide deltorphin II. The carrier is expressed in the liver and in some cancer cells. OATP2B1 (SLCO2B1) transports oestrone-3-sulphate and dehydroepiandrosterone. The carrier is most strongly expressed in the liver and, to a lesser extent, in the lung, kidney, brain, intestine and placenta. OATP1A2 (SLCO1A2) transports bile salts, organic anions and organic cations. More specifically, the carrier has been shown to transport the thyroid hormones  $T_4$  and  $T_3$ , prostaglandin  $E_2$ , and ouabain. The carrier is expressed in the endothelial cells of the brain, and in the kidney and liver.

#### 3.5.1.4.2 Organic anion and cation transporters (SLC22)

Transporters of the SLC22 family are polyspecific, which means that they transport multiple different substrates. The family can be divided into

various subgroups according to the substrates and transport mechanism. One of the subgroups comprises the organic cations transporter OCT subgroup. The OCT transporters transport organic cations, including weak bases (Koepsell and Endou, 2004). The transport process is electrogenic and independent of  $\text{Na}^+$ . A second subgroup of transporters is the organic anion transporters, OATs, which transport anions. Since transporters of the SLC22 family are expressed in tissues such as the intestine, liver and kidney, they are important in drug absorption and excretion (see Figure 3.5.7).

OAT1 (SLC22A6) is strongly expressed in the kidney. It is localised to the basolateral membrane in renal proximal tubule epithelial cells. The substrates are organic anions which are exchanged for  $\alpha$ -ketoglutarate. Drug molecules such as antibiotics, diuretics, anti-neoplastic drugs, and anti-inflammatory drugs are recognised as substrates (Koepsell and Endou, 2004). Moreover, endogenous compounds such as cyclic nucleotides, prostaglandins and uric acid are substrates. OAT3 (SLC22A8) is strongly expressed in the liver, with weaker expression in the kidney (Koepsell and Endou, 2004). It is localised to the basolateral membrane in renal proximal tubule epithelial cells. The substrates are organic anions, which may be exchanged for dicarboxylates. Drug molecules such as cimetidine and ochratoxine A are recognised as substrates (Koepsell and Endou, 2004). OCT1 (SLC22A1) is mainly expressed in liver tissue. It is localised to the sinusoidal membrane, and the basolateral membrane in enterocytes and renal epithelial cells. The substrates are organic cations and some weak bases; however, some anions are also transported. Drug compounds such as desipramine, aciclovir, ganciclovir and metformin are recognised as substrates. Moreover, endogenous compounds such as serotonin and prostaglandins  $\text{E}_2$  and  $\text{F}_{2\alpha}$  are substrates. OCT3 (SLC22A3) is expressed in the liver, placenta and kidney. The substrates are organic cations and some weak bases; however, some anions are also transported.

### 3.5.2 Conclusions

In this chapter a number of carriers, likely to be relevant in the overall pharmacokinetics of many drugs in the human body, have been described. Knowledge about these transporters is important in describing ADME properties of new chemical entities and drug compounds. It may thus be useful in describing unusual kinetics, or in order to predict the impact of interaction with transporters on absorption, clearance, excretion or

metabolism. Knowledge about the carriers as described in this chapter may also be applied in the drug discovery phase to rational design of prodrugs and analogues as substrates for absorptive carriers in the intestine, in order to increase intestinal permeation properties and thus oral bioavailability.

## References

- Bretschneider B, Brandsch M, Neubert R (1999). Intestinal transport of beta-lactam antibiotics: analysis of the affinity at the H<sup>+</sup>/peptide symporter (PEPT1), the uptake into Caco-2 cell monolayers and the transepithelial flux. *Pharm Res* 16: 55–61.
- Brodin B, Nielsen CU, Steffansen B, Frokjaer S (2002). Transport of peptidomimetic drugs by the intestinal di/tri-peptide transporter, PepT1. *Pharmacol Toxicol* 90: 285–296.
- Broer S, Cavanaugh JA, Rasko JE (2005). Neutral amino acid transport in epithelial cells and its malfunction in Hartnup disorder. *Biochem Soc Trans* 33: 233–236.
- Dantzig AH (1997). Oral absorption of  $\beta$ -lactams by intestinal peptide transport proteins. *Adv Drug Deliv Rev* 23: 63–76.
- Ganapathy ME, Ganapathy V (2005). Amino acid transporter ATB0, + as a delivery system for drugs and prodrugs. *Curr Drug Targets Immune Endocr Metabol Disord* 5: 357–364.
- Gopal E, Fei YJ, Miyauchi S, *et al.* (2005). Sodium-coupled and electrogenic transport of B-complex vitamin nicotinic acid by slc5a8, a member of the Na/glucose co-transporter gene family. *Biochem J* 388: 309–316.
- Gray JH, Owen RP, Giacomini KM (2004). The concentrative nucleoside transporter family, SLC28. *Pflügers Arch* 447: 728–734.
- Hagenbuch B, Meier PJ (2004). Organic anion transporting polypeptides of the OATP/SLC21 family: phylogenetic classification as OATP/SLCO superfamily, new nomenclature and molecular/functional properties. *Pflügers Arch* 447: 653–665.
- Hediger MA, Romero MF, Peng JB, *et al.* (2004). The ABCs of solute carriers: physiology, pathological and therapeutic implications of human membrane transport proteins. Introduction. *Pflügers Arch* 447: 465–468.
- Koepsell H, Endou H (2004). The SLC22 drug transporter family. *Pflügers Arch* 447: 666–676.
- Nielsen CU, Brodin B, Jorgensen FS, Frokjaer S, Steffansen B (2002). Human peptide transporters: therapeutic applications. *Expert Opin Ther Patents* 2002: 1329–1350.
- Palacin M, Kanai Y (2004). The ancillary proteins of HATs: SLC3 family of amino acid transporters. *Pflügers Arch* 447: 490–494.
- Thwaites DT, Anderson CM (2007). Deciphering the mechanisms of intestinal imino (and amino) acid transport: the redemption of SLC36A1. *Biochim Biophys Acta* 1768: 179–197.
- Verrey F, Closs EI, Wagner CA, *et al.* (2004). CATs and HATs: the SLC7 family of amino acid transporters. *Pflügers Arch* 447: 532–542.



# 3.6

## Efflux transporters

*Carsten Uhd Nielsen, Birger Brodin and Bente Steffansen*

In the previous chapter the absorptive transporters in the intestine and the kidney were discussed. In this chapter, the focus is on efflux transporters – membrane proteins that transport compounds from the cell to the exterior. In 1976 Juliano and Ling discovered that the over-expression of a membrane protein in colchicine-resistant Chinese hamster ovary (CHO) cells conferred resistance to a wide range of anti-cancer drugs (Juliano and Ling, 1976). The protein was termed P-glycoprotein 170 (P-gp) and the phenomenon was termed multidrug resistance (MDR). The consequence of expression of this glycoprotein was cellular export of structurally unrelated compounds. This caused a reduced retention and increased excretion of anti-cancer compounds from the cell. P-gp turned out to be the first member of a large superfamily of ATP-dependent efflux transporters. These are now termed ABC transporters, for ATP-binding cassette transporters. It has been found that ABC transporters are part of MDR, which is a cause of therapeutic failure in chemotherapy. ABC transporters are present in the normal human cell, where they are a natural part of the body's defence against xenobiotic compounds, i.e. compounds that are foreign to the body. Since ABC transporters act by pumping their substrates out of the cell by utilising ATP, they are often referred to as efflux transporters. From a pharmaceutical point of view efflux transporters affecting the ADME properties of drug candidates are of special interest in the present context. For the absorption part, it is relevant to consider the expression of efflux transporters in the intestine. The distribution aspect of efflux transporters is relevant for drugs that are intended to act in the CNS, since efflux mechanisms have been shown to prevent some drugs, such as ivermectin and digoxin, from accessing the brain. In terms of metabolism, efflux transporters in the intestinal epithelia and hepatocytes have been shown to work together with metabolising enzymes such as CYP3A4 and glutathione-S-transferases to decrease intracellular accumulation of various compounds. Efflux transporters are



also relevant in the excretion of drugs from the systemic circulation via intestinal or renal efflux. It is evident from this that efflux transporters must be taken into consideration when dealing with the ADME properties during drug discovery and in pharmaceutical and preclinical development (see Chapter 3.7). In the present chapter we will describe the expression and function of efflux transporters in tissues that are relevant for the biopharmaceutical scientist.

### **3.6.1 ATP-binding cassette (ABC) transport proteins in the intestine**

The ABC drug-transporting proteins, often referred to as efflux transporters, are in general from either the multidrug resistance (MDR) or the multidrug-resistance-associated protein (MRP) type. The transporters are listed in the Table 3.6.1 (Chan *et al.*, 2004), and in the following section the focus will be on the efflux transporters that are most relevant in the drug discovery and preclinical setting.

#### **3.6.1.1 MDR transporters**

The most studied efflux transporter is P-gp (MDR1, ABCB1). P-gp belongs to the MDR/TAP subfamily within the ABC superfamily. In the intestine, the expression of P-gp is confined to the apical membrane of the enterocyte. The expression increases from the crypt to the tip of the villus, and on the segmental level the expression increases from the proximal to the distal part of the small intestine (Chan *et al.*, 2004). The mechanism behind transport via P-gp is highly complex, and not yet well understood. However, P-gp acts by pumping substrate out of the cell or the cell membrane by utilising ATP. The ‘hydrophobic vacuum cleaner’ hypothesis predicts that P-gp pumps substrates either from the outer membrane of the lipid bilayer, or from the inner membrane of the bilayer into the extracellular space (Gottesman and Pastan, 1993). This implicates that P-gp recognises its substrate after the substrate has partitioned into the cell membrane. Substrate may thus enter the cell membrane from either the extracellular or intracellular side.

P-gp has an extremely broad substrate specificity, with a preference for lipophilic and cationic compounds; however, these general structural features are by no means restrictive. This is illustrated by the diversity in the substrates identified for P-gp, including anti-cancer drug substances such as vinblastine, doxorubicin, etoposide and paclitaxel, cardiac drug

**Table 3.6.1** Efflux transporters that are relevant in biopharmaceutics and drug disposition

<i>Transporter</i>	<i>Gene</i>	<i>Location</i>	<i>Expression</i>	<i>Substrate</i>
MDR1/P-gp	<i>ABCB1</i>	Apical	Intestine, liver, kidney, blood–brain barrier	Anti-cancer drugs, cardiac drugs, endogenous compounds, HIV drugs, fluoroquinolones, immunosuppressive drugs (Chan <i>et al.</i> , 2004)
MDR3	<i>ABCB4</i>	Apical	Liver	Phospholipids, digoxin, paclitaxel, vinblastine
BSEP	<i>ABCB11</i>	Apical	Liver	Bile acids
MRP1	<i>ABCC1</i>	Basolateral	Intestine, brain, kidney, lung, liver	Glutathione and glutathione conjugates
MRP2	<i>ABCC2</i>	Apical	Intestine, liver, kidney	Glutathione and glutathione conjugates as well as non-conjugated anionic molecules
MRP3	<i>ABCC3</i>	Basolateral	Intestine, liver, kidney	Bile acids, drugs
MRP4	<i>ABCC4</i>	Apical	Intestine, kidney, brain, liver	Bile acids, drugs
MRP5	<i>ABCC5</i>	Basolateral	Colon, liver, kidney, brain	Glutathione, adefovir, 6-mercaptopurine
MRP6	<i>ABCC6</i>	Basolateral	Kidney, liver	Some anti-cancer drugs, BQ123
MRP7	<i>ABCC10</i>			
MRP8	<i>ABCC11</i>			
MRP9	<i>ABCC12</i>			
BCRP	<i>ABCG2</i>	Apical	Intestine, liver	

*Notes:* For further detail consult a current review (suggested references: Seelig and Gerebtzoff, 2006; Gottesman and Ling, 2006; Huang and Sadec, 2006; Kerb, 2006; Teodori *et al.*, 2006; Varma *et al.*, 2006).

substances such as digoxin and some  $\beta$ -blockers, endogenous compounds such as steroid hormones and bile salts, HIV drug substances such as indinavir and saquinavir, fluoroquinolones such as sparfloxacin, and immunosuppressive drug substances such as ciclosporin A and tacrolimus (Chan *et al.*, 2004). In general, P-gp substrates are thus amphipathic compounds with a molecular weight ranging from approximately 300 to 2000 Da. It has been suggested that P-gp binds substrates through an 'induced-fit mechanism', where the shape and size of the substrate changes the packing of the transmembrane segments in order to accommodate the substrate (Loo and Clarke, 1999; Loo *et al.*, 2003).

Thus, in addition to the function of P-gp in regulating absorption of several compounds, a further dimension is added, giving evidence for the notion that P-gp functions in conjunction with metabolising enzymes. P-gp may thus play a dual role in limiting the oral bioavailabilities of drug substrates, i.e. by reducing their absorption and by delivering them to metabolic enzymes. In the liver and intestine the P-gp function is present in metabolically active cells. Phase I enzymes such as CYP P450s and phase II enzymes such as glutathione-S-transferases are key factors in limiting drug bioavailability. There is also some degree of overlapping substrate specificity between CYP3A4 and P-gp (Wacher *et al.*, 1995, 1998; Benet *et al.*, 1999). It is therefore important to consider both the efflux properties and the metabolic properties of drug candidates. This is shown in Figure 3.6.1, where the action of both P-gp and metabolising enzymes is illustrated.

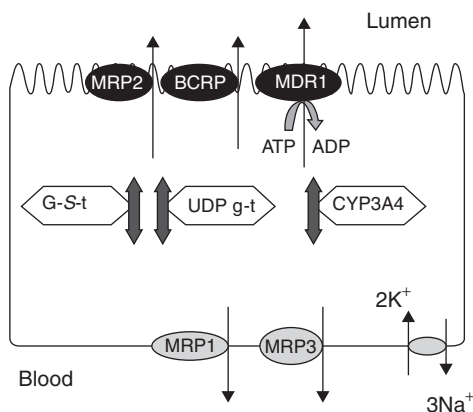


**Figure 3.6.1** Principal efflux transporters and intracellular enzymes in the intestinal epithelium. MDR1, the multidrug-resistance protein alias P-gp; G-S-t, glutathione-S-transferase; UDP g-t, UDP glucuronosyl transferase; MRPs, multidrug-resistance-associated transport proteins; BCRP, breast cancer resistance protein.

### 3.6.1.2 MRP transporters

The MRP transporters are active transporters belonging to the MRP/CFTR subfamily within the ABC superfamily.

MRP1 expression is widespread within the body. MRP1 is expressed in the basolateral membrane of polarised epithelial cells, and in the intestine, brain, kidney, lung and liver. MRP1 exports conjugated metabolites such as glutathione- and glucuronide-containing compounds from the cell. Furthermore, MRP1 and P-gp have overlapping substrate affinities. Examples are vincristine, paclitaxel and etoposide.

MRP 2 is expressed in the apical membrane of polarised epithelial cells of the intestine and kidney as well as in the liver. The expression increases from the crypt to the tip of the villus, and on the segmental level the transporter expression decreases from the proximal to the distal part of the small intestine (Chan *et al.*, 2004). The substrates are both conjugated and unconjugated anionic compounds such as glucuronides and glutathiones, as well as anti-cancer compounds such as vincristine and doxorubicin. There exist overlapping expression patterns with metabolising enzymes such as glutathione-S-transferases, which are phase II metabolising enzymes that catalyse the conjugation of a compound with glutathione. Furthermore, UDP-glucuronosyltransferases are membrane-bound phase II metabolising enzymes that are relevant in detoxification and subsequent metabolism and elimination of drug compounds. This is illustrated in Figure 3.6.1.

MRP3 is expressed in the basolateral membrane of polarised epithelial cells of the intestine and kidney. It is also expressed in the liver, kidney and lung. The expression increases from the crypt to the tip of the villus, and on the segmental level the transporter expression increases from the proximal to the distal part of the small intestine (Chan *et al.*, 2004). The substrates are conjugated compounds and bile acids. MRP3 transports some of the same substrates as recognised by MRP2 and the bile salt export pump (BSEP).

### 3.6.1.3 BCRP transporter

BCRP, breast cancer-resistance protein (ABCG2), belongs to the White subfamily (Chan *et al.*, 2004). BCRP is expressed in the intestine and liver. In the small intestine and the colon, it is expressed in the apical membrane, and in the liver it is expressed in the hepatocyte canalicular membrane (see Figures 3.6.1 and 3.6.2). BCRP has overlapping substrate

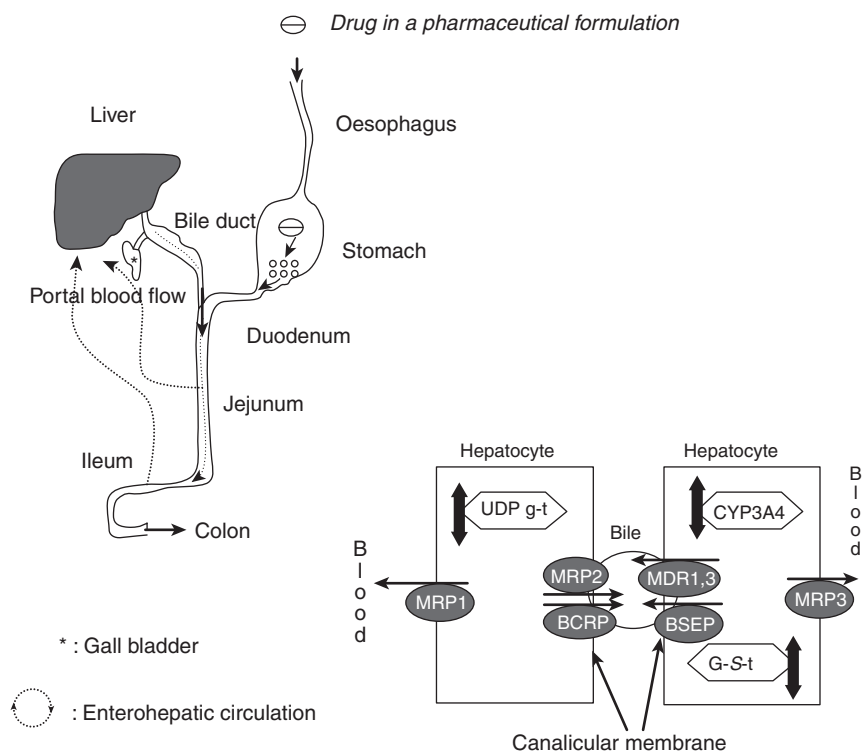


**Figure 3.6.2** Principal efflux transporters and intracellular enzymes in the liver. MDR1, multidrug-resistance protein alias P-gp; G-S-t, glutathione-S-transferase; UDP g-t, UDP glucuronosyl transferase; MRPs, multidrug-resistance-associated transport proteins.

specificity with P-gp, and it is therefore likely that it plays a similar role to P-gp in influencing drug absorption and disposition.

### 3.6.2 Efflux transporters in the liver

In Figure 3.6.2 the intake of a solid pharmaceutical formulation is illustrated. After ingestion, the drug formulation starts to disintegrate in the stomach and dissolution of the drug substance is initiated. After emptying of the stomach into the intestine, the solute drug substance is possibly absorbed across the intestinal epithelium. At the intestinal barrier, efflux transporters may – as illustrated in Figure 3.6.1 – limit the absorption of drug substrates and/or, after absorption, take part in its elimination. The

absorbed drug substance is circulated via the portal blood flow to the liver. The liver is a major metabolising and detoxifying organ. Here efflux transporters play a major role, together with metabolising enzymes, in the overall pharmacokinetics of the absorbed drug substrate(s). The intact drug substrate or its metabolites may pass into the bile, which is subsequently emptied into the duodenum. The formation of bile is a critical function of the liver, since it is the route for excretion of bilirubin, hormones, cholesterol and xenobiotics such as drugs. The drug or its metabolites may then either be excreted into the faeces or be available for a new absorption cycle. In the liver, some of the above-mentioned transporters are expressed. In the following section other efflux transporters in the liver are described.

### **3.6.2.1 The bile salt export pump (BSEP)**

In the canalicular membrane of human hepatocytes, the bile salt efflux pump, BSEP (ABCB11) causes a vectorial transport of bile salts from the blood to the bile. The BSEP is almost exclusively expressed in the liver. It belongs to the subfamily B (MDR/TAP). BSEP substrates include glycocholate, taurochenodeoxycholate, and tauroursodeoxycholate. In addition to bile salts, the transporter is also able to transport certain anti-cancer compounds such as vinblastine and taxol. Mutations in BSEP are the causes of some hereditary and acquired cholestatic disorders.

### **3.6.2.2 MDR transporters**

In the liver, another MDR transporter is expressed. MDR3 (ABCB4) is a canalicular phospholipid translocator. Besides transporting phospholipids, MDR3 may transport compounds such as digoxin, vinblastine and paclitaxel. The impact of this transporter in drug disposition and overall pharmacokinetics of lipophilic drug substances is not yet well investigated.

### **3.6.3 Efflux transporters in the kidney**

The kidney is the principal organ for elimination of a number of xenobiotics and metabolic waste products but, as discussed in Chapter 3.5, several re-absorption processes also take place rescuing nutrients from renal elimination. In the kidney, plasma is filtered through the glomerular capillaries into the renal tubules. This is known as glomerular filtration.

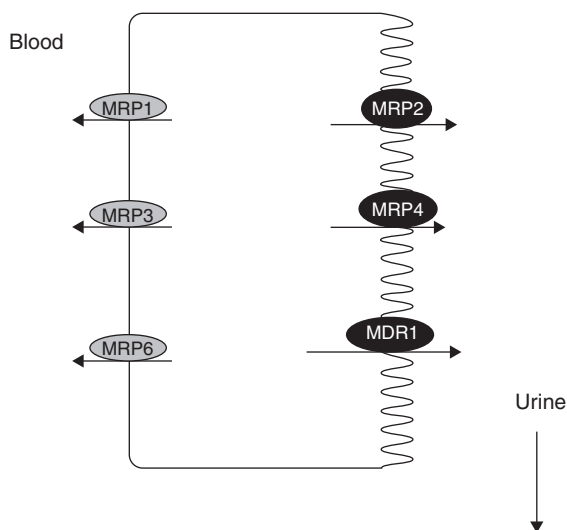


**Figure 3.6.3** Principal efflux transporters in the renal epithelium. MDR1, multi-drug-resistance protein alias P-gp; MRPs, multidrug resistance-associated transport proteins.

The filtrate passes down the tubules, where nutrients, salts and most of the water are reabsorbed. This increases the circulation time of drug substances or nutrients, which are substrates for absorptive transporters, and for a drug substance this may increase the overall bioavailability by reducing elimination. At the same time efflux transporters mediate the excretion of either intact drugs or their metabolites into the urine. This is illustrated in Figure 3.6.3 for efflux transporters present in the kidney. The expression of both influx and efflux transporters may give rise to various drug–drug interactions in treatments with multiple-drug regimens. The likelihood of drug–drug interactions depends on a variety of factors such as the transport capacity of the transporters, the relative binding of the substrate, the presence of inhibiting drugs, and expression patterns of the relevant transporters, as well as individual genotypes.

### 3.6.3.1 MRP transporters

The multidrug-resistance-associated transport protein MRP4 (ABCC4) is present in the renal epithelium. MRP4 is furthermore expressed in the intestine and at the blood–brain barrier. The transport protein is expressed at the apical membrane of the renal proximal tubules as illustrated in Figure 3.6.3. MRP4 substrates include methotrexate,

glucuronides and bile acids. MRP6 (ABCC6) is highly expressed in the basolateral membrane of the renal epithelium. MRP6 substrates include anti-cancer drugs such as etoposide, doxorubicin and cisplatin; the substrates are thus quite similar to those of MRP3.

### 3.6.4 Efflux transporters in the brain

For the majority of the previous chapter and the present one, the focus has been on transporters that are present in epithelial tissues. In this section we will look at the presence of efflux transporters in endothelial cells. Endothelial cells form the capillaries of the blood circulation system. The capillaries differ significantly between the periphery and central system as illustrated in Figure 3.6.4. In the periphery the capillaries are fenestrated, which means that the diffusion barrier between the individual cells is very low. In the brain, however, the capillaries form tight junctions, which means that the paracellular diffusion barrier is very high (with the exception of the capillaries in the choroid plexus). This implies that there will be little or no transport of hydrophilic compounds

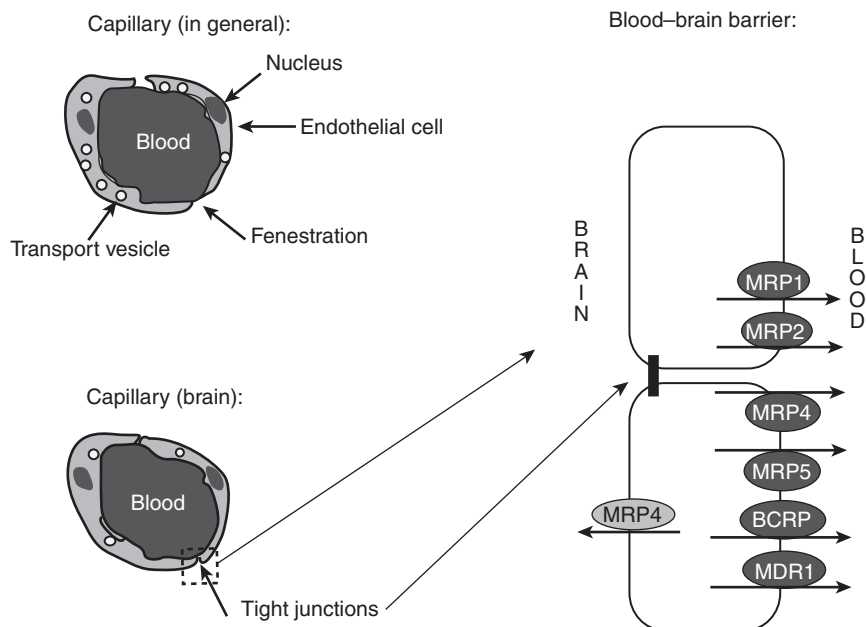


**Figure 3.6.4** Principal efflux transporters in the blood–brain barrier. MDR1, multidrug-resistance protein alias P-gp; MRPs, multidrug-resistance-associated transport proteins; BCRP, breast cancer-resistance protein.



across the barrier. As in all transporting epithelia, the cells therefore have an asymmetric distribution of transport proteins, which gives rise to a polarised transport. As illustrated in Figure 3.6.4, endothelial cell efflux transporters are present both in the membrane facing the blood side and in the membrane facing the brain side. The consequence of the tight junction is that drugs intended to work in the CNS must permeate the endothelial cell via the transcellular route, and this will favour lipophilic compounds. However, these types of compounds may be substrates for efflux transporters, thus rendering transepithelial transport low or absent. Furthermore, intracellular metabolism followed by cellular efflux will maintain a low accessibility to the cells of the brain.

### 3.6.5 Conclusions

In this chapter, the efflux transporters expressed in the intestine, kidney, liver and brain have been described. It is important to remember that the chapter is an overview with respect to the currently available literature. For expert knowledge regarding specific transporters, overlapping substrate specificity between metabolising enzymes and transporters, genetic polymorphisms of transporters, drug–drug interactions etc, readers are encouraged to consult the current available literature, as the field is developing rapidly. The presence of efflux transporters is a natural part of the body's defence against xenobiotics. In the drug discovery and preclinical development processes, transporters are highly relevant to consider, in order to get new drugs through registration. Thus the US FDA has published guidelines for evaluation of drug–drug interactions with focus on transporters and metabolising enzymes (FDA, 2006). The following Chapter 3.7 'Preclinical evaluation of drug transport' will describe examples of how knowledge regarding transporters' influence on *in vitro* ADME properties of drug candidates may influence the preclinical process.

### References

- Benet LZ, Izumi T, Zhang Y, Silverman JA, Wachter VJ (1999). Intestinal MDR transport proteins and P-450 enzymes as barriers to oral drug delivery. *J Control Release* 62: 25–31.
- Chan LM, Lowes S, Hirst BH (2004). The ABCs of drug transport in intestine and liver: efflux proteins limiting drug absorption and bioavailability. *Eur J Pharm Sci* 21: 25–51.

- FDA (2006). *Drug Development and Drug Interactions*. <http://www.fda.gov/Drugs/DevelopmentApprovalProcess/DevelopmentResources/Labeling/DrugInteractionsLabeling/ucm080499.htm> (accessed 3 June 2009).
- Gottesman MM, Ling V (2006). The molecular basis of multidrug resistance in cancer: the early years of P-glycoprotein research. *FEBS Lett* 580: 998–1009.
- Gottesman MM, Pastan I (1993). Biochemistry of multidrug resistance mediated by the multidrug transporter. *Annu Rev Biochem* 62: 385–427.
- Huang Y, Sadee W (2006). Membrane transporters and channels in chemoresistance and -sensitivity of tumor cells. *Cancer Lett* 239: 168–182.
- Juliano RL, Ling V (1976). A surface glycoprotein modulating drug permeability in Chinese hamster ovary cell mutants. *Biochim Biophys Acta* 455: 152–162.
- Kerb R (2006). Implications of genetic polymorphisms in drug transporters for pharmacotherapy. *Cancer Lett* 234: 4–33.
- Loo TW, Clarke DM (1999). The transmembrane domains of the human multidrug resistance P-glycoprotein are sufficient to mediate drug binding and trafficking to the cell surface. *J Biol Chem* 274: 24759–24765.
- Loo TW, Bartlett MC, Clarke DM (2003). Substrate-induced conformational changes in the transmembrane segments of human P-glycoprotein. Direct evidence for the substrate-induced fit mechanism for drug binding. *J Biol Chem* 278: 13603–13606.
- Seelig A, Gerebtzoff G (2006). Enhancement of drug absorption by noncharged detergents through membrane and P-glycoprotein binding. *Expert Opin Drug Metab Toxicol* 2: 733–752.
- Teodori E, Dei S, Martelli C, Scapecchi S, Gualtieri F (2006). The functions and structure of ABC transporters: implications for the design of new inhibitors of Pgp and MRP1 to control multidrug resistance (MDR). *Curr Drug Targets* 7: 893–909.
- Varma MV, Perumal OP, Panchagnula R (2006). Functional role of P-glycoprotein in limiting peroral drug absorption: optimizing drug delivery. *Curr Opin Chem Biol* 10: 367–373.
- Wacher VJ, Wu CY, Benet LZ (1995). Overlapping substrate specificities and tissue distribution of cytochrome P450 3A and P-glycoprotein: implications for drug delivery and activity in cancer chemotherapy. *Mol Carcinog* 113: 29–134.
- Wacher VJ, Silverman JA, Zhang Y, Benet L (1998). Z. Role of P-glycoprotein and cytochrome P450 3A in limiting oral absorption of peptides and peptidomimetics. *J Pharm Sci* 87: 1322–1330.



# 3.7

## Preclinical evaluation of drug transport

*Anna-Lena Ungell*

Transport of drugs across biological membranes is characterised by the membrane permeability. This characteristic of membranes is an important factor for the disposition of drugs because of the control it exerts over both the bioavailability and transport into and out of tissues and organs of the body such as the intestine, liver, kidney and central nervous system (CNS). Membrane permeability as well as other biological parameters (e.g. potency, metabolism and solubility in biological media) of a drug molecule can change dramatically with the molecular structure. All these biological properties essentially follow different rules of the quantitative structure–property relationship (QSPR). Parts of the molecule may be changed to optimise each single property separately, but in most cases the biological properties may be connected with the same region of the molecule, and thus optimisation of one property may dramatically attenuate the others. Therefore, screening of compounds using multiple techniques in parallel has become the rationale during preclinical evaluation of drugs.

Drug transport is a multifactorial process determined by several rate-limiting steps, i.e. the events and processes occurring before and during the transport across the membrane. Conceptually, one may divide all the factors influencing the potential for a drug to be transported into three proposed groups (Ungell, 2005). First are those factors associated with the chemical structure and physicochemical properties of the drug molecule, such as water solubility, lipophilicity ( $\log D$ ,  $\log P$ ), acid/base properties ( $pK_a$ ), and molecular weight/volume. Second are factors within the biological system – the intestinal lumen, plasma or intraluminal milieu – e.g. pH, ion composition, bile acids and soluble enzymes. The third group consists of factors that represent the anatomy and physiology of the membrane, e.g. surface area, transit times, blood flow, enzymes and transporters (Ungell, 1997, 2005; Ungell and Abrahamsson, 1997). In addition to this complexity of drug transport, there are also differences in

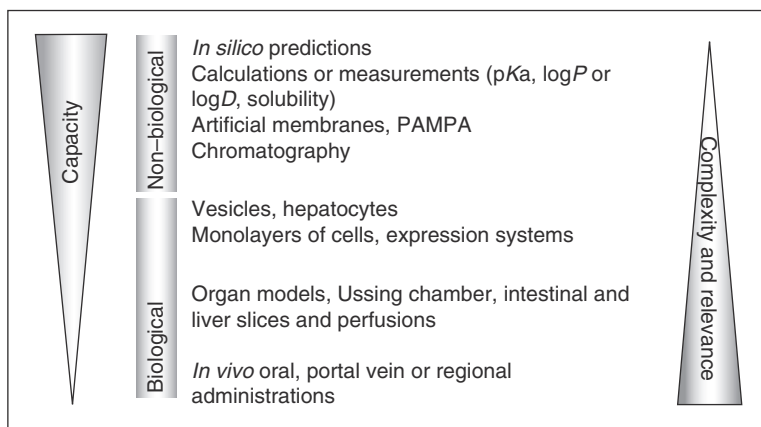


**Figure 3.7.1** Schematic drawing illustrating an overview of models for the determination of drug transport in relation to complexity and relevance *in vivo* in humans. PAMPA, parallel intraluminal membrane permeability approach.

*in vitro* and *in vivo* methodologies, since an *in vitro* system is a static system with well-defined conditions and may very well lack the proper milieu, dynamics and changes that can occur *in vivo*. This may be one explanation why *in vitro*–*in vivo* correlations might fail.

*In vivo* animal kinetic studies can provide a good basis for prediction of drug transport kinetics in humans. However, *in vivo* kinetic studies will be too complex to guide the chemist to change a specific property of the molecule, and the capacity is low. On the other hand, no single *in vitro* method may provide all the important information needed around key factors influencing drug transport for the huge diversity of drug molecules to be tested during the preclinical phases. Therefore, the majority of preclinical methods are flexible *in vitro* techniques offering solutions to different problems at different preclinical stages, and also permitting rapid feedback to medicinal chemists. In addition, due to the small amount of compound synthesised during early drug discovery, *in vitro* techniques offer a special advantage over *in vivo* ones (see Figure 3.7.1).

### 3.7.1 Mechanisms of drug transport across membranes

Drugs permeate cellular membranes not only by passive diffusion, but also by multiple and parallel processes (see Figure 3.7.2). In the gastrointestinal (GI) tract, passive diffusion can occur transcellularly

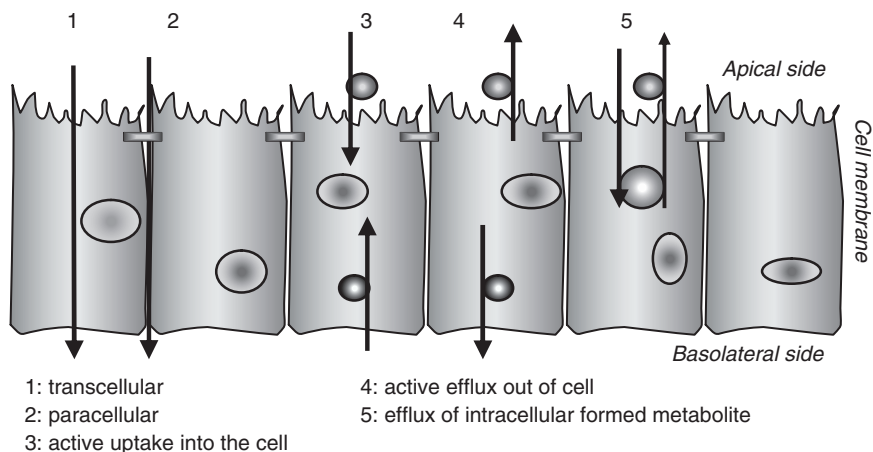


**Figure 3.7.2** Mechanisms of drug transport across an epithelial membrane.

across the lipid membrane or paracellularly between the epithelial cells through water-filled pores in the tight junctional complex. Usually, lipophilic drugs permeate more easily by a transcellular route and small polar and ionisable solutes are restricted to the paracellular route. The transcellular route can also be transversed via carrier-mediated processes for drugs that are substrates for transporter proteins, favouring uptake into or efflux out of the epithelial cell (Tsuji and Tamai, 1996; Hunter and Hirst, 1997). In other organs, e.g. the liver and kidneys, transporters are thought to regulate intracellular concentrations of drug compounds and thus may influence both intracellular metabolism and toxicity. In these organs, drug clearance (CL) can be a mixture of both enzymatic reactions and transporter interaction (Hunter and Hirst, 1997). The relative contributions of active and passive transport across membranes are variable between compounds, species and methods, as well as being influenced by the concentration and ion gradient applied (Ungell and Karlsson, 2003). For example, at low concentrations within the intestinal lumen, i.e. for low-solubility drugs with very high potencies, the involvement of efflux transport processes has a greater impact on the effective transport than it does for highly soluble compounds administered at high doses. In addition, in the systemic circulation, compounds may be protein bound and the fraction that is unbound might be small. This will reduce the effective concentration at the transporter protein. Similarly, a compound given at high doses can saturate processes at the intestinal level, but in the systemic circulation and at other tissue barriers, the concentration might be low and the risk for drug-transporter interactions increases.

The models used for the preclinical evaluation of compounds are often focused on investigating specific processes that are important for drug transport (see Figures 3.7.1 and 3.7.2). This is because the processes the methods describe are quite different, since molecular properties resulting in transport via carrier proteins are completely different from those favouring simple passive diffusion (see Figure 3.7.2) (Ungell, 2004). Firstly, passive transcellular diffusion is often guided by partitioning into and out of a lipid bilayer membrane characterised by well-known properties such as lipophilicity, polar surface area (PSA) etc. (Artursson *et al.*, 2001; Lipinski *et al.*, 2001; Stenberg *et al.*, 2001; Van de Waterbeemd *et al.*, 2001; Egan and Lauri, 2002; see also Section 2.1.1).

Secondly, the aqueous pathway of the paracellular route is dependent on molecular weight/volume, flexibility (number of rotatable bonds) and charge (Artursson *et al.*, 1993; Veber *et al.*, 2002). This pathway is considered less in the screening since most compounds are lipophilic and of higher molecular weight. However, the literature describes this pathway as being undervalued since it can contribute to the absorption of small ionised molecules (Matsson *et al.*, 2005). Thirdly, structural requirements for carrier-mediated processes depend on binding of the compound to the carrier (affinity) and translocation; thus they are driven by both the size and structure of the transported molecule (Vig *et al.*, 2006) (see Section 3.3.2.5.1). Thus, using only passive transcellular estimates (e.g.  $\log D$ ) will not predict net permeability correctly if transporters are involved.

In view of this, it is important to understand the different factors influencing drug transport and potential transporter interaction when interpreting *in vitro* and *in vivo* data. Thus, the method to be used should be selected on the basis of the mechanisms of transport to be studied (Figures 3.7.1 and 3.7.2).

### 3.7.2 Tools to assess drug transport during phases of drug discovery

The preclinical phase of drug discovery is divided into different phases, from target identification (TI), through lead generation (LG) and lead optimisation (LO) to the selection of a candidate drug suitable for development (see Figure 3.7.3). These phases are named differently among industries and can generally be divided into early discovery phase and late discovery phase. Early discovery starts after the high-throughput screening (HTS) of large combinatorial libraries on a specific target, through generation of potential lead series of new entities, and ends by

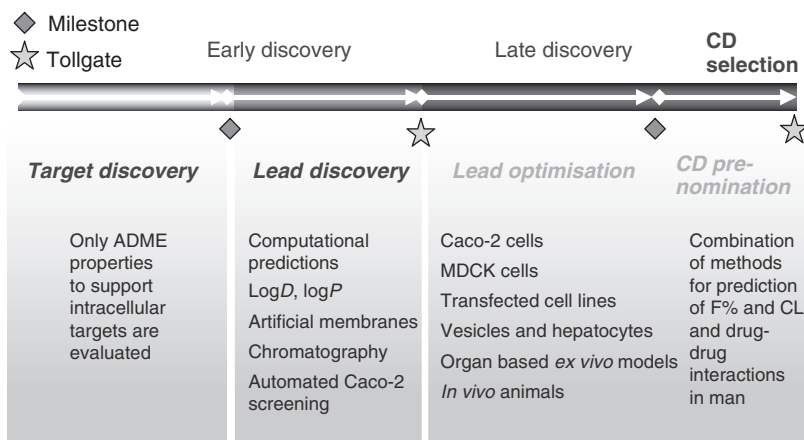


**Figure 3.7.3** Schematic drawing of the main drug discovery phases. From target identification (TI), via lead generation (LG) towards lead optimisation (LO) and pre-candidate selection (pre CD) and candidate drug selection (CD). After the CD selection, the development phase starts and the clinical testing in humans proceeds. MDCK, Madin–Derby canine kidney cells.

delivering series of compounds into the late discovery phase where the optimisation of a few series occurs. The late discovery phase ends with the selection of precandidates that are usually submitted to short toxicological programmes before a drug can be selected as a candidate.

Generally, in the early discovery, ADME properties with problems are identified and series of compounds are designed to build a structure–activity relationship (SAR). In the late discovery phase these problems are solved by stepwise optimisation of the different properties. A short description of some *in vitro* tools used in the different preclinical phases to optimise drug entities with respect to drug transport is given next. A summary of the tools is presented at the end of each section and in Figure 3.7.3.

### 3.7.2.1 Early discovery phase

The ideal *in vitro* technique for evaluation of drug transport at this stage needs to expedite a wide spectrum of molecules in order to range large and diverse data sets for ADME property information. Simple techniques addressing solubility, passive transcellular diffusion across a membrane, and metabolic stability, using rat or human liver microsomes, are commonly used in parallel with computational and physicochemical or pre-formulation approaches such as lipophilicity, logD or logP and aqueous solubility measurements (see also Part 2).



Nowadays, computer-based prediction models are valuable tools to estimate permeability properties of molecules with unfavourable biopharmaceutical properties, and require no synthesis as well as being almost unlimited in capacity (Ungell, 2004). First, a compound set is selected that is appropriate for the model to be built (active or passive processes). The next step is to both obtain experimental data and select the appropriate molecular descriptors. Multiple molecular properties of different complexity can be generated via computation using commercially available programs, for example, GRID ([www.moldiscovery.com](http://www.moldiscovery.com)), HYBOT ([www.timtec.net/software/hybot-plus.htm](http://www.timtec.net/software/hybot-plus.htm)), VolSurF ([www.moldiscovery.com](http://www.moldiscovery.com)), Molconn-Z ([www.tripos.com](http://www.tripos.com)), Cerius2 ([www.accelrys.com/](http://www.accelrys.com/)) (Ungell, 2004). The interrelationship between the most important generated descriptors is then mathematically described in a series of equations to obtain a calculated estimate of the apparent permeability coefficient,  $P_{app}$ , by, for example, the use of statistical multivariate analysis, such as principal component analysis (PCA) and partial least square (PLS) (Simca Umetrics AB; [www.umetrics.com](http://www.umetrics.com)).

Correlation between calculated and experimentally observed permeability values is then performed to obtain the final QSPR model. The last part of the building is the validation of the model. An external test set of compounds can provide an insight into how good the model is and ensure proper evaluation of predictions. Multiple *in silico* permeability models of varying complexity and success have been presented in the literature and many predict Caco-2 (human colon carcinoma cells) permeability or interaction with a certain transporter (Artursson *et al.*, 1996; Stenberg *et al.*, 2001; Ungell, 2004; Vig *et al.*, 2006). It should be mentioned that models generated from Caco-2 data can only be used for drug permeability in the intestine and do not generally predict permeability or disposition in all other tissues of the body, since tissues contain differences in expression of transporters and lipid composition of the membranes.

Experimental physicochemical measurements are often performed at this early stage of drug discovery. Capillary electrophoresis and chromatographic measurements using columns with different packing materials (immobilised phospholipids onto a silica surface (IAMS), liposomes and reversed phase C18, as well as measurement of  $\log P$  and  $\log D$  (Hartmann and Schmitt, 2004) are well-suited high-throughput methods for early predictions of permeability or lipophilicity ( $k'$ ) (Camenisch *et al.*, 1997; Hartmann and Schmitt, 2004; Örnkov *et al.*, 2005). Recently, artificial membranes (parallel intraluminal permeability approach, PAMPA) made of mixtures of lecithin or membrane phospholipids and inert organic solvents on a permeable support have also been developed to describe the

transcellular passive membrane permeation process (Camenisch *et al.*, 1997; Kansy *et al.*, 1998, 2004; Ottiger and Wunderli-Allenspach, 1999). However, using passive transcellular permeability as a single tool for optimising compounds can under- or over-predict permeability for compounds that are mainly restricted to either paracellular or carrier-mediated transport, respectively (Ungell, 2004). Thus, if the methods are used without knowledge of drug transport mechanisms, data can provide misleading information for prediction of drug transport in humans.

Evaluation of drug transport can also be made in this early phase using biological tools such as automated cell monolayer permeability methods, e.g. Caco-2 cells (see below), with high throughput, and both absorptive and secretory transport may be studied if needed. In most cases, at this stage of drug discovery, ranking compounds or series of compounds into levels or banding of permeability (low/moderate/high) (Ungell and Karlsson, 2003) may be enough to fill the purpose. The Caco-2 data can be used for validation of the physicochemical or computational predictions or for a 'quick and dirty' indication of carrier-mediated transport. For instance, if the passive permeability indicates a highly permeable compound, but the Caco-2 cell data show a low level of permeability, efflux transporters might be involved, attenuating drug transport. However, the exact identity of which transporter is involved is usually of no concern at this stage.

#### 3.7.2.1.1 *Summary of models used in the early discovery phase*

- Computation of surface descriptors for permeability; building of QSPR models, and computation of physicochemical properties
- Physicochemical properties, experimentally, e.g.  $\log D$  using chromatography or PAMPA
- Automated Caco-2 cell screening in recommended pH gradient of 6.5/7.4, one or few time points
- Bidirectional Caco-2 permeability for transporter involvement.

#### 3.7.2.2 **Late discovery phase**

In this stage of drug discovery, in-depth mechanistic evaluation of drug transport is performed to optimise compound structures in order to avoid poor permeability properties or drug–drug interactions in the clinic. Information from the models is used to solve problems by a stepwise optimisation of the molecules. Numerous techniques such as cell cultures,

membrane vesicles, hepatocytes, transfected cells, intestinal slices or sacs, Ussing chamber technique, *in vitro* and *in situ* intestinal and liver perfusions, *in vivo* cannulated animals, and *in vivo* gavaged animals (see Figure 3.7.1; Borchardt, 1996; Barthe *et al.*, 1999; Irvine *et al.*, 1999; Balimane *et al.*, 2000; Salphati *et al.*, 2001; Ungell, 2002, 2005; Miret *et al.*, 2004; Balimane and Chong, 2005; Li, 2005; Sahi, 2005) can be used in parallel to complement physicochemical knowledge and obtain a better understanding of drug transport during preclinical screening. A short description of some models used follows next.

### 3.7.3 Cell cultures

Caco-2 cells serve as an easy screen of drug permeation and for prediction of human intestinal permeability and fraction of the oral dose absorbed ( $f_a$ ) in man (Ungell and Karlsson, 2003; Ungell, 2004). The cells are easy to culture and show good experimental reproducibility and robustness, and much is described in the literature about their performance. The heterogeneous properties of the Caco-2 cells may be one explanation for the differences in morphology, paracellular permeability and expression of enzymes and transporters that have been reported from different research groups (Chong *et al.*, 1996; Chen *et al.*, 2002; Ungell, 2003). The culturing conditions, e.g. the age of the cells and the passaging process as well as nutritional conditions, can dramatically alter the biological characteristics and transport properties of the Caco-2 cell monolayers (Anderlé *et al.*, 1998; Li *et al.*, 2003; Ungell, 2003; Seithel *et al.*, 2006). The cell culture protocol therefore has to be standardised for screening, and experiments should only be performed within a limited and well-defined number of passages (Ungell and Karlsson, 2003; Seithel *et al.*, 2006). Since the cells are of colonic origin, their predictability to  $f_a$  has been debated (Balimane and Chong, 2005), and active transport of some compounds in these cells shows weak predictability for humans (Chong *et al.*, 1996; Lennernas *et al.*, 1996; Salphati *et al.*, 2001).

Experiments using the Caco-2 model and also other cell culture models are easy to perform. After seeding on microporous filters for a specified number of days (normally 14–21), the cultivation media is exchanged to transport buffer solution. Thereafter, the substance is added on one side, either apically or basolaterally, and samples are withdrawn from the opposite side at predefined time points. All experiments should be performed under stirring conditions and at 37 °C. Permeability of the cell monolayer ( $P_{app}$ ; apparent permeability coefficient,  $\text{cm s}^{-1}$ ) is calculated from the determination of the amount of drug transported to the

receiver side at the different time points and is also related to both the surface area of the monolayers and the donor concentration (Ungell and Karlsson, 2003).

A set of carefully selected compounds, based on available clinical  $f_a$  and Caco-2 permeability data forms the basic prediction curve (Artursson *et al.*, 2001; Ungell and Karlsson, 2003; Artursson and Tavelin, 2003) used for settings of levels of absorption or a ranking between compounds, and for classification of permeability according to a Biopharmaceutics Classification System (BCS) (see Section 3.7.8 and Chapter 4.2). An example of such levels can be obtained in the literature (Ungell and Karlsson, 2003).

It should be noted that the Caco-2 cells are not passive membranes. A multiplicity of uptake and efflux transporters contributing to enhancing or attenuating transport of compounds, as well as enzymes, have been identified in these cells (Ungell, 2004).

The MDCK cell line is also frequently used by several pharmaceutical industries to measure intestinal drug transport despite its origin from dog kidney (Horio *et al.*, 1989; Irvine *et al.*, 1999; Artursson and Tavelin, 2003; Balimane and Chong, 2005), and the cells are generally thought to serve more as a passive membrane model than Caco-2 cells do (Ungell, 2004). MDCK cells have also replaced Caco-2 in many research organisations because the cell cultivation is only 3–7 days compared with 14–21 days for Caco-2 cells (Irvine *et al.*, 1999; Ungell, 2004). However, even though a good correlation between MDCK and Caco-2 cells has been obtained for many compounds (Irvine *et al.*, 1999), and studies indicate their usefulness, MDCK cells are not of human origin. Thus, the MDCK monolayers may be sufficient for estimating passive epithelial transport, but not for mechanistic studies or for predicting active uptake or efflux across the intestinal epithelium, since the influence of background expression or dog transporters may obscure data (Goh *et al.*, 2002).

Stably transfected cell lines are used nowadays to screen for transporter-mediated permeability, i.e. as either specific uptake, efflux or inhibitory effect on permeability (see also Chapters 3.3, 3.4, 3.5 and 3.6). MDCK-MDR1 is one of the stable transfected cell lines that are frequently used as a tool for investigating the influence of human P-glycoprotein (P-gp) on transepithelial transport (Horio *et al.*, 1989; Keogh and Kunta, 2002; for assay see later).

Other cell lines forming monolayers, such as the human colon goblet cell line HT-29 (and subclones), Caco-2 cell subclone TC7, the rat small intestinal cell line IEC-18, microvillus-expressing human colon carcinoma cells LS180, and the rat duodenal cell line 2/4/A1, have all been developed to investigate mainly intestinal drug transport (Artursson

and Tavelin, 2003; Ungell and Karlsson, 2003; Brandon *et al.*, 2006). Most of these other cell lines can provide data for mechanistic information, but are too demanding of resources and sensitive to cell culture variables to be used routinely in drug screening in the industry. Cell lines for hepatic drug uptake and metabolism have also been developed to serve as a tool for biotransformation studies in conjunction with drug transport, e.g. HepG2 and IGROV-1 cells (Brandon *et al.*, 2006).

#### 3.7.3.0.1 Summary of cell culture-based models in late discovery

- Caco-2 cells for overall net transport in the intestine
- MDCK wild-type for passive permeability with low involvement of transporters
- Transfected cells for transporter-mediated permeation in all organs
- Other cell lines for identifying different transport routes, transporter involved and biotransformation.

#### 3.7.3.1 Organ-based *ex vivo* models for drug transport

Although cell monolayers and transporter-transfected cell lines are offered as rapid tools to determine drug transport, the optimisation of pharmacokinetic properties in the later stages of drug discovery should be related to the transport mechanism(s) during disposition *in vivo*. Several more complex methods such as *in vitro* organ-based or *ex vivo* techniques have therefore been developed, e.g. vesicles, hepatocytes, sandwich cultures, intestinal or liver slices, intestinal sacs, Ussing chamber technique, intestinal or liver perfusions (Olinga *et al.*, 1997, 2001; Akhteruzzaman *et al.*, 1999; Balimane *et al.*, 2000; Salphati *et al.*, 2001; Ungell, 2002; Hoffmaster *et al.*, 2004; Li, 2005; Sahi, 2005; Shitara *et al.*, 2005; Zamek-Glisczynski *et al.*, 2006).

Vesicles can be isolated from both brushborder and basolateral membranes in the kidney tubular epithelial cells, and from intestinal enterocytes. Furthermore, vesicles can be obtained from the sinusoidal and bile canicular membranes in the liver isolated both from humans and preclinical species such as the rat and dog (Sahi, 2005; Shitara *et al.*, 2005; Zamek-Glisczynski *et al.*, 2006). Vesicles are used for an in-depth evaluation of transporter interactions in general without the confounding influence of drug metabolism. Nowadays, vesicles can also be obtained as overexpressed transfected membranes (both mammalian and baculovirus-infected insect cells (sf9) with a specific transporter (www.Solvo.com)). Usually, the uptake of a compound into the vesicles is studied at certain

concentrations and incubation times to obtain kinetic parameters ( $K_m$  and  $V_{max}$ ) or, as in competition experiments, to determine an inhibitory effect on transport of a specific substrate. When efflux via transporters is being studied, ATP is added to the incubation media and transport into the inside-out vesicles can be studied (Sahi, 2005).

One disadvantage of vesicles is the day-to-day variation in vesicle preparation and a leakage of drugs from the vesicles during washing and filtration, which can affect drug accumulation. A relatively high level of expression of transporters in the material is needed to secure low variability in data (Sahi, 2005). In addition, transporter interaction for highly permeable compounds is hard to study due to the high passive (intrinsic) permeability (i.e. background permeability). Despite these drawbacks, vesicles can be used in the late discovery stage for mechanistic studies of drug transport to identify the involvement of a specific transporter (Sahi, 2005; Shitara *et al.*, 2005; Zamek-Gliszcynski *et al.*, 2006).

Isolated and cultured hepatocytes have been used for a long time as an *in vitro* model of the liver (Shitara *et al.*, 2005). Hepatocytes are isolated by liver perfusion of either an animal or human liver, followed by harvesting of live cells in the perfusate (Ishigami *et al.*, 1995; Akhteruzzaman *et al.*, 1999). Several studies indicate that both fresh and cryopreserved hepatocytes retain at least part of their viability and active transport and metabolism, as well as being inducible (Shitara *et al.*, 2005). An effect on transporter expression of using different types of extracellular matrix and dexamethasone during isolation has also been reported (Luttringer *et al.*, 2002). Uptake of compounds into the hepatocytes can be extrapolated to obtain *in vivo* clearance assuming a well-stirred model (Akhteruzzaman *et al.*, 1999). However, since only the uptake of compounds, but not the efflux, can be studied using this method, data for CL predictions are not complete.

Instead of freshly harvested hepatocytes, cryopreserved hepatocytes can be used and these are also available commercially ([www.bdbioscience.com](http://www.bdbioscience.com)). Hepatocytes can also be cultivated to form a multilayer structure called a sandwich culture, offering a better organ-like model for prediction of hepatobiliary disposition than fresh hepatocytes (Hoffmaster *et al.*, 2004). This model is, however, very complex and requires very careful handling and is therefore not used in routine screening in the industry. The models representing the hepatic CL of drugs – hepatocytes, sandwich cultures, liver slices and liver perfusions – have also been proven to generally predict *in vivo* disposition of drugs and to explain drug–drug interactions in humans (Sahi, 2005; Zamek-Gliszcynski *et al.*, 2006). However, care should be taken with

respect to species differences in the capacity and expression of transporters in these models that can affect predictions of actively transported compounds (Zamek-Gliszcynski *et al.*, 2006).

The intestinal sac method is a simple method experimentally, and is based on the preparation of a 2–3-cm-long tube of the intestinal part of interest, which is tied off at the ends after eversion on a glass rod (Barthe *et al.*, 1999; Ungell, 2002). Samples of fluid are taken from the buffer solution in the flask and also from the inner parts of the sac fluid. Several modifications have been made with this method since it was introduced in the 1950s, especially with regard to increasing the viability of the tissue (Barthe *et al.*, 1999). A clear advantage of this method is that in contrast to the Ussing chamber and cell culture models, it needs no specialised equipment and can easily be learned by the experimentalist. Even though this method clearly has a lot of practical advantages, the general usage in an industrial setting is low.

The main part of data presented using tissue slices concerns metabolism, and only a limited number of reports exist dealing with uptake and/or accumulation in slices of liver, kidney and/or intestine (Olinga *et al.*, 1997, 2001; De Kanter *et al.*, 2002; Sahi, 2005; van de Kerkhof *et al.*, 2006). The slice method is based on rapid excision of the tissue and cutting it into thin slices ( $<100\text{ }\mu\text{m}$ ), which are then incubated with the drug solution. A variant of the tissue slice technique, i.e. precision-cut slices, has also been reported in the literature, offering better viability of the tissue slices and, thus, more relevant metabolic activities (Olinga *et al.*, 1997, 2001; De Kanter *et al.*, 2002; van de Kerkhof *et al.*, 2006).

The Ussing chamber technique has been used for drug transport studies using excised intestinal tissues from different animals and humans and different regions of the GI tract (Ungell *et al.*, 1997; Polentarutti *et al.*, 1999; Wu-Pong *et al.*, 1999; Sjöström *et al.*, 2000; Ungell, 2002). The intestinal segments are quickly cut open into planar sheets, which may be stripped of the serosa and the muscle layers and then mounted between two diffusion half-cells (Polentarutti *et al.*, 1999). The integrity and viability of the tissue must be verified simultaneously when using this technique, because it will strongly impair transport of the drug molecules (Polentarutti *et al.*, 1999), and electrical values and markers for integrity have been suggested to ensure good predictive data (Ungell, 2002). Rat intestinal segments in Ussing chambers have been reported to correlate well to permeability coefficients of human jejunum *in vivo* (Ungell, 2002). Correctly used as a mechanistic low-capacity screening tool, data from the Ussing chamber technique

are well suited to predict the human fraction absorbed (Wu-Pong *et al.*, 1999; Sjöström *et al.*, 2000; Ungell, 2002).

Both isolated *ex vivo* intestine and *in situ* intestinal perfusions are known from the literature (Fagerholm *et al.*, 1996; Lindahl *et al.*, 1998; Balimane *et al.*, 2000; Augustijns and Mols, 2004; Sahi, 2005). A small part of the intestine is cannulated at both ends and perfused with a buffer solution at a flow rate of approx  $0.2 \text{ ml min}^{-1}$  (Fagerholm *et al.*, 1996). The blood side can also be cannulated and perfused with a separate perfusion system, or sampling from the blood side can be performed directly from a mesenteric vein. The permeability coefficient is calculated by the difference in concentration between given and collected fluid, and correction for intestinal fluid flow is made using polyethylene glycol (PEG) 4000 as a non-absorbable marker. Intestinal perfusion data from the rat correlate well with human permeability for passively transported compounds (Fagerholm *et al.*, 1996). *In situ* perfusions using anaesthetised animals have also successfully been used for in-depth mechanistic studies of the efflux of drugs (Fagerholm *et al.*, 1996; Lindahl *et al.*, 1998; Augustijns and Mols, 2004).

The liver perfusion setup is similar to the intestinal one (Geng *et al.*, 1995; Ishigami *et al.*, 1995). The animal is anaesthetised and catheters are inserted in the portal vein for inflow and hepatic vein as outflow. The media perfusing the liver are variable in the literature and consist of an oxygenated Krebs–Henseleit solution buffered to pH 7.4 complemented with 20% washed red blood cells (RBCs), 1–4% albumin, and 5–17 mmol/l of D-glucose (Geng *et al.*, 1995). Usually, the liver is perfused in a single-pass fashion without recirculating the solution. The difference in drug concentration between inflow and outflow is used for calculation of drug transport (Geng *et al.*, 1995).

The main disadvantage of all perfusion methods is the use of anaesthesia, which has been reported to affect drug transport (Ungell, 2002). The perfusion methods could have a better position in the industry since they reflect the complexity of organs of the body, but they are too time- and animal-consuming to fulfil the purpose of screening.

#### 3.7.3.1.1 Summary of organ-based and *ex vivo* models

- Vesicles from different membranes and recombinantly expressed transporters in vesicles
- Hepatocytes, primary, fresh and cryopreserved
- Sandwich cultures



- Tissue slices and precision-cut slices
- Ussing chambers
- Intestinal and liver perfusions.

### 3.7.4 Optimising experimental conditions

Care should be taken with respect to suboptimal conditions for studying drug transport using any of the experimental models available. Several factors, such as pH and media compositions, will affect the outcome of data and, thus, influence interpretation especially with respect to intestinal absorption. A pH gradient of 6–6.5 on the apical side and pH 7.4 on the basolateral side has been recommended for intestinal absorption studies to obtain a more *in vivo*-like permeability value (Fallingborg *et al.*, 1989; Yamashita *et al.*, 2000; Neuhoﬀ *et al.*, 2003, 2005a). If the secretion (efflux) of a compound is studied, then a non-pH gradient system should be used to discard false predictions of efflux of weak bases (Neuhoﬀ *et al.*, 2003), and if active uptake is evaluated, e.g. for weak acids or for compounds taken up by proton-dependent mechanisms, then two different pH systems, one without and one with a pH gradient, should be used to obtain maximal information on passive and active drug transport (Neuhoﬀ *et al.*, 2005a). For liver or hepatocyte uptake studies, a non-pH gradient should be used for all studies mimicking drug transport in the systemic circulation (Geng *et al.*, 1995). The measurement of plasma protein binding is important for full interpretation of drug transport *in vivo* (Neuhoﬀ *et al.*, 2005b). It has been recommended to use BSA/HSA (bovine serum albumin/human serum albumin) to increase the sink condition in *in vitro* systems and, thus, mimic the *in vivo* blood sink (Geng *et al.*, 1995; Neuhoﬀ *et al.*, 2005b). Indeed, highly protein-bound compounds will be affected by the addition of protein on the basolateral side, hence, both transport in the absorptive direction metabolism and the efflux of compounds may change (Neuhoﬀ *et al.*, 2005b).

Many compounds being researched today are sparingly soluble. This affects not only the data quality and recovery (mass balance) using *in vitro* methods, but also the *in vitro* and *in vivo* correlation (Yamashita *et al.*, 2000; Krishna *et al.*, 2001; Ungell and Karlsson, 2003). Different *in vitro* models have been used for evaluation of experimental solvents in *in vitro* experiments, and several systems, e.g. surfactants or biorelevant media, have been proposed (Ingels and Augustijns, 2003; Ungell, 2005; Ingels *et al.*, 2006). Solvents used for intestinal studies have been more evaluated than the solvents for hepatic models. General caution should be

taken with respect to the possible effect of solvent systems on intracellular enzymes and on transporter function before using them during screening for drug–drug transport (e.g. inhibition of P-gp; Nerurkar *et al.*, 1996; Bogman *et al.*, 2005).

Due to the increased number of highly lipophilic compounds emerging from early drug discovery and difficulties with adsorption to plastics, a mass balance or recovery calculation has to be performed to ensure good and consistent data quality. An example of such an approach can be found in Ingels *et al.* (2004).

#### 3.7.4.0.1 Summary of optimised conditions

- A pH 6.5/7.4 system is recommended for absorptive studies
- A pH 7.4/7.4 revealing active transport that is not pH dependent
- Combination of the above pH conditions for active drug uptake or secretion which is pH dependent
- Use BSA on the blood plasma side to mimic *in vivo* conditions for highly protein-bound compounds
- Use solvents to increase solubility with care
- Always check for recovery.

### 3.7.5 Screening for transporter interaction

Transporter proteins may potentially mediate drug–drug interactions in the clinic, and are therefore regularly evaluated during drug discovery, e.g. using MDCK-MDR1 and other transfected cell lines, Caco-2 bidirectional transport assays, uptake into vesicles with recombinantly expressed transporters, etc. One of the most frequently used models for active transport in the preclinical setting is bidirectional transport across a monolayer, which provides information around asymmetry of drug transport at a given concentration, and an efflux ratio (ER) ( $B \rightarrow A/A \rightarrow B$ ) or uptake ratio (UR) ( $A \rightarrow B/B \rightarrow A$ ) is calculated (see Figure 3.7.4). An asymmetry over the membrane of approx  $ER > 2$  indicates that the compound is secreted into the apical compartment by the cells (Polli *et al.*, 2001) and similarly, a  $UR < 0.5$  indicates uptake. These ratios can therefore give valuable information for interpretation of compound pharmacokinetics *in vivo*. However, the ratios (ER or UR) are concentration dependent and also dependent on the test system used, and should also be evaluated in relation to passive transport of the compound (Hochman *et al.*, 2002). Troutman and co-workers (Troutman and Thakker, 2003a) have suggested calculating a ratio between the net efflux component (difference between  $A \rightarrow B$  and  $B \rightarrow A$  normalised to  $A \rightarrow B$ ) called

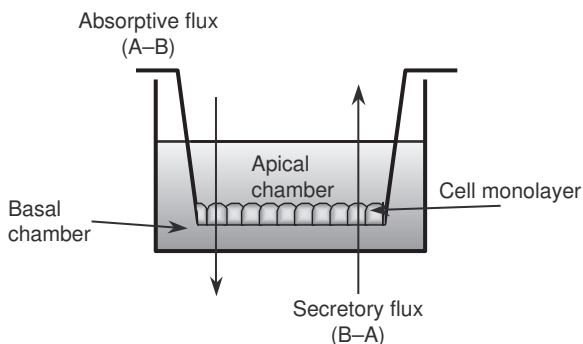


**Figure 3.7.4** An experimental setup using monolayers of cells. Cells are cultivated on filters in the plastic inserts. During the experiment, transport buffer solution is added to both the apical and basolateral side and drug to be tested on one side. The sampling of the solution on the receiver side (opposite the side where the drug is added) is made at predetermined time intervals, and the permeability coefficient,  $P_{app}$ , can be calculated.

absorption quotient (AQ), or secretion quotient (SQ), depending on which of the two transport directions are exceeding the other (Equations 3.7.1 and 3.7.2).

$$AQ = (A \rightarrow B) - (B \rightarrow A) / (A \rightarrow B) \quad (3.7.1)$$

$$SQ = (B \rightarrow A) - (A \rightarrow B) / (B \rightarrow A) \quad (3.7.2)$$

These parameters can be enough for a screening mode and will guide the chemist to an overall change in the molecular property of the drug candidate with respect to passive and active components, whereas the exact identity of the transporter/s involved is not always needed.

In some industries, the involvement of P-gp (*MDR1* gene product) is evaluated relatively early in drug discovery. The reason for the interest in P-gp is that in numerous clinical investigations possible interaction between drugs and P-gp seems to influence the kinetics of these drugs (Keogh and Kunta, 2006). The method used is bidirectional studies in MDCK-MDR1, and asymmetry is calculated as ER (see above). This asymmetry in permeability using MDCK-MDR1 cells (see Figure 3.7.4) can be corrected using wild-type (wt) MDCK cells (lacking human P-gp), e.g.  $ER_{corr} = ER_{MDR1} / ER_{wt}$  to obtain a more clear human P-gp interaction value. Important knowledge using this correction is that the expression of transporters in a non-transfected cell line of non-human origin used as background cell (i.e. MDCKwt) might be different from the transformed cell, resulting in substrate-specificity differences and a risk of misinterpretation (Goh *et al.*, 2002). Bidirectional transport in cell

lines can also be studied in combination with the use of inhibitors to specific transporters, thus providing a first and rough insight in which a transporter/family of transporters is/are responsible for the unidirectional or bi-directional transport and drug-drug interactions (Troutman and Thakker, 2003b; Keogh and Kunta, 2006; Rautio *et al.*, 2006). However, since many inhibitors and substrates to transporters show overlapping specificities, the interpretation of the data is complex. The relative contribution of each transporter to the overall transport of the compound is also complex and remains difficult to quantify. Therefore, data obtained from such *in vitro* studies are mainly used as rough guidance in designing new chemical entities in drug discovery.

Decision trees for identifying P-gp substrates can be found in the literature (Zhang *et al.*, 2006), and an example of a decision tree is shown in Figure 3.7.5 for a general screening for evaluation of the involvement of transporters and metabolism using several different techniques.

Transporter inhibition data (P-gp) are currently also evaluated during preclinical evaluation due to an increased number of reports showing raised and potentially toxic levels of compounds after concomitant administration with other therapeutic agents (Fromm *et al.*, 1999;

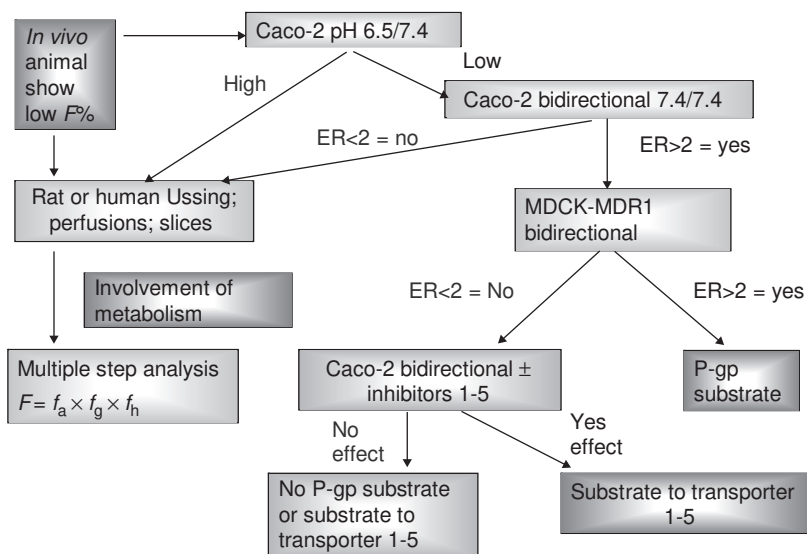


**Figure 3.7.5** Decision tree for evaluation of drug transport across GI membranes using several preclinical models. After each method is used, yes or no indicates the new direction and a new model is suggested. Such a decision tree can be made for each evaluation.  $F$ , bioavailability;  $f_a$ , fraction absorbed;  $f_g$ , fraction escaping gut metabolism;  $f_h$ , fraction escaping metabolism/extraction in the liver.

Sadeque *et al.*, 2000; Englund *et al.*, 2004). A preclinical technique that can be used for evaluation of P-gp inhibition is the taxol or digoxin transport inhibition assay (Gao *et al.*, 2001; Keogh and Kunta, 2006; Rautio *et al.*, 2006). A similar decision tree for evaluation of potential inhibitors to P-gp to the one for identifying P-gp substrates has also been proposed recently (Zhang *et al.*, 2006).

#### 3.7.5.0.1 Summary of screening using tools

- Caco-2 bidirectional studies and calculation of ER and UR and/or AQ and SQ
- MDCK-MDR1 bidirectional studies to identify P-gp substrates
- Caco-2 bidirectional studies in the absence and presence of inhibitors to identify involvement of a transporter or transporter family
- Caco-2 or MDCK-MDR1 cells for estimating P-gp inhibition to aid design of drug–drug interaction studies in the clinic.

### 3.7.6 Influence of metabolism during transport

Cytochrome P450 isoforms, such as CYP3A4, CYP2D6, 2C19 and 2C9, are involved in the biotransformation of lipophilic compounds of both endogenous and exogenous origin in the intestine and liver (Paine *et al.*, 2006; Daly, 2006). The main CYP450 isoforms in the intestine can vary between animal species and the intestinal region. In addition, phase II enzymes, the conjugating enzymes uridine diphosphate glucuronosyl transferases (UGTs) and glutathione-S-transferases (GSTs) and sulpho-transferases (SULTs) are also relevant for inactivation of drugs and either may influence the data from the different *in vitro* techniques or should be taken into account for *in vivo* interpretation (Zamek-Gliszczynski *et al.*, 2006). The clinical relevance of intestinal metabolism during absorption of drugs has often been debated (Groothuis, 2005), and the interest in relevant models for studying the influence of metabolism during drug transport has increased.

Using the Ussing chamber system with rat and human intestinal segments, the use of either radiolabelled or cold testosterone resulted in different permeability values (Ungell, 2005). When radiolabelled testosterone was used, high apparent permeability values ( $P_{app}$ ) were obtained. However, when unlabelled testosterone and ultraviolet (UV) detection were used to analyse the parent compound, the values of permeability were less than one-tenth of that obtained as total transport in both rat and human intestine (Ungell, 2005). Testosterone is assumed to be completely absorbed in humans. However, since the intestine significantly

contributes to extraction of the compound before it enters the liver, the number of intact testosterone molecules reaching the systemic circulation is probably less than complete. Therefore, care should be taken to extrapolate transport values to humans if the compound is metabolically unstable. Metabolic activity in the liver hepatocytes may also obscure total transport similarly to the results obtained in the Ussing chamber. Indeed, there are now several publications showing direct interaction between metabolism and efflux of metabolites via several transporters (Zamek-Gliszcynski *et al.*, 2006; Shitara *et al.*, 2006; Kusuhara and Sugiyama, 2002; Suzuki and Sugiyama, 2000; Benet *et al.*, 2004; Jeong *et al.*, 2005). This means that careful monitoring of the content of both parent compound and metabolites in different compartments of the *in vitro* methodology is needed for correct interpretation of data.

CYP450 3A4, which is the most important CYP isoform in the human intestine, is absent or at a low level in the parent clone of the Caco-2 cell (Ungell and Karlsson, 2003). This can explain the low predictability of permeability obtained by this model for drugs that are substrates to this enzyme family and may, thus, overestimate the extent of absorption *in vivo*. Caco-2 cell monolayers have also been used to evaluate the importance of ester hydrolysis of prodrugs in parallel with transport (Narawane *et al.*, 1993; Augustijns *et al.*, 1998). However, carboxyesterase activity within the Caco-2 cell line seems to be more liver than intestine specific (Imai *et al.*, 2005). This indicates that degradation of ester bonds during transport studies using the Caco-2 cell model can overestimate the involvement of intestinal esterases, especially when studying ester link-based prodrug activation.

#### 3.7.6.0.1 Summary of influence of metabolism on drug transport

- The presence of enzymes will affect data interpretation
- Species differences in enzymes and transporters exist
- Model differences in presence of enzymes and transporters exist
- Metabolites can be substrates to transporters.

### 3.7.7 Use of preclinical models for prediction of drug transport in humans

Regionally, within the gastrointestinal tract, both the properties of the intestinal membrane, i.e. lipid composition, surface area, protein content of transporters and enzymes, as well as the components and pH of the

intestinal luminal fluid change (Neuhoff *et al.*, 1989; Artursson *et al.*, 1993; Narawane *et al.*, 1993; Erickson *et al.*, 1995; Homsey *et al.*, 1995; Ungell *et al.*, 1997; Makhey *et al.*, 1998; Ungell, 2002; Seithel *et al.*, 2006; Zimmermann *et al.*, 2005). Data on functional studies for CL in isolated perfused livers have also suggested zone-dependent metabolism, especially phase II conjugation favouring the periportal region of the liver Zamek-Gliszcynski *et al.*, 2006). Hence, the transport (and metabolism) characteristics of a drug may change by region, a process that is very difficult to mimic in a static *in vitro* system (Homsey *et al.*, 1995). This illustrates the importance of having more complex organ-based models for better prediction of drug transport *in vivo*.

Selection of a drug candidate for development (see Figure 3.7.1) is usually based on both *in vivo* and *in vitro* ADME data in relation to the *in vivo* efficacy of the drug. In general, the most frequently used data for prediction of bioavailability ( $F$ ) in man is the *in vivo* hepatic clearance ( $CL_h$ ) data from animals (Rowland and Tozer, 1980; Poggesi, 2004) (see Figure 3.7.6).

$F$  in humans is estimated from allometrically scaled  $CL_h$  and hepatic blood flow ( $Q_h$ ) from *in vivo* studies using two to three animals and assuming complete absorption (i.e.  $f_a = 1$ ) and no intestinal loss of compound (e.g.  $f_g = 1$ ) (according to Equations 3.7.3–3.7.5 (Rowland and Tozer, 1980; Poggesi, 2004):

$$F = f_a \times f_g \times f_h \quad (3.7.3)$$

$F$	=	$f_a$	×	$f_g$	×	$f_h$
<i>In vivo</i> human po versus iv Or scaled from animal data		Predictions from Physicochemical parameters <i>In silico</i> Caco-2, MDCK Intestinal perfusions Ussing Intestinal sacs Human better than animal		Intestinal slices Intestinal perfusions Ussing  Biotransformation studies to calculate grade of extraction		Cell lines Hepatocytes Liver perfusions Liver slices  Biotransformation studies to calculate grade of extraction

**Figure 3.7.6** Models for prediction of bioavailability in humans. po, oral; iv, intravenous;  $F$ , bioavailability;  $f_a$ , fraction absorbed;  $f_g$ , fraction escaping gut metabolism;  $f_h$ , fraction escaping metabolism/extraction in the liver.

or:

$$F = f_a \times (1 - \text{CL}_h / Q_h) \quad (3.7.4)$$

or simply:

$$F = (1 - \text{CL}_h / Q_h) \quad (3.7.5)$$

However, an accurate prediction of human drug absorption based only on animal *in vivo* data might not be successful, since a variation in expression of transporters and enzymes between animal species exists. An alternative approach has been discussed (Ungell, 2005) and proposes to use predicted  $f_a$  obtained from Caco-2 cells and/or human intestinal segments (or other reliable and validated human *ex vivo* tools) combined with the allometrically scaled human CL (obtained from *in vivo* animal studies or *ex vivo* human hepatic models) according to Equation 3.7.4, for a better estimate of human  $F$  value. This suggestion assumes that  $f_g = 1$ , but that  $f_a$  can influence the estimate from *in vivo* scaled  $F$ . Thus, the use of predicted  $f_a$  values from human-relevant *in vitro* assays to support *in vivo* animal data would by this rationale probably give better confidence in the selection of clinical candidates (Li, 2005) (see Figure 3.7.1). However, if gut extraction is assumed to be substantial, none of the above models will correctly predict  $F$  in humans, and corrections for intestinal extraction need to be performed.

At this stage of drug discovery, the development of potential clinical formulations also starts and the predicted values for human drug transport will be used as information to guide the formulation development. To aid the development of a specific formulation, drug permeability (and solubility) data can also be used for prediction of human plasma profiles using commercially available tools such as GastroPlus™ (Parrott and Lave, 2002; Kuentz *et al.*, 2006).

#### 3.7.7.0.1 Summary of prediction of drug transport in humans

- *In vitro* data from humanised drug transport systems to be used to support *in vivo* animal data to obtain better predictions of human drug transport and bioavailability.

### 3.7.8 The Biopharmaceutics Classification System

The Biopharmaceutics Classification System (BCS) was developed to aid interpretation of solubility and permeability data for formulation development (Amidon *et al.*, 1995; FDA, Center for Drug Evaluation and



Research (2000); Yu *et al.*, 2002). BCS classifications are generally used to bridge between different versions of clinical formulations of a marketed product or clinical material in phase III, to reduce the need for bioequivalence studies (Yu *et al.*, 2002; Polli *et al.*, 2004). So far this guidance is helping the biowaiver to identify the class I drugs used in immediate-release formulations.

Four different classes of drugs are used: high permeability/high solubility (class I), high permeability/low solubility (class II), low permeability/high solubility (class III) and low permeability/low solubility (class IV) (see Chapter 4.2) (Ungell and Abrahamsson, 2001; Yu *et al.*, 2002; Polli *et al.*, 2004). Since the introduction of this classification system, its validity and applicability have been the subject of extensive research and debate (Yu *et al.*, 2002; Polli *et al.*, 2004). Opinions have been forwarded concerning the boundaries and criteria to be fulfilled for the different classes as well as suggested standard compounds. Two variants of this BCS system have been proposed in the literature; a six-class system (Bergström *et al.*, 2003), based on molecular surface properties of drugs, and a Biopharmaceutics Drug Disposition Classification System (BDDCS) that takes into account both metabolism and transporters (Wu and Benet, 2005).

Classification of drug compounds following these guidelines requires accurate and thoroughly validated models to assess permeability and solubility. If the model is not good enough, or if the validation of the technique is not properly made, the classification of new chemical entities can be inaccurate and misleading. The original guidance proposes several types of methods to be used: pharmacokinetics studies using human subjects for evaluation of fraction absorbed using mass balance, absolute bioavailability or intestinal perfusion approaches; or intestinal perfusion models using the rat or even cell models such as the Caco-2 model. If an *in vitro* system will be used, each laboratory is recommended to use a number of reference molecules with known clinical  $f_a$  for validation of the permeability properties of their model, to set boundaries of low and high permeability, and to show the presence of active transport. When the *in vitro* model is carefully validated, it can also be used earlier in the screening as a prediction curve for  $f_a$  in humans (Ungell and Karlsson, 2003).

#### 3.7.8.0.1 Summary of BCS classification

- BCS needs a thorough validation of the *in vitro* technique
- A set of 10–20 reference compounds with known  $f_a$  in humans is needed to set boundaries between classes.

## References

- Akhteruzzaman S, Kato Y, Kouzuki H, *et al.* (1999). Carrier-mediated hepatic uptake of peptidic endothelin antagonists in rats. *J Pharmacol Exp Ther* 290: 1107–1115.
- Amidon GL, Lennernas H, Shah VP, Crison JR (1995). A theoretical basis for a biopharmaceutic drug classification: the correlation of *in vitro* drug product dissolution and *in vivo* bioavailability. *Pharm Res* 12: 413–420.
- Anderlé P, Niederer E, Rubas W, *et al.* (1998). P-glycoprotein (P-gp) mediated efflux in Caco-2 cell monolayers: the influence of culturing conditions and drug exposure on P-gp expression levels. *J Pharm Sci* 87: 757–762.
- Artursson P, Palm K, Luthman K (2001). Caco-2 monolayers in experimental and theoretical predictions of drug transport. *Adv Drug Del Rev* 46: 27–43.
- Artursson P, Tavelin S (2003). Caco-2 and emerging alternatives for prediction of intestinal drug transport: a general overview. In: van de Waterbeemd H, Lennernas H, Artursson P, eds. *Drug Bioavailability: estimation of solubility, permeability, absorption and bioavailability*. Weinheim: Wiley-VCH, 72–89.
- Artursson P, Ungell A-L, Löfroth J-E (1993). Selective paracellular permeability in two models of intestinal absorption: cultured monolayers of human intestinal epithelial cells and rat intestinal segments. *Pharm Res* 10: 1123–1129.
- Augustijns P, Annaert P, Heylen P, *et al.* (1998). Drug absorption studies of prodrug esters using the Caco-2 model: evaluation of ester hydrolysis and transepithelial transport. *Int J Pharm* 166: 45–53.
- Augustijns P, Mols R (2004). HPLC with programmed wavelength fluorescence detection for the simultaneous determination of marker compounds of integrity and P-gp functionality in the Caco-2 intestinal absorption model. *J Pharm Biomed Anal* 34: 971–978.
- Balimane PV, Chong S (2005). Cell culture-based models for intestinal permeability: a critique. *Drug Discov Today* 10: 335–343.
- Balimane PV, Chong S, Morrison RA (2000). Current methodologies used for evaluation of intestinal permeability and absorption. *J Pharmacol Toxicol Methods* 44: 301–312.
- Barthe L, Woodley J, Houin G (1999). Gastrointestinal absorption of drugs: methods and studies. *Fundament Clin Pharmacol* 13: 154–168.
- Benet LZ, Cummins CL, Wu CY (2004). Unmasking the dynamic interplay between efflux transporters and metabolic enzymes. *Int J Pharm* 277: 3–9.
- Bergström CAS, Strafford M, Lazorova L, *et al.* (2003). Absorption classification of oral drugs based on molecular surface properties. *J Med Chem* 46: 558–570.
- Bogman K, Zysset Y, Degen L, *et al.* (2005). P-glycoprotein and surfactants: effects on intestinal talinolol absorption. *Clin Pharmacol Ther* 77: 24–32.
- Borchardt RT, Smith PL, Wilson G (1996). *Models for Assessing Drug Absorption and Metabolism*. Pharmaceutical Biotechnology vol 8. New York: Plenum Press.
- Brandon EF, Bosch A, Deenen TM, *et al.* (2006). Validation of *in vitro* cell models used in drug metabolism and transport studies: genotyping of cytochrome P450, phase II enzymes and drug transporter polymorphisms in the human hepatoma (HepG2), ovarian carcinoma (IGROV-1) and colon carcinoma (CaCo-2, LS180) cell lines. *Toxicol Appl Pharmacol* 211: 1–10.

- Camenisch G, Folkers G, van de Waterbeemd H (1997). Comparison of passive drug transport through Caco-2 cells and artificial membranes. *Int J Pharm* 147: 61–70.
- Chen W, Tang F, Horie K, Borchardt R (2002). Caco-2 cell monolayers as a model for studies of drug transport across human intestinal epithelium. In: Lehr C-M, ed. *Cell Culture Models of Biological Barriers: in vitro test systems for drug absorption and delivery*. London, New York: Taylor and Francis, 143–163.
- Chong S, Dando SA, Soucek KM, Morrison RA (1996). *In vitro* permeability through Caco-2 cells is not quantitatively predictive of *in vivo* absorption for peptide-like drugs absorbed via the dipeptide transporter system. *Pharm Res* 13: 120–123.
- Daly AK (2006). Significance of the minor cytochrome P450 3A isoforms. *Clin Pharmacokinet* 45: 13–31.
- De Kanter R, De Jager MH, *et al.* (2002). Drug-metabolizing activity of human and rat liver, lung, kidney and intestine slices. *Xenobiotica* 32: 349–362.
- Egan WJ, Lauri G (2002). Prediction of intestinal permeability. *Adv Drug Del Rev* 54: 273–289.
- Englund G, Hallberg P, Artursson P, Michaelsson K, Melhus H (2004). Association between the number of coadministered P-glycoprotein inhibitors and serum digoxin levels in patients on therapeutic drug monitoring. *BMC Med* 2: 8.
- Erickson RH, Gum JR Jr, Lindstrom MM, McKean D, Kim YS (1995). Regional expression and dietary regulation of rat small intestinal peptide and amino acid transporter mRNAs. *Biochem Biophys Res Commun* 216: 249–257.
- Fagerholm U, Johansson M, Lennernas H (1996). Comparison between permeability coefficients in rat and human jejunum. *Pharm Res* 13: 1336–1342.
- Fallingborg J, Christensen LA, Ingelman-Nielsen M, *et al.* (1989). pH-Profile and regional transit times of the normal gut measured by radiotelemetry device. *Aliment Pharmacol Ther* 3: 605–613.
- FDA, Center for Drug Evaluation and Research (2000). *Guidance for Industry, Waiver of in vivo Bioavailability and Bioequivalence Studies for Immediate-release Solid Oral Dosage Forms based on a Biopharmaceutics Classification System*. <http://www.fda.gov/downloads/Drugs/GuidanceComplianceRegulatoryInformation/Guidances/UCM070246.pdf> (accessed 2 June 2009).
- Fromm MF, Kim RB, Stein CM, Wilkinson GR, Roden DM (1999). Inhibition of P-glycoprotein-mediated drug transport: a unifying mechanism to explain the interaction between digoxin and quinidine. *Circulation* 99: 552–557.
- Gao J, Murase O, Schowen RL, Aube J, Borchardt RT (2001). A functional assay for quantitation of the apparent affinities of ligands of P-glycoprotein in Caco-2 cells. *Pharm Res* 18: 171–176.
- Geng WP, Schwab AJ, Goresky CA, Pang KS (1995). Carrier-mediated uptake and excretion of bromosulphophthalein-glutathione in perfused rat liver: a multiple indicator dilution study. *Hepatology* 22: 1188–1207.
- Goh LB, Spears KJ, Yao D, *et al.* (2002). Endogenous drug transporters in *in vitro* and *in vivo* models for the prediction of drug disposition in man. *Biochem Pharmacol* 64: 1569–1578.
- Groothuis GMM (2005). Clinical relevance of drug metabolism in the small and large intestine: more than absorption alone. *Pharmaceutisch Weekblad* 140: 328–331.

- Hartmann T, Schmitt J (2004). Lipophilicity – beyond octanol/water: a short comparison of modern technologies. *Drug Discov Today Technol* 1: 431–439.
- Hochman JH, Yamazaki M, Obe T, Lin JH (2002). Evaluation of drug interactions with P-glycoprotein in drug discovery: *in vitro* assessment of the potential for drug-drug interactions with P-glycoprotein. *Curr Drug Metab* 3: 257–273.
- Hoffmaster KA, Turncliff RZ, LeCluyse EL, *et al.* (2004). P-glycoprotein expression, localization, and function in sandwich-cultured primary rat and human hepatocytes: relevance to the hepatobiliary disposition of a model opioid peptide. *Pharm Res* 21: 1294–1302.
- Homsy W, Caille G, du Souich P (1995). The site of absorption in the small intestine determines diltiazem bioavailability in the rabbit. *Pharm Res* 12: 1722–1726.
- Horio M, Chin K-V, Currier SJ, *et al.* (1989). Transepithelial transport of drugs by the multidrug transporter in cultured Madin-Darby canine kidney cell epithelia. *J Biol Chem* 264: 14880–14884.
- Hunter J, Hirst BH (1997). Intestinal secretion of drugs: the role of P-glycoprotein and related drug efflux systems in limiting oral drug absorption. *Adv Drug Deliv Rev* 25: 129–157.
- Imai T, Imoto M, Sakamoto H, Hashimoto M (2005). Identification of esterases expressed in caco-2 cells and effects of their hydrolyzing activity in predicting human intestinal absorption. *Drug Metab Disp* 33: 1185–1190.
- Ingels FM, Augustijns PF (2003). Biological, pharmaceutical and analytical considerations with respect to the transport media used in the absorption screening system, Caco-2. Minireview. *J Pharm Sci* 92: 1545–1558.
- Ingels F, Beck B, Oth M, Augustijns P (2004). Effect of simulated intestinal fluid on drug permeability estimation across Caco-2 monolayers. *Int J Pharm* 274: 221–232.
- Ingels F, Augustijns P, Ungell A-L (2006). Selection of solvent systems for membrane-, cell- and tissue-based permeability assessment. In: Augustijns P, Brewster ME, eds. *Solvent Systems and their Selection in Pharmaceuticals and Biopharmaceutics*. New York: Springer, 179–220.
- Irvine JD, Takahashi L, Lockhart K, *et al.* (1999). MDCK (Madin-Darby Canine Kidney) cells: a tool for membrane permeability screening. *J Pharm Sci* 88: 28–33.
- Ishigami M, Tokui T, Komai T, *et al.* (1995). Evaluation of the uptake of pravastatin by perfused rat liver and primary cultured rat hepatocytes. *Pharm Res* 12: 1741–1745.
- Jeong EJ, Liu X, Jia X, Chen J, Hu M (2005). Coupling of conjugation enzymes and efflux transporters: impact on bioavailability and drug interactions. *Curr Drug Metab* 6: 455–468.
- Kansy M, Senner F, Gubenator K (1998). Physicochemical high throughput screening: parallel artificial membrane permeation assay in the description of passive absorption process. *J Med Chem* 41: 1007–1010.
- Kansy M, Avdeef A, Fischer H (2004). Advances in screening for membrane permeability: high-resolution PAMPA for medicinal chemists. *Drug Discov Today Technol* 1: 349–355.
- Keogh JP, Kunta JR (2006). Development, validation and utility of an *in vitro* technique for assessment of potential clinical drug-drug interactions involving P-glycoprotein. *Eur J Pharm Sci* 27: 543–554.

- Krishna G, Chen K-J, Lin CC, Nomeir AA (2001). Permeability of lipophilic compounds in drug discovery using *in-vitro* human absorption model, Caco-2. *Int J Pharm* 222: 77–89.
- Kuentz M, Nick S, Parrott N, Röthlisberger D (2006). A strategy for preclinical formulation development using GastroPlus™ as pharmacokinetic simulation tool and a statistical screening design applied to a dog study. *Eur J Pharm Sci* 27: 91–99.
- Kusuhara H, Sugiyama Y (2002). Role of transporters in the tissue-selective distribution and elimination of drugs: transporters in the liver, small intestine, brain and kidney. *J Controlled Rel* 78: 43–54.
- Lennernas H, Palm K, Fagerholm U, Artursson P (1996). Comparison between active and passive drug transport in human intestinal epithelial (Caco-2) cells in vitro and human jejunum in vivo. *Int J Pharm* 127: 103–107.
- Li AP (2005). Preclinical in vitro screening assays for drug-like properties. *Drug Discov Today Technol* 2: 179–185.
- Li Q, Sai Y, Kato Y, Tamai I, Tsuji A (2003). Influence of drugs and nutrients on transporter gene expression levels in Caco-2 and LS180 intestinal epithelial cell lines. *Pharm Res* 20: 1119–1124.
- Lindahl A, Sandstrom R, Ungell AL, Lennernas H (1998). Concentration- and region-dependent intestinal permeability of fluvastatin in the rat. *J Pharm Pharmacol* 50: 737–744.
- Lipinski CA, Lombardo F, Dominy BW, Feeney PJ (2001). Experimental and computational approaches to estimate solubility and permeability in drug discovery and development settings. *Adv Drug Del Rev* 46: 3–26.
- Luttringer O, Theil F-G, Lavé T, *et al.* (2002). Influence on isolation procedure extracellular matrix and dexamethasone on the regulation of membrane transporters gene expression in rat hepatocytes. *Biochem Pharmacol* 64: 1637–1650.
- Makhey VD, Guo A, Norris DA, *et al.* (1998). Characterization of the regional intestinal kinetics of drug efflux in rat and human intestine and in Caco-2 cells. *Pharm Res* 15: 1160–1167.
- Matsson P, Bergström CAS, Nagahara N, *et al.* (2005). Exploring the role of different drug transport routes in permeability screening. *J Med Chem* 48: 604–613.
- Miret S, Abrahamse L, de Groene EM (2004). Comparison of *in vitro* models for the prediction of compound absorption across human intestinal mucosa. *J Biomolec Screen* 9: 598–606.
- Narawane M, Podder SK, Bundgaard H, Lee VHL (1993). Segmental differences in drug permeability, esterase activity and ketone reductase activity in the albino rabbit intestine. *J Drug Target* 1: 29–39.
- Nerurkar MN, Burton PS, Borchardt RT (1996). The use of surfactants to enhance the permeability of peptides through Caco-2 cells by inhibition of an apically polarized efflux system. *Pharm Res* 13: 528–534.
- Neuhoff S, Ungell A-L, Zamora I, Artursson P (2003). pH dependent bidirectional transport of weakly basic drugs across Caco-2 cell monolayers: implications for drug–drug interactions. *Pharm Res* 20: 1141–1148.
- Neuhoff S, Artursson P, Zamora I, Ungell A-L (2005a). Impact of extracellular protein binding on passive and active drug transport across Caco-2 cells. *Pharm Res* 23: 350–359.

- Neuhoff S, Ungell A-L, Zamora I, Artursson P (2005b). pH dependent passive and active transport of acidic drugs across Caco-2 cell monolayers. *Eur J Pharm Sci* 25: 211–220.
- Olinga P, Groen K, Hof I, *et al.* (1997). Comparison of five incubation systems for rat liver slices using functional and viability parameters. *J Pharmacol Toxicol Methods* 38: 59–69.
- Olinga P, Hof IH, Merema MT, *et al.* (2001). The applicability of rat and human liver slices to the study of mechanisms of hepatic drug uptake. *J Pharmacol Toxicol Methods* 45: 55–63.
- Örnskov E, Gottfries J, Erickson M, Folestad S (2005). Experimental modelling of drug membrane permeability by capillary electrophoresis using liposomes, micelles and microemulsions. *J Pharm Pharmacol* 57: 435–442.
- Ottiger C, Wunderli-Allenspach H (1999). Immobilised artificial membrane (IAM)-HPLC for partition studies of neutral and ionised acids and bases in comparison with the liposomal partition system. *Pharm Res* 16: 643–650.
- Paine MF, Hart HL, Ludington SS, *et al.* (2006). The human intestinal cytochrome P450 ‘pie’. *Drug Metab Dispos* 34: 880–886.
- Parrott N, Lave T (2002). Prediction of intestinal absorption: comparative assessment of GASTROPLUS™ and iDEA™. *Eur J Pharm Sci* 17: 51–61.
- Poggesi I (2004). Predicting human pharmacokinetics from preclinical data. *Curr Opin Drug Discov Devel* 7: 100–111.
- Polentarutti B, Peterson A, Sjöberg Å, *et al.* (1999). Evaluation of viability of excised rat intestinal segments in the Ussing chamber: investigation of morphology, electrical parameters and permeability characteristics. *Pharm Res* 16: 446–454.
- Polli JW, Wring SA, Humphreys JE, *et al.* (2001). Rational use of *in vitro* P-glycoprotein assays in drug discovery. *J Pharmacol Exp Ther* 299: 620–628.
- Polli JE, Yu LX, Cook JA, *et al.* (2004). Summary workshop report: biopharmaceutics classification system – implementation challenges and extension opportunities. *J Pharm Sci* 93: 1375–1381.
- Rautio J, Humphreys JE, Webster L, *et al.* (2006). *In vitro* P-glycoprotein inhibition assays for assessment of clinical drug interaction potential of new drug candidates: a recommendation for probe substrates. *Drug Metab Dispos* 34: 786–792.
- Rowland M, Tozer TN (1980). *Clinical Pharmacokinetics: concepts and applications*. Philadelphia: Lea & Febiger.
- Sadeque AJ, Wandel C, He H (2000). Increased drug delivery to the brain by P-glycoprotein inhibition. *Clin Pharmacol Ther* 68: 231–237.
- Sahi J (2005). Use of *in vitro* transporter assays to understand hepatic and renal disposition of new drug candidates. *Expert Opin Drug Metab Toxicol* 1: 409–427.
- Salphati L, Childers K, Pan L (2001). Evaluation of a single-pass intestinal-perfusion method in rat for the prediction of absorption in man. *J Pharm Pharmacol* 53: 1007–1013.
- Seithel A, Karlsson J, Hilgendorf C, Björquist A, Ungell A-L (2006). Variability in mRNA expression of ABC- and SLC transporters in human intestinal cells: comparison between human segments and Caco-2 cells. *Eur J Pharm Sci* 28: 291–299.

- Shitara Y, Sato X, Sugiyama Y (2005). Drug–drug interaction involving transporters. *Annu Rev Pharmacol Toxicol* 45: 689–723.
- Shitara Y, Horie T, Sugiyama Y (2006). Transporters as a determinant of drug clearance and tissue distribution. *Eur J Pharm Sci* 27: 425–446.
- Sjöström M, Sjöberg Å, Utter L, *et al.* (2000). Excised human intestinal segments as a mechanistic tool for verifying transport properties of drug candidates. AAPS Annual meeting Abstracts, 2000. *Pharm Sci Suppl* 2(4): abstract 57. [http://www.aapsj.org/abstracts/AM\\_2000/3057.htm](http://www.aapsj.org/abstracts/AM_2000/3057.htm) (accessed 2 June 2009).
- Stenberg P, Norinder U, Luthman K, Artursson P (2001). Experimental and computational screening models for the prediction of intestinal drug absorption. *J Med Chem* 44: 1927–1937.
- Suzuki H, Sugiyama Y (2000). Role of metabolic enzymes and efflux transporters in the absorption of drugs from the small intestine. *Eur J Pharm Sci* 12: 3–12.
- Troutman MD, Thakker DR (2003a). Novel experimental parameters to quantify the modulation of absorptive and secretory transport of compounds by P-glycoprotein in cell culture models of intestinal epithelium. *Pharm Res* 20: 1210–1224.
- Troutman MD, Thakker DR (2003b). Efflux ratio cannot assess P-glycoprotein-mediated attenuation of absorptive transport: asymmetric effect of P-glycoprotein on absorptive and secretory transport across Caco-2 cell monolayers. *Pharm Res* 20: 1200–1209.
- Tsuji A, Tamai I (1996). Carrier-mediated intestinal transport of drugs. *Pharm Res* 13: 963–977.
- Ungell A-L (1997). *In vitro* absorption studies and their relevance to absorption from the GI tract. *Drug Devel Indust Pharm* 23: 879–892.
- Ungell A-L (2002). Transport studies using intestinal tissue *ex-vivo*. In: Lehr C-M, ed. *Cell Culture Models of Biological Barriers: in vitro test systems for drug absorption and delivery*. London, New York: Taylor & Francis, 164–188.
- Ungell A-L (2004). Caco-2 replace or refine? *Drug Discov Today Technol* 1: 423–430.
- Ungell A-L (2005). Prediction of human drug absorption using *in silico* and *in vitro* techniques. In: Pouton C, ed. Drug candidate optimization, formulation and early development. *Bulletin Technique Gattefossé* 98: 19–31.
- Ungell A-L, Abrahamsson B (2001). Biopharmaceutical support in candidate drug selection. In: Gibson M, ed. *Pharmaceutical Preformulation and Formulation. A practical guide from candidate drug selection to commercial dosage formulation*. Englewood: HIS Health Group, 97–143.
- Ungell A-L, Karlsson J (2003). Cell cultures in drug discovery: an industrial perspective. In: van de Waterbeemd H, Lennernäs H, Artursson P, eds. *Drug Bioavailability: estimation of solubility, permeability, absorption and bioavailability*. Weinheim: Wiley-VCH, 90–131.
- Ungell A-L, Nylander S, Bergstrand S, Sjöberg Å, Lennernäs H (1997). Membrane transport of drugs in different regions of the intestinal tract of the rat. *J. Pharm Sci* 87: 360–366.
- van de Kerkhof EG, Ungell A-LB Sjöberg Å-K, *et al.* (2006). Innovative methods to study human intestinal drug metabolism in vitro: precision-cut slices compared with Ussing chamber preparations. *Drug Metab Disp* 34: 1893–1902.

- Van de Waterbeemd H, Smith DA, Beaumont K, Walker DK (2001). Property-based design: optimization of drug absorption and pharmacokinetics. *J Med Chem* 44: 1313–1333.
- Veber DF, Johnson SR, Cheng H-Y, *et al.* (2002). Molecular properties that influence the oral bioavailability of drug candidates. *J Med Chem* 45: 2615–2623.
- Vig BS, Stouch TR, Timoszyk JK, *et al.* (2006). Human PEPT1 pharmacophore distinguishes between dipeptide transport and binding. *J Med Chem* 49: 3636–3644.
- Wu C-Y, Benet LZ (2005). Predicting drug disposition via application of BCS: transport/absorption/elimination interplay and development of a biopharmaceutics drug disposition classification system. *Pharm Res* 22: 11–23.
- Wu-Pong S, Livesay V, Dvorchnik B, Barr WH (1999). Oligonucleotide transport in rat and human intestine Ussing chamber models. *Biopharm Drug Disp* 20: 411–416.
- Yamashita S, Furubayashi T, Kataoka M, *et al.* (2000). Optimized conditions for prediction of intestinal drug permeability using Caco-2 cells. *Eur J Pharm Sci* 10: 195–204.
- Yu LX, Amidon GL, Polli JE, *et al.* (2002). Biopharmaceutics classification system: the scientific basis for biowaiver extensions. *Pharm Res* 19: 921–925.
- Zamek-Gliszczynski MJ, Hoffmaster KA, Nezasa K-I, Tallman MN, Brouwer KLR (2006). Integrating of hepatic drug transporters and phase II metabolizing enzymes: mechanisms of hepatic excretion of sulfate, glucuronide, and glutathione metabolites. *Eur J Pharm Sci* 27: 447–486.
- Zhang L, Strong JM, Qiu W, *et al.* (2006). Scientific perspectives on drug transporters and their role in drug interaction. *Mol Pharm* 3: 62–69.
- Zimmermann C, Gutmann H, Hruz P, *et al.* (2005). Mapping of multidrug resistance gene 1 and multidrug resistance-associated protein isoform 1 to 5 mRNA expression along the human intestinal tract. *Drug Metab Disp* 33: 219–224.





## Part 4

### Describing and predicting bioavailability

4.1	<i>In vitro</i> dissolution	257
4.2	The Biopharmaceutics Classification System in drug discovery and development	277
4.3	Biosimulation studies	297

The aim of Part 4 is to exemplify how bioavailability may be described and predicted. Regulatory authorities have put effort into identifying when bioavailability may be predicted from dissolution studies. Moreover, the US Food and Drug Administration (FDA) has, with support from biopharmaceutical scientists, introduced the Biopharmaceutics Classification System (BCS) in order to classify drug substances according to whether their permeability and/or solubility is rate limiting for bioavailability (FDA Center for Drug Evaluation and Research, 2000).

In Chapter 4.1, dissolution studies are described, focusing on theory and the methods applied to predict bioavailability by dissolution studies, i.e. *in vitro*–*in vivo* correlation. In Chapter 4.2, the BCS is described, as well as the Biopharmaceutics Drug Disposition Classification System (BDDCS) which is a further development of the BCS. The BDDCS classifies drug substances based on whether metabolism and transporters play a role in addition to solubility and permeability in determining the bioavailability of (pro)drug substances and candidates (Gupta *et al.*, 2006; Benet *et al.*, 2008; Custodio *et al.*, 2008). Chapter 4.2 also gives an industrial perspective on how the BCS and BDDCS may be used in the global development process of drug candidates in pharmaceutical industry.

Chapter 4.3 introduces and describes how biosimulation studies may be applied to predict the bioavailability of oral (pro)drug substances and candidates. Some commercially available programs for biosimulating oral absorption are discussed. For further reading on biosimulation in drug development a newly published book edited by Bertau *et al.* (2008) may be a more detailed resource.

## References

- Benet LZ, Amidon GL, Barends DM, *et al.* (2008). The use of BDDCS in classifying the permeability of marketed drugs. *Pharm Res* 52: 483–488.
- Bertau M, Mosekilde E, Westerhoff HV, eds (2008). *Biosimulation in Drug Development*. Weinheim: Wiley -VCH, 1–512.
- Custodio JM, Wu C-H, Benet LZ (2008). Predicting drug disposition absorption/elimination/transporter interplay and the role of food on drug absorption. *Adv Drug Del Rev* 60: 717–733.
- FDA, Center for Drug Evaluation and Research (2000). *Guidance for Industry, Waiver of in vivo Bioavailability and Bioequivalence Studies for Immediate-release Solid Oral Dosage Forms based on a Biopharmaceutics Classification System*. <http://www.fda.gov/downloads/Drugs/GuidanceComplianceRegulatoryInformation/Guidances/UCM070246.pdf> (accessed 3 June 2009).
- Gupta E, Barends DM, Yamashita E, *et al.* (2006). Review on global regulations concerning biowaivers for immediate release solid dosage forms. *Eur J Pharm Sci* 29: 315–324.

# 4.1

## *In vitro* dissolution

*Betty Lomstein Pedersen and Anette Müllertz*

An important characteristic for a drug substance, to be formulated in a solid oral dosage form, is the rate at which it goes into solution, from a pharmaceutical formulation from the pure drug substance. This is called the dissolution rate and is relevant since generally only a dissolved drug substance will be absorbed in the gastrointestinal (GI) tract.

Dissolution rates are determined by standardised dissolutions tests, described in the *European Pharmacopeia* (Ph Eur) and the *US Pharmacopeia* (USP), and also in pharmacopoeias covering other countries. The term ‘dissolution’ is used for all oral dosage forms, such as formulations that aim at a fast release of drug substance (immediate-release or conventional formulations) as well as those with a modified-release profile (controlled, delayed, extended, prolonged or sustained-release formulations). The term ‘intrinsic dissolution’ covers the dissolution of pure drug substance under controlled conditions.

In general, dissolution testing of pharmaceutical formulations is carried out with one of two purposes in mind: to support selection made during the development of new pharmaceutical formulations, or to perform quality control during production of pharmaceutical products.

When developing formulations for a specific drug substance, a desired dissolution profile is often defined and the development process will aim at reaching a delivery system with this profile. This work often takes place using compendial buffers as dissolution media. More sophisticated dissolution media, simulating the GI fluids, can be used in order to elucidate the potential influence of GI conditions (e.g. food effects) or to obtain a closer correlation with the *in vivo* situation. Development of new pharmaceutical formulation technologies takes place both in the industry and in academia, using *in vitro* dissolution testing as a central part.

For oral drug products on the market, a dissolution test assuring the quality of the product will often be included in the registration material. This dissolution test has been shown to be discriminative for the specific product during the development period and is easy to perform and

reproduce, thus batch-to-batch quality control dissolution tests do not normally include complex media simulating the intestinal fluids. According to the USP, selection of appropriate conditions for routine quality testing should, where possible, be based on discriminatory capability, robustness, stability of the drug substance in the dissolution medium, and the relevance to *in vivo* performance.

As described above, *in vitro* dissolution tests serve as a tool for assessing the biopharmaceutical dissolution properties of a pharmaceutical solid oral dosage form, during its development phase, as well as a quality control of the final marketed product. Furthermore, *in vitro* dissolution data are central for evaluating whether *in vivo* bioavailability studies are needed when changes are made to a marketed product regarding production site, manufacturing process or formulation (International Pharmaceutical Federation (FIP), 1997). If a dissolution method has been proven to be predictive of *in vivo* behaviour, the dissolution test might reduce or even obviate the necessity of performing expensive human bioequivalence studies. These circumstances will be expanded on in Chapter 4.2 by Dr Wu. However, the relationship between *in vitro* dissolution and *in vivo* bioavailability/absorption is still far from being fully explored, and it is important to keep in mind the limitations of the dissolution test when it is used as a predictor of *in vivo* performance.

During the past two decades, the focus has been on developing and optimising dissolution methods in both scientific, as well as regulatory communities. *In vitro* dissolution as a tool in biopharmaceutical evaluations has attracted a lot of interest; dissolution test methodology has been incorporated in the pharmacopoeias, and a large number of regulations and guidelines have been issued on bioavailability, bioequivalence and *in vitro* dissolution testing at both national and international levels (FIP, 1997).

In the present chapter, dissolution will be described and discussed with regard to dissolution mechanism theories, factors influencing dissolution – *in vitro* and *in vivo* – dissolution equipment described in the pharmacopoeias, and selection of dissolution media for *in vitro* dissolution studies.

### 4.1.1 Dissolution mechanism theories

Dissolution is basically the process molecules undergo when they are transferred from the solid to the dissolved state. There are two steps involved in dissolution. The first is detachment of molecules from the solid surface to form hydrated molecules at the solid–liquid interface. The

second is the transport from this interface to the bulk solution. Depending on which step is rate limiting to mass transfer, the dissolution process can be either:

- reaction-rate controlled
- transport-rate controlled
- a function of both processes.

*Reaction rate-controlled* dissolution is controlled by the rate of detachment of the drug from its crystal lattice into the solvent. In this case the liberation and deposition of the solubilised molecule is slower than the following process of transport into bulk solution. *Transport rate-controlled* dissolution involves two fundamental processes of mass transfer: molecular diffusion and forced convection. The rate of drug transport away from the dissolving solid surface is a combination of diffusion in the direction perpendicular to the planar surface and convection in the direction of flow.

When the rate constants of both processes are approximately equivalent, the dissolution rate is *a function of both processes*, i.e. determined by both the rate of reaction at the interface and the rate of the transport process (Wurster and Taylor, 1965; Abdou, 1989).

The most common dissolution theory is called the film theory or the diffusion layer model (Abdou, 1989). This theory assumes that the dissolution rate is *transport-rate controlled*, and in fact most dissolution processes are controlled by this diffusion–convection-controlled step (Wang and Flanagan, 1999). A basic diffusion–convection-controlled model for solid dissolution was developed by Noyes and Whitney in 1897, and later modified by Nernst (1904) and Brunner (1904), Levich (1962), and Dressman *et al.* (1998), leading to the equation shown in Equation 4.1.1:

$$\frac{dX_d}{dt} = \frac{A D}{\delta} \left( C_s - \frac{X_d}{V} \right) \quad (4.1.1)$$

where  $dX_d/dt$  is the dissolution rate as a function of the surface area,  $A$ , available for dissolution, the saturation solubility,  $C_s$ , of the drug substance in the dissolution medium, the amount of drug already in solution,  $X_d$ , the diffusion coefficient of the drug substance,  $D$ , the volume,  $V$ , of dissolution medium, and the diffusion layer thickness,  $\delta$ , adjacent to the dissolving surface. It is assumed that there is a rate-limiting diffusion layer at the solid–liquid interface, which has been described in the literature as a thin stagnant layer of saturated solution (Wurster and Taylor, 1965) or as

a hydrodynamic boundary layer with a velocity and a concentration gradient (Levich, 1962).

The Noyes–Whitney equation (Equation 4.1.1) is exact for dissolution from a plane surface under sink conditions, because the concentration gradient in the diffusion layer is linear at steady-state (Wang and Flanagan, 1999). Sink conditions are present when the concentration of the drug substance in the bulk phase is low and does not have an influence on the dissolution process from the solid phase. This is normally considered to be in the region of 10–30% of the saturation solubility or lower.

For spherical particles, the Noyes–Whitney equation will not be accurate, because the concentration gradient in the diffusion layer is non-linear. The degree of non-linearity depends on the ratio of drug particle size to diffusion layer thickness (Wang and Flanagan, 1999). Even though the thickness of the diffusion layer can only be calculated accurately if the hydrodynamics in the system are well defined, there are several suggestions in the literature on how to calculate the thickness of the diffusion layer of a particle (Abdou, 1989). Furthermore, it is important to keep in mind that the dissolution of particles will be influenced by the particle shape and particle size distribution.

#### **4.1.2 Factors influencing dissolution *in vitro***

*In vitro* dissolution of a drug substance from either the pure solid drug or a pharmaceutical formulation is influenced by several factors. These factors can be related to the physicochemical characteristics of the drug substance, the pharmaceutical formulation and the conditions of the *in vitro* dissolution test.

First of all, the solubility of the drug substance in the dissolution media should be known. This will reveal if there will be problems maintaining sink conditions during the dissolution test. This is the case for many poorly soluble drug substances belonging to class 2 or 4 in the Biopharmaceutics Classification System (BCS) (see Chapter 4.2 for further details). If sink conditions cannot be achieved, several possibilities to solve this issue are available: in general the dose of drug can be reduced or the composition of the medium can be changed in several ways. Firstly, the pH of the medium can be changed, taking into account the acid/base properties of the drug substance; the dissolution can be carried out at a pH value where the solubility is higher, thus enabling sink conditions. The pH of the dissolution medium should only be chosen within a certain interval that is physiologically relevant (see later); thus a pH change is generally only

relevant for drugs with  $pK_a$  values in the physiological pH range. Acid/base properties of drug substances are further described in Chapter 2.1.

If changing the pH is not feasible, the drug solubility in the media can be changed by increasing the dissolution volume or by addition of surfactants. The solubility of most poorly soluble drugs is enhanced in the presence of surfactants. Surfactants often used for dissolution includes sodium lauryl sulphate (SLS) and polysorbate 60 or 80 (Tween 60 or 80) as well as various sorbitan esters (SPANs). In some rare instances, the use of ethanol to increase dissolution has also been reported.

Dissolution testing is carried out on pharmaceutical formulations, and the characteristics of the formulation have to be taken into consideration. Several approaches can be applied when formulating a poorly soluble drug, where the solubility and dissolution rate in the GI tract are often the limiting factors for the absorption.

Firstly the dissolution rate of a drug substance can be increased by decreasing its particle size and thereby increasing the surface area available for dissolution. Furthermore, surfactants can be added to the formulations in order to give a better wetting of the drug substance and possibly increase the solubility. For drug substances that exhibit polymorphism, i.e. where the compound can exist in two or more crystal structures, the choice of crystal structure will influence the dissolution rate if there is a difference in the solubility of each polymorphic form.

Another strategy that can be used for poorly soluble drugs is to stabilise the drug substance in an amorphous state by using polymers (Chokshi *et al.*, 2007; Thybo *et al.*, 2008). The high-energy amorphous state has a higher dissolution rate than the crystalline form and this might result in an increased bioavailability. The amorphous state is normally physically unstable, so if it has not been stabilised in some way there might be a transformation into a crystalline phase over time.

The important parameters of the dissolution test include the volume and composition of the dissolution medium as well as the hydrodynamics employed and the duration of the test. These parameters influence the dissolution by exerting effects on solubility, effective surface area or diffusivity of the drug substance (Dressman *et al.*, 1998; Nicolaidis *et al.*, 2001). The test conditions normally employed, and alternative suggestions, will be presented in a later section of this chapter.

### 4.1.3 Factors influencing dissolution *in vivo*

When considering the *in vivo* dissolution rate of a drug substance, this will be influenced by the interplay with the physiological conditions in the



**Table 4.1.1** Physicochemical and physiological parameters important to drug dissolution in the gastrointestinal tract; modified from Dressman *et al.* (1998)

<i>Factor</i>	<i>Physicochemical parameter</i>	<i>Physiological parameter</i>
Surface area of drug ( $S$ )	Particle size, wettability	Surfactants in gastric juice and bile
Diffusivity of drug ( $D$ )	Molecular size	Viscosity of luminal contents, diffusivity of mixed micelles
Boundary layer thickness ( $\delta$ )		Motility pattern, flow rate
Solubility ( $C_s$ )	Hydrophobicity, crystal structure, $pK_a$	pH, buffer capacity, bile, food
Amount of drug already dissolved ( $X_d$ )	Particle size, wettability, solubility	Permeability
Volume of solvent available ( $V$ )		Secretions, co-administered fluids

GI tract and the physicochemical properties of the drug substance as well as by the properties of the pharmaceutical formulation. In Table 4.1.1 these factors are summarised according to the parameters from the Noyes–Whitney equation.

The aim of investigating *in vitro* dissolution for an oral solid dosage form is, in the present context, to obtain an estimate of its *in vivo* dissolution. This is a difficult task, considering the very complex nature of the GI tract. Reference is made to Chapter 3.1 where the GI tract is described. The present section will focus on some of the characteristics of the GI tract that are important to the dissolution process. The *in vivo* dissolution may be influenced by volume, pH and composition of the GI fluids. Furthermore, the hydrodynamics and the transit times in the different parts of the GI tract may have an influence on the *in vivo* dissolution rate.

The volume of the fasted stomach can be as low as 20–50 ml (Davenport, 1977; Dressman *et al.*, 1998) but changes when a drug is administered together with fluid. In the fed state, the volume is dependent on the composition and the volume of the meal. The capacity of the human stomach is approximately 1–1.6 l (Kaarli, 1995). The volume of the fasted small intestine has been found to be 120–350 ml (Dillard *et al.*, 1965), while Fordtran and Lochlear (1966) reported volumes in the upper small intestine in the fed state of up to 1.6 l. There is a large fluid flow in the intestines, with an average of 9 l being presented to the

intestines per day. Approximately 2 l originate from oral ingestion and 7 l from endogenous secretions (Chang and Rao, 1994). The fluid volume is lower in the distal parts of the intestines, where approximately 1.5 l enters the colon daily and about 1.3 l is absorbed during the passage of the chyme in the colon.

The pH of gastric fluid in the fasting stomach is between 1.5 and 2.9 (Dressman *et al.*, 1990; Lindahl *et al.*, 1997; Kalantzi *et al.*, 2006), while the pH of the fed stomach is dependent on the composition of the meal; pH values up to 5 have been reported in the stomach contents after intake of a meal (Dressman *et al.*, 1990). In the fasted duodenum and upper jejunum, average pH values between 6 and 7.1 have been observed (Dressman *et al.*, 1990; Lindahl *et al.*, 1997; Fallingborg, 1989; Kalantzi *et al.*, 2006). Food intake results in a slight reduction in the upper intestinal pH; values in the range 5.5 to 6.5 have been reported (Fallingborg *et al.*, 1989; Persson *et al.*, 2005; Kalantzi *et al.*, 2006).

The surface tension in the GI fluids is much lower than that of water, which is  $72 \text{ mN m}^{-1}$ . Values between 30 and  $50 \text{ mN m}^{-1}$  have been reported in gastric fluids from fasted subjects (Finholt and Solvang, 1968; Efentakis and Dressman, 1998; Pedersen *et al.*, 2000; Kalantzi *et al.*, 2006). In the fasted small intestine, the surface tension has been measured to be between 30 and  $34 \text{ mN m}^{-1}$  (Pedersen *et al.*, 2000; Kalantzi *et al.*, 2006). In the fed state, the surface tension in the stomach is dependent on the composition of the meal, while it does not change in the upper small intestines between the fasted and fed state (Persson *et al.*, 2005; Kalantzi *et al.*, 2006).

Besides lowering the surface tension of the GI fluids, the presence of endogenous surfactants in the GI tract can be expected to increase the solubility of poorly soluble drug substances as well as giving a better wetting of solid particles compared to water. The main endogenous surfactants in the small intestines are bile salts and phospholipids from bile. After food intake, several surfactants from the meal may be present, e.g. proteins and dietary phospholipid. Digestion of food can also produce surfactants, such as fatty acids and monoglycerides generated by lipolysis of triacylglycerides from fats. Furthermore, it is also important to consider the presence of salts, impacting the ionic strength in the GI fluids. Then there is the issue of a possible interaction between a drug substance and the ingested food, which should be taken into account when developing an oral pharmaceutical formulation.

The residence times or transit times through the different compartments in the GI tract are shown in Table 3.1.2 in Chapter 3.1. It is

important to take these into account when deciding how long to conduct the dissolution test for. The data in Table 3.1.2 are average values and it might be important to consider the range of residence times in some cases. Absorption of drug substance occurs primarily in the intestine, so the gastric emptying of fluid or particle matter is one rate-limiting factor for the absorption process. In case of the fasted state, the gastric emptying is dependent on the motility phase present when the drug is ingested. In the fasted state there is a cyclic motility pattern present in the stomach and intestines. This pattern is described by three, sometimes four phases (Oberle and Amidon, 1987; Sarna, 1985). Phase I is the quiescent period with no activity. Phase II consists of intermittent and irregular contractions which gradually increase to a short period of intense contractions called phase III. Phase III is also called the housekeeper wave or the interdigestive migrating motor complex (MMC). Phase IV is the short transition period between phases III and I. The gastric emptying of aqueous solutions in fasted human subjects for 50 ml and 200 ml has been shown to give a  $t_{50\%}$  between 5 and 61 min, depending on which phase was present when the solution was ingested (Oberle *et al.*, 1990). The gastric emptying of non-disintegrating tablets, e.g. modified-release dosage forms, in the fasted state typically follows the MMC phase III, the housekeeper wave. This results in a large variation in the gastric emptying time within the 2 h that the MMC cycle usually lasts (Podczek *et al.*, 2007a,b). The presence of food in the stomach has been shown to delay the emptying of larger single units such as tablets and capsules, while emptying of small pellets was not greatly affected by the fed state (Davis *et al.*, 1986). Gastric residence times from a few minutes to many hours have been reported in the literature (Fallingborg *et al.*, 1989; Davis *et al.*, 1986; Podczek *et al.*, 2007c).

The intestinal transit times of pharmaceutical dosage forms including data from both the fasted and the fed state have been measured to be between 2 and 5 hours (Davis *et al.*, 1986). These data included the small intestinal transit time of solutions, pellets and large single-unit dosage forms.

*In vivo* the drug substance disappears after release from an oral dosage form, due to absorption to the systemic circulation. Therefore, it is often assumed that sink conditions are present *in vivo*. For simulations of dissolution in the stomach, sink conditions do not represent a problem, since absorption across the gastric mucosa is usually negligible. However, for highly permeable drugs with fast absorption, sink conditions might be maintained in the small intestine.

#### 4.1.4 Dissolution equipment described in the pharmacopoeias

The Ph Eur and the USP describe four different types of dissolution equipment for oral dosage forms: the basket (Apparatus 1, Figure 4.1.1) and the paddle (Apparatus 2, Figure 4.1.2), both appearing in the pharmacopoeias in the 1970s, and the reciprocating cylinder (Bio-Dis, apparatus 3, Figure 4.1.3) and the flow-through apparatus (apparatus 4, Figure 4.1.4) that were included in 1990s. One further piece of equipment for the determination of the intrinsic dissolution of a pure drug substance is described in the pharmacopoeias.

A number of other pieces of specialised dissolution apparatus have been proposed over the years, and the reader is referred to Shiu (1996) for further details. Furthermore, guidelines for dissolution testing of novel or special dosage forms from the FIP and American Association of Pharmaceutical Scientists (AAPS) has been published. These include dosage forms such as suspensions, chewable tablets, transdermal patches and implants (Siewert *et al.*, 2003).

The basket, paddle, flow-through apparatus and intrinsic dissolution will be described in more detail in the following sections. The reciprocating cylinder apparatus can be applied to material that is contained in the glass reciprocating cylinder and does not go through the mesh screen (see Figure 4.1.3). The reciprocating cylinder is advantageous over the closed systems (see later) in that the dosage form can move about freely and does not come into contact with the walls (Esbelin *et al.*, 1991). In the commercially available apparatus there are several glass vessels for each reciprocating cylinder and this makes it possible to change the dissolution medium several times in one test.

##### 4.1.4.1 The paddle and basket apparatus

The most commonly used pieces of dissolution equipment are the basket and the paddle apparatuses. They can be characterised as ‘stirred beaker’ methods and are simple, robust, well standardised and easy to use. They are also referred to as ‘closed systems’ because they use a fixed volume of dissolution medium (Shiu, 1996; Dressman, 2000). The basket method is generally preferred for capsules, whereas tablet dissolution is performed using the paddle method. If the paddle method is employed for capsules, sinkers can be used to keep the capsules from floating. Sinkers are made of non-reactive material, and several designs and sizes are available on the market.

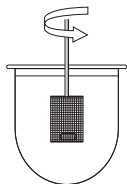


**Figure 4.1.1** Dissolution apparatus 1 (basket).

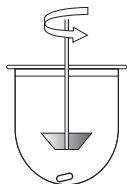


**Figure 4.1.2** Dissolution apparatus 2 (paddle).

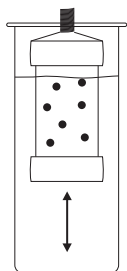


**Figure 4.1.3** Dissolution apparatus 3 (reciprocating cylinder).

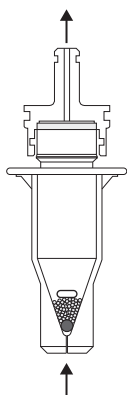


**Figure 4.1.4** Dissolution apparatus 4 (flow through).

For the basket and paddle apparatus, vessels of 1, 2 or 4 l can be employed. The 1 l vessel is the most commonly used, with typical volumes of 500, 900 or 100 ml dissolution medium. Dressman *et al.* (1998) suggest a medium volume of 300 ml to simulate the fasted stomach, 500 ml for the fasted small intestine, and up to 1000 ml for fed-state conditions in the stomach and small intestine. The USP suggests the use of medium volumes up to 2 l for poorly soluble drug substances. The quantity of the medium should be at least three times the amount required to form a saturated solution of the compound in order to obtain sink conditions.

In general, mild agitation is to be used during dissolution testing to allow maximum discriminating power. The FDA recommends rotating speeds of 50–100 rpm for the basket method and 50–75 rpm for the paddle method for testing solid oral dosage forms (FDA, Center for Drug Evaluation and Research, 1997). The Ph Eur (2.9.3) suggests the use of speeds between 50 and 100 rpm for both methods and that the speed must not exceed 150 rpm.

#### 4.1.4.2 Flow-through dissolution apparatus

In the flow-through apparatus, the dosage form is placed in a small vertical cylinder flow cell that is flushed continuously in an upward direction with a stream of dissolution medium (see Figure 4.1.4). The bottom cone is usually filled with 1 mm glass beads with one glass bead of 5 mm at the apex to protect the fluid entry tube. A laminar flow is secured by placing these small glass beads in the bottom of the flow cell (Zhang *et al.*, 1994). In the inner top of the cell, a glass-fibre filter can be placed. The dosage form can be placed on top of the glass beads as recommended in the pharmacopoeias, but can also be embedded in the glass beads. The placement of the dosage form will impact on the dissolution rate. Besides the placement of the dosage form, the main parameters determining the dissolution in the flow-through dissolution cell are the flow rate, the dissolution time and the composition of the dissolution media.

There are two sizes of flow cell described in the pharmacopoeias; one large cell with a diameter of 22.6 mm (shown in Figure 4.1.4) and one small cell with a diameter of 12 mm. The flow rates suggested in Ph Eur and USP are 4, 8 and 16 ml min<sup>-1</sup>. The intestinal fluids' axial velocity has been estimated to be in the region of 1.5 cm min<sup>-1</sup>, while the fluid flow inside the 22.6 mm cell is 1, 2 and 4 cm min<sup>-1</sup> for the dissolution medium flow rates of 4, 8 and 16 ml min<sup>-1</sup>, respectively (Fotaki *et al.*, 2005). The flow pattern in the flow-through dissolution equipment is unidirectional and probably unrepresentative of the segmental mixing in the intestine.

*In vitro–in vivo* correlations may be obtained by performing the dissolution test at a higher flow rate to compensate for the lack of destructive hydrodynamics. The *in vitro–in vivo* correlation between different flow rates as well as different dissolution media employed in the flow-through apparatus has been discussed by Sunesen *et al.* (2005).

One advantage is that the flow-through apparatus offers the possibility of maintaining sink conditions by continuous removal of dissolved drug (Zhang *et al.*, 1994; Perng *et al.*, 2003). However, the flow-through method has not been routinely used for immediate-release products, mainly because it is laborious and expensive due to the need for large volumes of medium. It is mainly used in cases where the performance of the paddle and basket apparatus is unsatisfactory. For several formulations though, the flow-through apparatus has been found to be superior to the paddle apparatus in achieving *in vitro–in vivo* correlation for several formulations (Ammar and Khalil, 1993; Butler and Bateman, 1998; Bloomfield and Butler, 2000).

#### 4.1.4.3 Intrinsic dissolution

The intrinsic dissolution rate is often measured on the pure drug substance in the early development phase during the development of new drugs in the industry. According to the USP:

The measurement of intrinsic dissolution rates is a tool in the functionality and characterisation of bulk drug substances and excipients. The intrinsic dissolution rate is defined as the dissolution rate of pure substance under the condition of constant surface area (USP 28, 1087).

When testing the intrinsic dissolution rate, the substance is compacted at high compression force to obtain a disk with a smooth surface area. This is normally done without adding any excipient such as lubricants or binders. The disk is preferably compressed in the disk holder but can also be compressed and then placed in a disk holder.

When studying different polymorphs of a substance, it might be necessary before measuring the dissolution rate to check if the high compression force imposes a change in the crystal structure.

The advantage of the intrinsic dissolution apparatus is that the area of drug is kept constant during dissolution and that the hydrodynamics are well defined. Equation 4.1.2, developed by Levich in 1962, can be used for calculations of intrinsic dissolution rate results:

$$J = 0.62D^{2/3}\nu^{-1/6}\omega^{1/2}C_s \quad (4.1.2)$$

where  $J$  is the flux,  $D$  is the diffusion coefficient,  $\nu$  is the kinematic viscosity,  $\omega$  is the rotational speed and  $C_s$  is the saturation solubility in the dissolution medium. Yu *et al.* (2004) have suggested that measurements of the intrinsic dissolution rates can be used for classifying drug substances into the BCS as low- or high-solubility drug substances. They measured the dissolution rate of 15 model drug substances and found that a dissolution rate of  $0.1 \text{ mg min}^{-1} \text{ cm}^{-2}$  was the class boundary unless the dose of the drug substance was extremely low or high (Yu *et al.*, 2004).

#### 4.1.5 Selection of dissolution media for *in vitro* dissolution studies

The testing conditions should be based on physicochemical characteristics of the drug substance and the environmental conditions the dosage form might be exposed to after oral administration (FDA, Center for Drug Evaluation and Research, 1997).

Very often the *in vitro* dissolution is more sensitive to variations than the *in vivo* performance. Thus, to achieve predictive *in vitro* data, it is important to identify and incorporate the rate-limiting physiological variable for *in vivo* dissolution (Shah and Lesko, 1995).

##### 4.1.5.1 Compendial dissolution media

According to the USP, the pH of a dissolution medium for an oral dosage form should be in the physiological range of 1.2 to 6.8. For modified-release dosage forms, pH values up to 7.5 could be evaluated, due to the potential release for the drug substance in the lower regions of the intestine. For certain drug substances it can also be of relevance to measure the pH change in the medium during the dissolution test.

Several buffer solutions are suggested in the Ph Eur and USP to perform dissolution at different pHs. In Table 4.1.2 the examples of dissolution media from the Ph Eur are shown. Reference is made to the pharmacopoeias for details on how to prepare these dissolution media.

The pharmacopoeias also recommend the use of media that are closer to the *in vivo* fluids, e.g. simulated (or artificial) gastric juice containing pepsin in addition to HCl and NaCl. Inclusion of pepsin in the dissolution medium might be appropriate when working with gelatine capsules. The media recommended by the Ph Eur as 'simulated intestinal fluid' contain a phosphate buffer (pH 6.8) and pancreas powder. However, it should be noted that these media do not have the lower surface tension that



**Table 4.1.2** Examples of dissolution media from Ph Eur's chapter on 'Dissolution test for solid dosage forms' monograph 2.9.3

<i>pH</i>	<i>Dissolution media</i>
1.0	0.2 M HCl
1.2	85 mM HCl, 50 mM NaCl
1.5	41.4 mM HCl, 50 mM NaCl
4.5	0.1 M phosphate or 22 mM sodium acetate and 28 mM acetic acid = acetate buffer
5.5 and 5.8	0.1 M phosphate buffer or 44 mM sodium acetate and 6 mM acetic acid = acetate buffer
6.8	50 mM phosphate buffer
7.2 and 7.5	50 mM phosphate buffer

characterises the human GI fluids; furthermore, the activity of the added enzymes is not controlled.

In order to simulate transfer from the stomach to the intestine, a change of media during dissolution is also recommended by the pharmacopoeias. This is especially relevant for enteric-coated or delayed-release dosage forms. The pharmacopoeias recommend two different methods for changing the pH during a dissolution test, both meant for the paddle and basket methods. 'Method A' is performed in one vessel, while 'method B' includes transfer of the dosage form from a vessel containing an acidic medium simulating the gastric fluid, to a vessel containing a medium buffered at pH 6.8. For 'method A', the first part of the study is performed in 750 ml 0.1 M HCl. After 2 h, 250 ml of 0.2 M phosphate buffer is added and the pH adjusted to 6.8. The test continues for 45 min or for the specified time. The dissolution medium for 'method B' prescribes 1 l 0.1 M HCl for 2 h and 1 l phosphate buffer, pH 6.8 for 45 min, or for the specified time.

#### 4.1.5.2 Biorelevant dissolution media

Media simulating the gastric and intestinal fluids to a much higher degree than the compendial media described above have also been developed; these are the so-called biorelevant media.

As already described, fasted-state gastric fluids are characterised by a lower surface tension than water, and a pH between 1.5 and 2.9, which is higher than the pH of compendial gastric media. Vertzoni *et al.* (2005) proposed a fasted-state gastric medium (fasted-state simulated gastric

**Table 4.1.3** Examples of biorelevant dissolution media. FaSSGF: fasted-state simulated gastric fluid; FeSSGF: fed-state simulated gastric fluid; FaSSIF: fasted-state simulated intestinal fluid; FeSSIF: fed-state simulated intestinal fluid

	FaSSGF	FeSSGF	FaSSIF	FaSSIF-v2	FeSSIF	FeSSIF-V2
Milk:buffer	–	1:1	–	–	–	–
Sodium taurocholate (mM)	0.08	–	3	3	15	10
Lecithin (mM)	0.02	–	0.75	0.2	3.75	2
Glycerol mono-oleate (mM)	–	–	–	–	–	5
Sodium oleate (mM)	–	–	–	–	–	0.8
Pepsin (mg ml <sup>-1</sup> )	0.1	–	–	–	–	–
Sodium chloride (mM)	34.2	237.02	106	68.62	173	125.5
Acetic acid (mM)	–	17.12	–	–	144	–
Sodium acetate (mM)	–	29.75	–	–	–	–
Sodium dihydroxy phosphate (mM)	–	28.66	–	–	–	–
Sodium hydroxide (mM)	–	–	–	34.8	–	81.65
Maleic acid (mM)	–	–	–	19.12	–	55.02
pH	1.6	5	6.5	6.5	5	5.8
Osmolality (mOsmol l <sup>-1</sup> )	120.7 ± 2.5	400	270 ± 10	180 ± 10	63 ± 10	390 ± 10
Buffer capacity	–	25	12	10	76	25

fluid; FaSSGF) with a pH of 1.6 and a reduced surface tension mediated by pepsin and low levels of taurocholate and phospholipids (see Table 4.1.3). FaSSGF was shown to give an *in vitro* dissolution profile of several drug models that predicted the *in vivo* dissolution in a satisfactory way.

Simulating the post-prandial stomach is complex, since the fed-state gastric fluids will be very dependent on the food ingested. Milk and nutritional drinks have been suggested as fed-state gastric media (Macheras *et al.*, 1987; Galia *et al.*, 1998; Klein *et al.*, 2004), used both pure and diluted with different buffers. Recently Jantratid *et al.* (2008) proposed the use of three media simulating the content of the fed stomach over time after meal intake. In order to simulate early digestion, pure milk adjusted to pH 6.5 was used; later digestion stages were simulated by milk:buffer 1:1 at pH 5, while milk:buffer 1:3 at pH 3 was used to

simulate late phases in digestion. The buffer capacity of the media and osmolality were also taken into account. However, the final proof of the adequacy of any of these media to simulate the actual *in vivo* dissolution of a given compound is yet to be demonstrated.

Many different media simulating the intestinal fluids have also been recommended. In 1998 Dressman and co-workers (Galia *et al.*, 1998) proposed a fasted-state simulated intestinal fluid (FaSSIF) and a fed-state simulated intestinal fluid (FeSSIF), the two media diverging by the level of taurocholate, the osmolality and the pH (see Table 4.1.3). These media have since been widely used in both industry and academia to characterise drugs and formulations. However, the FeSSIF media do not contain surface-active compounds like fatty acids and monoglycerides generated from digestion of lipids and other food components in the intestine. Other media containing lipid-digestion products have been included in biorelevant media used for solubility studies (Grove *et al.*, 2005; Nielsen *et al.*, 2005). Lipid-digestion products have been shown to be very important in simulating *in vivo* drug dissolution in the fed state (Sunesen *et al.*, 2005; Lue *et al.*, 2008). In these two publications, it is found that *in vivo-in vitro* correlation in the fed state can only be achieved by the use of biorelevant dissolution media containing lipid-digestion products. Recently, a modification of media simulating the upper small intestinal fluids was suggested (Jantratid *et al.*, 2008). Here the authors have included lipid-digestion products, and also simulate different stages of digestion, with different level of surfactants. However, the final proofs of the *in vivo* relevance of these media are still awaited.

#### 4.1.6 Conclusions

Standardised dissolution tests are described in the pharmacopeias and are used for quality control for most oral dosage forms. During development of an oral pharmaceutical formulation, dissolution tests are used on several levels: to determine the intrinsic dissolution rate of the drug substance, and to characterise the drug release from the formulations in the development phase. Usually a specific dissolution profile, employing a specific dissolution test, is desired and the development work aims to achieve this profile.

It is always relevant to consider the correlation with the *in vivo* situation, since formulation optimisation only makes sense if the *in vitro* dissolution profile reflects the *in vivo* conditions. Here it should be considered that the dissolution test apparatuses and media described in the pharmacopeias are very far from the *in vivo* situation. The *in vivo*

dissolution process is very complicated and the geometry and hydrodynamics prevailing in the *in vitro* dissolution test are very different from these. However, several publications have reported on achieving *in vitro*–*in vivo* correlation, so by using well-selected *in vitro* dissolution conditions, it seems to be possible to simulate the *in vivo* situation.

## References

- Abdou HM (1989). Theory of dissolution. In: Abdou HM, ed. *Dissolution, Bioavailability and Bioequivalence*. Easton: MACK Publishing Company, 11–36.
- Ammar HO, Khalil RM (1993). Discrepancy among dissolution rates for commercial tablets as a function of dissolution method. *Pharmazie* 49: 746–748.
- Bloomfield MS, Butler WCG (2000). Robustness testing, using experimental design, of a flow-through dissolution method for a product where the actives have markedly differing solubility properties. *Int J Pharm* 206: 55–61.
- Brunner E (1904). Reaktionsgeschwindigkeit in heterogenen systemen. *Zeitschrift f Physik Chemie* 47: 56–102.
- Butler WCG, Bateman SR (1998). A flow-through dissolution method for a two component drug formulation where the actives have markedly differing solubility properties. *Int J Pharm* 173: 211–219.
- Chang EB, Rao MC (1994). Intestinal water and electrolyte transport mechanism of physiological and adaptive responses. In: Johnson LR, ed. *Physiology of the Gastrointestinal Tract*, 3rd edn. New York: Raven Press, 2027–2081.
- Chokshi RJ, Zia H, Sandhu HK, Shah NH, Malick WA (2007). Improving the dissolution rate of poorly water soluble drug by solid dispersion and solid solution – pros and cons. *Drug Deliv* 14: 33–45.
- Davenport HW (1977). *Physiology of the Intestinal Tract. An introductory text*, 4th edn. Chicago: Year Book Medical Publishers, Inc.
- Davis SS, Hardy JG, Fara JW (1986). Transit of pharmaceutical dosage forms through the small intestine. *Gut* 27: 886–892.
- Dillard RL, Eastman H, McClean SW (1965). Volume–flow relationship during the transport of fluid through the human small intestine. *Gastroenterology* 49: 58–66.
- Dressman JB, Reppas C (2000). *In vitro*–*in vivo* correlations for lipophilic, poorly water-soluble drugs. *Eur J Pharm Sci* 11: S73–80.
- Dressman JB, Berardi RR, Dermentzoglou LC, *et al.* (1990). Upper gastrointestinal (GI) pH in young, healthy men and women. *Pharm Res* 7: 756–761.
- Dressman JB, Amidon GL, Reppas C, Shah VP (1998). Dissolution testing as a prognostic tool for oral drug absorption: immediate release dosage forms. *Pharm Res* 15: 11–22.
- Efentakis M, Dressman JB (1998). Gastric juice as a dissolution medium: surface tension and pH. *Eur J Drug Metab Pharmacokinet* 23: 97–102.
- Esbelin B, Beyssac E, Aiache JM, Shiu GK, Skelly JP (1991). A new method of dissolution *in vitro*, the ‘Bio-Dis’ apparatus: comparison with the rotating bottle method and *in vitro*: *in vivo* correlations. *J Pharm Sci* 80: 991–994.
- European Pharmacopoeia*, 6th edn (2009). <http://online6.edqm.eu/ep604/> (accessed 28 April 2009).

- Fallingborg J (1989). Intraluminal pH of the human gastrointestinal tract. *Dan Med Bull* 46: 183–196.
- FDA, Center for Drug Evaluation and Research (1997). *Guidance for Industry: dissolution testing of immediate release solid oral dosage forms*. <http://www.fda.gov/downloads/Drugs/GuidanceComplianceRegulatoryInformation/Guidances/UCM070237.pdf> (accessed 3 June 2009)..
- Finholt P, Solvang S (1968). Dissolution kinetics of drugs in human gastric juice – the role of surface tension. *J Pharm Sci* 57: 1322–1326.
- FIP (1997). Guidelines for dissolution testing of solid oral products, joint report of the Section for Official Laboratories and Medicines Control Services and the Section of Industrial Pharmacists of the FIP. *Dissol Technol* 4(4): 5–14.
- Fordtran JS, Lochlear TW (1966). Ionic constituents and osmolality of gastric and small intestinal fluids after eating. *Am J Dig Dis* 11: 503–521.
- Fotaki N, Symillides M, Reppas C (2005). *In vitro* versus canine data for predicting input profiles of isosorbide-5-mononitrate from oral extended release products on a confidence interval basis. *Eur J Pharm Sci* 24: 115–122.
- Galia E, Nicolaides E, Horter D, *et al.* (1998). Evaluation of various dissolution media for predicting *in vivo* performance of class I and II drugs. *Pharm Res* 15: 698–705.
- Grove M, Pedersen GP, Nielsen JL, Müllertz A (2005). Bioavailability of seocalcitol I: Correlating solubility in biorelevant media with oral bioavailability in rats – effect of medium and long chain triglycerides. *J Pharm Sci* 94: 1830–1838.
- Jantratid E, Janssen N, Reppas C, Dressman JB (2008). Dissolution media simulating conditions in the proximal human gastrointestinal tract: an update. *Pharm Res* 25: 1663–1676.
- Kalantzi L, Goumas K, Kalioras V, *et al.* (2006). Characterization of the human upper gastrointestinal contents under conditions simulating bioavailability/bioequivalence studies. *Pharm Res* 23: 165–176.
- Kararli TT (1995). Comparison of the gastrointestinal anatomy, physiology, and biochemistry of humans and commonly used laboratory animals. *Biopharm Drug Dispos* 16: 351–380.
- Klein S, Butler J, Hempenstall JM, Reppas C, Dressman JB (2004). Media to simulate the postprandial stomach I. Matching the physicochemical characteristics of standard breakfasts. *J Pharm Pharmacol* 56: 605–610.
- Levich VG (1962). Convective diffusion in liquids. In: Amundson NR, ed. *Physico-chemical Hydrodynamics*. Englewood Cliffs: Prentice-Hall Inc, 39–138.
- Lindahl A, Ungell AL, Knutson L, Lennernäs H (1997). Characterization of fluids from the stomach and proximal jejunum in men and women. *Pharm Res* 14: 497–502.
- Lue B-M, Nielsen FS, Magnussen TL, *et al.* (2008). Using biorelevant dissolution to obtain IVIVC of solid dosage forms containing a poorly-soluble model compound. *Eur J Pharm Biopharm* 69: 648–657.
- Macheras P, Koupparis M, Apostolelli E (1987). Dissolution of 4 controlled-release theophylline formulations in milk. *Int J Pharm* 36: 73–79.
- Nernst W (1904). Theorie der reaktionsgeschwindigkeit in heterogenen systemen. *Z Phys Chem* 47: 52–55.

- Nicolaides E, Symillides M, Dressman JB, Reppas C (2001). Biorelevant dissolution testing to predict the plasma profile of lipophilic drugs after oral administration. *Pharm Res* 18: 380–388.
- Nielsen FS, Müllertz A (2005). Development of *in vitro* methods for the evaluation of formulation performance. In: Pouton C, ed. Drug candidate optimization and early development. *Bulletin Technique Gattefossé* 98: 75–87.
- Noyes AA, Whitney WR (1897). The rate of solution of solid substances in their own solutions. *J Am Chem Soc* 19: 930–934.
- Oberle RL, Amidon GL (1987). The influence of variable gastric emptying and intestinal transit rates in the plasma level curve of cimetidine: an explanation for the double peak phenomenon. *J Pharmacokinet Biopharm* 15: 529–544.
- Oberle RL, Chen TS, Lloyd C, *et al.* (1990). The influence of the interdigestive migrating myoelectric complex on the gastric emptying of liquids. *Gastroenterology* 99: 1275–1282.
- Pedersen BL, Mullertz A, Brondsted H, Kristensen HG (2000). A comparison of the solubility of danazol in human and simulated gastrointestinal fluids. *Pharm Res* 17: 891–894.
- Perng CY, Kearney AS, Palepu NR, Smith BR, Azzarano LM (2003). Assessment of oral bioavailability enhancing approaches for SB-247083 using flow-through cell dissolution testing as one of the screens. *Int J Pharm* 250: 147–156.
- Persson EM, Gustafsson AS, Carlsson AS, *et al.* (2005). The effects of food on the dissolution of poorly soluble drugs in human and in model small intestinal fluids. *Pharm Res* 22: 2141–2151.
- Podczek F, Course NC, Newton JM, Short MB (2007a). The influence of non-disintegrating tablet dimensions and density on their gastric emptying in fasted volunteers. *J Pharm Pharmacol* 59: 23–27.
- Podczek F, Course N, Newton JM, Short MB (2007b). Gastrointestinal transit of model mini-tablet controlled release oral dosage forms in fasted human volunteers. *J Pharm Pharmacol* 59: 941–945.
- Podczek F, Mitchell CL, Newton JM, Evans D, Short MB (2007c). The gastric emptying of food as measured by gamma-scintigraphy and electrical impedance tomography (EIT) and its influence on the gastric emptying of tablets of different dimensions. *J Pharm Pharmacol* 59: 1527–1536.
- Sarna SK (1985). Cyclic motor activity: migrating motor complex. *Gastroenterol* 89: 894–913.
- Siewert M, Dressman J, Brown C, Shah V (2003). FIP/AAPS Guideline for Dissolution/In Vitro Release Testing of Novel/Special Dosage Forms. *AAPS Pharm Sci Tech* 4: 6–15.
- Shah VP, Lesko LJ (1995). Current challenges and future regulatory directions in *in vitro* dissolution. *Drug Inf J* 29: 885–891.
- Shiu GK (1996). Dissolution methodology: apparatus and conditions. *Drug Inf J* 30: 1045–1054.
- Sunesen VH, Pedersen BL, Kristensen HG, Müllertz A (2005). *In vivo in vitro* correlations for a poorly soluble drug, danazol, using the flow-through dissolution method with biorelevant dissolution media. *Eur J Pharm Sci* 24: 305–313.

- Thybo P, Pedersen BL, Hovgaard L, Holm R, Müllertz A (2008). Characterization and physical stability of spray dried solid dispersions of probucol and PVP-K30. *Pharm Dev Technol* 13: 375–386.
- US Pharmacopoeia (2009). <http://www.usp.org/> (accessed 28 April 2009).
- Vertzoni M, Dressman J, Butler J, Hempenstall J, Reppas C (2005). Simulation of fasting gastric conditions and its importance for the *in vivo* dissolution of lipophilic compounds. *Eur J Pharm Biopharm* 60: 413–417.
- Wang J, Flanagan DR (1999). General solution for diffusion-controlled dissolution of spherical particles. 1. Theory. *J Pharm Sci* 88: 731–738.
- Wurster DE, Taylor PW (1965). Dissolution rates. *J Pharm Sci* 54: 169–175.
- Yu LX, Straughn AB, Faustino PJ, *et al.* (2004). The effect of food on the relative bioavailability of rapidly dissolving immediate-release solid oral products containing highly soluble drugs. *Mol Pharm* 1: 357–362.
- Zhang GH, Vadino WA, Yang TT, Cho WP, Chaudry IA (1994). Evaluation of the flow-through cell dissolution apparatus: effects of flow rate, glass beads and tablet position on drug release from different types of tablets. *Drug Dev Ind Pharm* 20: 2063–2078.

# 4.2

## The Biopharmaceutics Classification System in drug discovery and development

*Chi-Yuan Wu*

There is both economic interest and medical need for exploring and improving the oral bioavailability of drugs in development. During the drug discovery process, drug candidates are screened for their ‘absorptive, distributive, metabolic and eliminative’ (ADME) properties. This is because ADME properties, which may also be called ‘drug metabolism and pharmacokinetic’ (DMPK) properties, are descriptive for evaluating the potential of the candidate to become a new drug product. Nowadays, DMPK issues are evaluated earlier in the discovery process than in former times and that is one of the reasons why the pharmaceutical industry has a higher success rate in introducing new drug substances into the market. The value of systematic approaches to predicting pharmacokinetic profiles is better appreciated, as this can drastically reduce the time and expense of drug development. Since pharmacokinetics are predicted from a limited set of input data, in the screening process a variety of algorithms have been proposed to evaluate the correlation between pharmacokinetic properties and pharmacological activities. For instance, methods to modify dissolution or aqueous solubility, decrease degradation of the drug candidate in gastric and intestinal fluids, enhance poor intestinal membrane permeation, and inhibit pre-systemic intestinal or hepatic metabolism have been proposed and studied.

Traditionally, the most pharmacologically active candidates were advanced to the next stage of development. Unfortunately, a significant percentage failed as a result of poor pharmacokinetic properties. An emerging strategy is to optimise both pharmacological activity and pharmacokinetic properties during drug discovery (see Figure 4.2.1). Bioavailability can be improved by modifying membrane permeability. Compounds with poor intestinal permeability have been associated with certain physicochemical properties, such as: low octanol/aqueous partitioning, the presence of strongly charged functional groups, high molecular



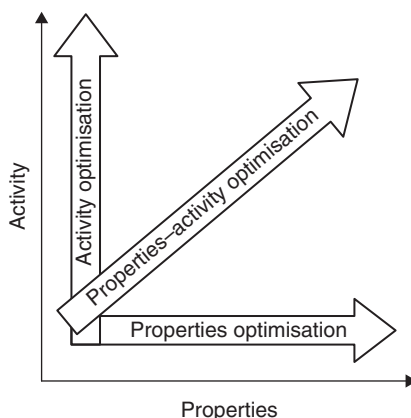


**Figure 4.2.1** Schematic representation of the pharmaceutical profiling optimisation.

weight, and a substantial number of hydrogen-bonding functional groups (Lipinski *et al.*, 1997). Lipinski's rule of five is further described in Section 2.4.1. Candidates that may benefit most from intestinal absorption-enhancing formulations usually have one or more of the above-mentioned characteristics. Typically, the drug candidates for which absorption-enhancement studies have been involved in their development, have been peptides, peptide analogues, or other polar, high molecular weight drug substances, such as heparin. For some candidates, their permeation through the intestinal epithelium is hindered by active efflux transporters that efflux or exsorb the candidates from the enterocyte back into the intestinal lumen, and/or by the candidate being degraded via drug-metabolising enzymes located in the enterocytes. The exsorptive transporters involved may include P-glycoprotein (P-gp), the family of multidrug-resistance-associated proteins (MRPs), and others. Exsorptive/efflux transporters are further described in Chapter 3.6. The main metabolising enzyme in enterocytes is cytochrome P450 3A (CYP3A). It has only recently been realised that besides physicochemical properties, these biochemical barriers (i.e. enzymes and transporters) also play an important role in controlling drug absorption.

In this chapter we will discuss and emphasise the importance of the fundamentals of the Biopharmaceutics Classification System (BCS). These fundamentals are to determine the solubility and intestinal permeability properties of candidates intended for oral absorption. However, the chapter will also discuss and emphasise how enzyme-transporter interplay can be incorporated into the BCS as a method for predicting drug disposition. The primary use of the BCS is, from a regulatory

perspective, for bioequivalence testing, i.e. to identify drugs for which *in vitro* dissolution testing could replace *in vivo* studies. However, if the BCS is useful for other reasons than regulatory issues, such as to predict drug disposition, its impact would certainly increase. Thus, we emphasise the innovative concept of the Biopharmaceutics Drug Disposition Classification System (BDDCS) implemented as a simple tool in early drug development to identify and determine the major factors for predicting the drug disposition process.

## 4.2.1 Prediction of oral drug absorption

### 4.2.1.1 The drug absorption process

The oral absorption of a drug candidate depends on the amount dissolving in the aqueous solution of the gastrointestinal tract. The term ‘oral bioavailability’ is defined by the European Medicines Agency (EMA) as the rate and extent to which the drug substance is absorbed from a pharmaceutical formulation and becomes available at the site of action (EMA, 2001). The term ‘absolute bioavailability’ is used by the American Food and Drug Administration (FDA) and many others as being equivalent to the term ‘absorption fraction’ ( $f_{\text{oral}}$ ).  $f_{\text{oral}}$  may be estimated from the dose-corrected ratio of the area under the blood concentration curve following oral administration ( $\text{AUC}_{\text{oral}}$ ) to that following intravenous administration ( $\text{AUC}_{\text{iv}}$ ), as seen from Equation 4.2.1.

$$f_{\text{oral}} = \frac{\text{AUC}_{\text{oral}}/D_{\text{oral}}}{\text{AUC}_{\text{iv}}/D_{\text{iv}}} \quad (4.2.1)$$

$D_{\text{iv}}$  and  $D_{\text{oral}}$  represent the intravenous and oral dose, respectively. However, oral bioavailability is also referred to as the fraction of the oral dose that reaches the systemic circulation. Thus, when drug-eliminating organs are arranged in series, such as the small intestine and liver (see Figure 4.2.2), bioavailability can be calculated as the product of the fractions of the dose that escape metabolism by each organ, where  $f_a$  is the fraction of an oral dose absorbed intact across the gut wall, and  $f_g$  and  $f_h$  are the fractions of the absorbed dose that escape metabolism by the intestine and liver, respectively. In fact, these three terms represent the most important properties that determine absorption after oral administration: permeability, solubility, and first-pass metabolism. The influence of these properties on the extent of absorption from the intestinal tract has attracted considerable attention (Amidon *et al.*, 1995; Norris *et al.*, 2000; Zhang

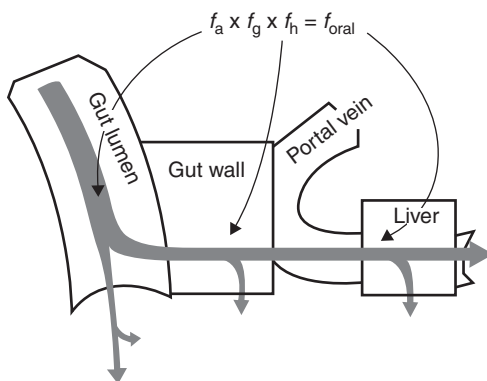


**Figure 4.2.2** Schematic simplified view of the absorption process. Oral bioavailability ( $f_{\text{oral}}$ ) is the product of the fraction of the drug dose absorbed into and through the gastrointestinal membranes ( $f_a$ ), the fraction of the absorbed dose that passes through the gut into the hepatic portal blood unmetabolised ( $f_g$ ), and the hepatic first-pass availability ( $f_h$ ). The concept emerging is that transporters would be involved with each of the absorption steps.

and Benet, 2001). Here, the discussion of these factors is divided into pre-membrane (before the drug passes across the mucosal membrane), and post-membrane (factors other than permeability and solubility). The interplay of all these factors will also be discussed.

#### 4.2.1.2 Pre-membrane prediction

The introduction of combinatorial chemistry and high-throughput pharmacological screening in drug discovery has resulted in a vast number of lead compounds. The compounds generated from a high-throughput discovery programme are generally more lipophilic and of higher molecular weight than conventional drugs (Lipinski, 2000; Lipinski *et al.*, 2001). The rate at which a drug goes into solution is an important determinant for its absorption from the gastrointestinal tract. Factors affecting the kinetics of drug dissolution can be identified by the Noyes–Whitney equation (Equation 4.2.2):

$$\left(\frac{dC}{dt}\right)_{\text{drug} \rightarrow \text{solution}} = \frac{DS}{V} \left[\frac{C_s - C}{h}\right] \quad (4.2.2)$$

where  $C$  is the concentration of solute in the bulk solution at time  $t$ ;  $C_s$  is the solubility of the solid;  $t$  is time;  $D$  is the diffusion coefficient of the drug in solution;  $S$  is the surface area of the exposed drug particle and  $h$  is the thickness of the diffusion layer.

*Dissolution* depends on the surface area of the dissolving solid and the solubility of the drug at the surface of the dissolving solid. Dissolution is further described in Chapter 4.1 and solubility in Chapter 2.1. Considering surface area and solubility factors separately, surface area is manipulated by processing and formulation, whereas solubility is manipulated mainly by changing the chemical structure or salt of the candidate. The solubility of a drug candidate is inversely proportional to the number and type of lipophilic functionalities within the molecule. The dissolution rate of a drug candidate is affected by its solubility, i.e. its actual concentration in the aqueous phases of the gastrointestinal (GI) fluids. The concentration of drug candidate in solution determines the driving force through it, and thus its membrane transfer into the body. Formulation scientists primarily use dissolution to evaluate the properties of the drug itself and thereby select appropriate formulations. Clinical scientists primarily use dissolution tests to establish *in vitro*–*in vivo* correlations between drug release from the dosage form and drug absorption.

Simple approaches are used for identifying easily computed descriptors that may be applied in predicting intestinal absorption of leads and that can dramatically improve the speed of selection of lead compounds. One widely used approach is *Lipinski's 'rule of five'* (Lipinski *et al.*, 1997). It is proposed that membrane transfer may be limited by various factors; i.e. poor permeability is more likely when:

- there are more than five H-bond donors (sums of OHs and NHs)
- there are more than 10 H-bond acceptors (sums of Ns and Os)
- molecular weight is over 500
- there is poor dissolution resulting from  $\log P > 5$ .

Lipinski's rule of five is described in more detail in Chapter 2.4. It should be kept in mind that substrates of any transporters are considered exceptions to the rule. Among several thousand drugs tested, some drug classes fell outside the rule of five: antibiotics, antifungals, vitamins and cardiac glycosides (Lipinski *et al.*, 1997). When the rule of five was developed, the knowledge about drug transporters was very limited. It is now believed that almost all drug substances are substrates for some transporter (Wu and Benet, 2005; Custodio *et al.*, 2008). Studies to date have not been able to show this because we are only just beginning to gain the knowledge and tools that allow investigation of substrates for absorptive and exsorpative transporters. In addition, unless a drug substance can passively gain intracellular access, it is impossible to simply investigate whether the molecule is a substrate for efflux transporters. Despite the fact that many

drug candidates are substrates for transporters, it is not uncommon for medicinal chemists in pharmaceutical industries to be advised to only optimise drug candidates by fine tuning the ‘rule of five’ factors.

#### 4.2.1.2.1 *The Biopharmaceutics Classification System*

In 1995 Amidon *et al.* devised a Biopharmaceutics Classification System (BCS) to classify oral drug substances, based on their dose-relevant aqueous solubility and intestinal permeability, determined as extent of oral absorption (Amidon *et al.*, 1995):

- class 1: high solubility, high permeability
- class 2: low solubility, high permeability
- class 3: high solubility, low permeability
- class 4: low solubility, low permeability.

The BCS was developed to serve as a regulatory tool for identifying those substances for which *in vivo*-based bioequivalence studies can be replaced by *in vitro* dissolution studies.

The recommended methods for determining solubility and permeability are discussed later in Section 4.2.2 (FDA, Center for Drug Evaluation and Research, 2000). Basically, the waiver of bioavailability/bioequivalence is only considered by the FDA for drugs with high solubility, high permeability and rapid dissolution (class 1). The replacement of *in vivo* bioequivalence studies by *in vitro* dissolution test studies yields certain benefits. The most rewarding benefit is minimisation of drug exposure in large numbers of volunteers. Other benefits are shortened development time and reductions of study costs. To summarise, the BCS addresses the following two factors of importance to oral drug bioavailability: (1) *drug solubility* identifies when limited solubility of a drug substance may give rise to incomplete release from the dosage form; (2) *drug permeability* addresses the efficiency of drug transport across the gut wall. However, a third important factor (3) is *drug stability or metabolism* such as chemical and enzymatic stability. Stability/metabolism should also be included in the BCS and this issue will be discussed in the next section.

#### 4.2.1.2.2 *Post-membrane prediction*

Solute concentrations of a given drug substance within the GI fluids are generally much higher than its systemic concentrations, simply because its

volume of distribution within the GI fluids is generally much smaller than the total systemic volume. Therefore, an intravenously administered dose, as well as the absorbed fraction of an oral dose that reaches the systemic circulation, generally results in much lower drug concentrations at the eliminating organ compared to the concentrations in the intestine. Consequently, transporters and metabolising enzymes in eliminating organs and the drug solubility in eliminating organ fluids may be relatively unimportant, because saturation of transporters (and enzymes) will be minimal, if present at all, and solubility considerations will be unimportant because it is generally believed that only solutes are absorbed. The interactive roles of the enzymes and transporters in absorptive and distributive organs, such as the intestine and liver, become more important.

#### 4.2.1.2.2.1 Intrinsic clearance

The most important factor, governing the extent and rate of first-pass metabolism, is commonly expressed by the Michaelis–Menten equation (Equation 4.2.3):

$$v = \frac{V_{\max} \times S}{K_m + S} \quad (4.2.3)$$

where  $v$  is the rate of metabolism,  $S$  is the substrate concentration, and  $V_{\max}$  is the maximal rate at which a drug substance is metabolised.  $K_m$ , the Michaelis constant, is the substrate concentration at which the rate of metabolism is one-half of  $V_{\max}$ . The intrinsic clearance ( $CL_{\text{int}}$ ) of a drug substance in an organ is defined as the maximum inherent efficiency of the organ in eliminating the substance (Wilkinson, 1987).  $CL_{\text{int}}$  may be determined by organ perfusion studies. The ‘true’  $CL_{\text{int}}$  value will be obtained if there is no protein binding of the substance and/or if drug delivery to the organ is not limited by blood perfusion.  $CL_{\text{int}}$  is thus regarded as a measure for the organ ‘eliminative activity’. Under linear conditions,  $CL_{\text{int}}$  can be obtained by measuring the rate of substrate disappearance (or rate of metabolite formation) at different substrate concentrations, i.e. when  $S$  is much smaller than  $K_m$ ,  $CL_{\text{int}}$  is given by Equation 4.2.4:

$$CL_{\text{int}} \approx \frac{v}{S} \approx \frac{V_{\max}}{K_m} \quad (4.2.4)$$

The concept of intrinsic clearance is important not only with regard to quantitative interpretation and prediction of drug interaction within the liver, but also with regard to prediction of pharmacokinetic parameters in general.

#### 4.2.1.2.2.2 *In vivo* clearance

*In vitro* hepatic  $CL_{int}$  is most commonly used for *in vitro*–*in vivo* correlation (Houston and Carlile, 1994, 1997; Obach *et al.*, 1997). The hepatic clearance after an intravenous dose is usually used for determining the *in vivo* hepatic clearance. However, in comparison between methods, i.e. from *in vitro* microsomes to whole organ (*in vivo*), interplay between the cell membrane and intracellular metabolic events should be taken into consideration. For example, hepatic uptake and efflux transporters play important roles in drug disposition and metabolism. When considering the transporter effect on hepatic  $CL_{int}$ , it may be more correctly determined by using methodologies that preserve the transporter/enzyme architecture of the liver (e.g. hepatocytes, sandwich-type hepatocytes, perfused liver etc.) rather than methods where the architecture is not preserved, such as in microsomes. Uptake and efflux transporters may modulate a drug candidate's metabolism by altering its accessibility to the metabolising enzymes, thus changing the estimated metabolic  $CL_{int}$ . The interplay of transporters and enzymes must be considered when defining the liver  $CL_{int}$  of a drug candidate (or its  $CL_{int}$  in other organs such as the intestine and kidney), as well as when evaluating potential drug–drug interactions. In general, *in vitro* microsomal studies that show metabolism changes for a drug candidate, when an interacting substrate is added, will be predictive for *in vivo* interaction between the compounds, but will not necessarily give a quantitative prediction. However, when an *in vitro* microsomal study shows no metabolic interaction, it cannot be concluded that an *in vivo* metabolic interaction will not occur, particularly for compounds where transporter–enzyme interplay can result in significant metabolism changes due to transporter inhibition.

#### 4.2.1.2.2.3 Drug–drug interactions

Table 4.2.1 summarises the predicted changes in area under the blood concentration curve (AUC) for drug candidates that are substrates of uptake or efflux transporters.

Following oral administration of drug candidates, significant interactions will occur for candidates that are substrates for both intestinal enzymes (e.g. phase I and II enzymes) and intestinal apical efflux transporters (e.g. P-gp, MRP2, BCRP). This is because concomitant inhibition of the intestinal enzymes and the apical efflux transporter both lead to reduced gut metabolism in a way that can synergistically increase the AUC (see Table 4.2.1). It is, therefore not surprising that drugs removed from the market at the FDA's recommendation (i.e. terfenadine,

**Table 4.2.1** Predicted direction of change in systemic AUC of drug/prodrug substrates when co-administered with inhibitors to enzymes and/or transporters expressed in the intestine

	<i>Intestine</i>	
	<i>Absorptive transporter inhibited</i>	<i>Eliminative transporter inhibited</i>
No enzyme inhibition	↓	↑
Metabolising enzymes inhibited	↔↓↑	↑↑
Drug-releasing enzymes inhibited (prodrugs)	↓↓	↔↓↑

mibefradil, cisapride, cerivastatin) are predominately orally dosed drugs that are substrates for both CYP3A and P-gp.

#### 4.2.2 Application of the Biopharmaceutics Classification System

At its core, the BCS is based on experimental methods applied to permeability and solubility studies. The objective of the BCS is to predict the *in vivo* pharmacokinetic performance of drug products from measurements of permeability and solubility. The definition of solubility and permeability is defined by FDA guidance (FDA, Center for Drug Evaluation and Research, 2000) as follows:

- *solubility*: a drug substance is considered highly soluble when the highest dose strength is soluble in 250 ml or less of aqueous media over the pH range of 1–7.5. The volume estimate of 250 ml is derived from typical bioequivalence study protocols that prescribe administration of a drug product to fasting human volunteers with a glass (about 8 ounces or approximately 230 ml) of water
- *permeability*: the permeability is based indirectly on the extent of absorption (fraction of dose absorbed, not systemic bioavailability) of a drug substance in humans and directly on measurements of the rate of mass transfer across the human intestinal membrane. Alternatively, non-human systems capable of predicting the extent of drug absorption in humans can be used (e.g. *in vitro* epithelial cell culture methods). A drug substance is considered to be highly permeable when the extent of absorption in humans is determined to be 90% or more of an administered dose based on a mass balance determination or in comparison to an intravenous reference dose.



The BCS system is based on the understanding that dissolution from the dosage form depends considerably on the *solubility* of the drug substance, and that absorption from the GI tract is dependent on *permeability* properties of the drug substance. However, dissolution is also affected by the formulation. Absorption from the intestine may be influenced by GI transit time or membrane permeability. Consequently, a waiver of bioequivalence studies may only be granted for products where more than 85% of the ingredient is dissolved in 30 min in all physiological media.

#### 4.2.2.1 Regulatory aspects

The BCS is primarily used to identify what drug candidates are appropriate for replacing *in vivo* study with *in vitro* dissolution testing, i.e. bioequivalence waiver. It is now accepted that if a BCS class 1 drug substance is released from the dosage form very rapidly *in vivo*, gastric emptying will become the rate-limiting process for drug absorption. Thus, bioavailability is not dependent on biopharmaceutical properties and therefore *in vivo* investigation may be waived. Additional criteria for bioequivalence eligibility are that the drug needs to be stable in the GI fluids, and it should be a non-narrow therapeutic index drug. The general concept is that differences in bioavailability (rate and extent) may only be observed between two essentially similar (generic) products if the two dosage forms exhibit different *dissolution*. However, this statement is only valid as long as the release from the dosage form represents the rate-controlling process for drug absorption. On the other hand, if the permeation through the intestinal membrane is rate limiting, dissolution properties may be of negligible importance. BCS class 3 drugs are also proposed for waiver of bioavailability/bioequivalence studies (Blume and Schug, 1999) because they are also characterised by high solubility, and because the bioavailability is less dependent on the release properties of the formulation than on the *in vivo* permeability. The reasoning for suggesting class 3 drugs for waivers of bioavailability/bioequivalence studies was that if two drug products, containing the same drug substance, have the same concentration–time profile at the intestinal membrane surface, then they will have the same rate and extent of bioavailability. However, this might not be true because it is obvious that for drug substances of class 3, excipients from the drug formulation may affect uptake transporters and consequently modify bioavailability (Wu and Benet, 2005). Similar conclusions can be reached for class 1 drug substances: if their dissolution is rapid under all physiological pH conditions, it can be expected that they will

also behave like an oral solution *in vivo*. Consequently, generic products of BCS class 1 and 3 drugs with different *in vitro* dissolution will not necessarily exhibit different *in vivo* performances, and vice versa. Until more is known about the importance of intestinal transporters, and until validated methodologies to predict the effects of formulation excipients on these transporters have been developed, expansion of *in vivo* bioequivalence waivers beyond class 1 substances is unjustifiable.

#### 4.2.2.2 Characterisation of candidate drugs

Permeability and solubility are of key importance in the selection of drug candidates for further development. Molecules with poor permeability and/or solubility usually have low and variable bioavailability, which becomes the hurdle to be dealt with before the molecule can reach the pipeline. Experimental methods and relevant acceptance criteria, regarding permeability and solubility, are needed during the early drug discovery phase. Such procedures have also been introduced into the industry, including high-throughput solubility and permeability screening. It has even been suggested that the drug substances listed in the BCS classes 1 and 2 are eliminated primarily via metabolism, while class 3 and 4 compounds are primarily eliminated unchanged into the urine and bile (Wu and Benet, 2005). The simple categorisation under the BCS has revealed the fact that the high permeability of the class 1 and 2 drug substances means they are also readily accessible to the metabolising enzymes within hepatocytes. Figure 4.2.3 shows the characteristic relationship between BCS classes and drug disposition. It is generally believed that chemicals are biotransformed to become more polar, thus becoming

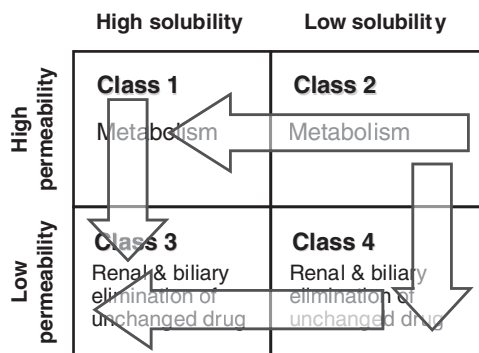


**Figure 4.2.3** Predicted routes of drug elimination based on BCS categories. The arrows indicate the direction of biotransformation.

more feasible for excretion pathways. For compounds with certain molecular weights (human: >500, rat: >350), biliary secretion may become a major excretion pathway. Note that the different permeability classes defined in the BCS do not necessarily reflect corresponding differences in permeability into hepatocytes, but rather reflect differences in access to the metabolising enzymes within the hepatocytes. Therefore, the BCS classification may correlate with the disposition characteristics of the drug substances. Certain drug substances are primarily eliminated through a metabolic pathway, the rest are removed through excretion by either biliary or renal elimination

#### 4.2.2.3 Formulation strategy

The BCS could be used as a framework to decide which types of formulation strategies are suitable for further development of a drug candidate. For candidates classified with low solubility, it is clear that bioavailability properties could be improved by formulation strategies that increase the dissolution rate and/or drug solubility, e.g. choosing the most water-soluble salt form, selecting the most soluble polymorph/anhydrate crystal form, providing the amorphous form with the most rapid dissolution, increasing solubility by super-saturation, or increasing the surface area of the crystals by micronisation, or by forming microemulsion, or nanoparticles. The optimal formulation should then provide a dissolution property that is no longer the rate-limiting step in the absorption process, i.e. situations that are comparable to those of class 1 and 3 compounds. The most straightforward way to achieve non-dissolution rate-limited absorption is to formulate the drug candidate in a solution. However, for different reasons, such as aqueous stability, it is not always feasible to formulate solutions, but rather solid dosage forms such as tablets and capsules are produced. Note that the influence of above-mentioned dissolution-enhancing strategies on biopharmaceutical classification are illustrated in Figure 4.2.4. It is very common to modify the absorption properties of low-solubility drug substances, by physical formulation strategies, into classes 1 or 3. However, it would be difficult to modify low-permeability properties by physical formulation approaches, from class 4 to class 2, or from class 3 to class 1. As illustrated in Figure 4.2.3, biotransformation alters the chemical properties of drug substances as well as their elimination characteristics (metabolism versus excretion). This is why chemical formulation approaches, such as a prodrug approach, can move candidate compounds vertically in Figure 4.2.4, i.e. between classes 3 and 1 or classes 4 and 2, as well as horizontally between

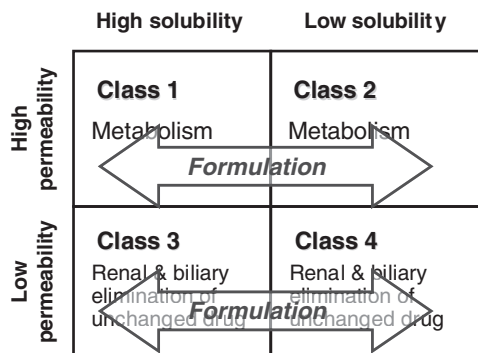


**Figure 4.2.4** Formulation approach based on BCS categories. The arrows indicate the formulation strategy between different BCS class compounds.

classes 1 and 2 or classes 3 and 4, whereas physical formulation approaches can only move drug candidates horizontally in Figure 4.2.4, i.e. between classes 1 and 2 or classes 3 and 4.

#### 4.2.2.4 Food–drug interactions

Alterations of bioavailability due to concomitant food intake can have serious implications for the clinical usefulness of a drug, and this is always in focus for clinical pharmacology profiling during drug development. It is well known that food can influence drug bioavailability, by changing the *extent* and the *rate* of availability. In December 2002, the FDA issued a guidance entitled *Food-effect Bioavailability and Fed Bioequivalence Studies* (FDA, Center for Drug Evaluation and Research, 2002). Fleisher *et al.* (1999) noted that food effects on the extent of bioavailability of drug substances could generally be predicted based on their BCS class. This observation that exposure of highly permeable and poorly soluble BCS class 2 compounds tends to be increased by high-fat meals, may be explained by increased GI fluid volume, which arises from co-administered meals stimulating GI secretions, and/or from biliary solubilisation that increases the dissolution rate. Alternatively it may be explained by food–drug interactions with transporters of BCS class 2 or 3 compounds (Wu and Benet, 2005). The fact that many water-soluble BCS class 3 substances show a sharp decrease in absorption when co-administered with a meal may either be explained by the food making a simple additional physical barrier that compromises simple diffusional permeability across the upper intestinal membrane, or by interference with the uptake mechanism between food and

class 3 drug substances. High-fat meal studies are recommended by the FDA, since such meal conditions are expected to provide the greatest effects on GI physiology, so that systemic drug availability is maximally affected and observed (FDA, Center for Drug Evaluation and Research, 2002).

#### 4.2.2.5 *In vitro*–*in vivo* correlation (IVIVC)

*In vitro* dissolution testing is an important tool in the development of solid drug products, as well as in batch quality controls. The aim of the dissolution test is to see that the drug is appropriately dissolved in the GI tract and made available for absorption. It is therefore highly desirable that the *in vitro* tests provide data that correlate well to the *in vivo* situation. Drug dissolution and intestinal permeability are the fundamental parameters governing the rate and extent of drug absorption and the expectations regarding *in vitro* dissolution and *in vitro* absorption (IVIVC) are summarised in Table 4.2.2. It is important to realise that the *in vitro* dissolution test only models the release and dissolution of the drug substance from the formulation, and it is only when these processes are rate limiting in the absorption process that IVIVC can be expected. In the case of class 1 drugs, the complete dose will already be dissolved in the stomach and, provided that absorption across the gut wall is negligible, the gastric emptying of the dissolved drug will be rate limiting for absorption. Thus, no IVIVC should be expected for class 1 compounds as long as the release of drug is faster than gastric emptying. Class 3 compounds exhibit a high variability in the rate and extent of absorption, but if dissolution is fast (such as 85% of drug dissolving in 15 min), the variation could be attributed to GI transit, luminal contents, and membrane

**Table 4.2.2** IVIVC expectations for immediate-release products based on the BCS

BCS class (rate-limiting step)	IVIVC expectations
1: gastric emptying	No IVIVC until product dissolution becomes rate-limiting step
2: dissolution	IVIVC expected provided that <i>in vitro</i> relevant dissolution test methods are used and drug absorption is limited by dissolution rate rather than by saturation solubility
3: permeability	No IVIVC until product dissolution becomes rate-limiting step
4	Limited or no IVIVC

permeation rather than dosage form factors. In this case, limited or no IVIVC is expected.

For class 2 compounds, a strong correlation between dissolution rate and the *in vivo* absorption could be difficult to establish. For example, if a rapid and complete dissolution of a class 2 compound is achieved by formulation approach, gastric emptying rather than dissolution becomes the rate-limiting step. Thus, it would be comparable to class 1 compounds. That is why no correlation would be expected in such a case. Another reason could be if absorption is limited by the saturation solubility in the GI tract rather than the dissolution rate. In this situation, the drug concentration in the GI tract will be close to the saturation solubility, and changes of the dissolution rate will not affect the plasma concentration–time profile, and consequently not the *in vivo* bioavailability. Standard *in vitro* dissolution tests are carried out under ‘sink conditions’, i.e. at concentrations well below the saturation solubility. Thus, only effects related to the dissolution rate can be predicted *in vitro*; the dissolution profile for class 2 compounds requires multiple sampling times and the use of more than one dissolution medium. For a compound that is primarily eliminated through a metabolic pathway, the other factors contributing to poor IVIVC of class 2 compounds are the interplay between transporters and enzymes. Therefore, a successful IVIVC can only be obtained after establishing a thorough understanding of the physicochemical properties as well as the uptake and elimination mechanism of the compounds.

### 4.2.3 The Biopharmaceutics Drug Disposition Classification System

The Biopharmaceutics Drug Disposition Classification System (BDDCS) was developed by Wu and Benet (2005) to predict the *in vivo* pharmacokinetic performance of drug products from measurements of permeability and solubility. The major difference between the BCS and BDDCS is the interpretation of the permeability term, which is looked upon, and consequently determined as, the extent of oral absorption in the BCS, but as the extent of metabolism (access to metabolic enzymes) in the BDDCS. In the BDDCS, the extent of metabolism is divided into drug substances that are extensively metabolised, i.e.  $\geq 70\%$  metabolism of an oral dose *in vivo* in humans, and those that are poorly metabolised; i.e.  $\geq 50\%$  of an oral dose *in vivo* in humans is excreted unchanged (Custodio *et al.*, 2008).

The BDDCS may be useful for prediction of overall drug disposition, including routes of drug elimination; the effects of efflux and

absorptive transporters on oral drug absorption; when transporter–enzyme interplay will yield clinically significant effects (e.g. low bioavailability and drug–drug interactions); the influence, mechanism and importance of food effects; and transporter effects on post-absorption systemic drug concentrations following oral and intravenous dosing. These predictions are based on a series of studies, over the past few years, in which the effect of transporter inhibition and induction on drug metabolism was investigated (Wu and Benet, 2005).

The author considers the difference between the BCS and BDDCS to be substantial. Thus, the fundamental interpretations of permeability behind the two classification systems are very different, i.e. the extent of oral absorption versus the extent of metabolism. However, the outcome from the two systems seems to be similar since, as Takagi *et al.* (2006) have pointed out, the provisional classification of the top 200 oral products on the world market is similar in the BCS and BDDCS. Thus, when the drug substance cimetidine is used as a reference for permeability, the distribution of 164 drug substances in the BCS is, respectively, 61:58:38:7 for class 1: class 2: class 3: class 4. This is very close to the distribution in the BDDCS, which is, respectively, 59:51:42:12. However, the classification part of the BDDCS is only of minor value, whereas the implication part of the BDDCS is the most innovative and valuable, because it may be applied for much more than biowaiver justification. The application of the BDDCS is described in detail in the original commentary paper as well as by Custodio *et al.* (Wu and Benet, 2005, Custodio *et al.*, 2008).

#### 4.2.3.1 The BCS from the point of view of drug disposition

As discussed earlier, Amidon *et al.* (1995) proposed using the BCS to categorise drugs into four classes according to their solubilities as well as their permeabilities through GI mucosa. Besides the regulatory applications of the BCS, it is also applied in the development process. The main merits of the BCS and BDDCS are the very clear and simple rules by which oral absorption and the extent of metabolism respectively are determined. In fact, the classification reflects the industrial optimisation process, i.e. the screening stage in new drug development. Until recently, mathematical modelling was widely used to explain and quantify the effect of a structure change on a defined biological activity.

In early drug development, the properties of candidates are always characterised to optimise pharmacokinetic performance. A typical example is depicted in Figure 4.2.5a, which shows that leads with optimal

pharmacokinetics usually have a medium partition coefficient. Properties of drug substances, such as permeability, solubility and metabolism that affect human absorption, can also be discussed in relation to the BCS. Lipinski and co-workers pointed out that identified leads from high-throughput screening (HTS-leads) tend to have higher molecular weight and lipophilicity than leads identified in the pre-HTS era (Lipinski *et al.*, 1997). In BCS terminology, this means that HTS leads tend to have limited dissolution and mainly belong to BCS class 2 (see Figure 4.2.5a).

Drug substances that are metabolised by, for example, CYP3A may have to be highly permeable in order to be metabolised within intracellular compartments. Consequently they may generally be classified as 1 or 2 in the BCS as illustrated by a darker shade in Figure 4.2.5b.

It has been suggested that drug substances should be passively *permeating* cell membranes, at least moderately, in order to be effluxed by P-gp. Such drug substances are, driven by concentration gradient, able to enter the cell by passive diffusion, but effective P-gp efflux can compete

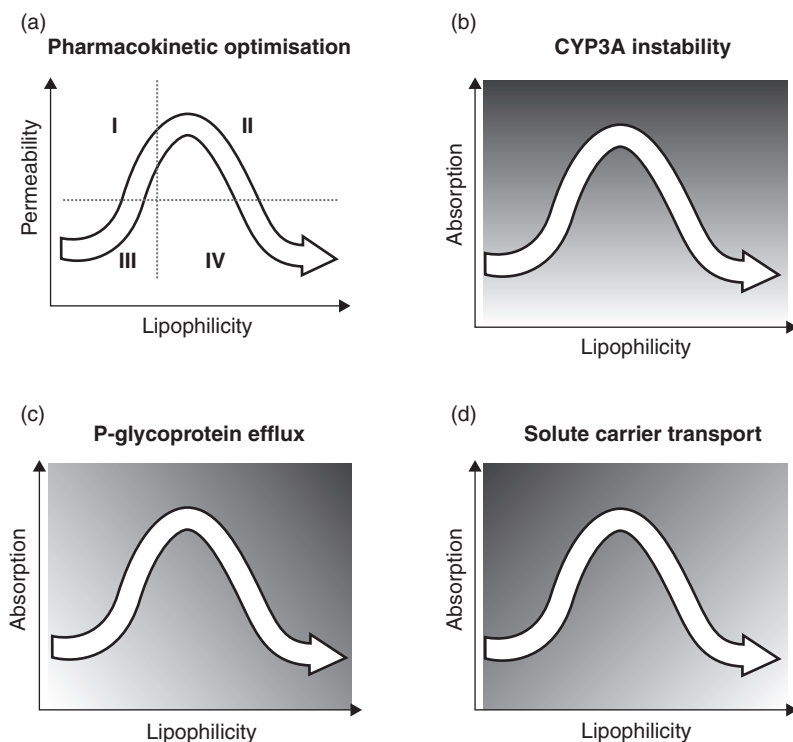


**Figure 4.2.5** The relationship between the BCS/BDDCS and drug disposition in terms of metabolic stability, P-gp efflux and solute carrier transport potential.



against its passive permeability. BCS class 1 compounds such as midazolam, with rapid transmembrane movement, may pass through the cell more quickly than P-gp can remove it (Tolle-Sander *et al.*, 2003). In contrast, compounds such as ranitidine (BCS class 3), whose passive permeability is low, may never reach the intracellular concentrations needed to be effluxed by P-gp. This is in agreement with the fact that the BCS class 2 apparently contains many P-gp substrates (Wu and Benet, 2005). Thus, in order to be P-gp substrates, drug substances should permeate biomembranes, at least moderately, by passive diffusion (Lentz *et al.*, 2000; Faassen *et al.*, 2003) and these compounds are generally characterised as lipophilic, which corresponds to P-gp substrates tending to be located in BCS class 1 or 2 as illustrated in Figure 4.2.5c by dark shading. Solute carrier substrates, on the other hand, are more hydrophilic and water soluble and need specific transport mechanisms to be efficiently absorbed. Such highly water-soluble drug substances tend to belong to BCS classes 1 and 3. This is illustrated in Figure 4.2.5d, by darker shading in classes 1 and 3. Figure 4.2.5 illustrates not only that the BDDCS is analogous to a pharmacokinetic optimisation process during pharmaceutical profiling, but also that lead identification by lead-HTS in drug development will result in more BCS class 2 compounds being developed and that this class of leads will have the highest risk of being substrates of CYP3A and P-gp. That partially explains why CYP3A substrates comprise half of the market's available drug substances, and also why there is a striking overlap in the substrates listed in both CYP3A and P-gp substrates (Wacher *et al.*, 1995).

The rationale for using permeability and solubility as parameters in the BCS for biowaiver of a bioequivalence study is derived from the fact that these two parameters directly determine the oral absorption profile of drugs. Consequently, IVIVC of bioavailability/bioequivalence can be discussed and evaluated based on those parameters. In the BDDCS classification criteria, 'permeability' is determined by the *extent of metabolism*, in contrast to the BCS which uses the *extent of oral absorption*. The importance of the BDDCS is not limited to a regulatory application to investigate the possible relationship between *in vitro* drug permeability and *in vivo* bioavailability. The scientific fact is that the extent of metabolism can be viewed as a subsequent step to permeability, another surrogate marker for predicting absorption; this is related to the permeability of drug substances, and their consequent access to metabolising enzymes, and further to the intracellular events that take place thereafter. The future application of the BDDCS in drug development may become more widespread when the present framework gains

increased recognition. This will probably be the case if the interplay of transporters and enzymes become better recognised. The BDDCS is a simple concept and tool that can be used in early drug development not only to determine the rate-limiting step in the oral absorption process, but also to better predict drug disposition in possible drug substance interactions with transporters and enzymes in the ADME process.

## References

- Amidon GL, Lennernäs H, Shah VP, Crison JR (1995). A theoretical basis for a biopharmaceutic drug classification: the correlation of *in vitro* drug product dissolution and *in vivo* bioavailability. *Pharm Res* 12: 413–420.
- Blume HH, Schug BS (1999). The biopharmaceutics classification system (BCS): class III drugs – better candidates for BA/BE waiver? *Eur J Pharm Sci* 9: 117–121.
- Custodio JM, Wu CY, Benet LZ (2008). Predicting drug disposition absorption/elimination/transporter interplay and the role of food on drug absorption. *Adv Drug Deliv Rev* 60: 717–733.
- EMA (2001). The European Agency for Evaluation of Medicinal Products Evaluation of Medicines for Human Use. *Note for Guidance on the Investigation of Bioavailability and Bioequivalence*. [http://healthtech.who.int/pq/info\\_applicants/BE/emea\\_bioequiv.pdf](http://healthtech.who.int/pq/info_applicants/BE/emea_bioequiv.pdf) (accessed 3 June 2009).
- Faassen F, Kelder J, Lenders J, Onderwater R, Vromans H (2003). Physicochemical properties and transport of steroids across Caco-2 cells. *Pharm Res* 20: 177–186.
- FDA, Center for Drug Evaluation and Research (2000). *Guidance for Industry, Waiver of in vivo Bioavailability and Bioequivalence Studies for Immediate-release Solid Oral Dosage Forms based on a Biopharmaceutics Classification System*. <http://www.fda.gov/downloads/Drugs/GuidanceComplianceRegulatoryInformation/Guidances/UCM070246.pdf> (accessed 2 June 2009).
- FDA, Center for Drug Evaluation and Research (2002). *Guidance for Industry, Food-Effect Bioavailability and Fed Bioequivalence Studies*. <http://www.fda.gov/downloads/Drugs/GuidanceComplianceRegulatoryInformation/Guidances/ucm070241.pdf> (accessed 2 June 2009).
- Fleisher D, Li C, Zhou Y, Pao LH, Karim A (1999). Drug, meal and formulation interactions influencing drug absorption after oral administration. Clinical implications. *Clin Pharmacokinet* 36: 233–254.
- Houston JB (1994). Utility of *in vitro* drug metabolism data in predicting *in vivo* metabolic clearance. *Biochem Pharmacol* 47: 1469–1479.
- Houston JB, Carlile DJ (1997). Prediction of hepatic clearance from microsomes, hepatocytes, and liver slices. *Drug Metab Rev* 29: 891–922.
- Lentz KA, Polli JW, Wring SA, Humphreys JE, Polli JE (2000). Influence of passive permeability on apparent P-glycoprotein kinetics. *Pharm Res* 17: 1456–1460.
- Lipinski CA (2000). Drug-like properties and the causes of poor solubility and poor permeability. *J Pharmacol Toxicol Methods* 44: 235–249.

- Lipinski CA, Lombardo F, Dominy BW, Feeney PJ (1997). Experimental and computational approaches to estimate solubility and permeability in drug discovery and development settings. *Adv Drug Deliv Rev* 3: 3–26.
- Norris DA, Leesman GD, Sinko PJ, Grass GM (2000). Development of predictive pharmacokinetic simulation models for drug discovery. *J Control Release* 65: 55–62.
- Obach RS, Baxter JG, Liston TE, *et al.* (1997). The prediction of human pharmacokinetic parameters from preclinical and *in vitro* metabolism data. *J Pharmacol Exp Ther* 283: 46–58.
- Takagi T, Ramachandran C, Bermejo M, *et al.* (2006). A provisional biopharmaceutical classification of the top 200 oral drug products in the United States, Great Britain, Spain, and Japan. *Mol Pharm* 3: 641–643.
- Tolle-Sander S, Rautio J, Wring S, Polli JW, Polli JE (2003). Midazolam exhibits characteristics of a highly permeable P-glycoprotein substrate. *Pharm Res* 20: 757–764.
- Wacher VJ, Wu CY, Benet LZ (1995). Overlapping substrate specificities and tissue distribution of cytochrome P450 3A and P-glycoprotein: implications for drug delivery and activity in cancer chemotherapy. *Mol Carcinog* 13: 129–134.
- Wilkinson GR (1987). Clearance approaches in pharmacology. *Pharmacol Rev* 39: 1–47.
- Wu CY, Benet LZ (2005). Predicting drug disposition via application of BCS: transport/absorption/elimination interplay and development of a biopharmaceutics drug disposition classification system. *Pharm Res* 22: 11–23.
- Zhang Y, Benet LZ (2001). The gut as a barrier to drug absorption: combined role of cytochrome P450 3A and P-glycoprotein. *Clin Pharmacokinet* 40: 159–168.

# 4.3

## Biosimulation studies

*Isabel Gonzalez-Alvarez and Marival Bermejo*

Mathematical models and simulations are powerful tools in all phases of medicine development, from drug discovery to clinical phases. Nevertheless, the pharmaceutical industry is just starting to implement biosimulation for registration purposes. The aim of this chapter is to describe the basic concepts about modelling and simulation within the framework of preclinical investigations and *dosage form evaluation*. As an example, some models developed for oral drug administration will be described because this route is the most used. However the same modelling concepts can be applied to any other administration route. This chapter is not intended to be comprehensive, but to give an overall view of the potential use of modelling and biosimulation in dosage form evaluation. In some cases, the reader is referred to papers in which the original methods are described, while in others the reader may be directed to the latest publications in which the methods are applied.

### 4.3.1 What is modelling and simulation?

The first step is to establish simple definitions of modelling and biosimulation in the context of dosage form evaluation. Thus, in this context, *modelling* is constructing a mathematical description of a system such as an oral route of drug administration. The model can then be used to simulate or optimise the system. All models are predictive, i.e. the simulation output predicts what could occur in the real world where the system is operating (Nørager *et al.*, 2005). In other words, a mathematical model explains the behaviour of a system such as the oral of drug administration route by functions and equations that may describe the relationship between variables representing the properties of the system. System variables of the oral route of drug administration are further presented in Section 4.3.3. The variables representing these properties can be measured outputs, time data, event occurrence, etc.

There are a couple of comments to add to the above model definition. First, the model is defined not only by equations or mathematical functions but also by a series of underlying assumptions that must be meaningful to ensure the model validity. Examples are the distribution probabilities used to describe the variation of random errors; the function probabilities associated with the system variables; or the mechanistic or empirical assumptions used to construct the model. Second, the model can be used to make predictions that depend on its empirical or mechanistic nature. In general, an empirical model uses mathematical equations to describe and reproduce experimental observations. It can therefore be applied within the range defined by the experimental data that have been used to construct the model, and the model can be useful for interpolation, but it will be less reliable outside these limits. A mechanistic model, based on some previous knowledge about the process, could be used for extrapolation. However, it should be used with caution, especially if the hypotheses supporting the model are applied outside the experimental data range.

*Simulation* is imitation of reality. In the context of dosage form evaluation, simulation is using a mathematical model to predict what will be the outcome of a given input in reality. Simulation can thus be used to study the effect of changing parameters in a model or to predict experimental results, without actually performing a physical experiment. It can be seen as numerical evaluation of a model system and it may be used to estimate the true characteristics of the system. A simulation is, in other words, an experiment that is run as a model of reality (Norager *et al.*, 2005).

Models can be classified in several ways. Examples of classifying models by, for example, types of equations are shown in Table 4.3.1.

Modelling and simulation allow the scientist to condense experimental data into groups of parameters, and to predict the response of a system to changed parameters. That implies prediction of outcome from different experimental designs and, eventually, one may avoid execution of data from less well-designed experiments. Of course the confidence of the predictions depends on the accuracy of previous assumptions and on the accuracy of the model itself. In this way, modelling and simulation should be seen as feedback processes. Thus, as new experimental data become available, the knowledge generated from these data should be incorporated in the model to refine it in a continuous fashion.

In dosage form development, models can be used for different purposes. If the starting point is an already accepted model, then the parameter values can be estimated from experimental data. With these values, as

**Table 4.3.1** Classification and examples of mathematical models (adapted from Endrenyi, 1981)

<i>Classification</i>	<i>Type of model</i>	<i>Example of equation and particular application</i>	
Type of equation	Linear	$y = a + bx$	Objective functions and constraints are linear
	Non-linear	Calibration curves $y = m^*(1 - e^{-b*x})$	Any of the objective functions or constraints are non-linear
	Integrated	First-order dissolution profile $y = y_0 * e^{-k*x}$ Plasma profile after iv dose of one compartment drug	
	Differential	$dy/dx = -k*y$ Plasma profile after iv dose of one compartment drug	
Presence of error terms, noise or randomness	Deterministic	$y = a + bx$	Performance is always the same for a set of initial values, parameters etc
	Stochastic	$y = a(f(\phi)) + b(f(\phi))x + \epsilon$	It incorporates some randomness either as a noise $f(\phi)$ in the parameters or as a random error term in the output
Time dependence	Static	$y = a + bx$	Describe a process/system not time dependent
	Dynamic	$x \neq t$ and $a$ and $b$ are not $f(t)$ $y = y_0 * e^{-k*x}$	Time is one of the variables of the model
Dependent variable	Explicit	$x = t$ $y = y_0 - k*x$	The dependent variable can be separated in one side of the equation

(continued)

**Table 4.3.1** (Continued)

Classification	Type of model	Example of equation and particular application	
	Implicit	$y_0 - y_p + K_m \ln\left(\frac{y_0}{y_p}\right) = V_m x$	The dependent variable and the one or more independent variables are not separated on opposite sides of an equation
$x = t$ ; dependent variable $y_p$			

well as a measurement of the uncertainty of the parameters and the residual variability, it is possible to obtain a *prediction* about the modelled property under different initial conditions. Finally, once the critical parameters determining the behaviour of a system have been characterised, it is possible to *optimise* the model performance by changing them. Typically, this is done to increase the process yield, achieve new specifications, or reduce/increase the process duration.

**4.3.2 How to construct and verify a model**

In this section, *inverse problems* will be described. To solve an inverse problem, one has to find the parameter values of the model that best describe the observed data. In other words, the objective is to identify the parameters of the input function that yield a given response. In this way, the modelling exercise is used as a tool to explore mechanisms and to generate a feasible hypothesis about the behaviour of the system, by means of comparing the goodness of fit indices of different models. The modelling procedure should include three steps: an exploratory data analysis (preliminary graphical analysis and statistical tests), model development and model validation (to validate its predictability). Detailed definitions of validation methods and references can be reviewed in the FDA population pharmacokinetic guidance (FDA, Center for Drug Evaluation and Research, 1999).

In general, the approach to solving an inverse problem is to reduce the overall difference between the experimental data points and the estimated points obtained by changing the values of the parameters. *These distances are used to calculate the objective function, which, in this case, has to be minimised (least squares regression).*

After the exploratory data analysis step, the second stage in a modelling approach is to select the dependent variable (the response or system property we want to predict), the independent variable(s) and the mathematical function(s) linking them, and, finally, the definition of the objective function. Linear and non-linear regressions by least squares are based on the following assumptions, which should be validated before model fitting:

- the selected model is the right one; if the model is not the right one, the lack of fit will be reflected in the residual sum of squares
- the independent variable ( $x$ ) has no error; in general, it is enough if the error in the independent variable is smaller than with the errors in the dependent variable ( $y$ )
- the errors (true residual variability) are independent, and follow a normal distribution with mean zero and the same variance; in some cases, if any of these assumptions are not true, it is possible to transform the dependent variable or to select some weighting scheme (see below).

The results should be interpreted with caution if some of the assumptions do not hold true. Fundamentals of linear regression (that can be applied to non-linear regression) can be reviewed elsewhere (Montgomery *et al.*, 2001; Motulsky and Christopoulos, 2004). Exploratory data analysis permits validation of the assumptions and allow the necessary actions to be taken if the assumptions are not met (FDA, Center for Drug Evaluation and Research, 1999). The mathematics of objective functions are further described in Appendix 4.3.1.

#### **4.3.3 How can a biosimulation model be applied for preclinical investigations and dosage form development?**

The concept of biosimulation is applicable for any biological process. In the process of drug absorption, several models have been developed to describe the main events taking place in the intestinal lumen (i.e. dissolution and transit) and the drug permeation through the intestinal epithelium. Also other pharmacokinetic processes (metabolism, distribution, elimination) have been modelled in addition to the pharmacological response. The current trend in biosimulation is the systems biology approach which incorporates integrative mechanistic models with the final aim of whole-body simulation by using *in silico*, *in vitro* and *in vivo*



input data (Dokoumetzidis *et al.*, 2007). In this section, some of the earliest models developed for the oral absorption route are briefly described to help the reader understand the evolution of this discipline and how the individual pieces are being integrated in more sophisticated models and software

#### 4.3.3.1 Modelling drug absorption

The oral route for drug administration is the most convenient, and preferred by patients and industry, so, in general, the main objective in the process of drug development is to develop drug products that are absorbed after oral administration, i.e. drugs with good oral bioavailabilities. This is a multifactorial problem that depends on three levels of parameters/factors. The first level of parameters arises from the physico-chemical characteristics of the drug substance, i.e. solubility,  $pK_a$ , lipophilicity, particle size, molecular surface area, crystalline form and stability. These parameters are further described in Part 2. The second level of parameters arises from the drug formulation, i.e. dosage form, disintegration and dissolution (mechanism and rate). The dissolution parameter is further described in Chapter 4.1. Finally, the third level of parameters is physiological variables, i.e. gastrointestinal pH, gastric emptying, intestinal motility and transit time, intestinal secretions, intestinal blood flow, and membrane permeability. These parameters are further described in Section 3; however, for pH in various biological media see Chapter 2.1, Table 2.1.2. The drug must be released from the dosage form and get into solution, which is the first essential step before its absorption. For this reason, *solubility* (and dissolution rate) and *permeability* across the intestinal membrane can be identified as key parameters for a new chemical entity in order for it to become a lead compound. These factors constitute the fundamental aspects of the BCS described in Chapter 4.2, which has evolved into a modern tool to speed up the drug development process (FDA, Center for Drug Evaluation and Research, 2000). Different mathematical model approaches, incorporating dissolution and permeability, have been developed to predict oral absorption and oral fraction absorbed for drug candidates. For instance, in some models the main goal is to explore the correlation between drug absorption (expressed as fraction absorbed or drug permeability) and drug physicochemical parameters. These models are then used to select the best drug candidate from a group of compounds, i.e. for *in silico* screening. The second approach consists of modelling the absorption process itself. This is done by incorporating some physiological variables

such as intestinal surface and considering the mass balance of the drug candidate at the absorption site. In the more advanced models, time events, such as gastrointestinal (GI) transit time are included as variables to predict plasma profiles after oral administration.

#### 4.3.3.1.1 *Molecular descriptors-based models to predict permeability and oral fraction absorbed*

One of the simplest models is based on the so-called ‘absorption potential’ that is a parameter used for predicting the oral fraction absorbed. The absorption potential is based on the pH-partition theory of Brodie and co-workers (Shore *et al.*, 1957) but considers not only the drug  $pK_a$  but also other factors such as solubility and dose. The proposed equation is shown in Equation 4.3.1:

$$AP = \ln\left(\frac{P \cdot F_{ni}}{Do}\right) \quad (4.3.1)$$

where AP is the absorption potential,  $P$  is the partition coefficient,  $F_{ni}$  the non-ionised fraction at pH 6.5 and  $Do$  the dose number ( $Do = \text{Dose} / 250 \cdot C_s$ ).

In order to establish a model describing the quantitative relationship between absorption potential and oral fraction absorbed ( $F_a$ ), Macheras and Symillides (1989) proposed the following equation:

$$F_a = \frac{(10^{AP})^2}{(10^{AP})^2 + F_{ni}(1 - F_{ni})} \quad (4.3.2)$$

Assuming that AP has an upper limit of 1000 and if  $Do > 1$ , a value  $Do = 1$  is used.

A second group of models derived from the pH-partition theory are the compartmental models from Wagner and Sedman (1973) and Higuchi and Ho (Higuchi *et al.*, 1981). In these models the lipid membrane and the aqueous media at both sides are both considered as compartments, and the diffusion from one compartment to the other is described as a function of the physicochemical characteristics of the compounds (mainly lipophilicity) (Wagner and Sedman, 1973; Plá-Delfina *et al.*, 1980; Higuchi *et al.*, 1981; Plá-Delfina and Moreno, 1981; Martin-Villodre *et al.*, 1986; Casabo *et al.*, 1987).

An example of the Higuchi–Ho model applied to a series of fluor-quinolones is shown in Figure 4.3.1.

In this model, the drug candidate absorption rate constant ( $k_a$ ) depends on its diffusion rate constants through the aqueous stagnant

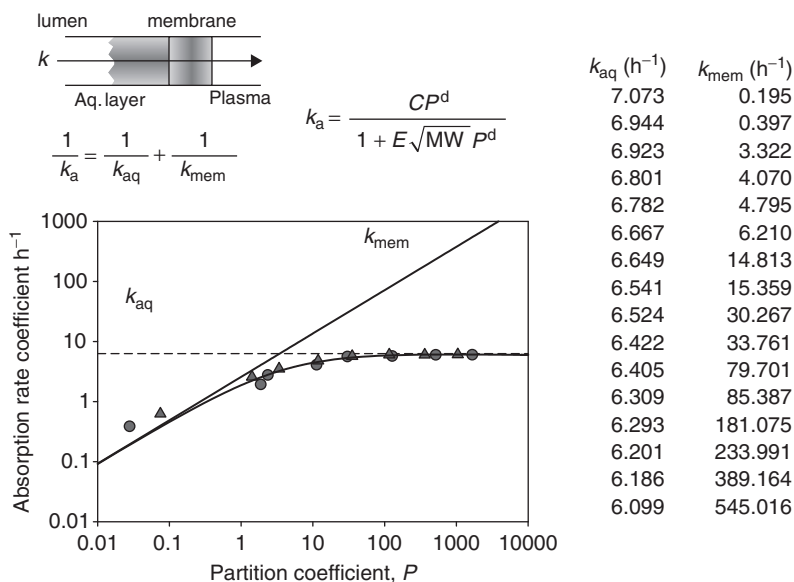


**Figure 4.3.1** Absorption–lipophilicity correlation obtained for a group of fluoroquinolone compounds. The curve in the plot represents the fitted values to the Higuchi–Ho absorption model. The lines are obtained by decomposing the absorption process in the two diffusional steps through the aqueous layer  $k_{aq}$  and through the membrane  $k_{mem}$ . The values of  $k_{aq}$  and  $k_{mem}$  are indicated from the most hydrophilic to the most lipophilic compounds to point out how the diffusion through the aqueous layer becomes the limiting step as the lipophilicity is increased. The equations are described in detail in the text. Adapted from Merino *et al.*, 1995; Bermejo *et al.*, 1999).

layer ( $k_{aq}$ ) and lipid membrane ( $k_{mem}$ ).  $k_a$  is the sum of  $k_{aq}$  and  $k_{mem}$  as can be seen from the left-hand equation given in Figure 4.3.1. Diffusion through the aqueous boundary layer decreases from the most hydrophilic to the most lipophilic compounds in the series. The aqueous diffusional rate constant ( $k_{aq}$ ) is expressed as a function of the molecular weight (MW); thus it is inversely proportional to the MW of the compounds as seen from Equation 4.3.3:

$$k_{aq} = J/\sqrt{MW} \quad (4.3.3)$$

where  $J$  is the inverse proportionality constant.

On the other hand, compound diffusion through a membrane is also quantified by means of its lipophilicity ( $P$ ) as seen from Equation 4.3.4.

$$k_{mem} = CP^d \quad (4.3.4)$$

where  $C$  and  $d$  are the parameters linking the coefficient to the membrane permeability. This equation is based on the Collander relationship for the partition coefficients obtained using different organic solvents. Thus  $C$  and  $d$  are needed to link the partition coefficient in the *in vitro* system and the *in vivo* partition coefficient; the latter is generally not known or measured (Collander, 1951). Combining both equations gives Equation 4.3.5:

$$k_a = \frac{CP^d}{1 + E\sqrt{MW}P^d} \quad (4.3.5)$$

in which  $E = C/J$

For more lipophilic compounds, diffusion through the stagnant water layer becomes the rate-limiting step, which leads to a 'plateau' in the absorption–lipophilicity correlation profile.

The model of Plá-Delfina and Moreno incorporates many of the principles described in the previous compartmental models; however, it also offers a global interpretation of the absorption–partition correlations which are obtained for many series of compounds when investigated in different intestinal segments (Delfina *et al.*, 1975, 1980; Plá-Delfina and Moreno, 1981). The main hypothesis, which is illustrated in Figure 4.3.2, is based on the assumption that intestinal absorption by passive diffusion is the result of two simultaneous processes described by the diffusion through aqueous channels ( $k_{a2}$ ) (porous or tight junctions) and diffusion through the lipophilic membrane ( $k_{a1}$ ). The correlation between absorption and lipophilicity can thus be represented by two hyperbolic functions, a direct one for the lipidic permeation and an inverse one for paracellular diffusion, with two asymptotic values, i.e.  $k_m$  for membrane permeation and  $k_p$  for aqueous diffusion.  $P$  represents the lipophilicity and the other symbols are parameters of the fit. This model can be applied to simulate the permeability of drug candidates across the small intestine, where both pathways are involved, and for candidates with MW low enough to use the aqueous paracellular permeability pathway. However, in the case of compounds with MW higher than 250 Daltons, and in the colon, the correlations are always hyperbolic.  $k_m$  represents the limiting value for the absorption rate constants of lipophilic compounds. This asymptotic value appears because the aqueous stagnant layer is the rate-limiting step in the diffusional process of more lipophilic compounds. Examples of these correlations are depicted in Figure 4.3.3 (Yu *et al.*, 1996).

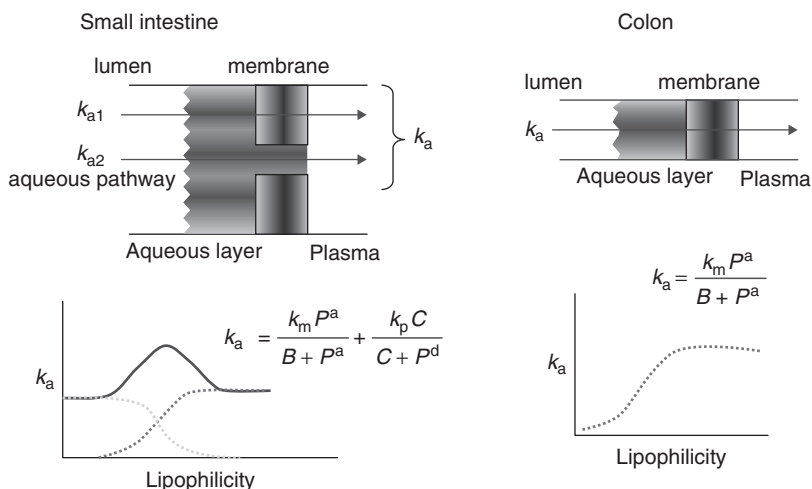


**Figure 4.3.2** Scheme representing the main assumptions of the biophysical absorption model of Plá-Delfina and Moreno. Absorption versus lipophilicity correlations in the small intestine are described as the sum of two hyperbolic equations: a direct hyperbola for the membrane permeation, and an inverse hyperbola for paracellular diffusion. See text for explanation.

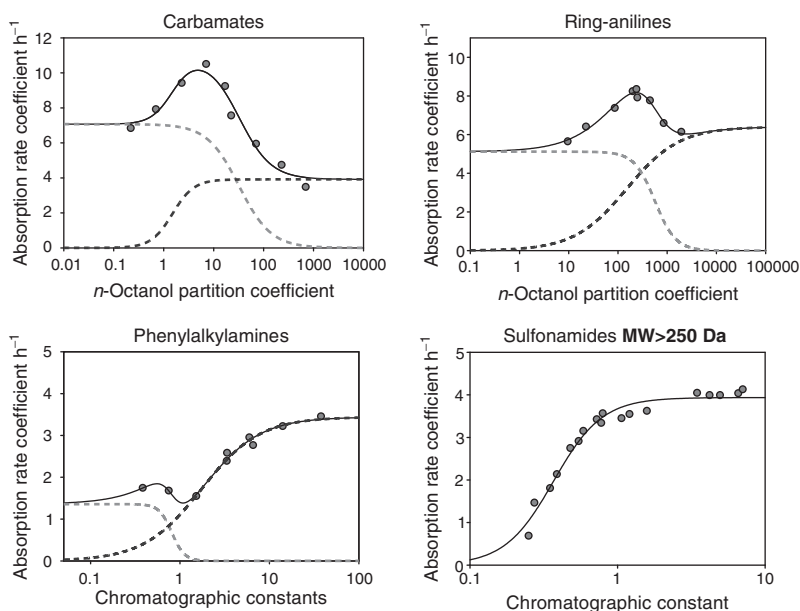


**Figure 4.3.3** Examples of absorption-partition relationships obtained in rat small intestine for different families of compounds. Adapted from Plá-Delfina *et al.*, 1980; Plá-Delfina and Moreno, 1981; Martín-Villodre *et al.*, 1986; Casabo *et al.*, 1987.

Besides lipophilicity, other molecular descriptors such as MW, polar surface area, and hydrogen-bonding capacity have been used in the literature to predict ADME properties. Table 4.3.2 summarises some of these molecular descriptors and their relationship to oral absorption.

**Table 4.3.2** Molecular descriptors used for drug-permeability predictions

<i>Molecular descriptor</i>	<i>References</i>
<i>Lipophilicity</i> : as drug partitioning into the cell membrane is one of the steps in membrane transport, lipophilicity is widely used as a predictor of drug permeability. Lipophilicity has two principal components, molecular size and hydrogen-bonding potential. This parameter has been used to predict <i>in vitro</i> permeability, and rat and human permeability using linear or hyperbolic correlations.	Casabo <i>et al.</i> , 1987; Dowty and Dietsch, 1997; Kamm <i>et al.</i> , 1999; Stenberg <i>et al.</i> , 1999; Bermejo and Ruiz-García, 2002
<i>Molecular weight</i> : this is a component of lipophilicity as well as the diffusion coefficient in biological membranes and fluids. It has been included as predictor variable of oral absorption in multiple linear and non-linear models along with other descriptors. A rather strong dependence between transcellular diffusion and molecular size has been observed. Compounds with MW < 200 are able to pass through the intestinal membrane by paracellular pathways along with diffusion through the transcellular route. Compounds with MW > 250 use the transcellular route but further increases of the MW (MW > 500) consequently lead to a decrease in membrane diffusion.	Camenisch <i>et al.</i> , 1996
<i>Hydrogen bonding capacity</i> : the absorption ability of a molecule depends on the number and strength of the hydrogen bonds that the molecule is able to form with water molecules, because the first step to entering into the membrane is desolvation of the molecule. Hydrogen-bonding capacity is detrimental for transport into the non-polar environment of the cell membrane. Thus, this property as well as lipophilicity is a good descriptor of drug permeation and it has been included in multiple linear regression models to predict Caco-2 permeability and human oral fraction absorbed.	Norinder <i>et al.</i> , 1999

(continued)

**Table 4.3.2** (Continued)

<i>Molecular descriptor</i>	<i>References</i>
<p><i>Polar surface area (PSA)</i>: PSA of a molecule is defined as the area of its van der Waals surface that arises from oxygen or nitrogen atoms plus the area of the hydrogen atoms attached to these hetero-atoms. As such, is clearly related to the capacity to form hydrogen bonds. Drugs with <math>PSA_d &lt; 60 \text{ \AA}^2</math> would be completely absorbed (fraction absorbed, <math>FA &gt; 90\%</math>). Drugs with <math>PSA^d &gt; 140 \text{ \AA}^2</math> would be absorbed less than 10%.</p>	Clark, 1999a, b; Palm <i>et al.</i> , 1996, 1997
<p><i>Non-polar surface area</i>: non-polar substituents facilitate membrane transport and hydrophobic compounds generally have higher permeabilities than hydrophilic ones (with similar hydrogen-bonding properties). Non-polar surface area can also correlate with membrane permeability. In general, this parameter is included in the correlations along with PSA.</p>	

Yoshida and Topliss (2000) have studied the quantitative structure–bioavailability relationships of 232 structurally diverse drugs. They have identified a group of structural variables for their model and quantified their influence on absorption and/or metabolism, and have included lipophilicity (expressed as the distribution coefficient at pH 6.5) as a significant factor influencing bioavailability. A quantitative structure–activity relationship (QSAR) study, performed by Sakaeda *et al.* (2001) included over 222 commercially available drugs, and it showed exclusion criteria to differentiate poorly absorbed drugs which are similar to the exclusion criteria described by the rule of five presented by Lipinski (Lipinski *et al.*, 2001). Essentially Lipinski’s rule stated that a compound has a low absorption or permeability if it shows MW higher than 500 Da, a  $\log P$  higher than 5, and there are  $>5$  hydrogen bond donors (OH and NH groups) in the molecular structure and  $>10$  hydrogen bond acceptors (notably N and O). Lipinski’s rule of five is further described in Chapter 2.4.1.

#### 4.3.3.1.2 Mass balance, time-independent models

In the simplest model it is assumed that the small intestine is a tube with area  $S = 2\pi RL$ , where  $R$  is the radius and  $L$  the length of the segment.

The mass balance in the segment can be described by Equation 4.3.6:

$$-\frac{dM}{dt} = \Phi (C_0 - C_f) = 2\pi R P_{\text{eff}} \int_0^L C dz \quad (4.3.6)$$

in which  $M$  is the amount of drug absorbed,  $\phi$  is the volumetric flow,  $C_0$  and  $C_f$  are the concentrations at the beginning and end of the segment respectively,  $L$  is the length of the segment,  $R$  is the radius,  $P_{\text{eff}}$  is the drug permeability and  $z$  the axial distance.

At steady state, the fraction absorbed ( $f_a$ ) is given by Equations 4.3.7–4.3.9:

$$f_a = 1 - \frac{C_f}{C_0} \quad (4.3.7)$$

$$f_a = 2 \frac{\pi R L P_{\text{eff}}}{\phi} \int_0^1 C^* dz^* \quad (4.3.8)$$

$$f_a = 2 A_n \int_0^1 C^* dz^* \quad (4.3.9)$$

where  $C^*$  and  $dz^*$  are dimensionless variables that corresponds to  $C_f/C_0$  and  $z/L$ .  $A_n$  is the absorption number, which is defined as the ratio between the transit time in the segment and the absorption time ( $R/P_{\text{eff}}$ ). Table 4.3.3 summarises the solutions for Equation 4.3.9.

**Table 4.3.3** Solutions to Equation 4.3.9

Comment	Conditions	Integral
Highly soluble drugs; permeability is the main parameter determining $f_a$	$C_0 \leq C_s$ and $C_f \leq C_s$	$f_a = 1 - e^{-2 A_n}$
Drug in solid form (suspension). If dissolution is faster than absorption then concentration is $C_s$	$C_0 > C_s$ and $C_f > C_s$	$f_a = \frac{2 A_n}{D_o}$
	$C_0 > C_s$ and $C_f \leq C_s$	$f_a = 1 - \frac{1}{D_o} e^{-2 A_n + D_o - 1}$

Notes:  $C_s$  is drug solubility,  $C_0$  and  $C_f$  are the concentrations at the beginning and at the end of the intestinal segment respectively.  $A_n$ : absorption number;  $D_o$ : dose number. See text for explanation.



This mass balance approach generally renders good predictions for high-solubility drug candidates, but for low-solubility candidates there are other more accurate approaches based on microscopic mass balance that provide better estimates (Oh *et al.*, 1993).

#### 4.3.3.1.3 Time-dependent models

The GI tract can be considered as one well-stirred mixing tank from which the drug is absorbed, or it can be represented by a series of tanks linked by linear transference processes. Several authors have constructed models following this scheme (Dressman *et al.*, 1984; Dressman and Fleisher, 1986; Oberle and Amidon, 1987). An example of applying this approach is described below and represented in Figure 4.3.4.

Solid drug is assumed to have an initial distribution of particle size. Each particle size group is considered separately. Particles are considered to be spherical (but other geometries can be accommodated into the model). Particle dissolution is described by the Noyes–Whitney equation which is described further in Chapter 4.1. The diffusion layer thickness is assumed to be constant for particles with a diameter larger than 30  $\mu\text{m}$ . The thickness is assumed to be equal to the particle radius for smaller

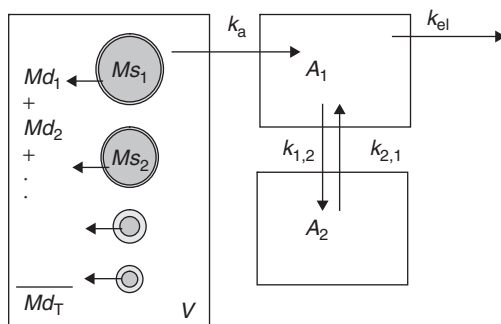


**Figure 4.3.4** Scheme of a dissolution/absorption/pharmacokinetic model adapted from Johnson, 2003. Drug in polydisperse particles is either in solid form  $Ms_i$  or dissolved in the intestinal fluids  $Md_i$ , where  $i$  represents a fraction of particles ( $1, 2 \dots n$ );  $V$  is the volume available in the intestinal lumen;  $A_1$  and  $A_2$  correspond to the drug mass in the central and peripheral pharmacokinetic compartments in the body;  $k_a$  is the first-order absorption rate constant and  $k_{el}$  the first-order elimination constant;  $k_{1,2}$  and  $k_{2,1}$  are the first-order distribution constants to and from the peripheral compartment respectively. Large particles have a diffusion layer of constant thickness, whereas particles smaller than 30  $\mu\text{m}$  have a diffusion layer equal to the particle radius.

particles. The derivation of the dissolution equations is described in several papers (Dressman and Fleisher, 1986; Hintz and Johnson, 1989).

The following series of coupled differential equations is used to simulate the process of drug dissolution, absorption and disposition:

$$\frac{dM_{s_i}}{dt} = -\frac{3D(M_{0i})^{1/3}(M_{s_i})^{2/3}}{\rho b_i r_{0i}} \left( C_s(t) - \frac{Md_T}{V(t)} \right) \quad (4.3.10)$$

$$\frac{dMd_i}{dt} = +\frac{3D(M_{0i})^{1/3}(M_{s_i})^{2/3}}{\rho b_i r_{0i}} \left( C_s(t) - \frac{Md_T}{V(t)} \right) - k_a(t) Md_i \quad (4.3.11)$$

$$Md_T = \sum_{i=1}^n Md_i \quad (4.3.12)$$

$$\frac{dA_1}{dt} = k_a(t) F Md_T - (k_{el} + k_{1,2}) A_1 + k_{2,1} A_2 \quad (4.3.13)$$

$$\frac{dA_2}{dt} = k_{1,2} A_1 - k_{2,1} A_2 \quad (4.3.14)$$

where  $M_{s_i}$  is the mass of drug in solid state in fraction  $i$ ;  $M_{0i}$  the initial mass in the fraction;  $Md_i$  the mass of dissolved drug;  $D$  the diffusion coefficient;  $\rho$  the drug density;  $r_{0i}$  the initial radius of fraction  $i$ ;  $b_i$  the thickness of the stagnant boundary layer around the particle;  $Md_T$  the summation of dissolved drug mass at any time from all particle size groups;  $V(t)$  the dissolution volume;  $A_1$  the mass of drug in the central compartment and  $A_2$  the amount of drug in peripheral compartment;  $k_{1,2}$  and  $k_{2,1}$  are the distribution rate constants and  $k_{el}$  the elimination rate constant from the central compartment.  $k_a(t)$  represents the absorption rate constant, the parenthesis  $(t)$  means that the parameter can be made time dependent. This model was used to simulate the plasma profile of nifedipine in a gastrointestinal therapeutic system (GITS)-type dosage form, using the disposition parameters from iv administration (Johnson, 2003).

These mixing tank models are simple and intuitive but the main disadvantage is the lack of physical basis for assuming that one physiological segment of the small intestine can be considered as one homogeneous and well-stirred tank, although such an assumption has been commonly used in classical pharmacokinetic modelling. On the other hand, the number of mixing tanks will affect the results. To approach this issue, a mathematical model was developed in order to describe the transit flow of a drug in the human small intestine. Seven mixing tanks was found to be the best number for describing this process. The model

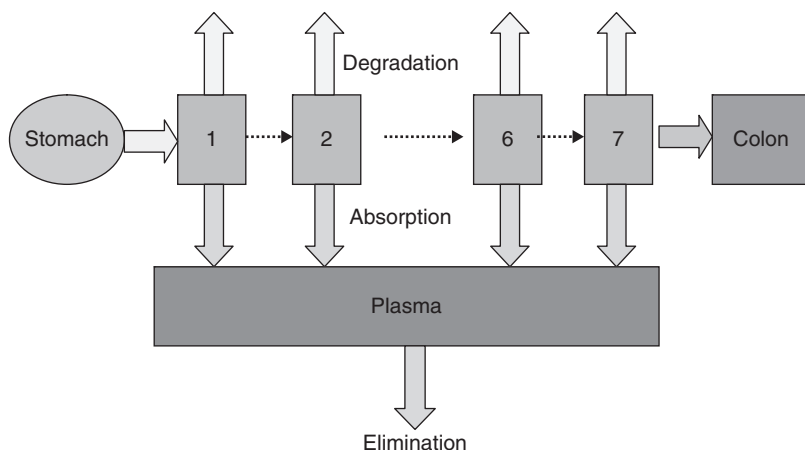


**Figure 4.3.5** Schematic representation of the compartmental transit and absorption model (CAT). See text for explanation.

was named compartmental transit and absorption (CAT). The initial model incorporated linear intestinal absorption and degradation in the lumen (Yu *et al.*, 1996; Yu and Amidon, 1999). In another paper, the model was extended to account for saturable absorption (Yu and Amidon, 1998). The CAT model, along with intravenous pharmacokinetic parameters, was used to estimate not only plasma concentration-time profiles, but also the fraction of dose absorbed. The model is briefly described here and illustrated in Figure 4.3.5.

In the model, the small intestine is divided into seven segments, plus the stomach and colon. Each segment is considered as a compartment where the drug transits from one to the other (following a linear kinetic) and is absorbed. In the first CAT models, absorption from the stomach and colon was considered to be negligible and the drug dissolution was instantaneous (Yu *et al.*, 1996; Yu and Amidon, 1998, 1999). The differential equations describing the change of mass with time in each compartment are as follows:

*Stomach:*

$$\frac{dM_s}{dt} = -K_{se}M_s \quad (4.3.15)$$

$K_{se}$  is the emptying rate constant and  $M_s$  a percentage of the dose.

*Small intestine:*

$$\frac{dM_n}{dt} = K_t M_{n-1} - K_a M_n - K_d M_n \quad (4.3.16)$$

$M_n$  ( $n = 1, 2, \dots, 7$ ) are the percentages of dose in each segment and  $K_t$ ,  $K_a$ ,  $K_d$  are the transit, absorption and degradation constants. In this case the constants are considered to be the same along the entire GI tract.

The rate of absorption can be defined from the absorption in each compartment:

$$\frac{dM_a}{dt} = \sum_{n=1}^{n=7} K_a M_n \quad (4.3.17)$$

In a similar way, the total amount degraded,  $M_d$ , can be estimated. The drug exiting from the last intestinal segment,  $M_c$ , passes to the colon, where absorption is considered to be negligible.

At time  $t \rightarrow \infty$ , the amount of drug in the stomach and intestine becomes zero, so:

$$100\% = M_a + M_c + M_d \quad (4.3.18)$$

The fraction absorbed is calculated by using the following expression:

$$f_{a \ t \rightarrow \infty} = \frac{M_a}{100} = \frac{\int_0^{\infty} \sum_{n=1}^{n=7} M_a K_a dt}{100} \quad (4.3.19)$$

The next step for predicting plasma profiles is to link the absorption process to a disposition compartmental model. For instance for a one-compartment drug:

$$\frac{dC}{dt} = \frac{D}{100} \left( \frac{dM_a}{dt} \right) \frac{1}{V} - k_{el} C \quad (4.3.20)$$

where  $k_{el}$  is the first-order elimination rate constant,  $V$  the distribution volume,  $C$  the plasma concentration and  $D$  the dose.

The original CAT model does not account for dissolution of the drug and the pH-dependent solubility of weak electrolytes. On the other hand, the absorption rate constant was modelled as a single parameter, without accounting for changes in factors such as surface area, transporter densities, efflux protein densities, and other regional factors within the intestinal tract. The CAT model can be made more accurate by treating the colon as an additional absorbing compartment. This applies in particular for low-solubility and low-permeability drugs and controlled-release formulations for which absorption in the colon can be significant. An example of application of the model to test the relevance of P-gp secretion in drug absorption has also been published (Yu and Amidon, 1999).

Modifications of the CAT model are implemented in simulation programs such as GastroPlus™ (based on the advanced CAT model (ACAT) (Agoram *et al.*, 2001)) and Simcyp© versions 7 and 8 (Advanced Dissolution, Absorption and Metabolism (ADAM) model).

The ACAT model includes allowance for changes in the transit constants from the upper to the lower segments. The model uses the concentration gradient across the apical and basolateral membranes to calculate the rate of drug transfer into and out of an enterocyte compartment for each lumen compartment, incorporating not only saturable absorption or efflux and intestinal metabolism but also the metabolic first-pass effect estimation. To estimate permeability values and the parameters of the metabolic processes, data coming from *in vitro* experiments can be used and they are scaled to the *in vivo* scenario using appropriate physiological scale factors.

The ADAM model, as implemented in Simcyp© Version 7, predicts the rates and extent of intestinal drug absorption and metabolism and their associated inter-individual variability (Dokoumetzidis *et al.*, 2007). The model is a population physiologically based mechanistic representation that accounts for the heterogeneity of the GI tract and considers the processes of dissolution, region-specific GI fluid dynamics, gut wall permeability and gut wall degradation and metabolism, with implicit consideration of active transport. The model incorporates a physiologically based treatment of fluid dynamics and basal fluid volumes within the GI tract, which includes the secretion and absorption of water for each ADAM intestinal segment. Physiological variability is applied to the GI tract surface area, transit times and fluid secretion/content/absorption in each segment by using a Monte Carlo approach. For dissolution, Simcyp© uses the Wang and Flanagan model (Wang and Flanagan, 1999) instead of the Noyes–Whitney model (Noyes and Whitney, 1897). Examples of application of the software to absorption of metoprolol and evaluation of the impact of P-gp have already been presented (Neuhoff *et al.*, 2008; Polak *et al.*, 2008).

An example with GastroPlus™ is shown in Figure 4.3.6. Data treated by the ACAT model are represented together with some plasma profiles predicted from physicochemical parameters and *in vitro* experiments, showing the good agreement of the simulated profile with the experimental plasma concentrations. On the other hand, the application of these modelling packages to the available clinical and pre-clinical data is extremely useful for model validation and refinement (Allan *et al.*, 2008).

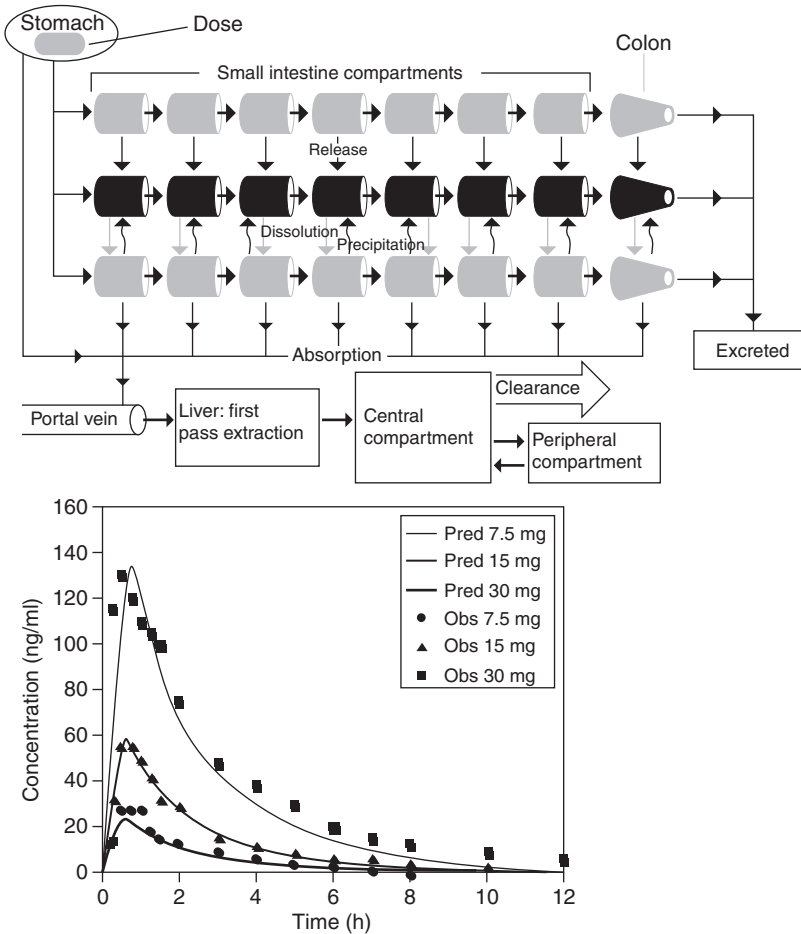


**Figure 4.3.6** (a) ACAT model schematic. The original CAT model with seven compartments was modified to include compartment-dependent physiological parameters and the colon. One to three compartment pharmacokinetic models were also included to estimate  $C_p$ -time profiles. (b) Predicted plasma profiles simulated for midazolam (experimental data from Bornemann *et al.*, 1985) as the dose is increased by a factor of 4, bioavailability increased from 25% to 38%. Reprinted from Agoram B, Woltosz WS, Bolger MB (2001). Predicting the impact of physiological and biochemical processes on oral drug bioavailability. *Adv Drug Deliv Rev* 50 (suppl 1): S41–S67, Copyright (2001), with permission from Elsevier.

#### 4.3.3.2 Modelling drug release and dissolution

There are numerous examples in the literature showing the critical role of drug dissolution on the rate and extent of absorption. The use of a mathematical model that relates some parameters of the dosage form to

the release of the drug and its dissolution facilitates the interpretation of the results of *in vitro* dissolution tests.

In some cases, the equations come from theoretical analysis of the process, as, for example, in zero-order or cubic root law kinetics. In many cases, other empirical equations are used. Table 4.3.4 summarises the equations (Equations 4.3.21–4.3.32) used to describe the dissolved amount of drug as a function of time. The theoretical bases for some of these equations are reviewed in detail by Costa and Sousa Lobo (2001).

Recently Dokoumetzidis and co-workers developed modified versions of the Noyes–Whitney and Weibull equations, explicitly including the solubility/dose parameter, for the analysis of dissolution data (Dokoumetzidis *et al.*, 2006). They applied these equations to metoprolol and ibuprofen dissolution and showed that the new equations performed better than the classical versions. On the other hand, the modified Weibull equation presented has a mechanistic meaning, as opposed to the purely empirical character of the original one.

According to the Noyes–Whitney equation, the rate of dissolution of a solid depends (among other factors) on its solubility and diffusivity in the dissolution media and on the surface area of the solid (see also Chapter 4.1). For drugs of low aqueous solubility, particle size (which determines the surface area) can have a significant impact on the dissolution rate. The drug in the dosage form is not generally present as a monodisperse powder but rather as a polydisperse system with a particular particle size distribution, which in most cases is log-normal. Hintz and Johnson (1989) developed a model for handling polydisperse particle dissolution based on a previous model by Dressman and Fleisher (Dressman *et al.*, 1984; Dressman and Fleisher, 1986,). This model generated Equation 4.3.33:

$$-\frac{dQ_{\text{solid}}^i}{dt} = \frac{3(Q_0^i)^{1/3}(Q_{\text{solid}}^i)^{2/3}}{\rho h r_0^i} \left( C_s - \frac{Q_{\text{diss}}^T}{V} \right) \quad (4.3.33)$$

in which  $Q_{\text{solid}}^i$  is described by Equation 4.3.34:

$$Q_{\text{diss}}^T = \sum_{i=1}^n Q_{\text{solid}}^i \quad (4.3.34)$$

where  $Q_{\text{solid}}^i$  represents the mass of solid drug in size fraction  $i$ ,  $Q_0^i$  the initial amount of drug in that size fraction,  $C_s$  is the drug solubility,  $V$  the volume of dissolution media,  $\rho$  the drug density,  $r_0^i$  the initial average radius of particles in fraction  $i$ ,  $h$  the thickness of the diffusion layer (controlling the dissolution rate), and finally  $Q_{\text{diss}}^T$  is the total amount

**Table 4.3.4** Dissolution models

<i>Model</i>	<i>Equation</i>	<i>Parameters</i>
Zero order	$Q_t = Q_0 + K_0 t$	$K_0$
First order	$Q_t = Q_\infty (1 - e^{-K_1 t})$ $\text{Ln}(Q_\infty - Q_t) = \text{Ln} Q_\infty - K_1 t$	$K_1$
Hixon–Crowell	$Q_i^{1/3} - Q_{\text{solid}}^{1/3} = K_s t$ $Q_\infty^{1/3} - (Q_\infty - Q_t)^{1/3} = K_s t$ $Q = Q_\infty - [\sqrt[3]{Q_\infty} - K_s t]^3$	$K_s$
Weibull	$Q_t = Q_\infty (1 - e^{-(t/T_d)^b})$	$b$ : shape parameter $T_d$ : time necessary to dissolve 63.2% of the dose When $b = 1$ ; first order
Higuchi	$Q_t = K_d \sqrt{t}$	$K_d$
Baker–Lonsdale	$\frac{3}{2} \left[ 1 - \left( 1 - \frac{Q_t}{Q_\infty} \right)^{2/3} \right] - \frac{Q_t}{Q_\infty} = K_d t$	$K_d$
Korsmeyer–Peppas	$\frac{Q_t}{Q_\infty} = K_k t^n$	$K_k$
Gompertz	$Q_t = Q_\infty e^{-e^{-(t-a)K}}$	$K, a$
Hopfenberg	$\frac{Q_t}{Q_\infty} = 1 - \left[ 1 - \frac{K_0 t}{C_0 a_0} \right]^n$ $C_0$ : uniform initial concentration of drug in the matrix; $a_0$ : initial radius for a sphere or cylinder or the half-thickness for a slab; $n = 1$ for a slab, $n = 2$ for a cylinder, $n = 3$ for a sphere	$K_0$ : erosion rate constant

*Notes:*  $Q_t$ , amount of drug dissolved;  $Q_0$ , amount dissolved at time 0;  $Q_\infty$ , amount dissolved when  $t \rightarrow \infty$ ;  $Q_i$ , initial amount in the dosage form (dose);  $Q_{\text{solid}}$ , amount remaining in the dosage form;  $K_x$ , dissolution rate constant. When dissolution is complete and in the absence of lag time, in general,  $Q_i = \text{dose} = Q_\infty$ ;  $Q_\infty$  can be treated as a parameter or fixed to the dose value or to 100% if the dependent variable is expressed as percentage dissolved.



dissolved from all the size fractions, which is used to calculate the dissolution gradient.

This equation was further modified (to Equation 4.3.35) to account for a time-dependent diffusion layer and for non-spherical geometries (Lu *et al.*, 1993).

$$-\frac{dQ_{\text{solid}}^i}{dt} = \frac{3(Q_0^i)^{2/3}(Q_{\text{solid}}^i)^{1/3}}{\rho(r_0^i)^2} \left( C_s - \frac{Q_{\text{diss}}^T}{V} \right) \quad (4.3.35)$$

Equation 4.3.35 is applied to small particles (<30  $\mu\text{m}$ ), whereas for particles bigger than 30  $\mu\text{m}$ , the diffusion layer thickness is fixed to a value of 30  $\mu\text{m}$ . This model was successfully applied to performing simulations of plasma profiles, by varying the absorption rate constant and dose/solubility ratio to explore in which scenarios the change in particle size leads to relevant changes in the maximum dose absorbed (Johnson and Swindell, 1996).

A similar approach to the dissolution process from a mechanistic point of view was used by de Almeida *et al.* (1997). They developed a Fortran subroutine which accounts for both the reduction in the number of particles as dissolution proceeds and the polydisperse nature of the powder. They applied the model to the dissolution of ibuprofen powders with different average diameters and their mixtures, and found a critical diameter of 22  $\mu\text{m}$  and a proportionality factor between particle diameter and boundary layer thickness of 0.26, indicating that for particles less than 22  $\mu\text{m}$  in diameter, the boundary layer thickness is approximately half the radius.

A review, including practical applications of other advanced methodologies such as Monte Carlo simulations or the fractal kinetics concept, can be found in Dokoumetzidis *et al.* (2005). There are several recent examples of the application of stochastic models used to describe the dissolution process (Lansky and Weiss, 1999, 2001, 2003; Lansky *et al.*, 2004; Schreiner *et al.*, 2005).

Modelling dissolution in the context of modelling release processes from the controlled-release dosage form can help to identify the controlling steps in the process and thereby to simulate the effects of the device parameters on the resulting release profile. Some recent reviews of these models are available in the following references: Grassi and Grassi (2005) and Siepmann and Peppas (2001) for a general overview; Grassi and Grassi (2005) for matrix devices and bio-erodible systems; Kanjickal and Lopina (2004) for polymeric systems; and Craig (2002) for solid dispersions of water-soluble polymers.

#### 4.3.3.3 *In vitro–in vivo* correlations

An *in vitro–in vivo* correlation (IVIVC) is a ‘predictive mathematical model describing the relationship between an *in vitro* property of a dosage form and an *in vivo* response’ (FDA, Center for Drug Evaluation and Research, 1997). The *in vitro* property is generally the rate or extent of drug dissolution or release, while the *in vivo* response is the plasma drug concentration or amount of drug absorbed. The main objective of developing and evaluating an IVIVC is to establish the *in vitro* dissolution test as a surrogate for human bioequivalence studies. There are several levels of IVIVC (see the FDA guidance document (1997) for more information) but the most informative one is level A correlation.

A level A correlation represents a point-to-point relationship between *in vitro* dissolution and *in vivo* input rate. In a linear correlation, the *in vitro* dissolution and *in vivo* input curves such as absorption rate may be directly superimposable or may be made to be superimposable by the use of a simple scaling factor. Non-linear correlations, while uncommon, may also be appropriate. Whatever model is used to establish a level A IVIVC, it should predict the *in vivo* plasma concentrations from the applied *in vitro* data.

Level A correlation is the only IVIVC that regulatory authorities allow for the prediction of plasma concentration profiles. The development of a level A IVIVC can be performed with two different approaches that are commonly described as the ‘one-step’ and ‘two-steps’ methods, respectively. In both cases it is necessary to develop formulations with different release rates such as slow, medium and fast. The *in vitro* dissolution profiles, as well the *in vivo* plasma concentration profiles in healthy human volunteers, have to be obtained for all these formulations. It is also necessary in the first step to obtain an *in vivo* ‘absorption’ or *in vivo* ‘dissolution’ profile from pharmacokinetic data. The second step consists of establishing the link, i.e. to modulate the link between *in vitro* and *in vivo* profiles and, finally, to validate the model, i.e. validate the prediction of the plasma levels from *in vitro* data.

##### 4.3.3.3.1 *Obtaining the absorbed fraction from plasma profiles*

This process is schematised in Figure 4.3.7. Once the *in vitro* (dissolution) and *in vivo* concentration profiles (plasma levels) have been obtained, in order to establish the correlation between them the first problem to be solved is how to calculate the *in vivo* amounts *absorbed* at each time

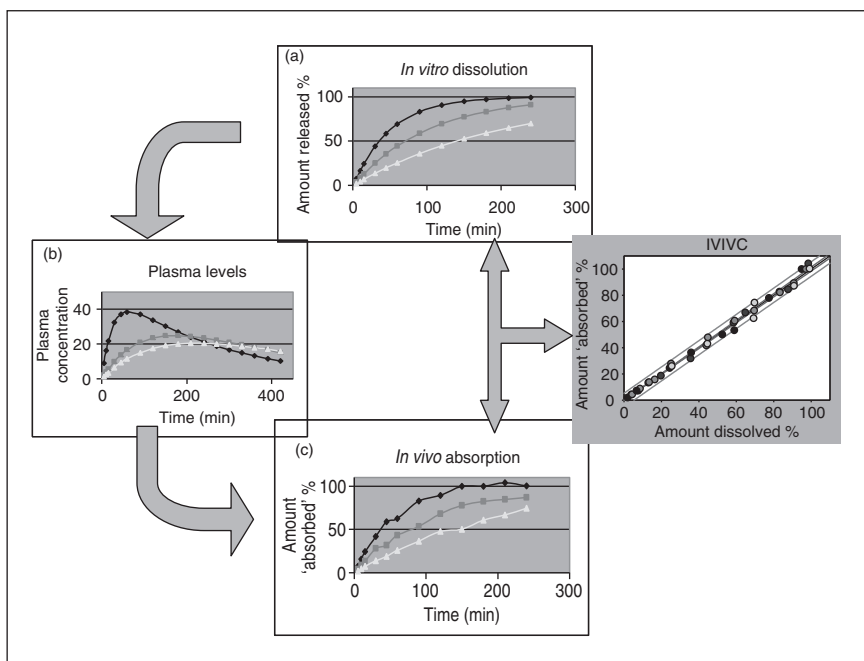


**Figure 4.3.7** Scheme of the development an *in vitro*–*in vivo* correlation in two steps: (a) dissolution profiles of formulations with different release rates, i.e. slow, medium, fast; (b) plasma profiles obtained in human volunteers after administration of the slow-, medium- and fast-release formulations; (c) amounts ‘absorbed’ versus time, calculated from the plasma levels (see methods in the text). The second step consists of establishing the link function between *in vitro* profiles (a) and *in vivo* profiles (c).

point, from the plasma profiles. At this point, it is convenient to remember the definition of fraction absorbed. Drug absorption must be distinguished from systemic availability. The systemic availability refers to the fraction of dose reaching the systemic circulation. Systemic availability  $F_{\text{sys}}$  can also be expressed by Equation 4.3.36:

$$F_{\text{sys}} = f_a * (1 - E_g) * (1 - E_h) \quad (4.3.36)$$

where  $f_a$  is the fraction absorbed,  $E_g$  the gut extraction ratio and  $E_h$  the hepatic extraction ratio. Absorption of a drug substance refers to its process of crossing the apical membrane of the enterocytes. So, the rate and extent of drug absorption may be considered simply as the rate and extent of drug permeating the apical membrane of the enterocytes. This section describes how the absorbed fraction  $f_a$  may be calculated from a plasma concentration profile, but the reader should bear in mind that in many

books and papers,  $F_{\text{sys}}$ , i.e. the fraction reaching the systemic circulation or available fraction, is misnamed and called fraction *absorbed*.

The mathematical methods for calculating the oral fraction absorbed are classified as model dependent or model independent. Model-dependent methods assume a particular compartmental pharmacokinetic model for the drug disposition, while the more general deconvolution methods are considered model independent as there is no need for assuming any particular pharmacokinetic model. Wagner–Nelson and Loo–Riegelman are examples of model-dependent methods:

The Wagner–Nelson method can be applied to one-compartment drugs. It is, essentially, a mass balance calculation. All the drug that has been absorbed up to a time point  $Q_{\text{at}}$ , is either in the body,  $Q_{\text{ct}}$ , or has been already eliminated,  $Q_{\text{et}}$ . The equations and an example of the Wagner–Nelson plot are illustrated in Figure 4.3.8. From the

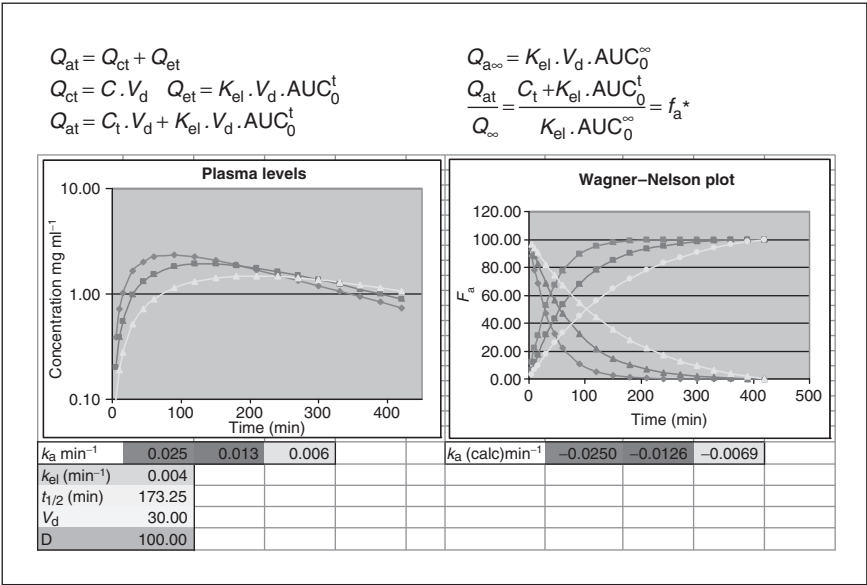


**Figure 4.3.8** Wagner–Nelson mass balance. At any time all the drug that has been absorbed is either in the body or has been already eliminated. The plasma levels (on the left) have been simulated for a one-compartment drug with different absorption rate constants. On the right the Wagner–Nelson plots and the remaining concentrations on the absorption site from which the absorption rate constant can be estimated.  $Q_{\text{at}}$  = amount absorbed at time  $t$ ;  $Q_{\text{ct}}$  = amount in the body at time  $t$ ;  $Q_{\text{et}}$  = amount eliminated at time  $t$ ;  $Q_{\text{a}\infty}$  = total amount absorbed;  $V_d$  = distribution volume;  $C_t$  = plasma concentration at time  $t$ ;  $k_{\text{el}}$  = elimination rate constant; AUC = area under the curve;  $f_a^*$ : fraction of the bioavailable dose.

plasma concentrations and the area under the curve (AUC calculated by the trapezoidal rule), and the elimination rate constant,  $k_{el}$  (obtained from the terminal slope), it is possible to obtain  $f_a$  at each time. In this case,  $f_a$  represents the fraction of the bioavailable dose that has already been absorbed at time  $t$ . Wagner–Nelson plots will always reach 100% even if bioavailability is not complete, because the fraction of bioavailable amount is the parameter calculated and not the fraction of the dose. On the other hand, in general, it is possible to perform Wagner–Nelson calculations without having intravenous data, as the elimination rate constant is estimated from the terminal slope of the plasma profiles. This latter approach is, of course, based on the assumption that the absorption is not influencing elimination (flip-flop).

In the case of a flip-flop, in which the decline of plasma concentration is absorption-rate limited, this leads to inaccurate estimation of the absorption rate constant; this could happen when evaluating controlled-release products.

A second problem that could arise when an intravenous reference is not available is the misidentification of the kinetic model of the drug. The results of Wagner–Nelson analysis are valid only if the one-compartment model represents the disposition kinetics. For two-compartment drugs it is necessary to account for the amount of drug in the peripheral compartment.

The Loo–Riegelman mass balance is similar to the Wagner–Nelson one. The problem now is the calculation of the amount and concentration of drug in the peripheral compartment. The equations summarised in Figure 4.3.9 are the exact solution of the Loo–Riegelman equation (a), published by Wagner, and an approximate solution. Both are easily implemented in Excel sheets. The approximate solution can be applied if the plasma concentrations have been obtained in short time intervals and if the change in concentration between two consecutive time points is approximated by a linear function. As can be seen, for these calculations the disposition parameters obtained from intravenous administration of the drug are necessary. Wagner–Nelson and Loo–Riegelman are model-dependent methods but in fact could also be considered as special cases of the more general deconvolution methods.

Deconvolution does not need to assume any kinetic model for drug disposition. Convolution can be applied to linear systems or, in other words, the convolution integral is the mathematical definition of a linear system.

The convolution principle may be expressed as follows:

$$C(t) = C_{(\delta)} * f(t) \tag{4.3.37}$$

The response function,  $C(t)$ , is obtained by convolution of the unit impulse response function,  $C_{(\delta)}$ , with the input function,  $f(t)$ . Mathematical convolution has been functionally expressed here by the asterisk. The fundamentals of this theory and the application in the pharmacokinetic field were set up in the 1980s (Veng-Pedersen, 1980a,b; Iga *et al.*, 1986; Veng-Pedersen and Miller, 1987), and there are many recent examples of their use (Gillespie and Veng-Pedersen, 1985; Modi *et al.*, 2000; Sirisuth *et al.*, 2002; Dutta *et al.*, 2005).

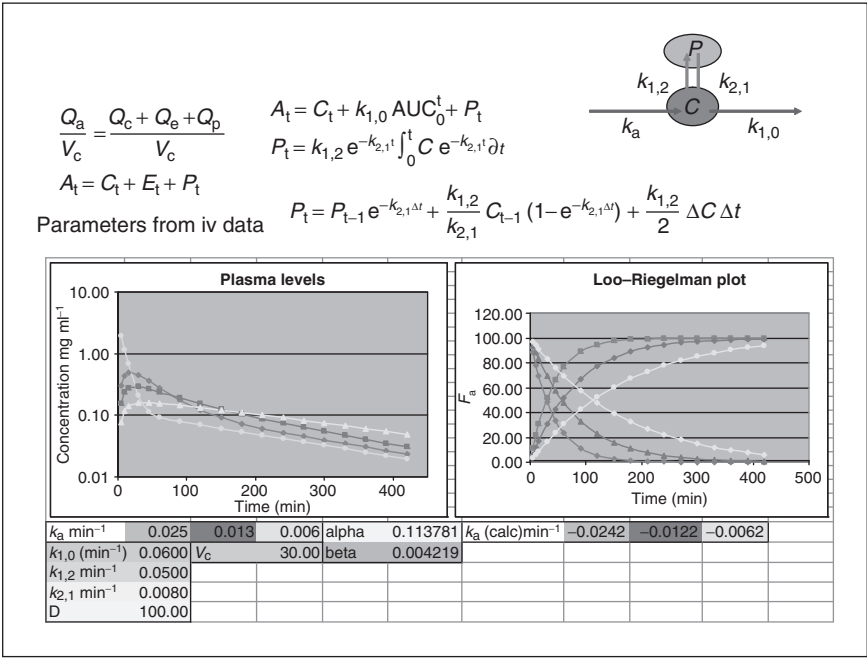


**Figure 4.3.9** Loo–Riegelman mass balance. At any time all the drug that has been absorbed is either in the central compartment or in the peripheral compartment, or it has already been eliminated. The plasma levels (on the left) have been simulated for a two-compartment drug with different absorption rate constants. On the right the Loo–Riegelman plots and the remaining concentrations on the absorption site from which the absorption rate constant can be estimated are shown.  $Q_a$ =amount absorbed;  $Q_c$ =amount in the central compartment;  $Q_p$ =amount in the peripheral compartment;  $Q_e$ =amount eliminated; the amounts are transformed in apparent concentrations ( $A$ ,  $C$ ,  $P$ ,  $E$ ) dividing by the  $V_c$ =central compartment volume;  $k_{1,0}$ =elimination rate constant from central compartment;  $k_{1,2}$ ,  $k_{2,1}$ =distribution rate constants.

Under conditions of linearity and time invariance, the transport of drug from the absorption site to the plasma can be completely expressed by the three functions in Equation 4.3.37.  $C_{(t)}$  refers to the concentration profile obtained when the drug is placed at the absorption site and the concentration is measured in plasma.  $C_{(\delta)}$  is also known as the characteristic or weighting function. In practical terms, it represents the concentration–time profile after an intravenous bolus, divided by the dose.  $f_{(t)}$  represents the transfer function that governs the movement of mass from the absorption site to the plasma. The knowledge of any two of these three functions allows determination of the third one. Deconvolution is the mathematical inverse of convolution. This refers to the situation where a knowledge of  $C_{(t)}$  and  $C_{(\delta)}$  is used to obtain the input function,  $f_{(t)}$  (Pithavala *et al.*, 1997). There are different deconvolution techniques: analytic deconvolution using Laplace transforms (Purves, 1995; Schalla and Weiss, 1999), implicit deconvolution by curve fitting (Veng-Pedersen, 1980), numeric deconvolution methods such as the point-area method (Yu *et al.*, 1996; Yeh *et al.*, 2001) among others. Analytic deconvolution and implicit deconvolution by curve fitting are described in Figures 4.3.10 and 4.3.11.

The Wagner–Nelson and Loo–Riegelman methods lead to calculation of the bioavailable fraction. In the deconvolution–convolution method, the *in vivo* input function that is obtained depends on the reference used during the deconvolution process.

Implicit deconvolution by curve fitting		
UIR	$C_{(\delta)(t)} = \frac{1}{D} \left( \frac{D}{V_c} e^{-k_{el} t} \right)$	}
Response	$C_{(t)} = \frac{F D k_a}{V_c (k_a - k_{el})} (e^{-k_{el} t} - e^{-k_a t})$	
Input	$f_{(t)} = F D k_a e^{-k_a t}$	

**Figure 4.3.10** Deconvolution by curve fitting implies the simultaneous curve fitting of the response function (i.e. the plasma curve after the oral administration) and the unit impulse response UIR (i.e. the response after a bolus divided by the dose). Once the disposition parameters are obtained, it is possible to extract the parameters of the input function.

Analytic deconvolution : Laplace transforms

$$c(t) = \int_0^t f(\tau) c_\delta(t-\tau) d\tau$$

Response	Input	Unit impulse response	
----------	-------	-----------------------	--

$f(t) = F D k_a e^{-k_a t}$	$\rightarrow \ell[f(t)] =$	$\frac{F D k_a}{(s + k_a)}$	input	Step 1
$c_\delta(t) = \frac{1}{D} \left( \frac{D}{V_d} e^{-k_{el} t} \right)$	$\rightarrow \ell[c_\delta(t)] =$	$\frac{1}{V_d(s + k_{el})}$	Unit impulse response	
$\ell[f(t)] \ell[c_\delta(t)] = \frac{F D k_a}{V_d(s + k_a)(s + k_{el})}$				Step 2
$\ell^{-1} \left[ \frac{F D k_a}{V_d(s + k_a)(s + k_{el})} \right] = \frac{F D k_a}{V_d(k_a - k_{el})} (e^{-k_{el} t} - e^{-k_a t})$				Step 3

**Figure 4.3.11** Steps to perform analytic convolution and deconvolution by using Laplace transforms. To convolve two functions: (1) take the Laplace transform of each one; (2) multiply the transformed functions; and (3) take the inverse transform.

If an intravenous bolus is used as a reference administration, the unit impulse response of the system corresponds to the disposition of the drug, and thus the input function incorporates all the previous processes, that is, dissolution, absorption and first pass.

In the case of using an oral solution as a reference, the unit impulse response already includes absorption and first pass besides disposition, so, by deconvolution, the input function that is estimated corresponds to the release or dissolution rate.

If the reference is an immediate release (IR) dosage form of the same drug, the unit impulse response incorporates the dissolution from the IR dosage form, and thus the input represents the release rate from the modified-release dosage form.

#### 4.3.3.3.2 Establishing the link function

With the methods described in the previous section, the input profiles (i.e. fraction absorbed versus time) are estimated from the plasma levels. The *in vitro* dissolution profiles have to be characterised, ideally, using the same time-sampling scheme and with a dissolution medium mimicking the *in vivo* dissolution conditions. The next step is to establish the correlation between the fraction absorbed and fraction dissolved at



similar time intervals. When dissolution *in vivo* is the limiting step for absorption, and the *in vitro* dissolution test reflects *in vivo* conditions, the *in vivo* input profiles and the *in vitro* dissolution profiles are superimposable, and then the link function between *in vitro* and *in vivo* fractions (for all three formulations) is a single linear correlation. In the second step, plasma concentrations are predicted from the *in vitro* dissolution data using the link model and by convoluting the unit impulse response characterised in the first step.

A one-step method involves simultaneous fitting of the *in vitro* and *in vivo* data, to obtain the parameters of the link function. Then, it is possible to compare directly the plasma concentrations predicted from the model and those observed. As there is no deconvolution step, the procedure does not require the reference administration (Buchwald, 2003).

Validation of the model consists of estimating the magnitude of error in predicting *in vivo* bioavailability, which is the ability of the model to predict  $C_{\max}$  and AUC from the IVIVC model and the dissolution profiles. The internal predictability correspond to the ability to predict  $C_{\max}$  and AUC from the data sets that have been used in the development of the correlations, whereas the external predictability refers to the ability of predictions for a data set not used in the development of the correlation.

The definition of a level A correlation, i.e. 'the *in vitro* and *in vivo* dissolution curves are superimposable', relates to the identity model. When these curves are not superimposable there are two possible strategies that may be adopted.

The first is to change the *in vitro* dissolution conditions in order to find conditions required for the curves to be superimposable. This strategy corresponds to the use and development of the so-called biorelevant dissolution media (Dressman and Reppas, 2000; Nicolaidis *et al.*, 2001; Vertzoni *et al.*, 2004) that are intended to simulate the main *in vivo* physiological variables such as pH of luminal fluids, the presence of surfactants and the volume available for dissolution.

The second approach is to find an alternative non-linear model that describes the relationship between the two curves or to include scaling factors, for either the time or the amplitude. Dunne and collaborators developed several non-linear mathematical models to obtain IVIVCs (Dunne *et al.*, 1997, 1999; O'Hara *et al.*, 2001). For the derivation of their equations, the authors considered the time at which a molecule goes into solution (either *in vivo* or *in vitro*) as a random variable (see Figure 4.3.12).  $F(t)$  represents the distribution function of the random variables. The practical meaning of the distribution function is the fraction of dose dissolved from each unit at time  $t$  under *in vitro* or *in vivo* conditions.

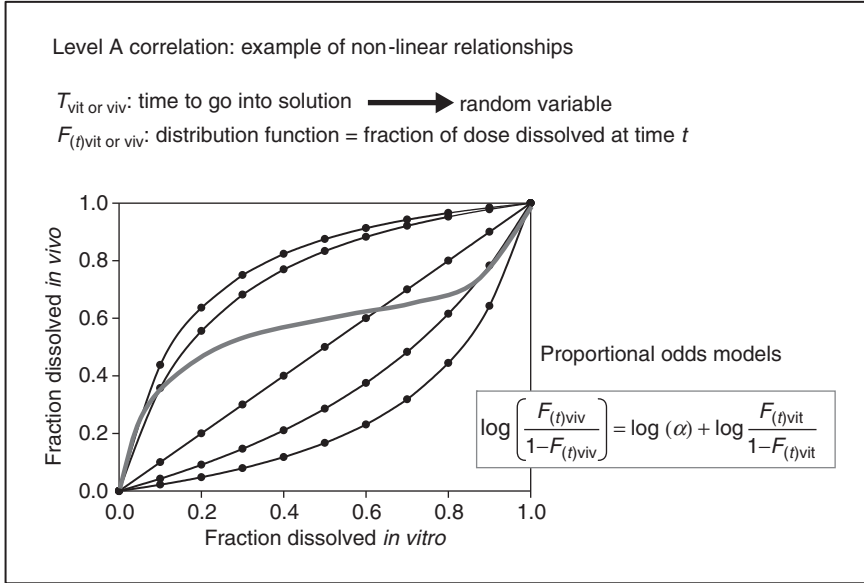


**Figure 4.3.12** Example of a non-linear IVVC relationship, the proportional odds model from Dunne *et al.* (1997). The time at which a molecule goes into solution either *in vivo* or *in vitro* is a random variable.  $F_{(t)}$  represents the distribution function of the random variable or, in practical terms, the fraction of dose dissolved from each unit at time  $t$  under *in vitro* or *in vivo* conditions. The odds function expresses the ratio of the probability that a molecule will enter into solution prior to time  $t$  to the probability that it will not. The proportional odds model states that at any time the odds function *in vivo* is proportional to the corresponding function *in vitro*.  $\alpha$  is the proportionality constant. When the proportionality constant equals one, the odds model collapse to the identity or linear model. Adapted from Dunne *et al.* (1997).

The odds function expresses the probability ratio of a molecule entering into solution or not, prior to time  $t$ . The proportional odds model states that at any time the odds *in vivo* function is proportional to the corresponding *in vitro* function; this may be described by Equation 4.3.38:

$$\left( \frac{F_{(t)viv}}{1 - F_{(t)viv}} \right) = \alpha \left( \frac{F_{(t)vit}}{1 - F_{(t)vit}} \right) \quad (4.3.38)$$

and in logarithmic expression by Equation 4.3.39:

$$\log \left( \frac{F_{(t)viv}}{1 - F_{(t)viv}} \right) = \log(\alpha) + \log \left( \frac{F_{(t)vit}}{1 - F_{(t)vit}} \right) \quad (4.3.39)$$

where  $\alpha$  is the proportionality constant. When the proportionality constant equals one, the odds model collapses to the identity or linear model.

Figure 4.3.12 represents a different relationship between the fraction of drug dissolved *in vivo* and *in vitro* for a range of values of  $\alpha$  from 0.2 to 7. The model increases its flexibility when the parameter  $\alpha$  change with time, but in these cases the relationship between the *in vivo* and the *in vitro* odds functions is no longer described by one of the curves in Figure 4.3.12 but by a shifted curve (grey line). One possible rationale to allow for  $\alpha$  changing with time is when there may be observed changes within the environment such as pH changes within GI fluids as the dosage forms proceeds along the GI tract.

Another example of a non-linear IVIVC model described in the literature is the one developed by Polli *et al.* (1996). The equations are based on the following mass balance equation:

$$M_a = M_o - (M_{ff} + M_{gi}) \quad (4.3.40)$$

where  $M_a$  is the amount absorbed at time  $t$ ,  $M_o$  represents the dose (initial amount of drug in the dosage form),  $M_{ff}$  is mass of drug still in the dosage form and  $M_{gi}$  the mass of drug in solution in GI fluids. The final equation is:

$$F_a = \frac{1}{f_a} \left( 1 - \frac{\alpha}{\alpha - 1} (1 - F_d) + \frac{1}{\alpha - 1} (1 - F_d)^\alpha \right) \quad (4.3.41)$$

where  $F_a$  is the fraction of the total amount of drug absorbed at time  $t$ ,  $f_a$  is the fraction of the dose absorbed at  $t = \infty$ ,  $\alpha$  is the ratio of the apparent first-order permeation rate constant ( $K_{papp}$ ) to the first-order dissolution rate constant ( $K_d$ ), and  $F_d$  is the fraction of drug dose dissolved at time  $t$ . For high  $\alpha$  values, i.e. when the absorption process is limited by the dissolution, the correlation is linear. But for lower  $\alpha$  values, when absorption is the rate-limiting step the correlation shows an 'L'-shape as can be seen in Figure 4.3.13. This would be the most usual situation for IR products of drug substances with high solubility and dissolution rate. This information is useful for identifying the limiting steps in the absorption process in new formulations. Drug products with high  $\alpha$  values would be those needing special attention in their technological variables, as any change in their dissolution profile will have a clear impact on their absorption rate. On the other hand, products with low  $\alpha$  values indicate that the rate-limiting step is membrane permeation and, thus, the absorbed fraction is not so sensitive to any modification in the dissolution of the product.

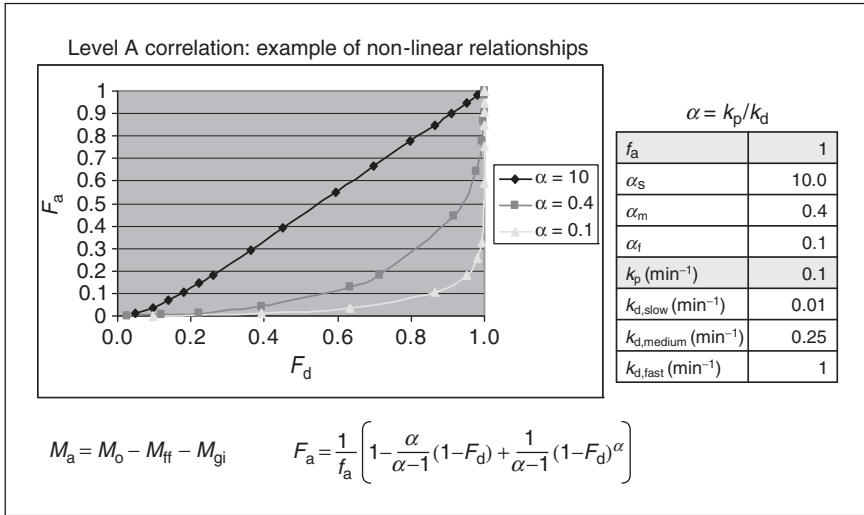


**Figure 4.3.13** Example of non-linear IVIVC. Model of Polli *et al.* (1996). The model is based on the mass balance:  $M_o$  is the dose (initial amount of drug in the dosage form);  $M_{ff}$  the mass of drug remaining in the dosage form;  $M_{gi}$  the mass of drug in solution in the GI fluids;  $\alpha$  represents the ratio between the permeation rate constant ( $k_p$ ) and the dissolution rate constant ( $k_d$ ). For explanation see text.

Once the IVIVC model has been adequately validated, the *in vitro* release profiles can be used to simulate the expected *in vivo* profiles and then to set the dissolution specifications that will ensure *in vivo* bioequivalence. A very useful and illustrative series of papers showing the basic concepts in IVIVC and how to program the calculation in Excel worksheets has been published by Langenbucher (2002, 2003a, b, 2005).

#### 4.3.4 Conclusions

A good modelling/biosimulation approach can be a useful tool in preclinical investigations and dosage form development, and there are many examples described in the literature that could help the reader to understand the advantages of using these simulations in terms of process optimisation, speeding development and maximising the information that can be extracted from large amounts of data. The following four examples have been selected from the literature for their relative simplicity, to show how to answer common questions in drug delivery, for instance, how to use modelling as a tool to explore the release mechanism from modified-release formulations (Cox *et al.*, 1999; Fukui *et al.*, 2002; Lutchman *et al.*, 2005), the use of simulation to explore the relevance

of differences in release rate on the *in vivo* exposure (Morita *et al.*, 2000; Yu *et al.*, 2001), how the release profile should be designed to achieve and maintain the target therapeutic plasma levels (Mrhar *et al.*, 1999; Morita *et al.*, 2000), or how to use simulations as tools for preclinical investigations and formulation development (Dannenfelser *et al.*, 2004, Kuentz *et al.*, 2006).

In many of these examples, specialised software is used to implement the models or simulations. In Appendix 4.3.2, a table with modelling and simulation software is included. The list has been adapted and updated from Rowland *et al.* (2004).

From the parameters obtained after model-fitting procedures, it is possible to perform deterministic simulations, i.e. without any noise or error in the predicted data. Of course, this is not the best representation of the reality, and even if this approach could be useful for understanding the system, the best-case situation would be to incorporate the real-life variability in the simulations. The non-linear mixed effect models (commonly used in the population pharmacokinetic field) include the so-called ‘fixed effects’ (the structural parameters) and ‘random effects’ (the variability parameters). Variability parameters are used to account for the possible sources of variation; these could be inter-subject variations, inter-occasion variability, and residual variability. These same concepts could be transferred to the dosage form evaluation field and the reader can find the general principles in specialised pharmacokinetic literature. Some recent references are Krishna (2004) and Bonate (2005).

## Appendix 4.3.1: Objective functions

### Least squares

In a fitting procedure we are looking for the set of parameters that produces predicted values of the dependent variable that are as close as possible to the experimental ones. The mathematical expression of this concept is the least square objective function (OF):

$$\text{OF} = \sum_{i=1}^n (y_{\text{exp}} - y_{\text{pred}})^2 \quad (4.3.42)$$

where  $y_{\text{exp}}$  represents the experimental data and  $y_{\text{pred}}$  refers to the values predicted by the model, giving a particular value for the parameters. Linear and non-linear regression by least squares means finding the combination of parameters that minimises this objective function.

### Weighted least squares

Even if the errors in each data point are independent and normally distributed, the magnitude of the error or variance may be different. When the magnitude of the errors in the dependent variable is high (as it is usual with biological data) and/or when the range covered is very wide (more than one order of magnitude), then an adequate weighting scheme becomes necessary:

$$\text{OF} = \sum_{i=1}^n w_i (y_{\text{exp}} - y_{\text{pred}})^2 \quad (4.3.43)$$

where  $w_i$  are the weights assigned to each residual value.

For instance, when the magnitude of the error is proportional to the magnitude of the dependent variable in the experimental range (so the coefficient of variation (CV) in the dependent variable is constant), then the usual weight is:

$$w_i = \frac{1}{(y_{\text{exp}})^2} \quad (4.3.44)$$

In Equation 4.3.44, if, instead of using the experimental data points the predicted ones are used, the method is called iteratively reweighted least squares, as the weights are changed in each iteration step.

### Extended least squares

In this method, a variance equation is included in the objective function expression and the parameters of the variance equation are estimated simultaneously with the model parameters.

$$\text{Variance} = f(P, P\nu, Px) \quad (4.3.45)$$

$$y_{\text{pred}} = f(P, x) \quad (4.3.46)$$

$$\text{OF} = \sum_{i=1}^{i=n} \frac{(y_{\text{exp}} - f(P, x))^2}{(\text{variance}, f(P, P\nu, x))} + \text{Ln}(\text{variance}, f(P, P\nu, x)) \quad (4.3.47)$$

where  $P$  are the model parameters and  $P\nu$  the variance parameters.

The second term in the objective function is a penalty term included in order to avoid the objective function becoming smaller due to the variance term becoming high regardless of the fit of the data.

More definitions of objective functions and a good review of linear and non-linear regression concepts applied to pharmacokinetics and biopharmaceutics can be found in Bourne's books (Bourne, 1995; Bourne *et al.*, 1986). Some basic principles are summarised in the next section.

### Appendix 4.3.2: How does non-linear regression work?

In linear regression, finding the solution of the objective function is quite straightforward. The process consists of obtaining the partial derivatives of the objective function (sum of squared residuals) with respect to the intercept and the slope (the line parameters) and equalling them to zero. The system of equations that is obtained has an algebraic solution (see Appendix 4.3.1). When the model and the equation are not linear, in general, the system of equations obtained after derivation of the objective function is not linear and does not have an algebraic solution. To find the solution it is necessary to use an iteration procedure, as well as to define the so-called initial estimates, as a starting point for the search of the parameters that minimise the objective function.

The majority of the searching algorithms or iteration methods can be classified as gradient-based methods or numerical methods. An example of gradient methods is the Gauss–Newton algorithm that is based on the Taylor's series linear approximation to the objective function.

Let us consider the Taylor's approximation (taking just the two first terms) to a non-linear function that it is being evaluated for a set of initial parameters  $P^0$ :

$$y_i = f(x_i, P) = f(x_i, P^0) + \sum_{j=1}^i \left[ \frac{\partial f(x_i, P)}{\partial P_j} \right]_{P=P^0} (P - P^0) \quad (4.3.48)$$

This expression is analogous to this one:

$$y = f(a) + (x-a)f'(a) \quad (4.3.49)$$

Reorganising the terms:

$$y_i - f(x_i, P^0) = \sum_{j=1}^i \left[ \frac{\partial f(x_i, P)}{\partial P_j} \right]_{P=P^0} (P - P^0) \quad (4.3.50)$$

The equation can be rewritten this way:

$$w = V_{i,j} * B \quad (4.3.51)$$

where  $w$  are the differences,  $y_i - f(x_i, P^0)$ ,  $B$  is the vector of parameters ( $P - P^0$ ), and  $V_{i,j}$  the matrix of partial first derivatives (called the Jacobian matrix). This matrix has as many columns as parameters and the number of rows corresponds to the number of data points.

This last equation is analogous to the linear regression equation (in matrix notation)  $y = x^*B$

Thus, the same solution can be applied, and the vector of parameters  $B$  is:

$$B = (V_{i,j}^T V_{i,j})^{-1} V_{i,j} w \quad (4.3.52)$$

(see Appendix 4.3.1).

From  $B$ , a new vector of parameters  $P^1$  is obtained. Then, the same calculation can be done again, that is:

$$P_{j+1} = P_j + (V_{i,j}^T V_{i,j})^{-1} V_{i,j} w \quad (4.3.53)$$

An example of the first step of the iterative process based on the Gauss–Newton algorithm is summarised in Table 4.3.5, taking the Michaelis–Menten equation as an example. The example is adapted from a similar one in Endrenyi's book (Endrenyi, 1981). This *one-step* calculation is repeated many times in the standard non-linear regression software until a convergence criterion is achieved. In non-linear regression, a starting point (initial estimates) is necessary, as well as a criterion to stop the search. In general, the convergence criterion is defined in terms of the relative improvement on the sum of squares (the objective function) with equations similar to Equation 4.3.54:

$$|(SS_{n+1} - SS_n)/SS_n| < \delta \quad (4.3.54)$$

where  $\delta$  is the convergence criterion and  $SS_{n+1}$  and  $SS_n$  the sum of squares obtained in the  $n + 1$  and  $n$  iterations.

The Nelder–Mead algorithm (or simplex method) (Nelder and Mead, 1965; Walters, 1991) is a numerical method based on the construction of a figure with  $p + 1$  vertices (where  $p$  is the number of parameters). In a problem with two parameters, the simplex would have three vertices. Each of these vertices represents a combination of values of  $P_1$  and  $P_2$  at which the objective function is evaluated. The point with the highest value for the objective function is projected over the simplex centroid, thus obtaining a new simplex figure and restarting the process again. A graphical representation of this procedure is shown in Figure 4.3.14. The lines represent combinations of parameter values rendering the same objective function value (in a similar fashion to pressure isobars).



**Table 4.3.5** Example of first iteration

$x = \text{concentration}$	$y_{\text{exp}} = \text{rate}$	$y_{\text{pred}}$	$\text{Residual} = (y_{\text{exp}} - y_{\text{pred}})$	$\text{Residual}^2$	$dy/dK_m = C/(K_m + C)$	$dy/dV_m = -V_m C/(K_m + C)^2$
0.010	0.01960	0.01275	0.00685	$4.69 \times 10^{-5}$	0.01961	-0.02499
0.030	0.05628	0.03679	0.01949	$3.80 \times 10^{-5}$	0.05660	-0.06942
0.070	0.10948	0.07982	0.02965	$8.79 \times 10^{-5}$	0.12281	-0.14004
0.100	0.16205	0.10833	0.05372	$2.89 \times 10^{-5}$	0.16667	-0.18056
0.300	0.32731	0.24375	0.08356	$6.98 \times 10^{-5}$	0.37500	-0.30469
0.500	0.44547	0.32500	0.12047	$1.45 \times 10^{-5}$	0.50000	-0.32500
1.000	0.57014	0.43333	0.13681	$1.87 \times 10^{-5}$	0.66667	-0.28889
3.000	0.70972	0.55714	0.15258	$3.33 \times 10^{-5}$	0.85714	-0.15918
5.000	0.73112	0.59091	0.14021	$1.97 \times 10^{-5}$	0.90909	-0.10744
6.000	0.75360	0.60000	0.15360	$2.36 \times 10^{-5}$	0.92308	-0.09231
8.000	0.70007	0.61176	0.08831	$7.70 \times 10^{-5}$	0.94118	-0.07197
10.000	0.71021	0.61905	0.09116	$8.31 \times 10^{-5}$	0.95238	-0.05896
			$w$	0.1270457	$V_{i,j}$	
				SS		

$V_m$	0.65	0.1151904	0.7651904			
$K_m$	0.5	-0.187224	0.3127757			
	$P^0$	$B = (P^1 - P^0)$	$P^1 = P^0 + B$			
$V_{i,j}$ transposed * $V_{i,j}$		Inverse ( $V_{i,j}$ transposed * $V_{i,j}$ )		SS/df		
5.087	-0.96427	0.36692	0.898826	0.0127046	0	
-0.96430	0.3936313	0.898834	0.7422832	0	0.0127046	
$V_{i,j}$ transposed * $w$		Inverse ( $V_{i,j}$ transposed * $V_{i,j}$ ) * SS/df = covariance matrix				
0.76657		0.0046615	0.0114192	= Var( $V_m$ )		
-0.1848		0.0114192	0.0602487	= Var( $K_m$ )		
					EE( $V_m$ )	0.0682752
					EE( $K_m$ )	0.245456

Notes: EE, standard estimation error; df, degrees of freedom (number of points – number of parameters); Var, variance;  $V_m$ , maximal velocity;  $K_m$ , Michaelis–Menten constant; SS, sum of squared residuals;  $V_{i,j}$ , matrix of first partial derivatives;  $w$ , differences between experimental and predicted values; in order to further reduce SS and estimate the parameters the next step would consist of taking  $P^1$  values and using them as new set of  $P^0$  values. The iteration process continues until convergence criteria are achieved. See text for detailed explanation. Adapted from (Endrenyi, 1981)

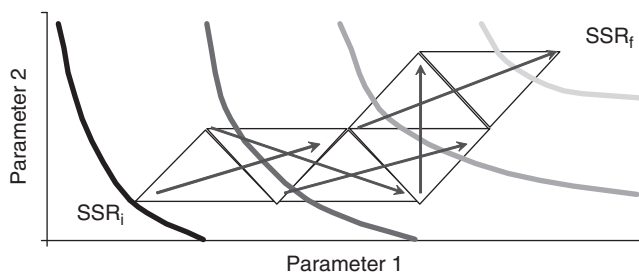


**Figure 4.3.14** Graphical representation of Nelder-Mead algorithm (or simplex method) in a problem with two parameters. The simplex has three vertexes. Each of these vertexes represents a combination of values of  $P_1$  and  $P_2$  (parameters) at which the objective function is evaluated. The point (combination of  $P_1$  and  $P_2$ ) with the highest value for the objective function is projected over the simplex centroid to obtain the new simplex figure. The lines represent combinations of parameters values rendering the same objective function value.  $SSR_i$ , initial value of the sum of squared residuals;  $SSR_f$ , final value of the sum of squared residuals.  $SSR_f < SSR_i$ .

Understanding how the values of the parameters are estimated in non-linear regression is very useful in order to design experiments and optimise the information that could be obtained from the experimental data.

Table 4.3.5 shows how the standard error of estimation is calculated. In order to get the variance of the parameter, the covariance matrix is computed. The inverse of the covariance matrix ( $V_{i,j}^T(\text{diag } w)V_{i,j}$ ) is the Fisher information matrix. Maximising the determinant of the Fisher information matrix will result in decreasing the variance of the parameter on the pre-specified model. In Figure 4.3.15,  $dy/dK_m$  is represented (one of the parameters of the example in Table 4.3.5) versus the concentration ( $x$ ) and its squared value. In order to reduce the estimation error, it is advisable to include in the experimental design those values of the independent variable at which  $dy/dK_m$  is higher (in absolute value), in order to make the variance-covariance matrix smaller. In summary, the estimation error will depend on the experimental design (as this impacts the amount of information about the parameters that is included in the data ( $V_{i,j}$ )) and on the residual variability. The residual error includes the pure error, as this could be the analytical error, random variability and the potential lack of fit (i.e. discrepancies between the experimental and predicted values if the model is not the correct one) (Franz *et al.*, 1996; Flaherty *et al.*, 2006).

There are various forms of optimality criteria that are used to select the points for a design: one popular criterion is *D-optimality*, which seeks to maximise  $|V_{i,j}^T(\text{diag } w)V_{i,j}|$ , the determinant of the *information*

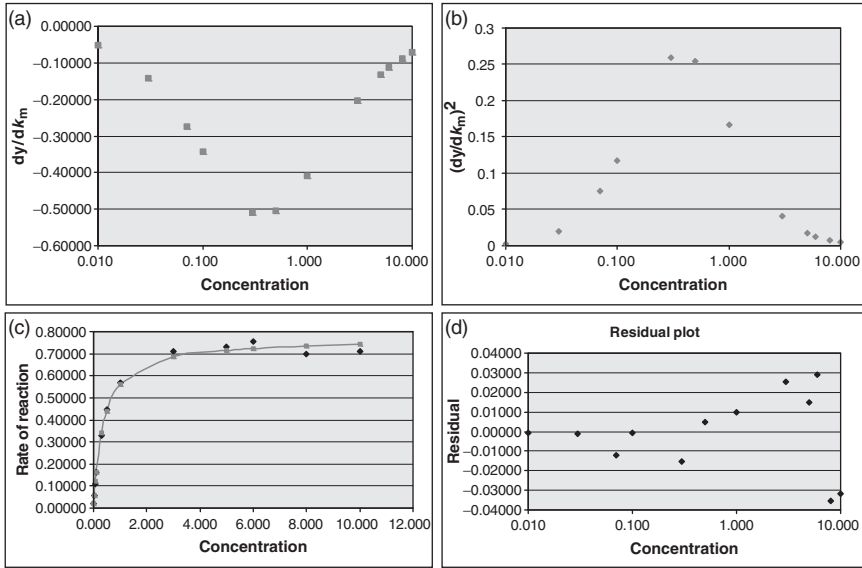


**Figure 4.3.15** (a) Derivate of the dependent variable with respect to the parameter ( $K_m$ ). (b) Squared value of the derivate in panel a. (c) plot of the dependent variable (rate of reaction) versus the independent one (substrate concentration). (d) Residual plot: differences between the experimental and the predicted values (residuals) versus concentration (independent variable). For explanation see text.

$matrix V_{i,j}^T (diag w) V_{i,j}$  of the design. This criterion minimises the generalised variance of the parameter estimates based on a prespecified model (Croarkin *et al.*, 2005).

### How well does the model fit the data?

Once the convergence criterion is achieved, it is useful to perform the fit again, by changing the initial estimates in order to check that the algorithm has found the true minimum instead of a local minimum. A second alternative is to perform the fit again but using a different iteration algorithm, if the software application allows doing so. It is advisable, besides the latter steps, to evaluate the sum of the squared residuals, and to inspect the graph with the experimental values and the fitted ones, to check how close the predicted curve is to the real data. On the other hand, the parameter values have to be evaluated, bearing in mind the assumptions of the model and their plausibility in the framework of the experiment. If the estimation errors of the parameters are high, that could indicate a bad experimental design or over-parameterisation of the model. This latter problem could be difficult to solve, as the range of

independent variable values could be restricted by other experimental constraints, and it is not always possible to remove a parameter from a non-linear model. Other criteria to judge the goodness of the fit are briefly discussed next.

### *Residual plot*

Provided that the residuals have a mean of zero and constant variance, are independent, and follow a normal distribution, the plot of the residual versus the independent variable should appear as randomly scattered around the zero value. Any trend in the residual plot indicates either that the variance is not constant or that the model is inadequate.

### *Coefficient of correlation R*

This indicates how closely a best-fit curve matches the given data and is also a measure of the joint variation of the dependent and the independent variable (adimensional covariance).

$$R = \frac{\sum_{i=1}^n (x_i - \bar{x}) (y_i - \bar{y})}{\sqrt{\sum_{i=1}^n (x_i - \bar{x})^2 \sum_{i=1}^n (y_i - \bar{y})^2}} \quad (4.3.55)$$

### *Coefficient of determination $R^2$*

The total variation of the dependent variable  $y$  around its mean can be explained in part by the model (the regression equation) and by random variation. In mathematical terms:

$$SC_{\text{total}} = SS_{\text{model}} + SS_{\text{residual}} \quad (4.3.56)$$

$$\sum (y_i - \bar{y})^2 = \sum (\hat{y} - \bar{y})^2 + \sum (y_i - \hat{y})^2 \quad (4.3.57)$$

where  $\hat{y}$  are the predicted values;  $y_i$  the experimental values and  $\bar{y}$  is the dependent variable mean.

From this equation it is possible to estimate how much of the variability of the dependent variable is explained by the model, defining  $R^2$  as:

$$R^2 = \frac{SS_{\text{model}}}{SS_{\text{Total}}} \quad (4.3.58)$$

The model is better at predicting the experimental data as this value approaches 1.

## Comparing models of different complexity

### *Akaike information criterion (AIC)*

This is a model-order selection criterion based on parsimony. More complicated models are penalised for the inclusion of additional parameters. The idea behind this parameter is that more complicated models with a large number of parameters would lead to a better fit but with fewer degrees of freedom and with less practical utility, so the criterion tries to find a balance between goodness of fit and model complexity. AIC is computed from the sum of squared residuals, and includes a penalising term for models with more parameters ( $P$ ):

$$\text{AIC} = \ln \text{SS}_{\text{res}} + 2P \quad (4.3.59)$$

The best model is the one with a lower AIC value

### *Snedecor's F test*

Snedecor's  $F$  test (or Fisher ratio) is used to compare the residual variances of models of increasing complexity (sum of squares divided by their degrees of freedom). To establish if the decrease in the sum of squared residuals produced by the inclusion of more parameters in the model is statistically significant, the  $F$  statistic is calculated:

$$F_{\text{calc}} = \frac{(\text{SC}_s - \text{SC}_c) / (\nu_s - \nu_c)}{\text{SC}_c / \nu_c} \quad (4.3.60)$$

where  $\text{SC}_s$  and  $\text{SC}_c$  correspond to the sum of squares of the simple and complex model respectively, and  $\nu_s$  and  $\nu_c$  are the degrees of freedom of each model (number of data points minus number of parameters).

The calculated value of  $F$  is compared with the tabulated  $F$  for the desired probability level (in general 0.05) and the degrees of freedom of the numerator and denominator. If the calculated  $F$  is lower than the tabulated  $F$ , then the decrease of the sum of squares is not significant so the simplest model should be chosen. When the calculated  $F$  value is higher than the tabulated one, then the improvement in the sum of squares is statistically significant, i.e. the complex model is better.

## Appendix 4.3.3: Software tools, companies and institutions developing biosimulation packages

Adapted from Rowland (Rowland *et al.*, 2004); other URL link including modelling software: [www.boomer.org/pkin/soft.html](http://www.boomer.org/pkin/soft.html)

### General tools for scientific computing

- Berkeley Madonna, University of California at Berkeley: [www.berkeleymadonna.com/](http://www.berkeleymadonna.com/)
- MATLAB-Simulink, The MathWorks, Inc: [www.mathworks.com](http://www.mathworks.com)
- MLAB: Civilized Software, Inc: [www.civilized.com/](http://www.civilized.com/)
- GNU Octave, University of Wisconsin: [www.octave.org/](http://www.octave.org/)

### Biomathematical and pharmacokinetics modelling software

- ADAPT II, Biomedical Simulations Resource, USC: [bmsr.usc.edu/](http://bmsr.usc.edu/)
- ModelMaker, ModelKinetix: [www.modelkinetix.com](http://www.modelkinetix.com)
- NONMEM, Univ. of California, San Francisco and Globomax Service Group: [www.globomaxservice.com](http://www.globomaxservice.com)
- Stella High Performance Systems Inc: [www.hps-inc.com/](http://www.hps-inc.com/)
- WinNonlin, WinnonMix, Trial Simulator, Pharsight Corp: [www.pharsight.com/products/prod\\_home.php](http://www.pharsight.com/products/prod_home.php)
- IntellipharmaPK, IntellipharmaCR, IntellipharmaC: [www.intellipharma.com/](http://www.intellipharma.com/)

### Toxicokinetic software

- ACSL Toxicology Toolkit, Aegis Technologies Group Inc: [www.aegistg.com/](http://www.aegistg.com/)

### Physiologically based custom-designed software

- Simulations Plus Inc: [www.simulations-plus.com](http://www.simulations-plus.com)
- SimCyp: [www.simcyp.com](http://www.simcyp.com)

## References

- Agoram B, Woltosz WS, Bolger MB (2001). Predicting the impact of physiological and biochemical processes on oral drug bioavailability. *Adv Drug Deliv Rev* 50 (suppl1): S41–S67.
- Allan G, Davis J, Dickins M, *et al.* (2008). Pre-clinical pharmacokinetics of UK-453 061, a novel non-nucleoside reverse transcriptase inhibitor (NNRTI), and use of *in silico* physiologically based prediction tools to predict the oral pharmacokinetics of UK-453 061 in man. *Xenobiotica* 38: 620–640.
- Bermejo M, Ruiz-García A (2002). Oral permeability predictions from *in silico* to in vivo models. In: Cooper E, ed. *Business Briefing: PharmaTech 2002*. London: World Markets Research Centre Ltd, 1–7.
- Bermejo M, Merino V, Garrigues TM, *et al.* (1999). Validation of a biophysical drug absorption model by the PATQSAR system. *J Pharm Sci* 88: 398–405.

- Bonate PL (2005). *Pharmacokinetic-pharmacodynamic Modeling and Simulation*. New York: Springer.
- Bornemann LD, Min BH, Crews T, *et al.* (1985). Dose dependent pharmacokinetics of midazolam. *Eur J Clin Pharmacol* 29: 91–95.
- Bourne DWA (1995). *Mathematical Modeling of Pharmacokinetic Data*. Lancaster: Technomic Publishing Company.
- Bourne DWA, Triggs, EJ, Eadie MJ (1986). *Pharmacokinetics for the Non-mathematical*. Boston: MTP Press.
- Buchwald P (2003). Direct, differential-equation-based *in-vitro-in-vivo* correlation (IVIVC) method. *J Pharm Pharmacol* 55: 495–504.
- Camenisch G, Folkers G, van de Waterbeemd H (1996). Review of theoretical passive drug absorption models: historical background, recent developments and limitations. *Pharm Acta Helv* 71: 309–327.
- Casabo VG, Nunez-Benito E, Martinez-Coscolla A, *et al.* (1987). Studies on the reliability of a bihyperbolic functional absorption model. II. Phenylalkylamines. *J Pharmacokinet Biopharm* 15: 633–643.
- Clark DE (1999a). Rapid calculation of polar molecular surface area and its application to the prediction of transport phenomena. 1. Prediction of intestinal absorption. *J Pharm Sci* 88: 807–814.
- Clark DE (1999b). Rapid calculation of polar molecular surface area and its application to the prediction of transport phenomena. 2. Prediction of blood–brain barrier penetration. *J Pharm Sci* 88: 815–821.
- Collander R (1951). Partition of organic compounds between higher alcohols and water. *Acta Chem Scand* 5: 774–778.
- Costa P, Sousa Lobo JM (2001). Modeling and comparison of dissolution profiles. *Eur J Pharm Sci* 13: 123–133.
- Cox PJ, Khan KA, Munday DL, Sujja-Areevath J (1999). Development and evaluation of a multiple-unit oral sustained release dosage form for S(+)-ibuprofen: preparation and release kinetics. *Int J Pharm* 193: 73–84.
- Craig DQ (2002). The mechanisms of drug release from solid dispersions in water-soluble polymers. *Int J Pharm* 231: 131–144.
- Croarkin C, Tobias P (2005). *NIST/SEMATECH e-Handbook of Statistical Methods*. <http://www.itl.nist.gov/div898/handbook/> (accessed 3 June 2009).
- Dannenfelser RM, He H, Joshi Y, Bateman S, Serajuddin AT (2004). Development of clinical dosage forms for a poorly water soluble drug I: Application of polyethylene glycol-polysorbate 80 solid dispersion carrier system. *J Pharm Sci* 93: 1165–1175.
- de Almeida LP, Simoes S, Brito P, Portugal A, Figueiredo M (1997). Modeling dissolution of sparingly soluble multisized powders. *J Pharm Sci* 86: 726–732.
- Dokoumetzidis A, Kosmidis K, Argyrakis P, Macheras P (2005). Modeling and Monte Carlo simulations in oral drug absorption. *Basic Clin Pharmacol Toxicol* 96: 200–205.
- Dokoumetzidis A, Papadopoulou V, Macheras P (2006). Analysis of dissolution data using modified versions of Noyes–Whitney equation and the Weibull function. *Pharm Res* 23: 256–261.
- Dokoumetzidis A, Kalantzi L, Fotaki N (2007). Predictive models for oral drug absorption: from *in silico* methods to integrated dynamical models. *Expert Opin Drug Metab Toxicol* 3: 491–505.



- Dowty ME, Dietsch CR (1997). Improved prediction of *in vivo* peroral absorption from *in vitro* intestinal permeability using an internal standard to control for intra- and inter-rat variability. *Pharm Res* 14: 1792–1797.
- Dressman JB, Fleisher D (1986). Mixing-tank model for predicting dissolution rate control or oral absorption. *J Pharm Sci* 75: 109–116.
- Dressman JB, Reppas C (2000). *In vitro*–*in vivo* correlations for lipophilic, poorly water-soluble drugs. *Eur J Pharm Sci* 11(suppl2): S73–80.
- Dressman JB, Fleisher D, Amidon GL (1984). Physicochemical model for dose-dependent drug absorption. *J Pharm Sci* 73: 1274–1279.
- Dunne A, O'Hara T, Devane J (1997). Level A *in vivo*–*in vitro* correlation: nonlinear models and statistical methodology. *J Pharm Sci* 86: 1245–1249.
- Dunne A, O'Hara T, Devane J (1999). A new approach to modelling the relationship between *in vitro* and *in vivo* drug dissolution/absorption. *Stat Med* 18: 1865–1876; discussion 1877.
- Dutta S, Qiu Y, Samara E, Cao G, Granneman GR (2005). Once-a-day extended-release dosage form of divalproex sodium III: development and validation of a Level A *in vitro*–*in vivo* correlation (IVIVC). *J Pharm Sci* 94: 1949–1956.
- Endrenyi L (1981). Kinetic Data Analysis: design and analysis of enzyme and pharmacokinetic experiments. New York: Plenum Press.
- FDA Center for Drug Evaluation and Research (1997). *Guidance for Industry. Extended Release Oral Dosage Forms: development, evaluation, and application of in vitro/in vivo correlations*. <http://www.fda.gov/downloads/Drugs/GuidanceComplianceRegulatoryInformation/Guidances/UCM070239.pdf> (accessed 3 June 2009).
- FDA Center for Drug Evaluation and Research (1999). *FDA Guidance for Industry. Population pharmacokinetics*. <http://www.fda.gov/downloads/ScienceResearch/SpecialTopics/WomensHealthResearch/UCM133184.pdf> (accessed 3 June 2009).
- FDA, Center for Drug Evaluation and Research (2000). *Guidance for Industry, Waiver of in vivo Bioavailability and Bioequivalence Studies for Immediate-release Solid Oral Dosage Forms based on a Biopharmaceutics Classification System*. <http://www.fda.gov/downloads/Drugs/GuidanceComplianceRegulatoryInformation/Guidances/UCM070246.pdf> (accessed 3 June 2009).
- Flaherty P, Jordan MI, Arkin AP (2006). Robust design of biological experiments. In: Weiss Y, Schoelkopf B, Platt J, eds. *Advances in Neural Information Processing Systems (NIPS) 18: proceedings of the 19th Annual Conference (NIPS 2005)*. Cambridge, MA: MIT Press: 363–370. [http://www.cs.berkeley.edu/~jordan/papers/FlaJorArk\\_nips05.pdf](http://www.cs.berkeley.edu/~jordan/papers/FlaJorArk_nips05.pdf) (accessed 3 June 2009).
- Franz RM, Cooper DC, Browne JE, Lewis AR (1996). Experimental design, modeling, and optimization strategies for product and process development. In: H.A. Lieberman HA, Rieger MM, Banker GS, eds. *Pharmaceutical Dosage Forms*. New York: Marcel Dekker, 437–519.
- Fukui A, Fujii R, Yonezawa Y, Sunada H (2002). Analysis of the release process of phenylpropanolamine hydrochloride from ethylcellulose matrix granules. *Chem Pharm Bull (Tokyo)* 50: 1439–1442.
- Gillespie WR, Veng-Pedersen P (1985). A polyexponential deconvolution method. Evaluation of the 'gastrointestinal bioavailability' and mean *in vivo* dissolution time of some ibuprofen dosage forms. *J Pharmacokinet Biopharm* 13: 289–307.

- Grassi M, Grassi G (2005). Mathematical modelling and controlled drug delivery: matrix systems. *Curr Drug Deliv* 2: 97–116.
- Higuchi WI, Ho NFH, Park JY, Komiya I (1981). Rate limiting steps and factors in drug absorption. In: Prescott LF, Nimmo WS, eds. *Drug Absorption*. New York: ADIS Press, 35–60.
- Hintz R, Johnson K (1989). The effect of particle size distribution on dissolution rate and oral absorption. *Int J Pharm* 51: 9–17.
- Iga K, Ogawa Y, Yashiki T, Shimamoto T (1986). Estimation of drug absorption rates using a deconvolution method with nonequal sampling times. *J Pharmacokinet Biopharm* 14: 213–225.
- Johnson KC (2003). Dissolution and absorption modeling: model expansion to simulate the effects of precipitation, water absorption, longitudinally changing intestinal permeability, and controlled release on drug absorption. *Drug Dev Ind Pharm* 29: 833–842.
- Johnson KC, Swindell AC (1996). Guidance in the setting of drug particle size specifications to minimize variability in absorption. *Pharm Res* 13: 1795–1798.
- Kamm W, Raddatz P, Gante J, Kissel T (1999). Prodrug approach for alphaIIb beta3-peptidomimetic antagonists to enhance their transport in monolayers of a human intestinal cell line (Caco-2): comparison of *in vitro* and *in vivo* data. *Pharm Res* 16: 1527–1533.
- Kanjickal DG, Lopina ST (2004). Modeling of drug release from polymeric delivery systems – a review. *Crit Rev Ther Drug Carrier Syst* 21: 345–386.
- Krishna R (2004). *Applications of Pharmacokinetic Principles in Drug Development*. New York: Kluwer Academic/Plenum Publishers.
- Kuentz M, Nick S, Parrott N, Rothlisberger D (2006). A strategy for preclinical formulation development using GastroPlus as pharmacokinetic simulation tool and a statistical screening design applied to a dog study. *Eur J Pharm Sci* 27: 91–99.
- Langenbucher F (2002). Handling of computational *in vitro/in vivo* correlation problems by Microsoft Excel: I. Principles and some general algorithms. *Eur J Pharm Biopharm* 53: 1–7.
- Langenbucher F (2003a). Handling of computational *in vitro/in vivo* correlation problems by Microsoft Excel II. Distribution functions and moments. *Eur J Pharm Biopharm* 55: 77–84.
- Langenbucher F (2003b). Handling of computational *in vitro/in vivo* correlation problems by Microsoft Excel: III. Convolution and deconvolution. *Eur J Pharm Biopharm* 56: 429–37.
- Langenbucher F (2005). Handling of computational *in vitro/in vivo* correlation problems by Microsoft Excel: IV. Generalized matrix analysis of linear compartment systems. *Eur J Pharm Biopharm* 59: 229–235.
- Lansky P, Weiss M (1999). Does the dose–solubility ratio affect the mean dissolution time of drugs?. *Pharm Res* 16: 1470–1476.
- Lansky P, Weiss M (2001). Modeling heterogeneity of properties and random effects in drug dissolution. *Pharm Res* 18: 1061–1067.
- Lansky P, Weiss M (2003). Classification of dissolution profiles in terms of fractional dissolution rate and a novel measure of heterogeneity. *J Pharm Sci* 92: 1632–1647.
- Lansky P, Lanska V, Weiss M (2004). A stochastic differential equation model for drug dissolution and its parameters. *J Control Release* 100: 267–274.

- Lipinski CA, Lombardo F, Dominy BW, Feeney PJ (2001). Experimental and computational approaches to estimate solubility and permeability in drug discovery and development settings. *Adv Drug Deliv Rev* 46: 3–26.
- Lu AT, Frisella ME, Johnson KC (1993). Dissolution modeling: factors affecting the dissolution rates of polydisperse powders. *Pharm Res* 10: 1308–1314.
- Lutchman D, Dangor CM, Perumal D (2005). Formulation of rate-modulating pellets for the release of ibuprofen: an extrusion-spheronization process. *J Microencapsul* 22: 643–659.
- Macheras PE, Symillides MY (1989). Toward a quantitative approach for the prediction of the fraction of dose absorbed using the absorption potential concept. *Biopharm Drug Dispos* 10: 43–53.
- Martin-Villodre A, Plá-Delfina JM, Moreno J, *et al.* (1986). Studies on the reliability of a bihyperbolic functional absorption model. I. Ring-substituted anilines. *J Pharmacokinet Biopharm* 14: 615–633.
- Merino V, Freixas J, Bermejo M, *et al.* (1995). Biophysical models as an approach to study passive absorption in drug development: 6-fluoroquinolones. *J Pharm Sci* 84: 777–782.
- Modi NB, Lam A, Lindemulder E, Wang B, Gupta SK (2000). Application of *in vitro* – *in vivo* correlations (IVIVC) in setting formulation release specifications. *Biopharm Drug Dispos* 21: 321–326.
- Montgomery D, Peck E, Vining G (2001). *Introduction to Linear Regression Analysis*. New York: Wiley.
- Morita R, Honda R, Takahashi Y (2000). Development of oral controlled release preparations, a PVA swelling controlled release system (SCRS). II. *In vitro* and *in vivo* evaluation. *J Control Release* 68: 115–120.
- Motulsky H, Christopoulos A (2004). *Fitting Models to Biological Data Using Linear and Non linear Regression: a practical guide to curve fitting*. New York: Oxford University Press.
- Mrhar A, Bogataj M, Grabnar I, Karba R (1999). Formulation of controlled release microspheres containing nicardipine: the role of pharmacokinetic modeling and computer simulation. *Eur J Drug Metab Pharmacokinet* 24: 55–61.
- Nelder JA, Mead RA (1965). Simplex method for function minimization. *Comput J* 7: 308–313.
- Neuhoff S, Yang J, Jamei M, Tucker G, Rostami-Hodjegan A (2008). Abstracts from the 10th European Regional ISSX Meeting, Simulation of the effect of P-glycoprotein on drug absorption in the human gastrointestinal tract. May 18th–21st 2008; Vienna, Austria. *Drug Metab Rev* 40: 169–170.
- Nicolaides E, Symillides M, Dressman JB, Reppas C (2001). Biorelevant dissolution testing to predict the plasma profile of lipophilic drugs after oral administration. *Pharm Res* 18: 380–388.
- Nørager S, Iakovidis I, Cabrera M, Özcivelek R (2005). White Paper: *Towards Virtual Physiological Human: multilevel modelling and simulation of the human anatomy and physiology*. <http://www.radicalhealth.eu/files/ec-vph-white-paper2005nov1.pdf> (accessed 3 June 2009).
- Norinder U, Osterberg T, Artursson P (1999). Theoretical calculation and prediction of intestinal absorption of drugs in humans using MolSurf parametrization and PLS statistics. *Eur J Pharm Sci* 8: 49–56.

- Noyes AA, Whitney WR (1897). The rate of solution of solid substances in their own solutions. *J Am Chem Soc* 19: 930–934.
- O'Hara T, Hayes S, Davis J, *et al.* (2001). *In vivo*–*in vitro* correlation (IVIVC) modeling incorporating a convolution step. *J Pharmacokinet Pharmacodyn* 28: 277–298.
- Oberle RL, Amidon GL (1987). The influence of variable gastric emptying and intestinal transit rates on the plasma level curve of cimetidine; an explanation for the double peak phenomenon. *J Pharmacokinet Biopharm* 15: 529–544.
- Oh DM, Curl RL, Amidon GL (1993). Estimating the fraction dose absorbed from suspensions of poorly soluble compounds in humans: a mathematical model. *Pharm Res* 10: 264–270.
- Palm K, Luthman K, Ungell AL, Strnadlund G, Artursson P (1996). Correlation of drug absorption with molecular surface properties. *J Pharm Sci* 85: 32–39.
- Palm K, Stenberg P, Luthman K, Artursson P (1997). Polar molecular surface properties predict the intestinal absorption of drugs in humans. *Pharm Res* 14: 568–571.
- Pithavala YK, Soria I, Zimmerman CL (1997). Use of the deconvolution principle in the estimation of absorption and pre-systemic intestinal elimination of drugs. *Drug Metab Dispos* 25: 1260–1265.
- Plá-Delfina JM, Moreno J (1981). Intestinal absorption–partition relationships: a tentative functional nonlinear model. *J Pharmacokinet Biopharm* 9: 191–215.
- Plá-Delfina JM, Moreno J, Duran J, Pozo A (1975). Calculation of the gastric absorption rate constants of 5-substituted barbiturated through the  $R_m$  values of substituent delta  $R_m$  constants in reversed-phase partition chromatography. *J Pharmacokinet Biopharm* 3: 115–141.
- Plá-Delfina JM, Moreno J, Riera P, *et al.* (1980). An experimental assessment of the Wagner-Sedman extraction theory for the intestinal absorption of antibacterial sulfonamides. *J Pharmacokinet Biopharm* 8: 297–309.
- Polak S, Jamei M, Turner D, *et al.* (2008). Abstracts from the 10th European Regional ISSX Meeting. Prediction of the *in vivo* behaviour of modified release formulations of metoprolol from *in vitro* dissolution profiles using the ADAM model (Simcyp®V8). May 18th–21st Vienna, Austria. *Drug Metab Rev* 40: 45–46.
- Polli JE, Crison JR, Amidon GL (1996). Novel approach to the analysis of *in vitro*–*in vivo* relationships. *J Pharm Sci* 85: 753–760.
- Purves RD (1995). Accuracy of numerical inversion of Laplace transforms for pharmacokinetic parameter estimation. *J Pharm Sci* 84: 71–74.
- Rowland M, Balant L, Peck C, (2004). Physiologically based pharmacokinetics in drug development and regulatory science: a workshop report (Georgetown University, Washington, DC, May 29–30, 2002). *AAPS Pharm Sci* 6: E6.
- Sakaeda T, Okamura N, Nagata S, *et al.* (2001). Molecular and pharmacokinetic properties of 222 commercially available oral drugs in humans. *Biol Pharm Bull* 24: 935–940.
- Schalla M, Weiss M (1999). Pharmacokinetic curve fitting using numerical inverse Laplace transformation. *Eur J Pharm Sci* 7: 305–309.
- Schreiner T, Schaefer UF, Loth H (2005). Immediate drug release from solid oral dosage forms. *J Pharm Sci* 94: 120–133.

- Siepmann J, Peppas NA (2001). Mathematical modeling of controlled drug delivery. *Adv Drug Deliv Rev* 48: 137–138.
- Shore PA, Brodie BB, Hogben CAM (1957). The gastric secretion of drugs: a pH partition hypothesis. *J Pharmacol Exp Ther* 119: 361–369.
- Sirisuth N, Augsburger LL, Eddington ND (2002). Development and validation of a non-linear IVIVC model for a diltiazem extended release formulation. *Biopharm Drug Dispos* 23: 1–8.
- Stenberg P, Luthman K, Ellens H, *et al.* (1999). Prediction of the intestinal absorption of endothelin receptor antagonists using three theoretical methods of increasing complexity. *Pharm Res* 16: 1520–1526.
- Veng-Pedersen PV (1980a). Novel deconvolution method for linear pharmacokinetic systems with polyexponential impulse response. *J Pharm Sci* 69: 312–318.
- Veng-Pedersen P (1980b). An algorithm and computer program for deconvolution in linear pharmacokinetics. *J Pharmacokinet Biopharm* 8: 463–481.
- Veng-Pedersen P, Miller R (1987). Deconvolution at steady state: determination of gastrointestinal bioavailability of sustained release theophylline. *Int J Clin Pharmacol Ther Toxicol* 25: 233–237.
- Vertzoni M, Fotaki N, Kostewicz E, *et al.* (2004). Dissolution media simulating the intraluminal composition of the small intestine: physiological issues and practical aspects. *J Pharm Pharmacol* 56: 453–462.
- Wagner JG, Sedman AJ (1973). Quantitation rate of gastrointestinal and buccal absorption of acidic and basic drugs based on extraction theory. *J Pharmacokin Biopharm* 1: 23–50.
- Walters FH, Parker LR Jr, Morgan SL, Deming SN (1991). *Sequential Simplex Optimization: a technique for improving quality and productivity in research, development, and manufacturing*. Boca Raton, FL: CRC Press.
- Wang JZ, Flanagan DR (1999). General solution for diffusion controlled dissolution of spherical particles. 1. Theory. *J Pharm Sci* 88: 731–738.
- Yeh KC, Holder DJ, Winchell GA, Wenning LA, Prueksaritanont T (2001). An extended point-area deconvolution approach for assessing drug input rates. *Pharm Res* 18: 1426–1434.
- Yoshida F, Topliss JG (2000). QSAR model for drug human oral bioavailability. *J Med Chem* 43: 2575–2585.
- Yu LX, Amidon GL (1998). Saturable small intestinal drug absorption in humans: modeling and interpretation of cefatrizine data. *Eur J Pharm Biopharm* 45: 199–203.
- Yu LX, Amidon GL (1999). A compartmental absorption and transit model for estimating oral drug absorption. *Int J Pharm* 186: 119–125.
- Yu LX, Lipka E, Crison JR, Amidon GL (1996). Transport approaches to the biopharmaceutical design of oral drug delivery systems: prediction of intestinal absorption. *Adv Drug Deliv Rev* 19: 359–376.
- Yu LX, Ellison CD, Conner DP, Lesko LJ, Hussain AS (2001). Influence of drug release properties of conventional solid dosage forms on the systemic exposure of highly soluble drugs. *AAPS PharmSci* 3: E24.

# Index

Page numbers in *italics* refer to figures and tables.

- AAPS *see* American Association of Pharmaceutical Scientists
- ABC *see* adenosine triphosphate-binding cassette
- absolute bioavailability 279
- absorption
  - absorption-enhancement 277
  - absorption–lipophilicity
    - correlation 304, 306
  - absorption–partition relationships 306
  - absorptive epithelial cells 117
  - absorptive transporters 193
    - amino acid transporters 195
    - BDDCS 291
    - dipeptides 195, 199
    - drug delivery importance 204
    - epithelial cells 196
    - genes 207
    - hexose transporters 201
    - influx transporters 208
    - intestinal absorption impacts 205
    - intestine 118, 121, 121, 195, 205
    - kidney 195, 208
    - kinetics 207
    - liver 208
    - nucleosides 202
    - nutrients 196
    - organic anion and cation transporters 209
    - organic anion-transporting polypeptides 208
    - peptide transporters
    - solute carrier family 194, 198, 201, 208
    - substrate specificity 207
    - tissue segments 205
    - tripeptides 195, 199
    - vitamins 196, 203
- barrier structure and function 115
  - brain 126
  - colon 118, 123
  - epithelial cells 117
  - epithelial morphology 115
  - eye 129
  - gastrointestinal tissue 118, 121
  - lungs 124
  - nasal cavity 124
  - nose 124
  - oesophagus 118, 119
  - olfactory epithelium 124
  - oral cavity 118, 119
  - pharynx 119
  - pyloric sphincter 118, 121
  - rectum 118, 123
  - respiratory tract 123
  - skin 125
  - small intestine 118, 121
  - tight junctions 117
- BCS 279, 294
- biosimulations 302, 305, 311, 312, 318
- dissolution 263
- fraction 279
  - biosimulations 303, 309, 319, 325
  - molecular descriptors-based models 303
  - plasma profiles 319
- intestine 118, 121, 121, 181, 195, 205
- pharmacokinetic models 310

- Plá-Delfina and Moreno model 306
- post-membrane predictions 282
- preclinical evaluations 226, 228, 229, 243
- pre-membrane prediction 280
- quotient (AQ) 239
- surface kinetics 162
- absorption, distribution, metabolism and elimination (ADME)
  - absorptive transporters 193
  - biosimulations 307
  - drug discovery 277
  - efflux transporters 213
  - peptide stabilisation 79
  - transport preclinical evaluations 228, 229, 243
- accumulation–time graphs 148
- 2'-acetate erythromycin
  - acid-catalysed degradation 42
  - hydrolysis 42, 42, 57, 57
  - kinetics of decomposition 60
  - pseudo first-order plots 56
- acetic acid 75
- acetylic salicylic acid (ASA) 8
  - Arrhenius plots 64
  - hydrolysis 36, 37
  - ionisation 9
  - ionisation/acidity constants 9, 17
  - kinetics of decomposition 62
  - pH metric titrations 17
  - structure 37
- aciclovir 8, 84
  - bioisosteric replacement 96
  - hydrolysis 38, 41, 55, 60
  - prodrug formation 94
  - specific acid-catalysed hydrolysis 41
  - valaciclovir hydrolysis 38
- acid/base functional groups 8, 20, 23, 24
- acid/base properties
  - amphiphilic drug candidates 12
  - aqueous solubility 7, 18
  - dissolution 260
  - distribution coefficient 24
  - drug candidates 5, 7, 18
  - industrial preformulation, early discovery 103
  - partition properties 23
  - physicochemical
    - characterisation 5, 7, 18
    - solubility–pH profiles 20
- acid-catalysed degradation 42
- acid-catalysed hydrolysis 41
- acid dissociation constants *see* ionisation/acidity constants
- acidity constants *see* ionisation/acidity constants
- active pharmaceutical ingredients (API), definitions 1
- active transport 155, 159
  - carrier-mediated transport
    - kinetics 154, 157
  - dynamic cellular systems 158
  - human transporter classification 175
- acycloxyalkoxy (AOA) 96
- acyl groups
  - acyl carbons 36, 65
  - acyloxyalkoxy-coumarinic-acids 96
  - $\alpha$ -acyloxyalkyl esters 95
  - $\alpha$ -acyloxyalkyl ethers 95
  - $\alpha$ -acyloxyalkyl thioethers 95
  - acyl oxygen protonisation 38, 41
  - hydrolysis 36, 38, 41
  - molecular structures 36, 36
- ADAM *see* Advanced Dissolution, Absorption and Metabolism
- adenosine diphosphate (ADP) 180
- adenosine triphosphate (ATP)
  - carrier-mediated transport
    - kinetics 157
  - human transporter classification 175, 177, 180, 186
  - powered pumps 177, 180, 186
- adenosine triphosphate-binding cassette (ABC) 159
  - efflux transporters 213, 214
  - Gene Ontology 187
  - human transporter classification 186
  - intestine 214

- Pfam database 191
- transport classification system 187
- ADME *see* absorption, distribution, metabolism and elimination
- ADP *see* adenosine diphosphate
- adrenaline 43, 84
- advanced compartmental transit and absorption (ACAT) 312, 314, 315
- Advanced Dissolution, Absorption and Metabolism (ADAM) 314
- affinity 166, 167
- AIC *see* Akaike information criterion
- Akaike information criterion (AIC) 339
- alcohol oxidation 44, 44
- aldehydes 44, 44
- alendronate 73
- E-alkenes 81, 82, 83
- allergies 47
- American Association of Pharmaceutical Scientists (AAPS) 265
- amides 95
  - bioisoteres 79, 80, 81
  - bond lengths and angles 83
  - bond replacement 79
  - hydrolysis 37
  - structure 37
- amidino group in mecillinam 40
- amifostine 84
- amines 8, 15
- amino acids 206
  - absorptive transporters 195, 198, 199
  - carrier-mediated transport kinetics 156
  - deamidation 40
  - epithelial cells 196
  - hydrolysis 38
  - peptide stabilisation 79
  - racemisation 47, 47
  - redox equilibrium 44
  - replacement 80
  - valaciclovir hydrolysis 38
- $\gamma$ -aminobutyric acid 193
- aminomethylene mimetics 81, 82
- amphiphilic drug candidates
  - acid/base properties 12
  - ionisation 12
  - ionisation/acidity constants 12
  - ionised species fraction 22
  - morphine 12
  - neutral species fraction 22
  - partition hypothesis 17
  - pH metric titrations 15
  - solubility in aqueous solution 22
  - species fractions 14, 16
- ampicillin 48, 55, 73, 84
- antioyrene 116
- antiports 154, 155, 157, 179
- AOA *see* acycloxyalkoxy
- API *see* active pharmaceutical ingredients
- apical surface specialisations 115
- apical to basolateral flux 147, 149, 150
- AQ *see* absorption quotient
- aqueous diffusional rate constants 303
- aqueous solubility 5, 7, 14, 18
- aqueous solution 6, 18, 51
- aqueous stability 288
- area under curve (AUC) 284
- Arrhenius equation 62
- Arrhenius plots 64
- ASA *see* acetylic salicylic acid
- ascorbic acid 203
- asparagine 40
- atenolol 140
- ATP *see* adenosine triphosphate
- AUC *see* area under curve
- azathioprine
- azidothymidine (AZT) 96
- AZT *see* azidothymidine
- Baker–Lonsdale dissolution 317
- balsalazide 84
- bambuterol 84
- barrier tissue
  - fluxes 137, 142
  - passive diffusion 135
  - see also* absorption...
- base-centred unit cells 30, 30
- base properties 11
  - see also* acid/base properties
- basket apparatus 265, 266
- basolateral-apical flux 147, 149, 150
- basolateral influx transporters 208



- BCRP *see* breast cancer-resistance proteins
- BCS *see* Biopharmaceutics Classification System
- BDDCS *see* Biopharmaceutics Drug Disposition Classification System
- benaxeprilat 84
- benazepril 84
- benzoic acid 75
- BHPH *see* bis-(*p*-hydroxyphenyl)-pyridyl-2-methane
- bile acids 196
- bile formation 218
- bile salt export pumps (BSEP) 215, 219
- binding analysis 165, 168, 169, 238
- bioavailability
  - absorption-enhancement 277
  - absorptive transporters 193
  - alendronate 73
  - ampicillin 73
  - BCS 23, 255, 277, 279
  - BDDCS 255
  - biosimulations 255, 297, 308, 326
  - classification 255
  - cytochrome P450 277, 293
  - decomposition mechanisms 35
  - definitions 1
  - describing 255
  - desmopressin 73
  - dissolution 255, 257
  - dosage form evaluation 297
  - efflux transporters 277
  - erythromycin 73
  - experimental methods 2
  - exsorptive transporters 277
  - food-drug interactions 289
  - P-glycoprotein 277, 293
  - in vitro* dissolution 255, 257, 262
  - in vitro*–*in vivo* correlation 255, 280
  - ivermectin 73
  - kinetics of decomposition 52
  - mathematical models 297
  - membrane permeability 277
  - models 297
  - morphine 73
  - omeprazole 73
  - optimisation
    - bioisoteric replacement 71, 76
    - chemical approaches 6, 71
    - dissolution 6, 71, 72
    - drug candidates 6
    - intestinal peptidases 6
    - Lipinski's rule of five 6, 71
    - oral drug candidates 6
    - peptidases 6
    - peptide stabilisation 6, 76
    - prodrug formation 6, 71, 84
    - salt formation 6, 71, 72, 75, 76
    - solubility rate 6, 71, 72
    - stabilisation 6
  - permeability optimisation 277
  - preclinical investigations 244, 297
  - simulations 297
  - solid-state drug candidates 30
  - solubility 23
  - succinate ester 73
  - transport preclinical evaluations 244
- bioequivalence 278, 286, 294
- biofluids, kinetics of decomposition 52
- bioisosteric replacement
  - amide-based bioisoterics 79, 81
  - bioavailability optimisation 71, 76
  - PEPT1 82, 96
  - peptidomimetics 79
  - valine 96
- biological process gene ontology 183
- biomathematical modelling software 340
- Biopharmaceutics Classification System (BCS)
  - absorption predictions 279
  - application 285
  - BDDCS 292, 293
  - bioavailability 23, 255, 277, 279
  - bioequivalence 278, 286, 294
  - dissolution 278, 286, 288, 290
  - drug development 277
  - drug discovery 277
  - drug disposition 292

- elimination routes 287
- enzyme-transporter interplay 278
- food-drug interactions 289
- formulation strategies 288, 289
- in vitro* dissolution 278, 286
- in vitro*–*in vivo* correlation 290, 294
- in vivo* studies 286
- metabolism 282, 294
- oral bioavailability 279
- oral drug absorption predictions 279
- permeability 277, 278, 282, 285, 287, 292
- pre-membrane absorption 282
- regulatory aspects 286
- solubility 23, 278, 282, 285, 287, 289, 292
- stability 282, 288
- transport preclinical evaluations 245
- Biopharmaceutics Drug Disposition Classification System (BDDCS)
  - BCS 292, 293
  - bioavailability 255, 278, 291
  - permeability 291
  - preclinical evaluations of drug transport 245
  - solubility 291
- bioreversible ester linkages 94
- biosimulations
  - absorption 305, 311, 312, 318
    - fraction 303, 309, 319, 325
    - modelling 302
    - potential 303
  - ACAT 314
  - ADAM 314
  - Akaike information criterion 339
  - bioavailability 255, 297, 308, 326
  - coefficient of correlation 338
  - coefficient of determination 338
  - compartmental models 303, 310, 312, 314, 321
  - computing tools 340
  - convolution 322
  - correlation coefficient 338
  - coupled differential equations 311
  - covariance matrix 336
  - deconvolution 322
  - determination coefficient 338
  - diffusion 303, 305, 318
  - dissolution 302, 311, 313, 315, 325
  - dosage form evaluation
  - dose factors 303
  - dose/solubility ratio 318
  - drug disposition 311
  - extended least squares 331
  - Fisher ratio 339
  - fit factors 337
  - fraction absorbed 303, 309, 319, 325
  - F* test 339
  - Gastroplus 314
  - gradient methods 332
  - Higuchi–Ho model 303
  - information matrix 336
  - in silico* screening 301, 302
  - in vitro* data 301
  - in vitro* dissolution 315
  - in vitro*–*in vivo* correlation 319
  - in vivo* data 301
  - iterations 332
  - least squares 330, 331
  - linear regressions 301, 330
  - link functions 325
  - lipophilicity 302, 304, 305
  - mass balance 302, 308, 321, 322, 324, 328
  - mathematical models 299, 317, 340
  - Michaelis–Menten equation 333
  - molecular descriptors-based models 303
  - Nelder–Mead algorithm 333
  - non-linear regression 301, 332
  - numerical methods 332
  - objective functions 330
  - oral absorption modelling 302
  - passive diffusion 305

- pH 302, 303, 313
- pharmacokinetics modelling
  - software 340
- pH-partition theory 303
- physicochemical characteristics 302
- physiologically based custom-designed software 340
- physiological variables 302
- Plá-Delfina and Moreno model 305
- plasma profiles 318
- polydisperse particle dissolution 316
- preclinical investigations 301
- quantitative structure–bioavailability 308
- release modelling 315
- residual plots 338
- scientific computing tools 340
- simplex method 333
- Snedecor's *F* test 339
- software packages 339, 340
- solubility 302, 303, 313, 318
- standard error of estimation 336
- time-dependent diffusion 318
- time-dependent models 310
- time-independent model 308
- toxicokinetic software 340
- transit times 302, 312
- weighted least squares 331
- biotransformation 288
- bisacodyl 84
- Bjerrum difference plots
  - ephedrine 15
  - monoprotic bases 15
  - morphine 26, 26
  - pH metric titrations 15
  - solubility–pH profiles 20
- blood
  - blood–brain barrier 221, 126, 127, 128,
  - blood–retinal barrier 129
  - concentration curves 284
  - flow 302
  - monoprotic bases 12
- body-centred unit cells 30, 30
- bond lengths and angles 83
- boundary layer thickness 262
- bovine serum albumin (BSA) 238
- brain 126, 127
  - blood–brain barrier 126, 127, 128, 221
  - efflux transporters 221, 221
  - intracellular enzymes 221
- breast cancer-resistance proteins (BCRP) 215, 217
- Brøndsted–Bjerrum equation 64
- Brøndsted–Lowry acids 7
- Brøndsted–Lowry bases 7
- BSA *see* bovine serum albumin
- BSEP *see* bile salt export pumps
- buffers 52, 66, 67, 269
- buprenorphine
  - distribution 16
  - ionisation 15
  - pH metric titrations 15
  - solubility in aqueous solution 22
  - solubility–pH profiles 22, 22
  - species distribution 16
- CA *see* coumarinic acid
- Caco-2 cell models
  - flux ratios 150
  - permeability 166, 140, 147, 149
  - transporter interaction screening 239, 240
  - transport preclinical evaluations 230, 232, 239, 240
- calibration curves 299
- candesartan 84
- capillary electrophoresis 230
- carba ethylene 81
- carbamates 95
- carbimazole 84
- carbonate esters 95
- carbon hydrogen nitrogen
  - microanalysis 108
- carboxylic acid 8, 20, 24, 36
- carboxyls
  - hydrolysis 35, 36
  - structures 36, 37
  - water-catalysed reactions 35
- carriers
  - active transporters 154, 157
  - adsorption surfaces 162

- carrier-mediated transport
  - kinetics 153
    - antiports 154, 157
    - binding analysis 165, 168, 169
    - carrier classification 154
    - carrier functions 154
    - competitive inhibitors 165
    - compound-transporter interactions
      - 164
    - dynamic cellular systems 158, 168
    - efflux transporters 158
    - electrochemical gradients 156
    - enzymes 160, 162
    - flux 160
    - identification of carrier type
      - 160
    - inhibitors 164, 165, 168
    - investigation methods 171
    - ion concentration 154
    - Langmuir equation 162
    - mathematics 160
    - maximal velocity 162
    - measurements 171, 172
    - mechanisms 154
    - Michaelis–Menten constant
      - 163
    - Michaelis–Menten equation
      - 160, 162
    - mixed kinetics 169
    - multiple carriers 169, 170
    - non-competitive inhibitors
      - 169
    - one directional transport 155
    - passive diffusion 169
    - peptide transporters 158, 167, 172
    - rate constants 161
    - saturable transporter kinetics
      - 160
    - steady-state conditions 160
    - study methods 171
    - substrate adsorption surfaces
      - 162
    - substrate-enzyme reactions
      - 160
    - substrates 154, 155, 164
    - symports 154, 156, 158, 167
    - translocation 156
    - transportates 164
    - uncompetitive inhibitors 168
    - uniports 154, 155
    - velocity 160, 162, 166
  - classification 154, 175, 177
  - functions 154
  - human transporter classification
    - 175, 177
- CAT *see* compartmental transit and absorption
- catalysts, hydrolysis 35, 39
- CBER *see* Center for Biologics Evaluation and Research
- CCK *see* cholecystokinin
- CDER *see* Center for Drug Evaluation and Research
- cefuroxime axetil 84
- cell cultures 232
- cell layers 115, 116
- cell shape 115, 116
- cellular component gene ontology 183
- Center for Biologics Evaluation and Research (CBER) 71
- Center for Drug Evaluation and Research (CDER) 71
- central nervous system (CNS) 128, 193
- channels
  - facilitated diffusion 178
  - human transporter classification
    - 175, 177
- charged amino acids 198, 198, 199
- charged solutes 144, 145
- chemical approaches to bioavailability
  - 6, 71
- Chinese hamster ovary (CHO) 213
- chloramphenicol 84
- CHO *see* Chinese hamster ovary
- cholecystokinin (CCK) 209
- chromatography 230
- ciclosporin 77
- cilia 115
- cimetidine 292
- cis-trans* isomerisation 46, 57
- citric acid 75
- CL *see* clearance

- classification
  - bioavailability 255
  - drug substances 2
  - epithelial morphology 115
  - see also* Biopharmaceutics Classification System; Biopharmaceutics Drug Disposition Classification System; human transporter...
- clearance (CL) 283
- cleavage 76, 78
- clinical studies, industrial
  - preformulation 101
- clopidogrel 84
- CNS *see* central nervous system
- CNT *see* concentrative nucleoside transporters
- coefficient of correlation 338
- coefficient of determination 338
- coefficient of variation 331
- colchicine-resistant cells 213
- colistimethate 84
- Collander relationship 304
- colon 118, 123
- compartmental models
  - biosimulations 303, 310, 312, 314, 321
  - flux measurements 138
- compartmental transit and absorption (CAT) 312, 314, 315
- compatibility issues 111
- compendial dissolution media 269
- competitive inhibitors 165, 166
- composition factors 261, 263
- compound diffusion 304
- compound-transporter interactions 164
- computing tools 340
- concentration 337
  - dependence on uptake 168
  - flux 148, 150
  - ion concentration 154
  - kinetics of decomposition 52, 54, 57
  - rate of reaction 337
  - residuals 337
  - velocity dependence 163
- concentration gradients 137
- concentration profiles 324
- concentrative nucleoside transporters (CNT) 159, 203
- conjunctival epithelium 129
- consecutive reactions 59
- construction, models/modelling 300
- convergence criterion 333
- convolution 322, 324, 325
- cornea 129
- correlation
  - absorption–lipophilicity 304, 306
  - coefficient 338
  - transport preclinical evaluations 230, 238
  - see also in vitro–in vivo* correlation
- coumarinic acid (CA) 96
- coupled differential equations 311
- covariance matrix 336
- crystallinity 105, 302
- crystals
  - biosimulations 302
  - lattices 29, 29
  - solid-state characterisation 29
- cubic lattice structures 29, 29
- CV *see* coefficient of variation
- cycloguanil 84
- CYP *see* cytochrome P
- cytochrome P (CYP) 68
- cytochrome P450 213, 214, 242, 277, 293
- DADLE (opioid peptides) 96, 97
- databases
  - absorptive transporters 194
  - human transporter classification 183, 186, 191
- deamidation 40
- decision trees 240, 241
- decomposition kinetics 6, 51
  - see also* kinetics...
- decomposition mechanisms
  - drug candidates 5, 35
  - hydrolysis 35
  - non-oxidative photolytic degradation 46
  - oxidation 43

- physicochemical
    - characterisation 5, 35
    - polymerisation 47
    - racemisation 47
- deconvolution 322, 324, 325
- degradation, 2'-acetate erythromycin 56
- dependent variables, mathematical models 299, 337
- dephosphorylated aminofostine 84
- depth, unit cells 29
- dermis structures, skin 125, 126
- desmopressin 73, 77
- determination coefficient 338
- deterministic models 299
- development
  - BCS 277
  - industrial preformulation 101, 102, 106
- diclofenac 20, 24, 25
- differential equations/models 299, 311
- differential scanning calorimetry (DSC) 106, 110
- diffusion/diffusivity 143, 143
  - biosimulations 303, 305, 318
  - coefficient 135
  - convection controlled models 259
  - dissolution 262, 316
  - layer model 259
  - rate constants 303
- digestion 118
- dihydroriboflavin 45
- dihydroxyethylene 81
- dimensions, unit cells 29
- dimerisation 55
- 5'-O-dipeptide ester 96
- dipeptides 96, 156, 158, 179, 195, 199
- dipivefrine 84
- direct measurements, transport kinetics 172
- disposition 292, 311
  - see also* Biopharmaceutics Drug Disposition Classification System
- dissociation 76
- dissolution 259
  - absorption 263
  - absorption/pharmacokinetic model 310
  - acid/base properties 260
  - Baker–Lonsdale dissolution 317
  - basket apparatus 265
  - BCS 278, 286, 288, 290
  - bioavailability 6, 71, 72, 255, 257
  - biorelevant media
  - biosimulations 302, 311, 313, 315, 325
  - buffer solutions 269
  - compendial media 269
  - composition factors 261, 263
  - diffusion layer model 259
  - equipment 265, 266
  - film theory 259
  - first-order dissolution 299, 317
  - flow-through equipment 265, 267
  - gastric fluids
  - gastrointestinal tissue 121
  - gastrointestinal tract 262, 336
  - Gompertz dissolution 317
  - Higuchi dissolution 317
  - Hixon–Crowell dissolution 317
  - Hopfenberg dissolution 317
  - intestinal fluids
  - intrinsic dissolution equipment 265, 268
  - in vitro*–*in vivo* correlation 290
  - Korsmeyer–Peppas dissolution 317
  - mathematical models 317
  - mechanism theories 258
  - media 269, 270, 271
  - Monte Carlo simulations 318
  - Noyes–Whitney equation 259, 260, 262, 316, 336
  - paddle apparatus 265
  - particle size 261
  - pH 260, 263
  - physicochemical characteristics 260
  - physicochemical properties 262, 336
  - physiological conditions 262, 336

- pre-membrane absorption
  - prediction 280
- rate constants 259
- release process modelling 318
- residence times 263
- solid-state drug candidates 30
- solubility 23, 260, 262, 316
- stomach
- surface area 261, 316
- surface tension 263
- surfactants 261, 263
- volume factors 261, 262
- Weibull dissolution 316, 317
- distribution 7
  - buprenorphine 16
  - ephedrine 15
  - pH profile 25, 27
- distribution coefficient 24
  - diclofenac 20, 24
  - industrial preformulation 105
  - monoprotic acids 24
  - monoprotic bases 24
  - morphine 27
  - propranolol 25
- disulfiram 84
- disulphides 95
- DMPK *see* drug metabolism and pharmacokinetic properties
- dosage form evaluation 297
- dose factors 303
- dose/solubility ratio 318
- driving force 154, 156, 157
- drug absorption modelling 302
- drug candidates
  - absorption barrier structure and function 115
  - acid/base properties 5, 7
  - aqueous solubility 5, 7
  - base properties 11
  - bioavailability optimisation 6, 71
  - chemical stability 18
  - decomposition kinetics 6
  - decomposition mechanisms 5, 35
  - definitions 1
  - distribution 7
  - industrial preformulation 6
  - lipophilicity 5
  - membrane transport 113
  - partition properties 23
  - passive diffusion 135
  - physicochemical
    - characterisation 5
  - solid-state properties 5, 7, 29
  - solubility 5, 7, 18
  - total concentration 9
- drug discovery 228, 229, 277
- drug disposition 292, 293, 311
  - see also* Biopharmaceutics Drug Disposition Classification System
- drug–drug interactions 231, 284
- drug excretion 213
- drug metabolism and pharmacokinetic (DMPK) properties 277
- drug product 2
- drug release modelling, biosimulations 315
- drug stability 5
- drug substances
  - classification 2
  - decomposition kinetics 6
  - definitions 1
- drug transport
  - delivery impacts 205
  - delivery importance 204
  - drug discovery 228
  - epithelial membrane 227
  - see also* preclinical evaluation...
- DSC *see* differential scanning calorimetry
- DVS *see* dynamic vapour sorption
- dynamic cellular systems 158, 168
- dynamic mathematical models 299
- dynamic vapour sorption (DVS) 106
- early development 101, 102, 106
- early discovery 101, 102, 228, 229
- efflux ratio (ER) 239
- efflux transporters 215
  - ATP-binding cassette 213, 214
  - BDDCS 291
  - bile salt export pumps 219
  - bioavailability 277
  - blood–brain barrier 221
  - brain 221

- breast cancer-resistance proteins 215, 217
- carrier-mediated transport kinetics 158
- endothelial cells 221
- epithelial tissue 214, 217, 218, 219
- intestine 214, 216, 217
- kidney 219, 220
- liver 217, 218
- membrane transport 158, 213
- metabolism 213
- multidrug resistance 213, 214, 219
- multidrug resistance-associated transport proteins 214, 217, 220
- electrical fields 145
- electrical potential 144, 145
- electrochemical gradients 156, 157
- electrolytes 64
- electron distribution 76
- electron donors 45
- electron pairs 36, 40
- electrophoresis 230
- elimination 287, 291, 321
- EMA *see* European Medicines Agency
- enalapril 84
- endothelial cells 126, 127, 221
- ENT *see* equilibrative nucleoside transporter 122
- enterocytes 122
- enthalpy 110
- enzymes
  - commission numbers 76, 78
  - efflux transporters 214
  - hydrolytic cleavage 76, 78
  - intestine 216
  - kinetics of decomposition 52, 67
  - liver 218
  - transporter interplay 278
  - transport preclinical evaluations 242
- ephedrine
  - Bjerrum difference plots 15, 15
  - ionisation 11, 17
  - ionisation/acidity constants 11, 15, 17
  - ionisation/base constant 11
  - neutralisation 18
  - pH metric titrations 17
- epidermis structures, skin 125, 126
- epinephrine (adrenaline) 43, 84
- epithelial cells 117, 196
- epithelial classifications 116
- epithelial membrane 227
- epithelial morphology 115, 116
  - brain 126
  - eye 129
  - gastrointestinal tissue barriers 118
  - respiratory tract 123
  - skin 125
- epithelial tissue 214, 217, 218, 219
- equilibrative nucleoside transporter (ENT) 203
- equilibrium potentials 154
- equipment, dissolution 265, 266
- ER *see* efflux ratio
- error predictions 326
- erythromycin 73, 84
  - see also* 2'-acetate erythromycin
- esomeprazole 84
- esters 37, 95
  - hydrolysis 38, 39, 55, 60, 65, 66, 93
  - hydrolytic acyl transfers 38
  - linkages 93
- European Medicines Agency (EMA) 2
- European Pharmacopeia (Ph Eur), solubility 18, 18
- excretion, efflux transporters 213
- ExPASy server 183
- experimental methods 2
  - condition optimisation 238
  - ionisation/acidity constants 14
- exsorpive transporters 277
- extended least squares 331
- ex vivo* models 234
- eye 129, 130
- eye drops 130
- eyelids 129
- FA *see* fraction absorbed
- face-centred unit cells 30, 30
- facilitated diffusion 178, 179
- famciclovir 84



- fasted-state simulated gastric fluid (FaSSGF) 271, 271
- fasted-state simulated intestinal fluid (FaSSIF) 271, 272
- FBP *see* folate-binding protein
- FDA *see* Food and Drug Administration
- fed-state simulated gastric fluid (FeSSGF) 258, 271
- fed-state simulated intestinal fluid (FeSSIF) 271
- Fick's law 136
- film theory 259
- FIP *see* International Pharmaceutical Federation
- first-order dissolution 299, 317
- first-order kinetics 52, 57
- Fisher ratio 339
- flip-flop 321
- flow-through equipment 265, 266, 267
- fluoroalkenes 81, 82
- fluoroquinolones 303, 304
- 5-fluorouracil (5-FU) 8, 76
- (Z)-flupentixol 84
- fluphenazine 84
- flurbiprofen 19, 20
- flux 135, 136
  - barrier tissue 137, 142
  - Caco-2 cell models 147, 149
  - carrier-mediated transport kinetics 160
  - charged solutes 144, 145
  - compartmental models 138
  - concentration values 148, 150
  - flux-time graphs 148
  - ratios 145, 150
  - saturable transport 162
  - unstirred layers 141
- folate-binding protein (FBP) 204
- folding 121
- Food and Drug Administration (FDA) 2
- food-drug interactions 289
- food effects 289, 291
- formatted protein sequences 183
- formulation
  - BCS 288, 289
  - biosimulations 302
  - decomposition mechanisms 35
  - kinetics of decomposition 52
- fosinopril 84
- fosphenytoin 84
- fractal kinetics 318
- fraction absorbed (FA) 303, 309, 319, 325
- free-radical transfers 43
- F* test 339
- 5-FU *see* 5-fluorouracil
- full development 101, 102, 111
- GABA *see*  $\gamma$ -aminobutyric acid
- $\gamma$ -aminobutyric acid (GABA) 193
- ganaciclovir 84, 96
- gas exchange 124
- gastric emptying 290, 302
- gastric fluids 12, 271, 271
- gastrointestinal tissue 118, 121
- gastrointestinal therapeutic system (GITS) 311
- gastrointestinal tract (GI) 118, 119, 262, 336
- Gastrolus 314
- Gauss-Newton algorithm 332
- Gene Ontology (GO) 183, 185, 187
- general solubility equation (GSE) 28
- genes 177, 183, 185, 207
- GI *see* gastrointestinal tract
- GITS *see* gastrointestinal therapeutic system
- D*-Glu[1-(2-hydroxyethyl)thymine]Ala 62
- Glu(aciclovir)-Sar 41, 62, 94
- glucose transporters (GLUTs) 155, 158, 201
- Glu(hydroxyethylamine)-Sar 94
- Glu(OBzl)-Sar 65
- L*-glutamate transporters 193
- glutathione-S-transferases (GSTs) 213
- GLUTs *see* glucose transporters
- P-glycoprotein (P-gp) 186, 213, 214, 240, 277, 293, 293
- GO *see* Gene Ontology
- Gompertz dissolution 317
- gradient methods 332
- GSE *see* general solubility equation
- GSTs *see* glutathione-S-transferases

- half lives 51, 53, 55, 57, 58, 59
- haloperidol 84
- HATs *see* heteromeric amino acid transporters
- height, unit cells 29
- Henderson–Hasselbalch equation 11
- heparin 277
- hepatic intrinsic clearance 284
- hepatocytes 235
- heteromeric amino acid transporters (HATs) 198
- hexagonal lattice structures 29, 29
- hexoses 196, 201, 201
- HGNC *see* Human Genome Nomenclature Committee
- hidden Markov models (HMMs) 186
- high-pressure liquid chromatography (HPLC) 104
- high-throughput screening (HTS)
  - criteria 129
- Higuchi dissolution 303, 317
- Hixon–Crowell dissolution 317, 317
- HMIT *see* H<sup>+</sup>-*myo*-inositol 317
- HMMs *see* hidden Markov models
- H<sup>+</sup>-*myo*-inositol (HMIT) 201
- Hopfenberg dissolution 317
- HPLC *see* high-pressure liquid chromatography
- HSA *see* human serum albumin
- HTS *see* high-throughput screening
  - criteria
- HUGO *see* Human Genome Organization
- human colon carcinoma cells
  - see* Caco-2 cell models
- Human Genome Nomenclature Committee (HGNC) 183, 185
- Human Genome Organization (HUGO) symbols 185
- human serum albumin (HSA) 238
- human transporter classification 175
  - active transport 175
  - adenosine triphosphate 175, 177, 180, 186
  - adenosine triphosphate-binding cassette 186
  - antiporters 179
  - ATP-powered pumps 177, 180, 186
  - carriers 175, 177
  - channels 175, 177
  - databases 183, 186, 191
  - diffusion 178
  - facilitated diffusion 178
  - Gene Ontology 183, 187
  - genes 177, 183, 185
  - Human Genome Nomenclature Committee 183, 185
  - Human Genome Organization 185
  - Internet 183, 185
  - passive transport 175
  - peptide transporters 179, 186
  - Pfam database 183, 186, 191
  - primary active transport 180
  - profile hidden Markov models 186
  - proteins 175
  - pumps 180
  - secondary active transport 179
  - solute carrier family 185, 186, 187, 191
  - symporters 179
  - transport classification system 180, 185, 187
  - transport mechanisms 177, 186
- hydrochloric acid 75
- hydrogen bond acceptors/donors 71
- hydrogen bonding capacity 76, 307, 307
- hydrolysis
  - 2'-acetate erythromycin 42, 42, 57, 57
  - acetylic salicylic acid 36, 37, 64
  - aciclovir 38, 41, 55, 60
  - acyl carbons 36
  - acyl groups 36, 38, 41
  - acyl oxygen protonisation 38, 41
  - amides 37
  - amino acids 38
  - carboxyls 35, 36
  - catalysts 35, 39
  - decomposition mechanisms 35
  - drug stability 5
  - electron pairs 36, 40

- esters 38, 39, 55, 60, 65, 66, 93
- Glu(aciclovir)-Sar 41
- intramolecular nucleophilic attack 40
- ionic strength 64
- kinetics of decomposition 55
- nucleophilic attack 36, 40
- prodrug candidates 35, 38
- two-electron transfer 35
- valaciclovir 38, 55, 60
- valine 38, 41, 55, 60
- water-catalysed reactions 35, 63
- hydrolytic acyl transfers 38
- hydrolytic cleavage 76, 78
- hydrolytic degradation 72
- hydrophilicity 76
- hydrophilic nutrients 154
- hydroxyethylene 81
- hydroxyethylmine 94
- bis*-(*p*-hydroxyphenyl)-pyridyl-2-methane (BHPH) 84
- hygroscopicity 106
- hypodermis 125
- IAMS *see* immobilised phospholipids onto a silica surface
- ibuprofen dissolution 316, 318
- identification, carrier-mediated transport kinetics 160
- IF *see* intrinsic factor
- imides 37
- immediate release (IR) 264, 325
- immobilised phospholipids onto a silica surface (IAMS) 230
- implicit mathematical models 299
- indirect measurements, transport kinetics 172
- industrial preformulation
  - acid/base properties 103
  - compatibility issues 111
  - crystallinity 105
  - development 101, 102, 106
  - distribution coefficient 105
  - drug candidates 6
  - DSC thermograms 106, 110
  - early development 101, 106
  - early discovery 101, 102
  - enthalpy 110
  - full development 101, 111
  - hygroscopicity 106
  - ionisation/acidity constants 104
  - late discovery 101, 105
  - lead optimisation 101, 104
  - lipophilicity 103, 104
  - melting point 106, 110
  - oxalate salts 106
  - physicochemical
    - characterisation 6, 101
  - polymorphism investigations 110
  - ranking 102
  - salt screening 108
  - solubility 103, 105, 109
  - stability 103, 105, 106
  - thermal stability 106, 109
  - thermogravimetric analysis 106, 109
- influx transporters 208
- information matrix 336
- inhibition
  - carrier-mediated transport
    - kinetics 164, 165, 168
  - concentration dependence 168
  - constants 166, 167
  - transporter interaction screening 240
- in silico* screening 301, 302
- in situ* techniques 231, 237
- integrated models 299, 299
- International Pharmaceutical Federation (FIP) 258, 272
- International Union of Biochemistry and Molecular Biology (IUBMB) 180
- intestinal fluids 12, 271, 271
- intestinal motility 302
- intestinal peptidases 6
- intestinal sac method 236
- intestine
  - absorption 118, 121, 195, 205
  - absorptive transporters 195
  - ATP-binding cassette 214
  - biosimulations 271, 302
  - dissolution 271, 271
  - efflux transporters 214, 216, 217
  - enzymes 216
  - peptide transport 200

- perfusions 237
  - time dependent biosimulations 312
- intracellular enzymes 216, 218, 221
- intramolecular nucleophilic attack 40
- intrinsic clearance 283
- intrinsic dissolution equipment 265, 268
- intrinsic factor (IF) 204
- intrinsic solubility 19, 28
- inverse problems, models/modelling 300
- investigation methods, transport kinetics 171
- in vitro* clearance 284
- in vitro* data, biosimulations 301
- in vitro* dissolution
  - BCS 278, 286, 290
  - bioavailability 255, 257, 262
  - biosimulations 315
  - media 269
- in vitro* metabolism 52, 67
- in vitro* preclinical evaluations of transport 226, 228, 229, 231, 238, 243
- in vitro* release 52, 67
- in vitro-in vivo* correlation (IVIVC) 320
  - BCS 290, 294
  - bioavailability 255, 280
  - biosimulations 319
  - non-linearity 326, 327, 329
  - post-membrane absorption predictions 284
- in vivo* data, biosimulations 301
- in vivo* studies
  - BCS 286
  - preclinical evaluations of drug transport 226, 228, 238, 243
- ion concentration 154, 154
- ionic strength 52, 64, 65
- ionisation
  - acetylic salicylic acid 9, 17
  - acid/base properties of drug candidates 9
  - amphiphilic drug candidates 12
  - buprenorphine 15
  - diclofenac 20, 24
  - ephedrine 11, 17
  - lidocaine 21
  - monoprotic acids 9
  - monoprotic bases 11
  - morphine 26
  - propranolol 25
- ionisation/acidity constants
  - acetylic salicylic acid 9, 17, 17
  - acid/base property characterisation 7
  - amphiphilic drug candidates 12
  - bioisoteric replacement 76
  - biosimulations 302
  - diclofenac 20, 24
  - ephedrine 11, 15, 17
  - experimental determinations 14
  - industrial preformulation, lead optimisation 104
  - monoprotic acids 9
  - monoprotic bases 11
  - morphine 12, 26, 27
  - pH metric titration 14
  - propranolol 25
  - Yasuda-Shedlowski technique 17
- ionisation/base constants 11
- ionised species fraction 11, 12, 19, 20, 22
- IR *see* immediate release
- irreversible consecutive reactions 59
- irreversible reactions
  - first-order kinetics 52
  - kinetics of decomposition 52, 54, 58, 59
  - pseudo first-order kinetics 54, 58, 59
  - pseudo zero-order kinetics 52
  - second-order kinetics 54
- cis-trans* isomerisation 46, 57
- iterations 332, 334
- IUBMB *see* International Union of Biochemistry and Molecular Biology
- ivermectin 73
- IVIVC *see in vitro-in vivo* correlation
- keratin 115
- ketomethylene 81
- ketone 43

- kidney 195, 208, 219, 220, 233, 239, 240
- kinetic constants, 166
- kinetics
  - absorptive transporters 207
  - carrier-mediated transport kinetics 153
  - decomposition 6, 51
    - acetylic salicylic acid 62
    - Arrhenius equation 62
    - biofluids 52
    - Brøndsted–Bjerrum equation 64
    - buffers 52, 66, 67
    - concentration terms 52, 54, 57
    - electrolytes 64
    - enzymes 52, 67
    - excipient 52
    - first-order kinetics 52, 53, 57
    - half lives 51, 53, 55, 57, 58, 59
    - hydrolysis 55
    - in vitro* metabolism 52, 67
    - in vitro* release 52, 67
    - in vitro–in vivo* correlation 67
    - ionic strength 52, 64
    - irreversible reactions 52, 54, 58, 59
    - linear plots 53, 55, 58
    - Michaelis–Menten kinetics 51, 67
    - pH 52, 60
    - pseudo first-order kinetics 54, 57, 58, 59
    - pseudo zero-order kinetics 52
    - rate constants 51, 52, 53, 54, 56, 57, 58
    - rate of reaction 52, 53, 54, 57, 58, 59
    - reversible reactions 57
    - second-order kinetics 54
    - shelf lives 51, 53, 55, 57, 58, 59
    - solubility 52
    - temperature 52, 62
  - stability 6, 51
  - transport preclinical evaluations 226, 228
- Korsmeyer–Peppas dissolution 317
- lactams 37, 47, 193
- lactic acid 75
- lactone 84
- Langmuir equation 162
- lansoprazole 84
- Laplace transforms 324, 325
- latanoprost 84
- late discovery 101, 102, 105, 228, 231
- lattices 29, 29
- LC *see* liquid chromatography
- leads
  - definitions 1
  - generation (LG) 102, 228
  - optimization (LO) 101, 102, 104, 228
- least squares 330, 331
- LG *see* leads, generation
- licochalcone A 46, 57
- lidocaine 8, 20, 21, 37
- ligands 164
- light, decomposition mechanisms 5
- light-induced oxidation 45
- liquid chromatography (LC) 172
- linearity conditions 324
- linear models 299
- linear plots 53, 55, 58
- linear regressions 301, 330
- link functions 325
- Lipinski's rule of five 6, 71, 129, 129, 281
- lipophilicity
  - absorption–lipophilicity correlation 304, 306
  - bioisoteric replacement 76
  - biosimulations 302, 304, 305
  - diclofenac 25
  - drug candidates 5
  - industrial preformulation 103, 104
  - permeability 307
- liver
  - absorptive transporters 208
  - efflux transporters 217, 218

- intracellular enzymes 218
- perfusions 237
- LO *see* leads, optimization
- Loo–Riegelman mass balance 322, 323, 324
- lovastatin 84
- lungs 124
- lymecycline 84
- Madin-Derby canine kidney cells (MDCK) 233, 239, 240
- maleic acid 75
- mannitol 116
- mass balance 321, 323, 329
  - biosimulations 302, 308, 321, 322, 324, 328
- mass spectroscopy (MS) 172
- mass transport 135
- mathematical models
  - bioavailability 297
  - biosimulations 299, 317
  - dissolution 317
- mathematics of transport kinetics 160
- maximal velocity 162
- MCT *see* monocarboxylate transporter
- MDCK *see* Madin-Derby canine kidney cells
- MDR *see* multidrug resistance
- measurements, transport kinetics 171, 172
- mechanisms of transport kinetics 154
- mecillinam 37, 40, 84
- media composition 238
- media for dissolution 269, 270, 271
- melting point 106, 110
- membrane permeability 277
- membrane transport 113
  - absorption barrier structure and function 115
  - absorptive transporters 193
  - carrier-mediated transport kinetics 153
  - classification of human transporters 175
  - compound diffusion 304
  - diffusion 135
  - efflux transporters 158, 213
  - flux 135
  - human transporter classification 175
  - migration 135
  - passive diffusion 135, 226
  - permeability 135
  - preclinical evaluation 225
- 6-mercaptopurine 84
- mesalazine 84
- mesylic acid 75
- metabolism
  - BCS 282, 294
  - BDDCS 291
  - efflux transporters 213
  - metabolic clearance 284
  - metabolic stability 229, 293
  - transport preclinical evaluations 236, 242
- metabolizing enzymes 214
- methanesulphonic acid 75
- N-methylation 79, 80
- metiamazole 84
- metronidazole 84
- metoprolol 116, 140, 316
- Michaelis–Menten constant 163
- Michaelis–Menten curves 162
- Michaelis–Menten equation 160, 162, 283, 333
- Michaelis–Menten kinetics 51, 67
- microvilli 121
- migrating motor complex (MMC) C04, A011
- migration 135
- minerals 196
- mixed kinetics 169
- mixing tank models 310
- MMC *see* migrating motor complex
- models/modelling
  - bioavailability 297
  - construction 300
  - definitions 297
- molecular acid/base properties 5, 7
- molecular descriptors-based models 303, 307
- molecular function gene ontology 183
- molecular mass transport 135
- molecular partition 7
- molecular solubility 5, 7

- molecular structures
  - acyl functional groups 36
  - acyl groups 36, 36
  - carboxyl compounds 36
  - carboxyl functional groups 36
- molecular weight 71, 307, 307
- monocarboxylate transporter (MCT) 203
- monoclinic structures 29
- monoprotic acids
  - distribution coefficient 24
  - Henderson–Hasselbalch equation 11
  - intrinsic solubility 19
  - ionisation 9
  - ionisation/acidity constant 9
  - partition coefficient 23
  - pH metric titrations 17
  - solubility 19, 20
  - species fractions 10, 11, 19, 23
- monoprotic bases
  - Bjerrum difference plots 15
  - distribution coefficient 24
  - gastric juices 12
  - intestinal fluids 12
  - ionisation 11
  - ionisation/acidity constant 11
  - ionisation/base constant 11
  - partition coefficient 23
  - pH metric titrations 17
  - solubility 20
  - species fractions 12, 15, 20, 23
- Monte Carlo simulations 318
- morphine 8
  - acid/base property
    - characterisation 12
  - bioavailability 73
  - Bjerrum difference plots 26
  - distribution coefficient 27
  - ionisation 26, 26
  - ionisation/acidity constant 12, 27
  - oxidation 43
- morphine hydrochloride 27
- morphine sulphate 26, 26
- morphology, epithelium 115, 116
- MRP *see* multidrug resistance-associated proteins
- MS *see* mass spectroscopy
- multidrug resistance-associated proteins (MRP) 214, 215, 217, 220, 277
- multidrug resistance (MDR) 213, 214, 215, 219, 240
- multiple carriers 169, 170
- mycophenolate mofetil 84
- nabumetone 84
- $\text{Na}^+/\text{H}^+$  exchanger (NHE) 157
- naphthalenesulphonic acid 75
- napsylic acid 75
- nasal cavity 124
- Nelder–Mead algorithm 333, 336
- Nernst–Planck equation 144
- neutral amino acids 198
- neutralisation, ephedrine 18
- neutral species fraction 10, 12, 19, 20, 22, 23
- NH-acidic structure 8
- NHE *see*  $\text{Na}^+/\text{H}^+$  exchanger
- nicotinic acid 203
- non-competitive inhibitors 166, 169
- non-linear models
  - biosimulations 299
  - in vitro*–*in vivo* correlation 326, 327, 329
- non-linear regressions 301, 332
- non-oxidative photolytic degradation 46
- non-photolytic oxidation 43
- non-polar surface area 307
- non-stationary diffusion 143
- non-stationary flux conditions 150
- non-steady state conditions
  - barrier tissue fluxes 142
  - permeability in Caco-2 cells 149
- nose 124
- Noyes–Whitney equation 259, 260, 262, 280, 316, 336
- nucleophilic attack 36, 36, 39, 40, 40, 65
- nucleosides 206
  - absorptive transporters 202
  - epithelial cells 196
  - transport kinetics 156, 202
- numerical methods, biosimulations 332
- nutrients 196

- OAT *see* organic anion transporter
- OATPs *see* organic anion-transporting polypeptides
- OB *see* oral bioavailability
- objective functions (OF),
  - biosimulations 299, 330
- OCT *see* organic cation transporter
- octanol/water partition coefficient 71
- odds function 327, 327
- oesophagus 118, 119
- OF *see* objective functions
- olfactory epithelium 124
- olsalazine 84
- omeprazole 73, 84
- ondansetron 166
- one directional transport 155
- one-electron transfer, oxidation 43
- opioid peptides (DADLE) 96, 97
- oral absorption 279, 302
- oral bioavailability (OB) 6, 71, 76, 193, 279
- oral cavity 118, 119
- oral drug absorption 279, 302
- oral drug bioavailability optimisation 6, 71
- organ-based *ex vivo* models 234
- organic anion and cation transporters 209
- organic anion transporter (OAT) 210
- organic anion-transporting polypeptides (OATPs) 208, 209
- organic cation transporter (OCT) 210
- orthorhombic structures 29, 30, 30
- oxalate salts, early development 106
- oxcarbazepine 84
- oxidation
  - alcohols 44
  - aldehyde 44
  - decomposition mechanisms 43
  - dihydroriboflavin redox equilibrium 45
  - drug stability 5
  - electron donors 45
  - photolytic reactions 43, 45
  - primary alcohols 44, 44
  - riboflavin redox equilibrium 45
- oxomethylene 81
- oxygen, decomposition 5
- oxymethyl modified coumarinic acid-based linkers 96
- paddle apparatus 265, 266
- PAMPA *see* parallel intraluminal membrane permeability approach
- pantaprazole 84
- paracellular diffusion 226, 305
- paracetamol 84
- parallel intraluminal membrane permeability approach (PAMPA) 226, 230
- parallel irreversible reactions 58
- parecoxib 84
- parsimony 339
- partial least squares (PLS) 230
- partial retro-inverso peptides 80
- particle size 261, 302
- partition properties
  - absorption–partition relationships 306
  - acid/base property drug candidates 23
  - drug candidates 23
  - partition coefficient
    - acid/base property characterisation 7
  - amphiphilic drug candidates 17
  - biosimulations 304
  - drug disposition 292
  - Lipinski's rule of five 71
  - monoprotic acids 23
  - monoprotic bases 23
- passive diffusion 135, 175
  - biosimulations 305
  - carrier-mediated transport kinetics 169
  - concentration gradients 137
  - facilitated diffusion 179
  - membrane transport 226
  - molecular mass transport 135
  - permeability coefficient 137
  - preclinical evaluations 229
  - single carrier transport 169
  - stirred layers 137
  - unstirred layers 139, 141
- passive transport 175



- PCA *see* principal component analysis  
 PEG *see* polyethylene glycol  
 penciclovir 84  
 penicillin allergies 47  
 PEPT1 *see* peptide transporters  
 peptidases 6, 76, 78  
 peptides 206
  - absorption-enhancement 277
  - deamidation 40
  - epithelial cells 196
  - oral bioavailability 76
  - racemisation 47
  - stabilisation 6, 76, 78, 79
  - structure 80
  - transport 200
- peptide transporters (PEPT1) 159
  - absorptive transporters 193, 195, 199
  - bioisosteric replacement 82, 96
  - carrier-mediated transport kinetics 158, 167, 172
  - human transporter classification 179, 186
- peptidomimetics 79  
 peptidosulfonamides 80  
 peptidyl phosphonate 80  
 perfusions 128, 235, 237  
 perindopril 84  
 permeability
  - BCS 277, 278, 282, 285, 287, 289, 292
  - BDDCS 291
  - bioavailability 277
  - biosimulations 302
  - Caco-2 cell models 140, 147, 149
  - charged solute fluxes 144
  - cimetidine 292
  - coefficient 137
  - hydrogen bonding capacity 307
  - in vitro*–*in vivo* correlation 290
  - Lipinski's rule of five 71
  - lipophilicity 307
  - membrane transport 135
  - molecular descriptors 303, 307
  - molecular weight 307
  - non-steady state conditions 142
  - polar surface area 307
  - preclinical evaluations 229, 231
  - solubility 84
  - surface area 307
  - surface descriptor computation 229
  - unstirred layers 141
- perphenazine 84  
 Pfam database 183, 186, 191  
 P-gp *see* P-glycoprotein  
 pH
  - acid/base property characterisation 7
  - aqueous solubility, buprenorphine 22
  - biofluids 13, 51
  - biosimulations 302, 303, 313
  - buprenorphine 16, 22
  - diclofenac 25
  - dissolution 260, 263
  - distribution coefficient 24
  - ephedrine Bjerrum difference plots 15
  - flurbiprofen solubility–pH profile 20
  - gastrointestinal segment functional characteristics 121
  - hydrolysis 38
  - kinetics of decomposition 52, 60
  - metric titrations
    - aqueous solubility 14
    - Bjerrum difference plots 15
    - buprenorphine 15
    - ionisation/acidity constants 14
    - Yasuda–Shedlowski technique 17
  - morphine hydrochloride logD–pH profiles 27
  - oxidation 43
  - partition theory 303
  - preclinical evaluations of drug transport 238
  - proton transfer 7
  - rate profiles 60, 62, 66
  - salt formation 72
  - solubility 20, 20, 22, 22, 108, 313
- pharmaceutical formulation properties 262, 336

- pharmacokinetic dissolution/
  - absorption models 310
- pharmacokinetic modelling software 340
- pharmacokinetic property
  - optimisation 277
- pharmacological activity optimisation 277
- pharynx 119
- phenols 8, 15, 43, 44
- phenytoin 84
- Ph Eur *see* European Pharmacopoeia
- phosphate esters 95
- phosphinyl peptidomimetics 80
- phosphoric acid 75
- photolytic reactions 5, 43, 45, 46
- physicochemical characterisation
  - acid/base properties 5, 7
  - bioavailability optimisation 6
  - biosimulations 302
  - chemical approaches to
    - bioavailability 6, 71
  - decomposition kinetics 6, 51
  - decomposition mechanisms 5, 35
  - dissolution 260
  - drug candidates 5
  - industrial preformulation 6, 101
  - kinetics of decomposition 6, 51
- physicochemical parameters 262
- physicochemical properties 230, 262, 336
- physiological conditions 262, 336
- physiologically based custom-designed software 340
- physiological parameters 262, 302
- picmecillinam 84
- pivampillicin 84
- Plá-Delfina and Moreno model 305
- plasma profiles 299, 318, 319
- plasma protein binding 238
- PLS *see* partial least squares
- polar surface area (PSA) 307, 307
- polydisperse particle dissolution 316, 318
- polyethylene glycol (PEG) 77
- polymerisation 47, 48
- polymers 261
- polymorphism investigations 110
- polysorbates 261
- porins 178
- post-absorption 291
- post-membrane predictions 282
- post-prandial stomach simulations
- POT *see* proton-dependent
  - oligopeptide transporter
- potentiometric titrations 14
- precipitate from toluene 110
- preclinical evaluations of drug
  - transport 225, 232
    - absorption 226, 228, 229, 243
    - ADME 228, 229
    - BCS 245
    - BDDCS 245
    - bioavailability 244
    - Caco-2 cell models 230, 232, 239, 240
    - correlation 230, 238
    - cytochrome P450 242
    - drug discovery 228
    - early discovery 228, 229
    - enzymes 242
    - experimental condition
      - optimisation 238
    - ex vivo* models 234
    - in situ* techniques 231, 237
    - in vitro* techniques 226, 228, 229, 231, 238, 243
    - in vivo* kinetic studies 226, 228, 238, 243
    - late discovery 228, 231
    - MDCK cells 233, 239, 240
    - metabolism 236, 242
    - organ-based *ex vivo* models 234
    - perfusions 235, 237
    - permeability 229, 231
    - physicochemical properties 230
    - predictions 226, 243
    - quantitative structure–property relationship 225, 230
    - solubility 229, 238
    - transporter interaction screening 239
- preclinical investigations
  - bioavailability 297
  - biosimulations 301
- preformulation in the industry 6, 101

- pre-membrane prediction 280
- primary active transport 180
- primary alcohols 44, 44
- primary amines 8
- principal component analysis (PCA) 230
- prodrugs
  - bioavailability optimisation 6, 71, 84, 93
  - ester linkages 93
  - formation 6, 71, 84, 93
  - hydrolysis 35, 38
  - kinetics of decomposition 52
  - linkages 93
- proguanil 84
- pro-moiety introduction 84
- propacetamol 84
- proportional odds model 327, 327
- propranolol 25, 26
- protease enzymes 76, 78
- proteins
  - binding 238
  - deamidation 40
  - expression polarity 117
  - human transporter classification 175
  - racemisation 47
  - stabilisation 6
- proton concentration 7
- proton-dependent oligopeptide transporter (POT) 187
- proton-dependent symports 196, 206
- proton oligopeptide cotransporters 156
- proton transfer 7
- PSA *see* polar surface area
- pseudo first-order kinetics 54, 57, 58, 59
- pseudo first-order plots 56
- pseudopeptides 80
- pseudo zero-order kinetics 52
- pumps 157, 177, 180, 186, 215, 219
- purine nucleosides 202
- pyloric sphincter 118, 121
- pyrimidine nucleosides 202
- QSPR *see* quantitative structure–activity relationship
- QSPR *see* quantitative structure–property relationship
- quantitative structure–activity relationship (QSAR) 308
- quantitative structure–property relationship (QSPR) 225, 230
- quantitative structure–bioavailability 308
- quinapril 84
- rabeprazole 84
- racemisation 47, 47
- ramipril 84
- ranitidine 140
- ranking 102
- rate constants
  - biosimulations 303
  - carrier-mediated transport kinetics 161
  - dissolution 259
  - kinetics of decomposition 51, 52, 53, 54, 56, 57, 58
- rate law 166
- rate of reaction
  - concentration 337
  - kinetics of decomposition 52, 53, 54, 57, 58, 59
  - second-order kinetics 54
- reaction-rate-controlled dissolution 259
- rectum 118, 123
- redox equilibrium 44, 45
- reduced folate transporter (RFT) 203
- regulatory aspects, BCS 286
- release process modelling 318
- renal proximal tubule 200
- residence times 121, 263
- residuals 337, 338
- respiratory tract 123
- retro-inverso peptides 79
- reverse-phase HPLC (RP-HPLC) 104
- reversible inhibitors 166
- reversible reactions 57
- RFT *see* reduced folate transporter
- riboflavin 45, 45
- ring-opening hydrolysis 39
- RP-HPLC *see* reverse-phase HPLC

- rule of five 6, 71, 129, 281
- salicylic acid 75
- salt formation 6, 71, 72, 75, 76
- salt screening 108
- sandwich cultures 235
- SAR *see* structure–activity relationship
- saturable transport 160, 162
- scaling factors 326
- scientific computing tools 340
- secondary active transport 179
- secondary amines 8
- second-order kinetics 54
- secretion quotient (SQ) 239
- segment lengths 121
- SGLT *see* sodium-dependent glucose transporters
- shape factors 30, 76
- shelf lives 51, 53, 55, 57, 58, 59
- simple unit cells 30
- simplex method 333, 336
- simulations
  - bioavailability 297
  - definitions 297
  - gastric fluids, dissolution
  - intestinal fluids, dissolution
- simvastatin 84
- single carrier transport 169
- single nucleotide polymorphism (SNP) 207
- size factors 76
- skin 125, 126
- SLC *see* solute carrier family
- slice technique 236
- small intestine 118, 121, 122, 198, 199, 312
- SMCT *see* sodium-coupled transporters
- SMVT *see* sodium-coupled transporters
- Snedecor's *F* test 339
- SNP *see* single nucleotide polymorphism
- sodium-chloride-dependent symports 196, 206
- sodium-coupled transporters (SMCT, SMVT) 203
- sodium-dependent glucose transporters (SGLT) 159
- sodium-dependent symports 196, 206
- sodium lauryl sulphate 261
- sodium salt dissociation 76
- software packages 229, 339, 340
- solid-state characterisation 29
- solid-state limited solubility 28
- solid-state properties 5, 7, 18, 28
- solubility
  - in aqueous solution 18
    - amphoteric drug candidates 22
    - buprenorphine 22
    - flurbiprofen 19
    - monoprotic acids 19
    - monoprotic bases 20
  - BCS 23, 278, 282, 285, 287, 289, 292
  - BDDCS 291
  - bioavailability 23
  - biosimulations 302, 303, 313, 318
  - dissolution 23, 260, 262, 316
  - drug candidates 5, 7
  - European Pharmacopoeia 18, 18
  - industrial preformulation 103, 105, 109
  - kinetics of decomposition 52
  - lidocaine 21
  - Lipinski's rule of five 71
  - pH profiles 20, 20, 22, 22, 108, 313
  - prodrug formation 84
  - rate 6, 71, 72
  - solid-state limited solubility 28
  - transport preclinical evaluations 229, 238
- solute carrier family (SLC)
  - absorptive transporters 194, 198, 201, 208
  - epithelial cells 196
  - human transporter classification 185, 186, 187, 191
  - SLC15A1 185, 186, 187, 191, 195
  - uniports 155
- solute carrier transport 293
- solvation 28
- solvent volumes 262
- sorbitan esters 261

- specialisations, epithelial
  - classifications 116
- species fractions 14, 15, 16
- specific acid-catalysed hydrolysis 41
- specific base catalysts 65
- spontaneous decomposition 52
- spontaneous hydrolysis 35, 63, 64
- SQ *see* secretion quotient
- stability
  - BCS 282, 288
  - bioavailability optimisation 6
  - biosimulations 302
  - decomposition kinetics 6, 51
  - decomposition mechanisms 35
  - industrial preformulation 103, 105, 106
  - solubility in aqueous solution 18
- standard error of estimation 336
- static models 299
- statistical multivariate analysis 230
- steady-state conditions 160
- stochastic models 299
- Stokes–Einstein equation 136
- stomach 118, 120, 312
- stratum corneum 126
- structure–activity relationship (SAR) 228
- structures
  - acyl groups 36, 36
  - amide bond isosteres 80
  - carboxyl functional groups 36
  - opioid peptides 96, 97
  - peptides 80
- structure–bioavailability 308
- study methods, transport kinetics 171
- substrates
  - adsorption surfaces 162
  - carrier-mediated transport
    - kinetics 154, 155, 164
  - enzyme reactions 160
  - solubility 18
  - specificity 154, 207
  - translocation 155
- succinate ester 73
- succinic acid 75
- sulphotransferase (SULT) 242
- SULT *see* sulphotransferase
- superqualifiers 102
- surface area 121
  - biosimulations 302, 307
  - dissolution 261, 316 262
  - permeability 307
  - pH in biological media 13
- surface descriptor computation 229
- surface tension 263
- surfactants 261, 263
- Swiss Institute of Bioinformatics
  - BLAST Network service 183
- SwissPfam database 183, 186, 191
- symports 154, 155, 156, 158, 167, 179, 196, 206
- system variables, biosimulations 297
- target identification (TI) 228
- tartaric acid 75
- Taylor’s approximation 332
- TC *see* transporter classification
- TCDB *see* transporter classification database
- TEER *see* transepithelial electrical resistance
- temazolamide 84
- temperature 52, 62
- terbutaline 140, 140
- tertiary amines 8
- tetracycline 84
- tetragonal structures 29
- TGA *see* thermogravimetric analysis
- thalidomide 37
- thermal stability 106, 109
- thermogravimetric analysis (TGA) 106, 109, 110
- thiamine transporter (ThT) 203
- ThT *see* thiamine transporter
- TI *see* target identification
- tight junctions 117, 126
- time
  - accumulation–time graphs 148
  - flux–time graphs 148
  - time-dependent diffusion 318
  - time-dependent mathematical models 299, 310
  - time-independent model 308
- tissue segments 205
- tissue slices 236
- titrations

- morphine sulphate 26, 26
  - pH metric titrations 14
  - solubility–pH profiles 20
- TMS *see* transmembrane segments
- toxicokinetic software 340
- trandolapril 84
- transcellular diffusion 226, 229
- transepithelial electrical resistance (TEER) 126
- transition state mimetics 80
- transit times 263, 302, 312
- translocation 155, 156, 157
- transmembrane segments (TMS),
  - human transporter classification 183
- transport
  - carrier-mediated transport
    - kinetics 153
  - classification system
    - gene ontology 185
    - human transporter
      - classification 180, 185, 187
    - gene ontology 185
    - human transporter classification
      - 180, 185, 187
    - mechanisms 177, 186
    - neutral amino acid transport
      - 198
    - passive diffusion 135
    - rate-controlled dissolution 259
  - transportates, kinetics 164
  - transporter classification (TC) 180
  - transporter classification database (TCDB) 183
  - transporter-enzyme interactions 291
  - transporter interaction screening 239
  - transporter-substrate complex binding
    - 168
  - travoprost 84
  - triclinic structures 29
  - trifluorethylamine 81
  - trigonal structures 29
  - tripeptides 156, 158, 179, 195, 199
  - two-electron transfer 35
  - tyrosine 44
- UGT *see* uridine diphosphate
  - glucuronosyl transferase
- uncompetitive inhibitors 166, 168
- uniports 154, 155, 179, 196
- unit cells 30, 30
  - dimensions 29
  - shape 30
  - solid-state characterisation 29
- unstirred layers 139, 141
- uphill transport 156
- uptake 168
- uptake ratio (UR) 239
- UR *see* uptake ratio
- uridine 203
- uridine diphosphate glucuronosyl
  - transferase (UGT) 242
- US Pharmacopoeia (USP) 257
- Ussing chambers 144, 236, 242
- valaciclovir 8
  - absorptive transporters 193
  - bioisosteric replacement 96
  - hydrolysis 38, 55, 60
  - pH-rate profile 62
- valdecoxib 84
- valganciclovir 84, 96
- validation techniques 326
- valine 8
  - bioisosteric replacement 96
  - hydrolysis 38, 41, 55, 60
  - valaciclovir hydrolysis 38
- variance–covariance matrix 336
- velocity 160, 162, 163, 166
- verification techniques 300
- vesicles 234
- villi 121, 122
- vitamins 196, 203, 204
- volume factors 261, 262
- Wagner–Nelson method 203, 321, 324
- water-catalysed reactions 35, 63
- Weibull dissolution 316, 317
- weighted least squares 331
- width, unit cells 29
- X-ray powder diffraction (XRPD) 105, 108, 109
- Yasuda–Shedlowski technique 17
- zuclopentixol 84

